The Jurassic/Cretaceous boundary: a hidden mass extinction in tetrapods?

Jonathan P. Tennant

CID: 00661116

Imperial College London

Department of Earth Science and Engineering

Thesis submitted to fulfil the requirements for the degree of Doctor of Philosophy and Diploma of Imperial College

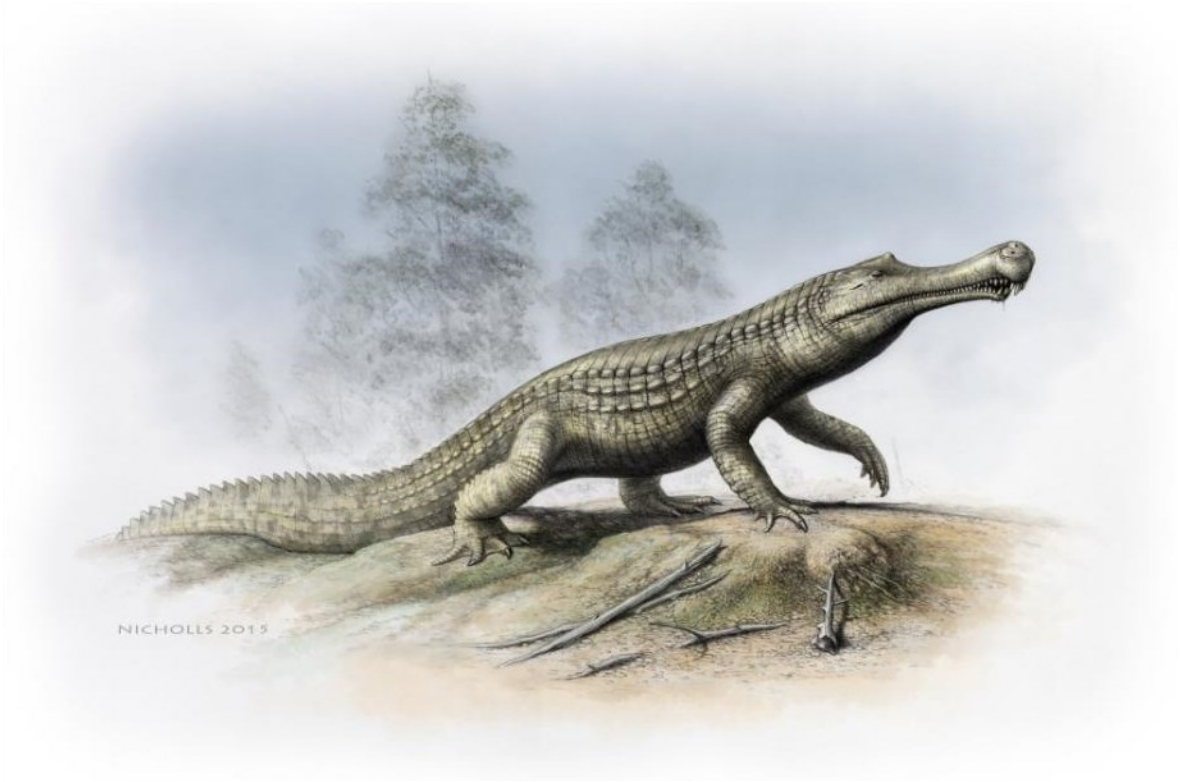


Image credit: Robert Nicholls (CC BY 4.0). Depicts *Sarcosuchus imperator*, a giant predatory crocodyliform from the Cretaceous of North Africa.

Declaration of originality

I declare that the works presented within this thesis are my own, and that all other work is appropriately acknowledged and referenced within.

Copyright declaration

The copyright of this thesis rests with the author, and it is made available under a Creative Commons Attribution (CC BY 4.0) license. Researchers are free to copy, distribute and transmit this thesis on the condition that it is appropriately attributed.



Jonathan Peter Tennant

Supervisors: Dr. Philip Mannion (Imperial College London); Prof. Paul Upchurch (University College London); Dr. Mark Sutton (Imperial College London).

Acknowledgements

First and definitely foremost, I want to extend my greatest thanks to Phil Mannion. As his first PhD student, I am sure he regretted his decision after day one, but stuck with it until the end, and has been a stoic mentor throughout. This project would have been a shadow of what it came to be without his guidance. I am still yet to get him on Twitter though. I am also hugely grateful to Paul Upchurch and Mark Sutton for their input and experience throughout this project. I also could not have completed this project without the encouragement and support from my girlfriend, friends, and family, and am hugely grateful to them. Each of you are amazing, and I love you all in your own special way.

I would like to extend my gratitude to NERC for funding this PhD project. Other institutes have provided various degrees of financial support throughout this research, and for that I would like to thank the Palaeontological Association, the Public Library of Science, and the Society of Vertebrate Paleontology. The whole Palaeontology community deserves collective thanks, and I would especially like to acknowledge the London vertebrate palaeontology community for their continuing support and advice throughout this PhD.

I'd also like to extend my thanks to Ross Mounce, Mike Taylor and the global 'open science' community for their encouragement in encouraging me to 'open up' this research project, and for providing advice on the various aspects of publishing and practising open scholarship. Graham Steel has also indirectly influenced the mind-set with which I approached this PhD. He once said at a conference, "G*etting younger people to be more open about their science: that's the revolution*." This inspired me to be completely open about all aspects of this PhD, from the research processes through to the outputs, including this thesis. As well as these, I feel that communities such as Wikipaleo and Twitter should be thanked for providing access to hundreds of research papers that I otherwise would not have had access to and without which I would not have been able to complete my research.

I am appreciative of anyone else who has ever offered encouragement directly or through social media. A special thanks to Ed Yong and Brian Switek as, although they don't know it, they encouraged me to start writing about science in the first place, which began my development along the path of science communication. I'd also like to extend my thanks to Barbara Ferreira of the European Geosciences Union for hosting my blog on the EGU network, which undoubtedly directly contributed to my development as a science writer, and has been an outlet for me to collect my thoughts.

Nic Bilham of the Geological Society, London, has been a strong mentor before and during this PhD, and always an incredible educator on the more social and policy-oriented aspects of scientific research. Without his guidance, I would never have really considered the broader impacts of my research and skills development as a junior researcher, so am indebted to him for this horizon broadening, and the initial risk he took in employing me. He also offered me one of the best [and indirectly targeted] pieces of advice I've ever had in my pursuit for knowledge: "*If you don't know what you're talking about, keep your mouth shut*." Needs no further explanation.

Thanks to [Dr!] James Lewis as, in spite of being a planetary geochemist, he has always had useful comments to make on various aspects of this project. Also, life at Imperial College would have been a lot duller without the presence of other characters in the department, so thanks to everyone for all the hallway chats, shenanigans, and various offerings of cake, coffee, and cookies.

For access to specimens, there are numerous people to thank for accommodating me and providing conversations about my research throughout: John Hutchinson for access to crocodile specimens at the RVC (London); Lorna Steel for access to specimens at the NHM (London), and useful discussion on crocodile anatomy; Didier Berthet at the MNHL (Centre de Conservation, Lyon); Zoltán Csiki-Sava at the FGGUB (Bucharest); Géraldine Garcia at UP (Poitieres); Amy Henrici at the CM (Pittsburgh); Carl Mehling of the AMNH (New York); Oliver Rauhut at the BSPG (Munich); Chris Sagebiel at UT (Austin); Daniela Schwarz at the MfN (Berlin); Herman Voogd from the TM (Haarlem); and Dale Winkler of the

SMU (Dallas). For those from non-English speaking countries, thanks for not making me feel any more stupid for not knowing your language. Without specimen access, much of this thesis would not have been possible, and I would like to thank each of you for your time and patience in allowing me to visit your collections. I would also like to thank Greg Price for useful discussion on the environmental changes occurring across the Jurassic/Cretaceous transition. Finally, I would like to offer my thanks to Robert Berner for freely providing his GEOCARBSULF data on request.

Finally, I am grateful for the efforts of all those who have collected Jurassic–Cretaceous tetrapod data, and to those who have entered this data into the Paleobiology Database, especially John Alroy, Matt Carrano, Roger Benson, and Richard Butler. I would also like to thank John Alroy and Graeme Lloyd for assistance with R during the Fossilworks Analytical Course in the summer of 2014. J. Alroy also provided the scripts for implementing SQS in R (bio.mq.edu.au/~jalroy/SQS.html) and in Perl. Silhouettes in figures were created by Gareth Monger, Scott Hartman, Michael Keesey, and Nobu Tamura, and are available from phylopic.org/.

If I have missed anyone out, it's either because I didn't want to thank you, or because writing an exhaustive list of everyone who has contributed in some way to my development as a scientist over the last few years would be a separate thesis in itself.

Published works by the author contributing to this thesis

Tennant, J. P., Mannion, P. D., and Upchurch, P. U. (in press) Sea level regulated tetrapod diversity through the Jurassic/Cretaceous transition, *Nature Communications*.

Tennant, J. P., Mannion, P. D., and Upchurch, P. (2016) Evolutionary relationships and systematics of Atoposauridae (Crocodylomorpha: Neosuchia): implications for the rise of Eusuchia, *Zoological Journal of the Linnean Society*, **177**, 854-936.

Tennant, J. P., Mannion, P. D., and Upchurch, P. (2016) Environmental drivers of crocodyliform diversity across the Jurassic/Cretaceous transition, *Proceedings of the Royal Society Series B: Biological Sciences*, **283**, 20152840. (link)

Tennant, J. P. Mannion, P. D., Upchurch, P., Sutton, M. and Price, G. (2016) Biotic and environmental dynamics across the Jurassic/Cretaceous boundary: evidence for a protracted period of faunal and ecological turnover, *Biological Reviews* (advanced online publication). (link)

Young, M. T., **Tennant, J. P.,** Brusatte, S. (2016) The first definitive Middle Jurassic atoposaurid (Crocodylomorpha, Neosuchia), and a discussion on the genus *Theriosuchus*, *Zoological Journal of the Linnean Society*, **176(2)**, 443-462. (link)

Mannion, P. D., Benson, R. B. J., Carrano, M. T., **Tennant, J. P.,** Judd, J. and Butler, R. J. (2015) Climate constrains the evolutionary history and biodiversity of crocodylians, *Nature Communications*, **6**, 8438. (link)

Tennant, J. P. and Mannion, P. D. (2014) Revision of the Late Jurassic crocodyliform *Alligatorellus*, and evidence for allopatric speciation driving high diversity in western European atoposaurids, *PeerJ*, **2**, e599. (link)

Young, M. T., Steel, L., Foffa, D., Price, T., Naish, D., and **Tennant, J. P.** (2014) Marine tethysuchian crocodyliform from the ?Aptian-Albian (Early Cretaceous) of the Isle of Wight, England, *Biological Journal of the Linnean Society*, **113(3)**, 854-871 (link).

Yi, H., **Tennant, J. P.,** Young, M. T., Foffa, D., Hudson, J. D., Challands, T. J,. Ross, D. A. and Brusatte, S. L. (in review) An unusual small-bodied crocodyliform from the Middle Jurassic of Scotland, UK, and potential evidence for an early diversification of 'advanced' neosuchians. *Transactions of the Geological Society of Edinburgh*.

Tennant, J. P. and Evers, S. (in prep.) How does diversity through time change through time?

"*An approximate answer to the right question is worth a great deal more than a precise answer to the wrong question*." – John Tukey.

"*You can come up with statistics to prove anything, Kent*." – Homer Simpson.

Table of Contents

Declaration of originality 2

Copyright declaration 2

Acknowledgements 3

Published works by the author contributing to this thesis 6

Table of Contents 9

List of Figures and captions 20

Abstract 36

List of institutional abbreviations 37

Introduction 38

Research overview 39

1 Biotic and Abiotic Dynamics Across the Jurassic/Cretaceous Transition 1-41

1.1 Introduction to the Jurassic/Cretaceous boundary 1-42

1.1.1 Stratigraphic age of the J/K boundary 1-43

1.1.2 The J/K boundary as an extinction event 1-44

1.1.2.1 The 'Big Five' mass extinctions 1-44

1.1.2.2 History of the J/K boundary extinction 1-45

1.1.2.3 Renewed evidence for an extinction event? 1-49

1.2 Palaeogeographic and environmental changes across the J/K boundary 1-50

1.2.1 Palaeogeography and palaeoceanography 1-50

1.2.2 Sea level and stratigraphy 1-53

1.2.3 Volcanism 1-57

1.2.4 Bolide impacts 1-60

1.2.5 Climate 1-61

1.3 Biotic changes across the Jurassic/Cretaceous transition 1-64

1.3.1 Incomplete and biased sampling in the fossil record 1-64

1.3.2 The quality of the Late Jurassic–Early Cretaceous fossil record 1-68

1.3.3 Vertebrates 1-76

1.3.3.1 Dinosaurs 1-76

1.3.3.2 Pterosaurs 1-81

1.3.3.3 Crocodylomorphs 1-82

1.3.3.4 Ichthyopterygians 1-84

1.3.3.5 Plesiosaurians 1-85

1.3.3.6 Testudinatans 1-86

1.3.3.7 Choristoderes 1-88

1.3.3.8 Lepidosaurians 1-89

1.3.3.9 Lissamphibians 1-90

1.3.3.10 Mammaliaforms 1-92

1.3.3.11 Fish groups 1-94

1.3.4 Invertebrates 1-95

1.3.4.1 Molluscs 1-96

1.3.4.2 Brachiopods 1-97

1.3.4.3 Corals 1-98

1.3.4.4 Echinoderms 1-99

1.3.4.5 Arthropods 1-99

1.3.4.6 Bryozoans 1-101
1.3.5 Microfossils 1-101
1.3.5.1 Foraminifera 1-102
1.3.5.2 Radiolarians 1-102
1.3.5.3 Phytoplankton 1-102
1.3.6 Plants 1-103
1.4 Scope of this thesis 1-104
2 Materials and Methods 2-108
2.1 Age of the Jurassic/Cretaceous boundary 2-109
2.2 Assembling a tetrapod occurrence dataset 2-110
2.2.1 The Paleobiology Database and Fossilworks 2-110
2.2.2 Data compilation 2-112
2.2.3 Crocodyliformes occurrences 2-116
2.2.3.1 A note on Cretaceous thalattosuchians 2-118
2.2.4 Defining taxonomic sub-groups 2-120
2.2.5 Latitudinal taxonomic subgroups 2-121
2.2.6 A note on data quality 2-122
2.3 Constructing a crocodyliform supertree 2-123
2.4 Time binning protocol 2-123
2.5 Reconstructing taxonomic diversity 2-125
2.5.1 A note on residual diversity estimates 2-126

2.6 Sample standardisation 2-128

2.6.1 Shareholder Quorum Subsampling 2-129

2.6.2 Applying SQS to Crocodylifomes 2-133

2.6.3 Bootstrapping SQS 2-135

2.7 Phylogenetic diversity estimates 2-135

2.7.1 Phylogenetic diversity estimation for non-crocodyliforms tetrapods 2-137

2.7.2 Phylogenetic diversity estimation for Crocodyliformes 2-138

2.7.2.1 Supertree construction protocol 2-138

2.7.2.2 Crocodyliformes 2-146

2.7.2.3 Notosuchia 2-146

2.7.2.4 Neosuchia 2-149

2.7.2.5 Eusuchia 2-153

2.7.2.6 Crocodylia 2-154

2.7.2.7 Excluded taxa due to unknown or uncertain affinities 2-154

2.7.3 PDE using the crocodyliform supertree 2-155

2.8 Calculating extinction and origination rates 2-156

2.9 Addressing the impact of sampling megabiases 2-158

2.9.1 Lithological changes across the J/K transition 2-164

2.10 Model-fitting procedure 2-165

2.10.1 Extrinsic parameter selection 2-166

2.10.2 Time series analysis 2-170

2.10.3 Autocorrelation of time series 2-171
2.10.4 Assessing the relative relative fit of extrinsic parameters 2-172
2.11 Building an atoposaurid character matrix 2-173
2.11.1 Taxon sampling 2-173
2.11.2 Data matrix 2-180
2.12 Phylogenetic analysis 2-183
2.12.1 Parsimony analysis 2-183
2.12.2 Bayesian inference 2-184
3 Tetrapod Diversity and Extinction Across the Jurassic/Cretaceous Boundary 3-187
3.1 Introduction 3-188
3.2 Results and discussion 3-188
3.2.1 Uncorrected taxonomic diversity 3-188
3.2.2 Global subsampled diversity 3-190
3.2.2.1 Comparison with results using TRiPS 3-194
3.2.3 Regional patterns of diversity across the J/K boundary 3-201
3.2.4 Latitudinal patterns of diversity change 3-213
3.2.5 Phylogenetic diversity estimation 3-217
3.2.6 Bootstrapped Shareholder Quorum Subsampling (SQS) 3-220
3.2.7 Patterns of global extinction and origination 3-226
3.2.8 Changes in lithological occupation across the J/K transition 3-232
3.2.9 Sampling, diversity and redundancy 3-235

3.2.10 The effect of sea level on sampling, and testing the 'common cause' hypothesis .3-242

3.2.11 Extrinsic drivers of Jurassic/Cretaceous tetrapod diversity 3-243

3.3 Summary 3-248

4 A Diversity Crash in Crocodyliformes Across the Jurassic/Cretaceous Boundary 4-251

4.1 Introduction 4-252

4.2 Results 4-253

4.2.1 Raw diversity across the Jurassic/Cretaceous boundary 4-253

4.2.2 Phylogenetic diversity across the Jurassic/Cretaceous boundary 4-255

4.2.3 Subsampled global diversity across the Jurassic/Cretaceous boundary 4-257

4.2.3.1 Global subsampled results when varying the quorum level.....4-261

4.2.4 Subsampled regional diversity across the Jurassic/Cretaceous boundary 4-264

4.2.5 Global origination and extinction rates through the Jurassic/Cretaceous boundary....4-267

4.2.6 Environmental drivers of diversity.....4-270

4.3 Discussion.....4-272

4.3.1 Crocodyliform extinction across the Jurassic/Cretaceous boundary.....4-272

4.3.2 The impact of sampling on Late Jurassic-Early Cretaceous non-marine crocodyliform biodiversity.....4-274

4.3.3 Environmental drivers of the Jurassic/Cretaceous crocodyliform diversity crash ..4-275

4.4 Summary 4-278

5 Evolutionary Relationships and Systematics of Atoposauridae (Crocodylomorpha: Neosuchia) Across the Jurassic/Cretaceous Boundary, and Implications for the Rise of Eusuchia.....5-282

5.1 Introduction 5-283
5.1.1 Taxonomic composition 5-283
5.1.2 Atoposaurids in time and space 5-285
5.1.3 Evolutionary relationships 5-286
5.2 Results 5-290
5.2.1 Parsimony analyses 5-290
5.2.1.1 Unordered analysis 5-291
5.2.1.2 Ordered analysis 5-293
5.2.1.3 Implied weighting 5-294
5.2.2 Bayesian analyses 5-296
5.2.3 Branch lengths and stratigraphic ranges 5-299
5.2.4 Results summary 5-301
5.3 Systematic Palaeontology 5-304
5.4 Definitive atoposaurid taxa 5-312
5.4.1 Alligatorium Jourdan 1862 5-312
5.4.1.1 *Alligatorium meyeri* (Jourdan, 1862) (type species) 5-312
5.4.2 Unnamed clade: Atoposaurus + Alligatorellus 5-317
5.4.3 Atoposaurus von Meyer 1850 5-317
5.4.3.1 *Atoposaurus jourdani* (Meyer, 1850) (type species) 5-320
5.4.3.2 *Atoposaurus oberndorferi* (Meyer, 1850) 5-322
5.4.4 Alligatorellus Gervais 1871 5-324

5.4.4.1 *Alligatorellus beaumonti beaumonti* (Wellnhofer, 1971) 5-332

5.4.4.2 *Alligatorellus bavaricus* Wellnhofer 1971 (re-ranked; (Tennant and Mannion, 2014)) 5-340

5.5 Osteoderm morphology in atoposaurid systematics 5-345

5.5.1 Alligatorellus bavaricus morphotype 5-346

5.5.2 Alligatorellus beaumonti morphotype 5-348

5.5.3 MfN MB. R. 4317.1-12 ('Alligatorellus sp.') morphotype 5-348

5.6 The taxonomic validity of Atoposaurus and Alligatorium 5-349

5.7 Putative atoposaurid taxa 5-354

5.7.1 Montsecosuchus (Buscalioni and Sanz, 1988) 5-355

5.7.1.1 *Montsecosuchus depereti* (Buscalioni and Sanz, 1988) 5-357

5.7.2 Theriosuchus Owen 1878a 5-361

5.7.2.1 The dentition of *Theriosuchus* 5-367

5.7.2.2 Unnamed clade: *Theriosuchus pusillus* + *Theriosuchus guimarotae* 5-371

5.7.2.3 *Theriosuchus pusillus* (Owen, 1878b) (type species) 5-372

5.7.2.4 *Theriosuchus guimarotae* (Schwarz and Salisbury, 2005) 5-380

5.7.2.5 *Theriosuchus grandinaris* (Lauprasert *et al.*, 2011) 5-386

5.7.2.6 *Theriosuchus* sp. 5-388

5.7.3 'Alligatorium' franconicum (Ammon, 1906) 5-395

5.7.4 Sabresuchus nov. gen. 5-398

5.7.4.1 *Sabresuchus ibericus* nov. comb. 5-402

5.7.4.2 *Sabresuchus sympiestodon* nov. comb. 5-407
5.7.5 Brillanceausuchus babouriensis (Michard et al., 1990) 5-411
5.7.6 Pachycheilosuchus trinquei (Rogers, 2003) 5-413
5.7.7 Wannchampsus kirpachi (Adams, 2014) 5-415
5.7.8 Karatausuchus sharovi (Efimov, 1976) 5-415
5.7.9 Hoplosuchus kayi (Gilmore, 1926) 5-416
5.7.10 Shantungosuchus chuhsienensis (Young, 1961) 5-417
5.7.11 Indeterminate remains previously attributed to Atoposauridae 5-418
5.8 Discussion 5-423
5.8.1 Western European Late Jurassic to Early Cretaceous Atoposaurid Diversity 5-423
5.8.2 Phylogenetic relationships and systematic implications 5-426
5.8.3 Evolutionary history of Atoposauridae, Theriosuchus and Sabresuchus 5-428
5.8.4 The transition to Eusuchia 5-429
5.8.4.1 Background 5-429
5.8.4.2 Development of the squamosal posterolateral process 5-430
5.8.4.3 Development of the secondary choanae 5-431
5.8.4.4 Development of vertebral procoely 5-435
5.8.4.5 Biconvex first caudal vertebra 5-438
5.9 Summary 5-439
6 Discussion and Conclusions 6-444
6.1 What was the scale of any extinction across the Jurassic/Cretaceous boundary? 6-444

6.1.1 The influene of different measures of diversity 6-445

6.1.2 Global versus regional patterns of diversity and extinction 6-446

6.2 How did the timing, magnitude, and tempo of the J/K boundary extinction vary between different groups? 6-448

6.3 What was the ecological response of different tetrapod groups to the J/K boundary extinction? 6-451

6.3.1 Marine and semi-aquatic groups 6-452

6.3.2 Terrestrial groups 6-454

6.3.3 Broader ecological implications 6-457

6.4 To what extent do abiotic factors correlate with biological changes through the Jurassic/Cretaceous boundary? 6-459

6.5 Future directions of research 6-462

6.5.1 Global correlation of the J/K boundary 6-462

6.5.2 Paying homage to the Red Queen 6-464

6.5.3 Macroevolutionary changes across the J/K transition 6-465

6.5.4 Taphonomic distortion of the J/K boundary extinction 6-467

6.5.5 Catastrophism and the J/K boundary extinction 6-468

Bibliography 6-471

Appendix 1 – Additional details regarding crocodyliform supertree construction. Note that these analyses were perform prior to the atoposaurid phylogenetic analyses in Chapter 5. 6-535

Appendix 2 – Mode of life for crocodyliform species used to construct supertree (see Section 2.6) ..6-548

Appendix 3 – Mode of life and first and last appearance data occurrences for crocodyliform genera used for supertree construction (see Section 2.6). 6-555

Appendix 4 – Machine readable versions of crocodyliform supertrees.....6-559

Appendix 5 – Age ranges for crocodyliform species used to construct supertree (see Section 2.6) 6-564

Appendix 6 – Atoposaurid character list.....6-570

Appendix 7 – Character codings for taxa used in phylogenetic analysis (see Chapter 4) 6-603

Appendix 8 – Full European and North American stage-level subsampling results for different tetrapod groups 6-609

Appendix 9 – Full results of the SQS results for tetrapod groups when varying the quorum level.6-639

Appendix 10 – Full model-fitting results for all tetrapod groups and extrinsic parameters including sampling proxies and environmental factors. 6-651

Appendix 11 – Appendix 11 – Spatial diversity (SQSPt, SQSPs, SQSRc, SQSRu) results for subsampled non-marine crocodyliforms (Chapter 4). 6-666

Appendix 12 - Complete results of phylogenetic diversity analyses for Crocodyliformes (Chapter 4). 6-677

Appendix 13 – Full results from model fitting procedure between crocodyliform diversity estimates and extrinsic sampling and environmental parameters (Chapter 4). 6-680

List of Figures and captions

Figure 1. Late Jurassic and Early Cretaceous (Oxfordian–Albian) palaeogeographic map showing the locations of major flood basalts, minor volcanic activity, and bolide impacts. 1-53
Figure 2. Sea-level curve showing shorter-term fluctuations through the Late Jurassic and Early Cretaceous. (Miller *et al.*, 2005). The blue horizontal line represents modern sea level, and the red line represents the J/K boundary. 1-57
Figure 3: (A) Late Jurassic (Oxfordian–Tithonian) and (B) Early Cretaceous (Berriasian–Albian) global fossil occurrences, with climatic regions overlain. Fossil occurrence data downloaded from The Paleobiology Database, November, 2014 (http://paleobiodb.org/). Palaeoclimate data from Paleomap project (http://www.scotese.com/). 1-64
Figure 4. Global taxonomic diversity curve for all animal species, with individual fossil collections and occurrences shown. The Jurassic/Cretaceous boundary is marked by a red line. Data extracted from the Paleobiology Database, January, 2014 (http://paleobiodb.org/). Constructed using the *strap* package (Bell and Lloyd, 2015) in R (version 3.1.1) (R Development Core Team, 2013). Abbreviations: Ox, Oxfordian; Ki, Kimmeridgian; Ti, Tithonian; Be, Berriasian; Va, Valanginian; Ha, Hauterivian; Ba, Barremian; Ap, Aptian; Al, Albian. 1-69
Figure 5. Changes in the 'quality' of the North American marine and non-marine tetrapod fossil record through time based on a measure of eveness (Good's u) (Good, 1953) (see 2-149). Data shown is the mean of that provided for different tetrapod groups in Appendix 8. 1-72
Figure 6. Changes in the 'quality' of the European marine and non-marine tetrapod fossil record through time based on a measure of eveness (Good's u) (Good, 1953) (see Section 2.5). Data shown is the mean of that provided for different tetrapod groups in Appendix 8. 1-74
Figure 7. Late Jurassic and Early Cretaceous fossil bearing collections based on continental location. (A) Terrestrial collections (vertebrates only); (B) Marine collections (vertebrates only; (C) Marine collections (invertebrates only). Data from the Paleobiology Database, accessed January, 2015 (http://paleobiodb.org/). Collections represent irreducible and discrete fossil-bearing localities. Only those that could be dated to Stage-level resolution were included. Constructed using the geoscale package (Bell and Lloyd, 2015) in R (version 3.1.1) (R Development Core Team, 2013).....1-76
Figure 8. Stratigraphic ranges of major Jurassic–Cretaceous theropod (A), sauropod (B) and ornithischian (C) dinosaur clades through the Middle Jurassic to Early Cretaceous. Theropods are adapted from Carrano et al. (2012); sauropods are adapted from Mannion et al. (2013). Clade dates are based on those available from The Paleobiology Database, and supplemented from the primary

literature. See text for details. Silhouettes from PhyloPic (http://phylopic.org/); Allosaurus fragilis and Diplodocus by Scott Hartman (CC BY-SA 3.0), and Stegosaurus by Andrew Farke (CC BY 3.0). Abbreviations as in Figure 4; additional abbreviations: Aa, Aalenian; Bj, Bajocian; Bt, Bathonian; Ca, Callovian. 1-78
Figure 9. Stratigraphic ranges of major Jurassic–Cretaceous crocodyliform clades. Adapted from Bronzati et al., (2012). Dates obtained from The Paleobiology Database. Abbreviations as in Figure 4. Silhouette of *Metriorhynchus geoffroyi* from PhyloPic, by Gareth Monger (CC BY 3.0). 1-84
Figure 10. Stratigraphic ranges of major Jurassic–Cretaceous turtle clades. Phylogenetic relationships are not illustrated. Dates obtained from the Paleobiology Database. Abbreviations as in Figure 4. Silhouette of a baenid turtle from PhyloPic, by Scott Hartman (CC BY-SA 3.0). 1-87
Figure 11. Stratigraphic ranges of major Jurassic–Cretaceous mammaliaform lineages. Dates obtained from The Paleobiology Database. Abbreviations as in Figure 4. Silhouette of Morganucodon watsoni from PhyloPic, by FunkMonk (CC BY-SA 3.0). 1-94
Figure 12. Jurassic marine (blue) and non-marine (brown) tetrapod body fossil occurrences. 2-113
Figure 13. Palaeolatitudinal distribution of all non-marine tetrapod occurrences through the Jurassic and Cretaceous. The Jurassic/Cretaceous boundary (145 Ma) is highlighted in red. Palaeolatitudes are based on Scotese rotations, and acquired from the Paleobiology Database 2-114
Figure 14. Cretaceous marine (blue) and non-marine (brown) tetrapod body fossil occurrences. 2-116
Figure 15. Late Jurassic marine (blue) and non-marine (red) crocodyliform occurrences. Palaeolatitudes are based on Scotese rotations, and acquired from the Paleobiology Database.. 2-119
Figure 16 Early Cretaceous marine (blue) and non-marine (red) crocodyliform occurrences. Palaeolatitudes are based on Scotese rotations, and acquired from the Paleobiology Database.. 2-120
Figure 19. Palaeolatitudinal distribution of all crocodyliform occurrences assigned to genera through the Jurassic and Cretaceous. The Jurassic/Cretaceous boundary (145 Ma) is highlighted in red. Palaeolatitudes are based on Scotese rotations, and acquired from the Paleobiology Database.. 2-134
Figure 17. Genus level supertree 2-140
Figure 18. Species level supertree 2-145
Figure 20. Palaeolatitudinal distribution of all marine tetrapod occurrences through the Jurassic and Cretaceous. The Jurassic/Cretaceous (145 Ma) and end-Cretaceous (66 Ma) boundaries are highlighted in red. Palaeolatitudes are based on Scotese rotations, and acquired from the Paleobiology Database 2-165
Figure 21. Raw taxonomic diversity for marine and non-marine Jurassic and Cretaceous tetrapods, grouped into approximately equal 10 million year time bins. 3-189

Figure 22. Global non-marine Late Jurassic/Early Cretaceous subsampled diversity for (a) major dinosaur groups; (b) testudines, crocodylomorphs, and pterosaurs; and (c) mammals, lepidosaurs and lissamphibians. Shaded areas represent stage boundaries. Silhouettes from PhyloPic courtesy of Michael Keesey, Brad McFeeters, Scott Hartman, Mark Witton, Ville Veikko Sinkkonen and Hanyong Pu (see http://phylopic.org/ for additional license information). 3-198
Figure 23. Global marine subsampled diversity for major Late Jurassic/Early Cretaceous pelagic clades. Sea level curve from Miller et al. Silhouettes from PhyloPic courtesy of Gareth Monger and Michael Keesey (see http://phylopic.org/ for additional license information). 3-199
Figure 24. Phylogenetic diversity estimates for different tetrapod clades. 3-218
Figure 25. Bootstrapped SQS diversity for non-marine and marine tetrapods. 3-221
Figure 26. Bootstrapped SQS diversity for the three major dinosaurian clades. 3-224
Figure 27. Bootstrapped SQS diversity for pterosaurs and non-marine crocodylomorphs. 3-224
Figure 28. Bootstrapped SQS diversity for marine tetrapod groups. 3-226
Figure 29. Normalised distribution of different lithofacies for each higher tetrapod group. 3-232
Figure 30. Outcrop area and collections for the (a) non-marine record of Europe; (b) marine record of Europe (c) non-marine record of North America; (d) marine record of North America. European outcrop area from Smith and McGowan (2007), and North American outcrop area from Peters and Heim (2010). Note the discontinuity between the availability of the rock record and the number of collections in the earliest Cretaceous of North America. 3-240
Figure 31. Jurassic (A) and Cretaceous (B) crocodyliform occurrences, superimposed onto reconstructed palaeomaps. Silhouettes: Isisfordia (M. Keesey), Goniopholis (S. Hartman), Notosuchus (N. Tamura), Steneosaurus (G. Monger), Elosuchus (M. Keesey), Protosuchus (M. Keesey); (C) Raw taxonomic diversity estimate (TDE) for Jurassic–Cretaceous marine (blue) and non-marine (red) crocodyliforms. Palaeomap: http://fossilworks.org/?a=mapForm. 4-255
Figure 32. Reconstructed phylogenetic diversity estimate (PDEt and PDEs) for marine (blue) and non-marine (red) crocodyliforms, based on the mean of all three reconstruction approaches. Eustatic sea-level is from Miller *et al.* (2005). 4-256
Figure 33. Phylogenetic diversity estimate (PDEt and PDEs) at the species level for marine and non-marine sub-groups. 4-257
Figure 34. Results obtained using SQSRs for marine and non-marine taxa. 4-260
Figure 35. Comparison between subsampled quorum level and subsampled richness (SQSRs) in the time bins either side of the J/K boundary. 4-262

Figure 36. Subsampled biodiversity. (A) Marine and non-marine curves (SQSRc); (B-F) Continent-level curves. Red filled circles represent SQSRc, and black filled circles are SQSRu. 4-265
Figure 37. Results obtained using SQSPt on a global and palaeocontinental level. 4-266
Figure 38. Non-marine (A) and marine (B) per capita extinction rates using the boundary-crosser and three-timer methods. 4-269
Figure 39. Stratigraphic (including uncertainty) and geographic ranges of known and putative ...5-286
Figure 40. Previously recovered inter-relationships between Atoposauridae and other major crocodyliform clades: (A) Adams (2014; (B) Rogers (2003); (C) Turner and Pritchard (2015).....5-288
Figure 41. Previously recovered intrarelationships within Atoposauridae. (A) Buscalioni and Sanz (1988); (B) Bronzati et al. (2012); (C) Turner, 2015. 5-290
Figure 42. (A) Strict consensus topology for phylogenetic analysis when all taxa are included, and all characters are considered to be unordered (i.e., non-additive). Atoposauridae is marked with a red star. (B) Strict consensus for phylogenetic analysis when all taxa are included, and selected characters are considered to be ordered (Appendix 6).....5-293
Figure 43. (A) Strict consensus topology for phylogenetic analysis when iterpcr script is employed, and Alligatorium franconicum and '*Alligatorellus*' sp. are excluded a priori. (B) Single most parsimonious tree for phylogenetic analysis when *Pachycheilosuchus trinquei* and '*Alligatorellus*' sp. (MB.R.3632) are excluded a priori. Absolute Bremer support values are provided adjacent to nodes. Atoposauridae is marked with a red star. 5-296
Figure 44. Single most parsimonious tree for phylogenetic analysis when implied weighting is employed with a weighting exponent of k=3. Selected characters are considered to be ordered, and no taxa were excluded a priori. Absolute Bremer support values are provided adjacent to nodes. 5-296
Figure 45 (A) Results of phylogenetic analysis using Bayesian inference, when all OTUs are active and selected characters are considered to be ordered. (B) Results of phylogenetic analysis using Bayesian inference, when '*Alligatorellus*' sp. (MB.R.3632) and *Theriosuchus* sp. (NMS G. 2014.52.1 and selected characters are considered to be ordered (see Appendix 6). 5-297
Figure 46. Relationship between branch lengths resulting from Bayesian phylogenetic analysis and total stratigraphic range implied from time-scaling analyses (see Figure 55) for all analysed OTUs. Pearson's p = 0.694, r = -0.089.....5-300
Figure 47. Relationship between branch lengths resulting from Bayesian phylogenetic analysis and total stratigraphic range implied from time-scaling analyses (see Figure 55) for all analysed OTUs excluding protosuchian and coelognathosuchian outgroups. Pearson's p = 0.834, r = -0.057. 5-301

Figure 48. A. Skull of the holotype of *Alligatorium meyeri* (MNHL 15646) in dorsal view. Synapomorphies for Atoposauridae are indicated (see text for details) B. Skull of the paratype of *Theriosuchus pusillus* (NHMUK PV R48330) in dorsal view. Shared characteristics with atoposaurids are indicated (see text for details). 5-308
Figure 49. (a) Geographic distribution of Late Jurassic atoposaurid specimen localities. (b) Approximate palaeogeographic distribution of Late Jurassic atoposaurids. 1: Cerin; 2: Kelheim; 3: Painten; 4: Solnhofen; 5: Guimarota; 6: Andrès; 7: Langenberg; 8: Uppen. Note that those localities not mentioned in the text all include occurrences of indeterminate remains of Theriosuchus. Palaeomap reconstruction from Ron Blakey, Colorado Plateau Geosystems, Arizona USA (http://cpgeosystems.com/paleomaps.html).....5-325
Figure 50. A. Skull of the holotype of *Alligatorellus beaumonti* (MNHL 15639) in dorsal view. See text for details. B. Skull of the holotype of *Alligatorellus bavaricus* (BSPG 1937 I 26) in dorsolateral view. Synapomorphies for Atoposauridae indicated (see text for details). *Alligatorellus beaumonti* (Gervais, 1871) (type species). 5-332
Figure 51. Photograph and line drawing of the skull of the holotype specimen of *Alligatorellus beaumonti* (MNHN 15639) in dorsal aspect. 5-333
Figure 52. (a) Line drawing of holotype specimen of *Alligatorellus beaumonti* (MNHN 15639); (b) photograph of holotype specimen. Abbreviations: AF, antorbital fenestra; Cav, caudal vertebra; Cev, cervical vertebra; Ch, chevron; Co, coracoid; CO, caudal osteoderm; DO, dorsal osteoderm; Dov, dorsal vertebra; DR, dorsal ridge; DS, dermal sculpting; EN, external nares; Fi, fibula; Fr, frontal; Hu, humerus; Il, ilium; Is, ischium; LTF, lateral temporal fenestra; Ma, manus; Man, mandible; Max, maxilla; MC, metacarpal; MP, manual phalanx; MT, metatarsal; Na, nasal; NO, nuchal osteoderm; Or, orbit; Pa, parietal; Pal, palatine; Pe, pes; PMn, premaxilla-maxilla notch; Pmx, premaxilla; PP, pedal phalanx; Pu, pubis; Ra, radius; Rad, radiale; Ri, rib; Sc, scapula; SO, sacral osteoderm; Sq, squamosal; STF, supratemporal fenestra; Sym, symphysis; Ti, tibia; Ul, ulna; Uln, ulnare; UP, ungual phalanx. 5-338
Figure 53. (A) Line drawing of referred specimen of *Alligatorellus beaumonti* (MNHN 15638) in dorsoventral view; (B) photograph of referred specimen. 5-340
Figure 54. (A) Line drawing of holotype specimen of *Alligatorellus bavaricus* (BSPG 1937 I 26) in dorsolateral view; (B) photograph of holotype specimen. 5-341
Figure 55. Photograph and line drawing of the skull of the holotype specimen of Alligatorellus bavaricus (LMU 1937 I 26) in dorsolateral aspect. 5-342

Figure 56. (A) Line drawings of the dorsal osteoderms of *A*. *bavaricus*; (B) line drawings of the cervical and dorsal osteoderm series of *A*. *beaumonti*; (C) Line drawing of a dorsal osteoderm of the specimen described as *Alligatorellus* sp. (MfN MB. R. 4317.1-12) (Schwarz-Wings et al., 2011). 5-347
Figure 57. Morphometric plots of the holotype specimens of the Late Jurassic atoposaurids *Alligatorellus*, *Alligatorium*, and *Atoposaurus*. (A) Skull length versus skull width; (B) skull length versus snout length; (C) skull length versus orbit length; and (D) PCA plot for all specimens based on six primary measurements. Squares represent French taxa, and circles represent German taxa. 5-354
Figure 58. Map of *Theriosuchus* and *Theriosuchus*-like specimens from the (a) Middle Jurassic, (b) Upper Jurassic, and (c) Lower Cretaceous and (d) Upper Cretaceous. See the discussion for the relevant references. Palaeomaps were modified version of high-resolution versions kindly provided by Ron Blakey (http://cpgeosystems.com/). 5-362
Figure 59. Chronostratigraphic chart of the *Theriosuchus* species, cf. *Theriosuchus* specimens and *Theriosuchus*-like specimens. See the Discussion for the relevant references. 5-363
Figure 60. Line drawings of the dentaries of *Theriosuchus* species in dorsal aspect. A, '*T*.' *ibericus*; B, *T. guimarotae*; C, '*T*.' *sympiestodon*; D, *T. pusillus*. Abbreviations: for, nutrient foramina; d, dentary tooth positions; fr, foramen row; nf, nutrient foramen; rar, raised alveolar rims; sym, symphysis. Scale bars represent 10mm. 5-365
Figure 61. Photographs and line drawings of *Theriosuchus* sp. from the late Bajocian-Bathonian Valtos Sandstone Formation of Skye, Scotland. A, ventral view; B, dorsal view; C, lateral view; D, medial view. Abbreviations: ant, anterior edge; for, nutrient foramina; c, crenulations; d, dentary tooth positions; fr, foramen row; rar, raised alveolar rims; rug, rugose texture; scu, sculpting; stip, stippled texture; sym, symphysis. Scale bar represents 10 mm. 5-388
Figure 62. Time-scaled phylogeny showing the relationships of Atoposauridae to the other taxa analysed in the present study (based on the topology provided in Figure 36). Atoposauridae is marked with a red star. Created using the strap package (Bell & Lloyd, 2015), using the geoscalePhylo() function and an 'equal' time-scaling method. 5-427
Figure 63. Relative positions of the choanae with respect to the main palatal bones in a range of neosuchian taxa. Citations are given were these reconstructions are based on in-text illustrations. (A) *Eutretauranosuchus delfsi* (Smith *et al.*, 2010; Pritchard *et al.*, 2012); (B) *Theriosuchus guimarotae* (Schwarz and Salisbury, 2005); (C) *Theriosuchus pusillus*; (D) *Sabresuchus sympiestodon*; (E) *Wannchampsus kirpachi*; (F) *Shamosuchus djadochtaensis* (Pol *et al.*, 2009); (G) *Koumpiodontosuchus aprosdokiti* (Sweetman *et al.*, 2015); (H) *Hylaeochampsa vectiana* (Clark and Norell, 1992). 5-433
Figure 64. Stage level subsampled (SQS) diversity results for European Chelonioidea. 6-620

Table 1. Selected publications and their interpreted statuses of the J/K extinction boundary based on a range of methodological approaches across a range of taxonomic and geographic scales. 1-48
Table 2. Raw occurrences for each taxonomic group, comprising Tetrapoda, analysed in this thesis, sub-divided into 10 million year time bin intervals. 1-70
Table 3. The number of per-taxon formation counts for all tetrapod groups analysed in the present study. Note that these values are not summed to provide 'tetrapod-level' estimates due to the issue of duplication. The per-groups also do not account for formations that cross more than one time bin. 1-72
Table 4. The number of per-taxon collection counts fir all tetrapod groups analysed in the present study. Note that these values are not summed to provide 'tetrapod-level' estimates due to the issue of duplication. The per-groups also do not account for collections that cross more than one time bin. 1-74
Table 7. Stage-level time binning scheme for the Jurassic/Cretaceous interval 2-110
Table 5. Raw counts of genus-level occurrences for all major tetrapod groups. Note that there are over 10 times the number of fossil occurrences in the terrestrial realm than there are for the marine realm. Data are grouped into approximately equal 10 million year time bins (see Section 2.2). 2-112
Table 18. Collections (colls), references (refs), raw genera (gen) and body fossil occurrences (occs) for each major taxonomic group analysed. 2-121
Table 6. Approximately equal 10 million year time bins. 2-125
Table 8. Raw counts of genera for each of the major taxonomic groups investigated, divided into approximately equal 10 million year time bins (see Section 2.2). 2-126
Table 9. Extrinsic variables used in the present study, their sources, and the environmental factors they represent.....2-167
Table 11. Extrinsic environmental parameters and sampling metrics used for the model-fitting procedure. Data are presented in approximately equal 10 million year time bins (see Section 2.2). Sources provided in text . NMA, Non-marine rock outcrop area; FMF, Fossiliferous marine formations; SQS div, Subsampled marine invertebrate diversity using Shareholder Quorum Subsampling (SQS) method; SST, Sea-surface temperature. 2-168
Table 12. Extrinsic environmental parameters and sampling metrics used for the model-fitting procedure. Data are presented in bins representing geological stages (see Section 2.2). Sources provided in text (Section 2.8). Abbreviations as Table 7. 2-169

Table 13. P-values from resulting Durbin-Watson tests for autocorrelation. 2-170
Table 19. The number of fossil-bearing formations for different tetrapod groups filtered by approximately equal 10 million year time bins. 2-160
Table 20. The number of fossil-bearing collections for different tetrapod groups filtered by approximately equal 10 million year time bins. 2-162
Table 13. Primary cranial measurements and counts for all OTUs analysed for phylogenetic analysis. Details of the source and observation status also provided. 2-177
Table 14. Stratigraphic ranges for all sampled OTUs for the atoposaurid phylogenetic analysis. FAD, First Appearance Datum; LAD, Last Appearance Datum. 2-178
Table 15. Primary axial, pectoral, and forelimb measurements and counts for all OTUs analysed for phylogenetic analysis. 2-178
Table 16. Primary appendicular and hindlimb measurements for all OTUs analysed for phylogenetic analysis. 2-180
Table 17. Ratios between primary measurements for OTUs used for phylogenetic analyses. 2-183
Table 23. Raw, uncorrected genus level counts for all taxonomic groups analysed at 10 million year time bin intervals. 3-190
Table 24. Global subsampled (SQS) diversity results for all non-marine tetrapod groups at the 10 myr time bin level.....3-191
Table 25. Global Good's u results for all non-marine tetrapod groups at the 10 myr time bin level....3-191
Table 26. Global SQS diversity results for all marine tetrapod groups at the 10 myr time bin level. ...3-194
Table 27. Global Good's u results for all marine tetrapod groups at the 10 myr time bin level. 3-194
Table 28. Global subsampled (SQS) diversity results for all non-marine tetrapod groups at the stage level. 3-195
Table 29. Global subsampled (SQS) diversity results for all marine tetrapod groups at the stage level. 3-200
Table 30. Regional (Africa) subsampled (SQS) diversity results for all marine tetrapod groups at the 10 million year time bin level. 3-202
Table 31. Regional (Asia) subsampled (SQS) diversity results for all marine tetrapod groups at the 10 million year time bin level. 3-203
Table 32. Regional (Europe) subsampled (SQS) diversity results for all marine tetrapod groups at the 10 million year time bin level. 3-204

Table 33. Regional (North America) subsampled (SQS) diversity results for all marine tetrapod groups at the 10 million year time bin level. 3-205
Table 34. (Left) Regional (Africa) subsampled (SQS) diversity results for all non-marine tetrapod groups at the 10 million year time bin level. (Right) Regional (Asia) subsampled (SQS) diversity results for all non-marine tetrapod groups at the 10 million year time bin level. 3-205
Table 35. Regional (South America) subsampled (SQS) diversity results for all marine tetrapod groups at the 10 million year time bin level. 3-209
Table 36. (Left) Regional (Europe) subsampled (SQS) diversity results for all non-marine tetrapod groups at the 10 million year time bin level. (Right) Regional (North America) subsampled (SQS) diversity results for all non-marine tetrapod groups at the 10 million year time bin level. 3-209
Table 37. Regional (South America) subsampled (SQS) diversity results for all non-marine tetrapod groups at the 10 million year time bin level. 3-213
Table 38. Subsampled latitudinal diversity changes in non-marine tetrapod groups in N3 latitudinal bin (60-90°N).....3-214
Table 39. Subsampled latitudinal diversity changes in non-marine tetrapod groups in N2 latitudinal bin (30-60°N).....3-215
Table 40. Subsampled latitudinal diversity changes in non-marine tetrapod groups in N1 latitudinal bin (0-30°N).....3-215
Table 41. Subsampled latitudinal diversity changes in non-marine tetrapod groups in S1 latitudinal bin (0-30°S).....3-215
Table 42. Subsampled latitudinal diversity changes in non-marine tetrapod groups in S2 latitudinal bin (30-60°S).....3-216
Table 43. Subsampled latitudinal diversity changes in non-marine tetrapod groups in S3 latitudinal bin (60-90°S).....3-216
Table 44. Subsampled latitudinal diversity for marine tetrapods in N3 latitudinal bin (60-90°N). .3-216
Table 45. Subsampled latitudinal diversity for marine tetrapods in N2 latitudinal bin (30-60°N). .3-216
Table 46. Subsampled latitudinal diversity for marine tetrapods in N1 latitudinal bin (0-30°N). ...3-217
Table 47. Subsampled latitudinal diversity for marine tetrapods in S1 latitudinal bin (0-30°S).....3-217
Table 48. Subsampled latitudinal diversity for marine tetrapods in S2 latitudinal bin (30-60°S). ..3-217
Table 49. Subsampled latitudinal diversity for marine tetrapods in S3 latitudinal bin (60-90°S). ..3-217
Table 50. 'Foote' extinction rates for all major marine and non-marine tetrapod groups at 10 million year time bin intervals. Abbreviations: Chel, Chelonioidea; Chor, Choristodera; Crocs, Crocodyliformes; Ichthy, Ichthyosauria; Lepid, Lepidosauria; Liss, Lissamphibia; Mamm, Mammaliaformes; Ornith,

Ornithischia; Plesio, Plesiosauria; Ptero, Pterosauria; Sauro, Sauropodomorpha; Test, Testudines; Thero, Theropoda. 3-227
Table 51. 'Foote' origination rates for all major marine and non-marine tetrapod groups at 10 million year time bin intervals. Abbreviations as Table 34. 3-227
Table 52. Three-timer extinction rates for all major marine and non-marine tetrapod groups at 10 million year time bin intervals. Abbreviations as Table 34. 3-228
Table 53. Three-timer origination rates for all major marine and non-marine tetrapod groups at 10 million year time bin intervals. Abbreviations as Table 34. 3-229
Table 54. 'Foote' origination rates for all major marine and non-marine tetrapod groups at stage level time bin intervals. Abbreviations as Table 34. 3-230
Table 55. 'Foote' extinction rates for all major marine and non-marine tetrapod groups at stage level time bin intervals. Abbreviations as Table 34. 3-230
Table 56. Three-timer extinction rates for all major marine and non-marine tetrapod groups at stage level time bin intervals. Abbreviations as Table 50. 3-231
Table 57. Three-timer origination rates for all major marine and non-marine tetrapod groups at stage level time bin intervals. Abbreviations as Table 34. 3-231
Table 21. Total lithological occurrences for tetrapod groups in the non-marine (top) and marine (bottom) realms. 3-234
Table 58. Correlations between global subsampled diversity and marine and non-marine tetrapod-bearing collections. 3-238
Table 59. Correlations between global subsampled diversity and marine and non-marine tetrapod-bearing formations. 3-239
Table 60. Correlations between raw metrics for non-marine tetrapods and European non-marine outcrop area, and between subsampled richness estimates for different non-marine tetrapod groups and European non-marine outcrop area. 3-241
Table 61. Correlations between raw metrics for marine tetrapods and European marine outcrop area, and between subsampled richness estimates for different marine tetrapod groups and European marine outcrop area. 3-241
Table 62. Correlations between raw metrics for non-marine tetrapods and North American non-marine outcrop area, and between subsampled richness estimates for different non-marine tetrapod groups and North American non-marine outcrop area. 3-242

Table 63. Correlations between raw metrics for marine tetrapods and North American marine outcrop area. Diversity for no individual tetrapod group was sufficiently continuous after subsampling for a regional comparison with marine outcrop area. 3-242
Table 64. Selected results of model fitting procedure. For complete results for both subsampled and raw taxonomic diversity, see Supplementary Information 7. Data for sea level (Miller *et al.*, 2005), and for palaeotemperature from the $\delta^{18}O$ proxy (Prokoph *et al.*, 2008) from original sources (see text for details).....3-247
Table 65. SQSRc for global marine crocodyliforms using 10 million year time bins.....4-258
Table 66.SQSRc for global non-marine crocodyliforms using 10 million year time bins. 4-258
Table 67. Global SQSPs results for marine crocodyliforms.....4-258
Table 68 Global SQSPs results for non-marine crocodyliforms. 4-259
Table 69. Global SQSPs results for marine crocodyliforms excluding Metriorhynchoidea. 4-259
Table 70. Global SQSPt results for marine crocodyliforms.....4-260
Table 71. Global SQSPt results for non-marine crocodyliforms. 4-261
Table 72 Richness vs quorum levels for marine crocodyliforms. 4-263
Table 73. Richness vs quorum levels for non-marine crocodyliforms. 4-263
Table 74. Stage level extinction and origination rates for global crocodyliforms. 4-269
Table 75. 10 million year time bin level extinction and origination rates for global crocodyliforms. ...4-269
Table 76. Extinction and origination rates for global non-marine crocodyliforms at the 10 million year time bin level.....4-270
Table 77. Stage-level extinction and origination rates for global non-marine crocodyliforms. 4-270
Table 78. Selected results that show strong significant correlations between environmental factors and crocodyliform macroevolutionary dynamics. Full results are provided in Appendix 13. 4-271
Table 79. All OTUs analysed in the present analysis, including data regarding their geographic range, temporal duration, source publications, and status following phylogenetic and systematic analysis. 5-302
Table 80. Stage level subsampled (SQS) diversity results for European Aves. 6-609
Table 81. Stage level subsampled (SQS) diversity results for European Choristoderes. 6-610
Table 82. Stage level subsampled (SQS) diversity results for European non-marine Crocodyliformes.6-611
Table 83. Stage level subsampled (SQS) diversity results for European non-marine Lepidosauria.6-612
Table 84. Stage level subsampled (SQS) diversity results for European Lissamphibia. 6-613

Table 85. Stage level subsampled (SQS) diversity results for European Mammaliaformes. 6-614
Table 86. Stage level subsampled (SQS) diversity results for European Ornithischia. 6-615
Table 87. Stage level subsampled (SQS) diversity results for European Pterosauria. 6-616
Table 88. Stage level subsampled (SQS) diversity results for European Sauropodomorpha. 6-617
Table 89. Stage level subsampled (SQS) diversity results for European Testudines. 6-618
Table 90. Stage level subsampled (SQS) diversity results for European Theropoda. 6-619
Table 91. Stage level subsampled (SQS) diversity results for European marine Crocodyliformes..6-621
Table 92. Stage level subsampled (SQS) diversity results for European Ichthyopterygia. 6-622
Table 93. Stage level subsampled (SQS) diversity results for European Sauropterygia. 6-623
Table 94. Stage level subsampled (SQS) diversity results for North American Aves. 6-624
Table 95. Stage level subsampled (SQS) diversity results for North American Choristodera.....6-625
Table 96. Stage level subsampled (SQS) diversity results for North American non-marine Crocodyliformes. 6-626
Table 97. Stage level subsampled (SQS) diversity results for North American non-marine Lepidosauria. 6-627
Table 98. Stage level subsampled (SQS) diversity results for North American Lissamphibia.....6-628
Table 99. Stage level subsampled (SQS) diversity results for North American Mammaliaformes..6-629
Table 100. Stage level subsampled (SQS) diversity results for North American Ornithischia. 6-630
Table 101. Stage level subsampled (SQS) diversity results for North American Pterosauria. 6-631
Table 102. Stage level subsampled (SQS) diversity results for North American Sauropodomorpha. ...6-632
Table 103. Stage level subsampled (SQS) diversity results for North American Testudines. 6-633
Table 104. Stage level subsampled (SQS) diversity results for North American Theropoda. 6-634
Table 105. Stage level subsampled (SQS) diversity results for North American Chelonioidea. 6-635
Table 106. Stage level subsampled (SQS) diversity results for North American marine Crocodyliformes. 6-636
Table 107. Stage level subsampled (SQS) diversity results for North American Ichthyopterygia. ..6-637
Table 108. Stage level subsampled (SQS) diversity results for North American Sauropterygia. 6-638
Table 109. SQS results when the quorum is varied at increments of 0.1 for marine Crocodyliformes at 10 million year (top) and Stage (bottom) time bin intervals. 6-639
Table 110. SQS results when the quorum is varied at increments of 0.1 for non-marine Crocodyliformes at 10 million year (top) and Stage (bottom) time bin intervals. 6-640

Table 111. SQS results when the quorum is varied at increments of 0.1 for Ichthyosauria at 10 million year (top) and Stage (bottom) time bin intervals. 6-641
Table 112. SQS results when the quorum is varied at increments of 0.1 for non-marine Lepidosauromorpha at 10 million year (top) and Stage (bottom) time bin intervals. 6-642
Table 113. SQS results when the quorum is varied at increments of 0.1 for Lissamphibia at 10 million year (top) and Stage (bottom) time bin intervals. 6-643
Table 114. SQS results when the quorum is varied at increments of 0.1 for Mammaliaformes at 10 million year (top) and Stage (bottom) time bin intervals. 6-644
Table 115. SQS results when the quorum is varied at increments of 0.1 for Ornithischia at 10 million year (top) and Stage (bottom) time bin intervals. 6-645
Table 116. SQS results when the quorum is varied at increments of 0.1 for Pterosauria at 10 million year (top) and Stage (bottom) time bin intervals. 6-646
Table 117. SQS results when the quorum is varied at increments of 0.1 for Sauropodomorpha at 10 million year (top) and Stage (bottom) time bin intervals. 6-647
Table 118. SQS results when the quorum is varied at increments of 0.1 for Sauropterygia at 10 million year (top) and Stage (bottom) time bin intervals. 6-648
Table 119. SQS results when the quorum is varied at increments of 0.1 for Testudines at 10 million year (top) and Stage (bottom) time bin intervals. 6-649
Table 120. SQS results when the quorum is varied at increments of 0.1 for Theropoda at 10 million year (top) and Stage (bottom) time bin intervals. 6-650
Table 121. Model fitting results for raw taxonomic diversity and subsampled diversity for Aves at the genus level. 6-651
Table 122. Model fitting results for raw taxonomic diversity and subsampled diversity for Chelonioidea at the genus level. 6-652
Table 123. Model fitting results for raw taxonomic diversity and subsampled diversity for Choristodera at the genus level. 6-653
Table 124. Model fitting results for raw taxonomic diversity and subsampled diversity for marine Crocodyliformes at the genus level. 6-654
Table 125. Model fitting results for raw taxonomic diversity and subsampled diversity for non-marine Crocodyliformes at the genus level. 6-655
Table 126. Model fitting results for raw taxonomic diversity and subsampled diversity for Ichthyosauria at the genus level. 6-656

Table 127. Model fitting results for raw taxonomic diversity and subsampled diversity for non-marine Lepidosauria at the genus level. 6-657
Table 128. Model fitting results for raw taxonomic diversity and subsampled diversity for Lissamphibia at the genus level. 6-658
Table 129. Model fitting results for raw taxonomic diversity and subsampled diversity for Mammaliaformes at the genus level. 6-659
Table 130. Model fitting results for raw taxonomic diversity and subsampled diversity for Ornithischia at the genus level. 6-660
Table 131. Model fitting results for raw taxonomic diversity and subsampled diversity for Pterosauria at the genus level. 6-661
Table 132. Model fitting results for raw taxonomic diversity and subsampled diversity for Sauropodomorpha at the genus level. 6-662
Table 133. Model fitting results for raw taxonomic diversity and subsampled diversity for Sauropterygia at the genus level. 6-663
Table 134. Model fitting results for raw taxonomic diversity and subsampled diversity for Testudines at the genus level. 6-664
Table 135. Model fitting results for raw taxonomic diversity and subsampled diversity for Theropoda at the genus level. 6-665
Table 136. Regional subsampled non-marine crocodyliform diversity (SQSPs) in Africa. 6-666
Table 137. Regional subsampled non-marine crocodyliform diversity (SQSPs) in Asia. 6-667
Table 138. Regional subsampled non-marine crocodyliform diversity (SQSPs) in Europe. 6-668
Table 139. Regional subsampled non-marine crocodyliform diversity (SQSPs) in North America. 6-669
Table 140. Regional subsampled non-marine crocodyliform diversity (SQSPs) in South America. 6-670
Table 141. SQSPt results on a regional level for Africa. 6-671
Table 142. SQSPt results on a regional level for Asia. 6-671
Table 143. SQSPt results on a regional level for Europe. 6-672
Table 144. SQSPt results on a regional level for North America. 6-672
Table 145. SQSPt results on a regional level for South America. 6-673
Table 146. SQSRc and SQSRu results on a regional level for Europe. 6-674
Table 147. SQSRc and SQSRu results on a regional level for Asia. 6-674
Table 148. SQSRc and SQSRu results on a regional level for Africa. 6-675
Table 149. SQSRc and SQSRu results on a regional level for North America. 6-675
Table 150. SQSRc and SQSRu results on a regional level for South America. 6-676

Table 151. Phylogenetic diversity (species) for all Crocodyliformes at the stage level (PDEs).....6-677
Table 152. Phylogenetic diversity (genera) for all Crocodyliformes at the stage level (PDEs). 6-678
Table 153. Phylogenetic diversity (species) for all Crocodyliformes at the 10 million year time bin level (PDEt). 6-679
Table 154. Phylogenetic diversity (genera) for all Crocodyliformes at the 10 million year time bin level (PDEt). 6-679
Table 155. Model fitting results for marine (top) and non-marine (bottom) crocodyliform raw taxonomic diversity and extrinsic environmental and sampling variables.....6-680
Table 156. Model fitting results for marine (top) and non-marine (middle) and marine excluding Metriorhynchoidea (bottom) subsampled crocodyliform diversity (SQSPs) and extrinsic environmental and sampling variables.....6-681
Table 157. Model fitting results for marine (top) and non-marine (bottom) subsampled crocodyliform diversity (SQSPt) and extrinsic environmental and sampling variables.....6-682
Table 158. Model fitting results for marine (top) and non-marine (bottom) subsampled crocodyliform diversity (SQSRc) and extrinsic environmental and sampling variables. 6-683
Table 159. Model fitting results for non-marine subsampled crocodyliform diversity (SQSRu) and extrinsic environmental and sampling variables. 6-683
Table 160. Model fitting results for total crocodyliform phylogenetic diversity (PDEs) at the genus (top) and species (bottom) levels and extrinsic environmental and sampling variables. 6-684
Table 161. Model fitting results for marine crocodyliform phylogenetic diversity (PDEs) at the genus (top) and species (bottom) levels and extrinsic environmental and sampling variables. 6-685
Table 162. Model fitting results for mpm=marine crocodyliform phylogenetic diversity (PDEs) at the genus (top) and species (bottom) levels and extrinsic environmental and sampling variables.....6-686
Table 163. Model fitting results for total crocodyliform phylogenetic diversity (PDEt) at the genus (top) and species (bottom) levels and extrinsic environmental and sampling variables. 6-687
Table 164. Model fitting results for marine crocodyliform phylogenetic diversity (PDEt) including (top two) and excluding (bottom two) Metriorhynchoidea at the genus and species levels and extrinsic environmental and sampling variables. 6-689
Table 165. Model fitting results for non-marine crocodyliform diversity at the genus (top) and species (bottom) levels and extrinsic environmental and sampling parameters.....6-689

Abstract

Reconstructing deep time trends in biodiversity remains a central goal for palaeobiologists, but our understanding of the magnitude and tempo of extinctions and radiations is confounded by uneven sampling of the fossil record. In particular, the Jurassic/Cretaceous (J/K) boundary, 145 million years ago, remains poorly understood. By applying a range of techniques for assessing changes in diversity, I demonstrate that both marine and non-marine tetrapod faunas show evidence for a protracted period of regional and global ecological and taxonomic reorganisation across the J/K boundary. Although much of the signal is exclusively European, almost every higher tetrapod group was affected by a substantial decline across the boundary, culminating in the extinction of several important clades and the ecological release and radiation of numerous modern tetrapod groups, including amphibians, birds and sharks. Groups such as pterosaurs and sauropods began their decline before the J/K boundary, whereas others (including mammaliaforms and ornithischians) did not appear to be affected at the J/K boundary, but declined subsequently in the earliest Cretaceous. However, the majority of clades document their greatest magnitude of decline through the Jurassic–Cretaceous boundary, indicating that the overall extinction tempo was staggered and occurred in a 'wave' through the J/K transition. These major shifts in tetrapod diversity are shown to be independent of both global and regional sampling proxies, except for the North American record for which evidence of the common cause hypothesis is strong. Variation in eustatic sea level was the primary driver of these patterns, controlling biodiversity through availability of shallow marine environments and via allopatric speciation on land. I further investigated the systematics of Atoposauridae, poorly known group of highly-specialised crocodyliforms that appear to have crossed through the J/K boundary. A detailed revision of their taxonomy and systematics indicates that they went extinct at the J/K boundary.

List of institutional abbreviations

AMNH, American Museum of Natural History, New York City, New York, USA; **BSPG**, Bayerische Staatssammlung fur Palaontologie und Geologie, Munich, Germany; **CHE**, Cherves-de-Cognac Collection, Musee d'Angouleme, France; **CM**, Carnegie Museum, Pittsburgh, Pennsylvania, USA; **DFMMh**, Dinosaurier-Freilichtmuseum Münchehagen, Germany; **FGGUB**, Faculty of Geology and Geophysics, University of Bucharest, Bucharest, Romania (LPB, Laboratory of Paleontology); **GZG**, Geowissenschaftliches Museum, Georg-August-Universitat, Gottingen, Germany (**BA**, Max Ballerstedt collection; **STR**, stratigraphic collection); **IVPP**, Institute of Vertebrate Paleontology and Paleoanthropology, Beijing, China; **MCDRD**, Muzeul Civilizatxiei Dacice şi Romane, Deva, Romania; **MfN**, Museum fur Naturkunde, Berlin, Germany (**MB.R**, Reptile Collection); **MGB**, Museo de Geologia del Ayuntameinto de Barcelona, Barcelona, Spain; **MHNL*,** Museum d'Histoire Naturelle, Lyon, France; **MO**, Musee de l'ile d'Oleron, Saint-Pierre-d'Oleron, France; **MTM**, Hungarian Natural History Museum, Budapest, Hungary; **NHMUK**, Natural History Museum, London, UK; **NMS**, National Museums Scotland, Edinburgh, UK; **PIN**, Paleontological Institute, Russian Academy of Sciences, Moscow, Russia; **PMC**, Laboratoire de Paleontologie des Vertebres de l'Universite Pierre et Marie Curie; **PRC**, Palaeontological Research and Education Centre, Mahasarakham University, Thailand; **SMU**, Southern Methodist University, Dallas, Texas, USA; **TM**, Teyler's Museum, Haarlem, Netherlands; **UP**, Universite de Poitiers, Poitiers, France; **UT**, University of Texas, Austin, Texas, USA.

*Note that at the time of visit, the collections from the MNHL were housed at the Centre de Conservation in Lyon, but remained under the same accession numbers.

Introduction

One of the central goals for palaeobiologists is to reconstruct the history and trajectory of life on Earth. The core and underpinning concept for modern palaeobiology is that occurrences of fossils, and the taxa that they represent, can be grouped in space and time, and by linking consecutive groups of these and counting the taxa that they represent, we can produce diversity 'curves'. These fossil occurrences also tell us something about the nature of extinction and speciation by providing us with apparent first- and last-appearance times for taxa. Therefore, in theory, by reading the fossil record we can identify periods of fluctuating diversity, extinction, and speciation, and apply quantitative methods to test theories applied to evolutionary laws.

Out of all major Phanerozoic interval boundaries, the Jurassic/Cretaceous (J/K) boundary, around 145 million years ago, remains plagued by this geological and biological uncertainty. Historical studies in the latter half of the 20th century recognised a distinct aberration in the biological patterns from Mesozoic background variation, and recognised the J/K boundary as a period of major faunal upheaval. While the issue of uneven sampling was commonly recognised (Raup, 1975; Sepkoski Jr *et al.*, 1981; Sepkoski Jr, 1982; Raup and Boyajian, 1988), methods for accounting for this were relatively simple or at a coarse scale, and produced roughly the same diversity curves as those produced using raw data. Only much more recently has the recognition of the pervasive issue of uneven sampling been able to be taken into account in a more rigorous, detailed, and quantitative manner, by identification and removal of 'sampling biases'. These advances, underpinned by our development of large, fossil occurrence databases, have led to renewed vitality in attempting to understand and compensate for the complex relationships between sampling and the fossil record. This concept of 'sampling biases' led to the development of a novel suite of techniques developed to counteract their influence, and each one has their own critics and advocates. Nonetheless, great leaps have been made in

reconstructing long-term trends in palaeobiodiversity, and with this a more detailed understanding of major events, such as mass extinctions.

Our current understanding of the J/K interval instead is relatively piecemeal, with events often referred to in passing within broader-scale studies, but with the common note that the interval is somewhat interesting, or worthy of additional investigation. This field of uncertainty prompted the development of this thesis. Originally, I set out with a simple task: to provide insight into the biological patterns that define the Jurassic/Cretaceous boundary, and unlock the processes that might be driving such patterns. In the wake of this comes the question that places this work in historical context: does a more nuanced reading of the Jurassic/Cretaceous boundary indicate that it represented a mass extinction as originally perceived (Raup and Sepkoski Jr, 1982; Raup and Boyajian, 1988), a minor extinction as more recent studies suggest, or something entirely different?

Research overview

Given that I started this thesis with a quote about the value of precision and asking the right questions, it would seem appropriate that I finish this initial overview with a precise set of questions to address. Originally when setting out on this research project, I wanted to answer the question: was there a mass extinction in tetrapods at the Jurassic/Cretaceous boundary? However, as the project developed, it transformed into several nested sub-questions that ask much more precise questions about the nature of changes through this interval.

- What was the *scale* of any extinction across the Jurassic/Cretaceous boundary?
- How did the *timing*, *magnitude*, and *tempo* of this vary between different groups?
- What was the *ecological response* of different tetrapod groups to any such extinction?
- To what extent do environmental factors *correlate* with biological changes through the Jurassic/Cretaceous boundary?

The individual chapters of this thesis reflect attempts to provide insight into the above questions at three different scales. Firstly, these questions are asked of all major tetrapod groups that were around in the Jurassic/Cretaceous interval, ranging from the largest sauropod dinosaurs to the smallest of amphibians. Working on this large scale allows in depth exploration of clade interactions and aspects of ecological replacement, the potential synchronicity of any J/K boundary event, the impact of broad-scale sampling issues, and the differential drivers of recovered patterns of diversity and extinction. Secondly, a medium-scale case study involving Crocodyliformes – the group that includes modern crocodylians and their ancestors – as an attempt to place stronger constraints on what we can say about the scale and mode of extinction, and how this variation influences our understanding of the external drivers of resulting patterns. Finally, macroevolution is put largely aside to explore the taxonomy and systematics of a particularly unusual group within Crocodyliformes known as atoposaurids. By exploring the components of this group, the fine-level dynamics of one specific J/K boundary-crossing clade are illuminated, and a richer understanding of the patterns of Crocodyliformes as a whole is developed. As such, this thesis is structured in a cascade style, with each successive chapter representing a more detailed investigation into the former, and each providing reciprocal insight to the other. To begin with, a detailed review of our current understanding of the biotic and abiotic patterns across the Jurassic/Cretaceous boundary is presented.

1 Biotic and Abiotic Dynamics Across the Jurassic/Cretaceous Transition

1.1 Introduction to the Jurassic/Cretaceous boundary

The Jurassic/Cretaceous (J/K) boundary has been traditionally represented as a transitional period in the history of life on Earth, coeval with significant environmental fluctuations and changes in Earth systems processes (Hallam, 1986; Ogg and Lowrie, 1986; Weissert and Mohr, 1996; Hart *et al.*, 1997; Gröcke *et al.*, 2003; Weissert and Erba, 2004; Zorina *et al.*, 2008; Sager *et al.*, 2013). An emerging picture of this interval indicates that it was a time of elevated extinction in marine invertebrate faunas (Hallam, 1986; Alroy, 2010c), coinciding in a faunal turnover in low-latitude, shallow marine groups (Aberhan *et al.*, 2006; Aberhan and Kiessling, 2012; Klompmaker *et al.*, 2013). In vertebrate groups, there is similar evidence for a faunal turnover in the marine (Steel, 1973; Benson and Druckenmiller, 2014) and non-marine (Upchurch *et al.*, 2011b; Butler *et al.*, 2013; Nicholson *et al.*, 2015) realms, culminating in the apparent Early Cretaceous radiations of numerous major extant groups, including eusuchian crocodyliforms, semi-aquatic turtles, and birds. Despite this overall, broad-scale importance, our understanding of this time interval is relatively poor compared to other major Phanerozoic stratigraphic intervals. This is, in part, due to two reasons:

1) Firstly, the lack of a robust, global chronostratigraphic framework for the J/K boundary (Zakharov *et al.*, 1996; Kudielka *et al.*, 2002; Sellwood and Valdes, 2006; Tremolada *et al.*, 2006; Wimbledon *et al.*, 2011; Li *et al.*, 2013; Taylor *et al.*, 2014; Naipauer *et al.*, 2015; Schnabl *et al.*, 2015). Other stratigraphic boundaries, such as the Cretaceous/Paleogene (K/Pg), have distinct geochemical markers that can be globally traced and dated, creating a near universally-accepted definition of the boundary (Schulte *et al.*, 2010). However, no such discrete event is currently traceable for the J/K boundary, hindering correlations between austral, boreal, Tethyan, and non-marine settings (Ogg and Lowrie, 1986; Bralower *et al.*, 1989; Ogg *et al.*, 1991; Bornemann *et al.*, 2003; Žák *et al.*, 2011; Bragin *et al.*, 2013; Dzyuba *et al.*, 2013; Schnabl *et al.*, 2015).

2) Secondly, a general perceived lack of importance of the J/K boundary, compared to other well-studied 'event boundaries', means that less research effort has been devoted to this time interval (Koeberl *et al.*, 1997; Kiessling, 2002; Kudielka *et al.*, 2002; Bornemann *et al.*, 2003; Tremolada *et al.*, 2006; Michalík *et al.*, 2009; Lukeneder *et al.*, 2010; Wimbledon *et al.*, 2011; Benson and Druckenmiller, 2014; Vennari *et al.*, 2014).

Such geological uncertainty has impacted upon our knowledge of the biological and evolutionary patterns and processes occurring through the J/K boundary. Currently, there is relatively little understanding of how biotic and abiotic patterns through this interval are linked, in spite of an emerging picture of biotic dynamics at this time (Alroy *et al.*, 2001; Upchurch *et al.*, 2011b; Benson and Druckenmiller, 2014). By synthesising our current understanding of major Earth system dynamics and environmental changes, this introductory chapter will provide the foundation for investigations into the potential mechanisms that underpinned macroevolutionary changes through the J/K boundary.

1.1.1 Stratigraphic age of the J/K boundary

Recently, there has been substantial progress in determining the age of the J/K stratigraphic boundary, along with attempts at a global correlation (Wimbledon *et al.*, 2011). Previous proposals for an age of 145.5 ± 0.8 million years (Ma) (Mahoney *et al.*, 2005) have now been widely accepted as the age of the J/K boundary (Gradstein *et al.*, 2012) (although see below). This represents the Tithonian–Berriasian boundary, with regional names of historic use such as Volgian and Portlandian no longer formally used, and instead integrated into these stage names. Of particular note in defining the J/K boundary is the biostratigraphic use of calpionellids (calcareous microplankton), which have helped to refine the dating of the base of the Cretaceous (Blau and Grün, 1997; Houša *et al.*, 2007; Casellato, 2010; Pruner *et al.*, 2010). Three biological markers, based on these calpionellids, have been identified

as potential biozones marking the base of the Berriasian (and thus the J/K boundary), comprising: (1) the base of the *Calpionella* Zone and the sudden decline in species of *Crassicollaria*; (2) the explosive radiation of small, globular forms of *Calpionella alpine;* and (3) the first appearances of two subspecies of *Nannoconus* (*N. steinmannii minor* and *N. kamptneri minor*) (Wimbledon *et al.*, 2011). Furthermore, magnetozone M18r has recently been identified as an indicator of the J/K boundary (Grabowski and Pszczółkowski, 2006; Grabowski *et al.*, 2010a; Grabowski *et al.*, 2010b; Grabowski, 2011; Grabowski *et al.*, 2013), although its use as a global identifier is hindered by its occurrence within a highly condensed section of local J/K boundary sequences (Schnabl *et al.*, 2015). These primary markers are supported by a suite of secondary biostratigraphic and magnetostratigraphic indicators (Wimbledon *et al.*, 2011; Schnabl *et al.*, 2015). However, others have argued for a younger, 140 Ma age for the J/K boundary, based on a combination of biostratigraphic markers, sedimentation rates, and isotopic analyses from an Argentinean site (Vennari *et al.*, 2014). As such, the absolute age of the J/K boundary remains uncertain, but a framework for its constraint is at least in place (Wimbledon *et al.*, 2011; Vennari *et al.*, 2014; Schnabl *et al.*, 2015). Here, for the purposes of discussing the timing of events, I follow the absolute age of 145.5 Ma (i.e., the Tithonian–Berriasian boundary) (Mahoney *et al.*, 2005) to remain consistent with the vast majority of previous studies (Wimbledon *et al.*, 2011).

1.1.2 The J/K boundary as an extinction event

1.1.2.1 The 'Big Five' mass extinctions

In the latter half of the 20th Century, numerous studies reassessed the geological, evolutionary and ecological significance of candidate past mass extinctions (Benton, 1994; Jablonski and Chaloner, 1994; Bambach, 2006). This was largely ignited by an overview of Phanerozoic mass depletion events by Newell in the mid-20th Century (Newell, 1952; 1963; 1967), which was subsequently quantified through compilation of fossil marine genus and family level lineage-duration compendia (Sepkoski Jr

et al., 1981; Raup and Sepkoski Jr, 1982; Sepkoski Jr, 1982; 1986). A significant outcome of this was that five major elevated extinction intervals are now commonly recognised during the Phanerozoic – the 'Big Five' mass extinctions (Benton, 1986; Benton, 1994; Jablonski and Chaloner, 1994; Bambach, 2006): (1) the end-Ordovician (443.4 ± 1.5 Ma) (Sutcliffe *et al.*, 2000; Finnegan *et al.*, 2012; McGhee *et al.*, 2012); (2) the late Devonian (Frasnian–Farmennian boundary, 372.2 ± 1.6 Ma) (Joachimski and Buggisch, 2002; Ricci *et al.*, 2013); (3) the end-Permian (252.17 ± 0.06 Ma) (Wignall and Twitchett, 1996; Payne and Clapham, 2012); (4) the end-Triassic (201.3 ± 0.2 Ma) (Hallam, 2002; Blackburn *et al.*, 2013); and (5) the end-Cretaceous (66 Ma) (Alvarez *et al.*, 1980; Schulte *et al.*, 2010). These mass extinctions were originally recognised based on literal readings of the fossil record (i.e., that it faithfully represented the biological record), using raw counts of observed taxa and their ranged-through occurrences through time, but have subsequently proved largely resilient to analyses accounting for uneven sampling (Alroy *et al.*, 2001; Smith, 2007; Alroy *et al.*, 2008; Smith *et al.*, 2012) (see 2.6).

1.1.2.2 History of the J/K boundary extinction

Early research into Phanerozoic macroevolutionary patterns led to the inclusion of the end-Jurassic as one of eight mass extinction events based upon a 20% level of extinction (Raup and Sepkoski Jr, 1982; 1984; Sepkoski Jr, 1986) (see Table 1 for an extensive record of studies). However, it was noted that this extinction was geographically and taxonomically constrained (Raup and Sepkoski Jr, 1982; 1984), leading to debate about its identification as a mass extinction on the same order of magnitude as the 'Big Five' (Hoffman, 1985; Benton, 1986; Hallam, 1986; Raup and Boyajian, 1988; Hallam and Wignall, 1997). Numerous subsequent studies (Sepkoski Jr, 1992; 1993; Barnes *et al.*, 1996; Rampino and Haggerty, 1996; Hallam, 1998; Benton, 2001; Ruban, 2005; Purdy, 2008) recovered evidence for a J/K extinction of similar magnitude to that originally proposed (Raup and Sepkoski Jr, 1982), although in all these cases the results were based on a literal reading of the fossil record. One of the most recent

analyses of Phanerozoic diversity identified the J/K boundary as one of nineteen major extinction intervals (Melott and Bambach, 2011), measured as a proportion of extinction (19.9% generic extinction), based on the latest version of the Sepkoski compendium, and overall very similar to original results investigating this time interval. Despite this relatively high apparent extinction intensity, an overall perceived lack of importance of the J/K boundary means that it has been largely neglected and often only referred to in passing in more recent studies of Phanerozoic biotic changes (Alroy *et al.*, 2001; Wignall, 2001; Bambach *et al.*, 2004; Bambach, 2006; Courtillot and Olson, 2007), or ignored altogether for investigations of historical extinctions (Harnik *et al.*, 2012). This likely relates to the lack of unambiguous evidence for dramatic environmental shifts or catastrophic events, or identification of significant biotic fluctuations (i.e., the extinction of a major group) through this period, ultimately leading to the J/K boundary being downgraded from mass extinction status (Hallam, 1986; Hallam and Cohen, 1989; Hallam and Wignall, 1997; Bambach *et al.*, 2002; Bambach *et al.*, 2004). In contrast, others have recovered a major peak in extinction rates, followed by a rapid increase in origination rates across the J/K boundary (Kiessling and Aberhan, 2007), with the magnitude of these events surpassing the Tr/J boundary mass extinction. Similarly, others explicitly documented a J/K boundary mass extinction (Smith, 2001), although subsequent work by the same author has demonstrated that such a signal is likely to be an artefact of the predominance of western European fossil occurrences within the Sepkoski compendium (Smith, 2007; Smith and McGowan, 2007; McGowan and Smith, 2008; Smith *et al.*, 2012), supporting the idea that any such event was localised in extent and caused by regional changes in facies or environment (Hallam, 1986).

Authors	Year of publication	Taxonomic Group	Geographic Scale	J/K Extinction Status (negligible, mild, intermediate, severe)
Raup & Sepkoski 1-46	1982	Marine animals	Global	Intermediate

Raup & Sepkoski	1984	Marine animals	Global	Intermediate
Sepkoski	1984	Marine animals	Global	Mild
Hoffman	1985	Marine invertebrates	Global	Intermediate
Hallam	1986	Mollsucs	Global	Severe
Patterson & Smith	1987	Echinoderms and fish	Global	Severe
Raup & Boyajian	1988	Marine invertebrates	Global	Intermediate
Benton	1989	Tetrapods	Global	Negligible
Roth	1989	Calcareous nannoplankton	Global	Intermediate
Dodson	1990	Dinosaurs	Global	Severe
Sepkoski	1992	Marine animals	Global	Mild
Sepkoski	1993	Marine animals	Global	Mild
Benton	1995	Animals	Global	Intermediate
Hallam	1998	Marine animals	Global	Intermediate
Fara	2000	Tetrapods	Global	Severe
Alroy *et al*.	2001	Marine invertebrates	Global	Intermediate
Benton	2001	All animals	Global	Mild
Peters & Foote	2001	Marine animals	Global	Mild
Smith	2001	Marine invertebrates	Global	Mild
Bambach *et al*.	2004	Marine animals	Global	Intermediate
Fara	2004	Lissamphibians	Global	Negligible
MacLeod	2004	Marine animals	Global	Intermediate
Foote	2005	Marine animals	Global	Intermediate
Peters	2005	Marine animals	Global	Intermediate
Rohde & Muller	2005	Marine animals	Global	Intermediate
Ruban	2005	Marine invertebrates	Global	Severe
Bambach	2006	Marine animals	Global	Intermediate
Slack *et al*.	2006	Pterosaurs	Global	Negligible
Wang & Dodson	2006	Dinosaurs	Global	Negligible
Kiessling & Aberhan	2007	Marine benthos	Global	Severe
Smith	2007	Marine animals	Global	Severe
Smith & McGowan	2007	Marine animals	Western Europe	Mild
Alroy *et al*.	2008	All animals	Global	Mild
Lloyd et al.	2008	Dinosaurs	Global	Severe
Purdy	2008	Marine animals	Global	Mild
Barrett *et al*.	2009	Dinosaurs	Global	Intermediate
Alroy	2010*a*	Marine animals	Global	Mild
Benson *et al*.	2010	Marine reptiles	Global	Severe
Rogov *et al*.	2010	Ammonites	Boreal	Negligible
Young *et al*.	2010	Metriorhynchoids	Global	Severe
Benson & Butler	2011	Marine reptiles	Global	Severe
Butler *et al*.	2011	Dinosaurs	Global	Intermediate
Feulner	2011	Marine animals	Global	Severe

Heim & Peters	2011	Marine animals	North America	Mild
Lloyd et al.	2011	Coccolithophorids	Global	Severe
Mannion *et al*.	2011	Sauropods	Global	Intermediate
Upchurch *et al*.	2011	Dinosaurs	Global	Intermediate
Wall *et al*.	2011	All terrestrial	Global	Intermediate
Carrano *et al.*	2012	Tetanurans	Global	Severe
Fischer *et al*.	2012	Ophthalmosaurids	Global	Mild
Lloyd	2012	Dinosaurs	Global	Intermediate
Lloyd *et al*.	2012	Coccolithophorids	Global	Severe
Mayhew *et al*.	2012	Marine animals	Global	Mild
Smith *et al*.	2012	Marine invertebrates	Europe, North America	Mild
Upchurch & Mannion	2012	Dinosaurs	Global	Intermediate
Butler *et al*.	2013	Pterosaurs	Global	Intermediate
Cascales-Miñana & Cleal	2013	Plants	Global	Negligible
Fischer *et al*.	2013*a*	Ichthyosaurs	Global	Mild
Fischer *et al*.	2013*b*	Ichthyosaurs	Global	Intermediate
Mannion *et al*.	2013	Eusauropods	Global	Mild
Novas *et al*.	2013	Theropods	Patagonia	Severe
Zanno & Makovicky	2013	Theropoda	Global	Severe
Benson & Druckenmiller	2014	Plesiosaurians	Global	Mild
Alroy	2014	Marine animals	Global	Intermediate
Tortosa *et al*.	2014	Ceratosauria	Global	Mild

Table 1. Selected publications and their interpreted statuses of the J/K extinction boundary based on a range of methodological approaches across a range of taxonomic and geographic scales.

The magnitude, timing, and taxonomic inclusivity of any potential J/K extinction event has remained in a state of flux for different fossil groups (Raup and Sepkoski Jr, 1982; Fara, 2000; Fara, 2004; Kiessling and Aberhan, 2007; Smith and McGowan, 2007; Benson and Butler, 2011; Alroy, 2014) (Table 1). Direct comparisons between these and other studies is often confounded by the different metrics used to quantify changes in diversity (e.g., counts of originations, extinctions, or taxonomic occurrences), and the taxonomic level of study (i.e., species, genus or family-level data) (Sepkoski Jr, 1992; 1993; Alroy *et al.*, 2001; Bambach *et al.*, 2004; Foote, 2005). Furthermore, the treatment of taxonomic data has

often varied greatly, with some studies taking a literal reading of the fossil record (Dodson, 1990; Peters, 2005; Rogov *et al.*, 2010), whereas others have applied a variety of sampling standardisation methods, ranging from the incorporation of information from phylogenetic relationships to create 'ghost lineages' (Young *et al.*, 2010; Fischer *et al.*, 2012; Mannion *et al.*, 2013), to the application of a range of subsampling protocols and modelling techniques (Alroy, 2000; Alroy *et al.*, 2001; Barrett *et al.*, 2009; Alroy, 2010a; Upchurch *et al.*, 2011b; Lloyd, 2012; Alroy, 2014). As such, methodological differences are likely to be at least partly responsible for disagreement in terms of whether the J/K boundary marks a mass extinction (Raup and Sepkoski Jr, 1982; 1984), a period of inflated extinction (Hallam, 1986; Bambach, 2006; Lloyd *et al.*, 2008; Benson and Butler, 2011), or represents a time of normal rates of background extinction and faunal turnover (Fischer *et al.*, 2012; Benson and Druckenmiller, 2014).

1.1.2.3 Renewed evidence for an extinction event?

Using large taxonomic occurrence databases and a range of sampling standardisation techniques, several recent studies (particularly regarding tetrapods, although not exclusively) have noted a sharp decline in diversity around the J/K boundary (Kiessling and Aberhan, 2007; Barrett *et al.*, 2009; Butler *et al.*, 2009c; Benson *et al.*, 2010; Benson and Butler, 2011; Mannion *et al.*, 2011; Upchurch *et al.*, 2011b; Aberhan and Kiessling, 2012; Friedman and Sallan, 2012; Upchurch and Mannion, 2012; Mannion *et al.*, 2015). Much of this research has incorporated our increasing awareness and understanding of the links between the geological and fossil records, and the impact that heterogeneous sampling might have on obscuring our reading of palaeobiodiversity patterns. These new studies and approaches are starting to elucidate biotic dynamics across the J/K boundary in detail, revealing that there might be a hitherto undetected complexity. For example, in dinosaurs, the magnitude of extinction varies depending on the proxies used to model sampling effort or the geological record in estimating 'residual' diversity (Upchurch *et al.*, 2011b). Marine tetrapod groups

also declined across the J/K boundary (Benson *et al.*, 2010; Benson and Butler, 2011), indicating that potentially significant events were impacting upon both marine and terrestrial ecosystems. These 'corrected' diversity curves largely supersede previous work that used raw counts of observed fossil occurrences as a measure of diversity (Dodson, 1990; Bardet, 1994), which have been shown repeatedly to be unreliable (Alroy, 2000; Alroy *et al.*, 2001; Peters and Foote, 2001; Peters, 2005; Alroy, 2008; Alroy *et al.*, 2008; Alroy, 2010c; Benson *et al.*, 2010; Peters and Heim, 2010; Benson and Butler, 2011; Benton *et al.*, 2011; Heim and Peters, 2011a; Upchurch *et al.*, 2011b; Dunhill *et al.*, 2012; Mayhew *et al.*, 2012; Benson *et al.*, 2013; Benton *et al.*, 2013a; Butler *et al.*, 2013; Dunhill *et al.*, 2014a; Dunhill *et al.*, 2014b; Benton, 2015; Mannion *et al.*, 2015; Benson *et al.*, 2016), and therefore offer new insights into diversity dynamics across the J/K boundary.

Consequently, there are currently differing interpretations of the intensity, timing, geographical extent, and taxonomic inclusivity of any putative extinction event across the J/K boundary. In this introductory chapter, I present a synthesis of our current understanding of diversity and major macroevolutionary patterns across the J/K boundary, and place this in an environmental framework describing the major perturbations to Earth systems that occurred during this interval. Such a synthesis is necessary as the basis for exploring biotic dynamics in the context of the extrinsic factors that potentially acted to mediate the patterns which we observe, and emphasise the importance of combining abiotic and biotic patterns when exploring macroevolution (Hallam and Cohen, 1989; Peters, 2005; Butler *et al.*, 2011; Mannion *et al.*, 2011; Smith *et al.*, 2012; Sookias *et al.*, 2012a).

1.2 Palaeogeographic and environmental changes across the J/K boundary

1.2.1 Palaeogeography and palaeoceanography

The continued fragmentation of Pangaea throughout the Late Jurassic and Early Cretaceous led to heterogeneous and large-scale tectonic processes on both regional (Nürnberg and Müller, 1991; Veevers *et al.*, 1991; Monger *et al.*, 1994; Adatte *et al.*, 1996; Hathway, 2000; DeCelles, 2004) and global (Scotese *et al.*, 1988; Scotese, 1991; Scotese *et al.*, 1999) scales. As Pangaea continued to fragment, major palaeogeographical events occurred, including the initiation of the opening of the Central Atlantic (Figure 1). This was accompanied by increased rates of plate spreading in the Middle to Late Jurassic, associated with high levels of continental motion (Scotese *et al.*, 1988; Hynes, 1990; Riccardi, 1991; Scotese, 1991; Seton *et al.*, 2012), with knock-on effects to other major Earth systems. Salinity might have been slightly higher within the Late Jurassic proto-Atlantic, particularly in restricted marginal basins (Sanford *et al.*, 2013) and at lower latitudes. Typically, however, the Atlantic must have been dominated by normal salinities, as evidenced by the presence of fully marine faunas (Leinfelder, 1993), although it is possible that high sea levels and the configurations of the continents allowed high-salinity waters in lower latitude epicontinental shelf seas to sink and form deep-water masses (i.e., the warm saline bottom water model (Brass *et al.*, 1982)). The opening of the South Atlantic during the Early Cretaceous rifting phases led to a gradual reduction in salinity (Evans, 1977). This rifting resulted in the connection of the present day Gulf of Mexico to southern Europe and the Tethys Ocean, with the Caribbean Ocean opening through continued motion of North and South America (Pindell and Kennan, 2009). Consequently, a global equatorial circulation current formed during the Albian, although this facilitated only restricted faunal interchange until the Late Cretaceous (Stinnesbeck *et al.*, 2014). In Africa, multiple rift phases were initiated during the latest Jurassic (Ford and Golonka, 2003), and Madagascar became isolated from Africa after the J/K boundary (Seton *et al.*, 2012). The evidence of land bridges between Laurasia and North America is complex, but a recent review suggests that they existed only at the Kimmeridgian/Tithonian boundary and the earliest Barremian, and that North America was otherwise isolated throughout this interval (Brikiatis, 2016b). Taken together, this evidence shows that the Late Jurassic to Early Cretaceous represents a time of

heightened levels of continental fragmentation and geographic isolation, combined with changing palaeoceanographic dynamics.

A wealth of palaeoceanographic data additionally comes from sites with rocks spanning the J/K boundary due to their targeting by the International Ocean Discovery Program (IODP) (and earlier incarnations). This program has included sites in (1) the Indian Ocean (Bown, 1992; Gradstein *et al.*, 1992; Kaminski *et al.*, 1992), with evidence for a cooler water regime; (2) the Pacific Ocean, which is thought to have had a stable circulatory regime (Matsuoka, 1992; Ogg *et al.*, 1992); and (3) the Atlantic Ocean with a distinct North–South salinity gradient (Deroo *et al.*, 1983; Kotova, 1983; Kaminski *et al.*, 1992). In the Late Jurassic, western Tethys and Atlantic ecosystems were fuelled by a high-nutrient flux, leading to high levels of phytoplankton and radiolarians, possibly driven by shifting circulatory regimes as continental configurations changed (Baumgartner, 1987; Weissert and Mohr, 1996; Danelian and Johnson, 2001).

Late Jurassic (Oxfordian) carbonate platforms experienced severe growth crises (Weissert and Mohr, 1996), and calcareous plankton subsequently underwent a significant global radiation in the Tithonian–Berriasian (Weissert *et al.*, 1998; Bornemann *et al.*, 2003; Falkowski *et al.*, 2004; Weissert and Erba, 2004), leading to Early Cretaceous biocalcification events (e.g., in the Pacific; (Kakizaki *et al.*, 2013)). However, the Early Cretaceous also saw a dramatic reduction in carbonate production, with a series of repeated ‘biocalcification crises’, notably in the Valanginian and Aptian (Weissert and Erba, 2004). ‘Disaster deposits’ in the Tethys Ocean resulted from localised but dramatic sea-level falls and cooling episodes (Chatalov *et al.*, 2015).

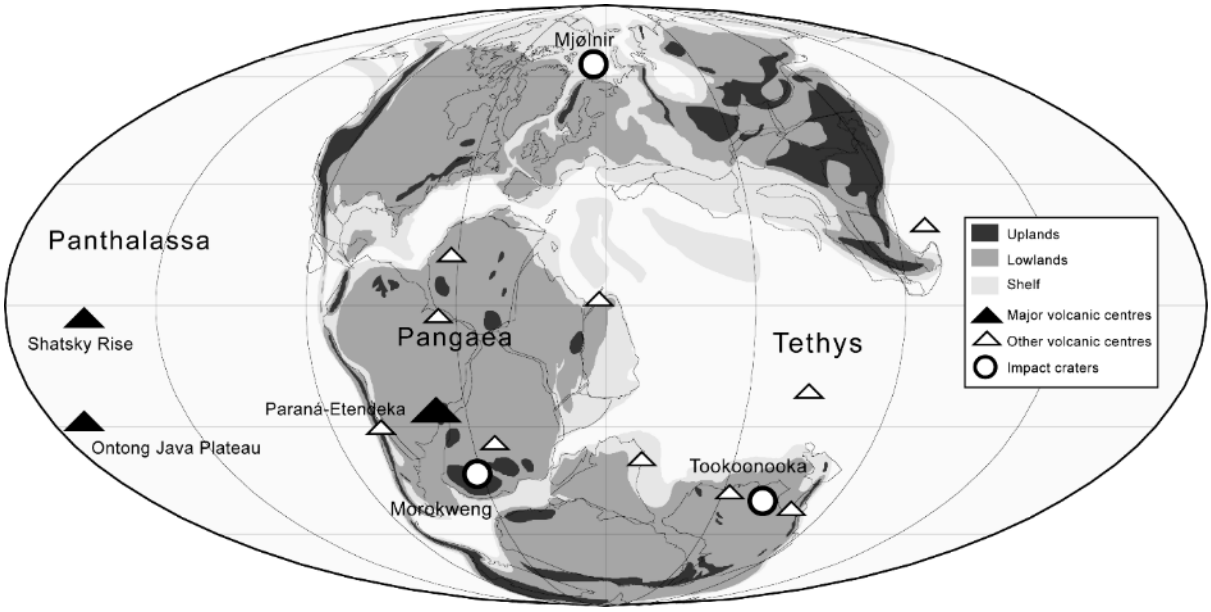


Figure 1. Late Jurassic and Early Cretaceous (Oxfordian–Albian) palaeogeographic map showing the locations of major flood basalts, minor volcanic activity, and bolide impacts.

1.2.2 Sea level and stratigraphy

Global (eustatic) sea-level curves show a peak in the Kimmeridgian–early Tithonian, prior to a lowstand at the J/K boundary, continuing into the Berriasian. This was followed by a slight rise, before plummeting again in the Valanginian–Hauterivian (Haq *et al.*, 1987; Hallam, 1988; 2001; Miller *et al.*, 2005; Haq, 2014) to the lowest sea level observed throughout the Cretaceous (Figure 2). This lowstand has been suggested previously to be the principle driver of a major extinction event at the end-Tithonian (Hallam, 1986), and is thought to have been responsible for high levels of production of nannoplankton-based carbonate (Roth, 1989; Erba *et al.*, 2004). The proportion of evaporitic rocks in the Late Jurassic parallels this sea-level pattern, coincident with, and possibly driven by, an increase in orogenic activity and associated mantle plume-related volcanism (Ronov *et al.*, 1980; Courtillot and Olson, 2007; Zorina *et al.*, 2008). Falling sea-levels at the J/K boundary decimated reef environments, as indicated by a marked decline in their areal extent and latest Jurassic diversity of reef-building organisms (Kiessling, 2008; Foote, 2014). Black shales were widely deposited throughout the Late

Jurassic and Early Cretaceous, often in marginal seas (Dypvik and Zakharov, 2012; Föllmi, 2012; Meyers, 2014). Multiple causes have been suggested for their deposition, including intense transgressive periods from rapidly changing sea-levels (Lipinski *et al.*, 2003), tectonic activity restricting flow patterns and increasing productivity (Wignall and Hallam, 1991; Weissert *et al.*, 1998), decreased erosion rates, and warmer, more arid climates (Kessels *et al.*, 2003; Föllmi, 2012). The Early Cretaceous saw several episodes of intense ocean water stagnation, possibly leading to anoxia, including the Valanginian Weissert and the late Hauterivian Faraoni oceanic anoxic events (Erba *et al.*, 2004; Hu *et al.*, 2012; Mattioli *et al.*, 2014). However, others have proposed that the Valanginian Weissert positive isotope carbon excursion was not part of a global oceanic anoxic event (Kujau *et al.*, 2012), and that episodes of anoxia were instead restricted to the Atlantic, Pacific, and Southern oceans, possibly with enhanced terrestrial carbon storage instead acting as the primary driver for the isotope excursion. A new global dataset comprising carbon isotope records from the Pacific, Tethyan, Atlantic and Boreal realms indicates that there was only a steady but slow decrease in carbon isotope values until the early Valanginian (Price *et al.*, 2016), a timing coincident with the Weissert event. However, there appears to be no globally traceable carbon isotope excursion to mark the J/K boundary.

The Late Jurassic to Early Cretaceous eustatic sea level curve shows a positive correlation with fluctuations in global continental flooding (Budyko *et al.*, 1987; Hay *et al.*, 2006) and terriginous sedimentation (Sahagian *et al.*, 1996; Ruban, 2010; Grabowski *et al.*, 2013; Haq, 2014; Zakharov *et al.*, 2014). High rates of sea-floor spreading, as a result of increasing levels of continental fragmentation throughout the Late Jurassic, are likely to be the primary drivers for these fluctuations (Hallam, 1988). The growth and decay of polar ice has also been suggested as a mechanism to account for shorter term, relatively rapid, and at times large amplitude, falls in sea level in the Early Cretaceous (Haq, 2014). Additionally, others have demonstrated that the Late Jurassic records the highest mass of sediment deposition in the Mesozoic, followed by a sharp decline at the J/K boundary (Hay *et al.*, 2006). This finding is reflected on a regional scale, with the European rock record documenting a

decline in sedimentary outcrop area from the Late Jurassic to Early Cretaceous, driven by a second order transgressive sea level phase (Smith and McGowan, 2005; Smith and McGowan, 2007). However, the fine-scale correlation of sea-level curves to global-scale sedimentation patterns through the J/K boundary is currently poorly understood (Hallam, 1986; Barnes *et al.*, 1996; Zorina *et al.*, 2008; Ruban, 2011). This is a result of aforementioned variations in regional tectonics and eustacy-driven sedimentation rates, leading to diachronous unconformities through the J/K boundary (Ogg *et al.*, 1991; Schnyder *et al.*, 2012).

The ratio of strontium isotopes ($^{87}Sr/^{86}Sr$) is an indicator of the rate of erosion of continental crust relative to enrichment from hydrothermal sources, and therefore acts as a proxy for marine sedimentation rate: peaks in the strontium curve correspond to minimum levels of associated sedimentation, and vice versa (Tardy *et al.*, 1989). The Phanerozoic global strontium isotope curve decreases from the Ordovician up until the Middle/Late Jurassic boundary, but increases across the J/K boundary (Jones and Jenkyns, 2001; McArthur *et al.*, 2001; Hannisdal and Peters, 2011), and can be detected on a local basis in J/K sequences (Jones *et al.*, 1994; Price and Gröcke, 2002). This is generally concordant with long-term systematic decreases in accommodation space and sedimentation rates associated with sea-level regression (Budyko *et al.*, 1987; Hallam and Cohen, 1989; Hay *et al.*, 2006), as well as decreasing levels of humidity and weathering rates that continued until the end-Jurassic (Ruffell and Batten, 1990; Hallam *et al.*, 1991). The decrease in erosion rates that occurred at the J/K boundary and into the Early Cretaceous is also tracked by a great decline in chlorine flux into the oceans (Hay *et al.*, 2006). Furthermore, the ratio of $\delta^{34}S$ increased consistently across the J/K boundary (representing decreasing biologically-driven sulfate reduction), which might have been responsible for toxic conditions in the marine realm (Kampschulte and Strauss, 2004). Together, these geochemical proxies provide strong evidence for a global shift in sedimentation patterns in concert with global-scale environmental perturbations, particularly focused in the marine realm.

Many regional studies have demonstrated that $\delta^{13}C$ values decreased through the J/K boundary, indicative of reduced oceanic productivity via a diminished flux of organic matter in the oceans and increasingly oligotrophic conditions (Weissert and Channell, 1989; Adatte *et al.*, 1996; Weissert and Mohr, 1996; Price and Gröcke, 2002; Prokoph *et al.*, 2008; Zakharov *et al.*, 2014). In the Panboreal realm, this negative trend is coincident with a high abundance of spores and prasinophytes (unicellular green algae), the latter of which might relate to an algal bloom driven by disturbances to marine ecosystems and/or shifts in oceanic productivity (Zakharov *et al.*, 2014). However, the global radiation of calcareous plankton in the Tithonian–Berriasian (Weissert *et al.*, 1998; Bornemann *et al.*, 2003; Falkowski *et al.*, 2004; Weissert and Erba, 2004) is not fully expressed within the $\delta^{13}C$ record. Within the Boreal-Tethyan region, a positive carbon isotope excursion has been identified (Dzyuba *et al.*, 2013). Such variation has led to the idea that carbon isotopes may be useful in adding to the characterisation of the J/K boundary (Michalík *et al.*, 2009; Michalík and Reháková, 2011; Dzyuba *et al.*, 2013), although recent global analyses have indicated that this might not be the case (Price *et al.*, 2016). In the Tethys, a negative isotope excursion at the J/K boundary has been suggested (Grabowski *et al.*, 2010b), possibly driven by increased continental weathering and erosion, or oxidation of organic-rich sediments exposed during localised sea-level transgression. These spatiotemporal variations indicate a geographically-controlled scenario for carbon and oxygen isotope fluctuations over the J/K boundary, corresponding to varying rates of organic matter burial and biological productivity.

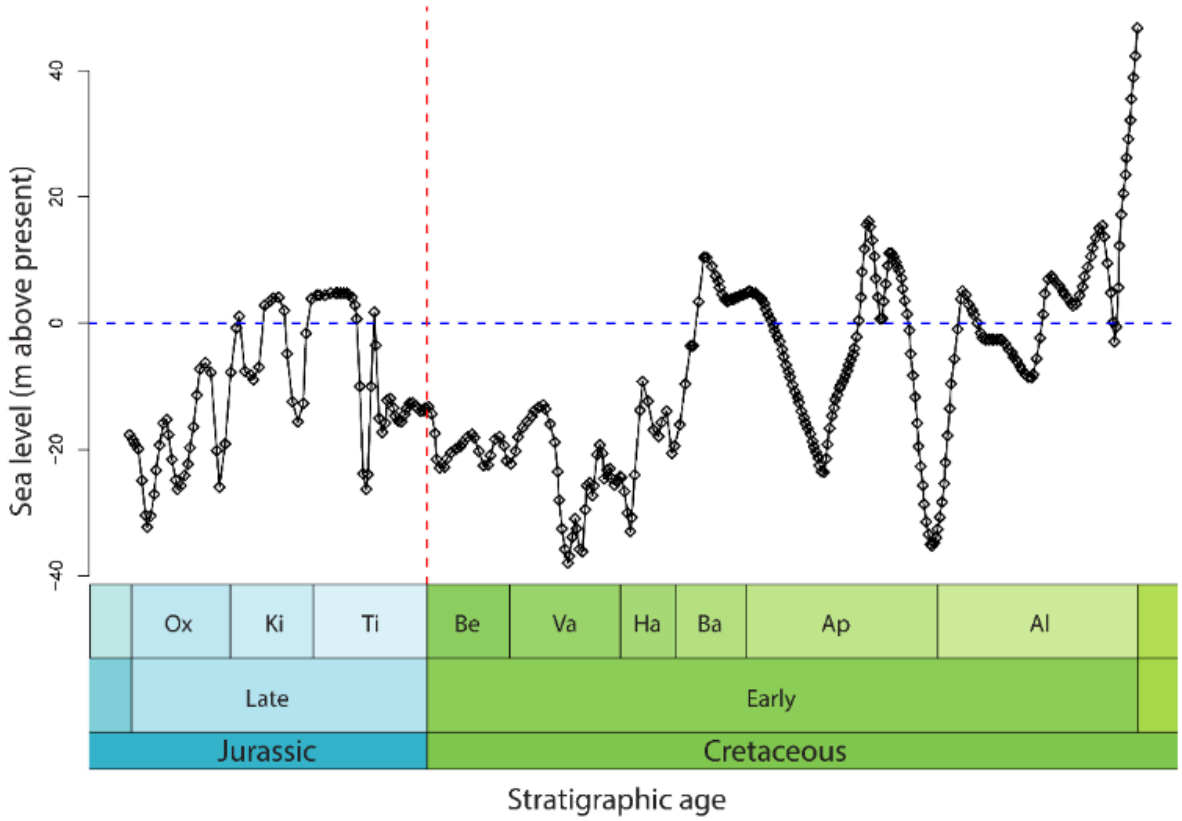


Figure 2. Sea-level curve showing shorter-term fluctuations through the Late Jurassic and Early Cretaceous. (Miller *et al.*, 2005). The blue horizontal line represents modern sea level, and the red line represents the J/K boundary.

1.2.3 Volcanism

Volcanic emissions have the potential to transmit large volumes of toxic and other harmful materials into the atmosphere, such as ash, sulphur dioxide and carbon dioxide. In general, these can have the following climatic and environmental effects (Bluth *et al.*, 1993; Wignall, 2001; Robock, 2002; Schaller *et al.*, 2011):

1) Lowering air-temperatures through direct insolation from ash and sulphate aerosols;

2) Increasing atmospheric toxicity and poisoning;

3) Acid rain and biocalcification crises;

4) Increasing atmospheric temperatures through release of greenhouse gases;

5) Oceanic anoxia.

The Shatsky Rise, a vast shield volcano with a surface area of around 480,000 km^2, formed in the northwest Pacific Ocean at the J/K boundary (Sager *et al.*, 2013). Recent $^{40}Ar/^{39}Ar$ age determinations of basaltic lava samples from Tamu Massif, the oldest and largest edifice of the submarine Shatsky Rise, provide an age of 144 Ma (Geldmacher *et al.*, 2014), approximately coincident with the currently accepted age of the J/K boundary. The impact of this extensive volcanism on Earth system cycles is currently poorly understood; however, it was significant enough to have affected the palaeotectonic motion of adjacent plates (Seton *et al.*, 2012).

Accompanying the Shatsky volcanism, and coincident with ongoing Gondwanan fragmentation (Wignall, 2001; Segev, 2002), was a host of smaller-scale and plume-related volcanic activity (Figure 1). These include:

1. 10–20 km thick sequences in the Jurassic to Early Cretaceous of Chile (Vergara *et al.*, 1995);
2. Evidence for a plume event (Wilson *et al.*, 1998) recorded in the Oxfordian deposits of northern Brazil (Baksi and Archibald, 1997), north-east Africa (Segev, 2002), and Western Africa (Maluski *et al.*, 1995), the latter of which continued erupting into the Valanginian–Hauterivian;
3. Plume-associated activity from the J/K boundary of the Liberian margin (Garfunkel, 1998) and the Equatorial Atlantic (southern India, northern South Africa, southeast Australia, the Antarctic peninsula, and Patagonia) concurrent with the final stage of the Karoo igneous province (Vaughan *et al.*, 1998; Féraud *et al.*, 1999; Vaughan and Pankhurst, 2008);
4. Berriasian–Hauterivian mantle plume activity in northern Israel (Segev, 2009);
5. A 1500 km wide magmatic province initiated in the Hauterivian–Barremian of Australia (Bryan *et al.*, 1997).

Alongside these were the Paraná flood basalts of South America and the Etendeka Traps of Namibia that were jointly emplaced during a major rifting phase throughout the late Valanginian and Hauterivian, possibly related to initiation of seafloor spreading in the South Atlantic (Harry and Sawyer, 1992; Jerram *et al.*, 1999; Seton *et al.*, 2012). The Paraná event (133 Ma) is estimated to have produced approximately 1.5 million km^3 of volcanic rock, implying a rate consistent with a mantle plume origin (Renne *et al.*, 1992). Although a link between the Paraná-Etendeka igneous province and the Weissert Event has been previously suggested (Erba *et al.*, 2004), some localised dates suggest that emplacement post-dated the isotope excursion (Martinez *et al.*, 2013). The most recent dating indicates that the emplacement of the Paraná-Etendeka igneous province coincides with the beginning of the Weissert event (Martinez *et al.*, 2015), but that overall the environmental impacts of the volcanism were minimal due to a relatively slow rate of emplacement (Dodd *et al.*, 2015). In the latest Barremian, the single largest volcanic province known on Earth was emplaced in the southwest Pacific, the Ontong Java Plateau (approximately 50 million km^3) (Coffin and Eldholm, 1994). This is concurrent with, and potentially a driver of, the marine biotic changes that culminated in oceanic anoxic event 1 (OAE1a) in the early Aptian (120 Ma) through sustained volcanic outgassing (Bralower *et al.*, 1989; Wignall, 2001; Weissert and Erba, 2004; Naafs *et al.*, 2016). In addition, a poorly known emplacement event occurred during the Berriasian, known as the Gascoyne large igneous province (Martinez and Dera, 2015). Presently, no link between this activity and any contemporary biotic or abiotic changes have been proposed. It is likely that this overall intensification of plume-related activity is related to the increased continental fragmentation rates in the Late Jurassic to Early Cretaceous. Recent evidence suggests that these large volcanic episodes can be tied to Early Cretaceous warming events driven by increasing CO_2 production, with colder episodes being driven by enhanced carbon burial and leading to dramatic cooling and fluctuations in sea level and the extent of polar ice caps (Bodin *et al.*, 2015).

1.2.4 Bolide impacts

Impacts from extra-terrestrial objects have the potential to cause massive disruption to Earth systems. These range from causing shockwaves, earthquakes, and wildfires and tsunamis upon impact, to depletion of ozone and the release of carbon dioxide and sulphur into the atmosphere, triggering an enhanced greenhouse effect and acid rain (O'Keefe and Ahrens, 1989; Toon *et al.*, 1997; Kaiho *et al.*, 2001). There are three known large bolide impacts that are approximately contemporaneous with the J/K boundary (Figure 1):

1. The 70–80 km diameter Morokweng impact crater in the Kalahari Desert, South Africa, dated at 145 ± 2 Ma (Corner *et al.*, 1997; Hart *et al.*, 1997; McDonald *et al.*, 2001; Henkel *et al.*, 2002; Reimold *et al.*, 2002; Maier *et al.*, 2006; McDonald *et al.*, 2006) and recognised from gravity and magnetic anomalies, as well as a bed enriched in extra-terrestrial elements with evidence of external impact (note that new, preliminary data suggests that the original diameter of this structure might have been up to 240 km, 1.3–2 times the size of the end-Cretaceous Chicxulub impact crater) (Misra *et al.*, 2014);
2. The 40 km wide Mjølnir crater in Norway, dated as 142 Ma (Dypvik *et al.*, 1996; Dypvik *et al.*, 2006);
3. The 22 km wide crater at Gosses Bluff, Northern Territory in Australia, dated at 142.5 Ma (Milton *et al.*, 1972; Milton and Sutter, 1987).

Additionally, the 55 km wide Tookoonooka impact structure from Queensland, Australia, has been dated to the Early Cretaceous at 125 ± 1 Ma (Bron and Gostin, 2012). Alongside these larger impacts, there were at least nine additional smaller (1-20 km wide) impacts from the Late Jurassic to Early Cretaceous, based on The Earth Impact Database (http://www.passc.net/EarthImpactDatabase/), in South America, Europe, Africa, Australia, and Asia. Presently, geochemical data are limited in extent, but there are multiple regional anomalies whereby trace metals (e.g., iron, cobalt and nickel, and

possibly iridium and chromium) are enriched around the J/K boundary, suggesting extra-terrestrial input on a global scale (Zakharov *et al.*, 1993; McDonald *et al.*, 2001; Kudielka *et al.*, 2002; McDonald *et al.*, 2006; Mizera *et al.*, 2010). On a regional level, dissipation of the energy release associated with the Mjølnir impact is estimated to have caused several short, near-field perturbations, including large magnitude earthquakes, displacement of a considerable amount of material from the impact site, and debris flows and high-amplitude tsunami waves (Dypvik *et al.*, 2006). Combined with the patterns outlined in Sections 1.2.1 and 1.2.2, there is considerable evidence for almost continuous environmental disruption throughout the J/K boundary and into the Early Cretaceous, including changes to Earth system processes and interference from singular, potentially catastrophic volcanic and extra-terrestrial events.

1.2.5 Climate

During the Late Jurassic, periods of enhanced continental erosion and oceanic productivity, combined with increased sedimentation rates, were most likely driven by a tropical climate with frequent monsoons (Hallam, 1994; Weissert and Mohr, 1996; Weissert and Erba, 2004). Variation in Late Jurassic and Early Cretaceous marine palaeotemperatures have been derived from oxygen isotope data based on well-preserved marine molluscs (bivalves and belemnites) and brachiopods largely from the Tethys and Boreal oceans (Gröcke *et al.*, 2003; Dera *et al.*, 2011; Price and Passey, 2013; Price *et al.*, 2013; Zakharov *et al.*, 2014). Following the Oxfordian warming period (Weissert and Erba, 2004; Jenkyns *et al.*, 2012), there was an increase in global temperatures in the Kimmeridgian (Anderson *et al.*, 1999; Scotese *et al.*, 1999; Bergman *et al.*, 2004; Price and Passey, 2013; Meyers, 2014). Increasing atmospheric temperatures through the Late Jurassic are consistent with results from the GEOCARBSULF model, although at a lower resolution (Berner, 1994; Berner, 2001; Berner and Kothavala, 2001; Berner, 2006; 2009; Price *et al.*, 2013). Numerous studies indicate a cooling and

aridity episode in the late Tithonian (a "cold snap"), followed by a temperature and humidity increase during the Berriasian (Hallam *et al.*, 1991; Price and Gröcke, 2002; Gröcke *et al.*, 2003; Jenkyns *et al.*, 2011; Grabowski *et al.*, 2013; Price *et al.*, 2013; Zhang *et al.*, 2014). These 'cold snaps' also occurred at the Middle–Late Jurassic boundary and early Aptian (Jenkyns *et al.*, 2011), and have been associated with marine biotic crises (McAnena *et al.*, 2013). When aridity reached its peak development during the earliest Cretaceous, arid regions extended across much of southern Eurasia, whilst higher latitudes were more humid (Hallam *et al.*, 1991) (Figure 3). Cooling may have been more significant at higher latitudes in the Boreal and Tethyan realms, creating a stronger latitudinal climatic gradient up to the J/K boundary (Žák *et al.*, 2011), and Australia appears to have been covered by glaciers from the Berriasian–Valanginian. However, some evidence suggests that high northern latitudes experienced a coupled oceanic-atmospheric warming (Zakharov *et al.*, 2014). Following cooling within the Tithonian and Berriasian, gradual warming occurred through the Early Cretaceous, beginning in the Valanginian and possibly punctuated by short, cooler interludes (Weissert and Channell, 1989; Berner and Kothavala, 2001; Bice *et al.*, 2003; Price and Rogov, 2009; Hannisdal and Peters, 2011; Jenkyns *et al.*, 2011; Price and Passey, 2013). For example, several studies have suggested that temperatures during the late Valanginian were consistent with sub-freezing polar conditions (Price and Mutterlose, 2004; Price and Passey, 2013). The gradual warming trend is detected in numerous regional localities, conceivably related to an increase in volcanic activity throughout the Early Cretaceous (Wang *et al.*, 2006; Sager *et al.*, 2013). From the Valanginian onwards, this volcanism might also be associated with concurrent oceanic anoxic events (Erba, 2004; Erba *et al.*, 2004). However, the idea of cool interludes conflicts with the work of other authors, who have found no evidence for such Early Cretaceous cooling; instead, these studies indicate that the Earth experienced consistently warm and stable temperatures, with a shallow latitudinal temperature gradient (Hay, 2008; Littler *et al.*, 2011; Pouech *et al.*, 2014). Following the late Tithonian "cold snap" (Jenkyns *et al.*, 2011), Cretaceous 'greenhouse' climates from the Valanginian onwards might also be associated with a concurrent oceanic anoxic

event (Erba, 2004; Erba *et al.*, 2004; Erba and Tremolada, 2004). Some evidence suggests that localised episodic climatic cooling during the Early Cretaceous (late Valanginian–earliest Hauterivian, late early Aptian, and latest Aptian–earliest Albian) correspond with high-amplitude fluctuations in sea level, driven by the growth and decay of polar ice caps (Bodin *et al.*, 2015). Furthermore, the Northern and Southern hemispheres might have experienced markedly different climatic regimes throughout the Late Jurassic and Early Cretaceous, which might have been due to the relative positions of the major oceans and landmasses (Jenkyns *et al.*, 2011). Overall, the Early Cretaceous (Berriasian–Barremian) is thought to have been a cooler period, but with steadily increasing temperatures, within the otherwise generally warmer Cretaceous 'greenhouse' world (Sames *et al.*, 2016).

In terms of terrestrial temperature change across the J/K boundary, data are much more limited. Data for the Late Cretaceous (Spicer and Parrish, 1990) are relatively abundant, and indicates peak temperatures in the mid-Cretaceous, followed by a Late Cretaceous decline. As these data are largely consistent with the marine record, it might suggest that the patterns of marine temperature change associated with the J/K boundary are matched in the terrestrial realm. Indeed, (Abbink *et al.*, 2001) described similar changes on the basis of quantitative sporomorph data, whereby climate from the middle Oxfordian to the Berriasian was characterised by stepwise warming and increasing aridity, followed by slight cooling.

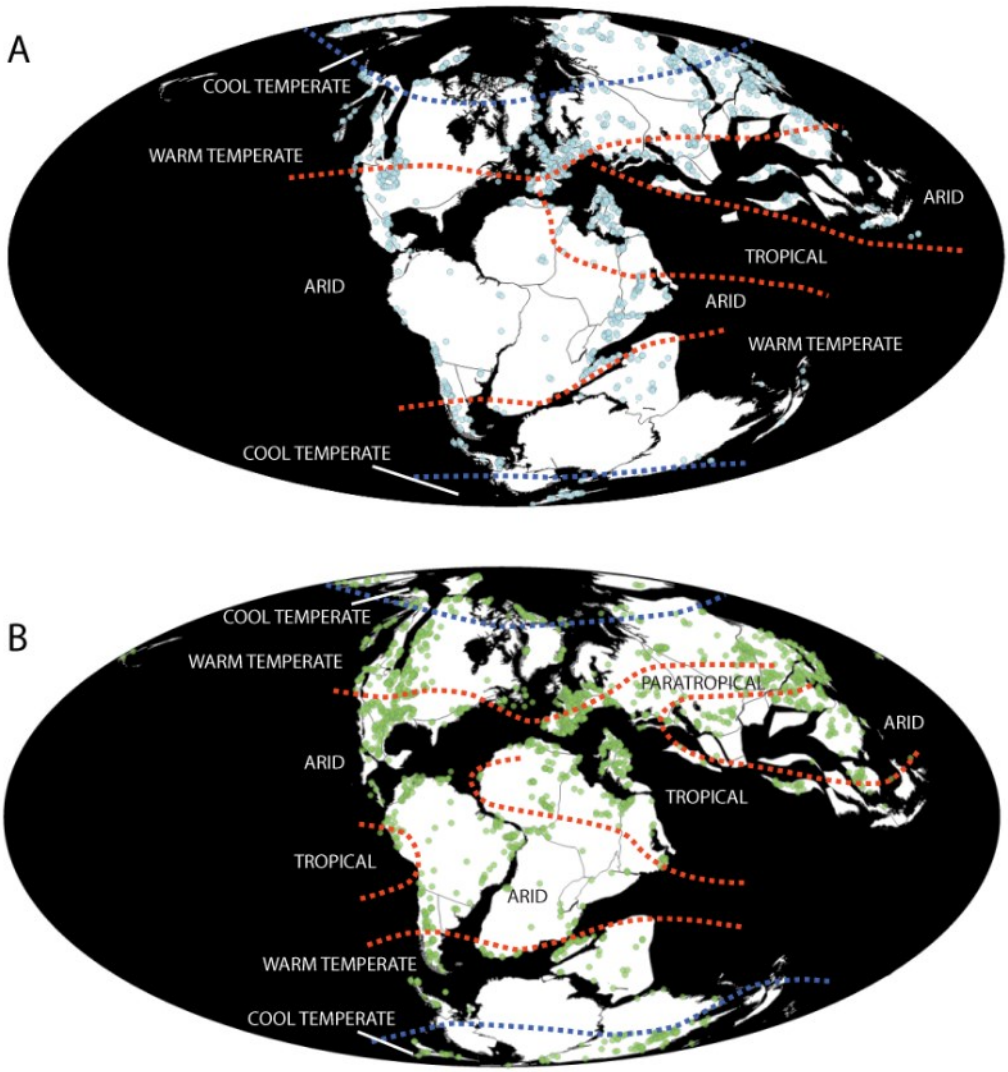


Figure 3: (A) Late Jurassic (Oxfordian–Tithonian) and (B) Early Cretaceous (Berriasian–Albian) global fossil occurrences, with climatic regions overlain. Fossil occurrence data downloaded from The Paleobiology Database, November, 2014 (http://paleobiodb.org/). Palaeoclimate data from Paleomap project (http://www.scotese.com/).

1.3 Biotic changes across the Jurassic/Cretaceous transition

1.3.1 Incomplete and biased sampling in the fossil record

Early investigations into the trajectory of diversity on a geological time scale typically used raw counts of fossil taxa, such as the numbers of species, genera, and/or families through time (Sepkoski Jr, 1982; 1984; 1986). These were often based on counting the number of lineages through time on a global

level, rather than explicit spatiotemporally-defined individual fossils occurrences. Our uneven sampling of the fossil record means that a literal reading of it is likely to be problematic, with observed patterns in diversity potentially artefacts of a biased, or highly structured, record. There are two main modes in which the fossil record can be biased by sampling: geological (including taphonomic biases) and anthropogenic; each of these act as filtering mechanisms between the observed and sampled record, and the original underlying biological record. The former of these biases concerns the nature in which the geological record preserves the biological record, through the processes of burial and decay and selective fossilisation (preservational or taphonomic bias), the amount of fossil-bearing rock preserved in a particular time and place (macrostratigraphic bias), and differences in the types of environments preserved through space and time (also a macrostratigraphic bias). This influences the frequency of opportunities to sample fossils, or the fossilisation potential of a particular depositional environment (Holland, 2000; Smith, 2001; Smith *et al.*, 2001; Peters, 2005; Smith and McGowan, 2007; McGowan and Smith, 2008; Smith and McGowan, 2008; Wall *et al.*, 2009; Heim and Peters, 2011b; a; Peters and Heim, 2011; Wall *et al.*, 2011; Dunhill *et al.*, 2013). Geological factors such as uplift and erosion also affect the accessibility of fossiliferous sediments. Anthropogenic sampling biases include the way we have sampled the fossil record, through increased collecting intensity at well-known sites, and/or time intervals of special interest (Alroy, 2010a; b; Mannion and Upchurch, 2011; Upchurch *et al.*, 2011b; Brocklehurst *et al.*, 2013; Fröbisch, 2013), but also include other human factors such as economics, political situations, or legal concerns. These anthropogencic filters can be broadly described as reflecting different aspects of sampling effort. Each of these general large-scale filters is influenced too by the underlying heterogeneity that creates biodiversity (i.e., the fact that between-clade differences exist), due to differences in the abundance and even distribution of taxa, different evolutionary rates and histories, and alpha and beta-level differences between communities and habitat-dependent variation.

Before we can start to explore and interpret macroevolutionary patterns in the fossil record, we need to be able to understand and deal with such sampling biases. Fortunately, there exists a variety of methods for quantifying and ameliorating these biases. Modelling techniques can be used that estimate the portion of standing diversity that cannot be explained by our sampling of the geological and fossil records, using sampling proxies such as numbers of fossiliferous collections, fossil-bearing stratigraphic formations, or rock outcrop area. These methods seek to explain whether diversity is driven by (1) sampling bias; (2) an external 'common cause' factor, such as sea level; and/or (3) redundancy, resulting from the non-independence of sampling metrics and diversity (Benton *et al.*, 2011; Benton *et al.*, 2013a). Resulting 'residual' diversity curves from these modelling approaches represent biological deviations from a null model in which observed diversity is driven purely by sampling (Smith, 2007; Barrett *et al.*, 2009; Mannion *et al.*, 2011; Butler *et al.*, 2013). However, the use and appropriateness of sampling proxies has been questioned by some studies (Crampton *et al.*, 2003; Benton *et al.*, 2011; Dunhill *et al.*, 2012; Benton *et al.*, 2013a; Dunhill *et al.*, 2013; Dunhill *et al.*, 2014a; Dunhill *et al.*, 2014b; Benton, 2015). Additional modelling approaches include probabilistic estimation using capture-mark-recapture models adapted from those used in ecology (Nichols and Pollock, 1983; Liow and Nichols, 2010; Liow, 2013; Liow and Finarelli, 2014), but are not considered further within this thesis except as a route for future exploration.

Subsampling techniques such as classical rarefaction account for heterogeneous sample sizes between different temporal groupings, setting a baseline subsampling threshold to the poorest-sampled bin as a measure of relative quality (Raup, 1975; Jackson and Johnson, 2001). Three new modes of randomised sub-sampling analysis were introduced based on subsampling from taxonomic occurrence lists using various weighting exponents, and used to assess the reliability of previous estimates of Phanerozoic diversity based on raw counts (Alroy *et al.*, 2001). The shareholder quorum subsampling (SQS) technique was subsequently developed (Alroy, 2010c; a), and works by assigning different weights to species occurrences depending on the frequency of their occurrence, and subsamples from

occurrence lists until a pre-defined quorum is met. As such, the key difference between the widely used classical rarefaction and SQS is that the former samples equally, whereas the latter samples fairly based on a measure of the evenness of the fossil record (see Section 2.6).

The phylogenetic relationships between taxa provide an additional source of information that can be utilised to reconstruct past diversity. A time-calibrated phylogenetic tree incorporates 'ghost lineages' that represent inferred gaps in the fossil record based on the known temporal distribution of lineages, with the first appearance time of a taxon extended back to that of its oldest known sister taxon occurrence (Wagner, 2000; Lane *et al.*, 2005; Cavin and Forey, 2007). Construction of these 'ghost lineages' can increase diversity in time bins where we know a taxon must have been present, but has not yet been sampled, by simply summing the within-bin total number of true and ghost lineages. However, there are drawbacks to this approach, primarily in that it cannot account for range extensions from the last appearance to the true extinction date of a lineage; i.e., 'zombie' lineages (Lane *et al.*, 2005), which can result in a Signor-Lipps effect of an artefactually smeared out extinction, and also imposes a skew on resulting diversity estimates by favouring ghost lineage counts in successively older time bins. Estimates of phylogenetic diversity may be a better representation of true diversity than residual diversity estimates, which vary highly in performance based on the scope and breadth of the proxy used (Brocklehurst, 2015).

Recent analytical studies have built on and surpassed earlier research into long-term macroevolutionary patterns via the development of databases such as *The Paleobiology Database* (www.paleobiodb.org) and *Fossilworks* (http://www.fossilworks.org), synchronous with the progress in analytical techniques outlined above. Macroevolutionary studies that have included the J/K interval explored the effects of uneven sampling on vertebrate diversity at regional and global levels (Barrett and Upchurch, 2005; Barrett *et al.*, 2009; Butler *et al.*, 2009c; Benson *et al.*, 2010; Benson and Butler, 2011; Mannion *et al.*, 2011; Upchurch *et al.*, 2011b; Butler *et al.*, 2012; Lloyd, 2012; Butler *et al.*, 2013;

Lloyd and Friedman, 2013; Newham *et al.*, 2014; Mannion *et al.*, 2015; Nicholson *et al.*, 2015), and are supplemented by a substantial wealth of taxonomic and systematic work. Combined with significant progress into our understanding of the diversity dynamics of marine invertebrates (Alroy, 2008; 2010b; c; 2014) these recent studies are beginning to reveal a much more nuanced view of broad macroevolutionary patterns across the J/K boundary.

1.3.2 The quality of the Late Jurassic–Early Cretaceous fossil record

Numerous studies have documented changes in global and regional sampling quality over the J/K boundary. Notable examples include the sharp decline in fossiliferous marine- (Benson *et al.*, 2010; Benson and Butler, 2011), pterosaur- (Butler *et al.*, 2009c; Butler *et al.*, 2012; Butler *et al.*, 2013) and dinosaur-bearing collections and formations (Mannion *et al.*, 2011; Upchurch *et al.*, 2011b), indicative of an overall regime shift in the relative quality of the fossil record through the J/K interval. The amount of terrestrial (Benson *et al.*, 2010; Peters and Heim, 2010) and marine (Smith, 2001; Smith and McGowan, 2007; McGowan and Smith, 2008; Smith *et al.*, 2012; Smith and Benson, 2013) rock outcrop area shows a shallow and steep decline, respectively, over the J/K boundary, with implications for the availability of possible fossil-bearing sites to sample. An additional measure of quality for the fossil record is specimen completeness, or the proportion of the skeleton that is known for a particular taxon as a whole. For example, sauropod dinosaurs (Mannion and Upchurch, 2010a), pterosaurs (Dean *et al.*), and birds (Brocklehurst *et al.*, 2012) all show reductions in average skeletal completeness over the J/K boundary, consistent with a drop in diversity in the three groups.

Using preliminary data from *The Paleobiology Database* and *Fossilworks* (downloaded on the 8th January, 2015), the total numbers of taxonomic occurrences, fossil-bearing collections, and raw species richness all show significant drops over the J/K boundary (Figure 4). This is discussed in more

detail in Chapter 3, but serves here as the basis for commenting on large-scale patterns in apparent diversity and sampling across the J/K interval.

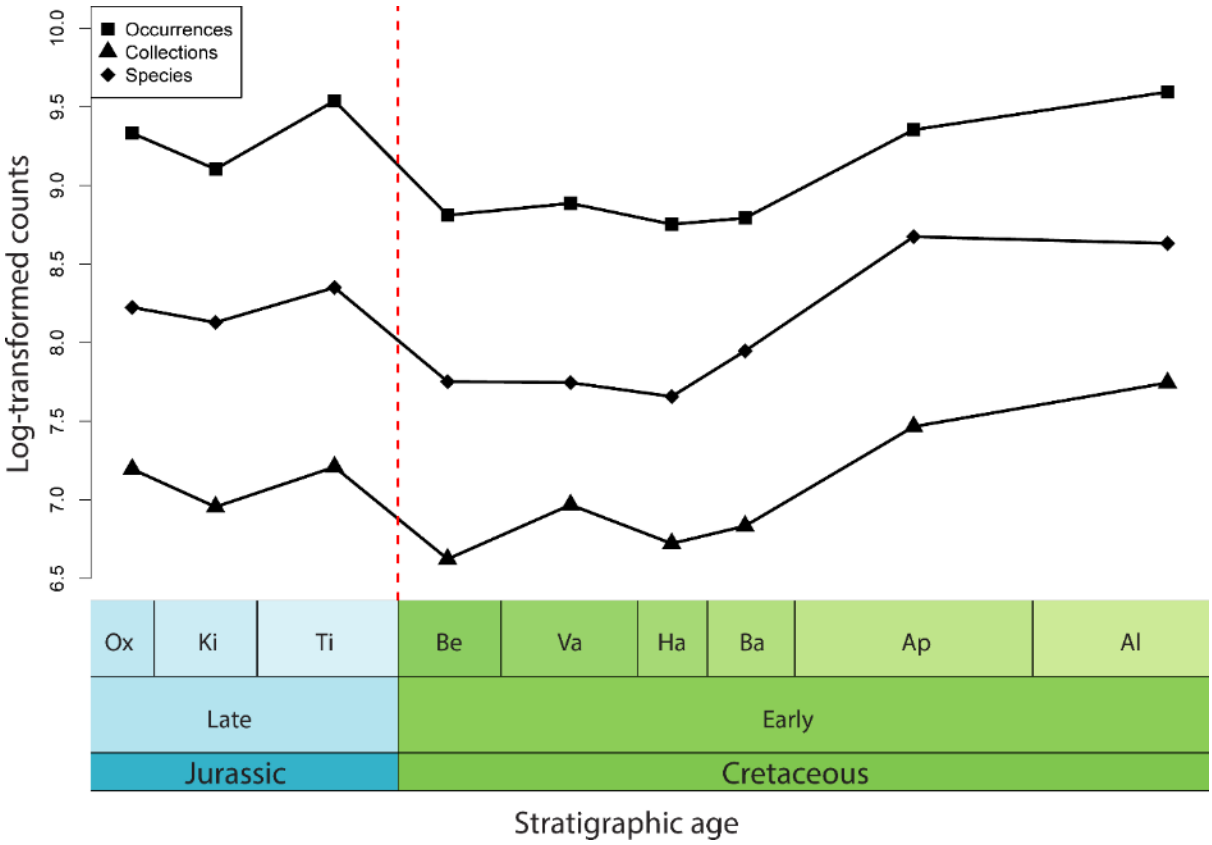


Figure 4. Global taxonomic diversity curve for all animal species, with individual fossil collections and occurrences shown. The Jurassic/Cretaceous boundary is marked by a red line. Data extracted from the Paleobiology Database, January, 2014 (http://paleobiodb.org/). Constructed using the *strap* package (Bell and Lloyd, 2015) in R (version 3.1.1) (R Development Core Team, 2013). Abbreviations: Ox, Oxfordian; Ki, Kimmeridgian; Ti, Tithonian; Be, Berriasian; Va, Valanginian; Ha, Hauterivian; Ba, Barremian; Ap, Aptian; Al, Albian.

Group	J1	J2	J3	J4	J5	J6	K1	K2	K3	K4	K5	K6	K7	K8	Sum per group
Aves	0	0	0	0	0	9	5	27	86	20	17	33	112	134	443
Choristoderes	0	0	0	14	2	15	6	3	18	2	0	1	8	102	171
Lepidosauromorphs	22	3	10	35	10	87	79	40	18	33	30	33	324	263	987
Lissamphibians	0	0	2	41	9	29	34	35	20	23	31	74	283	363	944
Mammaliaforms	28	5	8	74	35	213	115	46	22	56	154	176	731	1092	2755
Theropods	63	7	5	85	80	349	121	177	142	171	139	196	842	800	3177
Pterosaurs	6	1	52	25	23	118	46	38	49	120	51	30	58	33	650
Sauropodomorphs	150	2	7	72	53	572	66	83	58	101	55	61	76	233	1589
Ornithischians	49	3	3	23	48	253	131	174	114	217	77	182	1480	1006	3760
Crocodyliformes (terrestrial)	24	1	1	30	25	117	72	89	50	81	68	88	254	418	1318
Testudines	1	0	0	16	26	209	82	49	53	68	74	139	789	893	2399
Ichthyopterygians	40	5	72	8	28	55	10	18	11	63	15	0	1	0	326
Sauropterygians	29	10	36	7	107	137	26	17	26	32	36	65	96	67	691
Chelonioides	0	0	0	0	0	0	0	0	1	8	4	22	39	46	120
Crocodyliformes (marine)	1	0	45	49	80	131	12	2	7	1	4	0	5	52	389
Sum per time bin	413	37	241	479	526	2294	805	798	675	996	755	1100	5098	5502	19719
Sum aquatic	70	15	153	64	215	323	48	37	45	104	59	87	141	165	1526
Sum terrestrial	343	22	88	415	311	1971	757	761	630	892	696	1013	4957	5337	18193

Table 2. Raw occurrences for each taxonomic group, comprising Tetrapoda, analysed in this thesis, sub-divided into 10 million year time bin intervals.

The way in which we have sampled the fossil record spatially also affects our understanding of Late Jurassic and Early Cretaceous biotic patterns (Upchurch *et al.*, 2011b; Mannion *et al.*, 2012; Benson *et al.*, 2013; Vilhena and Smith, 2013). The northern hemisphere is generally sampled better than the southern hemisphere in the Late Jurassic (Figure 1), with a shift to increased global sampling effort for much of the Early Cretaceous. For terrestrial vertebrates, the Late Jurassic record is dominated by North American and east African (Tanzanian) collections, with multiple fossil-bearing sites from the well-sampled Morrison and Tendaguru formations, respectively. Much of our understanding of latest Jurassic terrestrial diversity comes from Lagerstätten, such as the Solnhofen Limestones (Tithonian of southeastern Germany) (Wellnhofer, 1970), and the Late Jurassic Daohugou Biota of northeastern China (Sullivan *et al.*, 2014). The earliest Cretaceous is devoid of terrestrial Lagerstätten, with the

stratigraphically youngest Cretaceous Lagerstätten deposits known from the Barremian of Spain (Las Hoyas), the Barremian–Aptian of China (Jehol), and the Aptian–Albian of Brazil (Crato and Santana). In the earliest Cretaceous (Berriasian–Hauterivian), terrestrial vertebrate fossils are known primarily from Asia and Europe, whereas North American and Gondwanan occurrences become common again only from the Barremian onwards. In Europe, this reflects a marked change from marine to non-marine environments in the geological record across the J/K boundary (Hallam, 1986). There is a decline in the total number of terrestrial vertebrate collections over the J/K boundary, before a dramatic increase in the Barremian, with around three-times the number of fossil-bearing collections known in the Aptian–Albian than for any Late Jurassic interval. However, this is likely to be largely driven by this aforementioned Lagerstätten effect, but nonetheless reflects an overall decline in sampling intensity through the J/K boundary. Australia and Antarctica completely lack a terrestrial fossil record through the J/K boundary, with the stratigraphically oldest Cretaceous occurrences known from the Aptian and Coniacian, respectively. A continuous Jurassic/Cretaceous stratigraphic terrestrial sequence is known from the Eromanga Basin of Eastern Australia, and coeval with other subsurface Gondwanan terrestrial deposits in India (Sajadi and Playford, 2002; Jha *et al.*, 2016). However, no tetrapod fossils have been formally reported from either of these basins, despite a rich palynoflora, and therefore whether this reflects a genuine biological absence or a taphonomic artefact requires further investigation.

Group	J1	J2	J3	J4	J5	J6	K1	K2	K3	K4	K5	K6	K7	K8	Sum per group
Aves	0	0	0	0	0	3	4	11	9	8	8	13	31	27	114
Choristoderes	0	0	0	5	2	4	2	3	7	1	0	1	8	11	44
Lepidosauromorphs	5	1	2	5	6	9	10	10	10	9	8	11	23	26	135
Lissamphibians	0	0	1	8	5	4	10	8	8	8	8	8	20	26	114
Mammaliaforms	3	1	1	9	4	7	9	8	8	10	8	11	28	31	138
Theropods	18	4	5	27	23	26	35	31	33	32	39	34	66	78	451
Pterosaurs	3	1	6	11	12	23	12	13	11	19	16	12	22	19	180
Sauropodomorphs	13	2	6	25	14	34	22	27	20	24	25	18	24	50	304
Ornithischians	9	3	3	8	17	19	24	33	32	35	28	39	72	89	411
Crocodyliformes (terrestrial)	5	1	1	13	12	20	12	15	13	25	18	25	42	51	253
Testudines	1	0	0	7	8	29	15	19	22	23	20	36	56	61	297
Ichthyopteryians	8	4	8	6	8	15	4	6	7	18	8	0	1	0	93
Sauropterygians	7	7	9	5	18	15	9	9	11	12	16	19	17	29	183
Chelonioides	0	0	0	0	0	0	0	0	1	4	4	10	16	17	52
Crocodyliforms (marine)	1	0	8	17	18	30	4	1	5	1	2	0	5	15	107

Table 3. The number of per-taxon formation counts for all tetrapod groups analysed in the present study. Note that these values are not summed to provide 'tetrapod-level' estimates due to the issue of duplication. The per-groups also do not account for formations that cross more than one time bin.

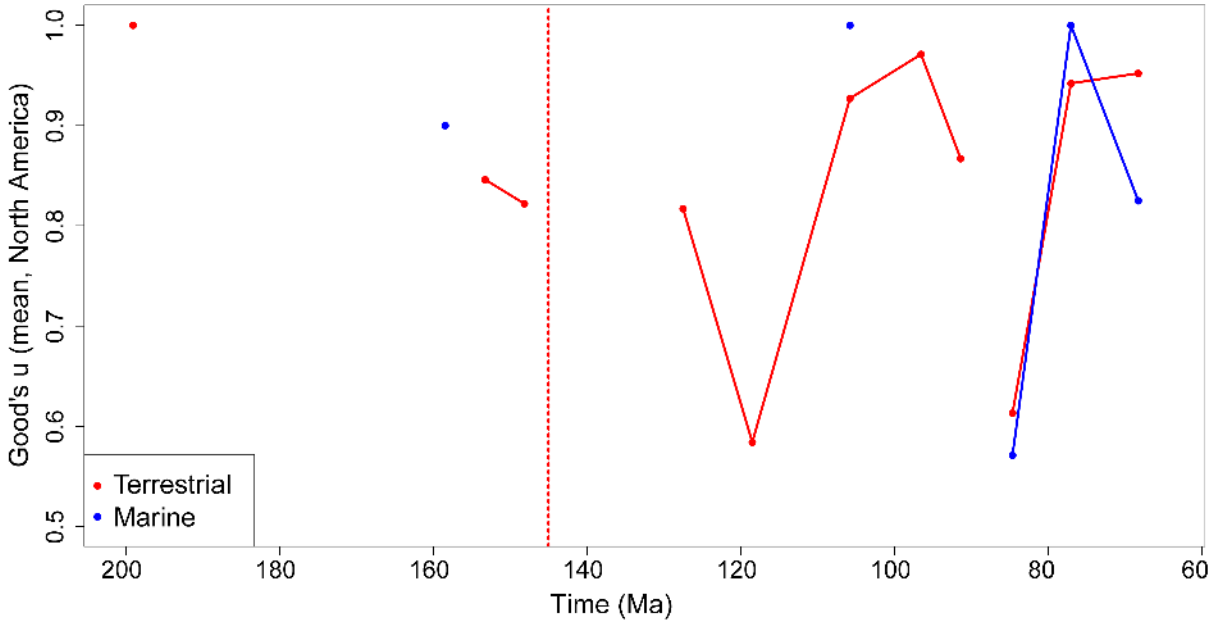


Figure 5. Changes in the 'quality' of the North American marine and non-marine tetrapod fossil record through time based on a measure of eveness (Good's u) (Good, 1953) (see 2-128). Data shown is the mean of that provided for different tetrapod groups in Appendix 8.

Almost our entire knowledge of Late Jurassic marine vertebrates comes from Europe, with a significant contribution from Africa (Figure 7B). There is a dramatic decline in the numbers of marine vertebrate collections through the J/K boundary, which begins to recover only in the Aptian, with North American collections dominating from the Albian onwards. A similar pattern is known for Late Jurassic marine invertebrates (Figure 7C), with a general European bias. African collections contribute much to our understanding of Kimmeridgian diversity, and North America to our knowledge of Tithonian diversity. There is a substantial decline in the number of marine invertebrate collections over the J/K boundary in all geographic regions, but a rapid recovery in the Valanginian, when Gondwanan collections begin to provide a more significant contribution. European collections dominate our knowledge of Early Cretaceous marine and terrestrial faunas (Smith and McGowan, 2007), exceeded only by North American collections in the Albian. Good's *u* (Good, 1953) is a relative measure of the eveness of the fossil record, or how well sampled it is, and has been applied widely in assessment of sampling changes for invertebrates (Alroy, 2010c; a; b) and vertebrate groups (Mannion *et al.*, 2015; Nicholson *et al.*, 2015). Regionally, at a stage-level resolution, there is a shift from well-sampled Late Jurassic marine and non-marine tetrapods (albeit with sparse data coverage) to a complete lack of sampling coverage in the earliest Cretaceous (Figure 5). Conversely, in Europe, there is fluctuating sampling coverage in the Late Jurassic for marine tetrapods, with a short hiatus in the earliest Cretaceous before the fluctuating pattern returns. In the non-marine tetrapod record of Europe, the Late Jurassic is generally more poorly sampled than the earliest Cretaceous, with fluctuating coverage levels through the J/K interval (Figure 6). The implications of these changes in sampling are discussed in more detail in Chapter 3. However, it is important to outline how these patterns contribute to our understanding of the temporal and spatial biases that determine our knowledge of Mesozoic biotas. Below, a detailed review of biotic patterns during the Jurassic–Cretaceous transition is provided in the context of these regional and global changes in sampling.

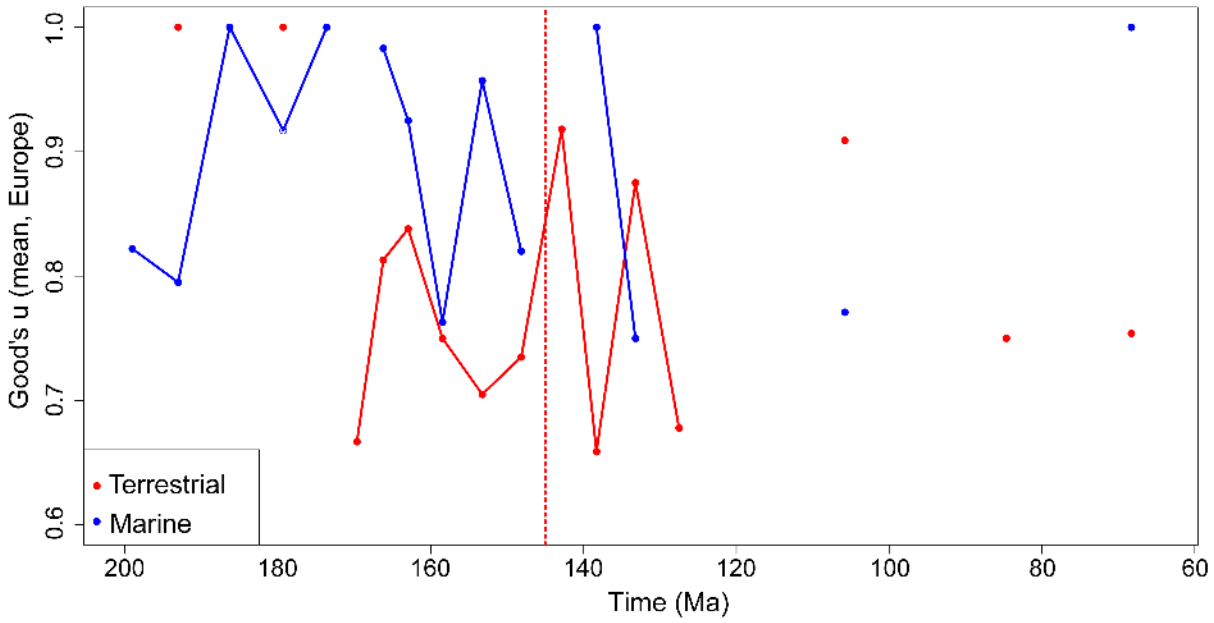


Figure 6. Changes in the 'quality' of the European marine and non-marine tetrapod fossil record through time based on a measure of eveness (Good's u) (Good, 1953) (see Section 2.6). Data shown is the mean of that provided for different tetrapod groups in Appendix 8.

Group	J1	J2	J3	J4	J5	J6	K1	K2	K3	K4	K5	K6	K7	K8	Sum per group
Aves	0	0	0	0	0	8	4	14	37	11	8	22	62	52	218
Choristoderes	0	0	0	6	2	12	1	3	13	2	0	1	24	36	100
Lepidosauromorphs	11	3	3	7	6	36	16	18	14	17	12	16	68	57	284
Lissamphibians	0	0	1	11	6	12	12	14	11	11	13	16	35	66	208
Mammaliaforms	14	4	1	12	10	31	19	15	13	19	17	20	76	91	342
Theropods	44	5	5	40	59	164	59	89	74	63	60	64	252	241	1219
Pterosaurs	6	1	10	12	16	55	21	24	26	28	31	20	36	28	314
Sauropodomorphs	63	2	7	49	39	177	39	55	41	48	38	42	46	133	779
Ornithischians	34	3	3	12	30	114	69	95	65	67	41	50	355	323	1261
Crocodyliformes (terrestrial)	15	1	1	14	18	72	29	41	23	35	34	62	107	131	583
Testudines	1	0	0	8	12	95	34	33	29	35	29	48	149	154	627
Ichthyopterygians	26	5	23	5	22	36	10	13	11	33	12	0	1	0	197
Sauropterygians	18	7	22	6	48	54	16	11	14	19	27	32	51	45	370
Chelonioides	0	0	0	0	0	0	0	0	1	8	4	14	24	29	80
Crocodyliformes (marine)	1	0	17	26	39	73	9	1	5	1	2	0	4	24	202

Table 4. The number of per-taxon collection counts for all tetrapod groups analysed in the present study. Note that these values are not summed to provide 'tetrapod-level' estimates due to the issue of duplication. The per-groups also do not account for collections that cross more than one time bin.

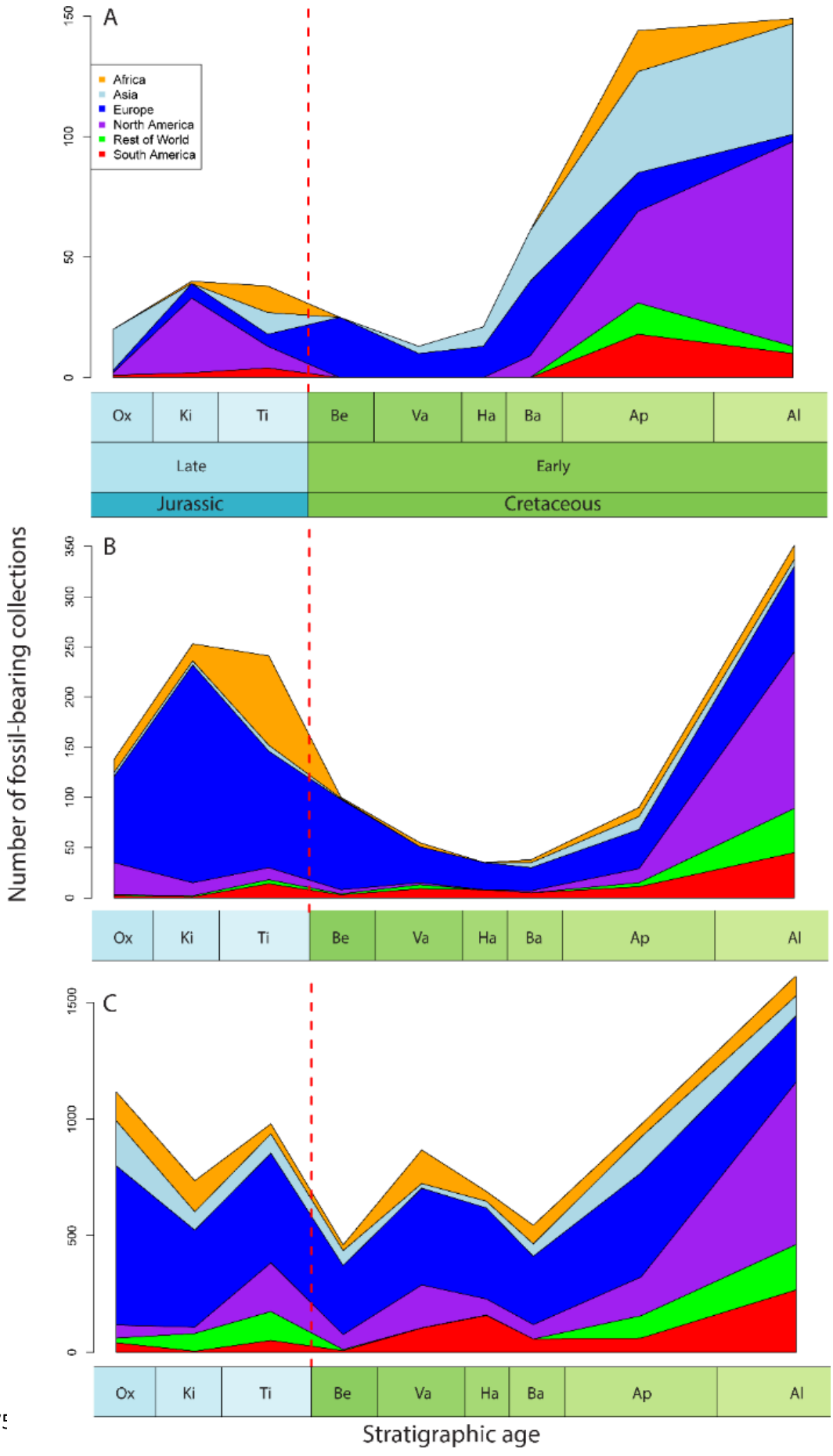

A
Africa
Asia
Europe
North America
Rest of World
South America
0
50
100
150
Ox
Ki
Ti
Be
Va
Ha
Ba
Ap
Al
Late
Early
Jurassic
Cretaceous
B
0
50
100
150
200
250
300
350
C
0
500
1000
1500
Number of fossil-bearing collections
Stratigraphic age

Figure 7. Late Jurassic and Early Cretaceous fossil bearing collections based on continental location. (A) Terrestrial collections (vertebrates only); (B) Marine collections (vertebrates only; (C) Marine collections (invertebrates only). Data from the Paleobiology Database, accessed January, 2015 (http://paleobiodb.org/). Collections represent irreducible and discrete fossil-bearing localities. Only those that could be dated to Stage-level resolution were included. Constructed using the geoscale package (Bell and Lloyd, 2015) in R (version 3.1.1) (R Development Core Team, 2013).

1.3.3 Vertebrates

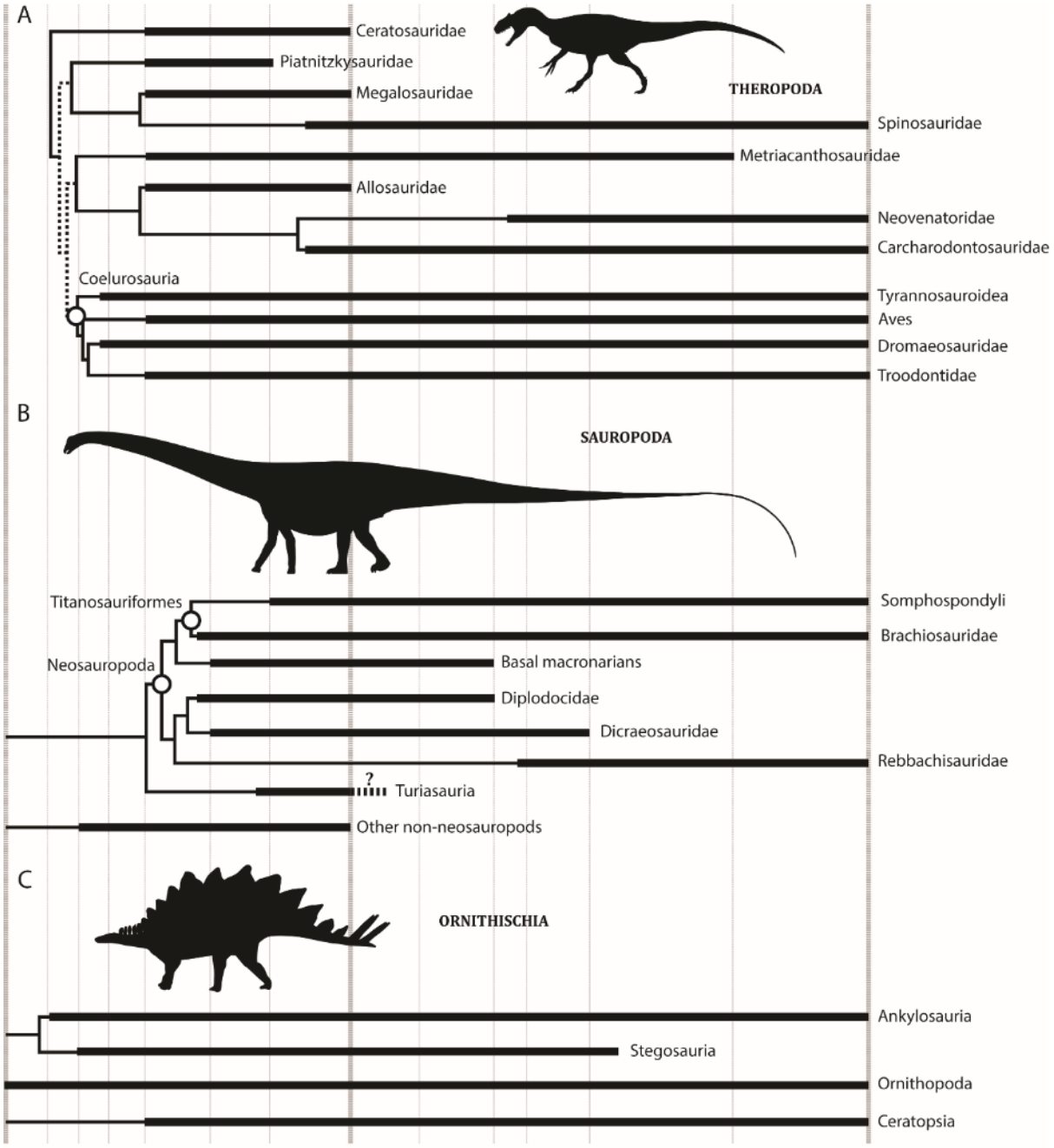
1.3.3.1 Dinosaurs

Of all Mesozoic vertebrate groups, dinosaurs have the best sampled and most studied fossil record. The number of raw non-avian dinosaur genera and species halved from the Tithonian to Berriasian (Lloyd *et al.*, 2008; Barrett *et al.*, 2009; Upchurch *et al.*, 2011b). This pattern is geographically focused in taxa from Europe and North and South America, with Africa and Asia seemgingly relatively unaffected (Upchurch *et al.*, 2011b). However, the precise details and magnitude of this diversity reduction are obfuscated by relatively poor preservation, sampling, and dating of earliest Cretaceous dinosaur-bearing terrestrial exposures, particularly in Gondwana, North America, and Asia (Upchurch *et al.*, 2011b; Upchurch and Mannion, 2012). The diversity dynamics of the three major dinosaur clades (Ornithischia, Sauropodomorpha and Theropoda) over the J/K boundary appear to have been very different to one another (Barrett *et al.*, 2009; Upchurch *et al.*, 2011b) (Figure 8). Apparent large-scale changes in the composition of dinosaurian faunas across the J/K boundary led to the original proposal that they co-evolved with the origin and early evolution of flowering plants (Bakker, 1978). This was based on an apparent ecological shift from higher browsing sauropod-dominated faunas to those composed of more diverse ornithischians. However, numerous recent discoveries in the Late Jurassic to Early Cretaceous interval indicate that such an ecological turnover is not as clearly defined as originally proposed, and the spatiotemporal structure of any such turnover does not support co-evolutionary relationships between herbivorous dinosaurs and either the origin of angiosperms (Barrett and Willis, 2001; Butler *et al.*, 2009a), or diversification of gymnosperms (Butler *et al.*, 2009b).

Theropods gradually reduced in diversity through the Late Jurassic, and appear to have been relatively unaffected across the boundary when using a residual diversity estimate based on collection counts (Upchurch *et al.*, 2011b; Upchurch and Mannion, 2012). However, evidence of a small decline was recovered based on a formations-based residual diversity estimate (Upchurch *et al.*, 2011b), a result also recovered based on a modified non-linear version of the residual method (Lloyd, 2012). Evidence for this decline is emphasised when birds are excluded, with non-avian theropod extinction intensity across the J/K boundary reaching a Mesozoic peak (excluding the K/Pg boundary) (Upchurch *et al.*, 2011b). This extinction seems to have primarily affected Laurasian faunas (Upchurch *et al.*, 2011b; Novas *et al.*, 2013), and appears to have been largely confined to medium- to large-bodied theropods that were more cosmopolitan in nature through the Late Jurassic (e.g., Ceratosauridae, Megalosauridae, and Piatnitzkysauridae), or that were confined to Euamerica (Allosauridae; Figure 8). Some smaller-bodied basal tyrannosauroids also went extinct at the J/K boundary (Brusatte *et al.*, 2016). Other large-bodied groups, including Carcharodontosauridae and Spinosauridae, have their earliest representatives in the latest Jurassic of Tanzania (Carrano *et al.*, 2012). The J/K boundary preceded the origins and diversification of several major lineages of tetanurans (Carrano *et al.*, 2012; Novas *et al.*, 2013; Zanno and Makovicky, 2013; Tortosa *et al.*, 2014). Smaller-bodied coelurosaurians (e.g., Troodontidae, Dromaeosauridae) have their origins in the Middle Jurassic (Hu *et al.*, 2009; Rauhut *et al.*, 2010), but remain largely absent from Early Cretaceous Gondwanan theropod faunas, which instead comprise a diverse array of small- and large-bodied taxa (e.g., carcharodontosaurids) (Sereno *et al.*, 1996; Novas *et al.*, 2005; Brusatte and Sereno, 2007; Evers *et al.*, 2015). Eumaniraptora, or the more inclusive Paraves, underwent a significant acceleration in diversification rates across the J/K boundary (Lloyd *et al.*, 2008). While the first definitive birds first appear in the Late Jurassic of Europe with *Archaeopteryx*, putative members of Aves have also been reported from the Late Jurassic (Oxfordian) of China (Xu *et al.*, 2011; Godefroit *et al.*, 2013a; Godefroit *et al.*, 2013b; Brusatte *et al.*, 2014). The first major radiation of Aves appears to have occurred in the Early Cretaceous of China

(Jehol Biota, Barremian–Aptian), indicated by the diversification of all major pygostylian lineages (O'Connor *et al.*, 2011a; O'Connor *et al.*, 2011b; Wang *et al.*, 2014; Huang *et al.*, 2016), although this apparent radiation is likely influenced by the Lagerstätten effect (see Section 1.3.2). Furthermore, the earliest Cretaceous fossil record of birds is extremely poor (Brocklehurst *et al.*, 2012), comprising only fragmentary and incomplete material (Dyke *et al.*, 2011). This pygostylian radiation was coeval with a rapid diversification of avian body plans during the Early Cretaceous (Benson *et al.*, 2014; Brusatte *et al.*, 2014; Wang *et al.*, 2014), although this was accompanied by an overall constrained ecological disparity (Mitchell and Makovicky, 2014).

Figure 8. Stratigraphic ranges of major Jurassic–Cretaceous theropod (A), sauropod (B) and ornithischian (C) dinosaur clades through the Middle Jurassic to Early Cretaceous. Theropods are adapted from Carrano et al. (2012); sauropods are adapted from Mannion et al. (2013). Clade dates are based on those available from The Paleobiology Database, and supplemented from the primary literature. See text for details. Silhouettes from PhyloPic (http://phylopic.org/); Allosaurus fragilis and Diplodocus by Scott Hartman (CC BY-SA 3.0), and Stegosaurus by Andrew Farke (CC BY 3.0). Abbreviations as in Figure 4; additional abbreviations: Aa, Aalenian; Bj, Bajocian; Bt, Bathonian; Ca, Callovian.



Sauropod diversity was high in the Late Jurassic (Kimmeridgian–Tithonian), followed by an apparent dramatic decline over the J/K boundary, based on both raw (Barrett and Upchurch, 2005; Upchurch and Barrett, 2005) and corrected (Benson and Mannion, 2011; Mannion *et al.*, 2011; Upchurch *et al.*,

2011b; Lloyd, 2012; Upchurch and Mannion, 2012) estimates of diversity. A similar signal was found by an earlier investigation of dinosaur diversity using similar techniques but at a finer temporal resolution (Barrett et al., 2009), although they recovered a moderate diversity decline leading up to the J/K boundary, followed by a diversity crash at the boundary. With the possible exception of Spanish taxa whose stratigraphic age cannot be constrained more precisely than late Tithonian-middle Berriasian (Royo-Torres et al., 2014), non-neosauropod eusauropods seem to have disappeared at the J/K boundary (Upchurch and Barrett, 2005; Mannion *et al.*, 2011; Mannion *et al.*, 2013) (Figure 8B), being replaced by titanosauriforms (Wilson, 2005), although a single non-titanosauriform lineage might have persisted into the earliest Cretaceous of North America (D'Emic and Foster, 2016). Late Jurassic representatives of Neosauropoda, comprising Macronaria and Diplodocoidea, were present on all sampled continents except Asia, and this diverse clade crossed the J/K boundary (Upchurch and Barrett, 2005; Mannion *et al.*, 2011). Basal macronarians are known to have survived into the earliest Cretaceous at least in Europe (Royo-Torres et al., 2014; Upchurch et al., 2015) and North America (D'Emic and Foster, 2016), although overall titanosauriform macronarian diversity was seemingly unaffected across the J/K boundary (Upchurch and Mannion, 2012; Mannion *et al.*, 2013). Cretaceous brachiosaurid diversity appears to have plummeted outside of North America (D'emic, 2012; Mannion *et al.*, 2013) and Africa (McPhee et al., 2016), although the clade possibly expanded into the northern tip of South America (Carballido et al., 2015), whilst Somphospondyli experienced a global radiation (D'emic, 2012; Mannion *et al.*, 2013). Within the narrow-toothed Diplodocoidea, diplodocids were thought to have gone extinct at the J/K boundary (Upchurch and Barrett, 2005), although recent discoveries in the earliest Cretaceous of Africa (McPhee et al., 2016) and South America (Gallina et al., 2014) indicates that at least one diplodocid lineage survived. This near-extinction of Diplodocoidea had little overall effect on sauropod speciation rates through the J/K interval (Sakamoto *et al.*, 2016). Cretaceous dicraeosaurid diplodocoids are also known only from South America (Salgado and Bonaparte, 1991; Mannion and Barrett, 2013) and Africa (McPhee et al., 2016), whereas

rebbachisaurids radiated in northern Africa, Europe and South America in the late Early Cretaceous (Carballido et al., 2012; Mannion and Barrett, 2013).

Ornithischians seem to have been relatively unaffected compared to the other dinosaur groups, with only a moderate decline in diversity at the J/K boundary (Barrett *et al.*, 2009; Upchurch *et al.*, 2011b) (Figure 8C). However, the magnitude of any extinction documented by recent investigations based on the residuals method is highly dependent on the mode of sampling correction used (i.e., through a collections- or formations-based residual diversity estimate) (Upchurch *et al.*, 2011b). Diversification rates in Ankylosauria increased rapidly at the J/K boundary (Lloyd *et al.*, 2008), with the North American origin of Ankylosauridae in the earliest Cretaceous (Arbour and Currie, 2015), possibly as they ecologically replaced Stegosauria (the other major group of thyreopheran ornithischians) in terrestrial ecosystems (Arbour *et al.*, 2016). Stegosaurians were in decline after the J/K boundary, becoming extinct by the end of the Early Cretaceous (Barrett and Willis, 2001; Maidment *et al.*, 2008). Basal ceratopsians originated in the Late Jurassic (Oxfordian), and were probably unaffected by the J/K boundary (Xu *et al.*, 2006; Benson *et al.*, 2013), and Neoceratopsia may have its origins in the earliest Cretaceous (Valanginian) of Asia (Farke *et al.*, 2014). Ornithopods seem to have been unaffected, with small basal forms instead proliferating around the J/K boundary (Han *et al.*, 2012; Escaso *et al.*, 2014; Xing *et al.*, 2014), and iguanodontians became increasingly abundant through the Early Cretaceous (Barrett and Willis, 2001).

1.3.3.2 Pterosaurs

Most Laurasian pterosaur taxa are known from Lagerstätten, including the Late Jurassic Solnhofen Limestones of southeastern Germany (Wellnhofer, 1970), the Late Jurassic Daohugou Biota (Sullivan *et al.*, 2014), and the late Early Cretaceous Jehol Biota (Xiaolin and Zhonghe, 2006) of northeastern China. In Gondwana, pterosaur specimens are scarce prior to the late Early Cretaceous (Codorniú and Gasparini, 2013), when Lagerstätten such as the Brazilian Crato Formation were deposited (Unwin and

Martill, 2007). Initial research into pterosaur diversity patterns hypothesised a peak in diversity at the J/K boundary (Slack *et al.*, 2006). However, more recent analyses have largely over-turned this pattern, interpreting diversity peaks to be predominantly the product of episodes of enhanced preservation (i.e., the Lagerstätten effect) (Butler *et al.*, 2009c; Butler *et al.*, 2013), despite other claims that Lagerstätten have little impact on the shape of pterosaur evolution (Dyke *et al.*, 2009).

Pterosaurs underwent a taxonomically-selective and staggered extinction phase up to the J/K boundary, with the majority of non-pterodactyloid pterosaurs (e.g., long-tailed rhamphorhynchoids) becoming extinct (Unwin, 2003), a pattern that is resilient to the impact of sampling biases (Barrett *et al.*, 2008; Butler *et al.*, 2009c; Butler *et al.*, 2013; Andres *et al.*, 2014; Upchurch *et al.*, 2014). Pterodactyloids, particularly ornithocheiroideans, flourished after the J/K boundary, diversifying into a range of species-rich sub-clades (Ji *et al.*, 1999; Butler *et al.*, 2013; Andres *et al.*, 2014). Many of these groups originated in the Late Jurassic along with a range of 'transitional' species (Liu *et al.*, 2012), but apparently did not radiate until the Cretaceous. Consequently, Late Jurassic and Early Cretaceous pterosaur faunas are quite distinct from one another, although some basal taxa, including the anurognathids (Wang *et al.*, 2009), passed through the J/K boundary.

1.3.3.3 Crocodylomorphs

Thalattosuchian crocodylomorphs, comprising the two major pelagic groups, Teleosauridae and Metriorhynchoidea, achieved the height of their diversity during the Late Jurassic (Kimmeridgian and early Tithonian, respectively). During this period, thalattosuchians achieved a broad ecological range, with a variety of feeding modes, craniofacial forms, dental morphologies, functional biomechanical behaviours, and a wide spectrum of body sizes (Pierce *et al.*, 2009a; b; de Andrade *et al.*, 2010a; Young *et al.*, 2010; Young *et al.*, 2011b; Buchy *et al.*, 2013; Young *et al.*, 2013a). Geosaurines, one subgroup of metriorhynchoids, possessed a suite of dental characteristics indicating a macrophagous feeding strategy, and it is likely that they were the apex or second-tier super-predators of Late Jurassic seas

(de Andrade *et al.*, 2010b; Young *et al.*, 2010; Young *et al.*, 2011a; Young *et al.*, 2011b; Foffa and Young, 2014). The other sub-group of metriorhynchoids, metriorhynchines, were smaller and progressively adapted towards an increasingly piscivorous and teuthophagous (squid-consumption) feeding style towards the latest Jurassic (Young *et al.*, 2011b). This ecological dichotomy in metriorhynchids is reflected in their high morphological disparity, although how this changed over the J/K boundary is difficult to discern (Young *et al.*, 2010). Thalattosuchian diversity declined through the J/K boundary based on both raw and subsampled estimates (Mannion *et al.*, 2015). Teleosaurids were previously thought to have gone extinct at the J/K boundary (Young *et al.*, 2014a; Mannion *et al.*, 2015), but a recent discovery shows that a single, highly-specialised lineage survived into the earliest Cretaceous of Gondwana, pushing the timing of their extinction into the Hauterivian (Fanti *et al.*, 2016b). Overall, few thalattosuchian lineages survived into the Early Cretaceous, and they went extinct in the Aptian at the latest (Martin *et al.*, 2014a; Young *et al.*, 2014a; Chiarenza *et al.*, 2015) (Figure 9). However, identification of the youngest metriorhynchid (Chiarenza *et al.*, 2015) has recently been challenged, with Fischer *et al.* (2015) arguing that it possibly represents a brachauchenine pliosaurid; therefore the timing of the final extinction for Thalattosuchia is currently contended.

Most basal mesoeucrocodylians, including the majority of shartegosuchids, are known only from the Jurassic, but at least some forms survived into the Cretaceous of Eurasia (Clark, 2011). Metasuchia, the dominant clade within Mesoeucrocodylia, comprises two major clades of crocodylomorphs: the extinct clade Notosuchia, and Neosuchia, which includes the extant Crocodylia. Basal neosuchians, including the semi-aquatic goniopholids, appear to have passed comparatively unscathed through the J/K boundary (de Andrade *et al.*, 2011b), although terrestrial atoposaurids seem to have been affected, with Cretaceous occurrences dominated by the shallow marine *Theriosuchus* lineage (Tennant and Mannion, 2014; Young *et al.*, 2016). This pattern of decline is reflected in subsampled diversity estimates of non-marine crocodyliforms, which decreased through the J/K boundary (Mannion *et al.*, 2015), although the structure of this decline is poorly understood. In the Early Cretaceous, the

terrestrial notosuchians diversified, adopting a novel suite of ecophenotypes (Carvalho *et al.*, 2005; Nobre *et al.*, 2008; Marinho and Carvalho, 2009; Kellner *et al.*, 2011; Bronzati *et al.*, 2015). Notosuchia may have its origin in the Early Jurassic based on its sister-taxon relationship with Neosuchia, but the first known occurrence is from the earliest Cretaceous (Berriasian) of Brazil (Carvalho *et al.*, 2010). Notosuchians reached a diversity peak in the Aptian–Albian (Carvalho *et al.*, 2010), but whether this represents the true timing of their early radiation is masked by a poor earliest Cretaceous fossil record (Benson *et al.*, 2013) (Figure 9).

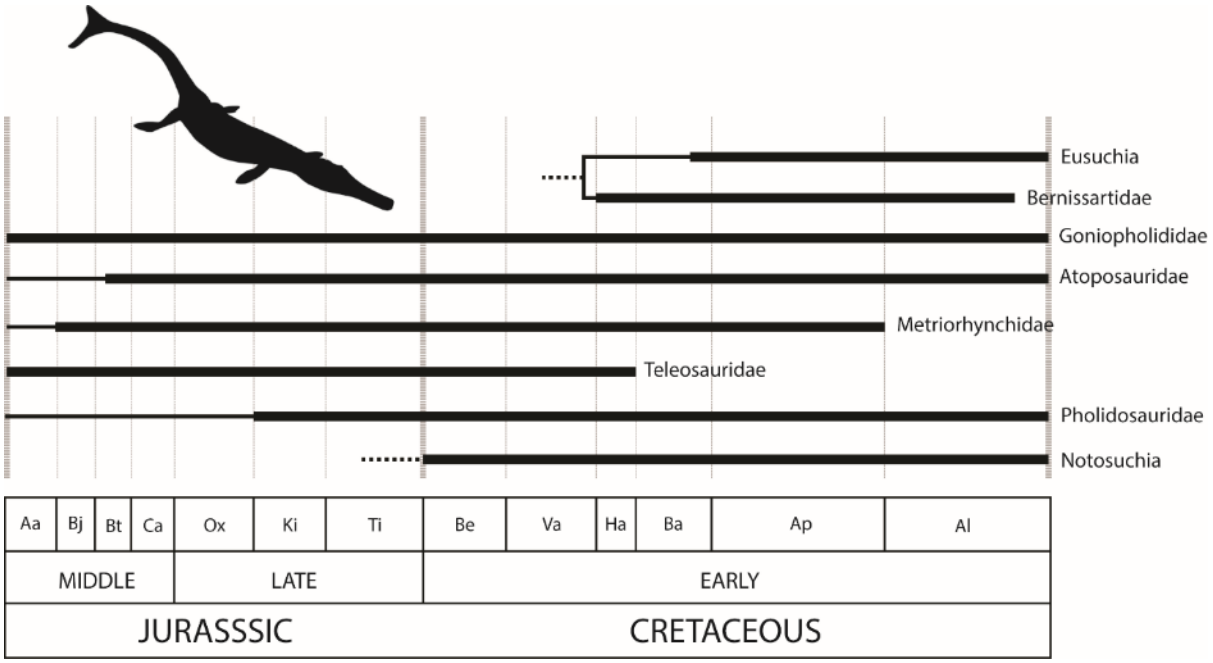


Figure 9. Stratigraphic ranges of major Jurassic–Cretaceous crocodyliform clades. Adapted from Bronzati et al., (2012). Dates obtained from The Paleobiology Database. Abbreviations as in Figure 4. Silhouette of *Metriorhynchus geoffroyi* from PhyloPic, by Gareth Monger (CC BY 3.0).

1.3.3.4 Ichthyopterygians

Recent analyses have demonstrated that summed marine reptile diversity declined dramatically at the J/K boundary (Benson *et al.*, 2010; Benson and Butler, 2011), with evidence that ichthyosaurs were severely affected (Bakker, 1993; Bardet, 1994; Sander, 2000; Benson *et al.*, 2010; Fernandez and Campos, 2015). However, subsequent discoveries and taxonomic revisions have challenged this view,

and instead it seems that ichthyosaurs actually passed through the J/K boundary relatively unscathed. The latest phylogenetic analysis show that 4 genera went extinct at the J/K boundary, highlighting variable interpretations of extinction intensity (Ji *et al.*, in press). Nearly all ichthyosaurs from the Late Jurassic onwards were members of Ophthalmosauridae. Whereas the subclade Platypterygiinae diversified during the Late Jurassic (Kimmeridgian) (Fischer *et al.*, 2012; Fischer *et al.*, 2013), only three ophthalmosaurine taxa survived into the Cretaceous, with the majority going extinct in the latest Jurassic, and the last known occurrences from the Aptian–Albian of Europe (Zammit, 2012; Arkhangelsky and Zverkov, 2014; Roberts *et al.*, 2014). However, this pattern is obscured by the paucity of earliest Cretaceous ichthyosaur specimens (Fischer *et al.*, 2012; Green and Lomax, 2014). *Malawania,* from the Early Cretaceous of Iraq, demonstrates that at least one basal non-ophthalmosaurid lineage passed through the J/K boundary (Fischer *et al.*, 2012; Fischer *et al.*, 2013). Ophthalmosaurines may have been ecologically conservative throughout their evolutionary history, whereas their sister group, Platypterygiinae, exhibited a much broader range of ecological diversity (Fischer *et al.*, 2014), a factor that might have played a role in their relative macroevolutionary histories. Recent evidence from the Early Cretaceous of South America indicates that dispersal pathways between the Northern and Southern Hemispheres might have been significant in controlling the relatively high survival rates for ichthyosaurs around the J/K boundary (Stinnesbeck *et al.*, 2014).

1.3.3.5 Plesiosaurians

Taxonomic diversity of Plesiosauria declined greatly across the J/K boundary, with the extinction of microcleidid and rhomaleosaurid taxa, known exclusively from Euamerica (Bakker, 1993; Benson and Druckenmiller, 2014), apart from a single Middle Jurassic occurrence from Argentina (Gasparini and Fernández, 1997). Recovery of this extinction did not begin until the Hauterivian–Barremian (Benson and Butler, 2011). The only plesiosaurian taxa that declined immediately prior to the J/K boundary were members of Cryptoclididae, which were restricted to the northern hemisphere (apart from a

tentative occurrence from the Kimmeridgian of India (Bardet *et al.*, 1991)), and Pliosauridae, with the exception of the pliosaurid subgroup Brachaucheninae (Ketchum and Benson, 2010; Benson and Druckenmiller, 2014). At least four plesiosaurian lineages are known to have crossed the J/K boundary, with the major clades Elasmosauridae and Leptocleididae both diversifying in the earliest Cretaceous (Benson and Druckenmiller, 2014), following a prolonged period of sustained extinction and replacement throughout the Late Jurassic (Benson and Bowdler, 2014). Coincident with this pattern of ecological turnover is evidence for a substantial decline in plesiosaurian morphological disparity during the Late Jurassic and Early Cretaceous (Benson and Druckenmiller, 2014), although recent discoveries hint that Early Cretaceous pliosaurs were highly ecomorphologically diverse (Fischer *et al.*, 2015).

1.3.3.6 Testudinatans

The timing of the origin of the Testudines, and diversification of its major extant clade Eucryptodira, remains controversial, but both events had occurred by at least the Late Jurassic (Danilov and Parham, 2006; Joyce, 2007; Sterli *et al.*, 2013b). Marine taxa experienced a substantial decrease in diversity across the J/K boundary based on residual diversity estimates (Benson *et al.*, 2010; Benson and Butler, 2011), although others have found only a moderate decline when applying a subsampling approach (Nicholson *et al.*, 2015). However, fully pelagic turtles might not have been present until the origin of Chelonioidea (sea turtles) in the Early Cretaceous of South America (Hirayama, 1998; Cadena and Parham, 2015) (Figure 10). Terrestrial turtles, on the other hand, appear to have been largely unaffected (Hirayama *et al.*, 2000), with more recent analyses applying subsampling methods documenting a steady increase in non-marine diversity through the J/K boundary, peaking in the Aptian (Nicholson *et al.*, 2015). However, this apparent 'global' increase is largely driven by data from Europe, with any other continent-level signal through the J/K boundary poorly resolved (Nicholson *et al.*, 2015). Many Laurasian taxa became endemic in the Late Jurassic, with three major biozones

forming in North America, Asia, and Europe (Hirayama *et al.*, 2000). In the Late Jurassic of Europe, an array of eucryptodiran groups, including basal forms, plesiochelyids, thalassemydids, and eurysternids, were abundant and occupied a range of coastal-marine and freshwater settings (Pérez-García *et al.*, 2008; Pérez-García *et al.*, 2011; Slater *et al.*, 2011; Anquetin and Joyce, 2014; Jansen and Klein, 2014; Pérez-García, 2014b; a; Anquetin and Chapman, 2016). Eucryptodires also dominated Asia, whereas North American faunas were composed primarily of paracryptodires, including the clades Baenidae, Solemydidae, and Pleurosternidae (Hirayama *et al.*, 2000; Lipka *et al.*, 2006; Joyce *et al.*, 2011; Pérez-García and Ortega, 2014).

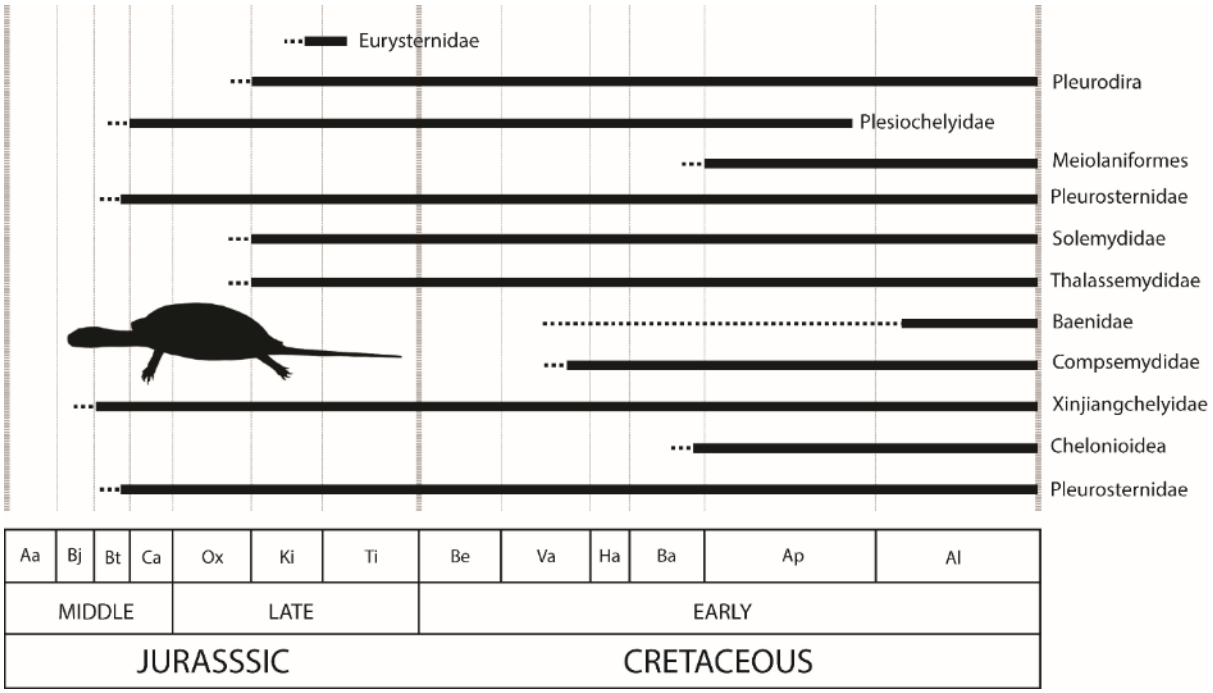


Figure 10. Stratigraphic ranges of major Jurassic–Cretaceous turtle clades. Phylogenetic relationships are not illustrated. Dates obtained from the Paleobiology Database. Abbreviations as in Figure 4. Silhouette of a baenid turtle from PhyloPic, by Scott Hartman (CC BY-SA 3.0).

Some basal eucryptodirans persisted into the Early Cretaceous of Europe (Pérez-García *et al.*, 2012), whereas others, such as eurysternids and thalassemydids, went extinct in the latest Jurassic (lower Tithonian). Coastal-dwelling plesiochelyids might have crossed the J/K boundary based on tentative reports from the Valanginian of Switzerland (de Lapparent de Broin, 2001). Only two species of the

diverse lineage Pleurosternidae survived into the Cretaceous, along with paracryptodirans, including the North American groups Baenidae and Compsemydidae (Pérez-García *et al.*, 2014). Groups dominant in Asia, such as the freshwater Xinjiangchelyidae (probable stem cryptodirans) (Zhou and Rabi, 2015), appear to have been unaffected by the J/K boundary (Danilov and Sukhanov, 2006), although there is some evidence suggesting that this group might be paraphyletic, in which case this taxonomic artefact likely masks a notable decline (Rabi *et al.*, 2010).

In the Early Cretaceous, derived eucryptodiran and paracryptodiran turtles became increasingly diverse in Europe (Pérez-García, 2012; 2014b; Pérez-García and Ortega, 2014; Püntener *et al.*, 2014), following the latest Jurassic extinction of many basal members of these groups. Basal panpleurodirans might have achieved a broad palaeobiogeographic distribution in shallow marine systems during the Late Jurassic (Bardet *et al.*, 2014), followed by the Early Cretaceous diversification of the second major clade of crown group turtles, Pleurodira (Joyce *et al.*, 2004; Danilov and Parham, 2008; Cadena *et al.*, 2013). In Gondwana, Early Cretaceous turtle faunas were dominated by two clades, Pleurodira and Meiolaniformes, although the geographic and temporal origins of this latter clade are poorly understood (Sterli *et al.*, 2013a), the latter first appearing in the Barremian of South America (Sterli, 2015). Of note is the absence of pleurodirans and meiolaniform turtles from Laurasian faunas during the Late Jurassic and Early Cretaceous (Perea *et al.*, 2014).

1.3.3.7 Choristoderes

Choristoderes were small- to medium-sized semi-aquatic middle-tier predators of Laurasian ecosystems, whose placement within Diapsida remains enigmatic (Ksepka *et al.*, 2005; Matsumoto *et al.*, 2009; Zhou and Wang, 2010). They are relatively rare components of the fossil record, known from only a dozen or so genera, but range through the Middle Jurassic to the Miocene (Evans and Klembara, 2005). The timing of the radiation of the important non-neochoristodere group, Monjurosuchidae, is a point of on-going study, although their origin might be in the Early Cretaceous of Asia (Gao and Fox,

2005; Averianov *et al.*, 2006; Richter *et al.*, 2010; Gao *et al.*, 2013). The earliest records of the major lineage Neochoristodera occur in Barremian (Early Cretaceous) deposits of Asia (Matsumoto and Evans, 2010) and North America (Britt *et al.*, 2006), and this lineage persisted well past the K/Pg boundary (Evans and Klembara, 2005). There appears to have been an ecological transition around the J/K boundary, from smaller basal forms (Late Jurassic), to larger taxa, primarily representing neochoristoderes (Early Cretaceous onwards), with non-neochoristoderes seemingly becoming extinct in Euamerica (Matsumoto and Evans, 2010).

1.3.3.8 Lepidosaurians

Lepidosauria comprises the diverse and extant groups Rhynchocephalia and Squamata (Evans and Jones, 2010). Numerous diverse lepidosaurian clades originated in the Middle Jurassic and passed through the J/K boundary (Conrad, 2008; Jones *et al.*, 2013), although their diversity dynamics have not been investigated through this period. These 'Jurassic-type' faunas persisted until the Aptian–Albian in North America and Europe, and became increasingly rare as they were replaced by more 'advanced' lepidosaur faunas (Evans and Chure, 1999; Nydam and Cifelli, 2002; Nydam, 2013). A pan-Laurasian fauna was present in the Late Jurassic (e.g., scincoids and anguimorphans), with several of these Laurasian taxa also known from the earliest Cretaceous of North Africa (Richter, 1994; Evans, 2003; Nydam, 2013; Rage, 2013), although Berriasian occurrences are restricted to western Europe (Evans *et al.*, 2012), Japan (Evans and Manabe, 1998; Evans and Manabe, 1999a; Evans and Manabe, 1999b), and North Africa (Evans and Sigogneau-Russell, 1997). Late Jurassic Gondwanan occurrences of Lepidosauria are restricted to a single occurrence from Tanzania, identified as a scincomorph squamate (Broschinski, 1999), although Early Jurassic Gondwanan occurrences are also known.

The origins of major extant squamate clades such as Lacertoidea (true lizards), Scincoidea (skinks), and the clade comprising Acrodonta and Pleurodonta (iguanians), appear to be either close to the J/K boundary (Pyron and Burbrink, 2012) or in the Early Cretaceous (Jones *et al.*, 2013; Rage, 2013), based

on a combination of molecular and fossil data. The origination time for Serpentes (snakes) is contentious, with some fossil evidence suggesting either the Middle Jurassic (Caldwell *et al.*, 2015) or Early Cretaceous (Martill *et al.*, 2015), but molecular evidence indicates a younger, early Late Cretaceous age (Jones *et al.*, 2013; Head, 2015). The first occurrences of Lacertoidea are in the Berriasian of western Europe (Evans *et al.*, 2012), before this group radiated into North America (Nydam, 2013) and Asia (Gao and Cheng, 1999) in the Barremian–Albian. Although lacking a pre-Cenozoic fossil record, amphisbaenian lacertoids (lizard worms) are thought to have originated around the J/K boundary (Longrich *et al.*, 2015). The earliest known scincoid is from the Albian–Cenomanian of North America (Nydam and Cifelli, 2002). Whereas the oldest acrodont is known from the late Early Jurassic of Asia (Evans *et al.*, 2002), the next stratigraphically oldest occurrence is from the Barremian of China (Li *et al.*, 2007). However, pleurodonts, the sister group to acrodonts, are not known until the Cenomanian of Argentina based on a fragmentary occurrence (Apesteguía *et al.*, 2005), and the Campanian of Mongolia (Norell and Gao, 1997).

Rhynchocephalians are only known from Euamerica in the Late Jurassic, and might have exhibited high ecological diversity, especially with respect to feeding strategy (Rauhut *et al.*, 2012). Their Cretaceous record extends to North Africa (Broschinski, 1999) and South America (Apesteguia and Carballido, 2014). Pleurosauridae represents a small and poorly-known basal clade of European marine rhynchocephalians, with a short duration from the Early Jurassic to the early Tithonian (Dupret, 2004; Bardet *et al.*, 2014). Sphenodontia, a group of basal rhynchocephalians that includes the only extant member (*Sphenodon*), appears to have been confined to Euamerica in the Late Jurassic, but is present in Africa in the Berriasian (Evans and Sigogneau-Russell, 1997), and extended into South America in the Albian (Reynoso, 2000; Apesteguia and Carballido, 2014).

1.3.3.9 Lissamphibians

Lissamphibia comprises anurans (frogs), caudatans (salamanders), albanerpetontids (salamander-like animals) and gymnophionans (caecilians). Within Lissamphibia, there was a small increase in total diversity over the J/K boundary (Fara, 2004). Molecular dates of lissamphibian radiations have wide uncertainty ranges, but it appears that several species-rich lineages, particularly within Anura, might have diversified around the J/K boundary (Marjanovic and Laurin, 2013). Anurans were largely unaffected across the J/K boundary at higher taxonomic levels, but more work on the systematics of the group is required to clarify its macroevolutionary history (Marjanović and Laurin, 2007). Anurans were diverse in the Late Jurassic of Euamerica, and absent in Gondwana (Evans and Milner, 1993), but in the Early Cretaceous we find their first fragmentary Gondwanan occurrences in South America (Chiappe *et al.*, 1998), Africa (Jacobs *et al.*, 1990), as well as in Asia (Evans and Manabe, 1998). Gymnophionan diversity is unknown across the J/K boundary, with the oldest occurrence in the Sinemurian of North America (Jenkins and Walsh, 1993), and the next and only Early Cretaceous occurrence from the Berriasian of Morocco (Evans and Sigogneau-Russell, 2001). See Gardner and Rage (2016) for a recent comprehensive review of lissamphibian material from Africa, Madagascar and the Arabian plate.

In the Late Jurassic of North America, the lissamphibian fossil record documents a mixture of stem caudates and anurans, as well as the first North American crown caudate (Henrici, 1998; Evans *et al.*, 2005; Gardner and DeMar Jr, 2013). There might be a 'hidden' Late Jurassic diversity in North America, as (Gardner and DeMar Jr, 2013) indicated that there could be as many as five unnamed anuran species, and an additional unnamed caudate, in the Quarry 9 and Rainbow Park localities alone. The Late Jurassic to Early Cretaceous record of central and western Asian salamanders and albanerpetontids is poor, with only a single stem salamander species known (Ivakhnenko, 1978; Skutschas, 2013). Salamanders from China are currently reforming our understanding of their Late Jurassic to Early Cretaceous evolution, but different views on the dating of associated beds make constraining their ages, and the timings of important radiations, problematic (Wang and Evans, 2006).

Several of these taxa occupy basal positions within Caudata, suggesting that events around the J/K boundary in eastern Asia might have been important in their early evolution (Yuan, 2000; Zhang *et al.*, 2009). The dynamics of salamander diversification in Laurasia remain obscured by fragmentary remains (Evans *et al.*, 2005), but the two major extant clades, Salamandroidea and Cryptobranchoidea, both appear to have passed through the J/K interval unperturbed. It is unknown when or where the split of Cryptobranchoidea into two large sub-clades, Hynobiidae and Cryptobranchidae, took place (Gao and Shubin, 2003), although major extant sub-lineages have been radiating since at least the Early Cretaceous (Gao and Shubin, 2003). Until recently, no stem salamanders were known in post-J/K boundary deposits, suggesting that they went extinct between the Kimmeridgian and end-Jurassic (Skutschas, 2013), but a new relict taxon from the Aptian–Albian of Siberia suggests that they survived in an isolated refugium (Skutschas, 2016). Albanerpetontids appear to have been confined to western Europe during the Late Jurassic, but are present in the Berriasian of Africa (Gardner *et al.*, 2003), and appeared in North America during the Aptian–Albian (Cifelli *et al.*, 1997; Gardner, 1999).

1.3.3.10 Mammaliaforms

The Late Jurassic was an important time in the rise of modern day mammal clades, with the diversification of Theria (comprising Eutheria and Metatheria) occurring around 160 Ma, during the Oxfordian (Luo *et al.*, 2011; Williamson *et al.*, 2014). Members of Theria remained relatively rare (although morphologically derived) (Sigogneau-Russell, 1998) through the J/K interval and into the Early Cretaceous. A recent analysis, however, placed these Jurassic occurrences outside of Theria (Krause *et al.*, 2014), implying that the earliest known occurrences of this group were in the Barremian (Ji *et al.*, 2002; Luo *et al.*, 2003). Only a single Late Jurassic Gondwanan mammaliaform occurrence is known, from Tanzania (Dietrich, 1927), in contrast with the diverse earliest Cretaceous (Berriasian) fauna known from Morocco (Sigogneau-Russell, 1995, 1999).

All major Late Jurassic mammalian clades persisted into the Early Cretaceous, including an array of forms such as basal cladotherians, multituberculates, triconodonts, and symmetrodontans, as well as rarer non-mammalian synapsids in Russia and Japan (Kielan-Jaworowska *et al.*, 2004; Zheng *et al.*, 2013) (Figure 11). Although no significant clades went extinct at the J/K boundary, more advanced mammalian groups (including multituberculates and eutriconodonts) displaced more primitive and contiguous mammaliaform lineages (i.e., dryolestids and docodonts) during the Late Jurassic, with docodonts surviving until at least the Berriasian of the UK (Cifelli *et al.*, 2012), and perhaps even later in Russia (Averianov and Lopatin, 2015). This apparent pattern of faunal replacement could represent a gradual or regional taxonomic turnover at the onset of the Cretaceous (Cifelli *et al.*, 2012), as evidenced by occurrences of tribosphenids in North America and Europe (Cifelli and Davis, 2015), but with their absence in Russia along with multituberculates being explained by an abundance of tritylodontids (Averianov and Lopatin, 2015). This conclusion was supported by the results of a series of analytical approaches to resolving Mesozoic mammaliaform diversity (Newham *et al.*, 2014), showing that it either dropped through the J/K boundary (using a residuals method), or increased slightly (using the SQS method), with little change from 'Jurassic-type' faunas over the boundary. However, regional North American diversity shows a decline (Newham *et al.*, 2014), suggesting that mammals responded disparately across the J/K boundary based on their geography.

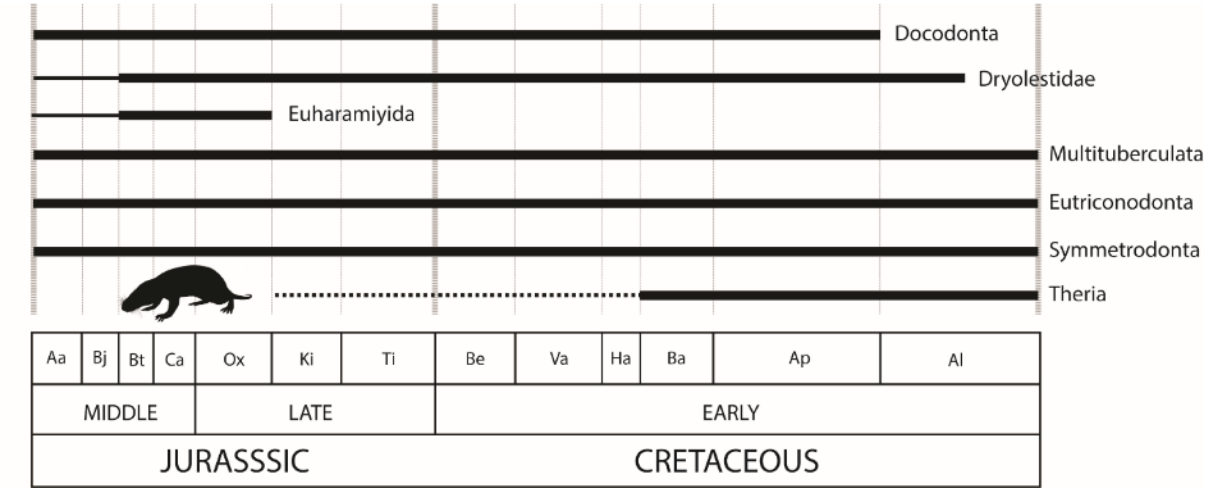


Figure 11. Stratigraphic ranges of major Jurassic–Cretaceous mammaliaform lineages. Dates obtained from The Paleobiology Database. Abbreviations as in Figure 4. Silhouette of Morganucodon watsoni from PhyloPic, by FunkMonk (CC BY-SA 3.0).

Within therians, or closely related forms, a broad array of ecophenotypes diversified in the Late Jurassic including scansorial, fossorial, insectivorous, carnivorous, gliding, and swimming forms, all with small body masses (<12kg) (Luo and Wible, 2005; Luo, 2007; Zheng *et al.*, 2013). Multituberculate disparity declined through the J/K boundary, and mean body size remained constant (Wilson *et al.*, 2012), coincident with generally low rates of phenotypic evolution and low disparity of mammals in the Late Jurassic to Early Cretaceous transition (Close *et al.*, 2015). This was coincident with a burst in taxonomic richness immediately preceding the boundary, followed by a minor fall in the Early Cretaceous (Wilson *et al.*, 2012), and the acquisition of key multituberculate characteristics (Yuan *et al.*, 2013).

1.3.3.11 Fish groups

Early studies found either a small increase (Benton and Walker, 1993) or small decrease (Carroll, 1988) in fish diversity over the J/K boundary. A recent analysis (Friedman and Sallan, 2012) based on the most recent version of the Sepkoski Compendium of marine animals (Sepkoski Jr *et al.*, 2002) was able to demonstrate that marine fishes experienced extinction rates across the J/K boundary of the same magnitude as that of the K/Pg boundary, coupled with reduced origination rates. This magnitude is relatively depressed when looking exclusively at marine chondrichthyans, but in marine osteichthyans the J/K extinction rate is higher than that for the K/Pg (Friedman and Sallan, 2012). This increased extinction rate at the J/K boundary coincides with one of two peaks in taxic diversity (the Late Jurassic and early Late Cretaceous), which has been attributed to increased preservation episodes (Friedman and Sallan, 2012). However, another recent analysis found little evidence for a significant change in fish diversity through the J/K boundary (Lloyd and Friedman, 2013), although results are absent for many sampling-corrected curves during the Late Jurassic in this study due to relatively poor sampling.

Actinopterygian diversity appears to be stable through the J/K boundary, although there is a diversity shift from marine to freshwater taxa (Cavin *et al.*, 2007). Teleost fish radiated during the Late Jurassic to Early Cretaceous, replacing many of their holostean-grade predecessors (Steel, 1973; Cavin, 2010).

Neoselachia, the clade including all modern forms of shark, and Batoidea (skates and rays) both underwent a phase of high diversification rates during the latest Jurassic (Kriwet, 2003; Rees, 2005). This was followed by a species-level diversity decline at the J/K boundary, resulting from decreased origination rates and heightened extinction rates (Kriwet and Klug, 2008; Kriwet *et al.*, 2009a). However, no major neoselachian clades went extinct at the J/K boundary, and their Early Cretaceous standing diversity was substantially higher than Late Jurassic levels (Underwood, 2006; Kriwet *et al.*, 2009a; Kriwet *et al.*, 2009b; Guinot *et al.*, 2012; Klug and Kriwet, 2013). A recent study showed that nearly all major extant lineages of sharks were already present in the latest Jurassic or earliest Cretaceous, with the origins of Squaliniformes, Squatiniformes, Orectolobidae, Lamniformes, and Carchariniformes occurring immediately prior to the boundary, and the timing of diversification of multiple important sub-lineages intimately associated with the J/K boundary (Sorenson *et al.*, 2014).

1.3.4 Invertebrates

As with vertebrate groups, early analyses of raw taxonomic invertebrate diversity have been superseded by global occurrence datasets and advanced analytical subsampling approaches (Alroy, 2000; Foote, 2000; Alroy *et al.*, 2001; Alroy, 2003; Foote, 2003; Bush and Bambach, 2004; Alroy, 2008; Alroy *et al.*, 2008; Alroy, 2010c; b; 2014). For all marine palaeofaunas, a diversity trough has been recovered at the J/K boundary (Alroy *et al.*, 2001), but at a range of intensities depending on the method used to correct for sampling biases (i.e., different occurrence weighting methods). This overall result was confirmed in subsequent studies (Alroy *et al.*, 2008; Alroy, 2010c) in both 'modern-type' and 'Palaeozoic-type' faunas (Sepkoski Jr *et al.*, 1981), with the former experiencing the greatest

diversity drop of the two; however, results are still variable with similar analyses by the same author finding no evidence for such decline (Alroy, 2010b). In the most recent analysis, a peak in extinction rates was detected for all marine invertebrate taxa at the J/K boundary (Alroy, 2014), similar in magnitude to that of the Silurian–Devonian boundary. A range of additional studies recovered this signal of decreasing diversity through the J/K boundary (Peters and Foote, 2001; Lu *et al.*, 2006; Smith *et al.*, 2012). Many of these analysed the dynamics of marine invertebrate faunas as a whole, rather than for individual geographical regions. As such, it is possible that this global diversity decline is a product of different regional-level patterns, with declines focused primarily in North America, Chile, and Europe (Smith, 2007; McGowan and Smith, 2008; Rogov *et al.*, 2010). Geographical variation was also noted in studies employing subsampling protocols (Alroy, 2010b), with results showing a more severe diversity drop in the northern hemisphere. In addition, some of these studies have grouped invertebrates together, rather than examine patterns in individual clades as others have done (Alroy, 2010b), which could potentially mask clade-specific variation.

1.3.4.1 Molluscs

Both raw and subsampled bivalve generic diversity declined at the J/K boundary (Skelton *et al.*, 1990; Jablonski *et al.*, 2003; Alroy, 2010b; Mondal and Harries, 2015), coincident with increasing phylogenetic clustering of extinction (Roy *et al.*, 2009). This drop is most pronounced in heteroconch and lucinoid bivalves, but is not as dramatic in other taxa, such as arcoids an pteriomorphs (Roy *et al.*, 2009). These extinctions might have been greater in taxa that inhabited shallow, rather than deeper water environments (Zakharov and Yanine, 1975), although more recent studies have not replicated this result (Skelton *et al.*, 1990). Endemic faunas became depleted in the southern hemisphere over the J/K boundary, except in the southern Andes and East Africa (Damborenea, 2002). A faunal transition zone, created by a strong Tethyan influence, existed between more northern regions (such as India, Arabia and northeast Africa) and southern faunas during the J/K interval (Kauffman, 1973;

Damborenea, 2002). Together, these factors suggest that a combination of tectonics, geography, and palaeoceanography exerted a strong control on bivalve diversity and distribution over the J/K boundary.

Early studies of ammonite diversity found evidence of a minor faunal turnover at the J/K boundary, with diverse Tethyan groups such as Perisphinctidae being replaced by Berriasellidae and Spiticeratinae (Sandoval *et al.*, 2001). Ammonite standing diversity varied greatly around the J/K boundary, with a substantial trough in diversity continuing into the Early Cretaceous (Vinarski *et al.*, 2011). Ammonite faunas are thought to have undergone a period of fluctuating provinciality over the J/K boundary, in concert with elevated speciation rates (Raup and Boyajian, 1988; Riccardi, 1991; Cecca *et al.*, 2005; Rogov *et al.*, 2010), leading to the diversification of several new ammonite lineages (Cecca, 1997; 1998; 1999). More recent explorations of diversity patterns, for all cephalopods, show a constant and severe decline in generic richness throughout the Late Jurassic, with diversity reaching a minimum in the Early Cretaceous before beginning to recover (Alroy, 2010b). Regionally, declines in ammonite diversity at the J/K boundary have been reported from South America and Madagascar (although this might instead relate to the opening of the South African seaway between the Tethys and South Pacific oceans) (Riccardi, 1991), and from India (Bardhan *et al.*, 1989; Bardhan *et al.*, 2007; Shome and Bardhan, 2009). However, the record from southeast Africa and Australasia over this period is too poor (Crame, 2002) for a pan-Gondwanan extinction event to be inferred.

At a raw taxonomic level, gastropod diversity appears unaffected at the J/K boundary (Vinarski *et al.*, 2011). However, sampling corrected generic diversity shows a decline at the J/K boundary to a level almost as low as at the Tr/J boundary (Alroy, 2010b), although this decline might have been initiated much earlier during the Middle to Late Jurassic (Mondal and Harries, 2015).

1.3.4.2 Brachiopods

Early studies found little evidence for a significant drop in brachiopod diversity at the J/K boundary (Ager, 1975; Ager and Walley, 1977; Hallam, 1986; Prosorovskaya *et al.*, 1993). However, (Alroy, 2010b) recovered a moderate diversity drop at the J/K boundary using subsampling methods, and of equal magnitude to the Tr/J boundary extinction, although whether this truly represents a global pattern is yet to be fully explored (Ruban, 2006; Curry and Brunton, 2007). Some evidence suggests that species-level diversity declined locally by up to 75% (e.g., in the Northern Caucasus), reflected in the loss of supraspecific taxa, a decrease in the rate of originations, and an increase in extinction rates (Ruban, 2006; 2011). This might be a reflection of latitudinal constraints on brachiopod distribution, with taxa largely restricted to low northern latitudes over the J/K boundary (Powell, 2009; Naimark and Markov, 2011). Terebratulids appear to have diversified as rhynchonellids declined at the J/K boundary, whereas there is a much more marked decline in observed terebratulid diversity than that of rhynchonellids during the Early Cretaceous, on both a regional and global scale (Vörös, 2010; Ruban, 2011).

1.3.4.3 Corals

Coral diversity appears to have increased linearly through the J/K boundary based on subsampled estimates (Alroy, 2010b); however, (Kiessling, 2008) found a substantial reef expansion in the early Late Jurassic, followed by a comparable decline in the latest Jurassic and over the J/K boundary. In the Late Jurassic, low latitude shallow marine regions were dominated by scleractinian coral reefs (Leinfelder, 2001; Martin-Garin *et al.*, 2012), with sea level exerting a strong control on their regional distribution (Bambach, 2006). In the Early Cretaceous, there was a shift towards rudist-dominated reef colonies in shallow environments (Scott, 1988; 1995). The precise timing of this scleractinian-to-rudist turnover is poorly constrained, but potentially relates to environmental changes during the Barremian (Scott, 1995; Höfling and Scott, 2002; Götz *et al.*, 2005), with Late Jurassic and earliest Cretaceous (Berriasian–Valanginian) faunas remaining compositionally consistent (Götz *et al.*, 2005). Extremely

high extinction and origination rates in scleractinian corals in the latest Jurassic might play a role in this faunal turnover, but they could also possibly relate to different environmental and/or preservational regimes in the Late Jurassic and Early Cretaceous (Simpson *et al.*, 2011).

1.3.4.4 Echinoderms

The impact of sampling on global patterns of pre-Cretaceous echinoderm diversity has yet to be explored in a manner similar to that of other marine invertebrate groups (Alroy, 2010b), hindering our understanding of their dynamics over the J/K boundary. At both the species and family-level, raw global echinoderm standing diversity increased from the Late Jurassic to Early Cretaceous, with diversity at an 'intermediate' level with respect to overall Phanerozoic diversity patterns (Raup, 1975; Markov *et al.*, 2012). On the other hand, crinoids appear to have suffered a major decline in diversity through the J/K boundary, following steadily inreasing diversity throghout the Jurassic (Gorzelak *et al.*, in press). Echinoderms might have experienced ecologically-selective perturbations through the Late Jurassic and over the J/K boundary (Aberhan *et al.*, 2012), although no major lineages went extinct at or around the boundary (Kroh and Smith, 2010); instead, there is evidence for the origins of major clades comprising multiple extant lineages occurring during the Early Cretaceous (Kroh and Smith, 2010). During the earliest Cretaceous, there is some evidence of low regional diversity (e.g., in the United Kingdom), before an increase in the Aptian (Smith and Benson, 2013). Disparity and diversity appear to have been decoupled in several geographically widespread boundary-crossing echinoderm lineages (Atelostomata, Disasteroidea), with a marked decline in disparity in the latter group coincident with a geographic range restriction to Europe (Eble, 2000). Uncorrected ('raw') crinoid diversity also declined through the J/K boundary, culminating in an extinction peak in the earliest Cretaceous (Gorzelak *et al.*, in press).

1.3.4.5 Arthropods

All major hexapod groups passed through the J/K boundary (Grimaldi, 2010; Nicholson *et al.*, 2014), and until recently their diversity dynamics were poorly understood at lower taxonomic levels (Clapham *et al.*, 2016). Total raw family-level insect diversity declined in the latest Jurassic, subsequent to a sharp increase in their diversity (Labandeira, 2005). Rarefied species richness estimates show that the largest recovered decline for insects occurred immediately after the J/K boundary (Clapham *et al.*, 2016), coincident with a decline in subsampled family richness before an explosive radiation to their highest pre-Cenozoic levels in the earliest Cretaceous. There was a Late Jurassic spike in origination rates that can be partially attributed to enhanced episodes of preservation (e.g., the Karatau deposits, Kazakhstan) (Ponomarenko, 1988; Labandeira and Eble, 2000; Karr and Clapham, 2015), but which also reflects a terrestrial revolution in insect faunas, with the rapid diversification of major holometabolan lineages including phytophagous and parasitoid taxa (Labandeira and Currano, 2013) (Misof *et al.*, 2014; Rainford *et al.*, 2014). This radiation was accompanied by a major extinction peak in insect families throughout the Late Jurassic, which might have resulted from competitive displacement of less derived insect faunas (Labandeira, 2005).

Multiple derived insect clades (e.g., Hemiptera, Coleoptera, Diptera, and Hymenoptera) appear to have dramatically increased in diversity in the Late Jurassic (Kimmeridgian), followed by a burst of intra-family diversification during the Early Cretaceous (Labandeira and Sepkoski, 1993; Labandeira, 2005). Origination rates at the family level in Apterygota increased after the J/K boundary, whereas the four other major insect groups (Palaeoptera, Polyneoptera, Paraneoptera, and Holometabola) experienced slightly depressed origination rates at the boundary, with no notable overall changes in extinction rates (Nicholson *et al.*, 2014). Major groups of Lepidoptera might have emerged in the Late Jurassic–Early Cretaceous interval, paving the way for them to become one of the most diverse insect groups today (Connor and Taverner, 1997; Kristensen and Skalski, 1998).

Myriapods are poorly known from the Jurassic and Cretaceous, but at least one group, Geophilomorpha, is known to have originated in the Late Jurassic, and no lineages are known to have gone extinct at the J/K boundary (Shear and Edgecombe, 2010). Whether or not chelicerates were affected at the J/K boundary is currently unknown, but extant families of scorpion (Chactidae, Hemiscorpiidae) have their first occurrences in the Early Cretaceous of South America (Dunlop, 2010), and some diverse lineages of spiders, including Juraraneidae, might have undergone rapid diversification events at the J/K boundary (Penney, 2003).

Decapod diversity suffered a dramatic decline over the J/K boundary in all three main groups (true crabs, hermit crabs, and lobsters and shrimp) (Klompmaker *et al.*, 2013). From the Late Jurassic to the Early Cretaceous, there was a replacement of highly diverse basal brachyuran (crab) lineages, such as Homolodromioidea, by other species-rich lineages, including Raninoidea and Calappoidea (Förster, 1985; Luque, 2015). This was accompanied by an environmental shift from reef-dwelling taxa to those preferring muddier, deeper, and colder waters (Krobicki and Zatoń, 2008).

1.3.4.6 Bryozoans

Late Jurassic and Early Cretaceous bryozoan faunas were almost entirely comprised of cyclostome stenolaemates (Taylor and Ernst, 2008), which reached their lowest post-Triassic diversity in the Tithonian (Taylor and Waeschenbach, 2015). Cheilostomes represent the largest group of extant bryozoans, and first occur in the fossil record in the Late Jurassic (Taylor, 1994). However, their diversification appears to have been constrained until the late Early Cretaceous (Taylor and Waeschenbach, 2015).

1.3.5 Microfossils

In the Early Cretaceous, microfossil groups became the most volumetrically significant biogenic constituent of deep sea sediments for the first time (Hart, 1999; Tremolada *et al.*, 2006; Lukeneder *et al.*, 2010; Pruner *et al.*, 2010; Olivier *et al.*, 2012).

1.3.5.1 Foraminifera

Global studies indicate that foraminiferan standing diversity was not affected at the J/K boundary, but that extinction rates in the Middle–Late Jurassic were of equal magnitude to the 'Big Five' mass extinctions, and accompanied by high origination rates (Kaminski *et al.*, 2010). This shifted to a regime of depressed origination and extinction rates after the J/K boundary (Kaminski *et al.*, 2010). Regional-scale studies indicate that foraminiferan species were in a state of geographical flux through the J/K boundary (Rogov *et al.*, 2010), indicating that diversity declined in a spatially-controlled manner (Ruban, 2006; 2010; 2011).

1.3.5.2 Radiolarians

Radiolarians experienced declining diversification rates throughout most of the Late Jurassic, in concert with a dramatic fall in their diversity (Kiessling, 2002). This shifted to an increase in origination rates and diversity in the late Tithonian and Early Cretaceous (Danelian and Johnson, 2001; Kiessling, 2002; Grabowski *et al.*, 2013), although (Kocsis *et al.*, 2014) recovered strongly depressed origination rates at the end of the Jurassic, and no significant changes in diversity through the J/K boundary. In relative terms, the J/K boundary saw three times as many boundary-crossing radiolarian genera as the Tr/J boundary, with Jurassic and Cretaceous faunas remaining largely unchanged (O'Dogherty *et al.*, 2009).

1.3.5.3 Phytoplankton

The J/K boundary saw a global revolution in calcareous phytoplankton, with a distinct impact on marine geochemical cycles and carbonate sedimentation (Bralower *et al.*, 1989; Bornemann *et al.*,

2003; Falkowski *et al.*, 2004; Weissert and Erba, 2004; Tremolada *et al.*, 2006; Wimbledon *et al.*, 2011). As noted above (Section 1.2.2), many studies demonstrate that $\delta^{13}C$ values decreased through the J/K boundary; rather than being indicative of increased oceanic productivity, such isotopic trends are typically associated with decelerating hydrological cycling and increasingly oligotrophic conditions (Weissert and Channell, 1989), despite global changes in calcareous phytoplankton production. Some estimates place the rate of extinction in calcareous nannoplankton at the J/K boundary at five times higher than that of background rates (Roth, 1989; Bown, Lees & Young, 2004), whereas the middle–late Tithonian saw significant radiations in both coccolithophores and nannoliths (Erba, 2006), with enhanced rates of speciation (Bown *et al.*, 2004; Săsăran *et al.*, 2014) and extinction (Lloyd *et al.*, 2012) occurring in both groups at the J/K boundary.

1.3.6 Plants

Cascales-Miñana *et al.* (2013) recently demonstrated that the 'Big Five' mass extinctions are not reflected in the record of vascular plants, and that there is no evidence for significant change at the J/K boundary (see also Cascales-Miñana and Cleal (2014)). The J/K boundary was also not identified as a mass extinction event in plants by McElwain and Punyasena (2007). In terms of higher-level diversity, pteridophytes were a relatively minor component of terrestrial ecosystems; instead, environments on land were dominated by gymnosperms, before angiosperms began their ascent in the Early Cretaceous (Niklas, 1988; Niklas and Tiffney, 1994; Philippe *et al.*, 2008; Coiffard *et al.*, 2012), possibly driven by tectonically influenced changes to atmospheric carbon levels and climate change (Barrett and Willis, 2001; Chaboureau *et al.*, 2014), or increasing environmental disturbance of angiosperm environments by herbivores (Barrett and Willis, 2001). However, in the earliest Cretaceous, floras were still dominated by cycadophytes, ferns, and conifers (Butler *et al.*, 2009a; Butler *et al.*, 2009b),

with angiosperms absent from pre-Hauterivian aged rocks, and there were no significant changes in the abundance of major plant groups across the J/K boundary (Barrett and Willis, 2001).

During the Jurassic, floral diversity and productivity were highest at mid-latitudes, due to the migration of productivity concentrations during greenhouse episodes (Rees *et al.*, 2000). In North America, the Kimmeridgian–Tithonian was a period of humid climates, echoed in the preserved floral diversity (Parrish *et al.*, 2004). In Eurasia there was a shift from Cheirolepidiaceae-dominated forests to a high diversity palynoflora composed of other conifers, cycads and pteridophytes (Abbink *et al.*, 2001; Zhang *et al.*, 2014), reflecting a change from a drier to a more humid climate over the J/K boundary. Important groups such as the aquatic clavatoracean charophytes were restricted to the Central Tethyan Archipelago throughout the late Tithonian to early Berriasian (Martín-Closas *et al.*, 2013). The complex palaeogeography of Europe at this time led to enhanced allopatric speciation and isolation of plants from nearby continents, with dispersal to Asia and North America initiated in the late Berriasian to early Valanginian (Martín-Closas *et al.*, 2013).

The South Pole and high latitudes were dominated by polar forests largely comprising podocarps and araucarians during the Early Cretaceous (Douglas and Williams, 1982; Dettmann, 1989). High latitude terrestrial regions of the southern hemisphere had similar forests from the latest Jurassic through to the close of the Cretaceous, with a steep floral zonation gradient (Dettmann, 1989). Floral groups in Australia (and associated landmasses) and Antarctica appear to have been unaffected at the J/K boundary, although, based on currently available data, any species-level effect is unknown (Dettmann, 1989), and in India Jurassic and Cretaceous palynofloral diversity was constant (Jha *et al.*, 2016).

1.4 Scope of this thesis

As summarised in this introductory synthesis, the Late Jurassic to Early Cretaceous interval represents a phase of major biotic upheaval and ecological reorganisation and a relatively poorly understood, but clearly important, period in the history of life on Earth. However, the precise magnitude of any extinction event is currently unknown, and clearly influenced by incomplete and spatially structured controls on fossil sampling. Such uncertainty occurs at all taxonomic levels, and obscures the pace, magnitude, and timing of potential changes in diversity reflecting major macroevolutionary changes (i.e., radiations and extinctions) that are hinted at from a raw reading of the fossil record. By untangling the role that these 'sampling biases' have on our understanding of diversity patterns, we can gain insight into the dynamics of faunal turnovers in the marine and terrestrial realms. By dealing with this perpetual issue, we can establish the basis for exploring the causes of these patterns, be they biotic or abiotic. What is clear is that there was a series of most likely unconnected, but dramatic, abiotic changes across the J/K transition, the combination of which might have been more severe than events documented at the end-Cretaceous mass extinction. These include singular events, such as bolide impacts or large-scale volcanism that are difficult to tie to long-term trends in diversity. Changes are also documented in Earth system cycles, such as palaeoclimate and atmospheric gas concentration shifts, and eustatic sea level. The result of this is the almost total reorganisation of marine and terrestrial ecosystems, with substantial evidence for a protracted mode of coupled ecological and faunal turnover. However, the degree to which these environmental and faunal patterns are linked, and therefore supportive of the press-pulse theory of extinction (Arens and West, 2008), with a combination of gradual changes ('press') and sudden, catastrophic disturbances ('pulse'), altering the composition of ecosystems, remains to be tested. As such, the J/K boundary represents a unique opportunity to investigate the environmental and ecological factors governing extinction and subsequent recovery dynamics.

This thesis will provide insight into the factors that governed tetrapod diversity and extinction patterns through the Jurassic/Cretaceous interval. Using a large fossil occurrence data set, combined with

advanced subsampling techniques, I will: (1) show that the shape of the Jurassic/Cretaceous fossil record is strongly influence by spatiotemporal variation in sampling; (2) demonstrate that it is possible to compensate for this variation by applying statistically rigorous protocols for alleviating the impact of incomplete sampling; (3) produce reliable estimates of diversity and origination and extinction rates through the J/K interval; (4) use these as the basis for investigating the environmental drivers behind tetrapod diversity for this time period; (5) provide a taxonomic case study to investigate detailed changes in a selected J/K boundary-crossing group. As mentioned in the introduction to this thesis, this will be undertaken with a hierarchical approach. Firstly, I will explore large-scale patterns for all tetrapod groups, and investigate the anthropogenic, geological, and environmental factors that influenced their diversity. Secondly, I will undertake a mid-level investigation using Crocodyliformes as an example, and examine the influence of different subsampling protocols on reconstructed diversity curves. Thirdly, I will undertake a thorough systematic and taxonomic examination of an important, but poorly known group of crocodyliforms known as atoposaurids. This group purportedly spanned the Middle Jurassic to the end of the Cretaceous (and possibly survived into the Cenozoic), and make an excellent case study for examining the response of a single, small clade to J/K boundary events.

Disclosure: Much of this Chapter is drawn on text published by Tennant *et al*. (2016). While the primary author wrote the majority of this text, parts of it have been contributed to by all other authors, as well as receiving input from the peer review process.

Tennant, J. P. Mannion, P. D., Upchurch, P., Sutton, M. and Price, G. (2016) Biotic and environmental dynamics across the Jurassic/Cretaceous boundary: evidence for a protracted period of faunal and ecological turnover, *Biological Reviews*, DOI: 10.1111/brv.12255.

2 Materials and Methods

2.1 Age of the Jurassic/Cretaceous boundary

The lack of understanding regarding biotic and abiotic dynamics across the J/K boundary is emphasised by the fact that it is the only Mesozoic interval without a Global Boundary Stratotype Section (GBSS) (Cohen *et al.*, 2013) (see Section 1.1.1). Recently, it has been argued that a J/K boundary age of 140 million years old (Ma) should be assigned, based on a combination of biostratigraphic markers, isotopes, and sedimentation rates (Vennari *et al.*, 2014). Traditionally, most research has followed the proposed age of 144.6 ± 0.8 Ma for the J/K boundary (Mahoney *et al.*, 2005), and a working group has also proposed this age more recently (Wimbledon *et al.*, 2011). However, this date has yet to be formally recognised by the International Commission on Stratigraphy (Cohen *et al.*, 2013), and the age of the base of the Berriasian remains uncertain. For the purposes of this thesis, the absolute age more commonly used (Mahoney *et al.*, 2005), and assigned in the International Chronostratigraphic Chart (Cohen *et al.*, 2013) of ~145.5 Ma is followed.

Abbreviation	Stage	Bin base (Ma)
K12	Maastrichtian	70.6
K11	Campanian	84.9
K10	Santonian	85.8
K9	Coniacian	89.3
K8	Turonian	94.3
K7	Cenomanian	99.7
K6	Albian	112.6
K5	Aptian	125.45
K4	Barremian	130
K3	Hauterivian	136.4
K2	Valanginian	140.2
K1	Berriasian	145.5
J11	Tithonian	150.8
J10	Kimmeridgian	155.7
J9	Oxfordian	161.2
J8	Callovian	164.7
J7	Bathonian	167.7
J6	Bajocian	171.6
J5	Aalenian	175.6
J4	Toarcian	183
J3	Pliensbachian	189.6
J2	Sinemurian	196.5
J1	Hettangian	201.6

Table 5. Stage-level time binning scheme for the Jurassic/Cretaceous interval

2.2 Assembling a tetrapod occurrence dataset

2.2.1 The Paleobiology Database and Fossilworks

When this PhD first began, both the Paleobiology Database (PaleoDB) and Fossilworks were a single, unified entity. However, they have now split, and represent a dual functionality. The PaleoDB is a non-governmental, non-profit, openly licensed (Creative Commons BY 4.0 International License) and public resource for palaeontological data. Founded in 1998, it is operated by a global network and community of palaeobiological researchers. Fossilworks is the original public interface to the PaleoDB, but now serves as a web-based portal to it. The data contained within the two are fully synchronous,

and enable different evaluations of the same core dataset, underpinned by a master taxonomic classification system and a synthesised global time scale. The main benefit of the PaleoDB compared to previous database efforts is that the context of fossil occurrences remains based on extraction of metadata from peer reviewed sources. Great care is exercised by the community in clarifying the spatial and temporal constraints on data, as well as the taxonomic history and uncertainty of specimens. At the time of writing, the PaleoDB contains 48,449 published references, with 280,335 taxa comprising 151,714 fossil collections and 1,155,026 taxonomic occurrences, input by 259 scientists from 132 institutions in 24 countries (08/12/2015) (Table 6). Over 260 formal publications have sourced data from the PaleoDB to date, including numerous studies on Mesozoic tetrapods (Benson and Butler, 2011; Butler *et al.*, 2011; Mannion and Upchurch, 2011; Upchurch *et al.*, 2011b; Benson and Upchurch, 2012; Brocklehurst *et al.*, 2012; Butler *et al.*, 2012; Mannion *et al.*, 2012; Benson *et al.*, 2013; Newham *et al.*, 2014; Pyenson *et al.*, 2014; Dunhill and Wills, 2015; Mannion *et al.*, 2015; Nicholson *et al.*, 2015). The PaleoDB forms the core dataset for this thesis.

Group	J1	J2	J3	J4	J5	J6	K1	K2	K3	K4	K5	K6	K7	K8	Sum per group
Aves	0	0	0	0	0	9	5	27	86	20	17	33	112	134	443
Choristoderes	0	0	0	14	2	15	6	3	18	2	0	1	8	102	171
Lepidosauromorphs	22	3	10	35	10	87	79	40	18	33	30	33	324	263	987
Lissamphibians	0	0	2	41	9	29	34	35	20	23	31	74	283	363	944
Mammaliaforms	28	5	8	74	35	213	115	46	22	56	154	176	731	1092	2755
Theropods	63	7	5	85	80	349	121	177	142	171	139	196	842	800	3177
Pterosaurs	6	1	52	25	23	118	46	38	49	120	51	30	58	33	650
Sauropodomorphs	150	2	7	72	53	572	66	83	58	101	55	61	76	233	1589
Ornithischians	49	3	3	23	48	253	131	174	114	217	77	182	1480	1006	3760
Crocodyliformes (terrestrial)	24	1	1	30	25	117	72	89	50	81	68	88	254	418	1318
Testudines	1	0	0	16	26	209	82	49	53	68	74	139	789	893	2399
Ichthyopteryians	40	5	72	8	28	55	10	18	11	63	15	0	1	0	326
Sauropterygians	29	10	36	7	107	137	26	17	26	32	36	65	96	67	691
Chelonioides	0	0	0	0	0	0	0	0	1	8	4	22	39	46	120
Crocodyliformes (marine)	1	0	45	49	80	131	12	2	7	1	4	0	5	52	389
Sum per time bin	413	37	241	479	526	2294	805	798	675	996	755	1100	5098	5502	19719
Sum aquatic	70	15	153	64	215	323	48	37	45	104	59	87	141	165	1526
Sum terrestrial	343	22	88	415	311	1971	757	761	630	892	696	1013	4957	5337	18193

Table 6. Raw counts of genus-level occurrences for all major tetrapod groups. Note that there are over 10 times the number of fossil occurrences in the terrestrial realm than there are for the marine realm. Data are grouped into approximately equal 10 million year time bins (see Section 2.3).

2.2.2 Data compilation

For the current study, tetrapods were selected as the study group for several reasons. Firstly, a newly compiled Mesozoic dataset has been built within the *Paleobiology Database* (PaleoDB; http://www.paleobiodb.org/), representing one of the largest and most comprehensive occurrence-based datasets ever assembled for tetrapod groups. Secondly, the impact of heterogeneous sampling on this group has been explored in a variety of ways for the different inclusive clades, suggesting that sampling biases have had a major impact on our reading of their raw fossil record (Butler *et al.*, 2009c; Benson *et al.*, 2010; Benson and Butler, 2011; Benton *et al.*, 2011; Butler *et al.*, 2011; Upchurch *et al.*, 2011b; Butler *et al.*, 2012; Benson *et al.*, 2013; Benton *et al.*, 2013a; Butler *et al.*, 2013; Martin *et al.*, 2014a; Newham *et al.*, 2014; Cleary *et al.*, 2015; Mannion *et al.*, 2015; Nicholson *et al.*, 2015). Thirdly,

different tetrapod groups have vastly variable spatiotemporal distributions, so offer a valuable perspective into heterogeneity of the fossil record. Finally, tetrapods occupied almost every possible environment or combination of environments throughout the Mesozoic era. This is reflected in their broad range of ecomorphologies, from small-bodied terrestrial animals to macropredaceous pelagic predators.

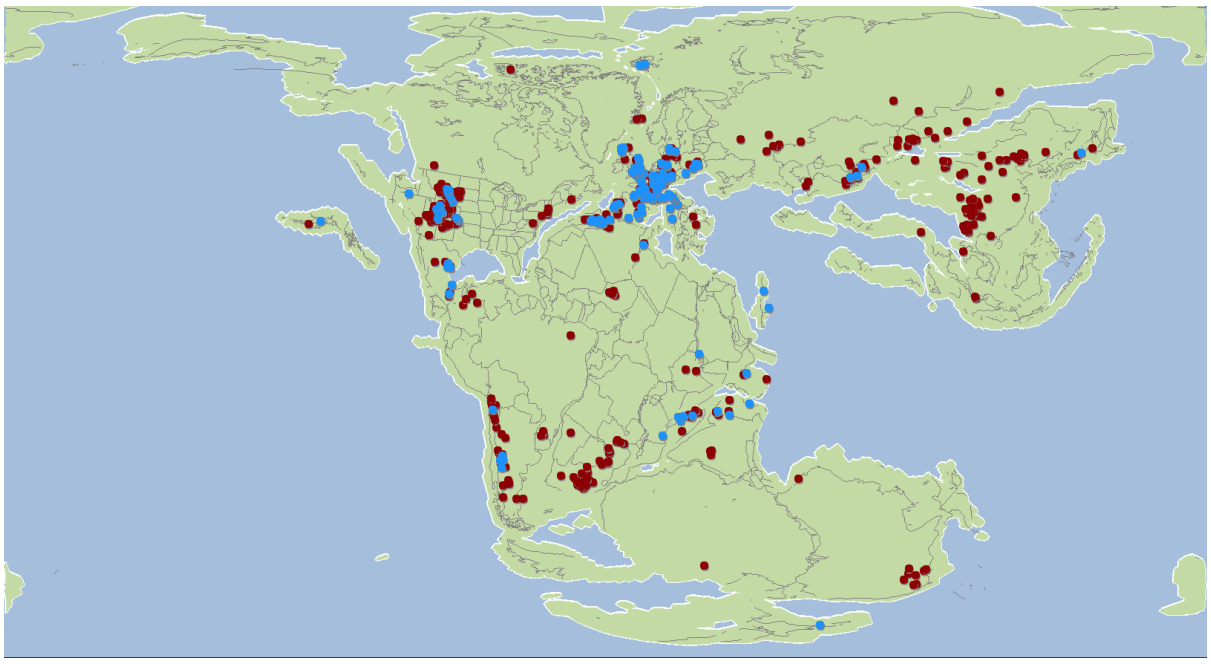


Figure 12. Jurassic marine (blue) and non-marine (brown) tetrapod body fossil occurrences.

Presently, data from 573 references have been entered into the PaleoDB by the author, representing primary published occurrences of fossil tetrapods from the Jurassic and Cretaceous. This builds on extensive work from several major contributors, including Matthew Carrano (2112 hours authorized = 58.4%), John Alroy (363 hours = 10.0%), Philip Mannion (354 hours = 9.8%), Roger Benson (279 hours = 7.7%), and Richard Butler (175 hours = 4.8%). Much of this work has focussed on systematically entering all published occurrences of Mesozoic tetrapods as part of an ongoing investigation into their macroevolutionary history, and great care has been taken to curate this database at the specimen level. This is important, as rather thanjust having names in the database to reconstruct taxonomic

diversity, occurrences dictate the shape of the taxonomic abundance curve, which is known to influence diversity estimates (Alroy *et al.*, 2001; Chao *et al.*, 2009; Alroy, 2010a; Chao and Jost, 2012). Additional contributors to the datatset are Martin Aberhan, Anna Behrensmeyer, Mark Bell, Kevin Boyce, Clint Boyd, Matthew Clapham, Will Clyde, Emmanuel Fara, Valentin Fischer, Jason Head, Austin Hendy, Pat Holroyd, John Hunter, Linda Ivany, Kirk Johnson, Wolfgang Kiessling, Matt Kosnik, Juergen Kriwet, Conrad Labandeira, Graeme Lloyd, Rick Lupia, David Nicholson, Robin O'Keefe, Mark Patzkowsky, Shanan Peters, Oliver Rauhut, Allister Rees, Ascanio Rincon, Dena Smith, Bruce Tiffney, Takehisa Tsubamoto, Mark Uhen, Matthew Vavrek, Loic Villier, Pete Wagner, Xiaoming Wang, Robin Whatley, and Scott Wing. Note that this is the list of those who have authorised data entry, and not necessarily those who have entered the data.

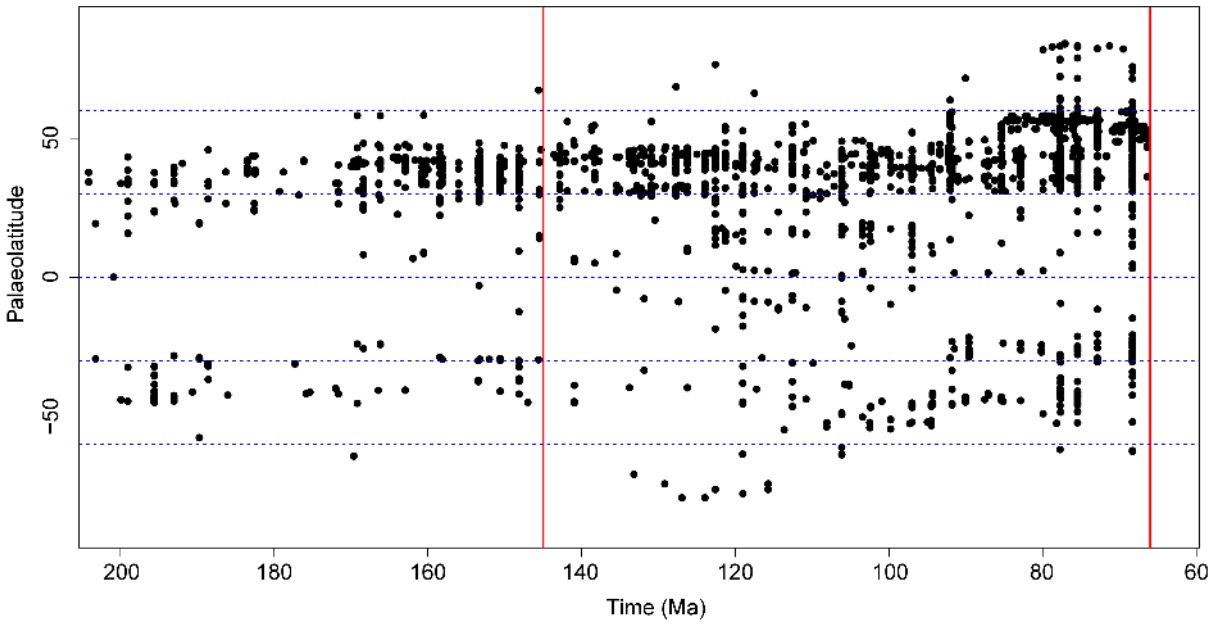


Figure 13. Palaeolatitudinal distribution of all non-marine tetrapod occurrences through the Jurassic and Cretaceous. The Jurassic/Cretaceous boundary (145 Ma) is highlighted in red. Palaeolatitudes are based on Scotese rotations, and acquired from the Paleobiology Database

Data for the bulk of this thesis were downloaded from the PaleoDB portal (https://paleobiodb.org/). The total dataset for Jurassic and Cretaceous Tetrapoda comprises 4907 species from 15472 occurrences, drawn from 7314 references (08/12/2015) (Carrano *et al.*, 2015b), following extensive

work to ensure that occurrences and taxonomic opinions reflect our current published knowledge. Each higher taxonomic group was downloaded individually, with inclusive clades excluded as needed (e.g., Testudines and Chelonioidea, Theropoda and Aves). Only occurrences from the Jurassic–Cretaceous interval (201–66 Ma) were downloaded (Figure 13). All lithologies and depositional environments were included, and data from all continents (and palaeocontinents) and latitudes (and palaeolatitudes) were also included, with spatial division being conducted *a posteriori*. Occurrences from all geographic and stratigraphic scales were included, and there was no discrimination based on the mode of preservation or method of collection. The taxonomy used for occurrences is the latest based on the published literature. This means that, where appropriate, original identifications were replaced where occurrences had been reidentified, and also with senior synonyms where needed. Despite issues with supra-specific assessments of biodiversity patterns (Robeck *et al.*, 2000; Hendricks *et al.*, 2014), I selected to use genera as it has been shown that genera and species diversity generally track each other for Mesozoic tetrapods, including crocodyliforms (Mannion *et al.*, 2015) and dinosaurs (Barrett *et al.*, 2009; Starrfelt and Liow, 2016), and is likely to be a more widespread relationship among different groups (Jablonski and Finarelli, 2009). Furthermore, this allows for the inclusion of specifically-indeterminate occurrences in the dataset (e.g., *Allosaurus* sp.), which would otherwise be excluded in a species-level analysis. Only body fossils are included, and occurrences defined at the sub-genus level were excluded, as were any generically indeterminate occurrences. Specifically indeterminate occurrences were included, as were occurrences with qualifiers such as aff., cf., ex. gr., n. gen., *sensu lato*, ?, and those within inverted commas. Ichnotaxa were excluded, due to difficulties in generic assignment, as were occurrences identified as form taxa. Further temporal data downloaded include the 10 million year time bins, the Fossil Record 2 bins, and interval dates based on interval names and geochronological records, where available. Reference numbers, the year of publication, collection name, and geographical information, including country, latitude, and

palaeolatitude, were also downloaded. The only further information acquired was the environment of deposition, the primary lithology, and the stratigraphic formation name.

PaleoDB collections represent discrete fossil groups, divided based upon their stratigraphic range, collection history, lithology and scale. This scheme resulted in two different binned datasets: (1) at the stage level, comprising 7312 occurrences from 6316 collections, representing 1275 genera drawn from 2313 published references; and (2) at the ~10 myr level, comprising 10874 occurrences from 9454 collections, representing 1954 genera drawn from a total of 3774 published references. Where time bins did not contain any occurrence data, these were treated as 'not applicable' (NA) data, rather than '0' data.

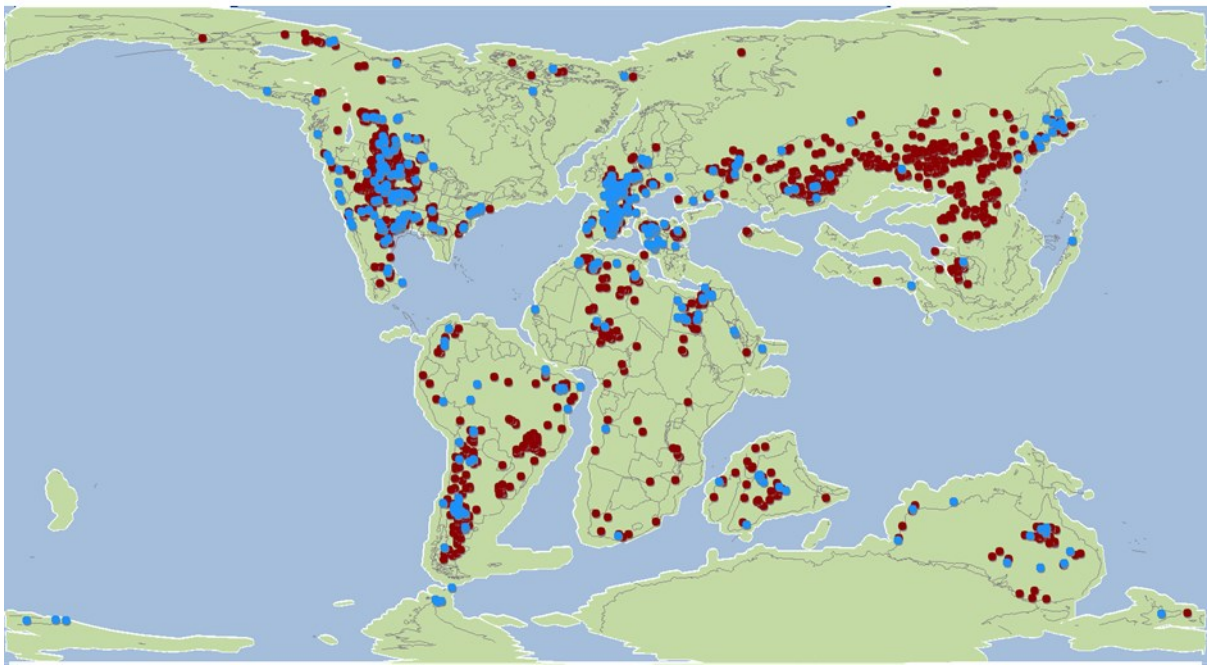


Figure 14. Cretaceous marine (blue) and non-marine (brown) tetrapod body fossil occurrences.

2.2.3 Crocodyliformes occurrences

The Crocodyliformes dataset used here spans the entirety of the Jurassic (Figure 15) to Cretaceous (Figure 16) (201–66 Ma), and is based on a newly compiled fossil occurrence data set (Carrano *et al.*,

2015a), comprising a near-comprehensive record of crocodyliforms. Body fossil occurrences that could be assigned to genera were downloaded from *The Paleobiology Database* (PaleoDB; http://www.paleobiodb.org/), accessed 29th July, 2015. This section of analysis was implemented independently of that outlined in Section 2.2.2. Genera were sub-divided into fully marine (comprising thalattosuchians, dyrosaurids, gavialoids, and some pholidosaurids) and non-marine (terrestrial, freshwater and coastal) taxa. The protocol of a recent study that checked for inconsistencies in the taxonomy of crocodyliforms in the PaleoDB (Mannion *et al.*, 2015) was followed by excluding spurious Mesozoic occurrences of *Crocodylus* and Cretaceous occurrences of teleosauroids (see Section 2.2.3.1). Note that this decision was based on insufficient evidence at the time to support definitive occurrences of Cretaceous teleosaurids, prior to the discovery of *Machimosaurus rex* (Fanti *et al.*, 2016b). This resulted in a dataset comprising 349 marine occurrences of 31 genera from 302 collections, and 825 non-marine occurrences of 132 genera from 809 collections.

To explore the impact of different binning schemes, these data were pooled into: (1) approximately equal length (~10 million year [myr], n = 14) time bins; and (2) stage-level time bins (n = 23). Raw in-bin counts of these genera were used to produce an uncorrected taxonomic diversity estimate (TDE) (Figure 31C). To avoid over-counting taxa in multiple time bins, resulting from uncertainty in their temporal durations, only occurrences that could be assigned to a single time bin were used, resulting in 681 non-marine occurrences from 669 collections, and 330 marine occurrences from 284 collections. Occurrences from the equivocally-aged Adamantina Formation of Brazil were included within the K6 bin for the analyses with 10 million year time bins following a recent study (Mannion *et al.*, 2015), but were excluded from stage-level analyses. This is due to the current lack of consensus on the age of the Adamantina Formation, with some studies recovering a Turonian–Santonian age based on ostracod data (Dias-Brito *et al.*, 2001), while others find a younger Campanian–Maastrichtian age, based on vertebrate fossils (Gobbo-Rodrigues *et al.*, 1999; Fernandes and Coimbra, 2008). Therefore the K6

interval is preferred to avoid redundancy in using vertebrate fossils to date vertebrate fossils, and due to higher stratigraphic resolution offered by ostracods.

2.2.3.1 A note on Cretaceous thalattosuchians

Several recent studies have now concluded that teleosauroids, as a subgroup within Thalattosuchia, went extinct at the J/K boundary (Young *et al.*, 2014a; Mannion *et al.*, 2015). The PaleoDB still contains numerous occurrences of Cretaceous thalattosuchians, including putative teleosauroids, which are briefly reviewed here. This is in light of considerable research focus on the taxonomy of thalattosuchians, combined with a long collecting history and wide geographic distribution.

The type locality for *Cricosaurus macrospondylus* is the late Valanginian of Germany (Young *et al.*, 2014a). An occurrence from the early Valanginian of France was previously identified as the now invalid genus, *Enaliosuchus* (Hua *et al.*, 2000). *Dakosaurus andiniensis* is known from two localities in the Berriasian of Argentina (Gasparini *et al.*, 2006; Young *et al.*, 2014a). In addition, a specimen described as *Dakosaurus* sp. is known from late Aptian deposits in the UK, comprising reworked fossils from the Kimmeridge Clay (Kimmeridgian age) (Benton and Spencer, 1995). *Geosaurus lapparenti* is known from three localities in France, ranging from the early Valanginian to late Hauterivian (Young *et al.*, 2014a). The oldest of these is of uncertain affinity. The late Valanginian locality is the type locality for *Dacosaurus* (=*Dakosaurus*) *lapparenti* (Debelmas and Strannoloubsky, 1957), but subsequently this specimen was referred to *Geosaurus*. *Geosaurus araucaniensis* is also known from the Berriasian of Argentina (Gasparini and Dellapé, 1976; Gasparini and Fernández, 2005), but more recent work determined that this specimen belongs to *Cricosaurus* (Young and de Andrade, 2009). The only Cretaceous occurrence of *Metriorhynchus* is from the late Berriasian of Germany (Young *et al.*, 2014a). *Neustosaurus gigondarum* is known exclusively from the early Valanginian of France (Raspail, 1842). Although this specimen was subsequently revised as belonging to *Geosaurus* (Piveteau, 1928),

the most recent analyses consider it to be a valid genus (Young and de Andrade, 2009). Cretaceous occurrences of *Peipehsuchus teleorhinus* are restricted to the poorly-dated Tzeliuching Formation of China, and cannot be constrained more than Lower Cretaceous at present (Young, 1937). Although originally described as a pholidosaurid (Li, 1993), *Peipehsuchus* was subsequently identified as a thalattosuchian (Jouve, 2009).

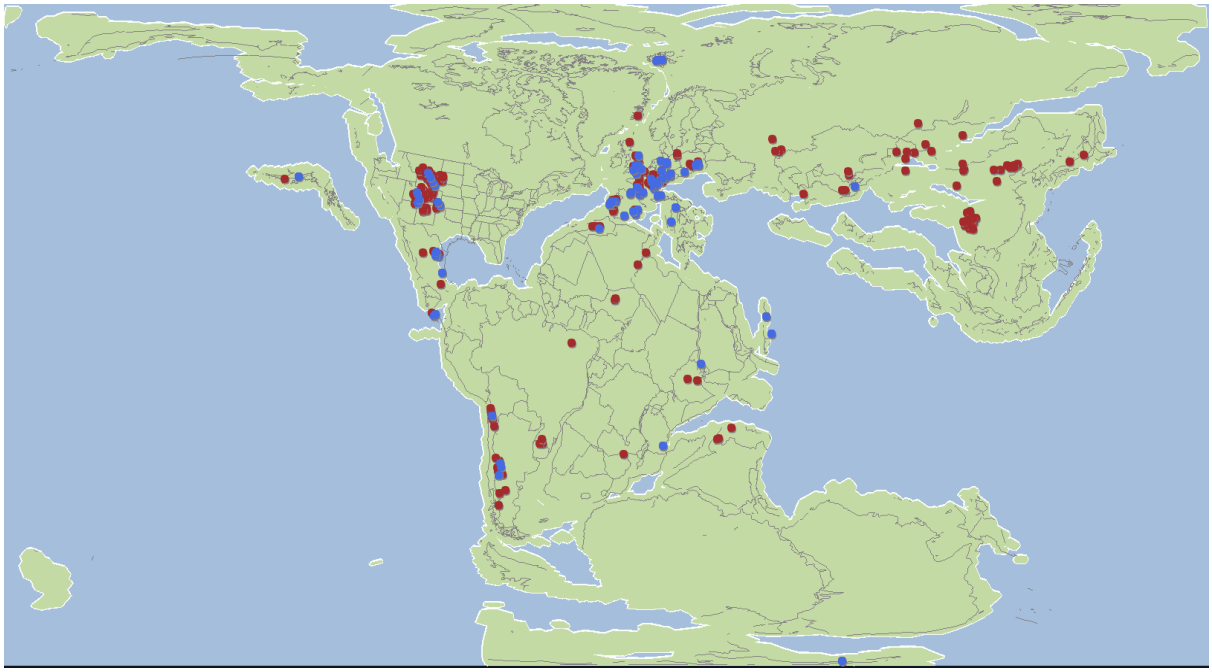


Figure 15. Late Jurassic marine (blue) and non-marine (red) crocodyliform occurrences. Palaeolatitudes are based on Scotese rotations, and acquired from the Paleobiology Database.

Machimosaurus is known from a range of Cretaceous localities, including the "Neocomian" of Spain (*Machimosaurus* sp., and *Machimosaurus hugii*, previously identified as *Steneosaurus* cf. *obtusidens*) (Royo y Gómez, 1927; Young *et al.*, 2014b) and the Lower Cretaceous of Tunisia (cf. *Machimosaurus* sp., along with cf. *Steneosaurus* sp.) (Schlüter and Schwarzhans, 1978). Putative occurrences are also reported from the Cenomanian of Sudan (*Machimosaurus* sp.) (Werner, 1994) and the "Senonian" (equivalent to Coniacian–Maastrichtian) of Brazil (cf. *Machimosaurus* sp.) (von Huene, 1931), but all of these remains are fragmentary and their taxonomic assignments remain unsubstantiated based on current evidence. An occurrence of *Teleosaurus* is known from the early Valanginian of the United

Kingdom, but has not been studied for more than a century (Etheridge, 1885), and its affinities remain unclear. Hence, there is no strong evidence for any teleosaurid taxon, besides the recently identified *Machimosaurus rex* (Fanti *et al.*, 2016b), to have passed the J/K boundary. Ultimately, this results in only six unambiguous thalattosuchian genera present in the Cretaceous (*Geosaurus*, *Cricosaurus*, *Neustosaurus*, *Peipehsuchus*, *Dakosaurus*, and *Teleosaurus*).

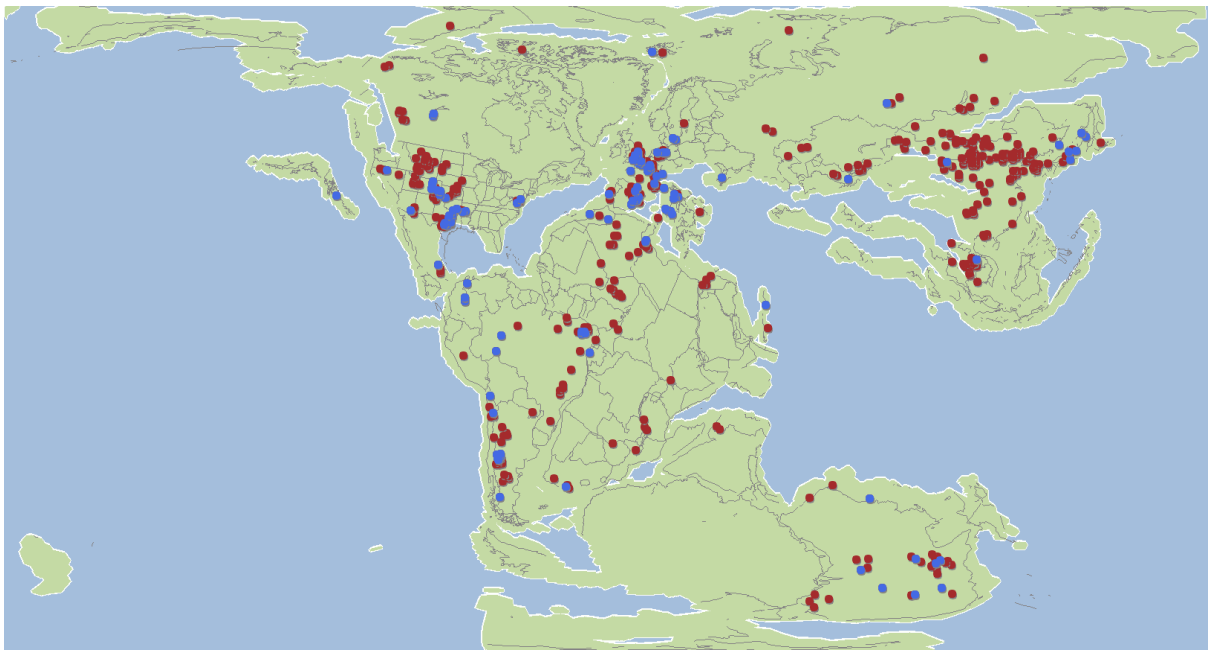


Figure 16 Early Cretaceous marine (blue) and non-marine (red) crocodyliform occurrences. Palaeolatitudes are based on Scotese rotations, and acquired from the Paleobiology Database.

2.2.4 Defining taxonomic sub-groups

Taxonomic categories are based on major clades that passed through the J/K boundary, or radiated in the Early Cretaceous (Table 9). For example, Lepidosauromorpha is included, but Mosasauroidea are excluded as a Late Cretaceous marine radiation. Choristodera is also treated as a separate group. Dinosaurs were partitioned into four separate sub-groups due to their proportionally large sample sizes: Sauropodomorpha, Ornithischia, Theropoda (excluding Aves) and Aves. For turtles, the more inclusive grouping of Testudines was used, but marine Chelonioidea were treated as a separate Cretaceous sub-group. Crocodyliformes were divided into two sub-groups: the first, comprising non-

marine forms including coastal, fluvial, and semi-aquatic taxa, and a second comprising fully marine (i.e., pelagic) taxa, including Thalattosuchia, Gavialoidea, Dyrosauridae, and some pholidosaurids (Appendix 2, Appendix 3) (Mannion *et al.*, 2015).

Taxon	Full data set				Stage				10 myr	
	Colls	Occs	Refs	Gen	Colls	Occs	Refs	Gen	Colls	Occs
Aves	211	314	53	55	64	105	134	130	159	250
Chelonioidea	95	109	31	21	48	56	53	27	75	85
Choristodera	226	232	53	5	163	167	83	11	211	216
Crocodyliformes (marine)	302	249	144	28	264	310	160	31	284	330
Crocodyliformes (non-marine)	807	823	187	73	474	484	316	131	667	681
Ichthyosauria	206	260	103	31	144	192	128	36	173	224
Lepidosauromorpha	594	614	89	93	365	381	159	153	545	564
Lissamphibia	561	631	101	67	468	522	135	78	537	600
Mammaliaformes	1908	2240	173	237	1420	1634	249	313	1791	2089
Ornithischia	1826	1896	409	160	841	868	733	275	1531	1590
Pterosauria	330	395	91	63	169	203	142	107	256	312
Sauropodomorpha	916	988	194	93	366	414	341	156	701	765
Sauropterygia	389	430	137	68	214	242	193	90	326	362
Testudines	875	1489	221	115	397	770	348	150	719	1266
Theropoda	1739	1806	327	166	919	964	600	266	1479	1540
SUM	**10985**	**12476**	**2313**	**1275**	**6316**	**7312**	**3774**	**1954**	**9454**	**10874**

Table 7. Collections (colls), references (refs), raw genera (gen) and body fossil occurrences (occs) for each major taxonomic group analysed.

Each taxonomic sub-group was further divided into approximately contiguous continental regions: Africa, Asia, Europe, South America, and North America. For each regional dataset, the record of fossil occurrences is patchy and discontinuous. This is especially prevalent for Gondwana, in which sampling occurs in distinct spatiotemporal clusters (Benson *et al.*, 2013). The full list of countries included in each regional data subset is given in Mannion *et al.* (2015), and these are taken to represent approximately contiguous palaeocontinental regions. The few tetrapod fossils from regions such as Australia, Indo-Madagascar, and Antarctica were included for global analyses, but too sparse to warrant analysing on a regional level.

2.2.5 Latitudinal taxonomic subgroups

In addition to regional heterogeneity in diversity patterns outlined above, a further geographic or spatial bias that might influence diversity through time are those regarding latitudinal biodiversity gradients (LBG). The LBG is a first-order pattern for many modern groups, persists to variable degrees throughout the fossil record (Mannion *et al.*, 2014), and has been explored in some detail for Mesozoic tetrapod groups (Mannion *et al.*, 2012; Mannion *et al.*, 2015). Palaeolatitudes are based on Scotese rotations and from the PaleoDB. The tropics (0-30°) and polar (60-90°) regions during the Jurassic/Cretaceous interval are almost completely devoid of fossils, and subsampled diversity estimates are patchy in both the non-marine (Table 36, Table 38, Table 39, Table 41) and marine (Table 42, Table 44, Table 45, Table 47) realms. The reason for keeping these analyses at the level of 10 million year time bins is that the data become too sparse to adequately subsample. However, as mentioned for the global analyses, this may obscure finer scale dynamics across the J/K boundary. The global tetrapod data were divided into latitudinal time bins for each group, comprising three bins for the northern hemisphere (0-30° [N1], 30-60° [N2], and 60-90° [N3]) and three for the southern hemisphere (0-30° [S1], 30-60° [S2], and 60-90° [S3]). The reason for such coarse bins is that sampling of the fossil record is already so incomplete for many time intervals that further subdivisions renders subsampling analysis near-impossible.

2.2.6 A note on data quality

The quality of the datasets used is undoubtedly influenced by worker effort on particular groups, as the taxonomic opinions for each occurrence are based explicitly on the peer reviewed published literature. Due to the inherent nature of Palaeobiology, not all taxonomic groups have been studied equally throughout the Mesozoic. For example, Dinosauria is undoubtedly the most thoroughly understood group, whereas others, such as Choristodera, or some sub-groups of Crocodyliformes remain poorly understood with relatively little taxonomic investigation through history. As such, while

it cannot be guaranteed that each data set is completely accurate to the extent that they reflect 'true' taxonomy, through collective effort it has ensured that it reflects the most up-to-date view on tetrapod taxonomy based on the current state of the field. Individually reviewing the taxonomic status of each occurrence is beyond the scope of this thesis, as such an effort would require an exhaustive global collaborative effort.

2.3 Constructing a crocodyliform supertree

2.4 Time binning protocol

The geological timescale used here is based upon the formally recognised Standard European Stages and absolute dates (Gradstein *et al.*, 2012). Many recent studies of tetrapod diversity have used geological stages (Benson *et al.*, 2010; Benson and Butler, 2011; Benson *et al.*, 2013), or grouped stage-level diversity data into approximately equal length intervals (Alroy, 2008; 2010b; Mannion *et al.*, 2015; Nicholson *et al.*, 2015) or finer sub-divisions (Barrett *et al.*, 2009; Benton *et al.*, 2013a; Brocklehurst *et al.*, 2013), to pool taxonomic occurrences. Both formally recognised stage bins and an approximately equal 10 million year time bin approach were used here. Occurrence data for each group were pooled into: (1) approximately equal length (~10 million year [myr], n = 14) time bins (Alroy *et al.*, 2008; Alroy, 2010b) (Table 8); and (2) stage-level time bins (n = 23) (Table 5). The reason for this dual scheme is that the former provides a finer scale resolution for investigating changes in diversity, whereas the latter ensures that time bins sample occurrence data at even time intervals (note that Jurassic and Cretaceous time bins are of uneven length, and range from around 2–13 million years). Recent work on Mesozoic tetrapods (Benson *et al.*, 2010; Benson and Butler, 2011; Mannion *et al.*, 2011; Mannion *et al.*, 2015) found that uneven time bin duration might not be problematic in creating spuriously high diversity in longer time bins (i.e., due to increasing potential to sample occurrences within that bin), and therefore stage level bins should be appropriate use for diversity studies. A further advantage of

using stage level time bins is the increased number of data points, which is important for increasing the statistical power of tests involving pairwise comparisons. Each occurrence has an associated stratigraphic range based on the temporal duration of its parent collection, which were used to assign individual minimum and maximum ages. Only occurrences that had their entire stratigraphic range included within a single time bin were included, in order to avoid over-counting single occurrences in multiple time bins, or incorporation of taxa with high uncertainty in their temporal durations. Although this means that certain geological formations, taxonomic sub-groups, or certain collections will be excluded from the binned datasets, this will likely be randomly distributed and should not affect the overall results of the present study.

Occurrences were divided into marine and non-marine partitions, with marine taxa representing only those which were fully pelagic. Semi-aquatic and coastal taxa were treated as non-marine in all cases (see Chapter 4). Where time bins did not contain any occurrence data, these were treated as non-applicable (NA) data, rather than 0 data. Taxonomic groups are based on major clades that either passed through the J/K boundary or radiated in the Early Cretaceous. Each taxonomic sub-group was further sub-divided into approximately contiguous palaeocontinental regions: Africa, Asia, Europe, South America, and North America. Sampling is too poor to analyse patterns in Antarctica, Australasia, or Indo-Madagascar, although these regions were included in the global analyses. Each fossil occurrence has an associated stratigraphic range based on the temporal duration of its parent collection, which in turn is based on the geological strata from which that collection is sampled. This was used to assign individual minimum and maximum ages to individual occurrences. Only occurrences that had their entire stratigraphic range contained within a single time bin were included. This approach avoids the over-counting single occurrences in multiple time bins and the spurious inclusion of taxa with high uncertainty in their temporal durations. Note that this means that the binning scheme is biased against taxa within formations or collections with higher levels of temporal uncertainty and poor stratigraphic constraints.

Abbreviation	10 million year time bin	Stage equivalent	Temporal range
K8	Cretaceous 8	Maastrichtian	72.1–66.0
K7	Cretaceous 7	Campanian	83.6–72.1
K6	Cretaceous 6	Turonian–Santonian	93.9–83.6
K5	Cretaceous 5	Cenomanian	100.5–93.9
K4	Cretaceous 4	Albian	113–100.5
K3	Cretaceous 3	Aptian	126.3–113
K2	Cretaceous 2	Hauterivian–Barremian	133.9–126.3
K1	Cretaceous 1	Berriasian–Valanginian	145.0–133.9
J6	Jurassic 6	Kimmeridgian–Tithonian	157.3–145.0
J5	Jurassic 5	Callovian–Oxfordian	166.1–157.3
J4	Jurassic 4	Bajocian–Bathonian	170.3–166.1
J3	Jurassic 3	Toarcian–Aalenian	182.7–170.3
J2	Jurassic 2	Pliensbachian	190.8–182.7
J1	Jurassic 1	Hettangian–Sinemurian	201.3–190.8

Table 8. Approximately equal 10 million year time bins.

2.5 Reconstructing taxonomic diversity

Taxonomic diversity reflects the observed or uncorrected (raw) number of taxa within a defined region, and is commonly referred to as taxonomic richness. It is the simple census of unique taxa that occur within a bin, irrespective of the frequency of occurrences of that taxon. Numerous studies have demonstrated that raw taxonomic, or taxic, diversity estimates are strongly biased by the abundance distribution of species. This is compounded by the availability of fossils in the geological record (see Chapter 3). Both of these factors mean that taxonomic diversity is actually a poor representative of true richness.

RAW COUNTS

Group	J1	J2	J3	J4	J5	J6	K1	K2	K3	K4	K5	K6	K7	K8	Sum per group
Aves	0	0	0	0	0	1	0	17	52	6	6	11	21	29	143
Choristoderes	0	0	0	1	0	1	2	1	8	1	0	1	2	1	18
Lepidosauromorphs	2	3	5	6	2	17	18	18	13	14	9	11	67	31	216
Lissamphibians	3	0	0	6	5	7	8	12	7	5	6	15	12	21	107
Mammaliaforms	9	3	7	24	19	48	43	18	15	18	27	24	66	59	380
Theropods	8	0	0	9	21	27	9	23	25	18	22	30	74	72	338
Pterosaurs	3	1	3	2	8	20	9	4	26	22	6	6	10	6	126
Sauropodomorphs	25	0	3	6	15	32	6	8	9	9	10	18	15	23	179
Ornithischians	10	2	1	1	15	25	17	20	17	27	13	23	111	58	340
Crocodyliformes (terrestrial)	6	0	0	2	6	18	9	12	10	12	18	38	21	31	183
Testudines	0	0	0	1	6	23	16	13	16	18	12	26	37	61	229
Ichthyopterygians	4	2	7	2	6	12	3	5	3	5	3	0	0	0	52
Sauropterygians	11	3	10	3	17	12	5	4	5	8	7	16	12	10	123
Chelonioides	0	0	0	0	0	0	0	0	1	7	1	16	25	35	85
Crocodyliformes (marine)	0	0	4	6	12	13	3	1	2	1	1	1	3	7	54
Sum per time bin	81	14	40	69	132	256	148	156	209	171	141	236	476	444	2573
Sum aquatic	15	5	21	11	35	37	11	10	11	21	12	33	40	52	314
Sum terrestrial	66	9	19	58	97	219	137	146	198	150	129	203	436	392	2259

Table 9. Raw counts of genera for each of the major taxonomic groups investigated, divided into approximately equal 10 million year time bins (see Section 2.3).

2.5.1 A note on residual diversity estimates

Two original methods for compensating for 'sampling bias' were proposed by Raup (1972): modelling, and subsampling or sample standardisation. Regarding the former, a commonly used approach has been the calculation of residual diversity estimates. These are based on the raw, or empirical, taxonomic diversity estimates, which are assumed to contain components of sampling error and true diversity. This modelling approach gained popularity among palaeontologists since its original implementation (Smith and McGowan, 2007), designed to estimate how the rock record influenced marine invertebrate diversity on a regional scale. Two factors are required to calculate residual diversity estimates: the raw taxonomic diversity, and a proxy for either sampling effort or availability. Commonly, these come in two forms, representing anthropogenic factors (e.g., the number of

fossiliferous collections) or geological factors (e.g., the number of fossiliferous formations, or available outcrop area). The use of each of these 'sampling proxies' has been questioned both theoretically and empirically (Dunhill, 2012; Dunhill *et al.*, 2012; Benton *et al.*, 2013a; Brocklehurst *et al.*, 2013; Dunhill *et al.*, 2014b; Benton, 2015; Brocklehurst, 2015), with no consensus reached as of yet as to what the most appropriate proxy might be on different scales and for different taxonomic groups. A residual diversity estimate is calculated by creating a linear model between ordered taxonomic diversity and an ordered chosen sampling proxy, and then subtracting this model from the observed taxonomic diversity to leave behind a residual diversity estimate. The result is essentially the deviations from the null model which supposedly represents diversity if it was uniform and driven purely by sampling. Here, the idea is that this subtraction 'removes' the sampling signal, leaving a purely biological diversity signal behind. One of the attractive reasons for applying this approach is that residual diversity curves in theory account for both the common cause hypothesis and any potential sampling bias, by rejecting the null hypothesis that sampling and diversity are inter-dependent. Since its original implementation it has been widely utilised, particularly among vertebrate researchers, as it produces a signal even at very low sampling levels (Barrett *et al.*, 2009; Butler *et al.*, 2009c; Benson *et al.*, 2010; Benson and Mannion, 2011; Benson and Butler, 2011; Benson *et al.*, 2013; Butler *et al.*, 2013; Newham *et al.*, 2014). The method was extended to allow modelling and assessment of non-linear relationships between sampling proxies and raw diversity, as well as by adding a simple test for significance as to whether residual diversity fluctuations deviate from background changes (Lloyd, 2012). However, a recent study revealed that residual diversity estimates poorly reflect true diversity estimates using a range of simulation parameters, and therefore performs relatively poorly compared to subsampling methods and phylogenetic methods (Brocklehurst, 2015). Additionally, sampling probabilities calculated for dinosaurs (Starrfelt and Liow, 2016), while strongly correlated with collection-based proxies (i.e., dinosaur-bearing collections), fail to capture any more than half of any putative sampling signal, and therefore might be more likely to introduce error when 'correcting' empirical diversity

curves. Based on these issues, residual diversity was not calculated for any tetrapod group. However, some of the proxies typically used for calculating residual diversity (e.g., tetrapod-bearing collections and formations, rock outcrop area) were used as sampling estimates for comparative analyses (see Chapter 4).

2.6 Sample standardisation

The shape of diversity curves is strongly influenced by uneven distributions of data (i.e., taxonomic occurrence abundances) in each of the time bins based on the amount of fossils available to sample (Alroy *et al.*, 2001; Alroy *et al.*, 2008). By using collection-based occurrence datasets that reflect the taxon-abundance curve, this variation in sampling can be compensated for by applying randomised subsampling techniques (Alroy *et al.*, 2001; Alroy, 2010a). Subsampling methods were also introduced into the palaeontological literature through investigations of Phanerozoic marine diversity (Raup, 1972), and they essentially draw on ecological methods for accounting for heterogeneity in sample size and distribution. Of these methods, classical rarefaction is perhaps the most widely implemented by palaeontologists, a technique which draws from comparable taxonomic lists until a certain threshold is reached, thus representing uniform sampling. Rarefaction can therefore be thought of as a sized-based subsampling method that achieves equal comparison between samples by subsampling to a fixed and equal coverage of the underlying sample pools. These methods have been implemented in a range of studies (Raup, 1975; Alroy *et al.*, 2001; Bush and Bambach, 2004; Bush *et al.*, 2004; Kowalewski *et al.*, 2006; Alroy *et al.*, 2008; Chao *et al.*, 2009), and more recently developed methods such as shareholder quorum subsampling (SQS) have been demonstrated to faithfully reflect true diversity patterns based on simulations. It is for this reason that subsampling techniques appear to out-perform current modelling approaches (see Section 2.5.1), and this approach is the one most favoured at the present.

2.6.1 Shareholder Quorum Subsampling

Shareholder quorum subsampling is the most recently developed of subsampling techniques, and works by standardising in-bin taxonomic occurrence samples based on an estimate of coverage to determine the relative magnitude of taxonomic biodiversity trends (Alroy, 2010a; b). This method is more accurate and precise in estimating relative diversity compared to previous methods, including rarefaction, that work through differential weighting of taxa based on their frequency of occurrence in sample sizes independent of the overall sample size coverage (Alroy *et al.*, 2001). SQS has been more widely applied to analyses of Phanerozoic diversity (Alroy, 2010c; Hannisdal and Peters, 2011; Mayhew *et al.*, 2012), for clade-specific investigations (Lloyd *et al.*, 2012), for estimating the magnitude of radiations, extinctions and their aftermath phases (Aberhan and Kiessling, 2014; Brusatte *et al.*, 2015; Cermeño *et al.*, 2015; Na and Kiessling, 2015), and even applied in some cases to modern groups (Cermeño *et al.*, 2013). The method has also recently gained popularity in application to tetrapod groups (Mannion *et al.*, 2012; Newham *et al.*, 2014; Mannion *et al.*, 2015; Nicholson *et al.*, 2015), due to the fact that it produces results even at low sample sizes, appears to eliminate sampling artefacts, and produces faithful representations of 'true' diversity. Furthermore, some studies have found that results from SQS are strongly correlated with results produced using residual diversity estimates (Smith *et al.*, 2012), which suggests that SQS captures, and most importantly compensates for, the underlying sampling signal. It also suggests that residuals might be an appropriate method for capturing a diversity signal, contrary to the results of Brocklehurst (2015). One recent study (available only as a non-peer-reviewed pre-print at the time of writing) has questioned the applicability of SQS due to its sensitivity to changes in the species-abundance distribution (Hannisdal *et al.*, 2016). Other methods such as TRiPS have been recently developed

(Starrfelt and Liow, 2016), but have not been shown to consistently outperform diversity estimation using SQS as of yet.

It is worth noting that SQS is a measure of relative, not absolute, diversity, and therefore is an unbiased estimator that provides information on the former, which is ultimately of interest in any attempt to interpret patterns of diversity through time. In this method, each taxon is treated as a 'shareholder', whose 'share' is its relative occurrence frequency (Alroy, 2010a). Taxa are randomly drawn from in-bin taxonomic occurrence lists, and when a summed proportion of these 'shares' reaches a certain threshold, or 'quorum' (q), subsampling stops and the number of taxa is tallied. Coverage, as a measure of sampling quality, is defined as the proportion of the frequency distribution of taxa within a sample, and given by the following equation, where O is the number of individual occurrences, and n_1 is the number of singleton occurrences (i.e., taxa sampled exactly once per bin):

$$u = 1 - n_1/O$$

Coverage is estimated by using randomised subsampling to calculate the mean value of Good's u (Good, 1953), the sum of the frequencies of sampled taxa within an occurrence list, and for each time bin, u is divided into q (Alroy, 2010a). Coverage of zero shows that either there are no sampled occurrences or all taxa are singletons, whereas higher coverage indicates more even sampling of taxa, and is therefore a measure of sample completeness independent of the overall sample pool size. The major difference of SQS to traditional subsampling methods (e.g., rarefaction) is that, instead of using a fixed uniform quota (Raup, 1975), it uses coverage, which is flexible in response to the changing taxon occurrence distribution. Importantly, by standardising based on coverage in this manner, instead of size (as in classical rarefaction), resulting species richness estimates can be replicated, which is an important property to preserve when characterising diversity (Alroy, 2010a; Chao and Jost, 2012). In all of the subsampling analyses, singletons were excluded (but still used to calculate Good's u), and dominant taxa (those with the highest frequency of occurrences per bin) were included. The reason

to exclude singletons is that they tell us nothing about the underlying taxon abundance distribution (i.e., the taxon-abundance distribution is 1:1), and can act to distort estimates of diversity. For each subsampling trial, this treatment of dominant taxa (o_1) means that when this taxon is encountered its share does not contribute towards *q*, but 1 is added to the subsampled diversity estimate for that bin (Alroy, 2010a). Additionally, occurrence lists might be biased by single large collections which can create the artificial appearance of poor coverage (Alroy, 2010a). This can be resolved by counting occurrences of taxa that only occur in single publications (p_1) as opposed to those which occur in single collections, and to exclude taxa that are only ever found in the most diverse collection (*t*). Together, this correction for dominant taxa and large collections means that Good's *u* is given by the following modified equation (Alroy, 2010a):

$$u_1 = (O - o_1 - p_1 + t)/O - o_1$$

SQS was applied to the occurrence datasets for each higher taxonomic group and for each time interval to provide an estimate of global subsampled taxonomic diversity. By subsampling higher taxonomic groups individually, instead of as a whole, the issue of taxon-specific factors that influence taxonomic identification of fossils, such as variation in identification difficulty, and degree and mode of preservation (Alroy, 2010a), is alleviated. This was conducted for both of the binning strategies (see above). SQS was implemented using a Perl script (version 4.3) provided by J. Alroy. The input for this script requires an occurrence dataset and pre-defined scale defining time bins from which to subsample (Table 8, Table 5). 1000 sub-sampling trials were run for each group, and the mean diversity is reported. Note that unfortunately the confidence intervals are not output using the Perl script (but see bootstrapping section below). For each sequential subsampling iteration, whenever a collection from a new publication was sampled from the occurrence list, subsequent collections were sampled until exactly three collections from that publication had been selected (Alroy, 2010a; 2014). A baseline quorum of 0.4 was set, as this has been demonstrated to be sufficient to accurately assess changes in

biodiversity (Alroy, 2010b), and the results from these are used as the basis for modelling the extrinsic parameters (see Chapter 3 and 4). In addition to this, the impact of different quorum levels was explored at increments of 0.1 on resulting diversity curves. Full results are reported in Appendix 9. Although it has been suggested that SQS can remove a underlying signal that controls both sampling and biodiversity (Hannisdal and Peters, 2011), others have found that the relationships between environmental variables and diversity were strengthened (Mannion *et al.*, 2015), and relationships between taxonomic diversity and sampling proxies were weakened, upon application of SQS, which suggests that such signal dampening is unlikely to be a problem for tetrapods.

SQS, like all other methods, is not without it's critics. Most recently, it has been suggested that it is highly sensitive to changes in the rank-abundance distribution, in that if you randomly lose species then this alters the sampled evenness (Hannisdal *et al.*, 2016), as measured through the shape parameter σ. These authors concluded that changes in eveness act to confound SQS, although it is unclear whether Good's *u* (Good, 1953) is as sensitive to these changes to an extent that SQS becomes a poor estimator for richness. Indeed, SQS is a superior method to traditional subsampling approaches, such as rarefaction, in that variations in eveness are explicitly taken into account by applying random sampling of the taxon-abundance curve to an equal frequency coverage. In addition, it appears that changes in SQS richness can be estimated as a product of normalised raw richness and raw eveness (as measured by Pielou's J; (Pielou, 1975)) for well sampled taxa (in this empirical example, Cenozoic coccolithophores and foraminiferans) (Hannisdal *et al.*, 2016). This suggests that changes in eveness will lead to changes in SQS richness, which we might expect. Indeed, a failsafe to combat this potential issue is built into the SQS algorithm, in which the quorum itself is subsampled based on recalculations of Good's *u* in each subsampling trial (Alroy, 2010a). The reported mean diversity therefore incorporates sensitivity to changes in the evenness of the sampled taxon pool.

Others have noted that modelling fossil sampling as a Poisson process might be a superior method (Starrfelt and Liow, 2016) to SQS, as this takes into account the processes of both fossilisation and detection (i.e., an observable occurrence). This method, called TRiPS (True Richnesss estimated using a Poisson Sampling model), is a maximum-likelihood estimate of true species richness that accounts for heterogeneous sampling between bins by estimating a sampling rate based on the number of observations per species per million years (Starrfelt and Liow, 2016), which is transformed into a per-bin (stage) probability and therefore should account for issues relating to differential time bin duration. The main difference in the outputs of this method and SQS is that the latter states when data is insufficient to return a reliable result (i.e., subsampled data cannot achieve the quorum level, and an NA result is reported), whereas TRiPS always produces a result, no matter how poorly sampled a time interval might be. Overall, the method is principally similar to SQS, and both aim to sample fairly from the underlying sample pool based on subsamples of equal coverage, or an estimate of sampling probability, both of which are underpinned by variance in the shape of the taxon-abundance curve. Unfortunately, the TRiPS method was published only towards the end of completing this thesis, and therefore I have not had a chance to analyse tetrapod diversity using it. However, this is an approach for future consideration.

2.6.2 Applying SQS to Crocodylifomes

SQS was also applied to the marine and non-marine genus-level occurrence datasets for each time interval to provide an estimate of global subsampled taxonomic richness, using two methods (each using the two binning strategies). The first of these, SQSP, was conducted using a Perl script (version 4.3) written and provided by J. Alroy, applied at 10 myr time intervals (SQSPt) and at the stage level (SQSPs). This version of SQS allows constraint over the number of taxonomic occurrences subsampled

based on their frequency per collection (Alroy, 2010a; b; c), and the procedure is essentially the same as that outlined above for broader tetrapod analyses.

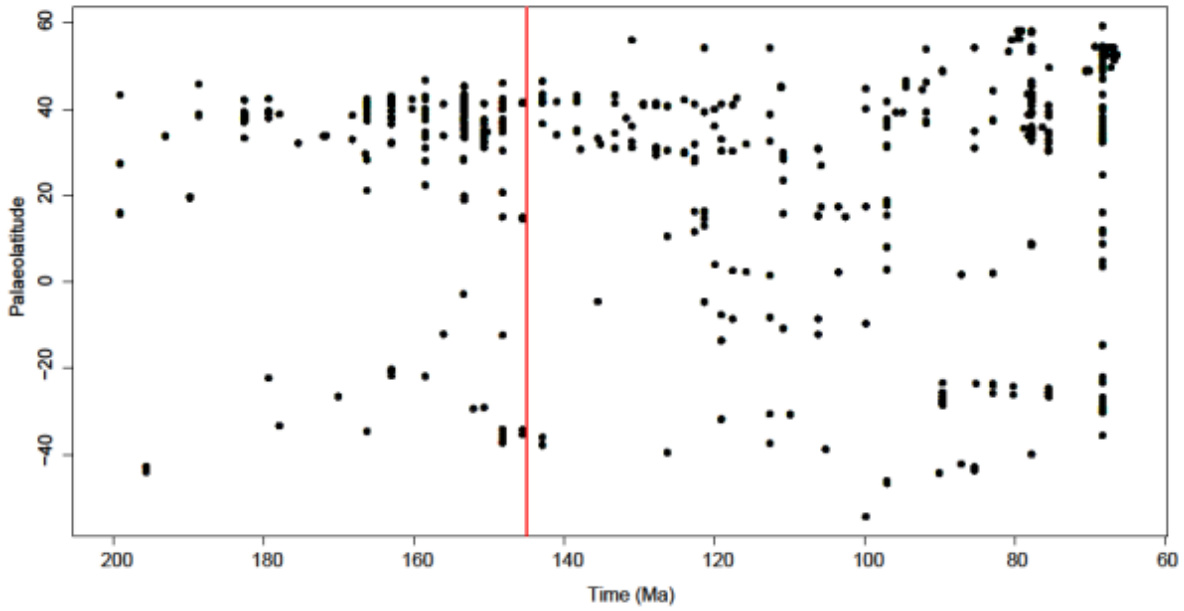


Figure 17. Palaeolatitudinal distribution of all crocodyliform occurrences assigned to genera through the Jurassic and Cretaceous. The Jurassic/Cretaceous boundary (145 Ma) is highlighted in red. Palaeolatitudes are based on Scotese rotations, and acquired from the Paleobiology Database.

Secondly, the SQS function (version 3.3) for R available on J. Alroy's personal website was employed. The major difference between this and the Perl script is that there is no restriction based on the number of publications per time bin, and no correction for single large collections (Alroy, 2010a; b; c). However, at the present it is unlear what the impact of this variation on tetrapod datasets is, as they are typically relatively under-sampled with respect to marine invertebrates, for which these methods were principally designed for. For all analyses, a baseline quorum of 0.4 was set, and 1000 iterations performed to obtain a subsampled biodiversity distribution (SQSR), conducted at 10 myr time intervals. Whereas the constrained analysis (SQSRc) restricted the dataset to occurrences that could be assigned to a single time bin, the stability of the resulting non-marine curves was tested by assessing the influence of retaining occurrences with uncertainty in their temporal duration from the original

dataset (unconstrained analysis [SQSRu]). Others have found that both of these versions of SQS (R and Perl) yield very similar results when applied to the same data at a moderate quorum (0.4) (Hannisdal *et al.*, 2016), although this was based on a group generally considered to have a 'good' fossil record (Cenozoic coccolithophores), and the variable utility of both methods has not yet been tested on any tetrapod group.

2.6.3 Bootstrapping SQS

In addition to the SQS trials using the Perl script, I also employed a second stream of analyses based on the form of SQS for R (version 3.3). The code for this is freely available from the site of John Alroy (http://bio.mq.edu.au/~jalroy/SQS-3-3.R), and an updated version is provided on my personal GitHub page. This update extends the function to have a bootstrapping component, and therefore is the first time sensitivity analyses have been applied to SQS. This version of SQS with R produces slightly different results to the Perl script (see Chapter 4), but does not influence the overall shape of diversity curves, at least for Crocodyliformes (Tennant *et al.*, 2016). For each clade 1000 bootstrap iterations were performed for SQS, replacing each taxon back in the list after each subsampling iteration. The median (50% confidence interval) and 5% and 95% confidence intervals as lower and upper bounds, respectively, were calculated from the outputs.

2.7 Phylogenetic diversity estimates

Phylogenies provide information on 'hidden' biodiversity that we know must have existed but that has not been preserved in the fossil record. Based on the bifurcation model of speciation, sister taxa originate at the same time as each other and therefore we can extrapolate their known fossil ranges so that they have equal origination times. The creation and incorporation of these 'ghost lineages'

increases biodiversity by extending unsampled taxonomic ranges into older time bins (Norell, 1993; Lane *et al.*, 2005). Therefore, phylogenetic diversity can be thought of as a minimum estimate of the failure to observe known lineages in the fossil record. Phylogenetic diversity has two components. The first is the raw, in bin taxonomic diversity. The second is based on the addition of ghost lineages implied by the phylogenetic relationships of those taxa. While phylogenetic methods might be superior for estimation of extinction and origination rates, conducting such analyses for all tetrapods would require a global collaboration effort and is beyond the scope of the present thesis. Generating a phylogenetic diversity estimate (PDE) has been shown to be a more accurate representation of true diversity than empirically measured, raw taxonomic diversity using simulation studies (Lane *et al.*, 2005; Brocklehurst, 2015), and therefore can be used as a comparative estimate with subsampling approaches. There are, however, limitations to using PDEs. Firstly, by only constructing backwards-extending ghost lineages, this imposes a skew towards higher diversity in older time bins. This exacerbates the PDEs failure to appropriately account for the Signor-Lipps effect, i.e. the failure of the last occurrence of a fossil taxon to accurately represent the extinction of that taxon, which can have the impact of making rapid extinction events appear more staggered then they were in reality. Additionally, phylogenetic approaches can have the adverse effect of imposing an asymmetry in analyses by only correcting origination times and not extinction times. They are also highly sensitive to changes in phylogenetic hypotheses and often the selective inclusion of only well-known taxa (Lane *et al.*, 2005). Resulting diversity estimates might also be over-estimated due to the way in which we model ancestor-descendant relationships through phylogenetics (i.e., a pure cladogenesis model), where ancestors/descendants might be incorrectly resolved as sister taxa, thus producing false ghost lineages (Lane *et al.*, 2005). In this model, bifurcating lineages will always lead to a minimum of two subsequent branches (depending on how polytomies are treated) from a single ancestral lineage which itself terminates in the branch splitting process, which makes recognition of ancestor-descendant pairs difficult to recognise in the fossil record (Foote, 1996). This problem is emphasised

in a recent simulation study (Brocklehurst, 2015), which found that in some cases PDE leads to over-estimation of true diversity, in spite of being the most closely correlated diversity metric with true diversity. Currently, tree building methods in palaeontology are not equipped to deal with this, by either introducing anagenesis or budding cladogenesis, and simply due to the nature of the fossil record we must assume a pure cladogenetic model of evolutionary relationships. One potential way to account for this issue is to assess convergence between tree assembly at different taxonomic levels, to see if the overall trends recovered are similar throughout the hierarchy. Such a result would suggest that the amount of cladogenesis (through varying the number of included taxa) has little effect on the overall structure of phylogenetic diversity.

2.7.1 Phylogenetic diversity estimation for non-crocodyliforms tetrapods

One of the major advantages of using PDEs is that they generate diversity estimates even in very poorly sampled intervals due to the continuous nature of phylogenetic branches, as opposed to discrete taxonomic occurrences. Therefore, investigation of PDEs here is for the sake of assessing convergence between different methods based on independent data sets, and to 'fill in the gaps' in our knowledge for time bins in which SQS fails to produce a result due to sampling issues.

To calculate PDEs, source trees were obtained from the primary research literature for the three major clades of dinosaurs (Sakamoto *et al.*, 2016), sauropterygians (Fischer *et al.*, 2015), ichthyopterygians (Fischer *et al.*, 2012), and pterosaurs (Upchurch *et al.*, 2014). Other tetrapod groups lack well-sampled trees for the study interval. To calculate phylogenetic diversity for each of these groups, first occurrence (FAD) and last occurrence (LAD) data were extracted from the PaleoDB. Trees were all time-scaled using the equal method in the R package *strap* (Bell and Lloyd, 2015) using the DatePhylo() function. This works by assigning an equal portion of time to zero-length branches available from the first directly ancestral branch of positive length.

2.7.2 Phylogenetic diversity estimation for Crocodyliformes

2.7.2.1 Supertree construction protocol

The utility of supertrees for macroevolutionary investigations has a history as long as that for the field of systematics (Bininda-Emonds, 2004). Supertrees have played a particularly strong role in our understanding of large-scale patterns in Mesozoic tetrapods, facilitated by an ever increasing understanding of the systematics of groups such as Therapsida and Archosauromorpha, and all inclusive clades (Brusatte *et al.*, 2008; Brusatte *et al.*, 2010; Irmis, 2010; Benson *et al.*, 2012; Sookias *et al.*, 2012a; Sookias *et al.*, 2012b; Benson and Choiniere, 2013; Foth and Rauhut, 2013; Benson *et al.*, 2014). While crocodyliform supertrees already exist (Gatesy *et al.*, 2004; Bronzati *et al.*, 2012), converting these into machine readable formats would have been just as much effort as constructing a new one from scratch. Furthermore, by creating my own tree, I can be explicit about the tree building protocol from the beginning, and make informed decisions about which taxa to include or exclude, rather than automating it and including potentially spurious taxa or relationships.

To produce a PDE, a new crocodyliform 'informal' supertree was constructed comprising 252 species (source trees indicated below) using Mesquite (version 2.75). This involves the 'bolting together' of different parts of independent but taxonomically overlapping and hierarchically nested trees to increase phylogenetic taxon sampling, without creating spurious relationships not found in any of the source trees. The advantage of this approach is that taxonomic sampling can be virtually comprehensive compared to approaches using just single trees (see above). One potential issue with informal supertree construction is that phylogenetic placement and conflict resolution is essentially a subjective decision. One possible way to account for this and maximise replicability is to be explicit with the justifications for each taxon substitution or addition decision, as is carried out below. An additional supertree was created at the genus level (146 genera) to account for uncertainty in the

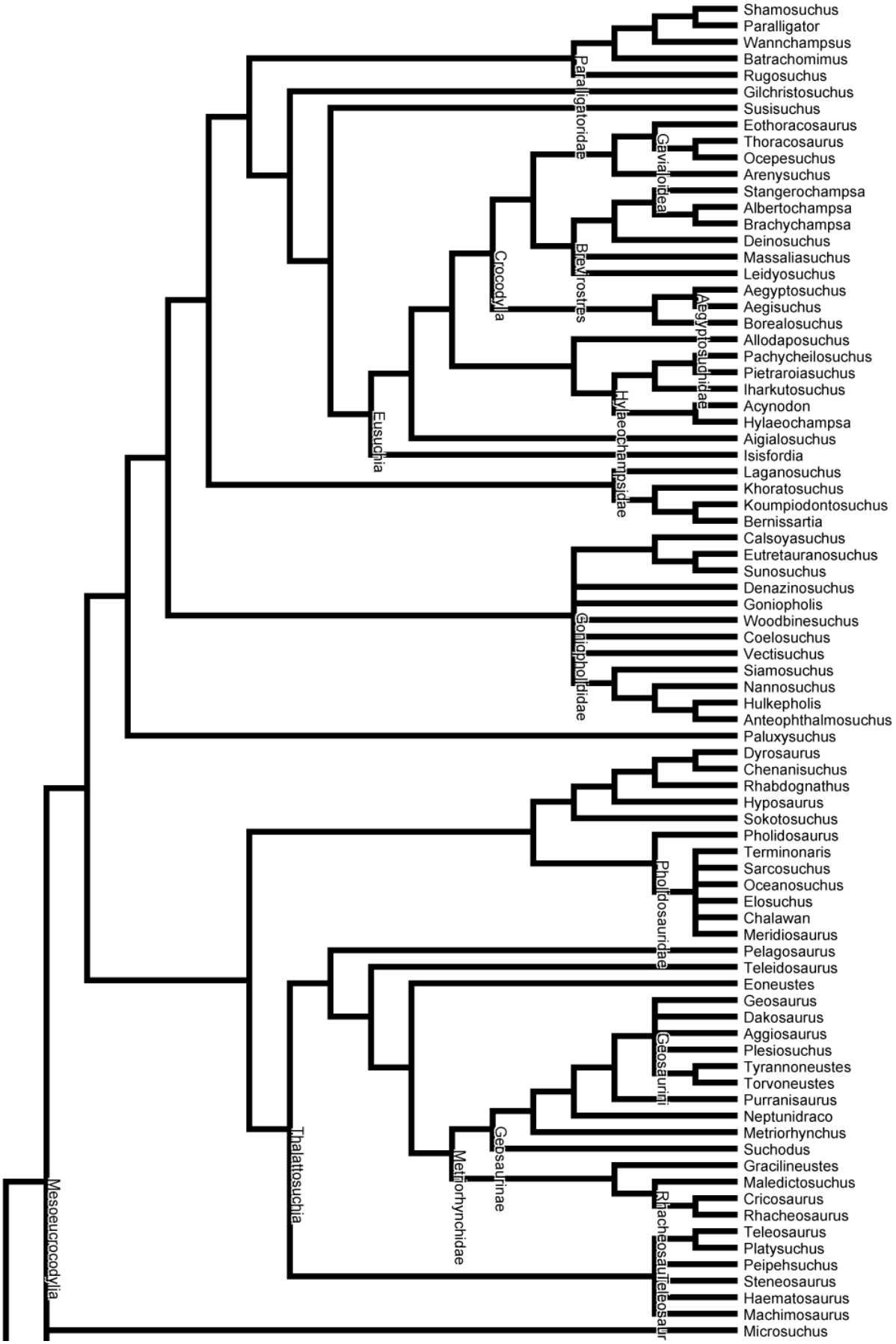
taxonomy of anomalously speciose genera, such as *Goniopholis*, *Steneosaurus*, and *Teleosaurus*. Here, details of the tree construction decisions are given in full. A complete list of taxa and sources are provided in Appendix 1, and additional details regarding the taxonomy, mode of life, and stratigraphic ranges in Appendix 2 and Appendix 3. Producing a supertree for all of Tetrapoda, or for each constituent higher clade, would require a much greater collaborative effort, and is not attempted beyond Crocodyliformes for the purposes of this thesis.

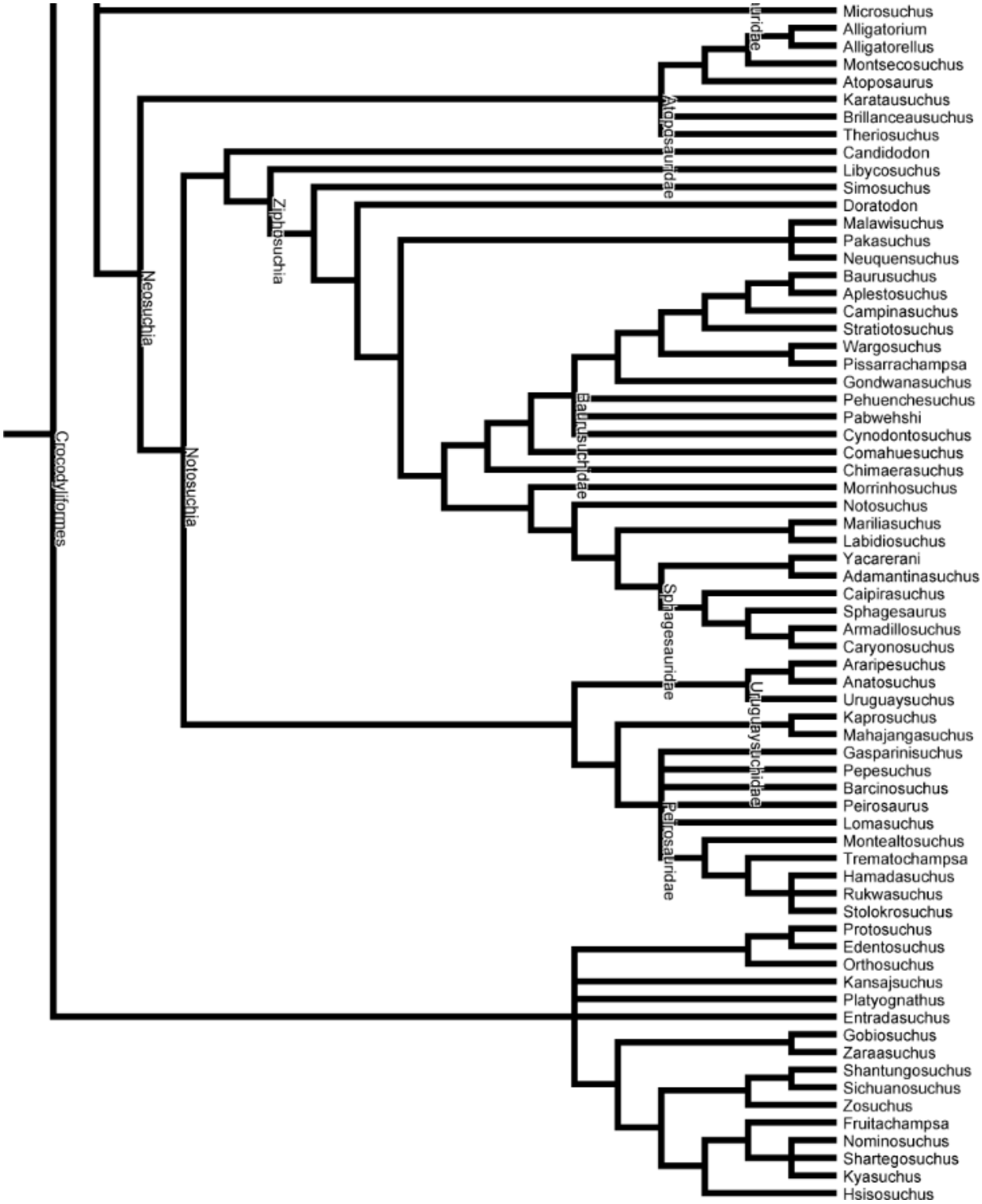
The taxonomy for these trees is based on a list of all Jurassic–Cretaceous crocodyliform species from the Paleobiology Database (accessed December 1, 2014). This is a comprehensive occurrence-based list that numerous researchers have contributed to (Carrano *et al*. 2015), and is a faithful representation of the current state of knowledge of crocodyliform taxonomy based on the published literature. Crocodyliform taxonomy and phylogenetics is a highly fluid field, and I expect to update this tree regularly as new discoveries are made. Information on phylogenetic relationships was obtained from a range of sources from the primary literature (see below; note that figures in this section refer to those within the references cited). Phylogenetic information could not be collected for some of the genera, which were omitted to reduce introducing unnecessary error into reconstructed diversity estimates. For time-scaling purposes, the full genus range implied by each of its constituent species was used, including specifically indeterminate remains. By comparing the two supertrees, it is possible to identify where taxonomic issues might confound the signal, as well as identify key areas for future taxonomic research. Both supertrees are in Appendix 5, and can be read into R by creating separate text-based files with a .tre file extension.

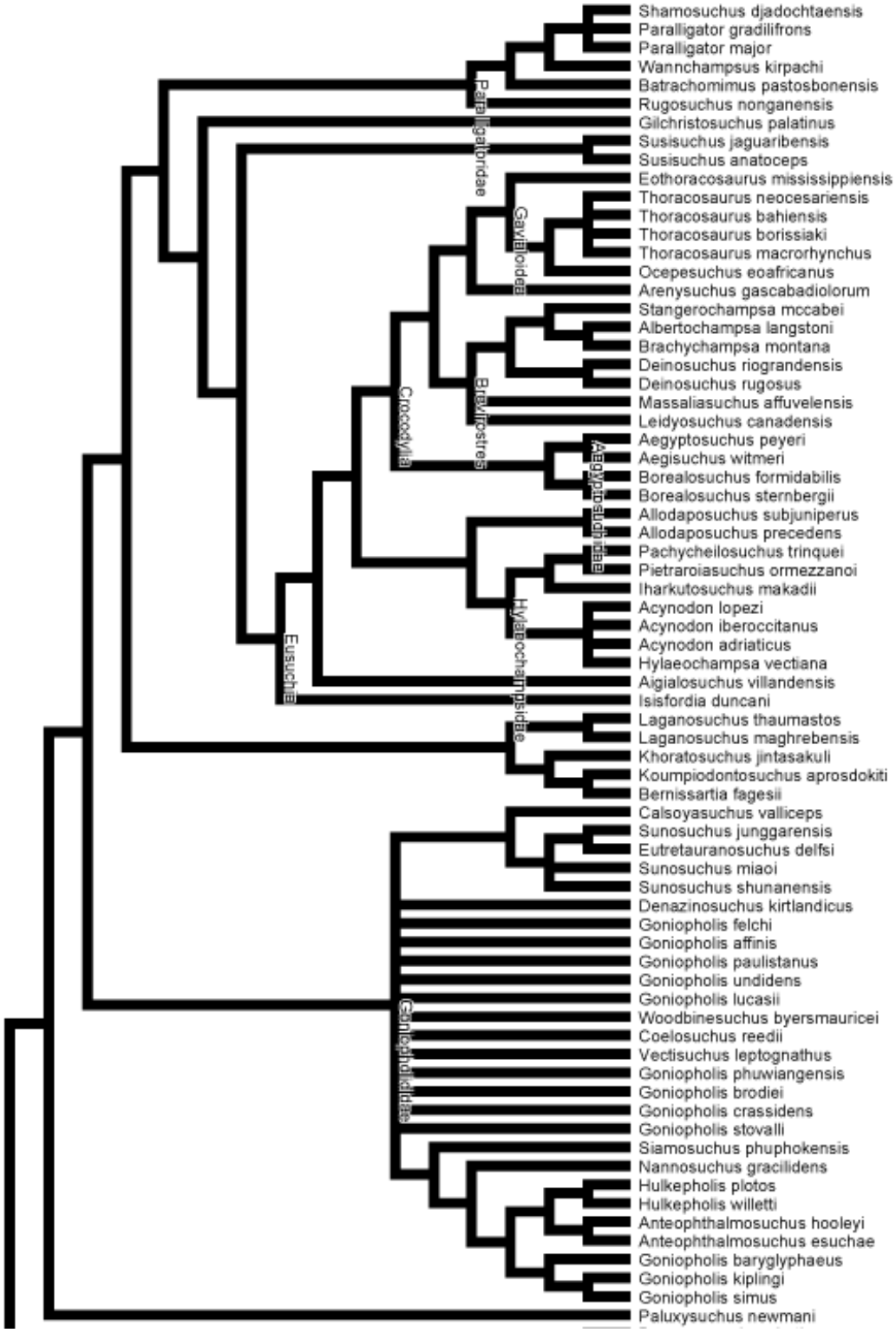
These supertrees contained multiple polytomies, which can skew biodiversity estimation by extending the durations of poorly resolved lineages to a more basal position than they should occupy, and therefore incorrectly inflating biodiversity in older time bins (Wagner, 2000). To combat this issue, three different methods of resolving polytomies were applied, and PDE was calculated as the mean of

the results using each of these. In instances where not all species of a multispecific genus have previously been included in a phylogeny, these are incorporated but a polytomy is created for all of the inclusive species. However, if there are only two species then they are included as sister taxa. Finally, PDE was calculated at both the stage level and for 10 million year time bins in order to facilitate direct comparison between resulting estimates and those obtained from subsampling trials. Images of the trees are provided below for visualisation purposes at the genus (Figure 18) and species (Figure 19) levels.

Figure 18. Genus level supertree


Shamosuchus
Paralligator
Wannchampsus
Batrachomimus
Rugosuchus
Gilchristosuchus
Susisuchus
Eothoracosaurus
Thoracosaurus
Ocepesuchus
Arenysuchus
Stangerochampsa
Albertochampsa
Brachychampsa
Deinosuchus
Massaliasuchus
Leidyosuchus
Aegyptosuchus
Aegisuchus
Borealosuchus
Allodaposuchus
Pachycheilosuchus
Pietraroiasuchus
Iharkutosuchus
Acynodon
Hylaeochampsa
Aigialosuchus
Isisfordia
Laganosuchus
Khoratosuchus
Koumpiodontosuchus
Bernissartia
Calsoyasuchus
Eutretauranosuchus
Sunosuchus
Denazinosuchus
Goniopholis
Woodbinesuchus
Coelosuchus
Vectisuchus
Siamosuchus
Nannosuchus
Hulkepholis
Anteophthalmosuchus
Paluxysuchus
Dyrosaurus
Chenanisuchus
Rhabdognathus
Hyposaurus
Sokotosuchus
Pholidosaurus
Terminonaris
Sarcosuchus
Oceanosuchus
Elosuchus
Chalawan
Meridiosaurus
Pelagosaurus
Teleidosaurus
Eoneustes
Geosaurus
Dakosaurus
Aggiosaurus
Plesiosuchus
Tyrannoneustes
Torvoneustes
Purranisaurus
Neptunidraco
Metriorhynchus
Suchodus
Gracilineustes
Maledictosuchus
Cricosaurus
Rhacheosaurus
Teleosaurus
Platysuchus
Peipehsuchus
Steneosaurus
Haematosaurus
Machimosaurus
Microsuchus
Paralligatoridae
Gavialoidea
Brevirostres
Crocodylia
Aegyptosuchidae
Hylaeochampsidae
Eusuchia
Goniopholididae
Pholidosauridae
Geosaurini
Geosaurinae
Metriorhynchidae
Rhacheosauri
Teleosaur
Thalattosuchia
Mesoeucrocodylia


Microsuchus
Alligatorium
Alligatorellus
Montsecosuchus
Atoposaurus
Karatausuchus
Brillanceausuchus
Theriosuchus
Candidodon
Libycosuchus
Simosuchus
Doratodon
Malawisuchus
Pakasuchus
Neuquensuchus
Baurusuchus
Aplestosuchus
Campinasuchus
Stratiotosuchus
Wargosuchus
Pissarrachampsa
Gondwanasuchus
Pehuenchesuchus
Pabwehshi
Cynodontosuchus
Comahuesuchus
Chimaerasuchus
Morrinhosuchus
Notosuchus
Mariliasuchus
Labidiosuchus
Yacarerani
Adamantinasuchus
Caipirasuchus
Sphagesaurus
Armadillosuchus
Caryonosuchus
Araripesuchus
Anatosuchus
Uruguaysuchus
Kaprosuchus
Mahajangasuchus
Gasparinisuchus
Pepesuchus
Barcinosuchus
Peirosaurus
Lomasuchus
Montealtosuchus
Trematochampsa
Hamadasuchus
Rukwasuchus
Stolokrosuchus
Protosuchus
Edentosuchus
Orthosuchus
Kansajsuchus
Platyognathus
Entradasuchus
Gobiosuchus
Zaraasuchus
Shantungosuchus
Sichuanosuchus
Zosuchus
Fruitachampsa
Nominosuchus
Shartegosuchus
Kyasuchus
Hsisosuchus
Crocodyliformes
Neosuchia
Notosuchia
Ziphosuchia
Atoposauridae
Baurusuchidae
Sphagesauridae
Uruguaysuchidae
Peirosauridae


Shamosuchus djadochtaensis
Paralligator gradilifrons
Paralligator major
Wannchampsus kirpachi
Batrachomimus pastosbonensis
Rugosuchus nonganensis
Gilchristosuchus palatinus
Susisuchus jaguaribensis
Susisuchus anatoceps
Eothoracosaurus mississippiensis
Thoracosaurus neocesariensis
Thoracosaurus bahiensis
Thoracosaurus borissiaki
Thoracosaurus macrorhynchus
Ocepesuchus eoafricanus
Arenysuchus gascabadiolorum
Stangerochampsa mccabei
Albertochampsa langstoni
Brachychampsa montana
Deinosuchus riograndensis
Deinosuchus rugosus
Massaliasuchus affuvelensis
Leidyosuchus canadensis
Aegyptosuchus peyeri
Aegisuchus witmeri
Borealosuchus formidabilis
Borealosuchus sternbergii
Allodaposuchus subjuniperus
Allodaposuchus precedens
Pachycheilosuchus trinquei
Pietraroiasuchus ormezzanoi
Iharkutosuchus makadii
Acynodon lopezi
Acynodon iberoccitanus
Acynodon adriaticus
Hylaeochampsa vectiana
Aigialosuchus villandensis
Isisfordia duncani
Laganosuchus thaumastos
Laganosuchus maghrebensis
Khoratosuchus jintasakuli
Koumpiodontosuchus aprosdokiti
Bernissartia fagesii
Calsoyasuchus valliceps
Sunosuchus junggarensis
Eutretauranosuchus delfsi
Sunosuchus miaoi
Sunosuchus shunanensis
Denazinosuchus kirtlandicus
Goniopholis felchi
Goniopholis affinis
Goniopholis paulistanus
Goniopholis undidens
Goniopholis lucasii
Woodbinesuchus byersmauricei
Coelosuchus reedii
Vectisuchus leptognathus
Goniopholis phuwiangensis
Goniopholis brodiei
Goniopholis crassidens
Goniopholis stovalli
Siamosuchus phuphokensis
Nannosuchus gracilidens
Hulkepholis plotos
Hulkepholis willetti
Anteophthalmosuchus hooleyi
Anteophthalmosuchus esuchae
Goniopholis baryglyphaeus
Goniopholis kiplingi
Goniopholis simus
Paluxysuchus newmani
Paralligatoridae
Gavialoidea
Crocodylia
Brevirostres
Aegyptosuchidae
Eusuchia
Hylaeochampsidae
Goniopholididae

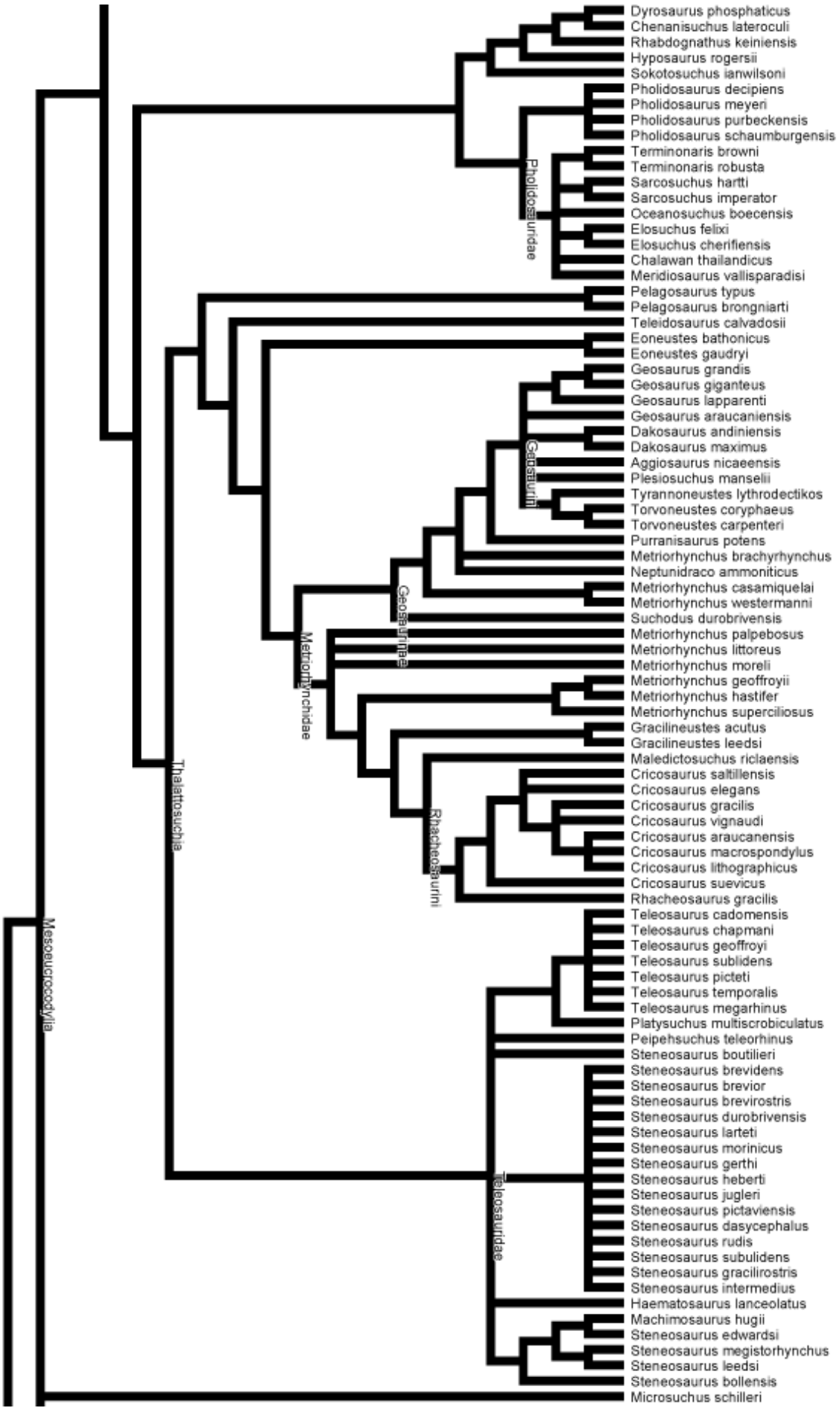

Dyrosaurus phosphaticus
Chenanisuchus lateroculi
Rhabdognathus keiniensis
Hyposaurus rogersii
Sokotosuchus ianwilsoni
Pholidosaurus decipiens
Pholidosaurus meyeri
Pholidosaurus purbeckensis
Pholidosaurus schaumburgensis
Terminonaris browni
Terminonaris robusta
Sarcosuchus hartti
Sarcosuchus imperator
Oceanosuchus boecensis
Elosuchus felixi
Elosuchus cherifiensis
Chalawan thailandicus
Meridiosaurus vallisparadisi
Pelagosaurus typus
Pelagosaurus brongniarti
Teleidosaurus calvadosii
Eoneustes bathonicus
Eoneustes gaudryi
Geosaurus grandis
Geosaurus giganteus
Geosaurus lapparenti
Geosaurus araucaniensis
Dakosaurus andiniensis
Dakosaurus maximus
Aggiosaurus nicaeensis
Plesiosuchus manselii
Tyrannoneustes lythrodectikos
Torvoneustes coryphaeus
Torvoneustes carpenteri
Purranisaurus potens
Metriorhynchus brachyrhynchus
Neptunidraco ammoniticus
Metriorhynchus casamiquelai
Metriorhynchus westermanni
Suchodus durobrivensis
Metriorhynchus palpebosus
Metriorhynchus littoreus
Metriorhynchus moreli
Metriorhynchus geoffroyii
Metriorhynchus hastifer
Metriorhynchus superciliosus
Gracilineustes acutus
Gracilineustes leedsi
Maledictosuchus riclaensis
Cricosaurus saltillensis
Cricosaurus elegans
Cricosaurus gracilis
Cricosaurus vignaudi
Cricosaurus araucanensis
Cricosaurus macrospondylus
Cricosaurus lithographicus
Cricosaurus suevicus
Rhacheosaurus gracilis
Teleosaurus cadomensis
Teleosaurus chapmani
Teleosaurus geoffroyi
Teleosaurus sublidens
Teleosaurus picteti
Teleosaurus temporalis
Teleosaurus megarhinus
Platysuchus multiscrobiculatus
Peipehsuchus teleorhinus
Steneosaurus boutilieri
Steneosaurus brevidens
Steneosaurus brevior
Steneosaurus brevirostris
Steneosaurus durobrivensis
Steneosaurus larteti
Steneosaurus morinicus
Steneosaurus gerthi
Steneosaurus heberti
Steneosaurus jugleri
Steneosaurus pictaviensis
Steneosaurus dasycephalus
Steneosaurus rudis
Steneosaurus subulidens
Steneosaurus gracilirostris
Steneosaurus intermedius
Haematosaurus lanceolatus
Machimosaurus hugii
Steneosaurus edwardsi
Steneosaurus megistorhynchus
Steneosaurus leedsi
Steneosaurus bollensis
Microsuchus schilleri
Pholidosauridae
Dakosaurini
Geosaurinae
Metriorhynchidae
Rhacheosaurini
Thalattosuchia
Teleosauridae
Mesoeucrocodylia



Figure 19. Species level supertree

2.7.2.2 Crocodyliformes

For crocodyliform taxa outside of Mesoeucrocodylia, figure 5 from one of the latest comprehensive investigations of basal crocodyliforms (Pol *et al.*, 2004) is followed as a starting point. The three species of *Hsisosuchus* (*H. chowi*, *H. chungkingensis*, and *H. dashanpuensis*) are resolved (Halliday *et al.*, 2015), and *Zosuchus*, *Shantungosuchus* (comprising *S. chuhsienensis* and *S. hangjinensis*) and *Sichuanosuchus* (*S. huidongensis* and *S. shuhanensis*) were placed as sister taxa to *Fruitachampsa*, along with *Shartegosuchus* (Clark, 2011). Additionally, both *Gobiosuchus* (comprising two species: *G. kielanae* and *G. parvus*) and *Protosuchus* (comprising three species: *P. micmac*, *P. haughtoni* and *P. richardsoni*) were forced into multi-specific polytomies. *Entradasuchus* is included within this assemblage of 'protosuchian'-grade taxa, in an unresolved basal position (Hunt and Lockley, 1995). Both *Orthosuchus* and *Edentosuchus* are included as successive sister taxa to *Protosuchus* (Pol *et al.*, 2004). *Dianosuchus* was placed within Protosuchia (Peng, 1996). *Platyognathus* was included in the unresolved polytomy at the base of Crocodyliformes due to its 'protosuchian' relationships with *Protosuchus* and *Shantungosuchus* (Wu and Sues, 1996). This position was used to place other shartegosuchids, *Kyasuchus* and *Nominosuchus*, in a basal polytomy with *Shartegosuchus*. *Zaraasuchus* was placed as the sister taxon to *Gobiosuchus* (Pol and Norell, 2004b) (fig. 11). For the position of Mesoeucrocodylia within Crocodyliformes, their currently accepted position based on the most recent and inclusive analysis of basal crocodyliforms was followed (Pol *et al.*, 2004). This excludes taxa such as *Hsisosuchus* and *Fruitachampsa* as basal mesoeucrocodylians, contrary to a recent study (Adams, 2014). This decision is based on the fact that Pol *et al*. (Pol *et al.*, 2004) sample a much broader range of basal crocodyliform taxa, and therefore there is increased confidence in their placement of these taxa. The position of *Microsuchus* is currently unstable (Leardi *et al.*, 2015), but here is placed in an unresolved position outside of Notosuchia and Neosuchia, within Mesoeucrocodylia.

2.7.2.3 Notosuchia

Notosuchia is based on a recent phylogeny of advanced notosuchians (Pol *et al.*, 2014) (fig. 31). This includes Uruguaysuchidae, Peirosauridae, Sphagesauridae and Baurusuchidae as subclades, with the latter two placed within Ziphosuchia. *Neuquensuchus* was repositioned from a basal crocodyliform to a ziphosuchian (Leardi *et al.*, 2015) (fig. 8), and placed with *Pakasuchus* and *Malawisuchus*, which is collapsed into a polytomy. These taxa comprise a basal assemblage of ziphosuchians, along with *Libycosuchus* and *Simosuchus* (Pol *et al.*, 2014). *Stolokrosuchus* is retained as a notosuchian (and sister taxon to Peirosauridae + Mahajungasuchidae) (Pol *et al.*, 2014), instead of the basal-most neosuchian as others have proposed (Adams, 2014). *Doratodon ibericus* and *Doratodon carcharidens* are placed within Ziphosuchia, one step higher than *Libycosuchus* (Company *et al.*, 2005).

2.7.2.3.1 Mahajangasuchidae

Mahajangasuchus and *Kaprosuchus* are placed as sister taxa to Peirosauridae, comprising Mahajangasuchidae.

2.7.2.3.2 Peirosauridae

Peirosauridae was placed within Notosuchia, together with Uruguaysuchidae + Mahajangasuchidae + *Stolokrosuchus*, comprising the sister group to Ziphosuchia. The internal relationships of Peirosauridae were revised according to the most recent analysis (Pol *et al.*, 2014) to conform to that of a recent study which attempted to evaluate their relationships (Sertich and O'Connor, 2014). Note that this revision of Peirosauridae also includes the 'trematochampsid' taxon *Trematochampsa.* Unfortunately, this placement of *Trematochampsa* renders the phylogenetic affinities of all other 'trematochampsids' as questionable, and therefore members previously assigned to this group are excluded from the supertree, pending further analysis of their taxonomy and phylogenetics. This uncertainty is unlikely to have a major impact on our understanding of crocodyliform diversity through the Jurassic/Cretaceous interval as they appear to comprise a largely Late Cretaceous Gondwanan radiation, but this does highlight the need for further directed research into their systematic

placement, and in particular their relationship to Notosuchia. *Barcinosuchus* is placed in a polytomy within Peirosauridae and closely related taxa (including *Lomasuchus* and *Montealtosuchus*) (Martinelli *et al.*, 2012). *Peirosaurus* and *Pepesuchus* are placed in an unresolved position at the base of Peirosauridae (Martinelli *et al.*, 2012).

2.7.2.3.3 Uruguaysuchidae

Araripesuchus is a paraphyletic taxon (Pol *et al.*, 2014). *Araripesuchus rattoides* is placed in the existing polytomy between several species of *Araripesuchus* and *Anatosuchus* (Sereno and Larsson, 2009) (fig. 43). *Uruguaysuchus* is included as the sister taxon to *Anatosuchus* + *Araripesuchus*, together comprising Uruguaysuchidae.

2.7.2.3.4 Baurusuchidae

Baurusuchidae is the sister clade to Sebecidae, which together comprise Sebecosuchia (Pol *et al.*, 2014). *Pabwehshi* is placed at the base of Baurusuchidae in a polytomy with *Cynodontosuchus* (Wilson *et al.*, 2001). *Gondwanasuchus* is placed as the sister taxon to all pissarachampsids and baurusuchines. *Aplestosuchus* is placed within Baurusuchidae, as the sister taxon to '*Baurusuchus*' *albertoi* based on figure 9 of Godoy *et al.* (2014). *Wargosuchus* is placed as the sister taxon to *Pissarachampsa*, which together with *Campinasuchus* comprises Pissarachampsinae. Pissarachampsinae and Baurusuchinae together comprise Baurusuchidae (Godoy *et al.*, 2014). *Pehuenchesuchus* is the most basal sebecosuchian (Turner and Calvo, 2005) (fig. 5). Baurusuchids were resolved within Sebecosuchia (Company *et al.*, 2005) and as such placed in a basal polytomy with *Pabwehshi* and *Cynodontosuchus*.

2.7.2.3.5 Sphagesauridae

The internal relationships of Sphagesauridae and 'advanced notosuchians' are based on a recent analysis of advanced notosuchians (Pol *et al.*, 2014) (fig. 31). Together, these form the sister taxon to Sebecosuchia, to the exclusion of *Comahuesuchus* and *Chimaerasuchus*.

2.7.2.4 Neosuchia

Neosuchia and Notosuchia are sister taxa, and together comprise Mesoeucrocodylia (Adams, 2014). Neosuchia is based on a recent broad-scale analysis of this group with wide taxonomic coverage (Adams, 2014) (fig. 13). Both species of *Laganosuchus* (*L. thaumastos* and *L. maghrebensis*) are placed within Neosuchia, outside of Eusuchia, and in a position basal to Bernissartiidae (Sereno and Larsson, 2009) (fig. 43).

2.7.2.4.1 Atoposauridae

Atoposauridae is placed at the base of Neosuchia (Martin *et al.*, 2010; Adams, 2014), and the most recently published analysis is followed (pending the results presented here in Chapter 5, which were conducted subsequent to the PDE analyses) for the internal relationships of this clade (Martin *et al.*, 2010). For *Alligatorium*, the two species *A. meyeri* and *A. franconicum* are used, although the only specimens of the latter are lost to science. The two species of *Alligatorellus* are also included (Tennant and Mannion, 2014). *Brillanceausuchus* (Michard *et al.*, 1990) and *Karatausuchus* (Efimov, 1976; Storrs and Efimov, 2000) have been considered to belong to Atoposauridae by some authors, but this has never been confirmed via phylogenetic analysis, and therefore they are excluded here.

2.7.2.4.2 Goniopholididae

The position of Goniopholididae is based on a recent analysis of Neosuchia (Adams, 2014). The internal relationships follow that of the most recent analysis to sample comprehensively from within the group (de Andrade *et al.*, 2011a). The “Hooley goniopholidid” is now named *Anteopthalmosuchus*, and the “Hulke goniopholidid” is *Hulkepholis* (Salisbury and Naish, 2011). *Sunosuchus thailandicus* was recombined recently as *Chalawan thailandicus* (Martin *et al.*, 2014b). *Goniopholis stovalli* is collapsed into a basal polytomy, as *Eutretauranosuchus* nests within *Sunosuchus* instead of being in a sister taxon relationship (Adams, 2014). *Denazinosuchus* is also placed in an unresolved basal position (de

Andrade *et al.*, 2011a). *Goniopholis* is a problematic genus, as there are an additional eight species of this taxon not included in recent analyses (de Andrade *et al.*, 2011a; Adams, 2014), but with a lack of work on them meaning that they are retained in the Paleobiology Database as valid species. For now, I tentatively include each of these species of *Goniopholis* as part of a basal polytomy with *G. stovalli* and *Denazinosuchus*, pending future taxonomic revision. *Goniopholis paulistanus* is excluded as it is explicitly stated as a *nomen dubium* belonging to Neosuchia (de Andrade *et al.*, 2011a). *Coelosuchus* is placed in a basal polytomy within Goniopholididae (Williston, 1906). Given the length of time that has passed since this assignment, this placement is regarded as extremely tentative. *Kanjasuchus* is included as a goniopholidid (Halliday *et al.*, 2015). These authors recovered it as part of a polytomous assemblage, along with *Calsoyasuchus*, *Sunosuchus* and others. As such, it is placed in a basal polytomy with these taxa along with *Entradasuchus*. These authors also considered *Turanosuchus* to be a *nomen dubium*, which is followed here. *Woodbinesuchus* is placed in a basal polytomy within Goniopholididae (Lee, 1997). *Vectisuchus* is placed as part of the basal polytomy within Goniopholididae based on figure 3 of Bronzati *et al.* (2012) .

2.7.2.4.3 Thalattosuchia

For Thalattosuchia (Teleosauroidea + Metriorhynchoidea), the cladogram based on a recent analysis of the group is used (Young *et al.*, 2013b) (fig. 15). Most recently, Thalattosuchia has been recovered in a more basal position and as the sister group to all remaining crocodyliforms (Wilberg, 2015). To assess the impact of this uncertain placement for Thalattosuchia, PDE was calculated with the clade traditionally positioned within Neosuchia, and also placed as the direct sister group to Crocodyliformes (Wilberg, 2015). Both results are reported in Appendix 13.

2.7.2.4.4 Teleosauroidea

Teleosauroidea is placed as the sister taxon to all other metriorhynchoids. Taxa that are not formally named (e.g., “Ricla crocodile” and “Mr Leeds Specimen”) are not included in the supertree. Those of

questionable genus referral (e.g., "*Metriorhynchus*" *westermanni*) are included in their current taxonomic status as recorded within the Paleobiology Database (as of December, 2014). The internal relationships of Teleosauridae follow the most up-to-date and comprehensively sampled analysis of their phylogeny (Young, 2014) (fig. 7). *Geosaurus araucaniensis* is placed in an unresolved basal position within Geosarini, based on its generic relationship with other species of *Geosaurus*. For *Machimosaurus*, just a single taxon is considered to be valid here, *Machimosaurus hugii* (Martin *et al.*, 2015b), and not with two or more species (Young *et al.*, 2014b). *Haematosaurus* is placed in an unresolved position at the base of Teleosauridae (Sauvage, 1874). Given the length of time that has passed since this assignment, this placement is regarded as extremely tentative. *Peipehsuchus* is placed within Teleosauridae in an unresolved basal position (Li, 1993). *Pelagosaurus brongniarti* is placed as sister taxon to *Pelagosaurus typus* based on its generic affinity, within Teleosauridae. *Steneosaurus* is clearly a problematic taxon. According to the Paleobiology Database, there are currently 20 valid species within this genus. Making a taxonomic statement about each of these taxa is beyond the scope of the present study. However, it is obvious that this taxon is in need of a comprehensive taxonomic reappraisal. For the purposes of the present study, all taxa not already included in previous analyses (Young *et al.*, 2014b) are placed in a generic polytomy at the base of Teleosauridae. Caution should be noted for doing this for such a large number of unstable species, as this is likely to create error in the phylogenetic diversity estimates, and therefore Middle and Late Jurassic diversity should be assessed at both the genus and species level. *Teleosaurus* suffers from similar taxonomic issues to *Steneosaurus* and *Goniopholis*. The additional six species are included in a polytomy with *Teleosaurus cadomensis*, as the sister taxon to *Platysuchus*.

2.7.2.4.5 Metriorhynchoidea

The node comprising the last common ancestor of *Pelagosaurus* and *Metriorhynchus* is taken as the point to attach Metriorhynchoidea (Young *et al.*, 2013b). *Metriorhynchus* is a paraphyletic taxon and

clearly in need of taxonomic revision. *M. littoreus, M. moreli, and M. palpebosus* are placed in an unresolved position at the base of Metriorhynchidae, based on their generic affinity. *Aggiosaurus* is placed at the base of Geosaurini (Young *et al.*, 2012). Both *Cricosaurus gracilis* and *Cricosaurus lithographicus* are placed within Metriorhynchidae (Herrera *et al.*, 2013). *Cricosaurus* species are arranged to conform to this relatively well-resolved topology, instead of representing a polytomy (Young *et al.*, 2013b). *Maledictosuchus* is placed at the base of Rhacheosaurini (Parrilla-Bel *et al.*, 2013) (fig. 17). *Purranisaurus* is placed as the sister taxon to Geosaurini within Metriorhynchidae (Cau and Fanti, 2011) (fig. 6). *Suchodus* is placed at the base of Geosaurinae according to Young and de Andrade (2009) (fig. 2), as the sister taxon to all other geosaurines. *Tyrannoneustes* is placed as the sister taxon to the *Torvoneustes* species, as part of the polytomy within Geosaurini, based on figure 21 of Young *et al.* (2013a).

2.7.2.4.6 Pholidosauridae

Pholidosauridae + Dyrosauridae is the sister taxon to Thalattosuchia, which together comprise the sister clade to Goniopholididae and other higher neosuchians (including Eusuchia) (Adams, 2014). *Pholidosaurus* constitutes the most basal member of Pholidosauridae (Martin *et al.*, 2014b), and comprises four species which are unresolved with respect to each other (*P. decipiens, P. meyeri, P. purbeckensis* and *P. schaumbergensis*). Similarly, *Terminonaris* includes the two species *T. browni* and *T. robusta*, *Sarcosuchus* includes *S. hartti* and *S. imperator*, and *Elosuchus* includes *E. cherifiensis* and *E. felixi*. *Chalawan* is positioned in a polytomy with *Elosuchus* and *Sarcosuchus* (Martin *et al.*, 2014b), which also collapses *Terminonaris, Oceanosuchus*, and *Meridiosaurus* into this polytomy.

2.7.2.4.7 Dyrosauridae

Dyrosauridae is placed as the sister group to Pholidosauridae. The position of this group is still uncertain within 'Tethysuchia' (Young *et al.*, 2014c). *Chenanisuchus* is placed as the sister taxon to *Dyrosaurus* (Jouve *et al.*, 2005).

2.7.2.4.8 Bernissartiidae

Koumpiodontosuchus is placed as sister taxon to *Bernissartia* (Sweetman *et al.*, 2015). *Khoratosuchus* is placed as sister taxon to *Bernissartia* and *Koumpiodontosuchus*, outside of Paralligatoridae and Eusuchia (Lauprasert *et al.*, 2009). Note that this topology places Bernissartiidae outside of Eusuchia.

2.7.2.4.9 Susisuchidae

Susisuchus, comprising the two species *S. anatoceps* and *S. juaguaribensis*, are placed according to Young *et al.* (2012) (fig. 26), who found them to be outside of Eusuchia as the sister taxon to *Isisfordia*, a position recently confirmed by a re-analysis of this group (Turner and Pritchard, 2015).

2.7.2.5 Eusuchia

Eusuchia follows a recent investigation into their systematics (Holliday and Gardner, 2012) (fig. 9), and is positioned as the sister taxon to Paralligatoridae following several more recent analyses (Adams, 2014; Turner, 2015; Turner and Pritchard, 2015). *Allodaposuchus* is placed within Eusuchia as the sister taxon to *Hylaeochampsa* (see below) (Adams, 2014; Puértolas-Pascual *et al.*, 2014). *Aigialosuchus* is placed as the basalmost member of Eusuchia, apart from *Isisfordia*, due to its uncertain position within this clade (Martin and Delfino, 2010). *Gilchristosuchus* is placed as the sister taxon to Eusuchia (Wu and Brinkman, 1993). This position also places it outside of Paralligatoridae, and more derived than *Bernissartia*. The '*Shamosuchus*' complex was historically considered to include ten species. Recently, Turner (2015) reviewed the taxonomy of this genus, finding only *Shamosuchus djadochtaensis*, *S. gradilifrons*, and *S. major* to be valid species. However, the latter two species were transferred to their own genus, *Paralligator* (Turner, 2015). *Shamosuchus sungaricus*, *S. borealis*, and *S. karakalpakensis* are considered to be *nomina dubia*, and *S. ancestralis, S. ulgicus, S. tersus*, and *S. ulanicus* are considered to be junior subjective synonyms of *S. gradilifrons* (Turner, 2015).

2.7.2.5.1 Hylaeochampsidae

Hylaeochampsidae includes the taxa *Acynodon*, *Hylaeochampsa, Iharkutosuchus, Pachycheilosuchus* and *Pietraroiasuchus* (Puértolas-Pascual *et al.*, 2014). *Acynodon lopezi* is added to the genus *Acynodon* to form a polytomy. The group is placed as the sister taxon to *Allodaposuchus* and within Eusuchia (Puértolas-Pascual *et al.*, 2014).

2.7.2.6 Crocodylia

The positions of Crocodylia, Gavialoidea and Aegyptosuchidae follow that of the most recent analysis to include all three (Holliday and Gardner, 2012). Along with *Thoracosaurus macrorhynchus*, the other three species of *Thoracosaurus* (*T. bahiensis, T. borissai* and *T. neocesariensis*) are placed in a polytomy in a position more derived than *Eothoracosaurus* at the base of Gavialoidea. *Ocepesuchus* is placed as the sister taxon to *Thoracosaurus* within Gavialoidea based on figure 5 of Jouve *et al.* (2008). *Arenysuchus* is placed within Crocodylia basal to *Eothoracosaurus*, based on its position within Crocodyloidea (Puértolas *et al.*, 2011) (fig. 5), a group which is relatively under-sampled in the present study due to its Late Cretaceous origins. *Albertochampsa langstoni* is placed as the sister taxon to *Brachychampsus* (Norell *et al.*, 1994). *Deinosuchus* is placed in a more derived position than *Leidyosuchus* within Brevirostres (Erickson and Brochu, 1999). Its two species, *D. riograndensis* and *D. rugosus*, are retained as sister taxa to each other based on generic affinity. *Massaliasuchus* is placed in a basal polytomy with *Leidyosuchus* within Brevirostres (Martin and Buffetaut, 2008). Five Cretaceous species attributed to *Crocodylus* are also still considered as valid within the database: *C. blavieri, C. humilis, C. proavus, C. selaslophensis,* and *C. vetustus*. However, these taxa are almost definitely invalid (Mannion *et al.*, 2015), with *Crocodylus* more likely originating in the Miocene, and therefore they are excluded.

2.7.2.7 Excluded taxa due to unknown or uncertain affinities

The following taxa appear within the Paleobiology Database, but are regarded either as *nomina dubia* or have insufficient information in the published literature to make confident decisions about their phylogenetic placement. They are therefore excluded to minimise uncertainty.

Amargasuchus minor, Artzosuchus brachicephalus, Baharijodon carnosauroides, Barreirosuchus franciscoi, Bottosaurus harlani, Brachydectes major, Brasileosaurus pachecoi, Caririsuchus camposi, Chiayusuchus cingulatus, Coringasuchus anisodontis, Dakotasuchus kingi, Dianchungosaurus lufegnesis, Diplosaurus felix, Eopneumatosuchus colberti, Hadangsuchus acerdentis, Heterosuchus valdensis, Hoplosuchus kayi, Ischyrochampsa meridionalis, Itasuchus jesuinoi, Kemkemia auditorei, Leiokarinosuchus brookensis, Lisboasaurus estesi, Lisboasaurus mitracostatus, Lusitanisuchus mitracostatus, Megalosaurus mersensis, Miadanasuchus oblita, Musturzabalsuchus buffetauti, Neustosaurus gigondarum, Notochampsa istedana, Pinacosuchus mantiensis, Prodiplocynodon langi, Stomatosuchus inermis, Stromerosuchus aegypticus, Tadzhikosuchus macrodentis, Tagarosuchus kulemzini, Unasuchus reginae, Zholsuchus procevus, Zhyrasuchus angustifrons.

2.7.3 PDE using the crocodyliform supertree

A new informal crocodyliform supertree was built at both the genus and species levels (Appendix 4), and used these as the basis for producing a phylogenetic diversity estimate (PDE). The sensitivity of this approach was tested by resolving polytomies in three different ways: (1) in an 'equal' fashion, by iteratively assigning an equal portion of time to zero-length branches available from the first directly ancestral branch of positive length (Brusatte *et al.*, 2008); (2) by randomly resolving polytomies (Bell and Lloyd, 2015); and (3) by resolving polytomies under the assumption that the order of first stratigraphic appearance reflects the order of branching (note that if the first appearances of two or more unresolved taxa are identical, then they are randomly resolved) (Bell and Lloyd, 2015). Tip taxa were dated using taxonomic first (FAD) and last (LAD) occurrences extracted from the PaleoDB

(Appendix 5), and time-scaled using the R functions DatePhylo() (for the 'equal' method) and timePaleoPhy() (for the random and ordered methods) in the packages *strap* (Bell and Lloyd, 2015) and *paleotree* (Bapst, 2012), respectively. The advantage of this method over traditional time-scaling is that this eliminates zero-length branches, which are ubiquitously present due to the divergence dates shared by sister taxa, by adding a minimum branch length which forces all branches to have a minimum temporal duration. Subsequent to the dating procedure, each supertree was divided into two subtrees for marine (86 species comprising 31 genera) and non-marine (169 species comprising 115 genera) taxa (Appendices 2 and 3), using the drop.tip() function in the *ape* package (Paradis *et al.*, 2004). This removed the appropriate terminal and corresponding internal branches from the original supertrees. For each subtree, phylogenetic diversity was calculated as the sum of all known occurrences plus ghost lineages for each time bin (PDEt for 10 myr bins, and PDEs for stage bins).

2.8 Calculating extinction and origination rates

Extinction and origination rates were calculated for the global occurrence datasets for each higher taxonomic group based on two different measures. Regional origination and extinction rates are not calculated here, as at this level it becomes impossible to distinguish between these and other events, including migration and localised extirpations. 'Foote' rates (Foote, 2000; Foote, 2003) are based on cohort analysis (i.e., the number of taxa that coexisted at a precise moment compared to earlier or later subsets of taxa), and are essentially a boundary-crosser method, which counts the number of taxa that must have crossed a boundary because they are known to exist both before and after it. The equations for calculating extinction (μ) and origination (λ) rates are:

$$\mu = ln(N_b + N_{bt})/N_{bt}$$

$$\lambda = ln(N_t + N_{bt})/N_{bt}$$

Taxa that cross both boundaries are given by N_{bt}, and N_b and N_t indicate taxa that cross the bottom and top boundaries of a bin, respectively. 'The Foote' methods are considered to be conservative estimates of rates, as they assume perfect sampling, and ignore singletons (Foote, 2003), but can also suffer from 'edge' effects (i.e., under-estimation of rates at the edge of analysed windows) and the back-smearing of extinction rates (Alroy, 2014). The advantage of boundary-crossing methods, with respect to in-bin methods, is that the former compensates for potential issues with grouping taxa within bins that might not have temporally co-existed (Foote, 2003), as all measured taxa must have co-existed in time at the point of boundary-crossing. Furthermore, they are relatively robust to long-term temporal trends in the quality of preservation (Foote, 2000). In addition, such rates have the quite desirable property of being robust to errors in estimated versus real temporal durations of fossil lineages (Liow, 2007; Liow and Stenseth, 2007; Liow *et al.*, 2008). Resulting rates are considered to be proportional and instantaneous *per capita*, meaning that they describe changes at an individual basis (i.e., per lineage) for whichever taxonomic level is being described, and explicitly within the time bin that they occur in (Foote, 2000; Peters and Foote, 2002; Foote, 2003; 2005). Although resulting rates are not normalised with respect to bin duration, which might artificially inflate or reduce rates depending on relative length, Foote (2005) demonstrated that rates tend to occur as 'pulses', as opposed to being spread throughout time bins, and therefore variable bin length is unlikely to bias resulting calculations.

The second method implemented here calculates three-timer (3T) rates (Alroy, 2008; 2014), with three-timers defined as taxa from cohorts which are found immediately before, within, and immediately after a bin (Alroy, 2010a). As such, 3T rates can be thought of as a moving window estimate (i.e., it involves data from either side of the sample window of interest). 3T rates are expressed as exponential decay rates, and are corrected for the fact that members of this group might be present but not sampled in the following bin (i.e., the Signor-Lipps effect (Signor and Lipps, 1982)). The equations for extinction (μ_1) and origination (λ_1) rates are:

$$\mu_1 = ln(N_{2t,i}/N_{3t,i}) + \ln(N_{3t}/(N_{3t} + N_{pt}))$$

$$\lambda_1 = ln(N_{2t,i+1}/N_{3t,i}) + \ln(N_{3t}/(N_{3t} + N_{pt}))$$

Here, N_{2t} represents the two-timer cohort, N_{3t} represents the 3T cohort, and the denominator represents the conditional probability of a taxon being sampled given that it is definitely present throughout the time bin (Alroy, 2008; 2010a), with N_{pt} being the number of taxa sampled immediately before and after an interval, but not within it (i.e., part-timers).

2.9 Addressing the impact of sampling megabiases

Sampling of the fossil record is a non-random, and strongly structured process. Each continent, country, stratigraphic formation, and fossil-bearing locality has been subject to intense sampling heterogeneity, due to historical, political, geological, geographic, logistic, and scientific reasons (Alroy *et al.*, 2001; Smith, 2001; Bush *et al.*, 2004; Peters and Heim, 2010; Benton *et al.*, 2011; Dunhill *et al.*, 2012; Benton *et al.*, 2013a; Dunhill *et al.*, 2013; Dunhill *et al.*, 2014a). The influence of this variation is often termed as 'megabias', and broadly grouped into either geological or anthropogenic factors. Geological factors represent the broad tectonostratigraphic factors that govern the amount of rock available to us for sampling fossils. Anthropogenic factors describe more the way in which humans have invariably influenced the way in which the fossil record is sampled through changing behaviour and activities. Both of these factors come together and leave their impression on how we interpret macroevolutionary signals. For example, intervals in which there is intensive sampling and a 'good' fossil record can provide the illusion of a radiation, based simply on the fact that we have more fossils present. Similarly, intervals which are relatively barren in fossils can provide the illusion that we are witnessing an extinction event, whereas in fact the absence of taxa is merely an artefact of their lack of preservation. Such potentially misleading signals emphasise the importance of accounting for this

heterogeneity using appropriate standardisation techniques (see Section 2.6), as well as interpreting macroevolutionary patterns in the context of broad-scale sampling variations.

To assess these influences, I used a range of data series representing different sampling proxies to account for the impact of heterogeneous sampling of the Jurassic/Cretaceous tetrapod fossil record. Sampling proxies have been broadly used to account for some aspect of sampling, including geological and anthropogenic factors, which introduce error into resulting diversity curves (Benson *et al.*, 2010; Benson and Butler, 2011; Benson *et al.*, 2013; Benton *et al.*, 2013a; Butler *et al.*, 2013; Dunhill *et al.*, 2013). This is based on the expectancy that as opportunities to sample fossils increase, one would expect the number of taxonomic units sampled, and hence raw diversity, to increase proportionally. The use of sampling proxies, therefore, is to alleviate this lack of evenness of sampling through space and time, by either standardising samples or 'correcting' raw diversity for sampling bias. Commonly used proxies include the number of fossil-bearing geological formations for the target group (Peters and Foote, 2001; Butler *et al.*, 2009c; Benson *et al.*, 2010; Benson and Butler, 2011; Butler *et al.*, 2011; Butler *et al.*, 2012; Benson *et al.*, 2013; Benton *et al.*, 2013a; Brocklehurst *et al.*, 2013; Newham *et al.*, 2014), rock outcrop area or volume (Smith, 2007; Smith and McGowan, 2007; Wall *et al.*, 2011; Smith *et al.*, 2012; Smith and Benson, 2013), and the number of fossiliferous collections (Alroy *et al.*, 2001; Alroy, 2008; Alroy *et al.*, 2008; Alroy, 2010c; a; Brusatte *et al.*, 2010; Butler *et al.*, 2011; Mannion and Upchurch, 2011; Brocklehurst *et al.*, 2013; Fröbisch, 2013; Cleary *et al.*, 2015). These proxies represent some factor of sampling bias that accounts for incomplete and heterogeneous spatiotemporal sampling of different palaeoenvironments and the fossil record, including variations in rock volume, accessibility of exposed units, and variations in collecting effort

Group	J1	J2	J3	J4	J5	J6	K1	K2	K3	K4	K5	K6	K7	K8	Sum per group
Aves	0	0	0	0	0	3	4	11	9	8	8	13	31	27	114
Choristoderes	0	0	0	5	2	4	2	3	7	1	0	1	8	11	44
Lepidosauromorphs	5	1	2	5	6	9	10	10	10	9	8	11	23	26	135
Lissamphibians	0	0	1	8	5	4	10	8	8	8	8	8	20	26	114
Mammaliaforms	3	1	1	9	4	7	9	8	8	10	8	11	28	31	138
Theropods	18	4	5	27	23	26	35	31	33	32	39	34	66	78	451
Pterosaurs	3	1	6	11	12	23	12	13	11	19	16	12	22	19	180
Sauropodomorphs	13	2	6	25	14	34	22	27	20	24	25	18	24	50	304
Ornithischians	9	3	3	8	17	19	24	33	32	35	28	39	72	89	411
Crocodyliformes (terrestrial)	5	1	1	13	12	20	12	15	13	25	18	25	42	51	253
Testudines	1	0	0	7	8	29	15	19	22	23	20	36	56	61	297
Ichthyopterygians	8	4	8	6	8	15	4	6	7	18	8	0	1	0	93
Sauropterygians	7	7	9	5	18	15	9	9	11	12	16	19	17	29	183
Chelonioides	0	0	0	0	0	0	0	0	1	4	4	10	16	17	52
Crocodyliforms (marine)	1	0	8	17	18	30	4	1	5	1	2	0	5	15	107

Table 10. The number of fossil-bearing formations for different tetrapod groups filtered by approximately equal 10 million year time bins.

Geological formations represent the formally defined units of global stratigraphy, and are defined as lithologically distinct and mappable rock units. The use of formation counts as a proxy for the rock record has been discussed in detail recently, in particular in their usage to 'correct' diversity curves for geological sampling bias (Benton *et al.*, 2011; Dunhill *et al.*, 2012; Benton *et al.*, 2013a; Dunhill *et al.*, 2013; Dunhill *et al.*, 2014a; Benton, 2015). This is due to the fact that they might not be directly comparable units because of inherent features including: (1) disparities in thickness; (2) varying preservation potentials for fossils; (3) discrepancies in the time of discovery and the amount of time to accumulate fossils, including sedimentation rate; (4) different naming procedures for geopolitical reasons; (5) the extent to which they are exposed and correlate with outcrop (map) area; (6) different sedimentological and environmental conditions of formation; and (7) different temporal durations. Irrespective of this variation, the fact that numerous studies have found significant correlations with additional, non-redundant proxies for the rock record (Peters and Foote, 2001; Peters, 2005), while

others have not (Crampton *et al.*, 2003; Dunhill, 2012; Dunhill *et al.*, 2013), suggests that fossil-bearing formation counts could represent an adequate proxy for the amount of rock record available for sampling, or at least that the association is worth testing.

In addition to this is the issue of 'redundancy', which arises from non-independence of sampling proxies and diversity when calculated at the same taxonomic level (Benton *et al.*, 2011; Benton *et al.*, 2013a; Dunhill *et al.*, 2014b; Benton, 2015) (e.g., comparing dinosaur-bearing formations to dinosaur diversity). One method for mitigating these potential issues is to use a sampling proxy that represents a more inclusive clade and that includes the target clade (Upchurch and Barrett, 2005; Mannion *et al.*, 2011; Brocklehurst *et al.*, 2013; Cleary *et al.*, 2015), such as comparing a tetrapod-bearing formations metric to dinosaur diversity. Therefore, for both the marine and non-marine realms, I calculated the number of marine (MBF) and non-marine (TBF) tetrapod-bearing formations at a global level, respectively, and also separately for North America and Europe, in order to test their relationships with uncorrected and subsampled diversity estimates for all tetrapod groups. Tetrapod-bearing formations are defined as any named geological formation that has ever yielded a published tetrapod body fossil, irrespective of the completeness of the specimens, and based on records within the PaleoDB. These formation counts were divided into marine and non-marine partitions, based on whether or not marine and non-marine fossils occurred within them. Some marine formations were included the non-marine tetrapod-bearing formations count because they have yielded some non-marine tetrapod fossils, and therefore represent opportunities to sample the latter. In addition to accounting for redundancy, the use of a tetrapod-level metric also accounts for failure to sample fossils from individual tetrapod groups, which would be obscured in lower level formation proxies. Furthermore, the use of a tetrapod-level proxy reflects the total potential of the geological record to yield fossils, and overcomes failure to yield fossils of individual groups based either on lower abundance of fossil groups, or genuine opportunities to sample them. TBF data series were divided into stage and 10 myr time bins in the same manner as for the occurrence data sets. Note that this

means that single formations with long temporal durations can be included in multiple time bins, as long as fossils occur within each bin a formation occupies.

Group	J1	J2	J3	J4	J5	J6	K1	K2	K3	K4	K5	K6	K7	K8	Sum per group
Aves	0	0	0	0	0	8	4	14	37	11	8	22	62	52	218
Choristoderes	0	0	0	6	2	12	1	3	13	2	0	1	24	36	100
Lepidosauromorphs	11	3	3	7	6	36	16	18	14	17	12	16	68	57	284
Lissamphibians	0	0	1	11	6	12	12	14	11	11	13	16	35	66	208
Mammaliaforms	14	4	1	12	10	31	19	15	13	19	17	20	76	91	342
Theropods	44	5	5	40	59	164	59	89	74	63	60	64	252	241	1219
Pterosaurs	6	1	10	12	16	55	21	24	26	28	31	20	36	28	314
Sauropodomorphs	63	2	7	49	39	177	39	55	41	48	38	42	46	133	779
Ornithischians	34	3	3	12	30	114	69	95	65	67	41	50	355	323	1261
Crocodyliformes (terrestrial)	15	1	1	14	18	72	29	41	23	35	34	62	107	131	583
Testudines	1	0	0	8	12	95	34	33	29	35	29	48	149	154	627
Ichthyopteryians	26	5	23	5	22	36	10	13	11	33	12	0	1	0	197
Sauropterygians	18	7	22	6	48	54	16	11	14	19	27	32	51	45	370
Chelonioides	0	0	0	0	0	0	0	0	1	8	4	14	24	29	80
Crocodyliformes (marine)	1	0	17	26	39	73	9	1	5	1	2	0	4	24	202

Table 11. The number of fossil-bearing collections for different tetrapod groups filtered by approximately equal 10 million year time bins.

To assess the impact of anthropogenic factors that might bias sampling, I used a metric based on the number of collections in the PaleoDB. Collections-based sampling metrics are representative of irreducible instances in which fossils have been sampled from a particular stratigraphic horizon at a discrete location. They have been commonly used as the basis to reconstruct standardised diversity through sub-sampling approaches (Alroy, 2010a; b; c). PaleoDB collections are a proxy for anthropogenic factors, such as sampling of fossil-bearing localities, and worker effort on fossils from those localities reflected in the published literature. They are underpinned by the availability of opportunities to sample from particular rock units, and therefore undoubtedly also capture an aspect of heterogeneity in the availability of fossil-bearing rock units. To account for this I used a 'higher level' metric of tetrapod-bearing formations and collections that should reduce any redundancy. I followed

the same time series analysis protocol (see Chapter 2) as for all other extrinsic factors to test the relationship between collection and formation counts and uncorrected and subsampled diversity.

Outcrop area has been used widely as a metric to quantify the availability of fossiliferous rock from which to sample (Crampton *et al.*, 2003; Smith, 2007; Smith and McGowan, 2007; McGowan and Smith, 2008; Smith *et al.*, 2012), and some other studies have used 'packages' as a way of estimating rock record volume (Peters and Foote, 2001; Peters, 2005). The use of outcrop area as a sampling proxy remains questionable due to inconsistency in its relationship with the amount of rock available to sample fossils from (i.e., exposure area) (Dunhill, 2012). Global records of the sedimentary rock record have not been compiled at stratigraphic scales finer than epochs (Wall *et al.*, 2009), and therefore testing the relationship between rock outcrop area and diversity is limited to a regional scale, which is the preferable approach when using this proxy (Dunhill, 2012). Regional records have been compiled for North America, based on sediment coverage area from the COSUNA dataset (Correlation of Stratigraphic Units of North America) (Peters and Heim, 2010), and for western Europe based an equal-grid sampling method of outcrop areas derived from geological maps (Smith and McGowan, 2007). I used the marine and terrestrial units from the COSUNA dataset (Peters and Heim, 2010), and the total rock estimate from western Europe (Smith and McGowan, 2007) to represent non-redundant quantifications of the amount of sedimentary rock available for sampling from North America and Europe, respectively. This aspect of non-redundancy is particularly important here (Smith, 2007; Benton *et al.*, 2011; Benton, 2015), as macrostratigraphic measures of the rock record are independent of the fossil record (Peters and Heim, 2010). By using both geological and collection-based proxies, it becomes possible to address the two major modes of bias that can be potentially introduced into fossil occurrence datasets.

In addition to the above, I also tested the relationship between global sampling and sea-level for evidence of the 'common cause' hypothesis, which explains that short-term fluctuations in both

sampling and diversity are related to a third, external factor, such as sea level, temperature, or continental weathering rates (Sepkoski Jr *et al.*, 1981; Peters, 2005; Peters and Heim, 2010; Hannisdal and Peters, 2011). Sea level has been the most investigated driver for such hypotheses, with proposals that reduction in sea level leads to increasing continental area and therefore higher diversity through a species-area effect, while higher sea levels can lead to greater continental flooding, habitat fragmentation and endemism ultimately promoting diversity (Upchurch and Barrett, 2005; Butler *et al.*, 2011), as well as sampling opportunities due to increasing preservation of these habitats. While a common cause factor might manifest itself on a smaller-scale regional level (Dunhill, 2011; Dunhill *et al.*, 2014a), others have found no significant correlation between short-term (i.e., detrended) fluctuations in global sampling effort or dinosaur diversity and sea level (Butler *et al.*, 2011). By using this complete set of proxies, it should be possible to distinguish whether relationships between diversity and sampling are correlated through sampling bias, redundancy, or common cause (Benton *et al.*, 2011; Benton *et al.*, 2013a).

2.9.1 *Lithological changes across the J/K transition*

A further dimension to consider for diversity analyses is the link between sampled diversity, the fossil record, and the structure of the geological record in terms of the 'geodiversity', or lithological diversity through time. Diversity studies considering the link between the rock record and the fossil record are now commonplace in the palaeontological literature, but an often ignored dimension is that of lithofacies diversity (Smith and Benson, 2013). Lithofacies comprise groupings of geological rock types that represent similar facies or depositional environments. Using the new occurrence-level based database for each higher tetrapod clade used throughout this thesis, primary ithological data were summed and analysed. The major rock types for each occurrence included: carbonates, claystones, conglomerates, mudstones, sandstones. shale, siltstones, other, and unknown. Simple counts were

calculated for each of these lithological classes at 10 million year time bin intervals for each group. This included occurrences that were not defined higher than the genus level to capture the total distribution of fossils for each group and the maximum possible lithological diversity. These lithological subgroups were then summed into coarse 'lithofacies' units representing carbonates, fine siliciclastics (mudstone, claystone, shale), and coarse siliclastics (sandstone, siltstone, conglomerates) for each tetrapod group (Figure 29).

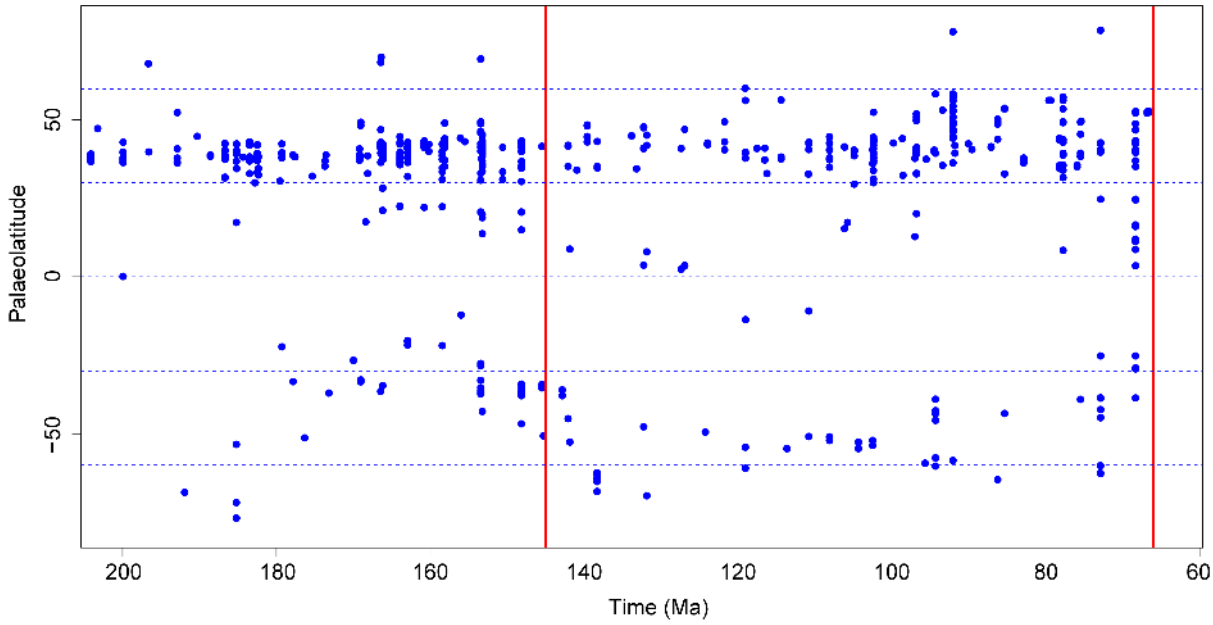


Figure 20. Palaeolatitudinal distribution of all marine tetrapod occurrences through the Jurassic and Cretaceous. The Jurassic/Cretaceous (145 Ma) and end-Cretaceous (66 Ma) boundaries are highlighted in red. Palaeolatitudes are based on Scotese rotations, and acquired from the Paleobiology Database

2.10 Model-fitting procedure

Biological diversity is regulated through the complex interaction between organisms and their environment, and the changes between abiotic and biotic factors through time. One of the key questions in palaeobiology is what were the mechanisms that acted to drive changes in biodiversity through deep time, and whether or not we can untangle the complicated web of biotic and abiotic

processes and their interaction with macroevolutionary patterns. Abiotic factors typically regard those which are organism-independent, and environmental or geological in nature, and include geochemical cycles, continental motion and orogenesis, erosion and weathering, volcanic eruptions or bolide impacts, and changes in climate, weather, and sea level patterns.

2.10.1 Extrinsic parameter selection

To explore the impact of abiotic patterns on diversity, a range of environmental variables were extracted from the primary literature (Table 12) to test whether extrinsic factors were the drivers of tetrapod diversity dynamics. These environmental proxies include: (1) eustatic sea level (Miller *et al.*, 2005); (2) palaeotemperature ($\delta^{18}O$) (Prokoph *et al.*, 2008); (3) the global carbon ($\delta^{13}C$) cycle (Prokoph *et al.*, 2008): (4) the global sulphate ($\delta^{34}S$) cycle (Prokoph *et al.*, 2008); (5) the global strontium ($^{87}Sr/^{86}Sr$) cycle (Prokoph *et al.*, 2008; Hannisdal and Peters, 2011); and (6) an estimate of global subsampled marine invertebrate biodiversity (Hannisdal and Peters, 2011), which are used here to assess whether patterns between tetrapods and marine invertebrates are congruent and driven by a common, underlying pattern. These environmental parameters were previously presented at the stage level, so were transformed into 10 myr time bin data by taking the arithmetic mean of values for groups of data points that fall within the individual time bin intervals (Table 13, Table 14). For the majority of tetrapod groups, subsampled diversity is too sparse too perform correlation tests with any sort of confidence at the stage level (i.e., there is too much missing data). To avoid drawing potentially spurious conclusions from inadequate data, the model-fitting analyses are largely restricted to diversity at 10 million year time intervals, for which resulting diversity time series are more continuous. For Crocodyliformes, correlation tests involving PDEs were constrained to the Bathonian–Albian interval, and J2 to K7 for PDEt, to remove potential skewing by edge effects associated with phylogenetic methods of estimating biodiversity. SQSPs was also constrained to the Bathonian–Albian,

as the results had little resolution outside of this interval. For the purposes of the present study, each of these factors are considered to be firstly independent of diversity, and each one is therefore analysed independently as a distinct factor that can influence diversity. However, in reality this is clearly not the case; for example, we would expect temperature and sea level to be intricately inter-linked through thermal expansion of seawater and melting of polar ice caps, which in turn will control the macrostratigraphic architecture of the geological record and the number and type of geological formations to sample from. The advantage of this approach is that it is possible to assess the relative strength of association of the individual parameters. These relative scores can be considered in combination simply by adding them together, as the scores are normalised (see below). This is a considerably more favourable, and less time consuming, approach then running large numbers (6 factorial) of multiple regressions for each estimate of diversity produced by the range analyses performed here.

Parameter	Source	Proxy for
Non-marine rock outcrop area (NMA)	Benson and Butler, 2011	Area of shallow marine habitat available
Fossiliferous marine formation (FMF)	Benson and Butler, 2011	Geological sampling of marine environments
Eustatic sea-level (1)	Miller *et al*., 2005	Area of shallow marine habitat available
Eustatic sea-level (2)	Haq *et al*., 1997	Area of shallow marine habitat available
$\delta^{18}O$	Prokoph *et al*., 2008	Inverse proxy for temperature
$\delta^{13}C$	Prokoph *et al*., 2008	Biological activity
$\delta^{34}S$	Prokoph *et al*., 2008	Organic nutrient inputs or shelf redox conditions
$^{87}Sr/^{86}Sr$	Prokoph *et al*., 2008	Inorganic nutrient inputs
Sea-surface temperature (based on $\delta^{18}O$)	Martin *et al*., 2014	Global sea-surface temperature
Global SQS marine animal diversity	Hannisdal and Peters, 2011	Subsampled marine animal diversity

Table 12. Extrinsic variables used in the present study, their sources, and the environmental factors they represent.

Bin	Mid-point	Sea level (Haq)	Sea level (Miller)	NMA	FMF	$\delta^{18}O$	$\delta^{13}C$	$^{87}Sr/^{86}Sr$	$\delta^{34}S$	SQS div	SST
Jurassic 1	196.05	16.316	NA	148	37	-0.603	0.108	0.708	17.728	13.4	23.5
Jurassic 2	186.75	46.989	NA	142	48	-0.830	0.402	0.707	17.548	18.84	23
Jurassic 3	176.5	66.562	NA	138.75	25	-1.202	1.618	0.707	17.679	7.94	28
Jurassic 4	168.2	82.897	-28.166	135.5	47	-2.388	1.112	0.707	17.272	6.375	23.5
Jurassic 5	161.7	69.766	-23.021	130	76	-1.232	1.299	0.707	16.385	6.66	23
Jurassic 6	151.5	131.638	-5.624	130	65	-2.146	1.669	0.707	16.154	7.685	21
Cretaceous 1	139.45	105.889	-21.686	127	67	-0.523	-0.814	0.707	16.812	7.01	21
Cretaceous 2	130.1	141.453	-8.771	125	55	-0.012	0.148	0.707	17.260	7.675	21
Cretaceous 3	119.65	154.439	-6.687	131	108	0.047	3.329	0.707	16.236	37.39	21
Cretaceous 4	106.75	181.656	6.137	129	163	-2.467	2.070	0.707	15.898	38.76	24
Cretaceous 5	97.2	227.843	46.260	118	114	-2.511	2.400	0.707	18.324	18.56	27
Cretaceous 6	88.75	222.289	22.429	119	65	-1.900	2.440	0.707	18.318	13.507	30.7
Cretaceous 7	77.85	226.317	33.348	110	146	-1.509	2.350	0.708	18.589	31.08	22
Cretaceous 8	69.05	203.145	28.610	109	130	-1.203	2.413	0.708	18.852	49.26	22

Table 13. Extrinsic environmental parameters and sampling metrics used for the model-fitting procedure. Data are presented in approximately equal 10 million year time bins (see Section 2.3). Sources provided in text . NMA, Non-marine rock outcrop area; FMF, Fossiliferous marine formations; SQS div, Subsampled marine invertebrate diversity using Shareholder Quorum Subsampling (SQS) method; SST, Sea-surface temperature.

Stage	Mid-point	Sea level (Haq)	Sea level (Miller)	NMA	FMF	$\delta^{18}O$	$\delta^{13}C$	$^{87}Sr/^{86}Sr$	$\delta^{34}S$	SQS div	SST
Hettangian	200.3	2.040	NA	150	35	-1.381	1.171	0.708	17.911	11.26	23
Sinemurian	195.05	30.591	NA	146	39	0.174	-0.954	0.708	17.544	15.54	24
Pliensbachian	186.75	46.989	NA	142	48	-0.830	0.402	0.707	17.548	18.84	23
Toarcian	178.4	52.573	NA	139	34	-1.202	1.618	0.707	17.668	6.81	30
Aalenian	172.2	80.552	NA	138.5	16	-1.202	1.618	0.707	17.689	9.07	26
Bajocian	169.3	95.085	-27.656	138	48	-2.388	1.112	0.707	17.420	6.8	24
Bathonian	167.2	70.709	-28.676	133	46	-2.388	1.112	0.707	17.124	5.95	23
Callovian	164.8	49.971	-26.008	128	60	-1.244	0.725	0.707	16.615	2.6	25
Oxfordian	160.4	89.560	-20.035	132	92	-1.220	1.872	0.707	16.154	10.72	21
Kimmeridgian	154.7	130.687	-3.254	130	51	-2.146	1.669	0.707	15.993	3.76	23
Tithonian	148.55	132.588	-7.995	130	79	-2.146	1.669	0.707	16.315	11.61	19
Berriasian	142.4	134.098	-19.034	127	57	-0.523	-0.814	0.707	16.637	7.63	21
Valanginian	136.35	77.680	-24.338	127	77	-0.523	-0.814	0.707	16.986	6.39	21
Hauterevian	131.15	118.780	-20.547	125	55	-0.102	0.079	0.707	17.144	7.55	20
Barremian	127.2	164.126	3.005	125	55	0.078	0.216	0.707	17.375	7.8	22
Aptian	119	154.439	-6.687	131	108	0.047	3.329	0.707	16.236	37.39	21
Albian	106.75	181.656	6.137	129	163	-2.467	2.070	0.707	15.898	38.76	24
Cenomanian	97.2	227.843	46.260	118	114	-2.511	2.400	0.707	18.324	18.56	27
Turonian	91.85	232.836	24.617	121	87	-2.173	2.787	0.707	18.652	18.47	32
Coniacian	88.05	219.126	19.750	118	47	-1.991	2.192	0.707	18.310	10.16	29
Santonian	84.95	214.906	22.920	118	62	-1.537	2.341	0.707	17.993	11.89	31
Campanian	77.85	226.317	33.348	110	146	-1.509	2.350	0.708	18.589	31.08	22
Maastrichtian	69.05	203.145	28.610	109	130	-1.203	2.413	0.708	18.852	49.26	22

Table 14. Extrinsic environmental parameters and sampling metrics used for the model-fitting procedure. Data are presented in bins representing geological stages (see Section 2.2). Sources provided in text (Section 2.8). Abbreviations as Table 13.

Prior to any model-fitting analyses, auto-correlation was examined for each extrinsic time series through application of the Durbin-Watson statistic. This test was applied to the residuals from each regression analysis, where the null hypothesis is that errors are serially uncorrelated, and the alternative hypothesis that they follow a first-order autoregressive process. All p-values were calculated using the durbinWatsonTest() function in the *car* package in R (Table 15). The maximum lag to compute the residual autocorrelations was set to 1, and the p-values were estimated by bootstrapping with 1000 replications, resampling from the observed residuals. The results show that non-marine rock outcrop area, sea level, strontium isotopes, and sea-surface temperature are all

significantly auto-correlated, with a first-order lag. The null hypothesis was not rejected for all other parameters, implying that they are primarily non-autocorrelated and independent of any long-term trend within the time series. This lack of autocorrelation is automatically compensated for in the arima modelling step, with any detrending simply producing the original time series through acknowledgement that there is an overall lack of autocorrelation. Nonetheless, this provides an important step in determining whether a time series is actually auto-correlated before applying any detrending or autoregressive modelling steps, which can lead to potential over-fitting of the data and introduction of error.

	p-value	
Factor	**10 myr**	**Stage**
NMA	0.0015	0.001
FMF	0.1674	0.1652
Sea level (Miller)	0.4943	0.3641
Sea level (Haq)	0.0351	0.0353
Oxygen	0.3964	0.2944
Carbon	0.4393	0.3976
Strontium	1.413E-07	1.74E-07
Sulphur	0.0021	0.0013
SQS diversity	0.2752	0.2831
SST	0.0198	0.0191

Table 15. P-values from resulting Durbin-Watson tests for autocorrelation.

2.10.2 Time series analysis

A time series comprises a sequence of logically connected points representing successive (i.e., naturally ordered) measurements throughout a time interval. For each of the datasets (i.e., those representing temporal diversity, and those representing extrinsic parameters), it is assumed that they are representative of a time series, as opposed to independent observations sampled from an underlying distribution. The reason for this is that for each series, it is logical to assume they are governed by the same ecological, environmental, and evolutionary laws and processes through time,

and therefore statistically dependant on each other, irrespective of whether or not a trend exists. This justifies the exploration of an autoregressive component in each of the datasets. Time series analysis essentially has two components: (1) to seek whether or not there is a dependency in the data series through time (i.e., a 'trend'), and (2) whether there are any independent characteristics of the series that can be used to make meaningful observations about the data through time. From this, cross examination of time series can be used to infer the relationships between two independent time series.

2.10.3 Autocorrelation of time series

Testing for auto-correlation is part of a subset of methods known as wavelet analysis, and is the examination of serial dependence within a time series (i.e., the statistical dependence of different values within the time series). Auto-correlation is the statistical similarity of different values as a function of the time lag between them, and determines whether there are repeated patterns or trends within a time series. The ARIMA method (Auto-regression with integrated moving average) applies moving averages, detrending, and regression methods to detect and remove any autocorrelation within a time series. The difference between using an integrated moving average model to a standard autoregressive model is that the number of lagged residuals to include in the regression analysis is determined by the auto-correlation function. An ARIMA process has three components: (1) the auto-regressive component, which removes the effect of previous observations; (2) the integrated component, which removes long-term trends within the data set by introducing an initial differencing step; and (3) the moving average component, which accounts for random error in previous observations (Wei, 1994). I used a first-order autoregressive model for each time series, as models of additional complexity will likely lead to over-fitting of estimated parameters to what are naturally relatively small time series (i.e., constrained by the number of observations).

The autoregressive function is set as ARIMA(p,d,q), where p is the number of autoregressive terms (the 'order' of the model), d is the number of non-seasonal (temporally structured) parameters needed to force stationarity about the mean for the time series (i.e., the degree of differencing), and q is the number of lagged 'forecast' errors from the prediction equation (the model), or the order of moving average component. To avoid making assumptions about the seasonality and error structure of the time series, q and d were consistently set to 0. The first-order autoregressive model is therefore input as ARIMA(1,0,0) (also denoted as AR(1)), and implies that the time series is stationary, contains a component of autocorrelation, and each successive value can be predicted based on the slope coefficient of the model and the previous observation .

The residuals of each of the selected environmental parameters were calculated by using the arima() function, which employs maximum likelihood to fit a first-order autoregressive (AR(1)) model to each time series (Gardner *et al.*, 1980) (http://search.r-project.org/R/library/stats/html/arima.html). This method removes the influence of any long-term background trend (i.e., a directed change in the mean value of the total time series through time) within the dataset, which can artificially inflate correlation coefficients (Box and Jenkins, 1976), and also accounts for serial autocorrelation (i.e., the correlation of a variable with itself through successive data points). A range of differencing techniques have been widely applied to correct time series when analysing fossil vertebrate data (Benson *et al.*, 2010; Butler *et al.*, 2011; Benton *et al.*, 2013a), and this method is used here because the maximum likelihood fitting approach accounts for missing values in the time series (i.e., not applicable), as opposed to treating them as zero data (Jones, 1980).

2.10.4 Assessing the relative relative fit of extrinsic parameters

The residuals of each time series were independently compared using linear regressions to each of the measures of diversity, using the lm() function. The relative fit of each variable was assessed using

the sample-size corrected Akaike Information Criterion (AICc) (Hurvich and Tsai, 1989), by calculating the likelihood and weight for each environmental parameter as a way of assessing the probability of each one among the candidate set of models. In addition, pairwise correlation tests were performed between the diversity estimates and each environmental parameter using parametric (Pearson's product moment correlation coefficient [r]) and non-parametric (Spearman's rank [ρ]) methods. For each pairwise statistical hypothesis test, both the raw and adjusted p-values are reported, the latter calculated using the p.adjust() function, and using the 'BH' model (Benjamini and Hochberg, 1995). This procedure controls for the false-discovery test when performing multiple hypothesis tests with the same data set, which can inflate type-2 error (i.e., to avoid falsely rejecting the null hypothesis). These adjustments were performed on 'families' of the data set, rather than on all correlation tests, to avoid the risk of setting the pass rate for statistical significance too low. All analyses were carried out in R version 3.0.2 (R Development Core Team, 2013) unless specified otherwise.

2.11 Building an atoposaurid character matrix

2.11.1 Taxon sampling

The final chapter of this thesis involves investigating the phylogenetic relationships of atoposaurid crocodyliforms, based on first-hand investigation of specimens and the construction of a new character matrix. Full details on this, including the taxonomic history of this group, are provided in Chapter 5, but details on the methods are given here for structural consistency.

All previously identified atoposaurid species were included (Table 78), with the exception of *Karatausuchus sharovi* (Efimov, 1976; 1996; Storrs and Efimov, 2000), which I was not able to observe directly, and for which there is insufficient morphological data published to adequately score it from the literature. I also excluded *Shantungosuchus chuhsienensis* (Young, 1961) for similar reasons, and

because this taxon is likely to be a protosuchian-grade crocodyliform (Wu *et al.*, 1994). All observations of specimens were made based on first-hand examinations. Measurements and ratios of key morphological characteristics are provided in Table 16, Table 18, Table 19 and Table 20, respectively. For specimens not personally observed, measurements were acquired using reported values and via ImageJ (http://imagej.nih.gov/ij/) (Schneider *et al.*, 2012) from published photographs of specimens. Most measurements and ratios provided are given to two decimal places and based on the holotype specimens, as opposed to multiple specimens. As such, I do not provide ratio ranges for species.

Both species of *Atoposaurus* (*A. jourdani* and *A. oberndorferi*) and *Alligatorellus* (*A. bavaricus* and *A. beaumonti*) were included, as well as *Alligatorium meyeri*, based on first-hand observations, and *Alligatorium franconicum* was scored based on figures and illustrations (Wellnhofer, 1971). These taxa have previously been regarded as representing multiple ontogenectic stages of a single lineage (Benton and Clark, 1988), and therefore to test this a number of primary anatomical measurements (skull width, snout length, and orbit length) were plotted for each of the species against skull length, and also carried out a covariance-based Principal Components Analysis (PCA) in R. PCA is a method that is often used to visualise the axes of greatest variation in a multi-dimensional dataset. It works by running a series of orthogonal multivariate linear regressions, and then selecting those vectors that describe the most variance for further scrutiny. The first principal component is that which describes the most variance, and each succeeding component describes proportionally less. If all three potential genera are part of the same lineage, then we might expect that the German specimens and the French specimens follow independent allometric trajectories, whereas if they do not then it is more likely that individual specimens represent individual taxa. Note that the specimen count for these putative taxa is very low for each, and therefore these resulting allometric trajectories are tentative, but the best possible way of assessing this based on the currently available data.

All species of *Theriosuchus* were included, with *T. pusillus*, *T. ibericus* and *T. sympiestodon* (supplemented by new material (Martin *et al.*, 2014c)) scored based on first-hand observations. The primary literature was used for *T. guimarotae* (Schwarz and Salisbury, 2005) and *T. grandinaris* (Lauprasert *et al.*, 2011). Scoring for *Montsecosuchus depereti* was based on personal observation, as were specimens described as *Alligatorellus* sp. (MB.R.3632, from the Late Jurassic of Germany) (Schwarz-Wings *et al.*, 2011), and *Theriosuchus* sp. (NMS G. 2014.52.1, from the Middle Jurassic of the Isle of Skye, UK) (Young *et al.*, 2016), with both incorporated to test their generic assignment. In addition, *Brillanceausuchus babouriensis* (Michard *et al.*, 1990) and *Pachycheilosuchus trinquei* (Rogers, 2003) were also included as previously identified putative atoposaurids, both based on personal observations.

Taxon	Total length	Tail length	Skull length	Skull width	Snout length	Orbit length	Orbit width	Supratemporal fenestra length	Supratemporal fenestra width	Symphysis length	Intermandibular angle	Premaxillary teeth	Maxillary teeth	Personally observed	Specimen	Source
"*Alligatorellus*" sp.	NA	NA	NA	NA	NA	NA	NA	NA	NA	NA	NA	NA	NA	Yes	Referred specimen	Schwarz-Wings *et al*., 2011
Alligatorellus bavaricus	288	165	40.9	18.5	13.7	13.1	9.3	5.7	4	7	45	NA	NA	Yes	Holotype	Wellnhofer, 1971; Tennant and Mannion, 2014
Alligatorellus beaumonti	193.4	165	35.5	17.2	13.6	9.2	8	5.7	3.6	7	43	NA	9	Yes	Holotype	Wellnhofer, 1971; Tennant and Mannion, 2014
Alligatorium franconicum	NA	NA	77	27.8	42.6	14.6	11	11.4	5.4	NA	36	NA	NA	No	Holotype of *A. paintenense*	Wellnhofer, 1971; Tennant and Mannion, 2014
Alligatorium meyeri	NA	NA	65.6	29	25.3	18	12.5	10.2	6.1	NA	45	NA	11	Yes	Holotype	Wellnhofer, 1971; Tennant and Mannion, 2014
Amphicotylus lucasii	NA	NA	480	288	320	48	40	56	40	NA	34	5	15	Yes	Referred specimen	Smith *et al*., 2010
Atoposaurus jourdani	188	111	20	15.6	8.3	8.6	5.8	NA	NA	NA	55	NA	NA	Yes	Holotype, referred specimen	Wellnhofer, 1971; Tennant and Mannion, 2014
Atoposaurus oberndorferi	130	96	26	13.1	NA	9.1	5.6	NA	NA	4	NA	NA	NA	Yes	Holotype	Wellnhofer, 1971; Tennant and Mannion, 2014
Brillanceausuchus babourensis	800	NA	75	42	34	11	12	14	6	NA	42	NA	15	Yes	Holotype	Michard *et al*., 1990
Eutretauranosuchus delfsi	NA	NA	416.6	211.9	251.8	58	39.9	53.2	31.8	NA	33	NA	17	Yes	Holotype	Pritchard *et al*., 2013
Hoplosuchus kayi	NA	NA	31	23	9.5	10	6.8	NA	NA	5	45	NA	14	Yes	Holotype	Gilmore, 1926
Karatausuchus sharovi	186	116.4	26.9	NA	10.4	8	5.6	3.2	1.7	NA	NA	NA	NA	No	Holotype	Storrs and Efimov, 2000
Koumpiodontosuchus aprosdokii	NA	NA	112	55	70	20	15	14	10	15	32	4	19	No	Holotype	Sweetman *et al*., 2015
Montsecosuchus depereti	NA	NA	53.4	29.7	20	13.2	9.3	6	5.7	6	61	NA	NA	Yes	Holotype	Buscalioni and Sanz, 1990
Pachycheilosuchus trinquei	NA	NA	NA	NA	NA	NA	NA	NA	NA	6	NA	NA	15	Yes	Holotype, referred specimens	Rogers, 2003
Pholidosaurus purbeckensis	NA	NA	NA	117	NA	33	33	41.7	41.7	NA	NA	NA	NA	Yes	Holotype	Salisbury, 2002
Protosuchus richardsoni	NA	133	113	86	44	25	5	17	14	NA	48	4	13	Yes	Holotype	Colbert and Mook, 1951
Sabresuchus ibericus	NA	NA	NA	NA	NA	NA	NA	NA	NA	12	NA	NA	14	Yes	Holotype	Brinkmann, 1992
Sabresuchus sympiestodon	NA	NA	NA	NA	NA	NA	NA	12	10	11	NA	NA	11	Yes	Holotype	Martin *et al*., 2010; 2014
Shamosuchus djadochtaensis	NA	NA	128	86	64	21	18	20	15	NA	42	NA	12	No	Holotype, referred specimen	Pol *et al*., 2009
Theriosuchus bhobhaltos	NA	NA	NA	NA	NA	NA	NA	NA	NA	12	NA	NA	NA	Yes	Holotype	Young *et al*., in press
Theriosuchus grandinaris	NA	NA	NA	NA	NA	NA	NA	NA	NA	12	NA	5	NA	No	Holotype	Lauprasert *et al*., 2011
Theriosuchus guimarotae	NA	NA	74.2	40.8	34.9	14.9	13.6	11.4	8.8	4	44	5	14	No	Holotype	Schwarz and Salisbury, 2005
Theriosuchus pusillus	NA	NA	84.3	55.7	35.7	22	16.1	12.9	11.6	12	45	5	14	Yes	Holotype, paratype	Owen, 1879
Wannchampsus kirpachi	NA	NA	64	44.8	24.6	17.2	16.2	8.5	8.7	17.3	40	NA	11	Yes	Holotype	Adams, 2014

Table 16. Primary cranial measurements and counts for all OTUs analysed for phylogenetic analysis. Details of the source and observation status also provided.

Several basal 'protosuchian'-grade taxa were selected along with a range of neosuchian taxa for outgroups. *Protosuchus richardsoni* (Colbert *et al.*, 1951) and *Hoplosuchus kayi* (Gilmore, 1926) were incorporated as protosuchians, both based on personal observations. Within Neosuchia, the goniopholidid *Amphicotylus lucasii* (Mook, 1942) was selected and scored based on personal observation, and *Eutretauranosuchus delfsi*, based on two publications (Smith *et al.*, 2010; Pritchard *et al.*, 2012), as these both preserve highly complete cranial material. In addition to these goniopholids, *Pholidosaurus purbeckensis* (Salisbury, 2002) was included as a further representative of 'coelognathosuchian' crocodyliforms (Martin *et al.*, 2014b). *Koumpiodontosuchus aprosdokiti* was also selected to represent Bernissartiidae (Sweetman *et al.*, 2015). The 'advanced neosuchian' *Wannchampsus kirpachi* (Adams, 2014) was also included based on personal observation due to its noted similarity with *Theriosuchus pusillus*, and *Shamosuchus djadochtaensis* (Pol *et al.*, 2009) was also included. Both of these taxa are likely to belong to the advanced neosuchian (and possibly eusuchian) group Paralligatoridae (Turner, 2015). *Protosuchus* was constrained as the ultimate outgroup taxon in each analysis. Stratigraphic range (i.e., temporal duration) data are all provided in Table 17.

Taxon	FAD	LAD
Alligatorellus bavaricus	152.1	148.55
Alligatorellus beaumonti	157.3	152.1
Alligatorium meyeri	157.3	152.1
Amphicotylus lucasii	157.3	152.1
Atoposaurus jourdani	157.3	152.1
Atoposaurus oberndorferi	152.1	148.55
Brillanceausuchus babouriensis	145	139.8
Eutretauranosuchus delfsi	155.7	150.2
Hoplosuchus kayi	152.1	148.55
Koumpiodontosuchus aprosdokiti	129.4	125
Montsecosuchus depereti	142.4	136.35
Pachycheilosuchus trinquei	113	106.75
Pholidosaurus purbeckensis	145.5	139.8
Protosuchus richardsoni	201.3	199.3
Shamosuchus djadochtaensis	77.85	72.1
Theriosuchus grandinaris	125	118
Theriosuchus guimarotae	157.3	152.1
Sabresuchus ibericus	129.4	125
Theriosuchus pusillus	145	139.8
Theriosuchus sp.	169.3	166.1
Sabresuchus sympiestodon	72.1	66
Wannchampsus kirpachi	125	114

Table 17. Stratigraphic ranges for all sampled OTUs for the atoposaurid phylogenetic analysis. FAD, First Appearance Datum; LAD, Last Appearance Datum.

Table 18. Primary axial, pectoral, and forelimb measurements and counts for all OTUs analysed for phylogenetic analysis.

Taxon	Cervical vertebrae	Dorsal vertebrae	Sacral vertebrae	Caudal vertebrae	Coracoid length	Scapula length	Humerus length	Ulna length	Radius length	Ulnare length	Radiale length	MC I	MC II	MC III	MC IV	MC V	Manus length	Forelimb length
"*Alligatorellus*" sp.	NA	NA	NA	NA	NA	NA	NA	NA	NA	NA	15.7	11.1	11.2	8.6	10.7	5.5	NA	NA
Alligatorellus bavaricus	7	15	3	40	NA	9.3	24.6	17	16.9	5	5	NA	NA	NA	NA	NA	21.5	63.1
Alligatorellus beaumonti	7	17	2	40	5.8	13	19.6	17.5	16.7	5.5	6.5	3.8	4.5	4.6	4.1	3	19	56.1
Alligatorium franconicum	7	15	2	NA	NA	NA	35	27.4	24	5.4	6.8	6.8	8.1	7.7	5.5	NA	31.7	94.1
Alligatorium meyeri	7	17	NA	NA	8.9	NA	NA	29.9	28.9	8.7	10.3	4.9	6.6	6.7	6.5	4.2	29.5	NA
Amphicotylus lucasii	NA	NA	NA	NA	NA	NA	NA	NA	NA	NA	NA	NA	NA	NA	NA	NA	NA	NA
Atoposaurus jourdani	6	17	2	50	2.2	4.2	11.2	9.9	9.5	5.3	3.8	4.1	4.8	5.7	4.4	NA	10.2	31.3
Atoposaurus oberndorferi	7	16	2	50	NA	7	15.6	13	13.1	3	3	2.2	2.5	2.6	2.6	1.6	10.5	39.1
Brillanceausuchus babourensis	7	19	NA	NA	NA	24	50	38	38	10	9	NA	9	11	9	5	35	123
Eutretauranosuchus delfsi	NA	NA	NA	NA	NA	NA	NA	NA	NA	NA	NA	NA	NA	NA	NA	NA	NA	NA
Hoplosuchus kayi	11	13	2	NA	NA	12.8	19.3	17.5	17.5	NA	NA	NA	NA	NA	NA	NA	NA	NA
Karatausuchus sharovi	8	NA	NA	46	NA	NA	8.8	6.1	6.1	NA	NA	NA	NA	NA	NA	NA	NA	NA
Koumpiodontosuchus aprosdokii	NA	NA	NA	NA	NA	NA	NA	NA	NA	NA	NA	NA	NA	NA	NA	NA	NA	NA
Montsecosuchus depereti	7	15	3	21	NA	35	27.1	21.1	19.6	3	7.5	4.3	5.3	5.3	5	0	23.3	71.5
Pachycheilosuchus trinquei	7	15	2	18	36.7	41.9	81.8	49.3	47.6	NA	11.1	NA	NA	NA	NA	NA	NA	NA
Pholidosaurus purbeckensis	NA	NA	NA	NA	NA	NA	NA	NA	NA	NA	NA	NA	NA	NA	NA	NA	NA	NA
Protosuchus richardsoni	9	15	2	39	25	48	66	52	52	11	14	11	11	12	11	8	52	170
Sabresuchus ibericus	NA	NA	NA	NA	NA	NA	NA	NA	NA	NA	NA	NA	NA	NA	NA	NA	NA	NA
Sabresuchus sympiestodon	NA	NA	NA	NA	NA	NA	NA	NA	NA	NA	NA	NA	NA	NA	NA	NA	NA	NA
Shamosuchus djadochtaensis	NA	NA	NA	NA	NA	NA	65	57	50	NA	NA	NA	NA	NA	NA	NA	NA	NA
Theriosuchus bhobhaltos	NA	NA	NA	NA	NA	NA	NA	NA	NA	NA	NA	NA	NA	NA	NA	NA	NA	NA
Theriosuchus grandinaris	NA	NA	NA	NA	NA	NA	NA	NA	NA	NA	NA	NA	NA	NA	NA	NA	NA	NA
Theriosuchus guimarotae	NA	NA	2	NA	18.6	NA	24.8	NA	NA	NA	NA	NA	NA	NA	NA	NA	NA	NA
Theriosuchus pusillus	NA	NA	NA	NA	NA	NA	40.3	32.2	29.6	8.6	10.3	NA	NA	NA	NA	NA	NA	NA
Wannchampsus kirpachi	NA	NA	NA	NA	NA	NA	NA	NA	NA	NA	NA	NA	NA	NA	NA	NA	NA	NA

2.11.2 Data matrix

A new character matrix was constructed (Appendix 7) based on a range of primary sources, with the majority of characters sampled from a few specific studies with extensive character lists relating to the phylogeny of Neosuchia (Clark *et al.*, 1994; Ortega *et al.*, 2000; Pol *et al.*, 2009; de Andrade *et al.*, 2011a) Clark (1994). 92 novel characters were also incorporated, following an extensive review of the literature, as well as via personal observations of specimens. Some of these were created by the splitting of previous characters. All characters were formatted to a standardised notation, and many characters were revised, quantified and/or clarified to remove ambiguity, including removal of problematic gaps between plesiomorphic and derived character states. The final data set comprises 329 characters (including autapomorphies – see 'Bayesian inference' below) scored for 24 OTUs (15 ingroup and 9 outgroup taxa) (Table 17). As with the majority of fossil crocodyliform data matrices, this one is dominated by cranial, mandibular and dental characters (263), augmented with 16 axial, 24 appendicular, and 26 osteoderm characters (Appendix 6). I opted to use a reductive (contingent) coding approach, which treats non-applicable character states as missing data when there is no logical basis for interpreting the character for any given OTU (Strong and Lipscomb, 1999). The advantage of this approach is that it facilitates the capture of grouping information between successive transformations between particular characters and state values (Brazeau, 2011).

Table 19. Primary appendicular and hindlimb measurements for all OTUs analysed for phylogenetic analysis.

Taxon	Ilium length	Pubis length	Ischium length	Femur length	Tibia length	Fibula length	MT I	MT II	MT III	MT IV	MT V	Pes length	Hindlimb length
"*Alligatorellus*" sp.	NA	NA	NA	74.7	68.3	61.9	NA	37.9	32.6	33.8	NA	NA	NA
Alligatorellus bavaricus	12	10.2	10.8	27.6	26.6	24.9	10	13	14.5	13	NA	29.2	83.4
Alligatorellus beaumonti	11	9.3	NA	26.3	23.6	24.2	11.5	14.5	14.5	13	3.5	19	68.9
Alligatorium franconicum	22	24	23	42.3	26.9	34.8	25	29	30	28	8	60	129.2
Alligatorium meyeri	NA	NA	NA	42	39.1	40.6	21.1	17.7	NA	NA	NA	42.6	123.7
Amphicotylus lucasii	NA	NA	NA	NA	NA	NA	NA	NA	NA	NA	NA	NA	NA
Atoposaurus jourdani	NA	NA	NA	16.7	15.7	13.9	12.6	15.9	16.1	14.8	NA	17	49.4
Atoposaurus oberndorferi	NA	5	NA	17.7	17.6	15.8	6.7	7.1	7	7.5	1.3	15	50.3
Brillanceausuchus babourensis	NA	NA	NA	45	43	43	NA	NA	NA	NA	NA	NA	NA
Eutretauranosuchus delfsi	NA	NA	NA	NA	NA	NA	NA	NA	NA	NA	NA	NA	NA
Hoplosuchus kayi	NA	NA	NA	25	23	23	NA	NA	NA	NA	NA	NA	NA
Karatausuchus sharovi	NA	NA	NA	12.1	13.1	13.1	NA	NA	NA	NA	NA	NA	NA
Koumpiodontosuchus aprosdokii	NA	NA	NA	NA	NA	NA	NA	NA	NA	NA	NA	NA	NA
Montsecosuchus depereti	20.1	NA	NA	38.5	30.7	31.7	13.2	17.6	18.8	14.3	NA	44	113.2
Pachycheilosuchus trinquei	40.9	38.5	35.6	75.1	74	72.3	41.5	45.6	0.1	NA	NA	NA	NA
Pholidosaurus purbeckensis	NA	NA	NA	NA	NA	NA	NA	NA	NA	NA	NA	NA	NA
Protosuchus richardsoni	51	56	30	100	83	83	37	40	39	37	15	80	263
Sabresuchus ibericus	NA	NA	NA	NA	NA	NA	NA	NA	NA	NA	NA	NA	NA
Sabresuchus sympiestodon	NA	NA	NA	NA	NA	NA	NA	NA	NA	NA	NA	NA	NA
Shamosuchus djadochtaensis	NA	NA	48	NA	69	71	NA	NA	41	38	NA	NA	NA
Theriosuchus bhobhaltos	NA	NA	NA	NA	NA	NA	NA	NA	NA	NA	NA	NA	NA
Theriosuchus grandinaris	NA	NA	NA	NA	NA	NA	NA	NA	NA	NA	NA	NA	NA
Theriosuchus guimarotae	13.7	NA	20	25.2	31.2	NA	NA	NA	NA	NA	NA	NA	NA
Theriosuchus pusillus	NA	NA	NA	53.3	53.6	51.7	31.9	28	31.5	28.4	NA	59	165.9
Wannchampsus kirpachi	NA	NA	NA	NA	NA	NA	NA	NA	NA	NA	NA	NA	NA

Taxon	Skull length: skull width	Skull length: snout length	Skull length: orbit length	Skull length: STF length	Skull width: orbit width	Skull width: STF width	Radius length: humerus length	Tibia length: femur length	Humerus length: femur length	Radius length: tibia lenth	Forelimb length: hindlimb length
"Alligatorellus" sp.	NA	NA	NA	NA	NA	NA	NA	0.91	NA	NA	NA
Alligatorellus bavaricus	2.21	2.99	3.12	7.18	1.99	4.63	0.69	0.96	0.89	0.64	0.76
Alligatorellus beaumonti	2.06	2.61	3.86	6.23	2.15	4.78	0.85	0.90	0.75	0.71	0.81
Alligatorium franconicum	2.77	1.81	5.27	6.75	2.53	5.15	0.69	0.64	0.83	0.89	0.73
Alligatorium meyeri	2.26	2.59	3.64	6.43	2.32	4.75	NA	0.93	NA	0.74	NA
Amphicotylus lucasii	1.67	1.50	10.00	8.57	7.20	7.20	NA	NA	NA	NA	NA
Atoposaurus jourdani	1.28	2.41	2.33	NA	2.69	NA	0.85	0.94	0.67	0.61	0.63
Atoposaurus oberndorferi	1.98	NA	2.86	NA	2.34	NA	0.84	0.99	0.88	0.74	0.78
Brillanceausuchus babourensis	1.79	2.21	6.82	5.36	3.50	7.00	0.76	0.96	1.11	0.88	NA
Eutretauranosuchus delfsi	1.97	1.65	7.18	7.83	5.31	6.66	NA	NA	NA	NA	NA
Hoplosuchus kayi	1.35	3.26	3.10	NA	3.38	NA	0.91	0.92	0.77	0.76	NA
Karatausuchus sharovi	NA	2.59	3.36	8.41	NA	NA	0.69	1.08	0.73	0.47	NA
Koumpiodontosuchus aprosdokii	2.04	1.60	5.60	8.00	3.67	5.50	NA	NA	NA	NA	NA
Montsecosuchus depereti	1.80	2.67	4.05	8.90	3.19	5.21	0.72	0.80	0.70	0.64	0.63
Pachycheilosuchus trinquei	NA	NA	NA	NA	NA	NA	0.58	0.99	1.09	0.64	NA
Pholidosaurus purbeckensis	NA	NA	NA	NA	3.55	2.81	NA	NA	NA	NA	NA
Protosuchus richardsoni	1.31	2.57	4.52	6.65	17.20	6.14	0.79	0.83	0.66	0.63	0.65
Shamosuchus djadochtaensis	1.49	2.00	6.10	6.40	4.78	5.73	0.77	NA	NA	0.72	NA
Theriosuchus sp.	NA	NA	NA	NA	NA	NA	NA	NA	NA	NA	NA
Theriosuchus grandinaris	NA	NA	NA	NA	NA	NA	NA	NA	NA	NA	NA
Theriosuchus guimarotae	1.82	2.13	4.98	6.51	3.00	4.64	NA	1.24	0.98	NA	NA
Theriosuchus ibericus	NA	NA	NA	NA	NA	NA	NA	NA	NA	NA	NA
Theriosuchus pusillus	1.51	2.36	3.83	6.53	3.46	4.80	0.73	1.01	0.76	0.55	NA
Theriosuchus sympiestodon	NA	NA	NA	NA	NA	NA	NA	NA	NA	NA	NA
Wannchampsus kirpachi	1.43	2.60	3.72	7.53	2.77	5.15	NA	NA	NA	NA	NA

Table 20. Ratios between primary measurements for OTUs used for phylogenetic analyses.

2.12 Phylogenetic analysis

2.12.1 Parsimony analysis

TNT version 1.1 (Goloboff *et al.*, 2000; Goloboff *et al.*, 2008) was used to perform a series of parsimony analyses. 47 multi-state characters were treated as ordered (additive) (Appendix 6). Starting with a random seed, 50 iterations of a ratchet search strategy were employed, which is a repeated pseudo-sampling protocol that uses character re-weighting to search tree space more effectively. No more than 20 substitutions were accepted during each phase of perturbation, and cycles were not auto-constrained. An equal probability was used for both up-weighting and down-weighting of characters in each cycle. The ratchet search function uses the tree bisection and reconnection (TBR) branch swapping algorithm to search for the most parsimonious trees (MPTs), which was repeated 1000 times. The MPTs were then subjected to a final exhaustive search for all remaining topologies of equal length, again using the TBR algorithm. All trees reported are the strict consensus topologies of all MPTs for each analysis, and zero-length branches were collapsed by default. The absolute Bremer branch support value (or decay index) for each node were calculated, which is a measure of the extra number of steps required to collapse a branch in the consensus topology (Bremer, 1994). An additional analysis was performed (with all OTUs included) utilising implied weighting, using a weighting exponent (k) of 3, as a method for favouring characters that are more likely to be homologous and penalising those more likely to be homoplastic and therefore producing a more 'reliable' topology (Goloboff, 1993; Goloboff *et al.*, 2003). Importantly, I wanted to test the effect of removal of taxa and combinations of taxa to test the stability of resulting topologies, for which the freely available *iterpcr* script was employed (Pol and Escapa, 2009).

2.12.2 Bayesian inference

In addition, Bayesian inference was used to test for topological congruence with the parsimony results using a different methodology, following the approach described by Lewis (2001). Relatively few paleontological studies have employed Bayesian methods thus far for phylogenetic analysis, and therefore I follow the standard protocol outlined in these studies (Müller and Reisz, 2006; Prieto-Márquez, 2010; Brusatte and Carr, 2016). MrBayes version 3.2.5 (Ronquist and Huelsenbeck, 2003) was used, and set to perform ten million generations running 4 simultaneous Markov chains, sampling a tree every one thousand chains, and setting a burn-in fraction of 0.25 (i.e., the first 25% of all sampled trees were discarded). The Markov Chain process started at a random seed, and fixed the states and rate frequencies to vary with an equal probability. The traditional Mk model was applied (Lewis, 2001), which assumes that a morphological character has an equal probability to change state at any time, and with equal probability along a branch. Recent analyses have demonstrated that this Mk model might perform more accurately than both equal- and implied-weights parsimony, although sometimes with an accompanying loss in precision (Wright *et al.*, 2015; O'Reilly *et al.*, 2016). The datatype was set as 'standard', which simply means that a variable number of states for each character was allowed, as employed in the standard 4by4 evolutionary model. I specified that all character state substitutions have equal rates (nst = 1), which is a simple model employed in molecular analyses equivalent to the Jukes-Cantor or Felsenstein81 models. All other parameters were retained at their default settings, and I did not employ a gamma shape parameter as some others have done (Slater, 2013; Brusatte and Carr, 2016; Sookias, 2016), as this model is best suited for molecular data and has not been unequivocally shown to be suitable for morphological data (although some recent simulations have found it to perform well in some cases (Wright *et al.*, 2015)). The data matrix includes characters with states that are locally, ambiguously, or unambiguously resolved as autapomorphic characters. These are not informative for the parsimony analyses, in which it is the shortest number of character state transformations (steps) leading to clades based on synapomorphies that is most

important, but they can have the effect of increasing terminal branch lengths for trees obtained using Bayesian inference (Lewis, 2001). Autapomorphies were included as others have suggested previously (Müller and Reisz, 2006), because inclusion of all available data is important for yielding new insights, as well as having an effect on deeper node support values. Ordered characters were treated in the same way as for the parsimony analyses, using the '*ctype ordered:*' command. Stationarity was achieved with a standard deviation of split frequencies less than 0.011.

Chapter 2: Materials and Methods

3 Tetrapod Diversity and Extinction Across the Jurassic/Cretaceous Boundary

3.1 Introduction

The primary aims of this chapter are to: (1) quantify the magnitude of extinction and diversity change of higher tetrapod clades across the J/K transition, and refine the timing of these events; (2) evaluate the impact of geological sampling biases; (3) assess the potential environmental drivers of resulting patterns; and (4) place such patterns in the ecological context of the radiation and extinction of major clades. This represents the first time that the relationship between both geological and environmental factors and standardised diversity has been explored on the scale of all major tetrapod groups.

3.2 Results and discussion

3.2.1 Uncorrected taxonomic diversity

'Raw' patterns of uncorrected, global genus-level diversity show a decline in almost all taxonomic groups across the J/K boundary (Figure 21). Marine tetrapod diversity was consistently almost an order of magnitude lower than non-marine diversity, and shows an approximate 75% decline across the J/K boundary. In non-marine faunas, small-bodied taxa (lepidosauromorphs, lissamphibians and mammals) exhibited either flat diversity or a small increase across the boundary, whereas medium- to large-bodied groups, including pterosaurs, crocodyliforms, turtles, and all three major dinosaur groups, reveal differential patterns of decline from 33–80% losses of standing diversity. Intriguingly, non-marine tetrapod diversity is consistently almost an order of magnitude higher than that for marine tetrapods. While such an observation could be an artefact of the fossil record, it is perhaps noteworthy that in the Early Jurassic, the diversity of both appears to be largely the same (i.e., in equilibrium), but becomes decoupled at some point during the Middle Jurassic at around the same time Pangaea began to fragment (~180 Ma). Such an event might have been important for changing the carrying capacity or diversity dependence (Marshall and Quental, 2016) of life on land relative to

life in the oceans, with geographical separation playing a decisive role in regulating the total number of species (or genera) on land. However, further interpretation of any such putative process will require additional assessments of species diversification rates and carrying capacity variation as a result of continental fragmentation.

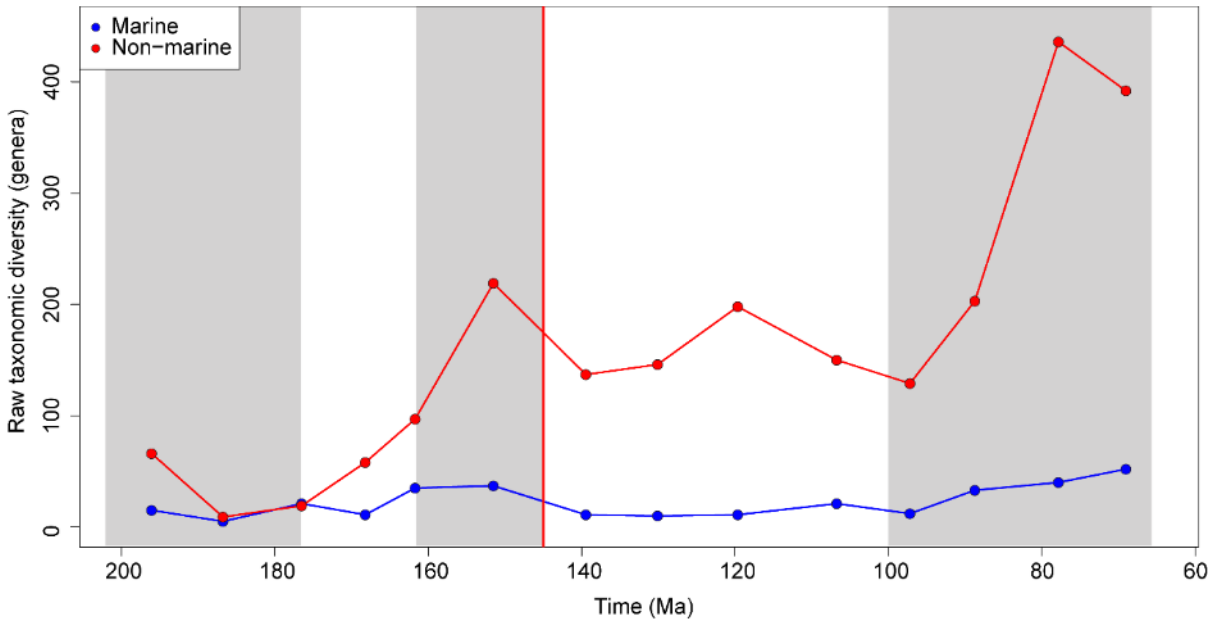


Figure 21. Raw taxonomic diversity for marine and non-marine Jurassic and Cretaceous tetrapods, grouped into approximately equal 10 million year time bins.

Group	J1	J2	J3	J4	J5	J6	K1	K2	K3	K4	K5	K6	K7	K8	Sum per group
Aves	0	0	0	0	0	1	0	17	52	6	6	11	21	29	143
Choristoderes	0	0	0	1	0	1	2	1	8	1	0	1	2	1	18
Lepidosauromorphs	2	3	5	6	2	17	18	18	13	14	9	11	67	31	216
Lissamphibians	3	0	0	6	5	7	8	12	7	5	6	15	12	21	107
Mammaliaforms	9	3	7	24	19	48	43	18	15	18	27	24	66	59	380
Theropods	8	0	0	9	21	27	9	23	25	18	22	30	74	72	338
Pterosaurs	3	1	3	2	8	20	9	4	26	22	6	6	10	6	126
Sauropodomorphs	25	0	3	6	15	32	6	8	9	9	10	18	15	23	179
Ornithischians	10	2	1	1	15	25	17	20	17	27	13	23	111	58	340
Crocodyliformes (terrestrial)	6	0	0	2	6	18	9	12	10	12	18	38	21	31	183
Testudines	0	0	0	1	6	23	16	13	16	18	12	26	37	61	229
Ichthyopteryians	4	2	7	2	6	12	3	5	3	5	3	0	0	0	52
Sauropterygians	11	3	10	3	17	12	5	4	5	8	7	16	12	10	123
Chelonioides	0	0	0	0	0	0	0	0	1	7	1	16	25	35	85
Crocodyliformes (marine)	0	0	4	6	12	13	3	1	2	1	1	1	3	7	54
Sum per time bin	81	14	40	69	132	256	148	156	209	171	141	236	476	444	2573
Sum aquatic	15	5	21	11	35	37	11	10	11	21	12	33	40	52	314
Sum terrestrial	66	9	19	58	97	219	137	146	198	150	129	203	436	392	2259

Table 21. Raw, uncorrected genus level counts for all taxonomic groups analysed at 10 million year time bin intervals.

3.2.2 Global subsampled diversity

Subsampled diversity estimates show a more nuanced pattern than the raw taxonomic estimates (results reported using a quorum of 0.4). Using 10 million year time bins on a global scale, the only non-marine group to show a notable drop in diversity across the J/K boundary is Crocodyliformes (Mannion *et al.*, 2015) (Table 22, Table 23, Table 24, Table 25) (including Thalattosuchia). Mammals and lissamphibians appear to have increased in diversity, with the former almost doubling, in marked contrast to previous studies documenting only a small increase (Newham *et al.*, 2014). A similar result was recently recovered, with subsampled diversity estimates based on SQS and the same source data finding an almost doubling in the diversity of non-dinosaurian, non-mammalian tetrapods across the J/K boundary (Benson *et al.*, 2016). Theropod and ornithischian dinosaurs both show a small increase in diversity across the J/K boundary, contrasting with results obtained using a residual diversity

approach (Upchurch *et al.*, 2011b), but a signal for sauropods in the earliest Cretaceous could not be recovered. Choristoderes and Aves, which were treated as separate radiations, are too poorly sampled throughout this interval to identify any diversity patterns with confidence. Marine crocodyliforms also suffered a decline across the J/K boundary (Mannion *et al.*, 2015), in contrast with a slight increase in sauropterygians (Benson and Druckenmiller, 2014). The dynamics of ichthyosaur diversity remain obscured through the J/K boundary. However, at this relatively coarse resolution overall, it is difficult to distinguish whether these patterns occurred through the J/K boundary (i.e., the Tithonian–Berriasian), or represent the lumping together of discrete signals from different time bins (i.e., the Kimmeridgian + Tithonian and Berriasian + Valanginian).

Group	J1	J2	J3	J4	J5	J6	K1	K2	K3	K4	K5	K6	K7	K8
Choristoderes	NA	NA	NA	1.00	NA	1.00	2.00	NA	4.54	NA	NA	NA	1.07	1.00
Crocodyliformes	2.14	NA	NA	1.64	2.30	3.22	2.75	4.21	3.26	NA	6.66	NA	4.94	4.99
Ornithischians	4.06	NA	NA	NA	8.81	3.43	3.37	4.39	3.51	10.83	5.55	9.74	10.82	5.29
Sauropodomorphs	3.12	NA	NA	1.53	7.77	3.88	NA	6.06	4.30	NA	4.46	NA	8.53	3.30
Theropoda	2.70	NA	NA	2.31	8.47	2.68	3.18	15.14	10.57	4.82	6.86	15.43	7.62	8.05
Aves	NA	NA	NA	NA	NA	1.00	NA	9.69	36.14	2.84	3.45	4.10	5.33	6.85
Lissamphibians	NA	NA	NA	2.14	NA	NA	5.45	6.83	4.28	2.40	2.58	5.83	2.25	4.38
Lepidosauromorphs	1.40	NA	3.35	2.56	NA	3.99	8.38	NA	6.52	NA	6.32	NA	9.57	5.36
Mammals	3.86	NA	NA	13.84	NA	8.15	15.40	6.51	NA	5.54	7.81	6.73	7.88	7.40
Pterosaurs	2.34	NA	1.48	1.08	NA	4.52	NA	2.08	NA	4.35	3.61	2.18	4.22	2.36
Testudines	NA	NA	NA	NA	1.87	3.87	4.48	9.14	NA	8.37	4.91	9.87	5.06	6.88

Table 22. Global subsampled (SQS) diversity results for all non-marine tetrapod groups at the 10 myr time bin level.

Group	J1	J2	J3	J4	J5	J6	K1	K2	K3	K4	K5	K6	K7	K8
Choristoderes	NA	NA	NA	1.00	NA	1.00	0.67	NA	0.80	NA	NA	NA	0.99	1.00
Crocodyliformes	0.76	NA	NA	NA	0.50	0.84	0.96	0.78	0.89	NA	0.61	0.52	0.89	0.96
Ornithischians	0.85	NA	NA	NA	0.52	0.94	0.86	0.86	0.83	0.82	0.62	0.51	0.92	0.94
Sauropodomorphs	0.85	NA	NA	0.79	0.54	0.97	NA	0.40	0.73	NA	0.59	NA	0.67	0.92
Theropoda	0.94	NA	NA	0.70	0.60	0.94	0.78	0.57	0.61	0.82	0.76	0.57	0.92	0.91
Aves	NA	NA	NA	NA	NA	1.00	NA	0.44	0.44	0.82	0.70	0.79	0.65	0.67
Lissamphibians	NA	NA	NA	0.71	NA	NA	0.64	0.50	0.40	0.75	0.75	0.85	1.00	0.98
Lepidosauromorphs	1.00	NA	0.43	0.81	NA	0.93	0.81	NA	0.76	NA	0.70	NA	0.89	0.95
Mammals	0.86	0.50	NA	0.69	0.40	0.79	0.74	0.66	NA	0.74	0.92	0.89	0.96	0.98
Pterosaurs	0.50	NA	1.00	0.91	0.50	0.84	0.56	0.78	NA	0.78	0.77	0.87	0.81	0.71
Testudines	NA	NA	NA	NA	0.80	0.97	0.80	0.50	NA	0.69	0.80	0.76	0.97	0.95

Table 23. Global Good's u results for all non-marine tetrapod groups at the 10 myr time bin level.

At a finer geological stage level, a markedly different global pattern emerges for subsampled diversity. This results from the differences in the size and shape of the sample pool (i.e., the taxonomic abundance distribution) due to the variation in the duration of time bins. In non-marine faunas, ornithischians and theropods show declines of around 33% and 75% diversity loss from the Tithonian to the Berriasian, respectively (Figure 22A). For ornithischians, this result is similar to that recovered from residual diversity estimates (Upchurch *et al.*, 2011b), and reflects the decline of stegosaurs. However, it cannot be ruled out that subsampled ornithischian diversity actually increases when applying a bootstrapping sensitivity test. This signal for theropods is highly distinct, as results based on residual diversity estimates show either a steady increase (collections-based) or small decline (formations-based) in theropod diversity through the J/K boundary (Upchurch *et al.*, 2011b), instead of the more prominent decline recovered here. Furthermore, this pattern remains when bootstrapping is applied, suggesting that the decline might have been even more severe across the J/K boundary. Sauropods are too poorly sampled in the Berriasian to reveal a signal, but their Valanginian diversity was only 37% of their Tithonian diversity, comprising the decline of non-neosauropods, diplodocids and basal macronarians (Mannion *et al.*, 2013), and representing a significant loss around the J/K transition. These results partly support the dramatic decline in sauropod diversity recovered using residual diversity estimates (Upchurch *et al.*, 2011b), prior to the Barremian radiation of titanosauriforms (Mannion *et al.*, 2013; Gorscak and O'Connor, 2016), although the exact timing of this is obscured by a generally poor titanosauriform fossil record during the J/K transition. Furthermore, the phylogenetic diversity estimates (PDEs) for each of the three major dinosaur clades provide some support for the subsampled results. Sauropods show the greatest evidence of decline across the J/K boundary, with a moderate decline in Theropoda, whereas ornithischian diversity remained stable.

Non-marine crocodyliforms still document a loss of more than 50% of diversity at the stage level (Mannion *et al.*, 2015) (Figure 22B), followed by the subsequent diversification of major non-marine

clades such as Notosuchia and Eusuchia in the Hauterivian–Barremian (Bronzati *et al.*, 2015). Pterosaurs are too poorly sampled at the stage level to reveal an SQS signal across the J/K boundary, but diversity in the Hauterivian was around 20% of Kimmeridgian levels, documenting low diversity subsequent to the extinction of non-pterodactyloid faunas (Butler *et al.*, 2013; Andres *et al.*, 2014). However, a component of this low diversity signal is possibly due to anomalously low within-bin sampling of the Hauterivian, and pterosaurs steadily increased in diversity through the remainder of the Early Cretaceous (Figure 22B), documenting the steadily increasing diversification of ornithocheiroid pterodactyloids (Andres *et al.*, 2014; Upchurch *et al.*, 2014). This overall pattern is quite similar to that obtained with the PDE, with pterosaurs showing a major diversity drop across the J/K transition overall, a slight increase across the J/K boundary that the SQS results do not contradict, and then a substantial recovery in the Hauterivian. Non-marine turtles declined by 33% of diversity through the J/K boundary (Figure 22B), in contrast to results obtained at a coarser resolution here and a recent study (Nicholson *et al.*, 2015) which found steadily increasing diversity. Some of this discrepancy with this study (Nicholson *et al.*, 2015) might also be due to differences in the treatment of coastal and freshwater taxa here, which are regarded as non-marine as opposed to fully marine (i.e., exclusively chelonioids [sea turtles]). Mammals suffered an overall loss in global subsampled diversity of 69% from the Kimmeridgian to the Valanginian (Figure 22C), similar to that recently recovered from subsampled and residual diversity estimates (Newham *et al.*, 2014), but the earliest Cretaceous rise in diversity reported by Newham *et al.* (2014) is not found. This is likely due to either the finer division of time bins used here, or the modified version of SQS (Section 2.6). Distinct from this broader pattern of decline, lepidosauromorphs greatly increased in diversity (48%) across the J/K boundary (Figure 22C), reflecting the diversification of major extant squamate clades, including Lacertoidea, Scincoidea and Iguania, in the earliest Cretaceous (Pyron and Burbrink, 2012; Jones *et al.*, 2013), and in approximate agreement with a large diversity increase in non-mammalian, non-dinosaurian tetrapods recently recovered by a similar analysis using SQS (Benson *et al.*, 2016).

Lissamphibian diversity is consistently low but discontinuously resolved through the J/K boundary (Figure 22C), reflecting overall poor Mesozoic sampling of this group.

Group	J1	J2	J3	J4	J5	J6	K1	K2	K3	K4	K5	K6	K7	K8
Crocodyliformes	NA	NA	1.42	1.89	2.31	3.24	2.23	NA	1.35	NA	NA	NA	2.36	1.72
Ichthyosaurs	1.73	1.60	1.86	1.73	2.08	2.96	NA	3.09	1.64	1.49	1.49	NA	NA	NA
Sauropterygians	4.41	NA	3.45	2.36	4.49	2.05	2.21	2.45	2.56	4.62	3.25	4.87	4.00	4.51
Chelonioides	NA	NA	NA	NA	NA	NA	NA	NA	NA	NA	NA	5.39	5.08	3.89

Table 24. Global SQS diversity results for all marine tetrapod groups at the 10 myr time bin level.

Group	J1	J2	J3	J4	J5	J6	K1	K2	K3	K4	K5	K6	K7	K8
Crocodyliformes	NA	NA	0.96	0.95	0.93	0.97	0.70	NA	0.67	NA	0.50	1.00	0.50	0.88
Ichthyosaurs	1.00	1.00	0.95	0.67	0.83	0.91	NA	0.63	0.71	0.92	0.78	NA	NA	NA
Sauropterygians	0.74	NA	0.86	0.50	0.90	0.95	0.73	0.50	0.75	0.50	0.79	0.78	0.88	0.71
Chelonioides	NA	NA	NA	NA	NA	NA	NA	NA	NA	NA	NA	0.81	0.80	0.83

Table 25. Global Good's u results for all marine tetrapod groups at the 10 myr time bin level.

3.2.2.1 Comparison with results using TRiPS

These results obtained using SQS for dinosaurs are largely at odds with those produced using a Poisson sampling model (TRiPS), which found no decline at the species and genus level overall and for the three individual sub-clades at a global level (Starrfelt and Liow, 2016). In this study, while all dinosaur groups seem to exhibit a shallow Tithonian–Berriasian decline, this decline is bound within confidence intervals that are firstly, the largest compared with almost any other time interval in the Mesozoic, and secondly could even indicate a rise in diversity in some groups (especially sauropods) due to the shape of the confidence distribution. This distinction is due to low sampling probabilities during the Berriasian (Starrfelt and Liow, 2016), producing wide uncertainties in the 'true' diversity recovered using TRiPS. The reason for the difference might be that while TRiPS documents this lack of extinction across the J/K boundary despite a shift in sampling probability, this is accounted for in SQS by applying an equal coverage sampling protocol across all bins, as measured by Good's *u* and set by varying the

quorum. Indeed, the same pattern of decline is recovered when the quorum increases incrementally, and is even emphasised when the eveness is set to to increase, a factor not incorporated into the TRiPS model where sampling probabilities are fixed (Starrfelt and Liow, 2016).

Table 26. Global subsampled (SQS) diversity results for all non-marine tetrapod groups at the stage level.

Bin	Crocodyliformes	Lepidosauromorpha	Lissamphibia	Mammaliaformes	Ornithischia	Pterosauria	Sauropodomorpha	Testudines	Theropoda
J1	1	1	NA	NA	NA	NA	3.83	NA	2.48
J2	3.12	NA	NA	2.02	2.3	NA	1.82	NA	1.8
J3	NA	NA	NA	NA	NA	NA	NA	NA	NA
J4	NA	1	NA	NA	NA	1.45	NA	NA	NA
J5	NA	NA	NA	NA	NA	NA	NA	NA	NA
J6	NA	NA	NA	NA	NA	NA	NA	NA	1.95
J7	NA	3.28	2.23	13.82	NA	1.08	1.49	NA	2.05
J8	1.51	NA	NA	NA	2.3	NA	4.69	1.81	6.01
J9	2.78	NA	NA	NA	NA	NA	3.46	1.86	5.87
J10	3.43	7.22	NA	16.92	3.7	4.91	5.46	4.46	3.32
J11	5.14	5.25	NA	NA	3.74	3.48	4.01	4.68	6.83
K1	2.35	7.75	5.45	12.4	2.52	NA	NA	3.12	1.42
K2	3.82	3	NA	5.27	3.03	NA	1.5	6.56	3.04
K3	2.28	NA	NA	NA	1.25	1	NA	2.39	NA
K4	4.36	5.84	5.15	7.43	4.86	3.34	3.82	NA	NA
K5	NA	NA	NA	NA	NA	3.61	NA	NA	3.15
K6	1	NA	NA	NA	5.65	4.14	2.02	5.18	2.96
K7	1	3.81	1	7.58	1	NA	NA	NA	NA
K8	NA	NA	NA	2.81	NA	NA	NA	NA	NA
K9	NA	NA	3.79	6.07	2.49	NA	NA	NA	2.04
K10	6.76	NA	2.8	12.61	NA	2.34	NA	9.59	NA
K11	1.54	6.25	2.72	6.47	4.77	1	NA	3.14	3.52
K12	5.07	8.06	4.33	7.72	5.32	2.35	3.34	7.07	7.78

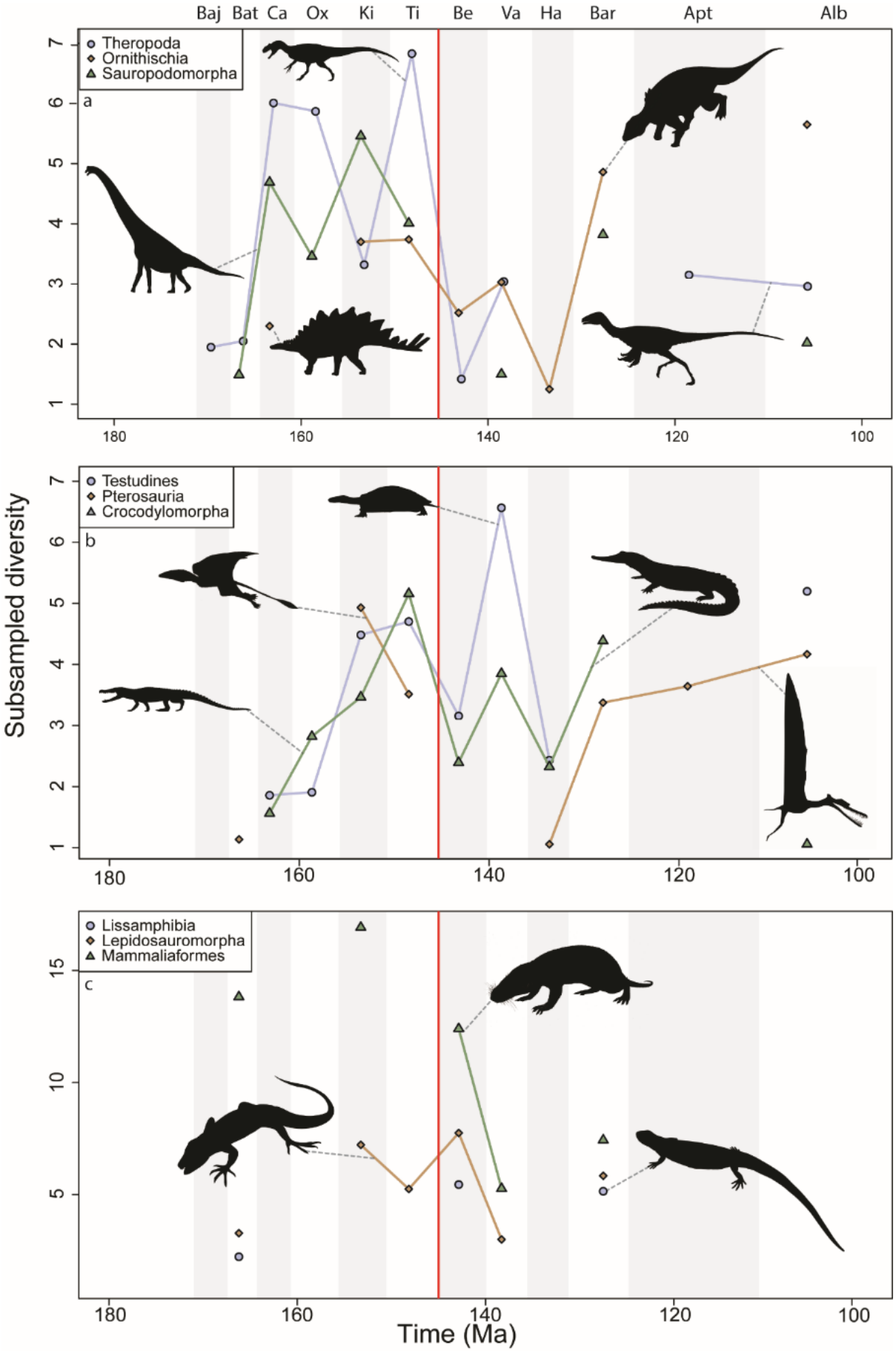

Baj Bat Ca Ox Ki Ti Be Va Ha Bar Apt Alb
Theropoda
Ornithischia
Sauropodomorpha
a
Testudines
Pterosauria
Crocodylomorpha
b
Lissamphibia
Lepidosauromorpha
Mammaliaformes
c
Subsampled diversity
Time (Ma)
180
160
140
120
100

Figure 22. Global non-marine Late Jurassic/Early Cretaceous subsampled diversity for (a) major dinosaur groups; (b) testudines, crocodylomorphs, and pterosaurs; and (c) mammals, lepidosaurs and lissamphibians. Shaded areas represent stage boundaries. Silhouettes from PhyloPic courtesy of Michael Keesey, Brad McFeeters, Scott Hartman, Mark Witton, Ville Veikko Sinkkonen and Hanyong Pu (see http://phylopic.org/ for additional license information).

In the marine realm, stage-based crocodyliform SQS diversity decreased by around 50% (Figure 23), reflecting the ongoing decline of Thalattosuchia prior to their extinction in the late Early Cretaceous (Martin *et al.*, 2014a; Young *et al.*, 2014a; Chiarenza *et al.*, 2015; Mannion *et al.*, 2015). The magnitude of this decline is slightly greater than that reported by some previous studies (Martin *et al.*, 2014a; Mannion *et al.*, 2015), most likely corresponding to usage of a finer resolution time scale that reduces or avoids the over-lumping of non-contemporaneous taxa. Ichthyosaurs and sauropterygians are too poorly sampled at the stage level in the earliest Cretaceous, but when a signal emerges in the Early Cretaceous (Hauterivian and Valanginian, respectively), diversity is consistently less than 50% of Late Jurassic levels (Figure 23), similar to previous estimates using residual diversity (Benson *et al.*, 2010; Benson and Butler, 2011). Surviving taxa were those with a more generalist feeding style (Fischer *et al.*, 2016), and diversified into additional ecologies, with some taxa becoming apex predators and others soft-prey specialists during the middle Early Cretaceous. More recently, a study of Cretaceous ichthyosaurs has suggested that they were taxonomically, phylogenetically and ecologically diverse (Fischer *et al.*, 2016), and that parvipelvians exhibited their greatest ecological disparity throughout the Valanginian–Barremian interval. This appears to post-date the apparent Berriasian–Hauterivian platypterygiine radiation (Fischer *et al.*, 2016), which the stage-level analyses here failed to recover. Moreover, based on PDEs, both sauropterygians and ichthyosaurs show evidence for a notable decline in diversity across the J/K boundary, which continued into the Hauterivian for both groups

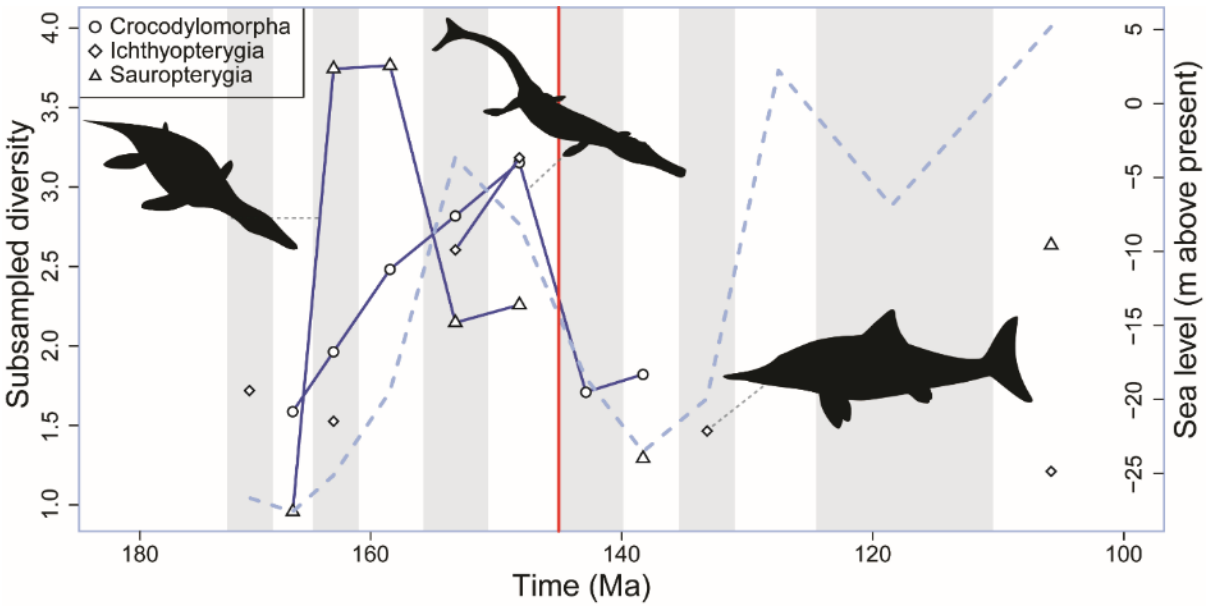


Figure 23. Global marine subsampled diversity for major Late Jurassic/Early Cretaceous pelagic clades. Sea level curve from Miller et al. Silhouettes from PhyloPic courtesy of Gareth Monger and Michael Keesey (see http://phylopic.org/ for additional license information).

Some notable differences between the results from some of the stage-level and 10 million year time bin analyses emphasise the effect that choice of time binning can have on our understanding of the magnitude of the J/K boundary extinction. Previously, studies of tetrapods have failed to find any correlation between time bin length and raw diversity (Benson *et al.*, 2010; Benson and Butler, 2011; Mannion *et al.*, 2011; Mannion *et al.*, 2015), suggesting that stage level bins are appropriate for diversity studies (i.e., diversity does not systematically increase with bin length, leading to artificial over-estimation). But future research should explicitly acknowledge that whereas 10 million year bins might give a 'fairer' method of grouping data, their relative coarseness means that some key aspects of palaeodiversity patterns can be obscured or at least be interpreted differently, which appears to be the case here for the J/K transition. Additionally, the time bin lengths for the Kimmeridgian, Tithonian, Berriasian, and Valanginian are quite similar (3.8–5.3 million years), and therefore interpreting stage level patterns through this interval appears to be sufficient to recover fair estimates of subsampled diversity. The conclusions drawn from these marine and non-marine results do not change markedly

if the quorum level is varied, although the magnitude of diversity decline increases with higher quorum levels.

Bin	Crocodyliformes	Ichthyosaurs	Sauropterygia
J1	NA	1.65	4.22
J2	NA	1.72	2.79
J3	NA	1.59	NA
J4	1.41	1.99	3.32
J5	NA	1	NA
J6	NA	1.75	NA
J7	1.62	NA	1
J8	1.99	1.56	3.74
J9	2.5	NA	3.76
J10	2.83	2.62	2.17
J11	3.16	3.19	2.28
K1	1.74	NA	NA
K2	1.85	NA	1.33
K3	NA	1.5	NA
K4	NA	NA	NA
K5	NA	NA	NA
K6	NA	1.25	2.65
K7	NA	NA	NA
K8	NA	NA	NA
K9	NA	NA	NA
K10	NA	NA	3.26
K11	NA	NA	NA
K12	1.8	NA	4.47

Table 27. Global subsampled (SQS) diversity results for all marine tetrapod groups at the stage level.

If the subsampling quorum level is increased (i.e., simulating more even sampling), it is possible to estimate with greater accuracy the magnitude of any diversity decline across the J/K boundary in groups that are relatively well sampled (SI 4). Marine crocodyliforms (primarily Thalattosuchia) suffered a maximum J/K boundary decline of 57% at a quorum of 0.6, only slightly higher than using a quorum of 0.4. Non-marine crocodyliforms exhibited a similar level of decline, 60% with a quorum of 0.5, from the Tithonian–Berriasian, slightly higher again than estimates using a quorum of 0.4. The magnitude of the lepidosauromorph radiation becomes dampened to just a 30% increase (quorum of

0.5), and in mammals the Berriasian–Valanginian decline becomes more striking with a 73% drop of diversity (quorum of 0.7). For dinosaurian clades across the J/K boundary, the maximum level of decline in ornithischians reached 37% (quorum of 0.8), and 76% in sauropods from the Tithonian–Valanginian (quorum of 0.6). The crash in theropod diversity is greatly emphasised at higher quorum levels, with a maximum estimated loss of 85% at a quorum of 0.7. Pterosaurs remain too poorly sampled throughout the majority of the Early Cretaceous to adequately assess global subsampled diversity patterns, as are turtles at quorum levels higher than 0.4. The magnitude of diversity decline in marine reptiles is also emphasised at higher quorum levels, matching previous estimates using residual diversity (Benson *et al.*, 2010; Benson and Butler, 2011), although the timing is difficult to pinpoint with ichthyosaurs suffering a maximum diversity loss of 71% from the Tithonian–Hauterivian, and sauropterygians losing 74% of their diversity from the Tithonian–Valanginian.

3.2.3 Regional patterns of diversity across the J/K boundary

It is important to determine whether or not these apparently global patterns are the product of grouping together disparate regional palaeocontinental level signals. The most comprehensive Jurassic–Cretaceous interval record comes from Europe (Figure 30A, B). Here, non-marine crocodyliforms experienced a 'double dip' diversity decline, with troughs in the Berriasian (37% loss) and Hauterivian (40% loss), before a major Barremian diversification (Bronzati *et al.*, 2015). This pattern is similar to that exhibited by turtles, which document a decline of 38% over the J/K boundary, with a recovery to their highest Mesozoic levels in the Valanginian, prior to a second, more severe diversity decline (69% loss) in the Hauterivian. This diversity decline reflects the regional extinction of diverse and widely palaeogeographically distributed European turtle faunas comprising coastal-dwelling plesiochelyids, thalassemydids and eurysternids (Anquetin and Joyce, 2014; Anquetin and Chapman, 2016). Lepidosaurs showed increasing diversity through the J/K boundary and lissamphibian

diversity patterns remain obscured, although they were twice as diverse during the Barremian as the Tithonian. European mammal diversity is poorly resolved at the stage level in the latest Jurassic, although this group suffered an overall loss of 58% of diversity from the Berriasian to the Valanginian. Ornithischian diversity increased through the J/K boundary, but steadily declined from the Berriasian to the Hauterivian (51% loss). Both sauropods and pterosaurs were in decline in Europe prior to the J/K boundary and, although their earliest Cretaceous dynamics are unknown, their diversity is consistently lower in the Hauterivian–Barremian than in the latest Jurassic. Theropods lost 76% of their diversity from the Kimmeridgian to Berriasian, but recovered rapidly in the Valanginian.

	Chelonioids	Crocodyliformes	Ichthyosaurs	Sauropterygians
J1	NA	NA	NA	NA
J2	NA	NA	NA	NA
J3	NA	NA	NA	NA
J4	NA	1	NA	NA
J5	NA	NA	NA	NA
J6	NA	NA	NA	NA
K1	NA	NA	NA	NA
K2	NA	NA	NA	NA
K3	NA	NA	NA	NA
K4	NA	NA	NA	NA
K5	NA	NA	NA	NA
K6	NA	NA	NA	NA
K7	NA	NA	NA	NA
K8	NA	2.52	NA	NA

Table 28. Regional (Africa) subsampled (SQS) diversity results for all marine tetrapod groups at the 10 million year time bin level.

	Chelonioids	Crocodyliformes	Ichthyosaurs	Sauropterygians
J1	NA	NA	NA	NA
J2	NA	NA	NA	NA
J3	NA	NA	NA	NA
J4	NA	NA	NA	NA
J5	NA	1	NA	NA
J6	NA	NA	NA	NA
K1	NA	NA	NA	1.64
K2	NA	NA	NA	NA
K3	NA	NA	NA	NA
K4	NA	NA	NA	NA
K5	NA	NA	NA	NA
K6	NA	NA	NA	NA
K7	NA	NA	NA	1.66
K8	1.47	1	NA	NA

Table 29. Regional (Asia) subsampled (SQS) diversity results for all marine tetrapod groups at the 10 million year time bin level.

The Early Cretaceous tetrapod record of Europe, despite being the best-sampled region globally, is still incredibly spatiotemporally sparse, and relatively poorly sampled compared to other time intervals. While there have been a number of discoveries in recent years, particularly of dinosaurs, there is still a strong spatial bias towards southwestern European localities, particularly those in the UK, France, and Spain, for the earliest part of the Cretaceous (Berriasian–Hauterivian). The effect of this is that our understanding of Early Cretaceous tetrapod faunas, even those of Europe, is strongly influenced by even smaller-scale taphonomic and ecological biases. For example, the dinosaurs of eastern Europe (Benton *et al.*, 2006) appear to have been much smaller-bodied than those of the Mediterranean Neo-Tethys (Csiki-Sava *et al.*, 2016).

	Chelonioids	Crocodyliformes	Ichthyosaurs	Sauropterygians
J1	NA	NA	1.55	4.38
J2	NA	NA	1.59	NA
J3	NA	1.59	1.82	3.16
J4	NA	1.77	NA	1.62
J5	NA	2.41	1.53	3.49
J6	NA	3.17	3.59	1.97
K1	NA	1.77	NA	1.47
K2	NA	NA	2.49	NA
K3	NA	1	2.34	NA
K4	NA	NA	1.68	2.02
K5	NA	NA	1.82	1
K6	NA	NA	NA	NA
K7	1	NA	NA	1.67
K8	NA	1	NA	NA

Table 30. Regional (Europe) subsampled (SQS) diversity results for all marine tetrapod groups at the 10 million year time bin level.

Much of this European pattern is reflected in the overall 'global' pattern of decline recovered in all non-marine tetrapod groups, suggesting that due to poor sampling of North America (Table 31) and Gondwana (Table 28, Table 32, Table 35, Table 33) during the earliest Cretaceous, most of this apparently global decline is the result of a regional signal focussed in Europe. Furthermore, the European pattern suggests that, conversely to a globally synchronous event across the J/K boundary as implied by the global analyses, the tempo of decline was staggered, with diversity decreasing in a cascading fashion across the J/K transition. Therefore, global patterns of tetrapod diversity are probably poor indicators of regional level dynamics, and care should be taken to distinguish between these signals.

	Chelonioids	Crocodyliformes	Ichthyosaurs	Sauropterygians
J1	NA	NA	NA	NA
J2	NA	NA	NA	NA
J3	NA	NA	NA	NA
J4	NA	NA	NA	NA
J5	NA	NA	2.24	2.39
J6	NA	NA	NA	NA
K1	NA	NA	NA	NA
K2	NA	NA	NA	NA
K3	NA	NA	NA	NA
K4	NA	NA	2	NA
K5	NA	NA	1	2.85
K6	2.46	NA	NA	3.91
K7	4.26	1.61	NA	3.28
K8	2.49	1.59	NA	2.96

Table 31. Regional (North America) subsampled (SQS) diversity results for all marine tetrapod groups at the 10 million year time bin level.

Table 32. (Left) Regional (Africa) subsampled (SQS) diversity results for all non-marine tetrapod groups at the 10 million year time bin level. (Right) Regional (Asia) subsampled (SQS) diversity results for all non-marine tetrapod groups at the 10 million year time bin level.

	Aves	Chroristoderes	Crocodyliformes	Lepidosauromorphs	Lissamphibians	Mammaliaformes	Ornithischians	Pterosaurs	Sauropodomorphs	Testudines	Theropods
J1	NA	NA	1.51	NA	NA	2.42	3	NA	1.98	NA	1.68
J2	NA	NA	NA	NA	NA	NA	NA	NA	NA	NA	NA
J3	NA	NA	NA	NA	NA	NA	NA	NA	NA	NA	NA
J4	NA	NA	NA	NA	NA	NA	NA	NA	1.44	NA	NA
J5	NA	NA	NA	NA	NA	NA	NA	NA	1.78	NA	NA
J6	NA	NA	1.53	NA	NA	NA	1.17	2.34	2.99	NA	2.34
K1	NA	NA	NA	NA	NA	NA	NA	NA	NA	NA	1.66
K2	NA	NA	NA	NA	NA	NA	NA	NA	NA	NA	NA
K3	NA	NA	1.62	NA	NA	NA	NA	NA	1.54	NA	NA
K4	NA	NA	2.16	NA	NA	NA	NA	NA	NA	NA	1.45
K5	NA	NA	NA	NA	1.4	NA	NA	1.67	1.92	NA	3.54
K6	NA	NA	NA	NA	NA	NA	NA	NA	NA	NA	NA
K7	NA	NA	NA	NA	NA	NA	NA	NA	NA	NA	1.77
K8	1.32	NA	1.49	1.34	NA	NA	NA	NA	NA	2.9	NA

	Aves	Chroristoderes	Crocodyliformes	Lepidosauromorphs	Lissamphibians	Mammaliaformes	Ornithischians	Pterosaurs	Sauropodomorphs	Testudines	Theropods
J1	NA	NA	3.13	1	NA	1.99	NA	NA	2.63	NA	1.57
J2	NA	NA	NA	NA	NA	NA	NA	NA	NA	NA	NA
J3	NA	NA	NA	NA	NA	NA	NA	NA	NA	NA	NA
J4	NA	NA	NA	NA	1	NA	NA	NA	NA	NA	NA
J5	NA	NA	1.69	NA	3.27	NA	4.36	NA	3.04	1.7	NA
J6	NA	NA	NA	NA	NA	NA	NA	NA	1.52	NA	2.75
K1	NA	2	NA	2.44	NA	NA	NA	1	NA	NA	NA
K2	NA	NA	NA	NA	NA	NA	NA	NA	NA	2.47	NA
K3	34.97	4.53	NA	2	1.48	4.62	2.15	NA	1.48	NA	6.7
K4	1	NA	NA	NA	NA	NA	3.12	NA	NA	5.12	NA
K5	1.66	NA	NA	NA	NA	3.52	1.35	NA	NA	4.76	2.02
K6	2.68	NA	4.93	NA	3.51	5.59	5.34	1	NA	5.19	6.9
K7	NA	NA	4.11	12.05	1	6.83	3.48	NA	NA	NA	15.56
K8	NA	NA	1.65	NA	NA	NA	NA	NA	3.54	3.47	9.18

In North America, diversity patterns can only be reconstructed for theropods and ornithischians in the late Early Cretaceous, which were both more diverse than their Late Jurassic counterparts, with all other groups too poorly sampled to retrieve a signal. In the non-marine record of North America, there are similar problems to Gondwana (see below) with distinguishing between false absences (i.e., a sampling failure) and true absences (i.e., a genuine lack of fossil occurrences and diversity) in the Early Cretaceous, with implications for the spatial structure of terrestrial diversity over the J/K boundary (Mannion *et al.*, 2015; Nicholson *et al.*, 2015). The North American non-marine fossil record is temporally discontinuous, but within a continuous macrostratigraphic sequence. This implies that sedimentary rock is available for sampling even during times when fossil record sampling and diversity are low or nil (Peters and Heim, 2010; Heim and Peters, 2011a) (Figure 30C, D), which suggests one of two things: either (1) the environments in which earliest Cretaceous tetrapods lived or were fossilised are not preserved in the available rock record; or (2) the lack of tetrapod fossils in the earliest Cretaceous represents genuine absence, following a J/K boundary extinction. Of interest is the timing of the apparent extinction, which coincides with the removal of a land bridge between North America and Eurasia around the J/K boundary. Such a land bridge was not re-established until the Hauterivian/Barremian (i.e., K2) (Brikiatis, 2016a), which is when there is a re-emergence of a diversity signal in dinosaur groups (Table 34). Furthermore, in the earliest Cretaceous, there was a breakdown of dinosaurian biogeographical connectivity between North America, and South America + Africa, at the family-level (Dunhill *et al.*, 2016), leading to increasing isolation of terrestrial faunas here. Further investigation into the facies, palaeoenvironment, and taphonomy of the earliest Cretaceous North American rock record should help to elucidate whether this apparent lack of diversity and extinction is a preservational artefact or genuine biological signal.

In Asia, the record of tetrapod diversity dynamics through the J/K boundary is patchy and discontinuous, with a Late Jurassic non-marine record composed primarily of crocodyliforms and lissamphibians possibly being replaced by an Early Cretaceous one comprising lepidosauromorphs and

choristoderes. Mammals, non-avian theropods, and birds appear to have explosively radiated during the Aptian in Asia, documented by the exceptionally well preserved Jehol Biota (Pan *et al.*, 2013; O'Connor and Zhou, 2015; Huang *et al.*, 2016; Wang *et al.*, 2016a), whereas sauropod and ornithischian diversity remained comparatively low. This high diversity is undoubtedly influenced by the Lagerstätten effect (i.e., episodes of greaty enhanced fossil record preservation), with the well-sampled Jehol Biota representing a window into the diverse Early Cretaceous Asian ecosystems (Huang *et al.*, 2016; Wang *et al.*, 2016b). However, the high diversity exhibited by this fauna remains in spite of the application of a fair subsampling protocol, and therefore it seems that this pattern of relative diversity reflects a genuine biological signal. Asian teleosaurid crocodylomorphs might have been more resilient to any regional changes across the J/K transition by inhabiting more freshwater environments than their European counterparts (Martin *et al.*, 2015a). Note that the specimens included in this study have not yet been formally described, and therefore were not included in the present dataset as potentially non-marine teleosaurids, as suggested (Martin *et al.*, 2015a). In general, the earliest Cretaceous record of Asia is poorer than Europe for two reasons: (1) the overall lack of occurrences; and (2) fossil-bearing sites often are spatiotemporally controversial, or dated within too wide a time-frame to be of any use for assessing diversity, especially through subsampling techniques, or any method which relies on well-constrained time bins. This is especially the case in Japan (Kusuhashi *et al.*, 2006; Matsukawa *et al.*, 2006; Matsumoto *et al.*, 2015), Thailand (Racey, 2009; Racey and Goodall, 2009), and China (Lucas and Estep, 1998; Tong *et al.*, 2009), and this uncertainty can have substantial consequences for our understanding of earliest Cretaceous diversity.

	Chelonioids	Crocodyliformes	Ichthyosaurs	Sauropterygians
J1	NA	NA	NA	NA
J2	NA	NA	NA	NA
J3	NA	NA	NA	NA
J4	NA	1	1.74	NA
J5	NA	1.18	NA	3.07
J6	NA	1.95	1.79	1
K1	NA	1.77	NA	NA
K2	NA	NA	NA	NA
K3	NA	1	1	1.52
K4	NA	NA	NA	NA
K5	NA	NA	NA	NA
K6	NA	NA	NA	NA
K7	1	NA	NA	NA
K8	NA	NA	NA	2.68

Table 33. Regional (South America) subsampled (SQS) diversity results for all marine tetrapod groups at the 10 million year time bin level.

Table 34. (Left) Regional (Europe) subsampled (SQS) diversity results for all non-marine tetrapod groups at the 10 million year time bin level. (Right) Regional (North America) subsampled (SQS) diversity results for all non-marine tetrapod groups at the 10 million year time bin level.

	Aves	Chroristoderes	Crocodyliformes	Lepidosauromorphs	Lissamphibians	Mammaliaformes	Ornithischians	Pterosaurs	Sauropodomorphs	Testudines	Theropods
J1	NA	NA	NA	1.34	NA	3.28	1	1.66	NA	NA	1
J2	NA	NA	NA	NA	NA	NA	NA	NA	NA	NA	NA
J3	NA	NA	NA	1	NA	NA	NA	1.43	NA	NA	NA
J4	NA	1	NA	2.49	1.54	13.41	NA	1.11	1.12	NA	2.19
J5	NA	NA	NA	NA	NA	NA	4.65	NA	NA	NA	1.76
J6	1	1	3.11	4.88	NA	9.03	2.24	3.66	3.71	3.91	4.97
K1	NA	NA	2.88	6.52	3	9.49	2.76	NA	1.95	4	2.48
K2	3.27	NA	3.95	3.71	6.84	4.08	2.94	2.05	NA	NA	7.68
K3	NA	NA	1.58	NA	NA	NA	1.54	NA	2.28	NA	NA
K4	NA	NA	2.4	3.22	NA	NA	NA	3.05	1.66	NA	1.75
K5	NA	NA	NA	NA	NA	NA	NA	1.65	NA	NA	NA
K6	2.15	NA	NA	NA	NA	NA	2.36	NA	NA	NA	NA
K7	NA	NA	3.63	NA	NA	NA	2.16	2.35	1	2.88	NA
K8	NA	NA	3.12	2.17	2.09	4.13	3.84	1.69	1.71	2.74	5.87

	Aves	Chroristoderes	Crocodyliformes	Lepidosauromorphs	Lissamphibians	Mammaliaformes	Ornithischians	Pterosaurs	Sauropodomorphs	Testudines	Theropods
J1	NA	NA	1	1	NA	NA	NA	NA	1.34	NA	NA
J2	NA	NA	NA	NA	NA	NA	NA	NA	NA	NA	NA
J3	NA	NA	NA	NA	NA	NA	NA	NA	NA	NA	NA
J4	NA	1	NA	NA	NA	NA	NA	NA	NA	NA	NA
J5	NA	NA	NA	NA	NA	NA	NA	NA	NA	NA	NA
J6	NA	1	1.91	2.92	2.48	5.36	2.84	NA	2.99	1.44	1.77
K1	NA	NA	NA	NA	NA	NA	NA	NA	NA	NA	NA
K2	NA	NA	NA	NA	NA	NA	4	NA	1.84	NA	3.65
K3	NA	NA	NA	NA	NA	NA	2	NA	NA	1.5	2.48
K4	NA	NA	NA	NA	1.77	3.91	3.47	NA	1.97	1.5	1.62
K5	2.1	NA	1.91	4.39	1	6.6	2.7	NA	NA	NA	3.08
K6	2.19	NA	1.46	NA	NA	4.39	5.3	1.56	NA	3.22	1.52
K7	2.1	1.08	2.21	6.95	2.11	6.62	9.42	1.87	1	4.23	4.92
K8	5.99	1	2.15	7.8	3.83	7.31	3.64	1	1	5.11	4.53

In Gondwana, there is almost no information about diversity in the earliest Cretaceous (Table 28, Table 32, Table 33, Table 35). The only group for which a subsampled signal can be recovered in the Berriasian of Africa is Theropoda, which documents a regional diversity decline of around 50% across the J/K boundary. Fossils from the earliest Cretaceous of Africa are almost entirely absent, virtually exclusively known from dinosaurian faunas of the Berriasian–Valanginian Kirkwood Formation (South Africa) (McPhee *et al.*, 2016), and a Berriasian microsite in Morocco (Sigogneau-Russell *et al.*, 1998). The Moroccan site at Anoual includes a diverse assemblage of mammals, lissamphibians, lepidosaurs, and turtles, as well as numerous indeterminate dinosaurs, the majority of which represent small maniraptoran theropods (Sigogneau-Russell *et al.*, 1998). However, many of these data are not added to total diversity estimates because they are single-publication occurrences from one large collection (see Section 2.6 and Alroy (2010a)), and therefore the tetrapod diversity of the earliest Cretaceous of Africa is under-estimated (McPhee *et al.*, 2016) in these subsampled results. In South America, only moderately low diversity can be detected for turtles, pterosaurs, and sauropods in the Late Jurassic, but a signal does not emerge again until the late Early Cretaceous. This lack of earliest Cretaceous signal remains despite the presence of a rich marine tetrapod fauna in the Rosablanca Formation of Colombia, comprising testudines, plesiosaurs, and ichthyosaurs (Fonseca, 2015), but which is dated to the late Valanginian–Hauterivian, and therefore occurrences are not confined to a single time bin as the subsampling analyses require. This overall pattern is similar to that of North America, with a well-sampled Late Jurassic fauna discontinuously sampled through the J/K boundary, with no signal emerging until the Barremian. The main issue for Gondwana is whether the overall lack of signal results from either sampling failure or genuinely low diversity, a problem exacerbated by the lack of a comprehensive, continuous, and well-dated geological record throughout this time.

	Aves	Chroristoderes	Crocodyliformes	Lepidosauromorphs	Lissamphibians	Mammaliaformes	Ornithischians	Pterosaurs	Sauropodomorphs	Testudines	Theropods
J1	NA	NA	NA	NA	NA	NA	NA	NA	NA	NA	NA
J2	NA	NA	NA	NA	NA	NA	NA	NA	NA	NA	NA
J3	NA	NA	NA	NA	NA	NA	NA	NA	NA	NA	NA
J4	NA	NA	NA	NA	NA	NA	NA	NA	NA	NA	NA
J5	NA	NA	NA	NA	NA	NA	NA	NA	1.49	NA	NA
J6	NA	NA	NA	NA	NA	NA	NA	1.5	NA	1.42	NA
K1	NA	NA	NA	NA	NA	NA	NA	NA	NA	NA	NA
K2	NA	NA	NA	NA	NA	NA	NA	NA	NA	NA	NA
K3	NA	NA	1.63	NA	NA	NA	NA	NA	NA	NA	NA
K4	NA	NA	3.3	NA	NA	NA	NA	3.15	NA	2.7	NA
K5	NA	NA	1	NA	NA	NA	NA	NA	1.97	NA	3.43
K6	1.75	NA	9.08	NA	NA	NA	1.5	NA	NA	NA	NA
K7	NA	NA	2.32	NA	1.51	NA	4.62	NA	NA	4.42	NA
K8	3.76	NA	2.95	NA	NA	NA	NA	NA	NA	NA	NA

Table 35. Regional (South America) subsampled (SQS) diversity results for all non-marine tetrapod groups at the 10 million year time bin level.

'Global' marine tetrapod dynamics across the J/K boundary are dominated by the South American and European fossil records, with the marine records in North America, Africa and Asia too discontinuous to document changes. In South America a small decline is observed in thalattosuchian diversity (10%), coupled with an apparent loss of all ichthyosaur and sauropterygian taxa across the J/K boundary. However, it should be noted that some taxa were excluded from the analyses as they cannot be constrained to any single time bin. For intervals in which sampling is too poor to produce a subsampled diversity signal, a result of NA (i.e., a gap in our knowledge) is reported. Even in these intervals there are often specimens present, but that these will just be singleton occurrences or not taxonomically identifiable to the genus level, and therefore exluded from diversity counts. In Europe there is the greatest loss in diversity, similar to the non-marine realm, with thalattosuchians showing a major decline (52%) alongside sauropterygians (48% loss) from the Tithonian to Valanginian. Ichthyosaurs are too poorly sampled in the earliest Cretaceous, but their Hauterivian diversity is 40% that of Tithonian levels, a signal which is recoverred with SQS at a moderate quorum (0.4), despite a relatively low sample size. This overall lack of signal in the Berriasian marine record can be attributed to a sampling failure (Good's $u = 0$). However, sampling in the Valanginian is better than the latest Jurassic (Kimmeridgian–Tithonian), indicating that the overall pattern of apparently global decline reflects a regional biological signal composed of diversity decreases in South America and Europe.

3.2.4 Latitudinal patterns of diversity change

At a coarse 10 million year time bin resolution, the smaller non-marine tetrapod groups such as lepidosaurs and mammaliaforms seem to increase in subsampled diversity (86% and 68%, respectively) across the J/K boundary in northern temperate biozones (30-60°N). This is distinct from ornithischian and sauropod dinosaurs, which both see a decrease in diversity from the J6 to K1 time bins (31% and

42%, respectively), and theropod diversity appears to remain constant. While the S1 (0-30°S) latitudinal belt is relatively well-sampled in the latest Jurassic, levels are consistently lower than for the N2 bin, with only theropods being as diverse. Changes across the J/K boundary in the Southern Hemisphere are impossible to assess due to the poor sampling of earliest Cretaceous groups, or their absence. During the Late Jurassic to Early Cretaceous, the majority of the Gondwanan landmass occupied a belt at approximately 30°–80° palaeolatitude, but extended in part south to the equator, imposing a considerable climatic gradient across the continent (McLoughlin, 2001). Such a factor could be responsible for the relatively poor fossil record and low recovered diversity signal in tetrapods throughout this time.

N3	K8	K7	K6	K5	K4	K3	K2	K1	J6	J5	J4	J3	J2	J1
Aves	NA	1.35	NA	NA	NA	NA	NA	NA	NA	NA	NA	NA	NA	NA
Choristodera	NA	NA	NA	NA	NA	NA	NA	NA	NA	NA	NA	NA	NA	NA
Crocodyliformes	NA	NA	NA	NA	NA	NA	NA	NA	NA	NA	NA	NA	NA	NA
Lepidosauromorpha	NA	NA	NA	NA	NA	NA	NA	NA	NA	NA	NA	NA	NA	NA
Lissamphibia	NA	NA	NA	NA	NA	NA	NA	NA	NA	NA	NA	NA	NA	NA
Mammaliaformes	3.3	NA	NA	NA	NA	NA	NA	NA	NA	NA	NA	NA	NA	NA
Pterosauria	NA	NA	NA	NA	NA	NA	NA	NA	NA	NA	NA	NA	NA	NA
Ornithischia	NA	2.27	NA	NA	NA	NA	NA	NA	NA	NA	NA	NA	NA	NA
Sauropodomorpha	NA	NA	NA	NA	NA	NA	NA	NA	NA	NA	NA	NA	NA	NA
Testudines	NA	NA	NA	NA	NA	NA	NA	NA	NA	NA	NA	NA	NA	NA
Theropoda	NA	2.62	NA	NA	NA	NA	NA	NA	NA	NA	NA	NA	NA	NA

Table 36. Subsampled latitudinal diversity changes in non-marine tetrapod groups in N3 latitudinal bin (60-90°N)

N2	K8	K7	K6	K5	K4	K3	K2	K1	J6	J5	J4	J3	J2	J1
Aves	6.65	4.17	2.95	3.23	1.17	35.23	NA	NA	1	NA	NA	NA	NA	NA
Choristodera	1	1.09	NA	NA	NA	4.47	NA	2	1	NA	1	NA	NA	NA
Crocodyliformes	1.98	NA	NA	NA	4.88	2.36	NA	NA	NA	NA	NA	NA	NA	1
Lepidosauromorpha	5.43	9.51	NA	5.17	NA	5.41	NA	7.32	3.93	NA	2.55	1	NA	1.35
Lissamphibia	4.45	2.32	4.92	2.01	2.03	2.49	3.84	3	NA	3.33	1.91	NA	NA	NA
Mammaliaformes	7.49	7.9	6.65	7.49	5.1	7.57	6.8	12.04	7.17	NA	13.09	NA	NA	3.44
Pterosauria	1.67	3.57	2.13	2.37	4.15	NA	1.74	6.2	4.47	NA	1.08	1.47	NA	1.67
Ornithischia	5.21	9.97	9.8	4.61	6.1	3.31	4.51	2.69	3.46	5.02	NA	NA	NA	1.4
Sauropodomorpha	1.73	2.68	NA	NA	4.72	3.79	5.42	1.97	3.34	NA	1.14	NA	NA	2.68
Testudines	6.08	5.71	7.01	4.62	5.88	NA	7.3	4.33	3.99	1.61	NA	NA	NA	NA
Theropoda	6.11	7.4	7.64	4.83	2.22	7.06	15.64	2.51	2.46	6.3	2.3	NA	NA	1.93

Table 37. Subsampled latitudinal diversity changes in non-marine tetrapod groups in N2 latitudinal bin (30-60°N)

N1	K8	K7	K6	K5	K4	K3	K2	K1	J6	J5	J4	J3	J2	J1
Aves	NA	NA	NA	NA	NA	NA	NA	NA	NA	NA	NA	NA	NA	NA
Choristodera	NA	NA	NA	NA	NA	NA	NA	NA	NA	NA	NA	NA	NA	NA
Crocodyliformes	1.98	NA	NA	NA	4.88	2.36	NA	NA	NA	NA	NA	NA	NA	1
Lepidosauromorpha	1.32	NA	NA	NA	NA	NA	NA	NA	NA	NA	NA	NA	NA	1
Lissamphibia	NA	NA	NA	1.83	2	NA	NA	NA	NA	NA	NA	NA	NA	NA
Mammaliaformes	NA	NA	NA	NA	NA	NA	NA	NA	NA	NA	NA	NA	NA	NA
Pterosauria	1.5	NA	NA	2.17	NA	NA	NA	NA	NA	NA	NA	NA	NA	NA
Ornithischia	NA	NA	NA	NA	NA	1.79	NA	NA	NA	NA	NA	NA	NA	NA
Sauropodomorpha	NA	NA	NA	1.89	NA	NA	NA	NA	NA	1.39	1.43	NA	NA	1.65
Testudines	NA	NA	NA	1.99	NA	NA	NA	NA	NA	NA	NA	NA	NA	NA
Theropoda	NA	1.77	NA	3.54	2.21	NA	NA	1	NA	NA	NA	NA	NA	NA

Table 38. Subsampled latitudinal diversity changes in non-marine tetrapod groups in N1 latitudinal bin (0-30°N)

S1	K8	K7	K6	K5	K4	K3	K2	K1	J6	J5	J4	J3	J2	J1
Aves	NA	NA	NA	NA	NA	NA	NA	NA	NA	NA	NA	NA	NA	NA
Choristodera	NA	NA	NA	NA	NA	NA	NA	NA	NA	NA	NA	NA	NA	NA
Crocodyliformes	5.31	NA	NA	NA	3.11	1.74	NA	NA	2	NA	NA	NA	NA	NA
Lepidosauromorpha	NA	NA	NA	NA	NA	NA	NA	NA	NA	NA	NA	NA	NA	NA
Lissamphibia	NA	1	NA	NA	NA	NA	NA	NA	NA	NA	NA	NA	NA	NA
Mammaliaformes	2.38	NA	NA	NA	NA	NA	NA	NA	NA	NA	NA	NA	NA	NA
Pterosauria	NA	NA	NA	NA	2.69	NA	NA	NA	2.35	NA	NA	NA	NA	NA
Ornithischia	NA	NA	NA	NA	NA	NA	NA	NA	1.19	NA	NA	NA	NA	NA
Sauropodomorpha	4.66	NA	NA	NA	NA	NA	NA	NA	2.41	1.75	NA	NA	NA	1.37
Testudines	NA	NA	NA	NA	3.54	NA	NA	NA	NA	NA	NA	NA	NA	NA
Theropoda	NA	NA	NA	NA	NA	NA	NA	NA	2.32	NA	NA	NA	NA	NA

Table 39. Subsampled latitudinal diversity changes in non-marine tetrapod groups in S1 latitudinal bin (0-30°S).

S2	K8	K7	K6	K5	K4	K3	K2	K1	J6	J5	J4	J3	J2	J1
Aves	2.45	NA	1.73	NA	NA	NA	NA	NA	NA	NA	NA	NA	NA	NA
Choristodera	NA	NA	NA	NA	NA	NA	NA	NA	NA	NA	NA	NA	NA	NA
Crocodyliformes	1.48	NA	4.47	1	NA	1.29	NA	NA	NA	NA	NA	NA	NA	1.5
Lepidosauromorpha	NA	NA	NA	NA	1	NA	NA	NA	NA	NA	NA	NA	NA	NA
Lissamphibia	1	NA	NA	NA	NA	NA	NA	NA	NA	NA	NA	NA	NA	NA
Mammaliaformes	1	NA	NA	NA	NA	NA	NA	NA	NA	NA	NA	NA	NA	2.38
Pterosauria	NA	NA	NA	NA	2.48	NA	NA	NA	1.51	NA	NA	NA	NA	NA
Ornithischia	NA	1	1.51	NA	NA	NA	NA	NA	NA	NA	NA	NA	NA	2.76
Sauropodomorpha	2.9	NA	NA	3.52	NA	1.51	NA	NA	NA	1.47	NA	NA	NA	1.94
Testudines	2.8	NA	NA	NA	2.33	NA	NA	NA	1.42	NA	NA	NA	NA	NA
Theropoda	1.93	NA	NA	NA	1	NA	NA	NA	NA	NA	NA	NA	NA	1.74

Table 40. Subsampled latitudinal diversity changes in non-marine tetrapod groups in S2 latitudinal bin (30-60°S).

S3	K8	K7	K6	K5	K4	K3	K2	K1	J6	J5	J4	J3	J2	J1
Aves	NA	NA	NA	NA	NA	NA	NA	NA	NA	NA	NA	NA	NA	NA
Choristodera	NA	NA	NA	NA	NA	NA	NA	NA	NA	NA	NA	NA	NA	NA
Crocodyliformes	NA	NA	NA	NA	NA	NA	NA	NA	NA	NA	NA	NA	NA	NA
Lepidosauromorpha	NA	NA	NA	NA	NA	NA	NA	NA	NA	NA	NA	NA	NA	NA
Lissamphibia	NA	NA	NA	NA	NA	NA	NA	NA	NA	NA	NA	NA	NA	NA
Mammaliaformes	NA	NA	NA	NA	NA	NA	NA	NA	NA	NA	NA	NA	NA	NA
Pterosauria	NA	NA	NA	NA	NA	NA	NA	NA	NA	NA	NA	NA	NA	NA
Ornithischia	NA	NA	NA	NA	1	NA	NA	NA	NA	NA	NA	NA	NA	NA
Sauropodomorpha	NA	NA	NA	NA	NA	NA	NA	NA	NA	NA	NA	NA	NA	NA
Testudines	NA	NA	NA	NA	NA	NA	NA	NA	NA	NA	NA	NA	NA	NA
Theropoda	NA	NA	NA	NA	NA	NA	NA	NA	NA	NA	NA	NA	NA	NA

Table 41. Subsampled latitudinal diversity changes in non-marine tetrapod groups in S3 latitudinal bin (60-90°S).

In the marine realm, the only latitudinal signal detected is for sauropterygians for N2, where diversity declines by around one quarter across the J/K transition, and for crocodyliforms in the S2 latitudinal belt there is a slight decline in the diversity of South American thalattosuchians. As with non-marine tetrapods, the polar and tropical regions are almost devoid of well-sampled tetrapod faunas, and subsampled diversity estimates are impossible to estimate in any consistent manner.

N3	K8	K7	K6	K5	K4	K3	K2	K1	J6	J5	J4	J3	J2	J1
Chelonioidea	NA	NA	NA	NA	NA	NA	NA	NA	NA	NA	NA	NA	NA	NA
Crocodyliformes	NA	NA	NA	NA	NA	NA	NA	NA	NA	NA	NA	NA	NA	NA
Ichthyopterygia	NA	NA	NA	NA	NA	NA	NA	NA	NA	NA	NA	NA	NA	NA
Sauropterygia	NA	NA	NA	NA	NA	NA	NA	NA	1.25	NA	NA	NA	NA	NA

Table 42. Subsampled latitudinal diversity for marine tetrapods in N3 latitudinal bin (60-90°N).

N2	K8	K7	K6	K5	K4	K3	K2	K1	J6	J5	J4	J3	J2	J1
Chelonioidea	2.65	5.04	3.35	NA	NA	NA	NA	NA	NA	NA	NA	NA	NA	NA
Crocodyliformes	1.57	1.65	NA	NA	NA	1	NA	NA	2.94	2.96	1.54	2.01	NA	NA
Ichthyopterygia	NA	NA	NA	1.53	1.72	2.35	2.55	NA	2.57	1.9	NA	1.86	1.63	1.72
Sauropterygia	3.5	3.85	3.69	3.22	3.36	NA	NA	1.49	2.1	4.01	1.66	3.38	NA	4.4

Table 43. Subsampled latitudinal diversity for marine tetrapods in N2 latitudinal bin (30-60°N).

N1	K8	K7	K6	K5	K4	K3	K2	K1	J6	J5	J4	J3	J2	J1
Chelonioidea	NA	NA	NA	NA	NA	NA	NA	NA	NA	NA	NA	NA	NA	NA
Crocodyliformes	3.05	NA	NA	NA	NA	NA	NA	NA	2	1	1	NA	NA	NA
Ichthyopterygia	NA	NA	NA	NA	NA	1	NA	NA	1.67	NA	NA	NA	NA	NA
Sauropterygia	NA	NA	NA	NA	NA	1.51	NA	NA	NA	NA	NA	NA	NA	NA

Table 44. Subsampled latitudinal diversity for marine tetrapods in N1 latitudinal bin (0-30°N).

S1	K8	K7	K6	K5	K4	K3	K2	K1	J6	J5	J4	J3	J2	J1
Chelonioidea	NA	NA	NA	NA	NA	NA	NA	NA	NA	NA	NA	NA	NA	NA
Crocodyliformes	1	NA	NA	NA	NA	1	NA	NA	NA	1	NA	NA	NA	NA
Ichthyopterygia	NA	NA	NA	NA	NA	NA	NA	NA	NA	NA	NA	NA	NA	NA
Sauropterygia	NA	NA	NA	NA	NA	NA	NA	NA	1	NA	NA	NA	NA	NA

Table 45. Subsampled latitudinal diversity for marine tetrapods in S1 latitudinal bin (0-30°S).

S2	K8	K7	K6	K5	K4	K3	K2	K1	J6	J5	J4	J3	J2	J1
Chelonioidea	NA	NA	NA	NA	2.34	NA	NA	NA	NA	NA	NA	NA	NA	NA
Crocodyliformes	NA	NA	NA	NA	NA	NA	NA	1.77	1.99	NA	NA	NA	NA	NA
Ichthyopterygia	NA	NA	NA	NA	1	NA	NA	NA	2.01	NA	1.75	NA	NA	NA
Sauropterygia	2.67	NA	NA	NA	NA	NA	NA	1.66	1	NA	NA	NA	NA	NA

Table 46. Subsampled latitudinal diversity for marine tetrapods in S2 latitudinal bin (30-60°S).

S3	K8	K7	K6	K5	K4	K3	K2	K1	J6	J5	J4	J3	J2	J1
Chelonioidea	NA	NA	NA	NA	NA	NA	NA	NA	NA	NA	NA	NA	NA	NA
Crocodyliformes	NA	NA	NA	NA	NA	NA	NA	NA	NA	NA	NA	NA	NA	NA
Ichthyopterygia	NA	NA	NA	NA	1.53	NA	NA	NA	NA	NA	NA	NA	NA	NA
Sauropterygia	1.66	NA	NA	NA	NA	NA	NA	NA	NA	NA	NA	NA	NA	NA

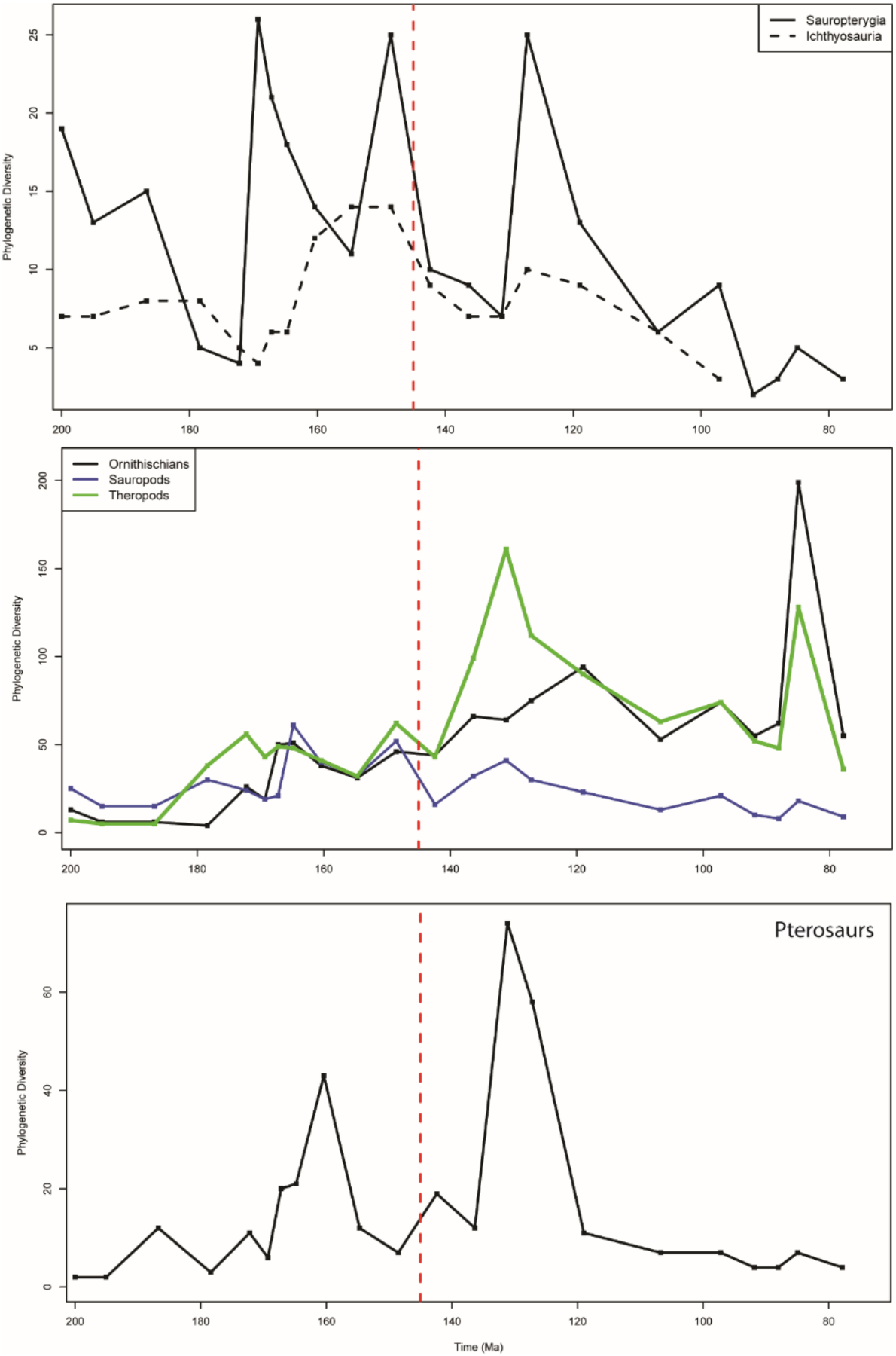
Table 47. Subsampled latitudinal diversity for marine tetrapods in S3 latitudinal bin (60-90°S).

3.2.5 Phylogenetic diversity estimation

Results using PDE are broadly congruent with the shape of diversity curves through the J/K transition obtained using SQS. In Sauropterygia, there is evidence of a dramatic decline across the J/K boundary, a factor that is not recovered by the SQS analyses due to poor sampling of the earliest Cretaceous. There is a similar pattern in ichthyosaurs, with a continuous decline over the J/K boundary until the

Valanginian, followed by a small Barremian peak, and the continuous decline until their final extinction in the Late Cretaceous. In theropods, the magnitude of the diversity decline using PDE is not as great as that implied by SQS. Both theropods and sauropods suffer a small decline across the J/K boundary, whereas diversity for ornithischians remains stable. For pterosaurs, the PDE indicates a long-term decline from the Oxfordian to the Tithonian, with a recovery through the boundary and then another small diversity drop in the Valanginian. This is followed by a large diversification in the Hauterivian, which is distinct from the low diversity recorded in this group then using SQS.

Figure 24. Phylogenetic diversity estimates for different tetrapod clades.


Sauropterygia
Ichthyosauria
Phylogenetic Diversity
Ornithischians
Sauropods
Theropods
Pterosaurs
Time (Ma)

3.2.6 Bootstrapped Shareholder Quorum Subsampling (SQS)

Two large scale bootstrapped SQS analyses were performed at the tetrapod level for marine and non-marine taxa. Non-marine tetrapods show an uncertain diversity pattern through the J/K boundary, with differences between the upper and lower confidence intervals suggesting that there might even have been an overall increase in diversity. There is a definitive crash in diversity in the Hauterivian, with very narrow confidence intervals. However, at least a part of this might be due to overall poor sampling, and the presence of multiple-occurrence single genera within each taxonomic subset of the tetrapod dataset. In marine tetrapods, the overall pattern of decline through the J/K transition remains notable. There is a continuous decline from the Tithonian to the Hauterivian, a pattern which remains constrained within the confidence intervals. However, these patterns fail to account for, or detect, the smaller-scale variations that are found at the finer clade level. Note also that these groups we analysed at this scale do not represent clades, but ecological groups.

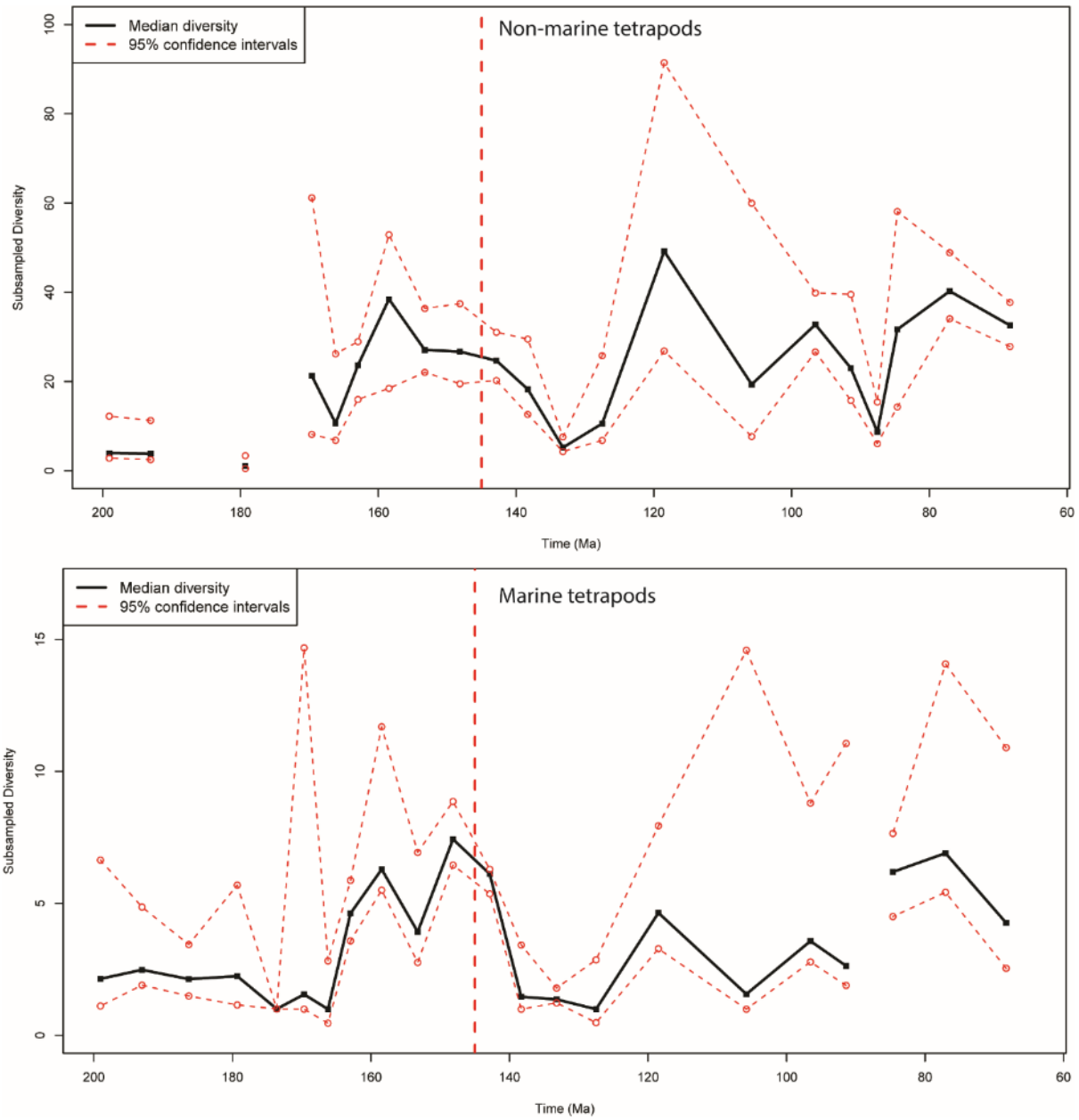


Figure 25. Bootstrapped SQS diversity for non-marine and marine tetrapods.

For individual clades, the bootstrapping procedure emphasises some of the uncertainty in the magnitude of diversity decline across the J/K transition. For theropods, the magnitude of decline remains very high and is their greatest diversity drop during the study interval. Sauropods remain too poorly sampled in the Berriasian to detect a diversity signal, but when a signal re-emerges in the Valanginian, diversity is consistently lower than at any time during the Late Jurassic. This pattern is

also mirrored by pterosaurs across the J/K transition. For ornithischians, the analyses cannot detect whether there is a slight increase, slight decrease, or no change in diversity across the J/K boundary. The lower confidence interval remains flat from the Kimmeridgian to the Albian, suggesting that the J/K transition was a time period of relative stability for ornithischian groups. For non-marine crocodylomorphs, bootstrapping highlights much uncertainty in the upper bounds of the potential diversity crash. Earliest Cretaceous diversity was consistently low but appears to have recovered in the Barremian and into the 'middle' Cretaceous.

In the marine realm, earliest Cretaceous diversity for ichthyosaurs remains unknown, but their Hauterivian diversity is consistently lower than their Tithonian diversity. This provides further evidence for a diversity loss but it is difficult to identify when this happened due to poor sampling of the earliest Cretaceous marine deposits. Sauropterygian diversity is also unknown in the Berriasian due to poor sampling, and when a signal re-emerges in the Valanginian it is as low as the lower bound of Tithonian diversity. Marine crocodylomorphs (Thalattosuchia) show evidence of a consistent decline into the earliest Cretaceous, supported by very narrow confidence intervals. Based on the upper bound of the subsampled Kimmeridgian diversity, it cannot be excluded that this drop began in the Kimmeridgian with a continuous pattern of decline across the J/K transition.

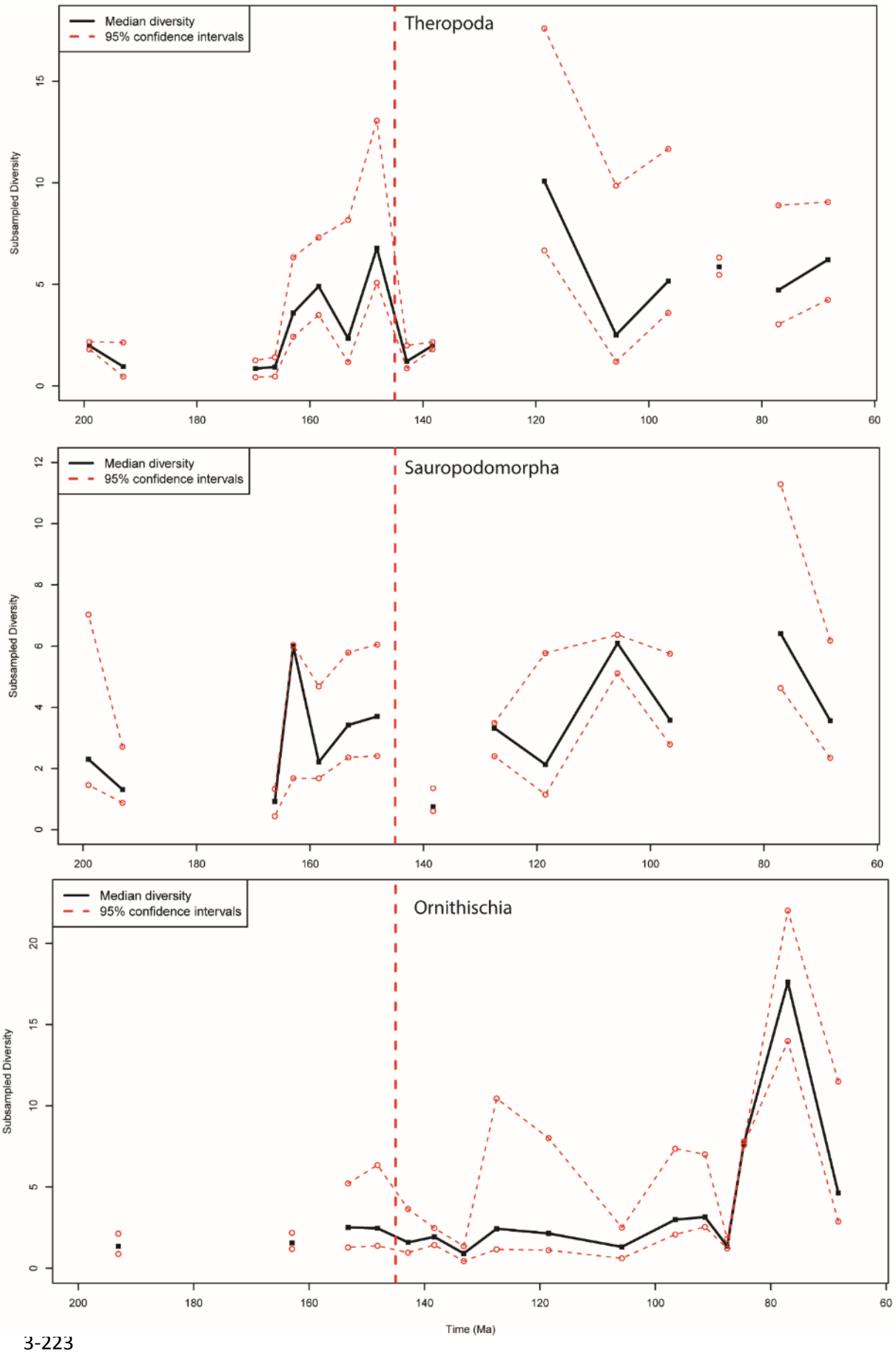
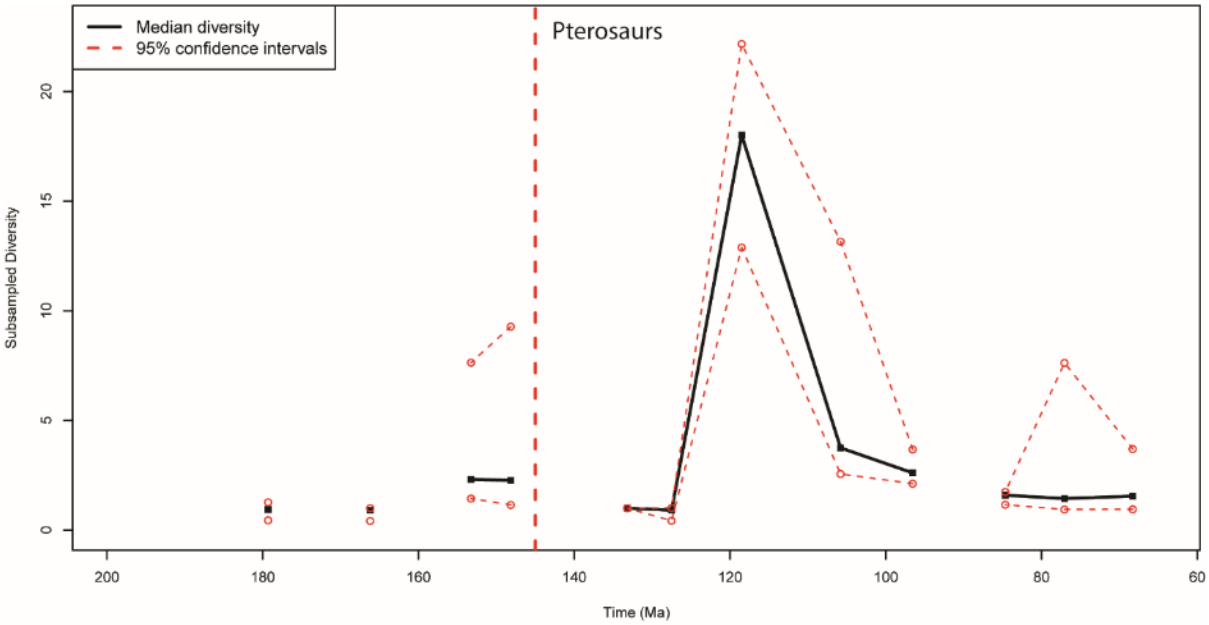

Median diversity
95% confidence intervals
Theropoda
Subsampled Diversity
Median diversity
95% confidence intervals
Sauropodomorpha
Subsampled Diversity
Median diversity
95% confidence intervals
Ornithischia
Subsampled Diversity
Time (Ma)

Figure 26. Bootstrapped SQS diversity for the three major dinosaurian clades.



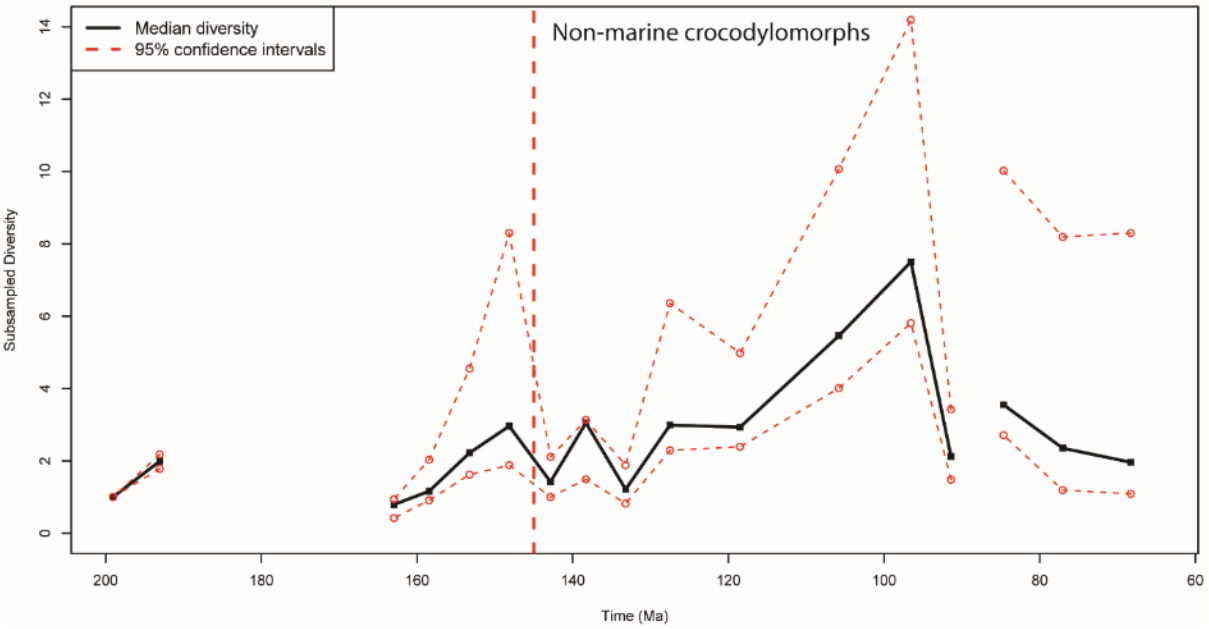


Figure 27. Bootstrapped SQS diversity for pterosaurs and non-marine crocodylomorphs.

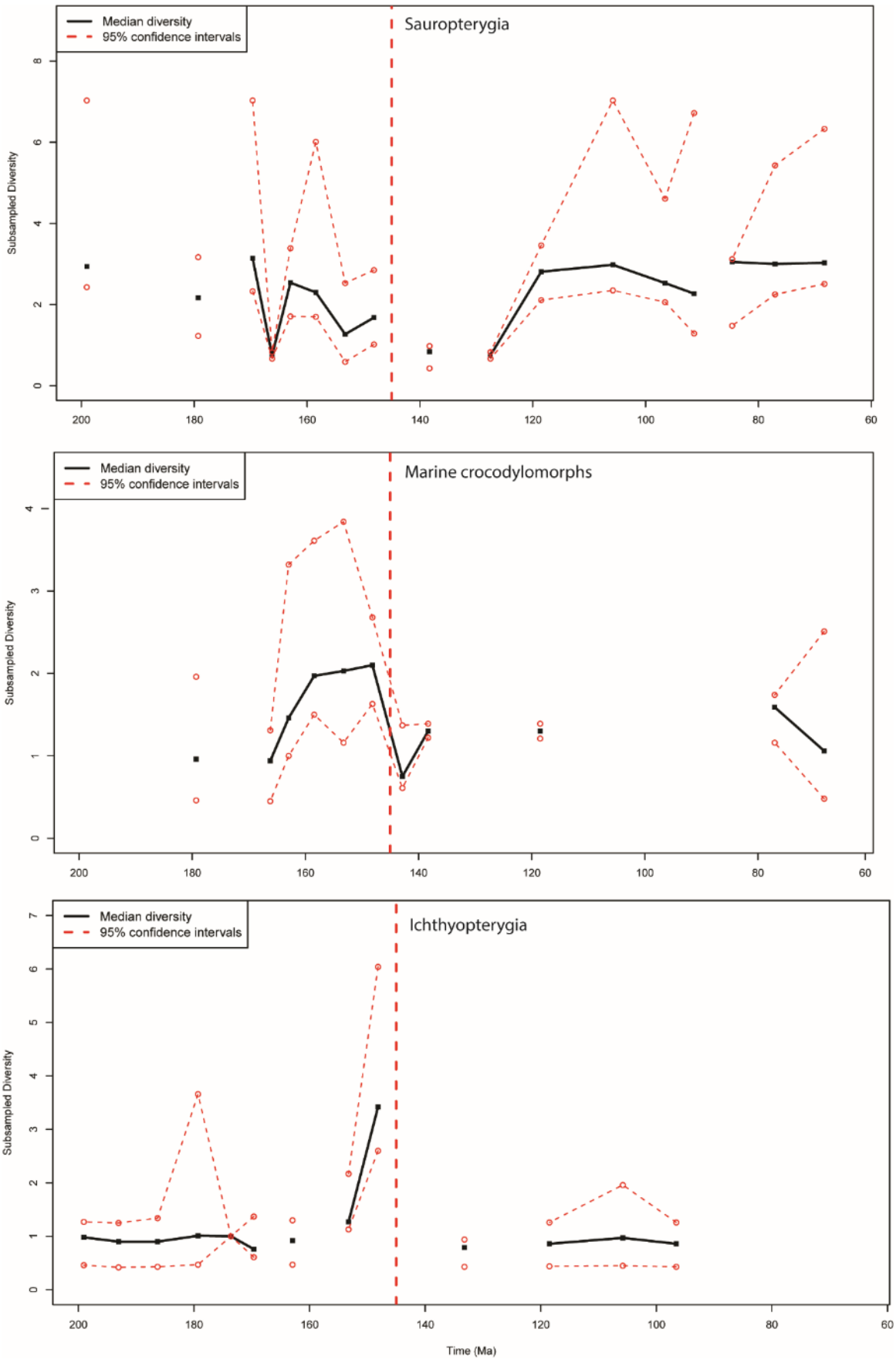

Median diversity
95% confidence intervals
Sauropterygia
Subsampled Diversity
Median diversity
95% confidence intervals
Marine crocodylomorphs
Subsampled Diversity
Median diversity
95% confidence intervals
Ichthyopterygia
Subsampled Diversity
Time (Ma)

Figure 28. Bootstrapped SQS diversity for marine tetrapod groups.

3.2.7 Patterns of global extinction and origination

The global patterns of diversity reported above are largely reflected in rates of extinction and origination. Crocodyliforms (marine and non-marine), ichthyosaurs, sauropterygians, sauropods, theropods, pterosaurs and turtles all experienced greatly elevated extinction rates at the end of the Tithonian, recorded in both boundary-crosser (BC) and three-timer (3T) estimates (Table 48, Table 49, Table 50, Table 51, Table 52, Table 53, Table 54, Table 55). However, in some groups (e.g., ichthyosaurs) it is still possible that an extremely poor earliest Cretaceous fossil record influences these results. In most groups, the earliest Cretaceous record is too poor to gauge accurate estimates of extinction. However, marine crocodyliforms, theropods and pterosaurs sustained high extinction rates into the Berriasian, which coincides with the greatest diversity losses recorded among all tetrapod groups. The highest end-Jurassic extinction rates were in sauropods, at more than six times higher than Jurassic turnover rates, and twice those in the 'middle' Cretaceous. In all other groups, the end-Jurassic was singularly the most intense period of extinction of all intervals throughout the Jurassic and Cretaceous (except for the end-Cretaceous mass extinction, which was not included in analyses). Confidence is lent to these results based on using both 3T and BC estimates, as not only do both converge on the same overall pattern, but the use of 3T extinctions compensates for deficiencies in the fossil record caused by the issue of incomplete sampling in the earliest Cretaceous by accounting for the Signor-Lipps effect. This can have the undesired effect of artificially clustering extinctions at the end of well-sampled intervals due to artificial range truncation (Foote, 2000; Peters and Foote, 2002; Foote, 2003; 2005; Holland and Patzkowsky, 2015), which can have the consequence of making a simultaneous extinction appear more gradual as extinctions are based on ranges and last occurrences of taxa rather than 'true' extinction times. Furthermore, the general pattern of elevated extinction rates is reflected

both at the 10 million year time bin level and at stage resolution, suggesting that, as with the diversity analyses, these patterns are resilient to heterogeneity in bin lengths across the J/K transition.

10 myr time bin	Aves	Chel	Chor	Crocs (non-marine)	Crocs (marine)	Ichthy	Lepid	Liss	Mamm	Ornith	Plesio	Ptero	Sauro	Test	Thero
K8	0.560	2.079	0.693	0.821	0.916	NA	1.078	1.179	1.224	1.122	0.368	0.511	0.405	1.145	0.965
K7	0.811	0.693	0.405	0.087	NA	NA	0.057	0.223	0.642	0.251	0.442	0.693	0.201	0.236	0.329
K6	NA	0.405	NA	0.154	NA	NA	0.054	0.405	0.095	NA	0.182	NA	NA	0.211	NA
K5	0.288	NA	NA	0.288	NA	0.693	0.134	0.223	0.310	0.348	NA	0.693	0.182	0.375	0.125
K4	NA	NA	0.405	0.405	NA	NA	0.167	0.336	NA	0.241	0.105	0.560	0.241	0.348	0.143
K3	NA	NA	0.405	NA	0.223	0.288	0.167	0.182	0.182	0.201	0.105	0.223	0.241	0.154	0.310
K2	0.405	NA	NA	0.288	0.288	NA	0.241	NA	0.405	0.318	0.118	NA	NA	0.080	0.201
K1	NA	NA	NA	0.182	0.223	0.916	0.336	0.336	0.811	0.118	0.154	0.511	0.201	0.288	NA
J6	NA	NA	NA	0.811	0.588	0.693	NA	NA	0.405	0.847	0.288	1.099	1.335	0.956	0.619
J5	NA	NA	NA	0.182	0.288	NA	0.105	0.182	0.693	0.405	NA	0.405	NA	0.223	0.134
J4	NA	NA	NA	NA	NA	0.693	NA	NA	NA	NA	NA	NA	NA	NA	NA
J3	NA	NA	NA	NA	NA	0.511	NA	NA	NA	NA	0.405	NA	NA	NA	NA
J2	NA	NA	NA	NA	NA	NA	NA	NA	NA	1.099	NA	0.693	NA	NA	NA
J1	NA	NA	NA	NA	NA	NA	NA	NA	NA	NA	NA	NA	NA	NA	NA

Table 48. 'Foote' extinction rates for all major marine and non-marine tetrapod groups at 10 million year time bin intervals. Abbreviations: Chel, Chelonioidea; Chor, Choristodera; Crocs, Crocodyliformes; Ichthy, Ichthyosauria; Lepid, Lepidosauria; Liss, Lissamphibia; Mamm, Mammaliaformes; Ornith, Ornithischia; Plesio, Plesiosauria; Ptero, Pterosauria; Sauro, Sauropodomorpha; Test, Testudines; Thero, Theropoda.

10 myr time bin	Aves	Chel	Chor	Crocs (non-marine)	Crocs (marine)	Ichthy	Lepid	Liss	Mamm	Ornith	Plesio	Ptero	Sauro	Test	Thero
K8	NA	NA	NA	NA	NA	NA	NA	NA	NA	NA	NA	NA	NA	NA	NA
K7	0.405	1.386	NA	0.492	0.405	NA	0.693	0.916	1.030	0.999	NA	0.288	0.105	0.788	0.665
K6	0.560	0.916	0.288	0.288	NA	NA	0.477	0.223	0.531	0.288	0.262	0.693	0.262	0.499	0.314
K5	0.288	NA	NA	0.288	NA	NA	0.251	0.405	0.435	0.080	0.095	NA	NA	0.241	0.125
K4	0.693	0.693	NA	0.118	0.223	0.405	0.087	0.182	0.619	0.375	0.105	0.223	NA	0.223	0.143
K3	NA	NA	0.405	0.405	0.223	NA	NA	0.336	0.182	0.105	0.201	0.405	0.087	0.288	0.310
K2	0.405	NA	NA	0.154	NA	0.288	0.241	0.182	0.223	NA	0.223	0.405	0.167	0.223	0.105
K1	NA	NA	0.405	0.336	NA	NA	0.095	NA	0.405	0.629	0.154	0.288	0.368	0.442	0.288
J6	0.693	NA	NA	0.223	NA	0.693	NA	NA	0.223	0.288	NA	0.405	0.182	0.470	NA
J5	NA	NA	NA	0.956	0.606	0.916	0.511	0.470	0.693	1.012	0.511	1.099	1.609	1.386	0.999
J4	NA	NA	0.693	0.405	0.511	NA	0.847	0.916	1.253	0.693	0.511	0.693	0.693	NA	0.693
J3	NA	NA	NA	NA	0.693	0.288	NA	NA	0.693	NA	NA	NA	NA	NA	NA
J2	NA	NA	NA	NA	NA	NA	NA	NA	NA	NA	NA	NA	NA	NA	NA
J1	NA	NA	NA	0.693	NA	0.693	NA	NA	NA	1.386	0.693	1.099	NA	NA	0.693

Table 49. 'Foote' origination rates for all major marine and non-marine tetrapod groups at 10 million year time bin intervals. Abbreviations as Table 48.

Origination rates in almost all groups were severely depressed in the earliest Cretaceous, which when combined with the high latest Jurassic extinction rates, explains the consistently low diversity recorded in most clades. Despite elevated origination rates in some groups during the Oxfordian (e.g., thalattosuchians) and Kimmeridgian (e.g., non-marine crocodyliforms, all dinosaurs, and pterosaurs), at between 2–10 times the background rate of other intervals during the Jurassic, these do not appear to have conferred any survivorship advantage through the J/K boundary. However, relatively high origination rates in ichthyosaurs and sauropterygians during the Kimmeridgian–Tithonian, representing the radiations of Platypterygiinae (Fischer *et al.*, 2012; Fischer *et al.*, 2013) and Xenopsaria (Benson and Druckenmiller, 2014), respectively, might have been responsible for their moderately high apparent survival rates through the J/K boundary based on 'ghost lineages' (Fischer *et al.*, 2012; Benson and Druckenmiller, 2014), following a diversity crash in cryptoclidid plesiosaurs at this time (Benson and Druckenmiller, 2014).

10 myr time bin	Aves	Chel	Chor	Crocs (non-marine)	Crocs (marine)	Ichthy	Lepid	Liss	Mamm	Ornith	Plesio	Ptero	Sauro	Test	Thero
K8	NA	NA	NA	NA	NA	NA	NA	NA	NA	NA	NA	NA	NA	NA	NA
K7	1.792	NA	NA	0.377	NA	NA	1.153	1.5	0.934	1.426	1.216	0.405	1.648	NA	0.78
K6	0.405	NA	NA	1.253	NA	NA	1.623	NA	NA	0.55	1.91	1.003	0.571	NA	1.245
K5	NA	0.69	NA	NA	NA	NA	0.236	NA	NA	NA	1.504	NA	1.196	NA	1.581
K4	NA	NA	NA	0.847	NA	0.223	0.93	1.97	1.34	1.466	NA	NA	0.348	NA	1.022
K3	NA	NA	NA	1.253	NA	0.916	0.236	1.5	1.34	NA	NA	NA	NA	NA	0.329
K2	NA	NA	NA	0.442	NA	0.223	0.93	1.06	0.241	1.936	NA	NA	NA	NA	NA
K1	NA	NA	NA	0.442	1.417	1.609	0.236	NA	0.934	NA	NA	0.821	NA	2.49	1.938
J6	NA	NA	NA	1.135	1.166	0.916	1.846	NA	2.381	1.849	NA	0.492	1.447	3	2.033
J5	NA	NA	NA	0.154	1.012	NA	0.236	NA	0.934	1.243	NA	0.598	NA	NA	NA
J4	NA	NA	NA	NA	0.318	NA	NA	NA	NA	NA	NA	NA	NA	NA	NA
J3	NA	NA	NA	NA	NA	NA	NA	NA	NA	NA	NA	NA	NA	NA	NA
J2	NA	NA	NA	NA	NA	0.223	0.236	NA	NA	NA	NA	NA	NA	NA	NA
J1	NA	NA	NA	NA	NA	NA	NA	NA	NA	NA	NA	NA	NA	NA	NA

Table 50. Three-timer extinction rates for all major marine and non-marine tetrapod groups at 10 million year time bin intervals. Abbreviations as Table 48.

10 myr time bin	Aves	Chel	Chor	Crocs (non-marine)	Crocs (marine)	Ichthy	Lepid	Liss	Mamm	Ornith	Plesio	Ptero	Sauro	Test	Thero
K8	NA	NA	NA	NA	NA	NA	NA	NA	NA	NA	NA	NA	NA	NA	NA
K7	1.504	NA	NA	1.253	NA	NA	0.236	3.19	0.647	2.236	2.197	1.34	2.428	NA	1.678
K6	1.792	NA	NA	1.764	NA	NA	1.846	NA	NA	1.936	1.91	2.708	1.36	NA	2.033
K5	NA	0.693	NA	NA	NA	NA	0.93	NA	NA	NA	1.91	NA	0.859	NA	1.245
K4	NA	NA	NA	0.56	NA	0.916	0.236	2.197	0.241	1.243	NA	NA	2.294	NA	1.176
K3	NA	NA	NA	1.54	NA	0.223	0.93	1.281	1.34	NA	NA	NA	NA	NA	2.12
K2	NA	NA	NA	0.154	NA	0.916	0.93	0.588	0.241	1.243	NA	NA	NA	NA	NA
K1	NA	NA	NA	0.442	0.318	0.223	0.93	NA	1.34	NA	NA	0.598	NA	2.079	1.022
J6	NA	NA	NA	0.442	0.318	0.916	0.236	NA	0.241	0.55	NA	0.31	1.041	2.485	1.245
J5	NA	NA	NA	2.234	1.571	NA	1.153	NA	3.074	2.948	NA	1.003	NA	NA	NA
J4	NA	NA	NA	NA	1.012	NA	NA	NA	NA	NA	NA	NA	NA	NA	NA
J3	NA	NA	NA	NA	NA	NA	NA	NA	NA	NA	NA	NA	NA	NA	NA
J2	NA	NA	NA	NA	NA	0.223	0.236	NA	NA	NA	NA	NA	NA	NA	NA
J1	NA	NA	NA	NA	NA	NA	NA	NA	NA	NA	NA	NA	NA	NA	NA

Table 51. Three-timer origination rates for all major marine and non-marine tetrapod groups at 10 million year time bin intervals. Abbreviations as Table 48.

This high extinction pattern for ichthyosaurs is distinct from that recovered by a previous study (Fischer *et al.*, 2012), which noted either suppressed extinction rates or little to no deviation from background rates across the J/K boundary based on a boundary-crosser estimate. Following this, it has been argued that the earliest Cretaceous was a period of quiescence for ichthyosaurs (Fischer *et al.*, 2012), representing a phase of moderate diversity but no speciation. However, a more likely explanation, supported by the results that account for the 'Signor-Lipps' effect (i.e., the artificial prolonging of extinction events), is that there were high extinction rates in ichthyosaurs in the latest Jurassic that led to their apparently low diversity throughout the earliest Cretaceous (when a signal is able to be recovered), consistent with other marine tetrapod groups. Overall, no major marine reptile lineage went extinct at the J/K boundary, and the moderately low lineage survivability exhibited by ichthyosaurs, plesiosaurians, and thalattosuchians might have been maintained by consistent levels of morphological disparity in each of these groups (Fischer *et al.*, 2012; Fischer *et al.*, 2013; Benson and Druckenmiller, 2014; Young *et al.*, 2014a; Chiarenza *et al.*, 2015; Fischer *et al.*, 2015; Fanti *et al.*, 2016a)

Stage	Aves	Chel	Chor	Crocs (non-marine)	Crocs (marine)	Ichthy	Lepid	Liss	Mamm	Ornith	Plesio	Ptero	Sauro	Test	Thero
Maastrichtian	0.693	1.204	NA	0.916	0.693	NA	1.078	0.827	0.788	1.076	0.288	0.223	0.452	0.960	0.811
Campanian	0.511	0.511	0.693	NA	0.074	NA	0.061	0.134	0.372	0.182	0.325	0.560	0.251	0.191	0.223
Santonian	NA	0.288	NA	NA	0.074	NA	0.054	0.134	0.049	0.065	NA	NA	NA	0.182	0.049
Coniacian	0.405	NA	NA	NA	NA	NA	0.061	0.693	0.223	0.074	NA	NA	NA	NA	0.049
Turonian	NA	NA	NA	NA	0.074	NA	0.065	NA	0.054	NA	0.143	NA	NA	0.051	NA
Cenomanian	NA	NA	NA	NA	0.223	0.511	0.154	0.154	0.268	0.325	NA	0.405	0.065	0.305	0.118
Albian	NA	NA	0.405	0.223	0.310	NA	0.182	0.336	NA	0.208	0.080	0.470	0.182	0.288	0.134
Aptian	NA	NA	0.405	NA	NA	0.223	0.167	0.182	0.154	0.167	0.080	0.182	0.182	0.125	0.223
Barremian	0.693	NA	NA	NA	0.201	NA	NA	NA	0.405	0.167	0.087	NA	NA	NA	0.095
Hauterivian	NA	NA	NA	0.182	NA	NA	0.095	NA	NA	NA	NA	NA	NA	0.080	NA
Valanginian	NA	NA	0.405	0.134	NA	0.511	0.095	NA	0.154	NA	0.105	NA	0.095	0.143	NA
Berriasian	NA	NA	NA	NA	0.134	0.288	0.336	0.336	0.336	0.095	0.105	0.405	0.095	0.095	0.134
Tithonian	NA	NA	NA	0.405	0.539	0.288	0.201	NA	0.405	0.511	0.223	0.693	0.875	0.693	0.539
Kimmeridgian	NA	NA	NA	0.368	0.134	NA	0.105	0.154	0.511	0.154	0.118	NA	NA	NA	NA
Oxfordian	NA	NA	NA	NA	NA	NA	NA	NA	0.288	0.288	NA	0.223	NA	0.288	NA
Callovian	NA	NA	NA	NA	NA	NA	NA	0.223	0.511	NA	NA	NA	NA	NA	NA
Bathonian	NA	NA	NA	NA	NA	NA	NA	NA	NA	NA	NA	NA	NA	NA	NA
Bajocian	NA	NA	NA	NA	NA	0.405	NA	NA	NA	NA	NA	NA	NA	NA	NA
Aalenian	NA	NA	NA	NA	NA	NA	NA	NA	NA	NA	NA	NA	NA	NA	NA
Toarcian	NA	NA	NA	NA	NA	0.405	NA	NA	NA	NA	0.405	NA	NA	NA	NA
Pliensbachian	NA	NA	NA	NA	NA	NA	NA	NA	NA	NA	NA	0.405	NA	NA	NA
Sinemurian	NA	NA	NA	NA	NA	NA	NA	NA	NA	NA	0.405	NA	NA	NA	1.386
Hettangian	NA	NA	NA	NA	NA	NA	NA	NA	NA	NA	NA	NA	NA	NA	NA

Table 52. 'Foote' origination rates for all major marine and non-marine tetrapod groups at stage level time bin intervals. Abbreviations as Table 48.

Stage	Aves	Chel	Chor	Crocs (non-marine)	Crocs (marine)	Ichthy	Lepid	Liss	Mamm	Ornith	Plesio	Ptero	Sauro	Test	Thero
Maastrichtian	NA	NA	NA	NA	NA	NA	NA	NA	NA	NA	NA	NA	NA	NA	NA
Campanian	0.511	1.099	0.693	0.405	0.431	NA	0.783	0.619	0.642	0.956	NA	0.223	0.251	0.693	0.615
Santonian	0.288	0.511	NA	NA	0.143	NA	0.201	0.134	NA	0.182	0.074	NA	0.201	0.223	0.049
Coniacian	0.405	NA	NA	NA	NA	NA	0.118	NA	0.095	0.074	NA	0.223	NA	NA	0.049
Turonian	0.693	0.693	NA	NA	0.143	NA	0.288	0.619	0.477	0.134	0.143	0.223	NA	0.274	0.191
Cenomanian	0.693	NA	NA	NA	0.154	NA	0.288	0.288	0.379	0.074	0.080	NA	NA	0.134	0.118
Albian	NA	NA	NA	0.182	0.087	0.288	0.095	0.182	0.560	0.325	0.080	0.182	NA	0.182	0.134
Aptian	NA	NA	0.405	0.223	0.310	NA	NA	0.336	0.154	0.167	0.154	0.336	0.125	0.236	0.288
Barremian	NA	NA	NA	NA	0.105	NA	0.241	0.182	0.154	NA	0.087	0.288	0.194	0.182	NA
Hauterivian	NA	NA	NA	NA	NA	0.223	NA	NA	0.154	NA	0.095	0.182	0.087	NA	NA
Valanginian	NA	NA	NA	NA	0.118	NA	NA	NA	0.154	0.087	NA	NA	NA	0.208	0.262
Berriasian	NA	NA	0.693	NA	0.134	NA	0.182	NA	0.182	0.336	0.201	NA	NA	0.182	NA
Tithonian	0.693	NA	NA	NA	0.134	0.511	NA	NA	0.405	0.154	NA	0.223	0.095	0.318	NA
Kimmeridgian	NA	NA	NA	0.201	0.619	0.405	0.442	0.288	0.511	0.693	0.118	0.560	0.799	1.099	0.827
Oxfordian	NA	NA	NA	0.318	0.223	NA	0.182	NA	0.288	0.288	NA	0.223	0.452	0.288	0.511
Callovian	NA	NA	NA	0.288	0.288	0.288	NA	0.405	NA	0.405	0.452	NA	0.288	0.405	NA
Bathonian	NA	NA	0.693	0.223	0.405	NA	0.693	0.916	0.981	0.693	0.288	0.511	0.405	0.693	NA
Bajocian	NA	NA	NA	0.288	NA	NA	NA	NA	NA	NA	0.405	NA	0.693	NA	NA
Aalenian	NA	NA	NA	NA	NA	NA	NA	NA	NA	NA	NA	NA	NA	NA	NA
Toarcian	NA	NA	NA	0.693	NA	0.223	NA	NA	NA	NA	NA	NA	NA	NA	NA
Pliensbachian	NA	NA	NA	NA	NA	NA	NA	NA	NA	NA	NA	NA	NA	NA	NA
Sinemurian	NA	NA	NA	NA	0.693	NA	NA	NA	NA	NA	NA	NA	NA	NA	NA
Hettangian	NA	NA	NA	NA	NA	0.693	NA	NA	NA	NA	0.916	0.693	NA	NA	1.609

Table 53. 'Foote' extinction rates for all major marine and non-marine tetrapod groups at stage level time bin intervals. Abbreviations as Table 48.

Stage	Aves	Chel	Chor	Crocs (non-marine)	Crocs (marine)	Ichthy	Lepid	Liss	Mamm	Ornith	Plesio	Ptero	Sauro	Test	Thero
Maastrichtian	NA	NA	NA	NA	NA	NA	NA	NA	NA	NA	NA	NA	NA	NA	NA
Campanian	0.693	NA	NA	NA	NA	NA	1.038	1.03	1.658	0.916	NA	0.452	NA	NA	0.84
Santonian	NA	NA	NA	NA	NA	NA	0.345	NA	NA	0.511	0.875	0.606	NA	1.01	NA
Coniacian	NA	NA	NA	NA	NA	NA	0.345	NA	NA	1.897	2.955	0.724	3.519	NA	NA
Turonian	0.693	NA	NA	NA	NA	NA	NA	NA	NA	0.916	1.569	NA	NA	NA	NA
Cenomanian	NA	NA	NA	NA	NA	NA	1.038	NA	NA	NA	1.569	NA	2.575	NA	1.805
Albian	NA	NA	NA	0.956	NA	0.305	1.038	2.02	1.658	1.427	NA	NA	1.322	NA	1.245
Aptian	NA	NA	NA	1.361	NA	0.305	0.345	NA	1.253	NA	NA	NA	NA	NA	0.552
Barremian	NA	NA	NA	0.262	NA	0.305	0.345	0.63	0.56	NA	NA	NA	NA	NA	NA
Hauterivian	NA	NA	NA	0.262	NA	NA	NA	0.63	NA	NA	NA	NA	NA	NA	1.245
Valanginian	NA	NA	NA	0.262	0.125	NA	NA	1.32	NA	NA	NA	NA	NA	NA	1.245
Berriasian	NA	NA	NA	0.55	0.818	NA	NA	NA	NA	1.204	NA	NA	NA	2.11	0.958
Tithonian	NA	NA	NA	0.956	1.378	1.404	1.731	NA	3.268	2.015	NA	0.724	NA	2.62	2.855
Kimmeridgian	NA	NA	NA	0.262	0.307	0.305	0.345	0.63	0.56	0.511	NA	NA	NA	1.01	NA
Oxfordian	NA	NA	NA	NA	0.125	0.305	0.633	NA	NA	0.511	0.875	NA	NA	NA	NA
Callovian	NA	NA	NA	NA	0.125	NA	NA	NA	NA	0.511	NA	NA	NA	NA	0.552
Bathonian	NA	NA	NA	NA	0.125	NA	NA	NA	0.56	0.511	NA	NA	NA	NA	NA
Bajocian	NA	NA	NA	NA	NA	NA	NA	NA	NA	NA	NA	NA	NA	NA	NA
Aalenian	NA	NA	NA	NA	NA	NA	NA	NA	NA	NA	NA	NA	NA	NA	NA
Toarcian	NA	NA	NA	NA	NA	0.999	NA	NA	NA	NA	NA	NA	NA	NA	NA
Pliensbachian	NA	NA	NA	NA	NA	0.999	0.345	NA	NA	NA	NA	NA	NA	NA	NA
Sinemurian	NA	NA	NA	NA	NA	0.305	1.038	NA	NA	NA	NA	NA	NA	NA	NA
Hettangian	NA	NA	NA	NA	NA	0.711	NA	NA	NA	NA	NA	NA	NA	NA	NA

Table 54. Three-timer extinction rates for all major marine and non-marine tetrapod groups at stage level time bin intervals. Abbreviations as Table 48.

Stage	Aves	Chel	Chor	Crocs (non-marine)	Crocs (marine)	Ichthy	Lepid	Liss	Mamm	Ornith	Plesio	Ptero	Sauro	Test	Thero
Maastrichtian	NA	NA	NA	NA	NA	NA	NA	NA	NA	NA	NA	NA	NA	NA	NA
Campanian	1.792	NA	NA	NA	NA	NA	1.038	3.231	1.658	3.114	2.955	1.705	NA	NA	2.056
Santonian	NA	NA	NA	NA	NA	NA	1.038	NA	NA	1.609	NA	1.299	NA	1.705	NA
Coniacian	NA	NA	NA	NA	NA	NA	0.345	NA	NA	0.511	0.875	1.012	1.322	NA	NA
Turonian	1.386	NA	NA	NA	NA	NA	NA	NA	NA	1.204	2.955	NA	NA	NA	NA
Cenomanian	NA	NA	NA	NA	NA	NA	1.443	NA	NA	NA	1.569	NA	1.727	NA	1.245
Albian	NA	NA	NA	0.668	NA	0.999	0.345	2.238	0.56	1.204	NA	NA	3.268	NA	1.399
Aptian	NA	NA	NA	1.649	NA	0.305	1.731	NA	1.658	NA	NA	NA	NA	NA	2.344
Barremian	NA	NA	NA	0.262	NA	0.305	0.345	1.034	1.253	NA	NA	NA	NA	NA	NA
Hauterivian	NA	NA	NA	0.262	NA	NA	NA	1.322	NA	NA	NA	NA	NA	NA	0.552
Valanginian	NA	NA	NA	0.262	0.125	NA	NA	0.629	NA	NA	NA	NA	NA	NA	0.552
Berriasian	NA	NA	NA	0.262	0.125	NA	NA	NA	NA	0.511	NA	NA	NA	1.012	1.245
Tithonian	NA	NA	NA	0.55	0.125	0.999	0.345	NA	0.56	0.511	NA	0.318	NA	2.11	1.651
Kimmeridgian	NA	NA	NA	2.054	0.462	0.711	0.633	2.42	2.575	2.708	NA	NA	NA	2.621	NA
Oxfordian	NA	NA	NA	NA	0.818	0.305	0.345	NA	NA	0.511	0.875	NA	NA	NA	NA
Callovian	NA	NA	NA	NA	0.531	NA	NA	NA	NA	0.511	NA	NA	NA	NA	0.552
Bathonian	NA	NA	NA	NA	0.818	NA	NA	NA	0.56	0.511	NA	NA	NA	NA	NA
Bajocian	NA	NA	NA	NA	NA	NA	NA	NA	NA	NA	NA	NA	NA	NA	NA
Aalenian	NA	NA	NA	NA	NA	0.305	NA	NA	NA	NA	NA	NA	NA	NA	NA
Toarcian	NA	NA	NA	NA	NA	0.999	NA	NA	NA	NA	NA	NA	NA	NA	NA
Pliensbachian	NA	NA	NA	NA	NA	0.305	0.345	NA	NA	NA	NA	NA	NA	NA	NA
Sinemurian	NA	NA	NA	NA	NA	0.305	0.345	NA	NA	NA	NA	NA	NA	NA	NA
Hettangian	NA	NA	NA	NA	NA	NA	NA	NA	NA	NA	NA	NA	NA	NA	NA

Table 55. Three-timer origination rates for all major marine and non-marine tetrapod groups at stage level time bin intervals. Abbreviations as Table 48.

3.2.8 *Changes in lithological occupation across the J/K transition*

For birds, dinosaurs, mammals, lissamphibians, lepidosaurs, crocodyliforms, and choristoderes, the vast majority of body fossil occurrences are found within a coarse siliclastic lithofacies, usually indicative of a higher energy depositional environment. For exclusively marine reptile groups (ichthyosaurs and sauropterygians), their fossil record is dominated by fine siliclastic occurrences. For pterosaurs, fossils are equally abundant in fine siliclastic facies as they are in carbonate ones.

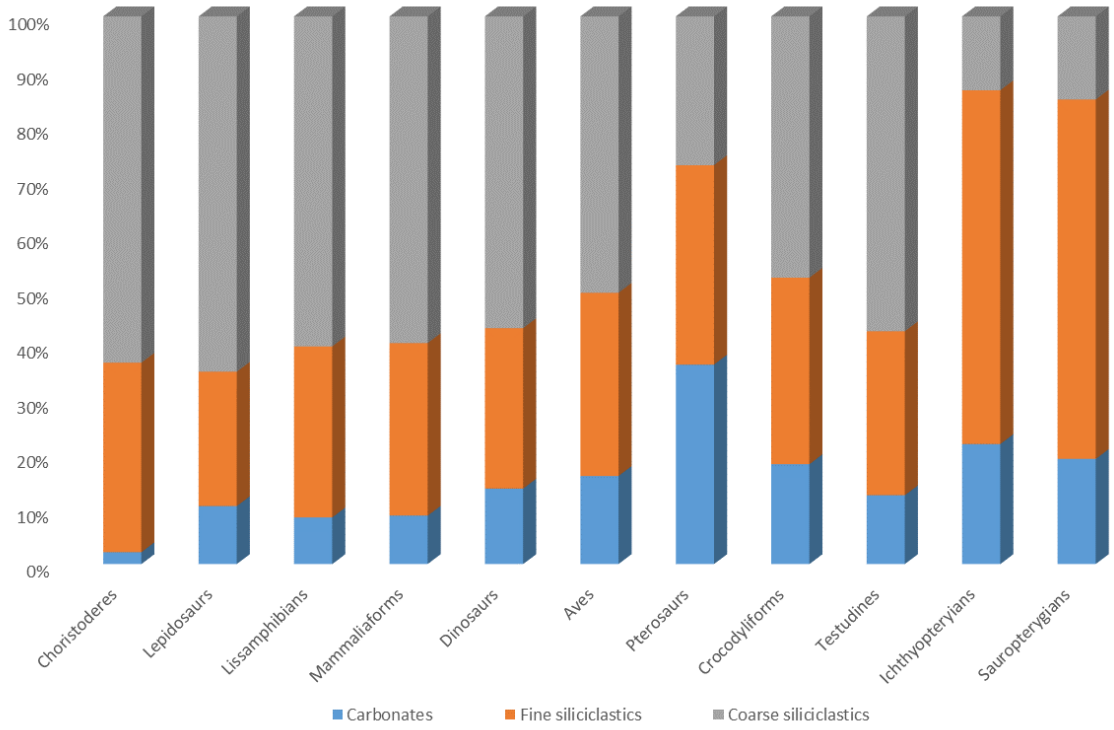


Figure 29. Normalised distribution of different lithofacies for each higher tetrapod group.

Lithology	Aves	Choristodera	Crocodyliformes (terrestrial)	Lepidosauromorpha	Lissamphibia	Mammaliaformes	Pterosauria	Ornithischia	Sauropodomorpha	Testudines	Theropoda	SUM
Carbonates	126	7	157	117	75	135	210	249	282	183	356	1897
Claystone	68	13	174	99	100	239	60	356	222	137	313	1781
Conglomerates	9	2	34	33	35	104	22	110	46	47	115	557
Mudstone	95	51	194	138	127	246	70	442	235	307	355	2260
Sandstone	86	119	536	455	448	961	145	1323	538	821	1275	6707
Shale	97	21	45	50	54	57	113	108	37	105	86	773
Siltstone	28	20	101	105	101	171	22	217	88	125	193	1171
Other	27	6	49	32	31	112	30	99	52	61	92	591
Unknown	216	54	299	214	185	1171	91	1489	426	889	975	6009
Total lithology occurrences per time bin	752	293	1589	1243	1156	3196	763	4393	1926	2675	3760	21746

Lithology	Chelonioidea	Crocodyliformes (marine)	Ichthyopterygia	Sauropterygia	SUM
Carbonates	33	101	87	126	347
Claystone	5	43	25	68	141
Conglomerates	4	16	1	9	30
Mudstone	8	40	17	95	160
Sandstone	22	33	28	86	169
Shale	11	40	86	97	234
Siltstone	8	8	6	28	50
Other	6	19	9	27	61
Unknown	31	118	88	216	453
Total lithology occurrences per time bin	128	418	347	752	1645

Table 56. Total lithological occurrences for tetrapod groups in the non-marine (top) and marine (bottom) realms.

For individual groups, a distinctly heterogeneous pattern emerges for lithofacies occupation over the J/K transition. Lepidosaurs increasingly occupy carbonate lithofacies from the Late Jurassic to Early Cretaceous, becomlng less frequent in both fine and coarse siliclastic facies. Although the number of occurrences is relatively small for lissamphibians, they also exhibit a similar pattern to lepidosaurs, with around half of all occurrences being from carbonate environments in the Berriasian–Barremian. This greatly reduces throughout the remainder of the Cretaceous in both groups, although there is a Cenomanian peak again for lepidosaurs. This pattern is reflected even more strongly by mammaliaforms, with latest Jurassic occurrences being exclusively from siliclastic environments, but with a dramatic shift to more than 70% carbonate facies occupation in the Berriasian–Valanginian. This pattern in smaller-bodied tetrapods is distinct from other dinosaurs, in which occupation of carbonate environments remains fairly constant at between 20–30% throughout the J/K transition. Pterosaurs show an inverse pattern to that smaller-bodied non-archosaur tetrapods, with a high proportion of carbonate lithofacies occupation during the Late Jurassic, reducing over the J/K transition, before rising again in the late Early Cretaceous, with occurrences becoming dominated by those occupying coarse siliclastic lithofacies. Crocodyliforms show a unique pattern of consistently increasing occupation of carbonate environments throughout the J/K transition, before declining in the Hauterivian–Barremian and remaining below 10% throughout the rest of the Cretaceous. This pattern is nearly identical to that of testudines, except for a moderate Late Cretaceous (K6) peak in carbonate lithofacies occupation. For exclusively marine groups, the Early Cretaceous numbers of ichthyosaur and sauropterygian occurrences are too small to draw meaningful conclusions from the patterns.

At the present, it is difficult to distinguish whether these represent environmental preferences or lithological bias for each group. As the numbers reported are proportional, they represent a fraction of the total occurrence distribution for each time bin, as opposed to absolute values which might be biased by over-sampling of particular lithologies. However, at the present, it is difficult to distinguish between whether lithofacies sampling varies due to changing availability of that lithology to sample from, or differing occupation of that lithofacies by any particular group. The impact of lithofacies variation and occupation will undoubtedly require further investigation to help refine our understanding of the geological constraints on tetrapod diversity.

3.2.9 Sampling, diversity and redundancy

The relationship between raw empirical diversity and estimates of global sampling based on tetrapod-bearing collections and formation counts for the non-marine (TBC and TBF, respectively) and marine (MBC and MBF, respectively) realms is almost consistently positive and strong for each taxonomic group analysed, even after correcting for false positives (i.e., the false discovery rate). This pattern is found in both the marine (e.g., for ichthyosaurs: AICc weight = 0.92, Pearson's r = 0.877, adjusted p = 0.04) and terrestrial (e.g., for mammaliaforms: AICc weight = 0.836, Pearson's r = 0.751, adjusted p = 0.018) realms. In every group for which a strong relationship between empirical taxonomic diversity and sampling is not found, there is also no strong relationship recovered for any of the other extrinsic parameters. Therefore the correlations between raw diversity of J/K tetrapods and sampling either reflect the effect of redundancy or demonstrate that sampling controls observed diversity (Benton *et al.*, 2013b; Benton, 2015). The possible issue of redundancy arises from the non-independence of a sampling proxy with diversity (Benton *et al.*, 2013b; Dunhill *et al.*, 2014b; Benton, 2015), which should be alleviated by the use of a higher level proxy such as tetrapod-bearing formations (Butler *et al.*, 2012; Newham *et al.*, 2014), as this captures more information about potential opportunities to sample that

might be missed by a lower level proxy. As such, redundancy appears to be the less likely explanation for these correlations.

The impact of rock outcrop area was also assessed as a non-redundant proxy for geological sampling on the shape of both empirical and subsampled diversity curves. This was only possible on a regional level (i.e., for North America and western Europe), where readily available estimates of rock outcrop area exist (Smith and McGowan, 2007; Peters and Heim, 2010). In Europe, raw, summed, non-marine tetrapod taxonomic richness is strongly correlated with non-marine western European rock outcrop area (Spearman's rho = 0.671, adjusted p = 0.034). This pattern is distinct from the North American record, in which raw marine tetrapod richness does not correlate with non-marine outcrop area. In contrast, when global subsampled diversity is compared to these global sampling metrics, for almost every group no statistical relationship exists for either collections or formations. The only exception to this pattern is theropod diversity, which retains a strong, positive correlation with global counts of non-marine collections even after subsampling (Pearson's r = 0.79, adjusted p = 0.044). However, rather than interpreting this as an instance of sampling controlling the shape of subsampled theropod diversity, it is more likely to reflect the fact that theropods are so well sampled globally that they closely mirror the global tetrapod record. Subsampled diversity, as a more accurate estimate of true diversity (Alroy, 2010c; a), is therefore apparently independent of higher taxonomic-level sampling metrics (i.e., MBFs/TBFs and MBCs/TBCs) at a global level (Table 58), which means the hypothesis that 'true' diversity controls sampling can be rejected, and so does not control the sampling metrics employed here.

Furthermore, for each taxonomic group in which there is a sufficiently continuous subsampled European record through the J/K boundary, there is no relationship between either European marine or non-marine outcrop area and subsampled diversity. European outcrop area is also independent of any other regional sampling metric, which probably reflects Europe having a more intensive sampling

history compared to the rest of the world. Furthermore, an estimate of European fossil record coverage based on Good's *u* is only weakly and non-significantly negatively correlated with western European marine (Pearson's r = -0.429, adjusted p = 0.625) and non-marine (Pearson's r = -0.348, adjusted p = 0.267) outcrop area. Similarly to Europe, no individual North American tetrapod group for which there is a sufficiently continuous record (only Ornithischia and Theropoda) exhibits a strong relationship between subsampled diversity and non-marine outcrop area. Good's *u* is also not correlated with either marine or non-marine outcrop area in North America, suggesting that increasing regional outcrop area (i.e., geological sampling) has little to no effect on the overall evenness and structure of tetrapod sampling for reconstructing diversity, irrespective of whether this means there are more opportunities to sample (collections) or not. Marine outcrop area in Europe shows no significant relationships with any of the used sampling metrics, or with raw or subsampled diversity, which is broadly congruent with the global level analyses. Given that the regional rock record metrics and subsampled diversity estimates are shown not to be the product of 'redundancy' (Benton, 2015) (a similar conclusion to that reached by Upchurch *et al.* (2011a) for North America and Europe), this further implies that the potentially redundant proxies (i.e., formation and collection counts) are capturing a genuine regional sampling signal. This provides some support for 'correcting' diversity curves by choosing a 'higher level' proxy that accounts for any potential redundancy. Such a conclusion is supported by studies that show a close short-term relationship between diversity curves produced using both SQS and residual estimates using sampling proxies (Smith *et al.*, 2012).

The results outlined above suggest that on a global level, both geological and anthropogenic sampling appear to control raw taxonomic diversity, but this is alleviated when subsampling is applied, as observed from the switch from almost universally significant positive correlations to no correlations (SI 7). Although caution is urged in the interpretation of non-significant results as evidence for no relationship, this shift in correlation strength occurs in almost every taxonomic group, independently of their sampling histories and overall diversity patterns. Therefore, although SQS was designed to

account for collections-based sampling issues (Alroy, 2010c; a), and problems relating to geological sampling biases were implicitly ignored (despite their wide documentation (Wall *et al.*, 2009; Peters and Heim, 2010; Smith *et al.*, 2012)), this method seems to also alleviate issues pertaining to geological sampling variation. These results collectively suggest that SQS is an adequate method to account for fossil record bias, as opposed to scrambling a common underlying signal influencing both sampling and diversity (Hannisdal and Peters, 2011). This utility of SQS most likely occurs because the relationship between regional collection counts and outcrop area is almost consistently strongly positively correlated in the non-marine and marine realms (SI 7); the exception to this is the marine record of Europe, in which outcrop area appears to be independent of raw and subsampled diversity.

Group	**Spearman's rank**			**Pearson's PMCC**		
Non-marine	**rho**	**p-value**	**Adjusted p-value**	**r**	**p-value**	**Adjusted p-value**
Aves	0.321	0.498	0.988	-0.174	0.708	0.865
Choristoderes	-0.500	1.000	1.000	-0.509	0.660	0.865
Crocodyliformes	0.273	0.448	0.988	0.015	0.967	0.967
Lepidosauromorphs	0.050	0.912	1.000	0.317	0.406	0.757
Lissamphibians	0.000	1.000	1.000	-0.340	0.371	0.757
Mammaliaformes	0.079	0.838	1.000	-0.292	0.413	0.757
Ornithischians	0.209	0.539	0.988	0.424	0.539	0.847
Pterosaurs	0.521	0.123	0.451	0.309	0.387	0.757
Sauropodomorphs	0.736	0.024	0.264	0.733	0.031	0.171
Testudines	-0.117	0.776	1.000	-0.094	0.810	0.891
Theropods	0.531	0.079	0.435	0.790	0.004	**0.044**
Marine						
Chelonioides	-0.500	1.000	1.000	-0.474	0.686	0.842
Crocodyliformes	0.690	0.069	0.138	0.740	0.036	0.144
Ichthyopterygians	0.612	0.060	0.138	0.479	0.166	0.332
Sauropterygians	0.335	0.263	0.351	0.061	0.842	0.842

Table 57. Correlations between global subsampled diversity and marine and non-marine tetrapod-bearing collections.

Group	Spearman's rank			Pearson's PMCC		
Non-marine	**rho**	**p-value**	**Adjusted p-value**	**r**	**p-value**	**Adjusted p-value**
Aves	0.071	0.906	1.000	-0.266	0.565	0.982
Choristoderes	-0.500	1.000	1.000	-0.528	0.646	0.982
Crocodyliformes	-0.079	0.838	1.000	-0.083	0.819	0.982
Lepidosauromorphs	0.262	0.496	1.000	0.017	0.982	0.982
Lissamphibians	-0.533	0.148	0.814	-0.417	0.264	0.968
Mammaliaformes	0.200	0.584	1.000	-0.083	0.820	0.982
Ornithischians	0.509	0.114	0.814	0.623	0.041	0.451
Pterosaurs	-0.030	0.946	1.000	0.271	0.448	0.982
Sauropodomorphs	0.317	0.410	1.000	0.520	0.152	0.836
Testudines	0.167	0.678	1.000	0.050	0.898	0.982
Theropods	0.147	0.651	1.000	0.178	0.579	0.982
Marine						
Chelonioides	0.333	1.000	1.000	-0.992	0.082	0.164
Crocodyliformes	0.571	0.151	0.302	0.579	0.132	0.176
Ichthyopterygians	0.552	0.104	0.302	0.598	0.068	0.164
Sauropterygians	0.126	0.683	0.911	0.130	0.671	0.671

Table 58. Correlations between global subsampled diversity and marine and non-marine tetrapod-bearing formations.

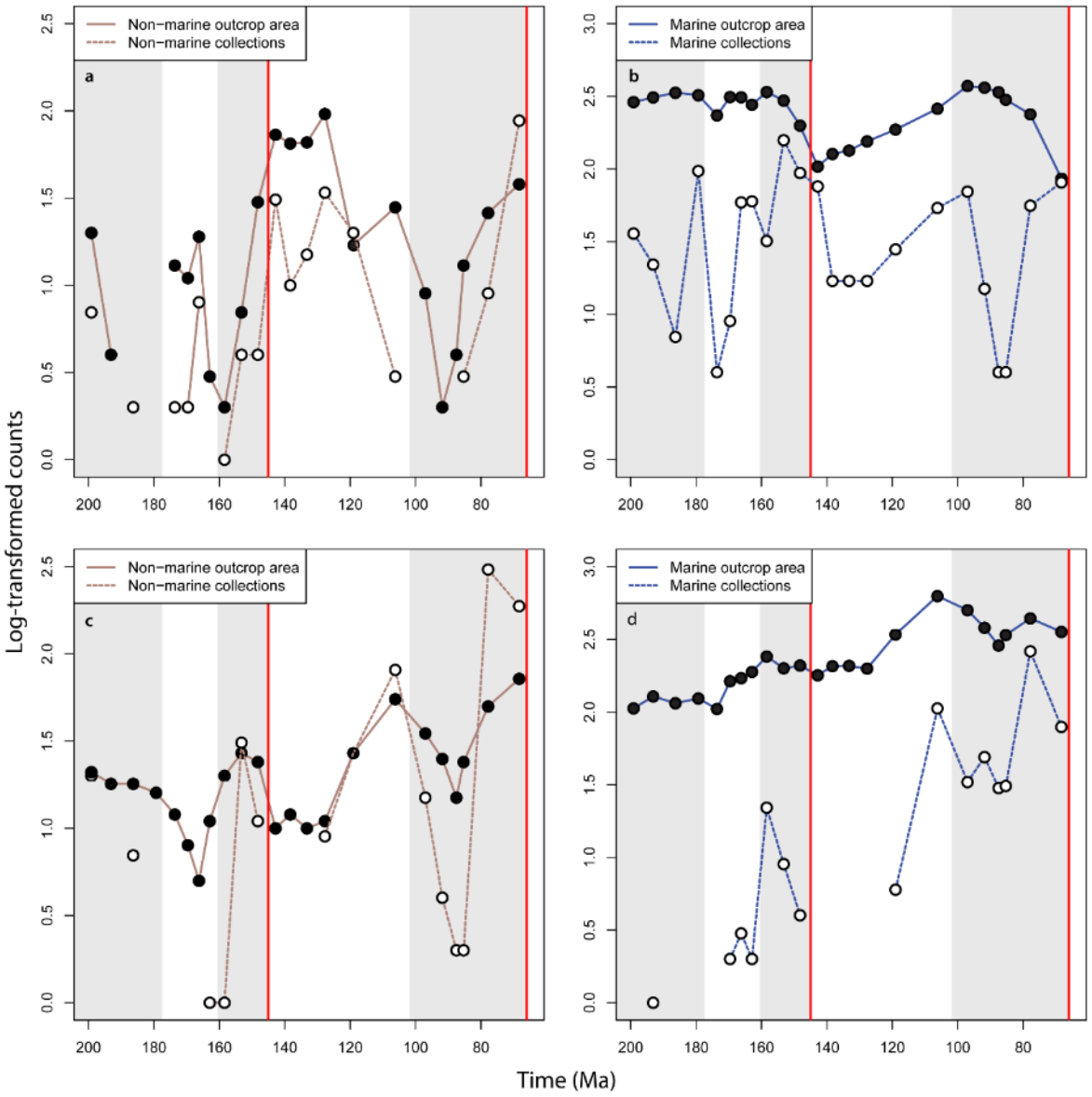


Figure 30. Outcrop area and collections for the (a) non-marine record of Europe; (b) marine record of Europe (c) non-marine record of North America; (d) marine record of North America. European outcrop area from Smith and McGowan (2007), and North American outcrop area from Peters and Heim (2010). Note the discontinuity between the availability of the rock record and the number of collections in the earliest Cretaceous of North America.

Europe	Spearman's rank			Pearson's PMCC		
	rho	p-value	Adjusted p-value	r	p-value	Adjusted p-value
Raw richness	0.671	0.006	**0.034**	0.513	0.042	0.167
Collections	0.468	0.070	0.140	0.474	0.064	0.167
Occurrences	0.512	0.045	0.135	0.446	0.084	0.167
Good's u	-0.147	0.616	0.660	-0.348	0.223	0.267
Formations	0.326	0.173	0.259	0.328	0.171	0.256
Global sea-level	-0.115	0.660	0.660	-0.153	0.557	0.557
Subsampled richness						
Crocodyliformes	0.036	0.964	0.964	0.381	0.400	0.599
Lepidosauromorpha	0.657	0.175	0.525	0.449	0.372	0.599
Ornithischia	0.091	0.811	0.964	0.323	0.363	0.599
Pterosauria	-0.107	0.840	0.964	0.277	0.547	0.657
Testudines	-0.257	0.658	0.964	0.034	0.949	0.949
Theropoda	0.527	0.123	0.525	0.605	0.064	0.383

Table 59. Correlations between raw metrics for non-marine tetrapods and European non-marine outcrop area, and between subsampled richness estimates for different non-marine tetrapod groups and European non-marine outcrop area.

Europe	Spearman's rank			Pearson's PMCC		
	rho	p-value	Adjusted p-value	r	p-value	Adjusted p-value
Raw richness	-0.217	0.318	0.547	-0.141	0.521	0.625
Collections	-0.164	0.456	0.547	-0.173	0.430	0.625
Occurrences	-0.228	0.293	0.547	-0.180	0.411	0.625
Good's u	-0.547	0.046	0.275	-0.429	0.126	0.625
Formations	0.179	0.438	0.547	0.174	0.451	0.625
Global sea-level	-0.069	0.795	0.795	-0.018	0.945	0.945
Subsampled richness						
Crocodyliformes	0.143	0.752	0.759	0.239	0.569	0.569
Ichthyopterygia	0.115	0.759	0.759	-0.309	0.385	0.569
Sauropterygia	0.321	0.368	0.759	0.347	0.325	0.569

Table 60. Correlations between raw metrics for marine tetrapods and European marine outcrop area, and between subsampled richness estimates for different marine tetrapod groups and European marine outcrop area.

North America	Spearman's rank			Pearson's PMCC		
	rho	p-value	Adjusted p-value	r	p-value	Adjusted p-value
Raw richness	0.429	0.113	0.332	0.509	0.053	0.133
Collections	0.154	0.584	0.683	0.454	0.089	0.133
Occurrences	0.146	0.602	0.683	0.474	0.074	0.133
Good's u	0.300	0.683	0.683	0.298	0.626	0.626
Formations	0.479	0.166	0.332	0.457	0.185	0.221
Global sea-level	0.463	0.063	0.332	0.702	0.002	**0.010**

Table 61. Correlations between raw metrics for non-marine tetrapods and North American non-marine outcrop area, and between subsampled richness estimates for different non-marine tetrapod groups and North American non-marine outcrop area.

North America	Spearman's rank			Pearson's PMCC		
	rho	p-value	Adjusted p-value	r	p-value	Adjusted p-value
Raw richness	0.346	0.206	0.309	0.278	0.315	0.464
Collections	0.446	0.097	0.292	0.561	0.030	0.089
Occurrences	0.386	0.157	0.309	0.388	0.153	0.305
Good's u	-0.073	0.839	0.965	-0.290	0.387	0.464
Formations	-0.012	0.965	0.965	-0.146	0.589	0.589
Global sea-level	0.581	0.016	0.098	0.630	0.007	**0.040**
Subsampled richness						
Ornithischia	0.150	0.708	0.708	0.268	0.485	0.485
Theropoda	-0.452	0.268	0.536	-0.404	0.321	0.485

Table 62. Correlations between raw metrics for marine tetrapods and North American marine outcrop area. Diversity for no individual tetrapod group was sufficiently continuous after subsampling for a regional comparison with marine outcrop area.

3.2.10 The effect of sea level on sampling, and testing the 'common cause' hypothesis

Global sea level is uncorrelated with global non-marine tetrapod-bearing formations (Pearson's r = 0.034, p = 0.92) and collections (Pearson's r = 0.301, p = 0.368), and marine tetrapod-bearing formations (Pearson's r = 0.195, p = 0.566) and collections (Pearson's r = 0.222, p = 0.512), and therefore the hypothesis that sea level acts as a common factor driving *both* global sampling and diversity of marine and non-marine tetrapods can be rejected. Additionally, these results imply that

regional rock records and estimates of subsampled regional diversity are not connected by a 'common cause' factor such as sea level (Butler *et al.*, 2011), with the possible exception of the marine realm in North America.

In North America, both marine and non-marine outcrop area are strongly correlated with fluctuations in eustatic sea level (Miller *et al.*, 2005) (Pearson's r = 0.702, adjusted p = 0.01 and Pearson's r = 0.63, adjusted p = 0.04, respectively). However, the marine tetrapod record is too patchy to detect any statistical relationship between outcrop area and subsampled diversity in this region. This implies that sea level exerts a strong control on the geological record of North America, but it cannot be determined whether or not this relationship influences regional subsampled diversity estimates. Therefore, it cannot be discounted that a 'common cause' relationship influences marine diversity estimates in North America because of the discontinuous nature of the fossil record (Peters and Heim, 2011). Distinct from North America, sea level is not related to European marine or non-marine outcrop area, similar to previous results from the United Kingdom (Dunhill *et al.*, 2014b). However, there is no relationship between western European non-marine outcrop area and the number of tetrapod-bearing marine formations (Pearson's r = 0.328, adjusted p = 0.256). This relationship is distinct from that recovered previously in an examination of an exclusively British fossil record (Dunhill *et al.*, 2014b), which is likely due to the higher resolution techniques employed in this study and the examination of an exclusively British fossil record. Furthermore, no relationship is recovered between marine outcrop area and tetrapod-bearing marine collections or formations for western Europe, suggesting that the local signal recovered by this previous analysis is strongly localised to the unique collecting and tectonic histories of Britain (Dunhill *et al.*, 2014b), where sampling has been largely focused on historical mining and collections from ephemerally exposed localities along coastlines.

3.2.11 Extrinsic drivers of Jurassic/Cretaceous tetrapod diversity

The rejection of hypotheses here proposing that subsampled tetrapod diversity reflects either a sampling artefact, signal redundancy, or a common external driver in the form of sea level, implies that subsampling provides an appropriate method for reconstructing patterns of diversity, and thus a suitable basis for assessing the extrinsic parameters that control diversity. Eustatic sea level is shown to be the principle mechanism controlling the true Jurassic–Cretaceous diversity of tetrapods, being strongly positively correlated with subsampled diversity of lepidosauromorphs (AICc weight = 0.727), mammals (AICc weight = 0.931), ornithischians (AICc weight = 0.391), theropods (AICc weight = 0.534), sauropods (AICc weight = 0.501), pterosaurs (AICc weight = 0.872), sauropterygians (AICc weight = 0.409), and non-marine crocodyliforms (AICc weight = 0.969) (Table 63). The relationship between sea level and dinosaur diversity differs from that recovered by a recent study which found no correlation between detrended fluctuations in global sampling effort or dinosaur diversity and sea-level (Butler *et al.*, 2011), and can most likely be explained by the contrasting approaches to reconstructing diversity (i.e., SQS here versus the residuals method in previous studies). However, this finding is more congruent with a range of studies that have documented sea level as the principal controlling factor on Phanerozoic diversity (Bardhan *et al.*, 1989; Hallam and Cohen, 1989; Smith *et al.*, 2001; Hannisdal and Peters, 2011). In these studies, higher sea level is considered to promote increasing diversity through the expansion of marine environments due to continental flooding, as well as increasing the preservation of near-shore habitats as sediment accumulation increases (Peters, 2005; Peters, 2006; Wall *et al.*, 2009; 2011). However, this relationship is not so clear cut, as increasing sea level can also decrease the accommodation rate and sediment deposition in coastal depocentres due to shortening of depositional systems, leading to higher energy sediment flux and consequently increasing probability that sediments will be removed from non-marine settings (Burgess and Hovius, 1998; Blum and Törnqvist, 2000). In addition, there is no overwhelming support for a strong relationship between sea level and marine crocodyliform diversity (Mannion *et al.*, 2015), a factor which is explored in greater detail in Chapter 4. In contrast to the general relationship with sea level exhibited by many

tetrapod groups, lissamphibian diversity shows a strong positive correlation (AICc weight = 0.796) with palaeotemperature (Prokoph *et al.*, 2008), with weaker support in non-marine turtles (AICc weight = 0.258) (Nicholson *et al.*, 2015), implying that these semi-aquatic groups are more sensitive to palaeoclimatic shifts than to changes in eustatic sea level. This relationship between palaeotemperature and lissamphibian and turtle diversity could be due to a late Tithonian 'cold snap' (Jenkyns *et al.*, 2011), followed by a global temperature increase during the Berriasian (Gröcke *et al.*, 2003), which are possible candidates for causing these groups to decline and then radiate during the earliest Cretaceous (Marjanović and Laurin, 2007; Marjanovic and Laurin, 2013; Nicholson *et al.*, 2015). Ichthyosaur diversity is negatively correlated with global subsampled marine invertebrate diversity (AICc weight = 0.42), suggesting that the global richness of the former is tied to broader patterns influencing the marine realm, rather than to a possible food source. For poorly-sampled groups, such as birds, choristoderes, and marine turtles, the controls on their diversity patterns were unable to be resolved. Where relatively lower AICc weights are recovered, this indicates that additional parameters that were not analysed here, such as post-extinction opportunism or competitive displacement (Mannion *et al.*, 2015), or passive aspects of trait evolution (Sookias *et al.*, 2012a), might also have played a significant role in affecting global diversity patterns for different groups. Alternatively, diversity in these groups might have been driven by a combination of factors, rather than any single underlying diversity regulator.

Overall, this recovery of changes in eustatic sea level as a causal factor in the extinction of tetrapods is concordant with results from a range of studies in vertebrates and invertebrates (Hallam and Cohen, 1989; Haubold, 1990; Hallam, 1992; Smith *et al.*, 2001; Bambach, 2006; Smith, 2007; Purdy, 2008). In particular, sea level regression leads to habitat restriction and therefore leads to extinction by changes to species-area relationships. Some studies have noted that it is not the actual regression which is the causal factor, but the subsequent early phase transgression in eustatic cycles that leads to the spread of anoxic bottom waters, which are unsuitable conditions for marine life (Hallam and Cohen, 1989).

Furthermore, this sea level regression is undoubtedly responsible for the regional shift in facies noted across the J/K boundary, as well as the almost total lack of stratigraphically continuous sections around the world. The fact that this regression is most notable on a regional basis in Europe, rather than on a global basis (Hallam, 1986; Hallam and Cohen, 1989), is concordant with the conclusion that the J/K extinction was primarily a regional event in Europe. While earlier research of this association noted that this regression was not followed by anoxia during the subsequent transgression (Hallam and Cohen, 1989), subsequent research has found more widespread evidence for oceanic anoxia during the earliest Cretaceous (Weissert and Channell, 1989; Weissert *et al.*, 1998; Erba *et al.*, 2004; Weissert and Erba, 2004; Martinez *et al.*, 2013; Martinez *et al.*, 2015), and such a factor might have been responsible for the widespread suppression of origination rates throughout this time. In South America, where there is a continuous geological and fossil record through the J/K boundary, there is little evidence of regional extinction or diversity declines in marine and non-marine faunas, and no apparent evidence of either anoxia or a regression throughout this time (Hallam, 1986). As such, any J/K boundary event here is minimal, with faunal transitions happening later on in the Early Cretaceous, as evidenced by the regional extinction of thalattosuchians and emergence of chelonioid turtles (Cadena and Parham, 2015). Such asynchronicity between the northern and southern hemispheres has been noted previously in several studies of marine tetrapods (Pierce *et al.*, 2009a; Benson and Butler, 2011).

Group	Parameter	AICc		Spearman's rank		Pearson's PMCC	
		Likelihood	Weight	rho	adjusted p-value	r	adjusted p-value
Crocodyliformes (marine)	Palaeotemp.	22.741	0.237	-0.524	0.634	-0.522	0.678
Crocodyliformes (non-marine)	Sea level	26.285	0.969	0.750	0.175	0.846	0.028
Lissamphibia	Palaeotemp.	38.260	0.796	0.700	0.301	0.742	0.154
Mammaliaformes	Sea level	51.394	0.931	-0.450	0.537	-0.666	0.301
Ornithischia	Sea level	60.106	0.391	0.200	0.681	0.047	0.898
Pterosauria	Sea level	33.261	0.872	0.714	0.406	0.647	0.581
Sauropodomorpha	Sea level	41.191	0.501	0.310	0.810	0.457	0.564
Sauropterygia	Sea level	41.820	0.409	0.055	0.906	0.065	0.985
Testudines	Palaeotemp.	50.648	0.258	0.343	0.880	0.462	0.891
Theropoda	Sea level	72.931	0.534	-0.018	0.968	0.037	0.954

Table 63. Selected results of model fitting procedure. For complete results for both subsampled and raw taxonomic diversity, see Supplementary Information 7. Data for sea level (Miller *et al.*, 2005), and for palaeotemperature from the $\delta^{18}O$ proxy (Prokoph *et al.*, 2008) from original sources (see text for details).

The relationship between sea level and tetrapod diversity has been previously examined in most detail for dinosaurs (Barrett and Upchurch, 2005; Butler *et al.*, 2011; Mannion *et al.*, 2011) and crocodyliforms (Martin *et al.*, 2014a; Mannion *et al.*, 2015), and the results lend strong support to these earlier studies, reinforcing the view that changes in sea level control the architecture of near-shore ecosystems. Support for this conclusion in a range of groups with vastly different ecologies, from pelagic open ocean swimmers and volant taxa, to small and large-bodied terrestrial groups, suggests that sea level influences these groups in a variety of ways. A relationship between sea level and terrestrial diversity can best be explained by rising sea levels leading to greater division of landmasses through creation of marine barriers. This alters the spatial distribution of near-shore habitats and affects the species-area relationship, which can lead to elevated extinctions. Such fragmentation can also be a potential driver of biological and reproductive isolation and allopatric speciation, the combination of which one would expect to see manifest in the diversity signal. However, evidence for these potential relationships between sea level, terrestrial diversity and sampling has previously remained elusive (Butler *et al.*, 2011). As there is evidence for a positive correlation between sea level and diversity in multiple terrestrial clades, this suggests that allopatric speciation has outweighed the species-area effect for non-marine tetrapods during the study interval.

Furthermore, the diversity of fully marine taxa was more probably affected by the opening and closure of marine dispersal corridors, whereas that of fully terrestrial and coastal taxa was more probably dependent on the extent of habitable ecosystems (including the availability of continental shelf area) (Benson and Butler, 2011). However, the global extent of this relationship between sea level and diversity is difficult to discern, and confounded by issues of linking a global parameter like eustatic sea level with spatially heterogeneous diversity patterns and sampling regimes. Irrespective of this, there

is strong evidence that a eustatic lowstand across the J/K boundary impacted upon global marine and non-marine faunas, a phenomenon that is most clearly marked in the data for Europe (Hallam, 1986). Future research should focus on how changing sea level effects habitat areas in regions dominated by shallow, epicontinental seas, which are distinct from open ocean environments in being relatively shallow over broad geographical areas.

These changes in sea level throughout the Mesozoic can be attributed to a first-order transgressive-regressive cycle driven by the ongoing fragmentation of Pangaea, and geothermal uplift at mid-oceanic ridges (Haq *et al.*, 1987; Miller *et al.*, 2005), and has previously been proposed to have driven regional extinctions across the J/K boundary (Hallam, 1986; Hallam and Cohen, 1989). Indeed, continental movement and reconfiguration is probably one of the dominant controls on patterns of sea level regression and transgression (Valentine and Moores, 1970; Valentine, 1971; Valentine and Moores, 1972; 1974). Therefore, it cannot be ruled out that tectonic reconfiguration was the driver of both continental breakup and eustatic changes, and therefore ultimately played a key role in determining tetrapod diversity patterns during the J/K transition.

3.3 Summary

Both marine and non-marine tetrapod faunas show evidence for a global ecological and taxonomic reorganisation across the J/K boundary. Whereas the diversity of groups such as pterosaurs and sauropods began to fall prior to the J/K boundary, and that of others such as mammals and ornithischians decreased subsequently in the earliest Cretaceous, the majority of clades document their greatest Jurassic–Cretaceous decline through the boundary itself. The magnitude of this drop in diversity ranges from around 33% for ornithischians to 75–80% loss for theropods and pterosaurs. This is coupled with elevated extinction rates, almost at the level of mass extinction, and strongly depressed origination rates throughout the earliest Cretaceous, that are sufficiently distinct from rates

throughout much of the rest of the Jurassic and Cretaceous to warrant future investigation. Together, this is strong evidence for several pulses of extinction and radiation, culminating in a 'wave' of ecological turnover through the J/K boundary. Ultimately, this could be related to the radiation of several important and extant clades during the earliest Cretaceous, such as birds and non-marine turtles.

Disclosure: Much of this Chapter is drawn on text currently in press (Tennant *et al*. in press). While the primary author wrote the majority of this text and performed all analyses, parts of it have been contributed to by all other authors, as well as receiving input from the peer review process.

Tennant, J. P., Mannion, P. D. and Upchurch, P. (in press) Sea level regulated tetrapod diversity dynamics through the Jurassic/Cretaceous interval, *Nature Communications*.

4 A Diversity Crash in Crocodyliformes Across the Jurassic/Cretaceous Boundary

4.1 Introduction

Crocodyliforms are a major group of pseudosuchian archosaurs that include living crocodylians. Originating in the Late Triassic (Nesbitt, 2011), they have a long and rich evolutionary history (Benton and Clark, 1988; Markwick, 1998; Brochu, 2003; Jouve *et al.*, 2008; Brochu *et al.*, 2009; Carvalho *et al.*, 2010; Holliday and Gardner, 2012; Martin *et al.*, 2014a; Bronzati *et al.*, 2015; Mannion *et al.*, 2015; Pol and Leardi, 2015). The Jurassic–Early Cretaceous interval records at least two independent marine radiations of diverse groups (Thalattosuchia and 'Tethysuchia' (Buffetaut, 1982; Jouve, 2009; Pierce *et al.*, 2009b; de Andrade *et al.*, 2010b; de Andrade *et al.*, 2010a; Young *et al.*, 2010; Young *et al.*, 2011b; Young *et al.*, 2014a; Chiarenza *et al.*, 2015; Herrera, 2015)), as well as a major phase of terrestrial diversification (Notosuchia (Sereno *et al.*, 2003; Zaher *et al.*, 2006; de Andrade and Bertini, 2008; Nobre *et al.*, 2008; Novas *et al.*, 2009; Carvalho *et al.*, 2010; Turner and Sertich, 2010; Kellner *et al.*, 2011; Pol *et al.*, 2014; Pol and Leardi, 2015)). It also includes the decline and eventual extinction of Thalattosuchia (Young *et al.*, 2014a; Chiarenza *et al.*, 2015; Mannion *et al.*, 2015), and radiation of Eusuchia (Martin and Delfino, 2010; Buscalioni *et al.*, 2011; Adams, 2014), the lineage leading to crown group Crocodylia (Brochu, 2003).

Although some studies have documented high lineage survival of marine crocodyliforms across the Jurassic/Cretaceous (J/K) boundary (Young *et al.*, 2014a; Chiarenza *et al.*, 2015), others have recovered an overall decrease in marine crocodyliform biodiversity (Martin *et al.*, 2014a; Mannion *et al.*, 2015), with evidence for a comparable decline among non-marine forms too (Mannion *et al.*, 2015). Uncertainty characterises the tempo of any decline as well, varying from an extinction event at the boundary (Bardet, 1994; Benson *et al.*, 2010), to a spatiotemporally staggered turnover (Benson and Druckenmiller, 2014) that might have comprised a pulsed, two-phase wave of extinctions (Young *et al.*, 2010). Alternate explanations for fluctuations in marine crocodyliform biodiversity across the J/K boundary have also been proposed, including close ties to changes in sea level (Mannion *et al.*, 2015)

and palaeotemperature (Martin *et al.*, 2014a; Mannion *et al.*, 2015), whereas the driver/s of patterns in non-marine crocodyliform biodiversity have yet to be identified for this interval. Thus, there is considerable uncertainty concerning both the patterns of diversity change across the J/K boundary for marine and non-marine crocodyliforms, and the identity of the causal factors that supposedly drove such fluctuations.

These disagreements are likely to at least partly stem from contrasting approaches to the reconstruction of palaeobiodiversity patterns. While recent analyses of crocodyliforms based on uncorrected (raw) taxonomic counts, phylogenetically-corrected biodiversity, and subsampling approaches (Martin *et al.*, 2014a; Mannion *et al.*, 2015) largely recover the same patterns, they differ in the magnitude of these changes and their potential driving factors. Here, a detailed analysis of Jurassic–Cretaceous crocodyliform biodiversity is presented, focussing in particular on dynamics across the J/K boundary, a relatively neglected phase in their evolutionary history. While crocodyliforms where included in the larger-scale tetrapod analysis in Chapter 3, only a single method of diversity reconstruction was employed. Here, this is built upon by exploring a range of different methods, including the effects of a new type of sensitivity analysis, to provide more detailed insight into the dynamics of crocodyliform diversity across the J/K boundary.

4.2 Results

4.2.1 Raw diversity across the Jurassic/Cretaceous boundary

An uncorrected ('raw') census (empirical TDE) of global non-marine crocodyliform generic biodiversity shows a steady increase from the Middle to Late Jurassic, peaking in the Kimmeridgian–Tithonian, before declining through the J/K boundary (Figure 31C). Subsequent to this decline is a Barremian diversity peak followed by a second decline in the late Early Cretaceous. Marine biodiversity largely

follows this Late Jurassic pattern, but there is a much greater biodiversity crash across the J/K boundary (loss of >75% genera), with this decline beginning in the Tithonian following a Kimmeridgian peak. Whereas marine biodiversity remained low throughout the Early Cretaceous, non-marine biodiversity partially recovered, but did not reach latest Jurassic levels again during the study interval. This general pattern of increasing biodiversity in the Late Jurassic, followed by a sharp decline through the J/K interval, is emulated by the PDE (Figure 33) and SQS (Figure 36) analyses. PDEt and SQSPt are strongly positively correlated with one another for both the marine (Pearson's r = 0.601, p = 0.115) and non-marine (Pearson's r = 0.796, p = 0.006) groups.

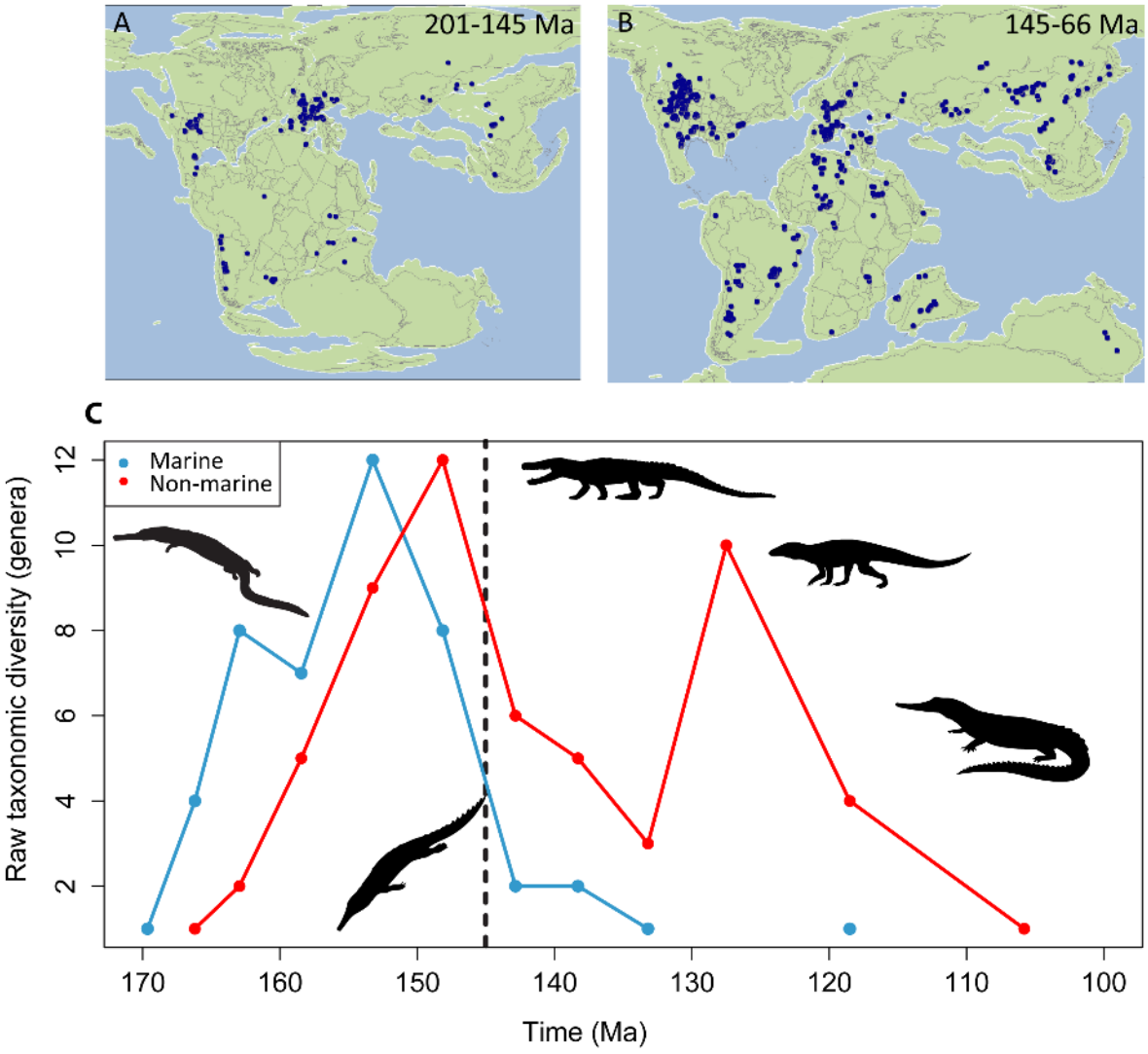


Figure 31. Jurassic (A) and Cretaceous (B) crocodyliform occurrences, superimposed onto reconstructed palaeomaps. Silhouettes: Isisfordia (M. Keesey), Goniopholis (S. Hartman), Notosuchus (N. Tamura), Steneosaurus (G. Monger), Elosuchus (M. Keesey), Protosuchus (M. Keesey); (C) Raw taxonomic diversity estimate (TDE) for Jurassic–Cretaceous marine (blue) and non-marine (red) crocodyliforms. Palaeomap: http://fossilworks.org/?a=mapForm.

4.2.2 Phylogenetic diversity across the Jurassic/Cretaceous boundary

After the J/K boundary decline, global non-marine biodiversity consistently exceeded that of the Late Jurassic based on the PDE results, with peaks in the Hauterivian–Barremian and Cenomanian (PDEt), or in the Aptian (PDEs) (Figure 32, Figure 33). The decline in non-marine crocodyliforms is emphasised at the 10 million year time bin level (PDEt), and almost negligible at the stage level for genera. This pattern is almost replicated at the species level, with both also failing to recover the late Early Jurassic decline observed in the TDE. In the marine realm, the decline in crocodyliform (thalattosuchian) diversity is almost identical for PDEs and PDEt, and similar to the TDE results in tracking the initiation of this decline prior to the J/K boundary. The fact that as with non-marine crocodyliforms, the PDE patterns retain the same general structure at both the species and genus levels suggests that both are tracking a consistent biological pattern, and one that is coincident with that produced using subsampling. Full results of the phylogenetic analyses are provided in Appendix 12.

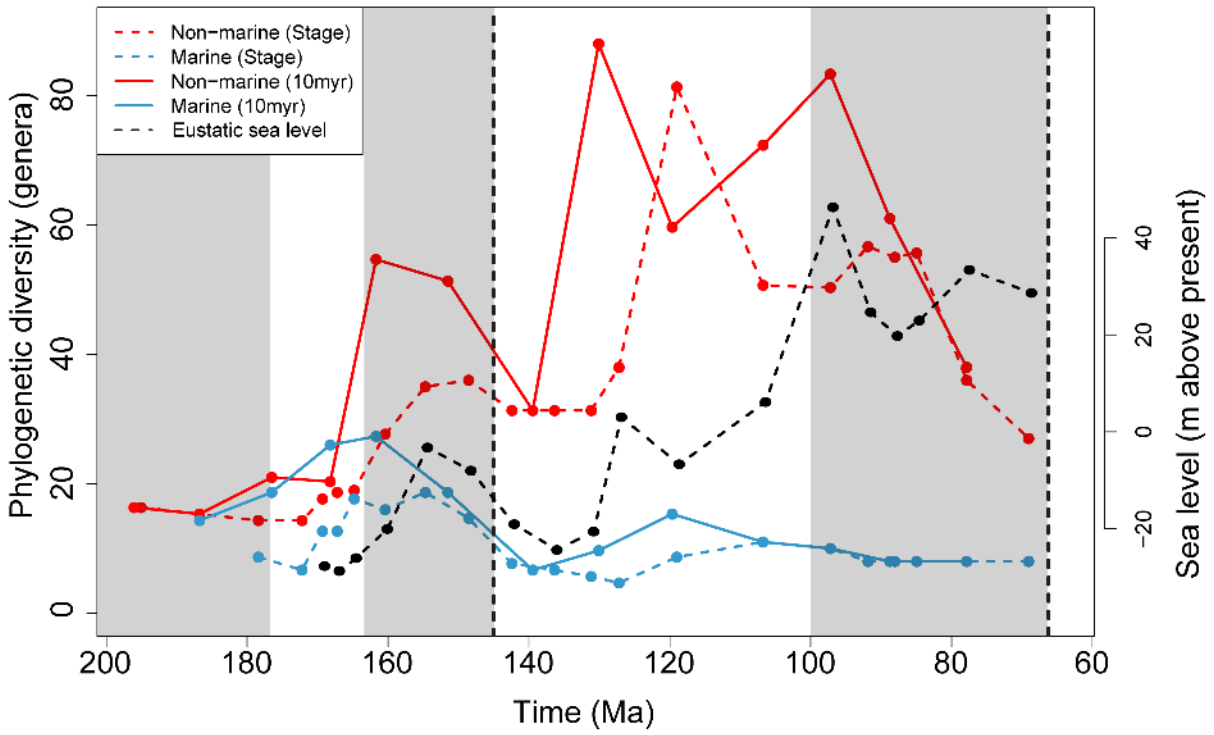


Figure 32. Reconstructed phylogenetic diversity estimate (PDEt and PDEs) for marine (blue) and non-marine (red) crocodyliforms, based on the mean of all three reconstruction approaches. Eustatic sea-level is from Miller *et al.* (2005).

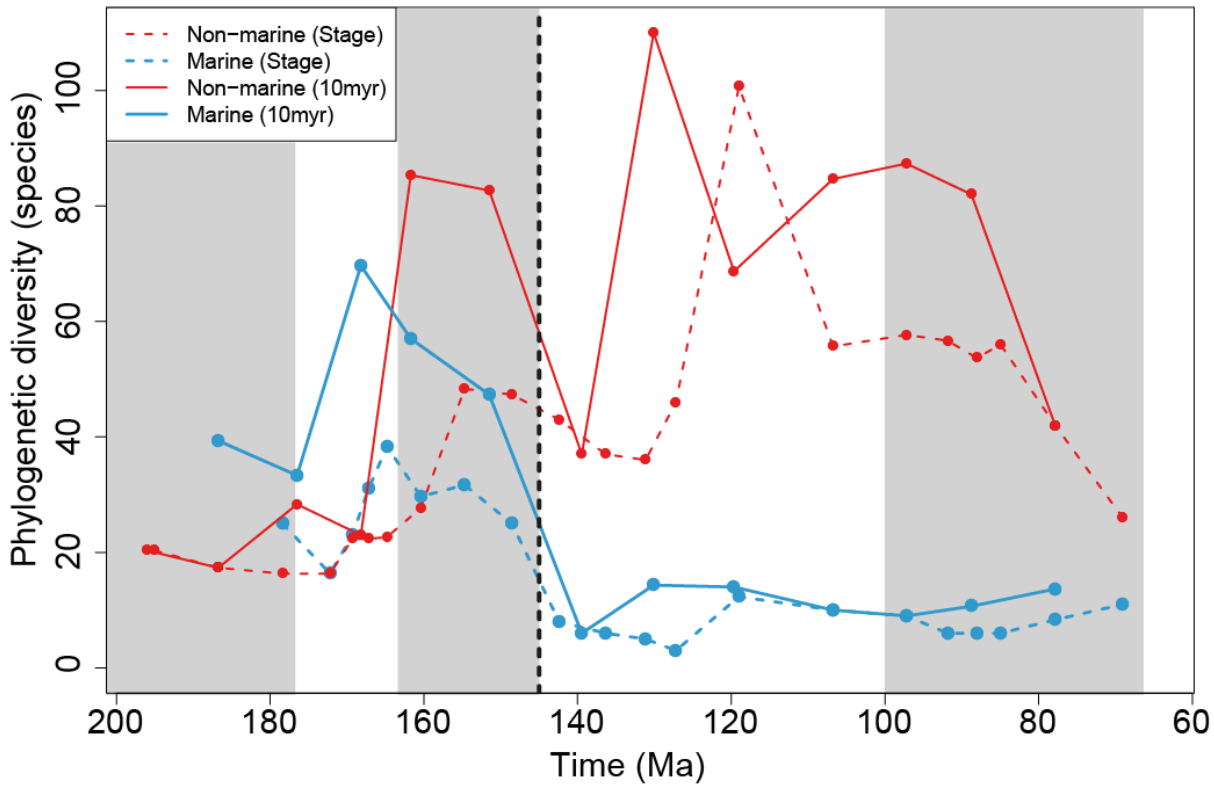


Figure 33. Phylogenetic diversity estimate (PDEt and PDEs) at the species level for marine and non-marine sub-groups.

4.2.3 Subsampled global diversity across the Jurassic/Cretaceous boundary

Subsampled results are inconsistent in the non-marine realm: whereas results from the SQSRc analysis show no change in diversity through the J/K boundary (Figure 36), both the SQSRu and SQSPt (Figure 37) analyses reveal declines of varying strength (57% and 15%, respectively), as do those for SQSRs (Figure 34). SQSPs shows a decline in diversity from the Tithonian to Berriasian in both the non-marine (54%) and marine realms (45%) (Table 66, Table 67). However, when metriorhynchoids are excluded from the SQSPs analyses, the remaining diversity of marine crocodyliforms (i.e., teleosauroids) remains consistent throughout the Late Jurassic, but with no recorded diversity in the Early Cretaceous, due to either a severe extinction in this group at the J/K boundary and a 'dead-clade walking' scenario, or a consistently poor fossil record. The maximum estimated genus extinction level is around 60–70% for non-marine crocodyliforms, and 75–80% for marine crocodyliforms. However, coverage for marine crocodyliforms is zero in the K2 interval (Hauterivian–Barremian) (Table 64), as all taxa are known only from singleton occurrences), and therefore subsampled diversity could not be calculated for this interval.

		Marine			
Bin	**Base**	**Collections**	**Raw genera**	**Subsampled diversity**	**Good's u**
Albian	112	NA	NA	NA	NA
Aptian	125	1	1	NA	NA
Barremian	130	NA	NA	NA	NA
Hauterivian	136.4	1	1	NA	NA
Valanginian	140.2	4	2	1.85	1
Berriasian	145.5	3	2	1.74	0.667
Tithonian	150.8	34	8	3.16	0.974
Kimmeridgian	155.7	60	12	2.83	0.942
Oxfordian	161.2	18	7	2.5	0.842
Callovian	164.7	35	8	1.99	0.959
Bathonian	167.7	33	4	1.62	0.95

Table 64. SQSRc for global marine crocodyliforms using 10 million year time bins.

			Terrestrial		
Bin	**Collections**	**Raw genera**	**Subsampled diversity**	**Standard deviation**	**Good's u**
K8	195	31	1.965	0.037	0.96
K7	89	21	1.963	0.037	0.916
K6	41	38	NA	NA	0.36
K5	24	18	7.677	0.061	0.613
K4	14	12	NA	NA	0.375
K3	21	10	2.789	0.036	0.889
K2	23	12	2.419	0.033	0.829
K1	22	9	1.258	0.035	0.9
J6	52	18	1.256	0.035	0.886
J5	43	7	1.074	0.03	0.538
J4	1	1	NA	NA	NA
J3	NA	NA	NA	NA	NA
J2	NA	NA	NA	NA	NA
J1	19	6	0.969	0.022	0.8

Table 65.SQSRc for global non-marine crocodyliforms using 10 million year time bins.

		Non-marine			
Bin	**Base**	**Collections**	**Raw genera**	**Subsampled diversity**	**Good's u**
Albian	112	2	1	1	1
Aptian	125	4	4	NA	NA
Barremian	130	23	10	4.36	0.783
Hauterivian	136.4	6	3	2.28	0.833
Valanginian	140.2	7	5	3.82	0.429
Berriasian	145.5	29	6	2.35	0.969
Tithonian	150.8	22	12	5.14	0.591
Kimmeridgi	155.7	19	9	3.43	0.826
Oxfordian	161.2	7	5	2.78	0.5
Callovian	164.7	4	2	1.51	0.75
Bathonian	167.7	1	1	NA	NA

Table 66. Global SQSPs results for marine crocodyliforms.

	Marine				
Bin	**Collections**	**Raw genera**	**Subsampled diversity**	**Standard deviation**	**Good's u**
K8	37	7	0.987	0.021	0.905
K7	4	3	NA	NA	0.5
K6	1	1	NA	NA	NA
K5	1	1	NA	NA	NA
K4	1	1	NA	NA	NA
K3	4	2	1.295	0.014	1
K2	1	1	NA	NA	NA
K1	7	3	1.247	0.012	1
J6	76	13	2.327	0.031	0.973
J5	43	12	1.731	0.027	0.929
J4	31	6	0.988	0.204	0.93
J3	30	4	0.964	0.017	0.976
J2	NA	NA	NA	NA	NA
J1	NA	NA	NA	NA	NA

Table 67 Global SQSPs results for non-marine crocodyliforms.

		Marine (excluding Metriorhynchoidea)			
Bin	**Base**	**Collections**	**Raw genera**	**Subsampled diversity**	**Good's u**
Albian	112	NA	NA	NA	NA
Aptian	125	NA	NA	NA	NA
Barremian	130	NA	NA	NA	NA
Hauterivian	136.4	NA	NA	NA	NA
Valanginian	140.2	NA	NA	NA	NA
Berriasian	145.5	NA	NA	NA	NA
Tithonian	150.8	8	2	1.51	1
Kimmeridgi	155.7	31	4	1.54	0.971
Oxfordian	161.2	11	3	1.54	0.917
Callovian	164.7	16	4	1.33	0.958
Bathonian	167.7	31	2	1.42	1

Table 68. Global SQSPs results for marine crocodyliforms excluding Metriorhynchoidea.

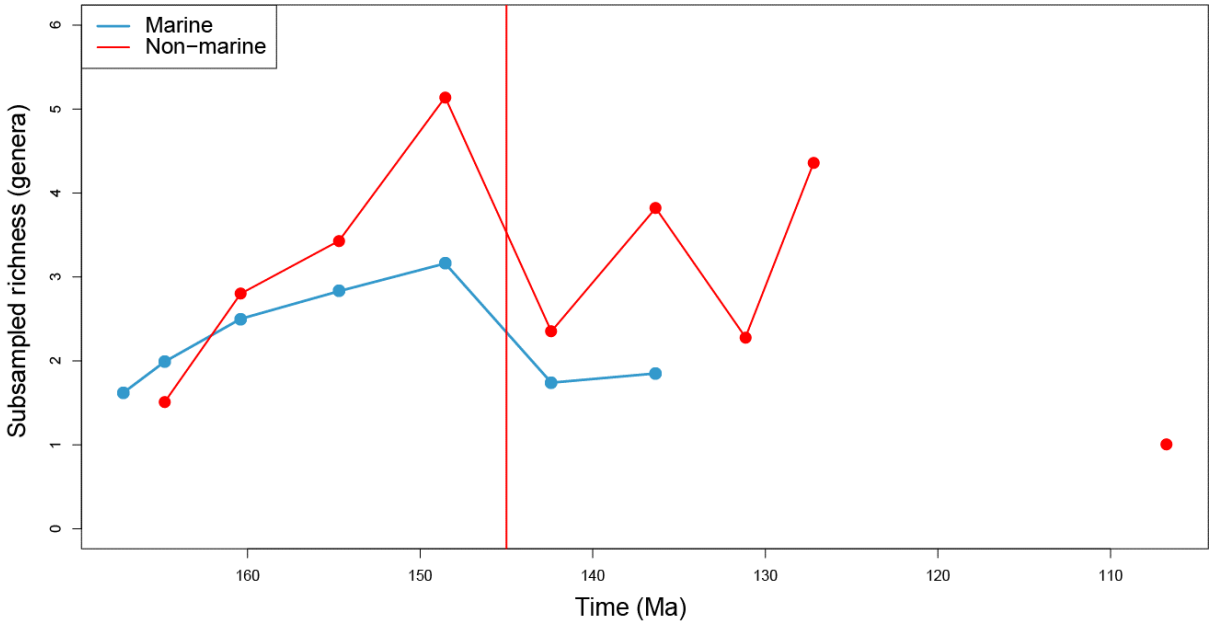


Figure 34. Results obtained using SQSRs for marine and non-marine taxa.

		Marine		
Bin	**Collections**	**Raw genera**	**Subsampled diversity**	**Good's u**
K8	41	7	1.72	0.905
K7	4	3	2.36	0.5
K6	1	1	NA	NA
K5	1	1	NA	NA
K4	1	1	NA	NA
K3	4	2	1.35	1
K2	1	1	NA	NA
K1	8	3	2.23	1
J6	100	13	3.24	0.973
J5	55	12	2.31	0.929
J4	36	6	1.89	0.93
J3	32	4	1.42	0.958
J2	NA	NA	NA	NA
J1	NA	NA	NA	NA

Table 69. Global SQSPt results for marine crocodyliforms.

	Terrestrial			
Bin	**Collections**	**Raw genera**	**Subsampled diversity**	**Good's u**
K8	271	31	4.99	0.96
K7	106	21	4.94	0.916
K6	49	38	NA	NA
K5	29	18	6.66	0.613
K4	16	12	NA	NA
K3	27	10	3.26	0.889
K2	35	12	4.21	0.829
K1	37	9	2.75	0.9
J6	65	18	3.22	0.886
J5	11	6	2.3	0.583
J4	3	2	1.64	0.667
J3	NA	NA	NA	NA
J2	NA	NA	NA	NA
J1	20	6	2.14	0.8

Table 70. Global SQSPt results for non-marine crocodyliforms.

4.2.3.1 Global subsampled results when varying the quorum level

The magnitude of the J/K boundary diversity decline increases as the quorum level is raised for both marine and non-marine datasets (Figure 35), suggesting that this is a genuine signal, and not obscured by temporal heterogeneity in sampling intensity. At quorum levels of 0.4, the relative diversity decline is virtually negligible using SQSRs, and implies that we are more likely to see genuine diversity declines between well sampled time intervals, the magnitude of which will increase as relative sampling intensity increases.

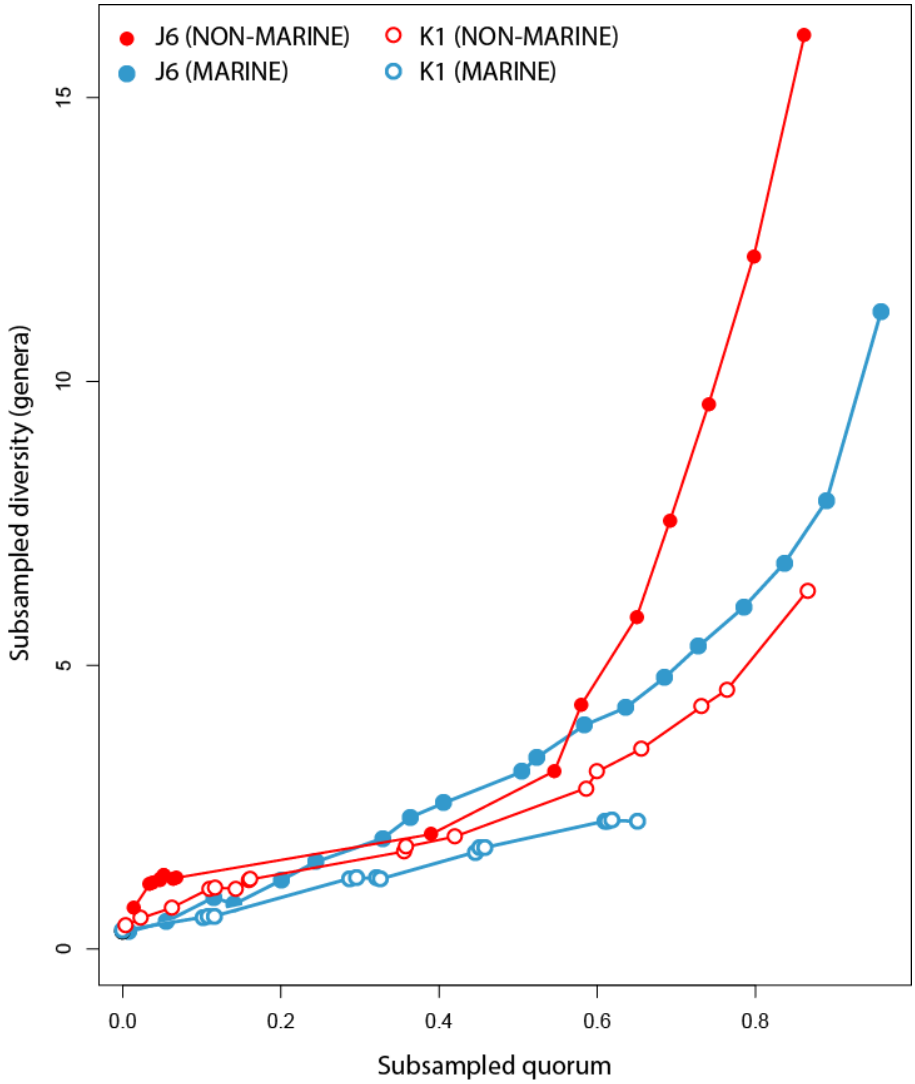


Figure 35. Comparison between subsampled quorum level and subsampled richness (SQSRs) in the time bins either side of the J/K boundary.

J6		K1	
Subsampled u	**Subsampled richness**	**Subsampled u**	**Subsampled richness**
0.008	0.305	0.000	0.322
0.055	0.484	0.000	0.306
0.115	0.909	0.000	0.319
0.141	0.791	0.000	0.326
0.201	1.216	0.102	0.563
0.244	1.535	0.108	0.576
0.329	1.952	0.116	0.581
0.364	2.324	0.287	1.245
0.406	2.573	0.296	1.251
0.505	3.124	0.321	1.249
0.524	3.379	0.326	1.235
0.584	3.945	0.446	1.709
0.636	4.252	0.452	1.779
0.685	4.780	0.458	1.789
0.728	5.333	0.610	2.256
0.786	6.032	0.613	2.246
0.837	6.803	0.619	2.267
0.890	7.900	0.651	2.251
0.959	11.232	NA	NA

Table 71 Richness vs quorum levels for marine crocodyliforms.

J6		K1	
Subsampled u	**Subsampled richness**	**Subsampled u**	**Subsampled richness**
0.014	0.724	0.004	0.412
0.034	1.138	0.023	0.543
0.038	1.177	0.062	0.727
0.047	1.238	0.110	1.065
0.047	1.204	0.117	1.081
0.052	1.300	0.143	1.066
0.052	1.305	0.160	1.224
0.064	1.233	0.161	1.226
0.068	1.255	0.356	1.720
0.390	2.023	0.358	1.800
0.546	3.137	0.420	1.982
0.580	4.305	0.586	2.835
0.650	5.852	0.600	3.126
0.692	7.549	0.656	3.530
0.741	9.601	0.732	4.271
0.798	12.208	0.764	4.569
0.862	16.099	0.866	6.316

Table 72. Richness vs quorum levels for non-marine crocodyliforms.

4.2.4 Subsampled regional diversity across the Jurassic/Cretaceous boundary

At a palaeocontinental level, poor sampling of earliest Cretaceous (Berriasian–Valanginian) terrestrial deposits generally obscures the spatial dynamics of non-marine crocodyliforms, especially in North America and Gondwana (Benson *et al.*, 2013). Within the Laurasian palaeocontinents, latest Jurassic (J6) biodiversity was generally high, but evidence of a decline on land can only be documented in Europe in the SQSPs, SQSRu and SQSRc analyses (39–45% decrease) (Figure 36, Figure 37). European non-marine biodiversity recovered rapidly in the Hauterivian–Barremian interval, reaching its highest level for any point during the Cretaceous. However, the relative magnitude of this recovery is dampened based on the SQSPs results. Based on the results using SQSRu, diversity through the J/K boundary in Asia declined only slightly (14% decrease). In Asia, Africa, and South America, Late Jurassic–Early Cretaceous biodiversity peaked in the Aptian (K3) (Figure 36, Figure 37), whereas in North America it appears to have been approximately constant. Full results of the regional analyses are provided for SQSPt, SQSPs, SQSRu and SQSRc in Appendix 11.

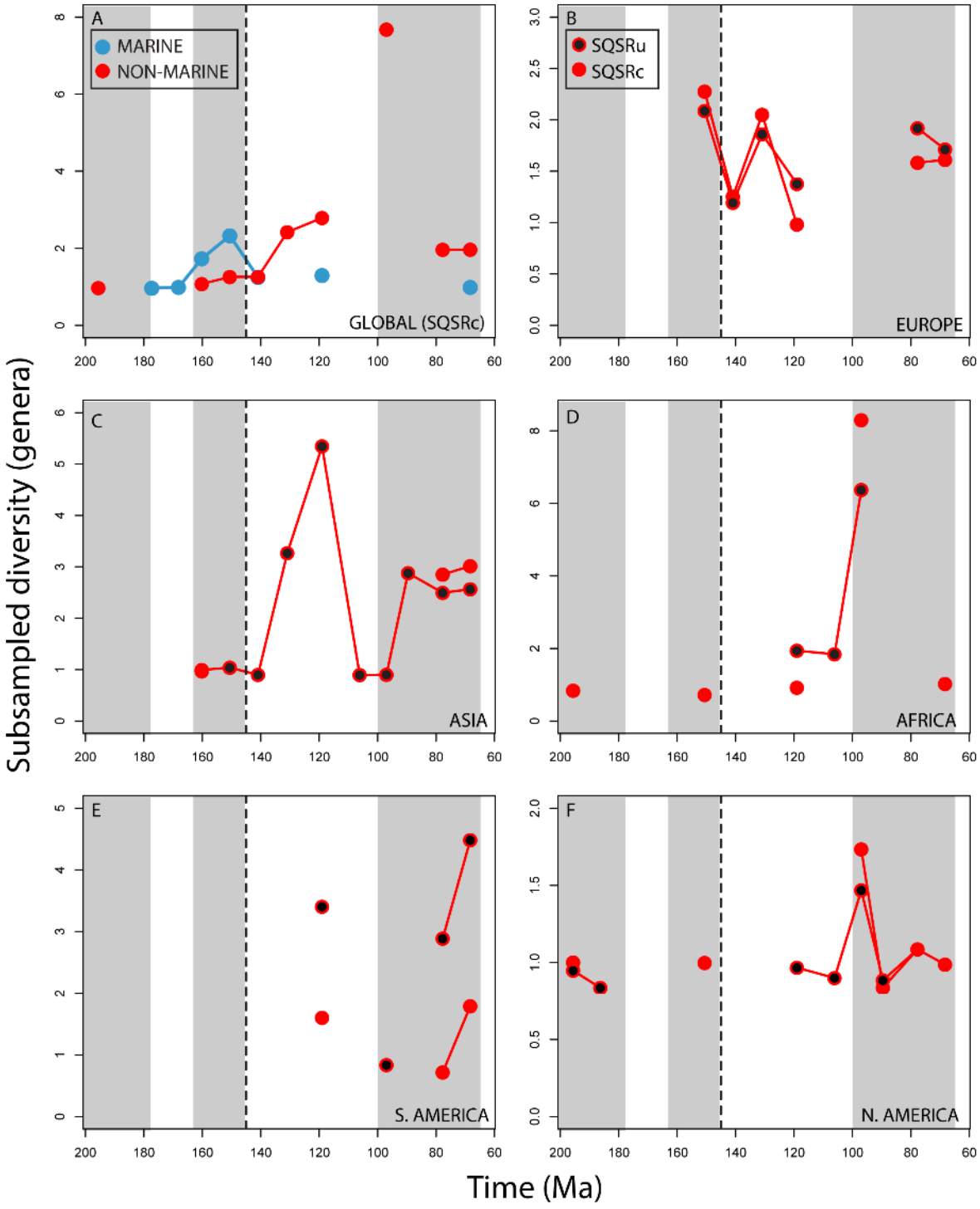


Figure 36. Subsampled biodiversity. (A) Marine and non-marine curves (SQSRc); (B-F) Continent-level curves. Red filled circles represent SQSRc, and black filled circles are SQSRu.

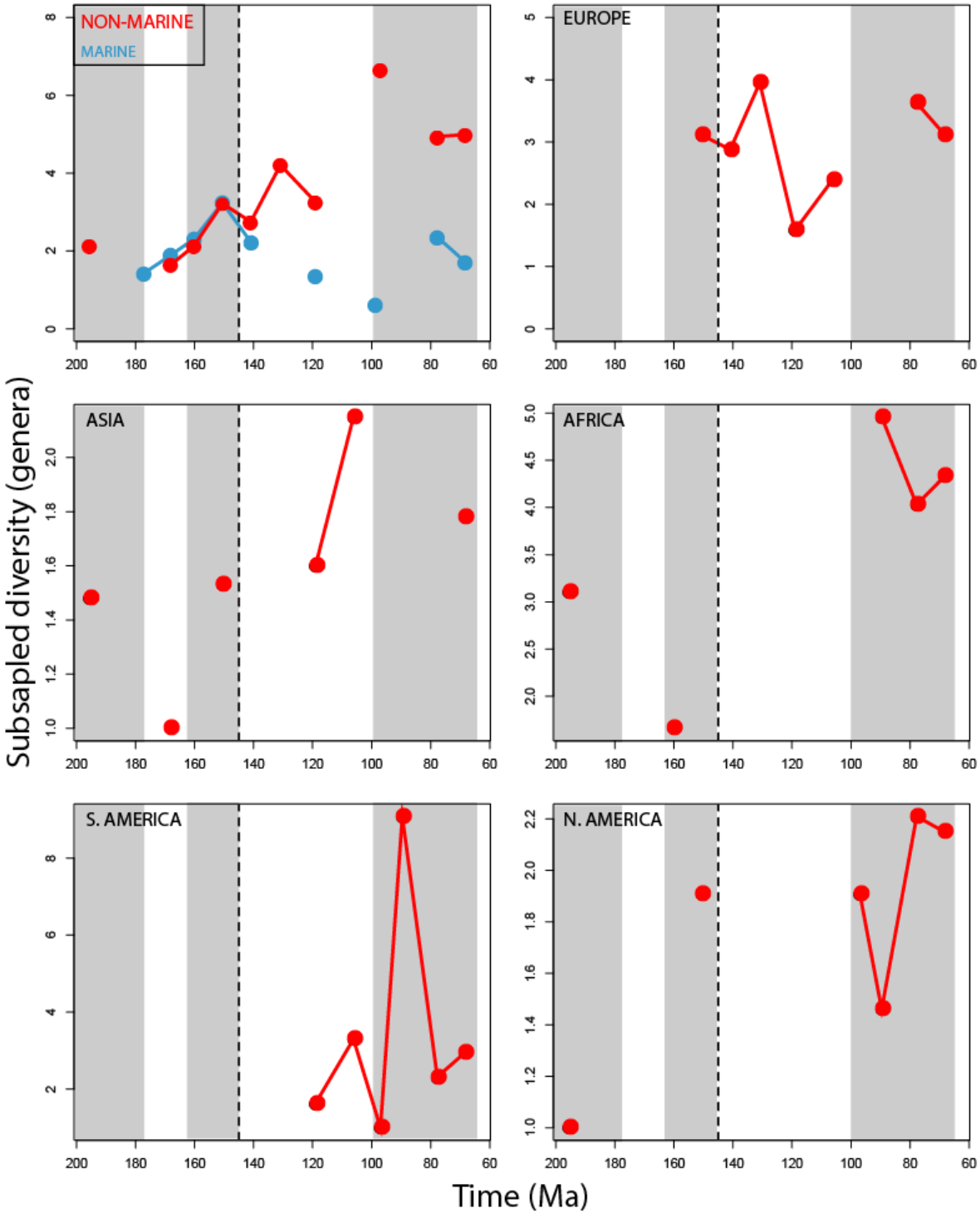


Figure 37. Results obtained using SQSPt on a global and palaeocontinental level.

4.2.5 Global origination and extinction rates through the Jurassic/Cretaceous boundary

Following relatively low rates in the Kimmeridgian, both Foote and 3T extinction rates in non-marine crocodyliforms peaked in the Tithonian (at around four times background rates), remaining relatively high in the Berriasian, before declining through the Valanginian–Barremian (Figure 38). 3T extinction rates are the highest for any stage interval during the Aptian, remaining high during the Albian, suggesting high rates of crocodyliform turnover throughout the late Early Cretaceous on a global scale. Origination rates show a constant pattern of decline in non-marine forms from the Kimmeridgian, where rates are exceptionally high, through the J/K boundary, remaining low throughout most of the Early Cretaceous. Origination rates also peak in the Aptian, remaining high in the Albian, mirroring extinction rates, and indicative of a rapid faunal turnover, part of which could be due to the relatively long durations of these time bins. In marine crocodyliforms, the trend is generally similar to that for non-marine crocodyliforms, with the highest extinction rates in the Tithonian and Berriasian (Figure 38). Extinction rates are unknown throughout the Early Cretaceous, plausibly due to the extremely low diversity of thalattosuchians throughout this time as their recovery was suppressed following the J/K transitional decline Origination patterns in marine forms are distinct from non-marine crocodyliforms, with very low rates in the Berriasian–Valanginian and no Aptian recovery for marine forms. This is strongly suggestive of a decoupling in the processes that governed the diversity recovery between marine and non-marine realms, and ultimately led to the Early Cretaceous extinction of thalattosuchians.

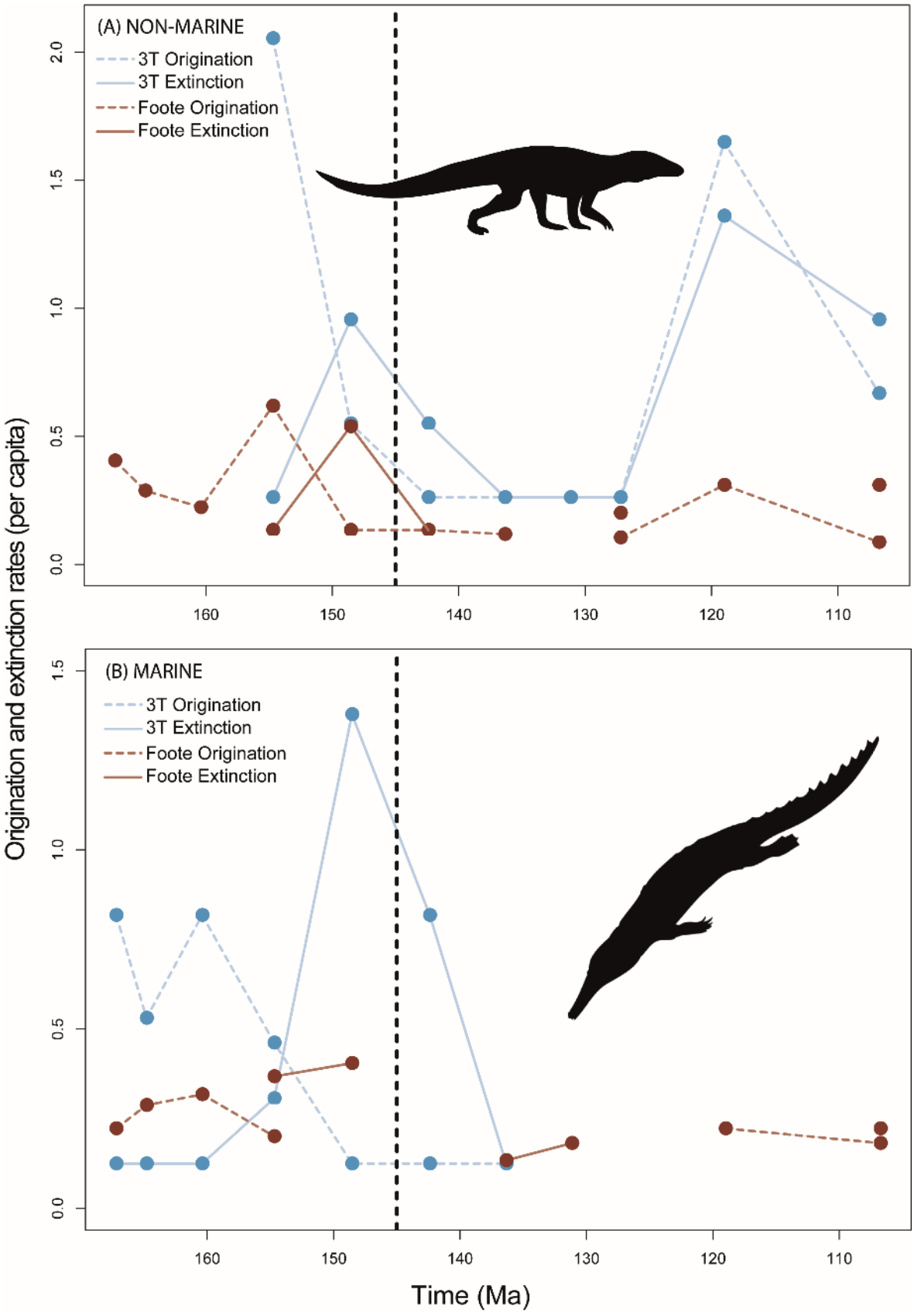

(A) NON-MARINE
3T Origination
3T Extinction
Foote Origination
Foote Extinction
(B) MARINE
3T Origination
3T Extinction
Foote Origination
Foote Extinction
Origination and extinction rates (per capita)
0.0
0.5
1.0
1.5
2.0
160
150
140
130
120
110
Time (Ma)

Figure 38. Non-marine (A) and marine (B) per capita extinction rates using the boundary-crosser and three-timer methods.

MARINE

Bin name	3T origination rate	3T extinction rate	Foote origination rate	Foote extinction rate
Albian	NA	NA	0.182	0.223
Aptian	NA	NA	0.223	NA
Barremian	NA	NA	NA	NA
Hauterivian	NA	NA	NA	0.182
Valanginian	0.125	0.125	NA	0.134
Berriasian	0.125	0.818	NA	NA
Tithonian	0.125	1.378	NA	0.405
Kimmeridgian	0.462	0.307	0.201	0.368
Oxfordian	0.818	0.125	0.318	NA
Callovian	0.531	0.125	0.288	NA
Bathonian	0.818	0.125	0.223	NA

Table 73. Stage level extinction and origination rates for global crocodyliforms.

MARINE

Bin name	3T origination rate	3T extinction rate	Foote origination rate	Foote extinction rate
K8	1.265	0.754	NA	0.916
K7	NA	NA	0.405	NA
K6	NA	NA	NA	NA
K5	NA	NA	NA	NA
K4	NA	NA	0.223	NA
K3	NA	NA	0.223	0.223
K2	NA	NA	NA	0.288
K1	0.348	1.447	NA	0.223
J6	0.348	1.196	NA	0.588
J5	1.601	1.041	0.606	0.288
J4	1.041	0.348	0.511	NA
J3	NA	NA	0.693	NA
J2	NA	NA	NA	NA
J1	NA	NA	NA	NA

Table 74. 10 million year time bin level extinction and origination rates for global crocodyliforms.

NON-MARINE

Bin name	3T origination rate	3T extinction rate	Foote origination rate	Foote extinction rate
K8	0.421	0.827	NA	0.821
K7	1.232	0.357	0.492	0.087
K6	1.743	1.232	0.288	0.154
K5	NA	NA	0.288	0.288
K4	0.134	0.827	0.118	0.405
K3	1.520	1.232	0.405	NA
K2	0.134	0.421	0.154	0.288
K1	0.421	0.421	0.336	0.182
J6	0.421	1.114	0.223	0.811
J5	2.213	0.134	0.956	0.182
J4	NA	NA	0.405	NA
J3	NA	NA	NA	NA
J2	NA	NA	NA	NA
J1	NA	NA	0.693	NA

Table 75. Extinction and origination rates for global non-marine crocodyliforms at the 10 million year time bin level.

Bin name	3T origination rate	3T extinction rate	Foote origination rate	Foote extinction rate
Albian	0.668	0.956	0.087	0.310
Aptian	1.649	1.361	0.310	NA
Barremian	0.262	0.262	0.105	0.201
Hauterivian	0.262	0.262	NA	NA
Valanginian	0.262	0.262	0.118	NA
Berriasian	0.262	0.55	0.134	0.134
Tithonian	0.55	0.956	0.134	0.539
Kimmeridgian	2.054	0.262	0.619	0.134
Oxfordian	NA	NA	0.223	NA
Callovian	NA	NA	0.288	NA
Bathonian	NA	NA	0.405	NA

Table 76. Stage-level extinction and origination rates for global non-marine crocodyliforms.

4.2.6 Environmental drivers of diversity

A summary of the results that show a strong significant correlation with crocodyliform biodiversity is presented in Table 77, with all results documented in Appendix 13. TDE shows no strong correlation with any of the extrinsic variables. Sea level is shown to exert the greatest control on marine

biodiversity for SQSPs (AICc weight = 0.433), with a significant contribution from $\delta^{13}C$ (AICc weight = 0.259). As SQSPs was constrained to the Bathonian–Albian, these results pertain almost exclusively to thalattosuchians. For SQSRc, no single variable satisfies all of the criteria for statistical significance (Appendix 13), but $\delta^{34}S$ and $^{87}Sr/^{86}Sr$ isotope cycling are strongly negatively correlated with marine biodiversity (Table 77), with some evidence for the importance of sea-level too. Although no combination of variables is significantly correlated with SQSPt, it is worth noting that the most important drivers appear to be sea level and palaeotemperature, the latter of which is negatively correlated with biodiversity. Marine PDEt shows a weak and conflicting relationship with sea level, depending on taxonomic scale (Appendix 13). Contrary to Martin *et al*. (2014a), there appears to be no positive relationship between marine biodiversity and sea-surface temperature (SST), even when Metriorhynchoidea are excluded (see Section 4.3.3).

Changes in eustatic sea level are shown to be the dominant controlling factor on global non-marine crocodyliform biodiversity based on the SQSPt (AICc weight = 0.949) reconstructions of biodiversity (Table 77), as well as for PDEs, with strong statistical support at both the genus and species levels. Sea level is also the strongest driver of non-marine PDEt (AICc weight = 1.0), but this is not supported by the additional correlation tests. SQSRu produces a slightly different association, with a combination of sea level and $\delta^{13}C$ exerting the most control on non-marine biodiversity. Furthermore, analyses for non-marine SQSPs show that there is a strong negative association with SST based on an independent $\delta^{18}O$ dataset (Martin *et al.*, 2014a) (AICc weight = 0.529).

Metric	Parameter	AICc		Spearman's correlation		Pearson's correlation	
		Likelihood	Weight	rho	*p*	r	*p*
SQSRc (marine)	$\delta^{34}S$	19.458	0.240	-0.786	0.048	-0.622	0.136
SQSPt (non-marine)	Sea-level (Miller)	26.285	0.949	0.750	0.025	0.846	0.004
SQSRu (non-marine)	$\delta^{13}C$	65.284	0.228	0.762	0.006	0.764	0.004
PDEs (non-marine, genera)	Sea level (Miller)	89.704	0.827	0.642	0.033	0.769	0.006
PDEs (non-marine, species)	Sea level (Miller)	94.021	0.852	0.873	0.001	0.801	0.003

Table 77. Selected results that show strong significant correlations between environmental factors and crocodyliform macroevolutionary dynamics. Full results are provided in Appendix 13.

4.3 Discussion

4.3.1 Crocodyliform extinction across the Jurassic/Cretaceous boundary

The majority of results provide strong evidence for a substantial decline in crocodyliform biodiversity across the J/K boundary. This is coupled with high extinction rates in the latest Jurassic (Tithonian), and depressed origination rates throughout the Early Cretaceous (Berriasian–Barremian). The magnitude of this extinction is estimated to have been a loss of approximately 55–75% of total crocodyliform biodiversity at the generic level, with an increase in extinction rate of up to five times that of adjacent time intervals. However, the possibility that at least part of this high extinction rate is due to poor sampling of earliest Cretaceous North American and Gondwanan crocodyliform faunas cannot be discounted (see below). These results support those of recent analyses of longer-term trends in marine (Benson *et al.*, 2010; Benson and Butler, 2011; Martin *et al.*, 2014a; Mannion *et al.*, 2015) and non-marine crocodyliform (Mannion *et al.*, 2015) biodiversity, and demonstrate that in spite of high lineage survivability (Young *et al.*, 2014a; Chiarenza *et al.*, 2015), there was an overall decline in biodiversity through the J/K boundary. In marine crocodyliforms, this tracks a two-phase thalattosuchian decline, with teleosauroids going extinct at the J/K boundary (Young *et al.*, 2014a), and metriorhynchoids declining in biodiversity during the Early Cretaceous, prior to their complete extinction by the Aptian (Chiarenza *et al.*, 2015). Note however that the timing of this metriorhynchoid extinction could instead be in the Valanginian, with the youngest metriorhynchid remains identified possibly belonging to a pliosaur (Fischer *et al.*, 2015). Furthermore, this timing of the extinction for Teleosauridae might be exclusive to Europe, with a single, highly-specialised lineage persisting into the Hauterivian of Gondwana (Fanti *et al.*, 2016b) representing a phenomenon often referred to as ‘dead clade walking’. The European extirpation of teleosaurids coincides with a steady reduction in the overall number of thalattosuchian fossil occurrences throughout the Early Cretaceous, despite increasingly better sampling of crocodyliform faunas, providing further support that this was a genuine

biodiversity decline. Note that these recent discoveries were published subsequent to the analyses performed as part of this chapter, and therefore were not included. However, they are unlikely to have affected the subsampled diversity curves substantially on either a regional or global basis and therefore do not impact upon the overall interpretation of declining diversity across the J/K boundary.

Even accounting for poor sampling in the earliest Cretaceous, a large biodiversity decrease is still apparent in the PDE reconstructions (Figure 32, Figure 33). It has previously been noted that tree instability through errors in phylogenetic tree topology has the effect of 'dampening' the magnitude of biodiversity loss, by back-smearing origination times and inflating biodiversity in older time bins (Wagner, 2000). Although this artefact might partially explain heightened biodiversity in the Kimmeridgian–Tithonian, it cannot produce the low biodiversity recovered in subsequent time bins. The J/K diversity crash in marine crocodyliforms, and the lack of coverage in the Hauterivian–Barremian, cannot be explained by geological megabias, as other groups of marine reptiles are consistently found in globally distributed deposits throughout this time (Benson *et al.*, 2010; Benson and Butler, 2011). Therefore the general lack of marine crocodyliforms in the Hauterivian–Barremian is regarded as reflecting a genuine biological signal, rather than a preservational artefact (Martin *et al.*, 2014a). In contrast, non-marine crocodyliform biodiversity recovered rapidly after the J/K boundary, with a peak in the Hauterivian–Aptian that appears to be composed of the radiations of notosuchians and eusuchians (Brochu, 2003; Carvalho *et al.*, 2010; Bronzati *et al.*, 2015; Pol and Leardi, 2015), and is a pattern partially mirrored in other terrestrial groups (e.g., dinosaurs; (Upchurch *et al.*, 2011b)). It is likely that this diversity increase from Notosuchia will become even greater with further collecting effort, as over the last 20 years we have witnessed an explosion in the number of notosuchian species discovered, including the first from Madagascar (Pol and Leardi, 2015).

4.3.2 The impact of sampling on Late Jurassic-Early Cretaceous non-marine crocodyliform biodiversity

The Northern Hemisphere is generally better sampled during the Late Jurassic than its southern counterpart (Figure 15, Figure 16, Figure 31). In Gondwana, there is a sharp reduction in the number of non-marine crocodyliform fossil occurrences across the J/K boundary. This could be due to several different factors: (1) regional crocodyliform extinction, with lineages terminating at the J/K boundary (true absence); (2) the lack of sedimentary rock availability for sampling fossils (false absence); or (3) the presence of crocodyliforms, but a failure to sample them amongst other tetrapod faunas (false absence). In North America, the earliest Cretaceous (Berriasian–Barremian) is largely devoid of tetrapod fossils (Benson *et al.*, 2013), and therefore it can be inferred that the lack of crocodyliforms is most likely the product of poor sampling. However, as discussed in Chapter 3, whether or not this is an artefact of a poor fossil record, incomplete sampling, or genuine absence requires further investigation. In Europe, the continental Berriasian record is relatively well-sampled, but still documents a decline in non-marine crocodyliform diversity (Figure 37). This European decline is tracked by a constriction in the apparent latitudinal ranges of Northern Hemisphere earliest Cretaceous crocodyliforms across the J/K boundary. In Asia, the first well-dated Cretaceous occurrences are from the Hauterivian–Barremian of the Russian Federation, and the low Berriasian–Valanginian biodiversity (SQSRu) found is based on rare semi-aquatic occurrences from poorly temporally constrained localities. Other small-bodied groups, such as lepidosaurs and mammals, are also rare in earliest Cretaceous Asian faunas, whereas dinosaur fossils are relatively well known (Benson *et al.*, 2013), although these groups all occupied different non-marine environments in Asia throughout this time, and have variable preservational potentials (Benson *et al.*, 2013). Despite these differences, the rarity of crocodyliform fossils suggests that at least a portion of the low biodiversity of this group in the earliest Cretaceous is a genuine signal, but it cannot be ruled out that part of this is due to incomplete sampling.

In Africa, the first identifiable Cretaceous crocodyliform occurrences are from the Aptian, represented by the notosuchians *Malawisuchus* and *Araripesuchus* from Malawi (Gomani, 1997), as well as *Machimosaurus rex* now from the Hauterivian of Tunisia (Fanti *et al.*, 2016b), the discovery of which post-dates the analyses here. In South America, the earliest Cretaceous record is restricted to just a single occurrence of the Brazilian neosuchian *Susisuchus*, which cannot be dated more precisely than the Berriasian–Barremian (Fortier and Schultz, 2009). In Patagonia, there are multiple occurrences of metriorhynchids from the Tithonian–Berriasian Vaca Muerta Formation, comprising at least three different genera: *Dakosaurus*, *Cricosaurus*, and *Purranisaurus* (Herrera *et al.*, 2013; Herrera, 2015). This represents a relatively high diversity in comparison to the rest of Gondwana, but relatively lower diversity than that exhibited by the well-sampled Tethyan regions. Unfortunately, due to the dating of these occurrences, many were not included in the subsampling analyses as they occupy more than a single time bin. However, it should be noted that there appears to have been an endemic fauna of Eastern Pacific metriorhynchids that might have crossed the J/K boundary. In addition to this, there are relatively high numbers of dinosaur-bearing collections and formations in the earliest Cretaceous of Gondwana (Benson *et al.*, 2013), including regions inhabited by crocodyliforms during other intervals of the Mesozoic. Therefore the absence of non-marine crocodyliforms from these regions at this time cannot be fully explained by sampling failure, and reflects at least in part a genuine lack of biodiversity, a pattern also observed in contemporaneous Gondwanan turtle faunas (Nicholson *et al.*, 2015).

4.3.3 Environmental drivers of the Jurassic/Cretaceous crocodyliform diversity crash

The corrected biodiversity curves presented are largely convergent, and show varying degrees of correlation with a range of environmental factors (Table 77), in contrast to raw taxonomic diversity.

This suggests that the methods employed here of reconstructing biodiversity are appropriate, and do not scramble an underlying biodiversity signal (Hannisdal and Peters, 2011).

After correcting for sampling, the positive relationship between episodes of warm sea-surface temperatures (SST) and marine crocodyliform biodiversity found by a recent study (Martin *et al.*, 2014a) could not be recovered. This lack of correlation occurs despite using the same SST dataset and a similar phylogenetic correction methodology to that study, and suggests that different time scaling methodologies or an intrinsically different dataset of marine crocodyliforms is responsible for this discrepancy. Furthermore, no relationship was recovered for the subsampled results based on SQSPs and SQSPt, and the SQSRc analysis actually produced a statistically weak negative correlation between SST and marine biodiversity (Appendix 13). This disagreement could be due to the different statistical procedure employed by the previous analysis (Martin *et al.*, 2014a), as well as the relatively short temporal duration of thalattosuchians (an issue which is alleviated by the use of a maximum-likelihood modelling approach). However, this discrepancy more likely pertains to the treatment of metriorhynchoid thalattosuchians. The positive correlation between biodiversity and SST was only previously identified when metriorhynchoids were excluded (Martin *et al.*, 2014a). These authors suggested that this indicated that metriorhynchoids responded differently to palaeotemperature changes than other marine crocodyliforms. However, a simpler explanation is that there is no strong palaeotemperature signal governing the long-term trends in marine crocodyliform biodiversity (Mannion *et al.*, 2015), an interpretation that is favoured by the present results. When metriorhynchoids are excluded from analyses using SQSPs, Late Jurassic teleosauroid diversity remains flat until their extinction at the J/K boundary (although their absolute extinction might have been much later during the Hauterivian (Fanti *et al.*, 2016b)), and the positive relationship with palaeotemperature was still not recovered (Pearson's r = -0.69, p = 0.197). If metriorhynchoids are excluded from the PDE analyses, a weak positive association is recovered between marine biodiversity (PDEs) and palaeotemperature (Spearman's ρ = 0.524, p = 0.098), but the AICc results support a

stronger relationship with $\delta^{34}S$ (AICc weight = 0.283). Furthermore, the relationship between PDEt and sea level is strengthened when metriorhynchoids are excluded at both the genus (AICc weight = 0.873) and species (AICc weight = 0.998) levels. Overall, these results support those of a more recent analysis (Mannion *et al.*, 2015) in that eustatic sea level was the most important factor in controlling the biodiversity of marine crocodyliforms. This correlation is most strongly recovered for PDEt and SQSPs, and periods of high biological activity in the oceans (indicated by $\delta^{13}C$) also appear to be a strong controlling factor for SQSPs. While some of the results do not fully support this relationship with sea level (SQSPt, SQSRc, PDEs), these results are non-significant and do not necessarily contradict the conclusions. Results for SQSRc also suggest that factors such as nutrient cycling and eustacy-influenced redox shifts (indicated by perturbations to the $\delta^{34}S$ cycle) were also important in regulating marine crocodyliform biodiversity, as secondary mechanisms underpinned by fluctuating sea levels.

Interestingly, the results also indicate that sea level influenced non-marine crocodyliform biodiversity. Rising sea levels increase the amount of shallow marine habitat available, resulting in high biodiversity during the Late Jurassic highstand. Sea level reached a global lowstand across the J/K boundary (Hallam, 1988; Miller *et al.*, 2005; Haq, 2014), reflected in a reduction of global crocodyliform biodiversity. Because most of the Late Jurassic crocodyliforms in the non-marine dataset are coastal or semi-aquatic forms (e.g., Atoposauridae, Goniopholididae), rather than fully terrestrial (e.g., Notosuchia), it seems likely that these major eustatic sea-level changes promoted high Late Jurassic biodiversity, as well as the elevated extinctions and subsequent low biodiversity of crocodyliforms in both the marine and non-marine realms. This conclusion should be treated with caution because much of this non-marine signal might be a reflection of changes in European basins across the J/K boundary.

Recovery of the quantitative association between sea level and marine crocodyliform diversity (see above) is also supported by qualitative observations and differences between northern hemisphere and southern Tethyan marine environments. A dramatic reduction in European thalattosuchian

diversity was recovered, which plausibly relates to the closure of shallow marine lagoonal environments (Young *et al.*, 2014a; Young *et al.*, 2014b), and a major environmental shift continuing into the Cretaceous. However, in Tunisia, these environments dominate Early Cretaceous sedimentary sequences (Benton *et al.*, 2000; Barale and Ouaja, 2002; Anderson *et al.*, 2007; Fanti *et al.*, 2012), and explains why a single relict teleosaurid lineage persisted into the Early Cretaceous (Fanti *et al.*, 2016b).

In Asia, relatively low earliest Cretaceous (K1) diversity might have been caused by changes in palaeotemperature, with a climatic shift from warmer and more arid Late Jurassic conditions to a much cooler regime (Krassilo.Va, 1973; Amiot *et al.*, 2011). However, if the rapidly increasing diversity in the K2-K3 intervals is considered when estimating maximum subsampled diversity, accounting for uncertainty in dating of some non-marine crocodyliform occurrences, then it appears that this climatic shift coincides with increasing Early Cretaceous non-marine crocodyliform diversity in Asia. Although the data are currently too sparse to statistically test, such a correlation would imply that there is, at least in Asia, and inverse relationship between increasing temperatures and non-marine crocodyliform diversity.

4.4 Summary

Using a combined approach to reconstructing palaeobiodiversity, it has been demonstrated that crocodyliforms suffered a major biodiversity decline across the Jurassic/Cretaceous boundary in both the marine and terrestrial realms. This is accompanied by elevated extinction rates in the latest Jurassic, nearly at the level of mass extinction status, and severely depressed origination rates in the Early Cretaceous. Sea-level changes were primarily responsible for this biodiversity decline, both in the marine realm and on land, reducing the amount of habitable shallow marine area for crocodyliforms. Secondary factors driving biodiversity changes included perturbations to the carbon and sulphur cycles that, together with sea-level fluctuations, indicate a prominent role for large-scale tectonic processes

in shaping crocodyliform biodiversity in the Late Jurassic to Early Cretaceous. Contrary to previous work, there is little evidence for a mediating effect of palaeotemperature on crocodyliform biodiversity during this interval. Overall this suggests that the fate of Mesozoic crocodyliforms was coupled more broadly to a combination of environmental factors and their wider impact on pelagic and shallow marine ecosystems. Results here support the hypothesis that sea-level change is the principal driving factor in shaping the evolution of shelf biotas, but it cannot be ruled out that additional ecological factors were also at play across the Jurassic/Cretaceous boundary.

Disclosure: Much of this Chapter is drawn from a related publication by Tennant *et al*. (2016). While the primary author wrote the majority of this text and performed all analyses, parts of it have been contributed to by the other authors, as well as receiving input from the peer review process.

Tennant, J. P., Mannion, P. D. and Upchurch, P. (2016) Environmental drivers of crocodyliform extinction across the Jurassic/ Cretaceous transition. *Proceedings of the Royal Society Series B: Biological Sciences* **283**, 20152840. doi: 10.1098/rspb.2015.2840.

5 Evolutionary Relationships and Systematics of Atoposauridae (Crocodylomorpha: Neosuchia) Across the Jurassic/Cretaceous Boundary, and Implications for the Rise of Eusuchia

5.1 Introduction

Atoposaurids comprise a clade of extinct neosuchian crocodyliforms, often characterised by their differentiated dentition and diminutive body size (Owen, 1879; Joffe, 1967; Buscalioni and Sanz, 1990b). This group has a long history of study, with specimens first identified from Late Jurassic deposits in France and Germany in the mid-19th century (Meyer, 1850; 1851). The current view is that atoposaurids were an important and diverse component of Eurasian Late Jurassic and Cretaceous terrestrial to semi-aquatic ecosystems, often with multiple sympatric lineages (Wellnhofer, 1971; Thies *et al.*, 1997; Martin *et al.*, 2010; Lauprasert *et al.*, 2011; Tennant and Mannion, 2014). A number of discoveries indicate that atoposaurids might also have been present in the Jurassic and Cretaceous of Africa (Michard *et al.*, 1990; Flynn *et al.*, 2006; Haddoumi *et al.*, 2015) and North America (Cifelli *et al.*, 1997; Cifelli *et al.*, 1999; Eaton *et al.*, 1999; Fiorelli, 1999).

5.1.1 Taxonomic composition

Despite their long history of study, the taxonomic composition of Atoposauridae remains uncertain and many putative atoposaurid species have never been incorporated into a phylogenetic analysis. In an extensive revision of the taxonomy of atoposaurids, three genera were recognised from the Late Jurassic of continental western Europe (*Alligatorellus*, *Alligatorium*, and *Atoposaurus*) (Wellnhofer, 1971), who followed previous authors by including *Theriosuchus* from the UK (Joffe, 1967), *Shantungosuchus* from China (Young, 1961), and *Hoplosuchus* from North America (Gilmore, 1926), in Atoposauridae (Steel, 1973). *Alligatorium* comprises the type species *A. meyeri* (Gervais, 1871), and the first detailed analysis of the European specimens (Wellnhofer, 1971) considered the referred species *Alligatorium depereti* (Vidal, 1915), *Alligatorium franconicum* (Ammon, 1906) and *Alligatorium paintenense* (Kuhn, 1961) to be valid, although all specimens of the latter two species were lost or destroyed during the Second World War. Subsequently, the Spanish species *Alligatorium depereti* was

considered to be distinct enough to warrant its own genus, *Montsecosuchus* (Buscalioni and Sanz, 1988; Buscalioni and Sanz, 1990b). In addition to these relatively well-known European specimens, a putative atoposaurid *Karatausuchus* was described from the Jurassic of Kazakhstan (Efimov, 1976), but a more recent analysis subsequently removed this taxon, as well as *Hoplosuchus* and *Shantungosuchus*, from Atoposauridae (Buscalioni and Sanz, 1988). At around the same time, a different analysis (Benton and Clark, 1988) considered only *Alligatorium* to be valid among atoposaurid taxa from the Late Jurassic of France and Germany, regarding *Alligatorellus* and *Atoposaurus* as juvenile individuals of this taxon. Together, this study among others considered *Theriosuchus* to represent an atoposaurid (Joffe, 1967; Benton and Clark, 1988). This was largely followed by the first formal phylogenetic analysis of Atoposauridae (Buscalioni and Sanz, 1988; Buscalioni and Sanz, 1990b), but these authors also accepted *Alligatorellus*, though not *Atoposaurus*, as valid. Most recently, it has been argued that *Alligatorellus*, *Alligatorium*, and *Atoposaurus* all represent valid atoposaurid genera, with each comprising two species (Tennant and Mannion, 2014). These authors also suggested that *Alligatorium paintenense* is likely to be a junior synonym of *Alligatorium franconicum*. In addition to the type species of *Theriosuchus*, *T. pusillus* (Owen, 1878b; a; 1879), four additional species have subsequently been named: *T. guimarotae* (Schwarz and Salisbury, 2005), *T. grandinaris* (Lauprasert *et al.*, 2011), *T. ibericus (Brinkmann, 1989; 1992)* and *T. sympiestodon* (Martin *et al.*, 2010; Martin *et al.*, 2014c). Some authors have further taken the view that *Theriosuchus* is distinct enough from all other atoposaurids to constitute its own clade, Theriosuchidae (Kälin, 1955; Buffetaut, 1982; 1983), but this taxonomic assignment has not been widely adopted. Two additional taxa have also been referred to Atoposauridae, with the first putative Gondwanan atoposaurid (*Brillanceausuchus babouriensis*) being identified from Cameroon (Michard *et al.*, 1990), and *Pachycheilosuchus trinquei* described from North America (Rogers, 2003). However, subsequent studies have placed *Pachycheilosuchus* outside of Atoposauridae, and it is likely to be a member of Hylaeochampsidae (Buscalioni *et al.*, 2011).

5.1.2 Atoposaurids in time and space

Based on our current understanding of Atoposauridae, the oldest diagnostic remains are: (1) a partial dentary from the Middle Jurassic (late Bajocian–Bathonian) of the Isle of Skye, United Kingdom (Young *et al.*, 2016), ascribed to *Theriosuchus* sp.; (2) isolated tooth crowns from the late Bathonian of France and the UK (Evans *et al.*, 1994; Kriwet *et al.*, 1997; Knoll *et al.*, 2013); (3) crocodyliform teeth, possibly referable to an atoposaurid, from the Bathonian Grand Causses of France (Knoll *et al.*, 2013; Knoll and López-Antoñanzas, 2014); and (4) teeth, mandibular and postcranial remains from the Bathonian of Madagascar (Flynn *et al.*, 2006) and Morocco (Haddoumi *et al.*, 2016) (Figure 39). These remains indicate that atoposaurids had attained their characteristic small body size and heterodont dentition, along with a broad geographic distribution, by the Middle Jurassic.

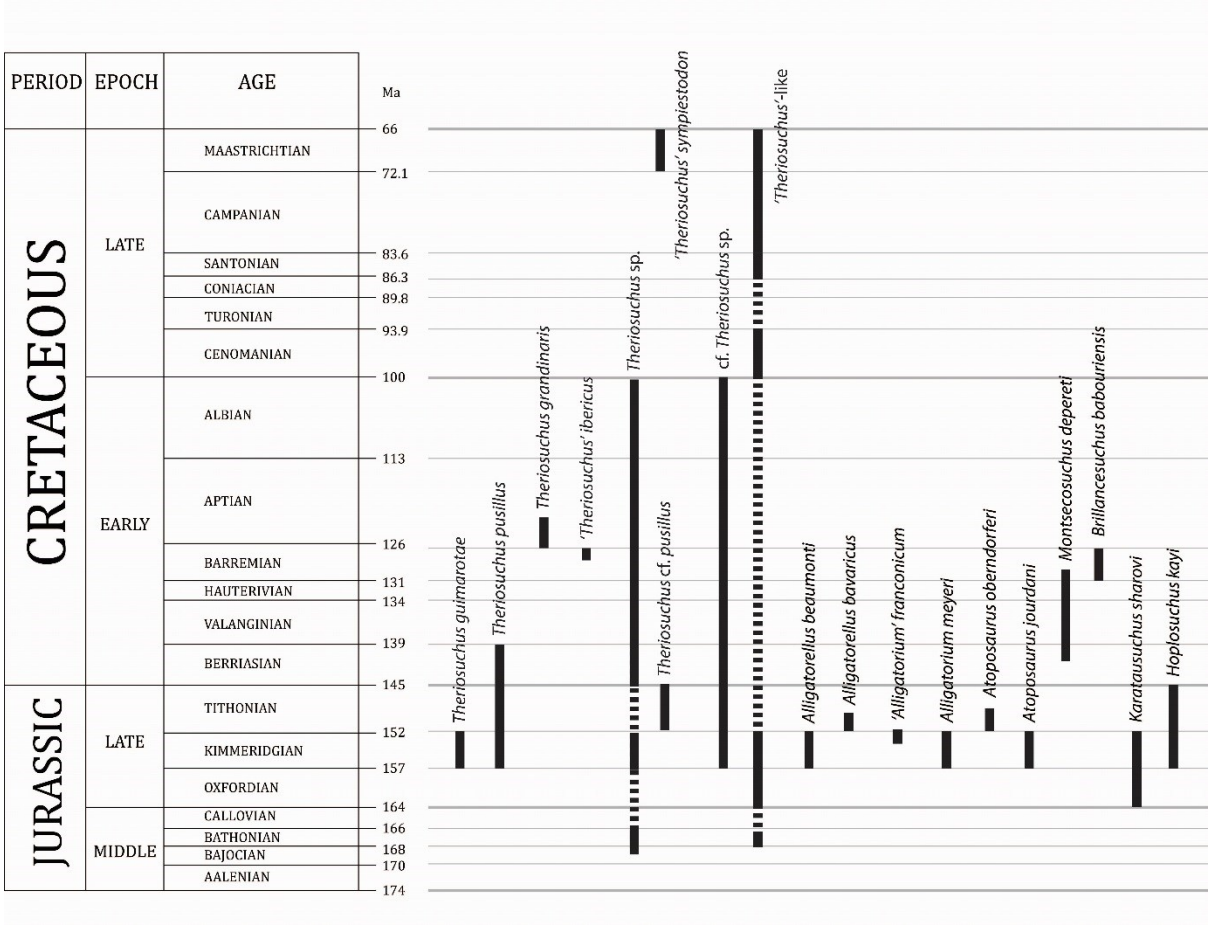


Figure 39. Stratigraphic (including uncertainty) and geographic ranges of known and putative (denoted with a "?") atoposaurid species.

In addition to the presence of *Alligatorellus*, *Alligatorium*, *Atoposaurus* and *Montsecosuchus* in the Late Jurassic and Early Cretaceous of western Europe, *Theriosuchus* is known from a number of Late Jurassic and Cretaceous localities in Europe (Owen, 1879; Buffetaut, 1983; Buscalioni and Sanz, 1984; Buscalioni, 1986; Buscalioni and Sanz, 1987a; b; Salisbury, 2002; Schwarz and Salisbury, 2005; Martin *et al.*, 2010; Salisbury and Naish, 2011; Martin *et al.*, 2014c; Tennant and Mannion, 2014; Young *et al.*, 2016). Reports based on isolated teeth also place *Theriosuchus* in the middle Cretaceous of North America (Pomes, 1990; Winkler *et al.*, 1990; Cifelli *et al.*, 1999; Eaton *et al.*, 1999; Fiorelli, 1999), alongside the putative atoposaurid *Pachycheilosuchus* (Rogers, 2003). Remains of *Theriosuchus* are also found in the latest Jurassic to Early Cretaceous of Thailand (Lauprasert *et al.*, 2011) and China (Wu *et al.*, 1996b). In addition, *Brillanceausuchus* from western Africa (Michard *et al.*, 1990) is the only putative Cretaceous Gondwanan occurrence of Atoposauridae, along with the fragmentary and poorly known Middle Jurassic remains mentioned by several authors (Flynn *et al.*, 2006; Haddoumi *et al.*, 2016). Finally, fragmentary putative atoposaurid remains from the Eocene of Yemen would mean that Atoposauridae passed through the end-Cretaceous mass extinction (Stevens *et al.*, 2013).

5.1.3 Evolutionary relationships

The monophyly of Atoposauridae has not been tested at a low taxonomic level since the first formal analysis (Buscalioni and Sanz, 1988; Buscalioni and Sanz, 1990b), and even species attributed to *Theriosuchus* have not been conclusively demonstrated to form a monophyletic genus. This is partly due to the taphonomy and preservation of these specimens, whereby incompleteness and the mode of preservation (i.e., dorsal flattening) restricts assessment of important characters. Furthermore, the generally small body size of atoposaurids has led to an overall lack of clarity in distinguishing between

plesiomorphic, juvenile, and paedomorphic characteristics (Joffe, 1967; Buffetaut, 1983; Clark, 1986; Buscalioni and Sanz, 1988; Tennant and Mannion, 2014), although the ontogeny of *Theriosuchus* is reasonably well understood among crocodyliforms (Joffe, 1967; Schwarz and Salisbury, 2005; Martin *et al.*, 2014c).

Most phylogenetic analyses recover atoposaurids as non-eusuchian neosuchians, part of the important crocodyliform lineage that includes living crocodiles (Benton and Clark, 1988; Buscalioni and Sanz, 1988; Buscalioni and Sanz, 1990a; Buscalioni and Sanz, 1990b; Salisbury *et al.*, 2006; Brochu *et al.*, 2009; Pol and Gasparini, 2009; Pol *et al.*, 2009; Martin *et al.*, 2010; Adams, 2013; 2014; Sertich and O'Connor, 2014). Whereas some analyses have found Atoposauridae to be outside of Neosuchia (Sereno *et al.*, 2003), this has not gained support from subsequent studies. Recent analyses consider atoposaurids to be within Neosuchia, but their position differs greatly, varying between: (1) basal to Goniopholididae and other neosuchians when investigating higher neosuchian or eusuchian relationships (Pol and Norell, 2004a; Gasparini *et al.*, 2006; Turner, 2006; Fortier and Schultz, 2009; Pol *et al.*, 2009; Figueiredo *et al.*, 2011; Adams, 2013; 2014) (Figure 40A); (2) in an uncertain position within basal Neosuchia (Pol and Apesteguía, 2005; Larsson and Sues, 2007; Turner and Buckley, 2008; Lauprasert *et al.*, 2009; Martin *et al.*, 2010); (3) just outside of Eusuchia (Rogers, 2003; Salisbury *et al.*, 2006) (Figure 40B); or (4) as the sister group to Paralligatoridae within Eusuchia (Figure 40C) that, together with Hylaeochampsidae, comprises the sister group to crown Crocodylia (Turner, 2015). However, among almost all of these analyses, atoposaurids have been relaitvely poorly sampled, and discussion of their relationships based on phylogenetic analyses remains highly limited, with very few exceptions (Martin *et al.*, 2010).

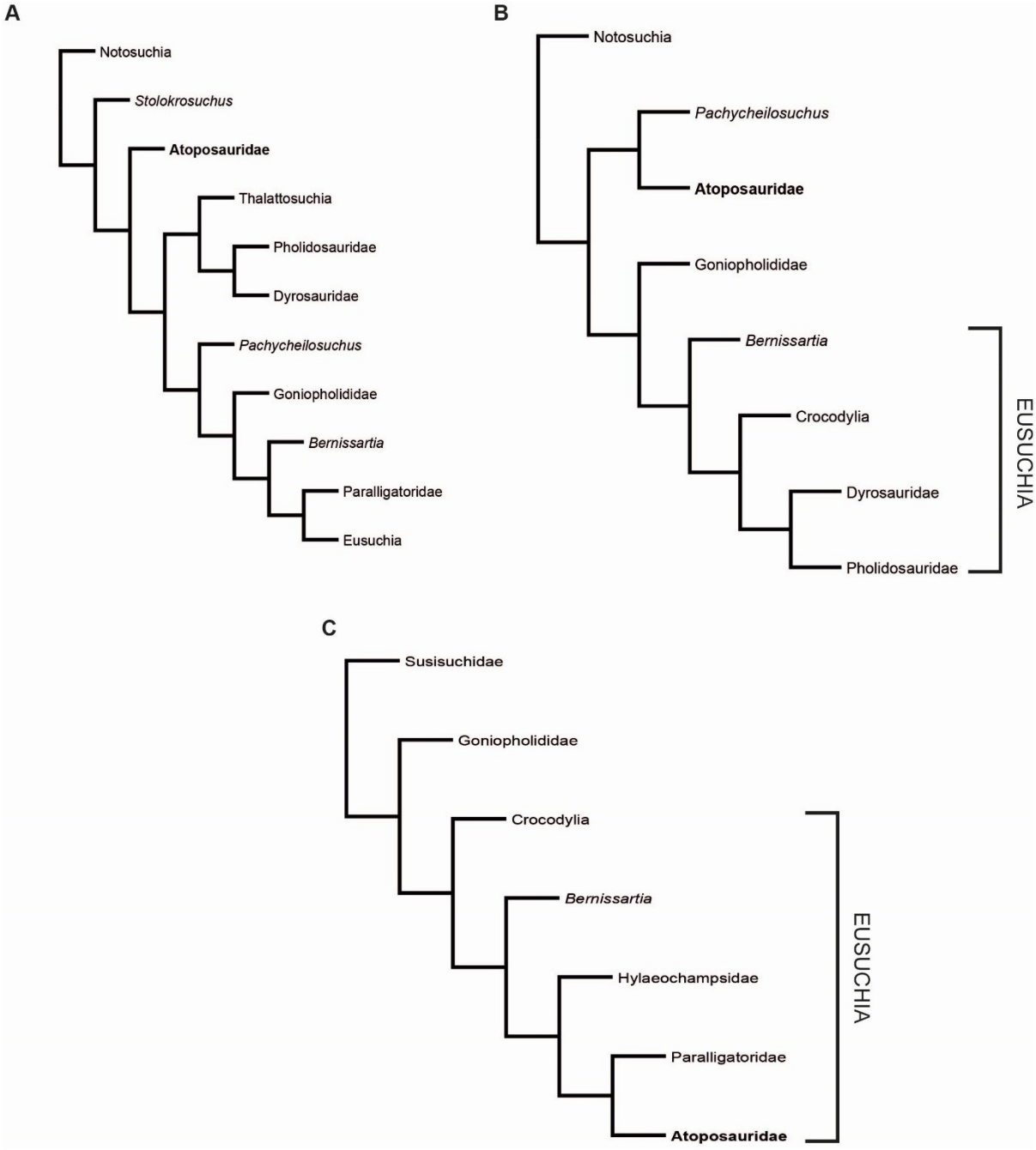


Figure 40. Previously recovered inter-relationships between Atoposauridae and other major crocodyliform clades: (A) Adams (2014; (B) Rogers (2003); (C) Turner and Pritchard (2015).

The first analysis of atoposaurid inter-relationships recovered two sub-clades comprising *Montsecosuchus* + *Theriosuchus*, and *Alligatorium* + *Alligatorellus* (Buscalioni and Sanz, 1988) (Figure 41A), although the position of *Montsecosuchus* was unstable. A subsequent analysis recovered the same topology, but also included *Atoposaurus*, which was placed as the most basal atoposaurid (Karl

et al., 2006). However, these two studies predated the identification of several new species of *Theriosuchus*. The recent construction of a crocodyliform supertree included *Alligatorium*, *Alligatorellus*, *Atoposaurus*, *Montsecosuchus*, *Pachycheilosuchus*, and *Theriosuchus guimarotae*, *T. pusillus*, and *T. sympiestodon*, and placed them all within Atoposauridae (Bronzati *et al.*, 2012), as the sister group to Goniopholididae and more advanced neosuchians (Figure 41B). However, these authors were unable to fully resolve the internal relationships of the group beyond finding *Alligatorellus* and *Atoposaurus* to be sister taxa, and that the three *Theriosuchus* species formed a clade. Most recently, a pair of investigations into the origins and evolution of Eusuchia included *Theriosuchus guimarotae*, *T. pusillus*, and *T. sympiestodon* (Turner, 2015; Turner and Pritchard, 2015), finding them to be paraphyletic with respect to *Alligatorium* (Figure 41C).

Consequently, the full plethora of putative atoposaurid species has never previously been included in any phylogenetic analysis. In studies that have included atoposaurids, *Montsecosuchus* and the putative atoposaurids *Brillanceausuchus* and *Karatausuchus* have been almost completely disregarded. As a result, neither the phylogenetic position of Atoposauridae within Neosuchia, nor its intra-relationships are clear at present.

In this chapter, a full systematic reassessment of all species previously assigned to Atoposauridae is undertaken, determining the composition and internal relationships of the group, as well as its position within Neosuchia. This is based on the construction of a new phylogenetic character matrix, analysed using parsimony and Bayesian approaches. Revised diagnoses are provided for all genera and species assigned to Atoposauridae, as well as the first phylogenetic definition for the clade, and the taxonomic and phylogenetic status of putative atoposaurids is discussed. Lastly, the implications of these phylogenetic results for atoposaurids across the Jurassic/Cretaceous boundary and the evolution of Eusuchia are explored.

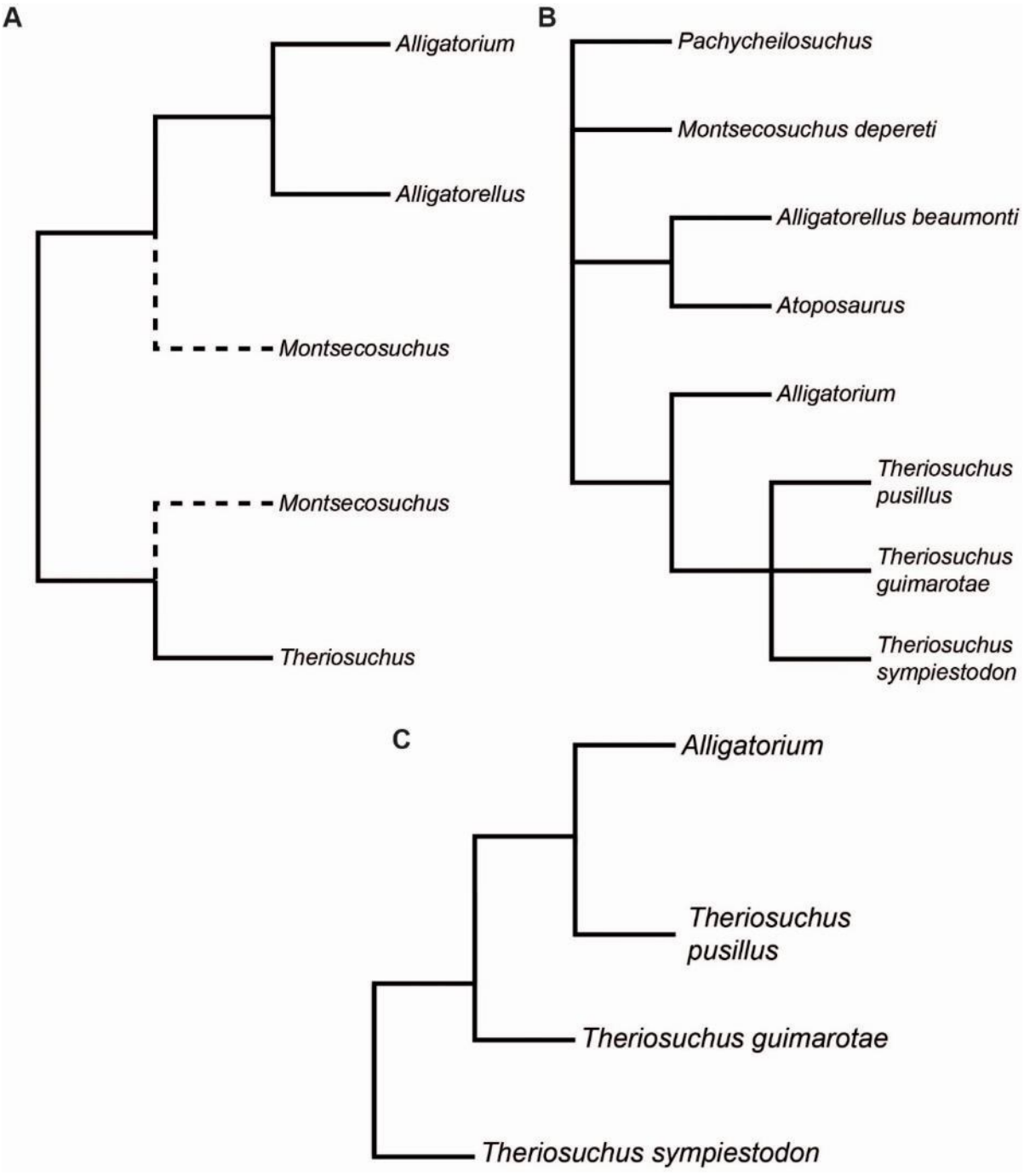


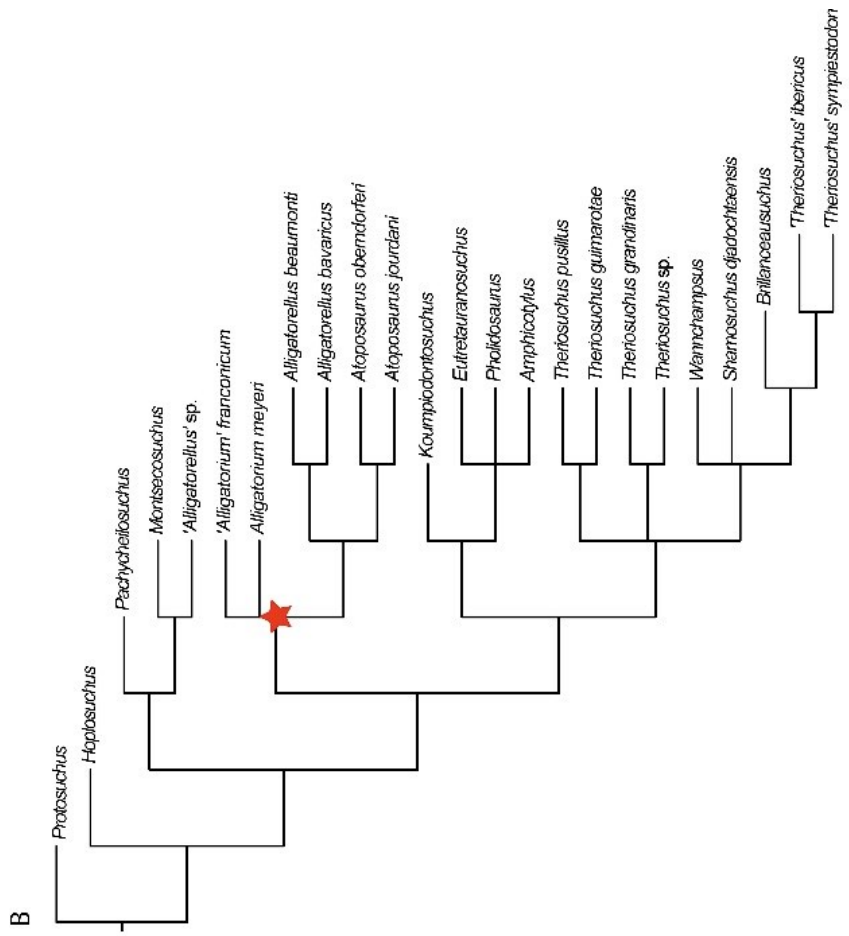
Figure 41. Previously recovered intrarelationships within Atoposauridae. (A) Buscalioni and Sanz (1988); (B) Bronzati et al. (2012); (C) Turner, 2015.

5.2 Results

5.2.1 Parsimony analyses

5.2.1.1 Unordered analysis

A complete analysis involving all OTUs and all characters defined as unordered resulted in 7 MPTs, with a total length of 802 steps (Figure 42A). In this topology, Atoposauridae comprises all species of *Alligatorium*, *Alligatorellus*, and *Atoposaurus*, with the two species of *Alligatorium* (*A*. *meyeri* and *A*. *franconicum*) occupying an unresolved basal position. *Atoposaurus* and *Alligatorellus* are sister taxa, with each comprising two constituent species. Atoposauridae is in a more stemward position than a clade comprising *Koumpiodontosuchus* and coelognathosuchians. MB.R.3632 (Schwarz-Wings *et al.*, 2011) does not group with other *Alligatorellus* species, supporting the conclusions of a recent review of this genus (Tennant and Mannion, 2014), but instead clusters with *Montsecosuchus*, forming a basal clade with *Pachycheilosuchus*. *Theriosuchus* is resolved as polyphyletic, with a clade of *T*. *ibericus* + *T*. *sympiestodon* nested within Paralligatoridae, along with *Brillanceausuchus*, *Shamosuchus* and *Wannchampsus*. The remaining *Theriosuchus* species fall outside of this clade, with *T*. *guimarotae* + *T*. *pusillus*, and *T*. *grandinaris* + *Theriosuchus* sp. forming clades.


B
Protosuchus
Haplosuchus
Pachycheilosuchus
Montsecosuchus
'Alligatorellus' sp.
'Alligatorium' franconicum
Alligatorium meyeri
Alligatorellus beaumonti
Alligatorellus bavaricus
Atoposaurus oberndorferi
Atoposaurus jourdani
Koumpiodontosuchus
Eutretauranosuchus
Pholidosaurus
Amphicotylus
Theriosuchus pusillus
Theriosuchus guimarotae
Theriosuchus grandinaris
Theriosuchus sp.
Wannchampsus
Shamosuchus djadochtaensis
Brillanceausuchus
Theriosuchus' ibericus
Theriosuchus' sympiestodon

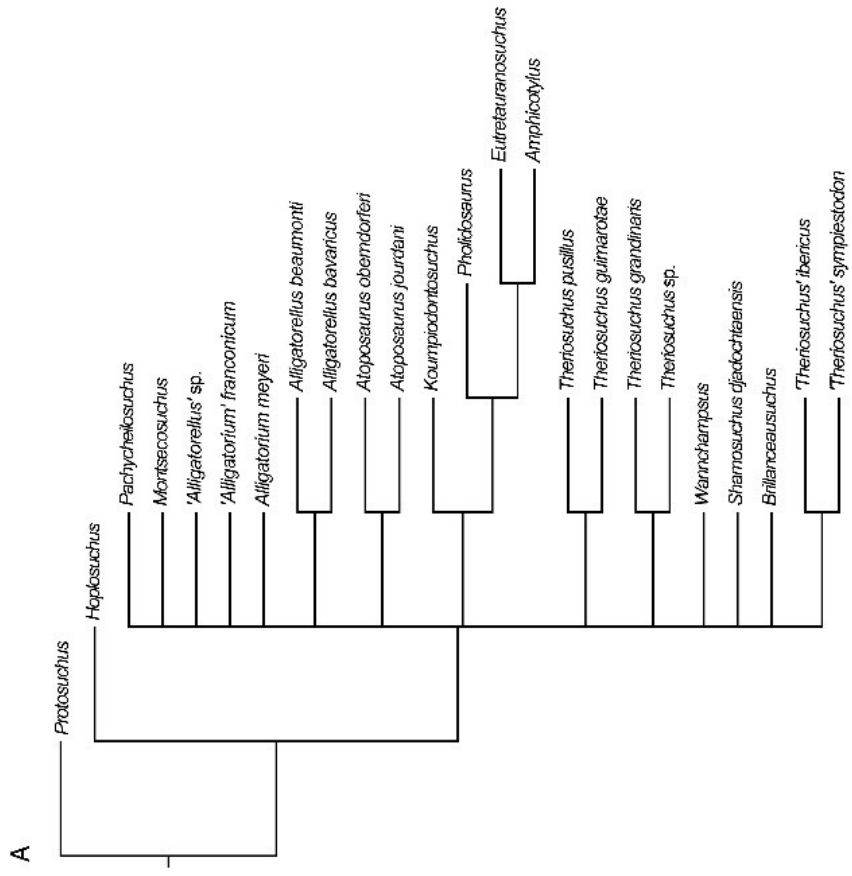

A
Protosuchus
Haplosuchus
Pachycheilosuchus
Montsecosuchus
'Alligatorellus' sp.
'Alligatorium' franconicum
Alligatorium meyeri
Alligatorellus beaumonti
Alligatorellus bavaricus
Atoposaurus oberndorferi
Atoposaurus jourdani
Koumpiodontosuchus
Pholidosaurus
Eutretauranosuchus
Amphicotylus
Theriosuchus pusillus
Theriosuchus guimarotae
Theriosuchus grandinaris
Theriosuchus sp.
Wannchampsus
Shamosuchus djadochtaensis
Brillanceausuchus
Theriosuchus' ibericus
Theriosuchus' sympiestodon

Figure 42. (A) Strict consensus topology for phylogenetic analysis when all taxa are included, and all characters are considered to be unordered (i.e., non-additive). Atoposauridae is marked with a red star. (B) Strict consensus for phylogenetic analysis when all taxa are included, and selected characters are considered to be ordered (Appendix 6).

5.2.1.2 Ordered analysis

When all taxa are included and 47 characters are treated as ordered (Appendix 6), a largely unresolved polytomy is recovered (Figure 42B) for the strict consensus of 11 MPTs of length 830 steps. *Theriosuchus* remains polyphyletic, forming the same clades as in the unordered analysis, and *Atoposaurus* and *Alligatorellus* are monophyletic genera.

The *iterpcr* function (Pol and Escapa, 2009) found '*Alligatorellus*' sp. (MB.R.3632) and *Alligatorium franconicum* to be the most unstable taxa. The instability of the former taxon is most likely due to a high proportion of missing data, whereas for the latter this is more likely a result of character conflict, coupled with the inability to study the specimen first-hand. When these taxa are removed *a priori*, the topology is almost completely resolved (Figure 43A), producing 11 MPTs of length 805 steps. The strict consensus identifies the remaining source of conflict to be the relationship between *Brillanceausuchus*, *Shamosuchus* and *Wannchampsus* (Figure 43A). Atoposauridae comprises *Alligatorium meyeri*, *Alligatorellus* and *Atoposaurus*. *Montsecosuchus* is allied with *Pachycheilosuchus*, with this clade outside of all other neosuchian taxa. Bremer support values show that Atoposauridae is moderately well supported with a node value of 2. The two species of *Alligatorellus* are strongly supported with a node value of 4, and the relationship between *Alligatorellus* and *Atoposaurus* is supported by a node value of 2. *T. pusillus* + *T. guimarotae* is strongly supported with a node support value of 4, and *T. sympiestodon* + *T. ibericus* has a node support value of 3.

One final analysis was performed that excluded *Pachycheilosuchus* along with MB.R.3632 *a priori*, but included *Alligatorium franconicum*. This was due to the unexpected placement of *Pachycheilosuchus* in resulting topologies, given the more derived position it usually occupies (Buscalioni *et al.*, 2011;

Adams, 2014; Turner, 2015). This resulted in a single MPT of length 792 steps (Figure 43B). *Alligatorium franconicum* shifts to a position at the base of the clade comprising *Koumpiodontosuchus* + coelognathosuchians, with no other changes to the topology. Bremer support values show that Atoposauridae is overall only weakly supported (Fig. 5B), with a node value of 1. The sister taxon relationship between *T. pusillus* + *T. guimarotae* is the most strongly supported node on the tree, with a Bremer support value of 5, followed by *T. sympiestodon* + *T. ibericus*, with a support value of 4. Most other nodes have a support value of 1.

5.2.1.3 Implied weighting

Application of implied weighting on the ordered dataset similarly recovers a monophyletic Atoposauridae, but one that also includes *Montsecosuchus* and MB.R.3632 (Figure 44). *Alligatorium meyeri* remains the most basal member of this clade, followed by *Montsecosuchus*, and MB.R.3632 groups with the two species of *Alligatorellus*. *Theriosuchus* still remains polyphyletic, but there are now three groupings, with the clade comprising *Theriosuchus grandinaris* + *Theriosuchus* sp. shifting to a more basal position (Figure 44). This possibly reflects the incompleteness of the specimens of both these taxa. *Alligatorium franconicum* remains as the basalmost member of the clade comprising *Koumpiodontosuchus* + coelognathosuchians. The Bremer node support for Atoposauridae is 0.23 (note that support values are non-integers due to changes to character weights during the implied weighting procedure), with internal support values of 0.15–0.23. *T. pusillus* + *T. guimarotae* remains the most strongly supported clade with a node support value of 0.81.

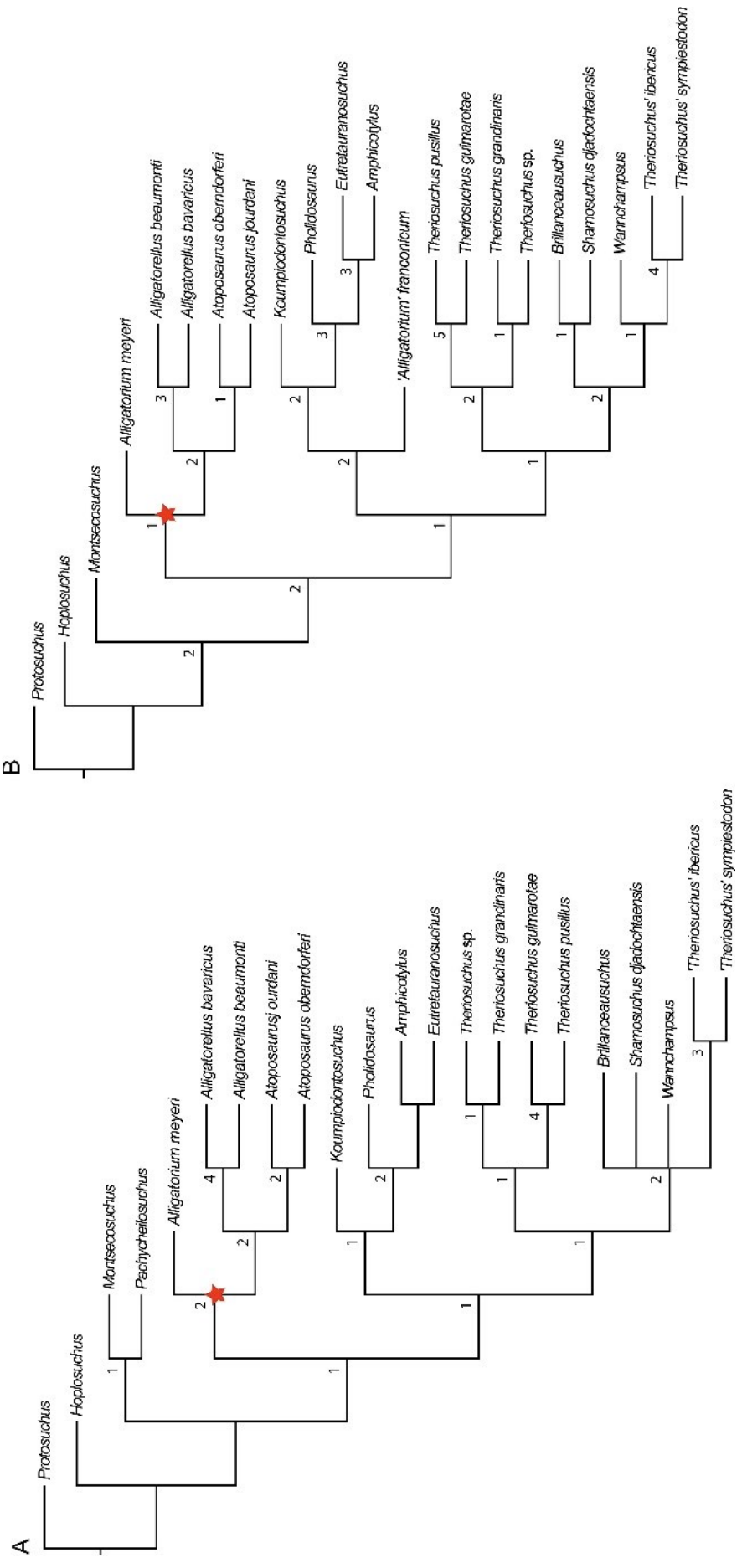

A
Protosuchus
Hoplosuchus
Montsecosuchus
Pachycheilosuchus
Alligatorium meyeri
Alligatorellus bavaricus
Alligatorellus beaumonti
Atoposaurusj ourdani
Atoposaurus oberndorferi
Koumpiodontosuchus
Pholidosaurus
Amphicotylus
Eutretauranosuchus
Theriosuchus sp.
Theriosuchus grandinaris
Theriosuchus guimarotae
Theriosuchus pusillus
Brillanceausuchus
Shamosuchus djadochtaensis
Wannchampsus
'Theriosuchus' ibericus
'Theriosuchus' sympiestodon
B
Protosuchus
Hoplosuchus
Montsecosuchus
Alligatorium meyeri
Alligatorellus beaumonti
Alligatorellus bavaricus
Atoposaurus oberndorferi
Atoposaurus jourdani
Koumpiodontosuchus
Pholidosaurus
Eutretauranosuchus
Amphicotylus
'Alligatorium' francoinicum
Theriosuchus pusillus
Theriosuchus guimarotae
Theriosuchus grandinaris
Theriosuchus sp.
Brillanceausuchus
Shamosuchus djadochtaensis
Wannchampsus
'Theriosuchus' ibericus
'Theriosuchus' sympiestodon

Figure 43. (A) Strict consensus topology for phylogenetic analysis when iterpcr script is employed, and Alligatorium franconicum and '*Alligatorellus*' sp. are excluded a priori. (B) Single most parsimonious tree for phylogenetic analysis when *Pachycheilosuchus trinquei* and '*Alligatorellus*' sp. (MB.R.3632) are excluded a priori. Absolute Bremer support values are provided adjacent to nodes. Atoposauridae is marked with a red star.

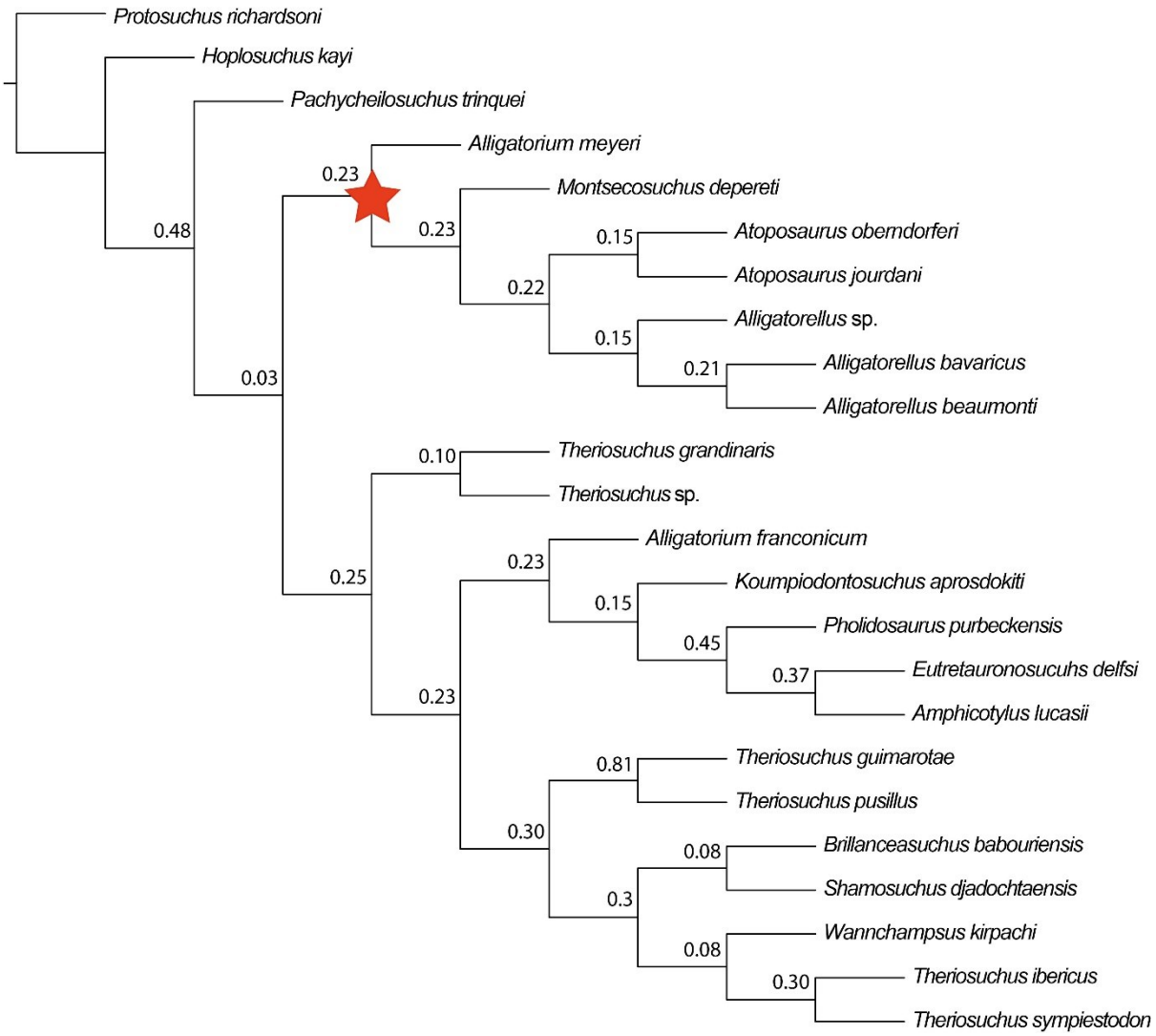


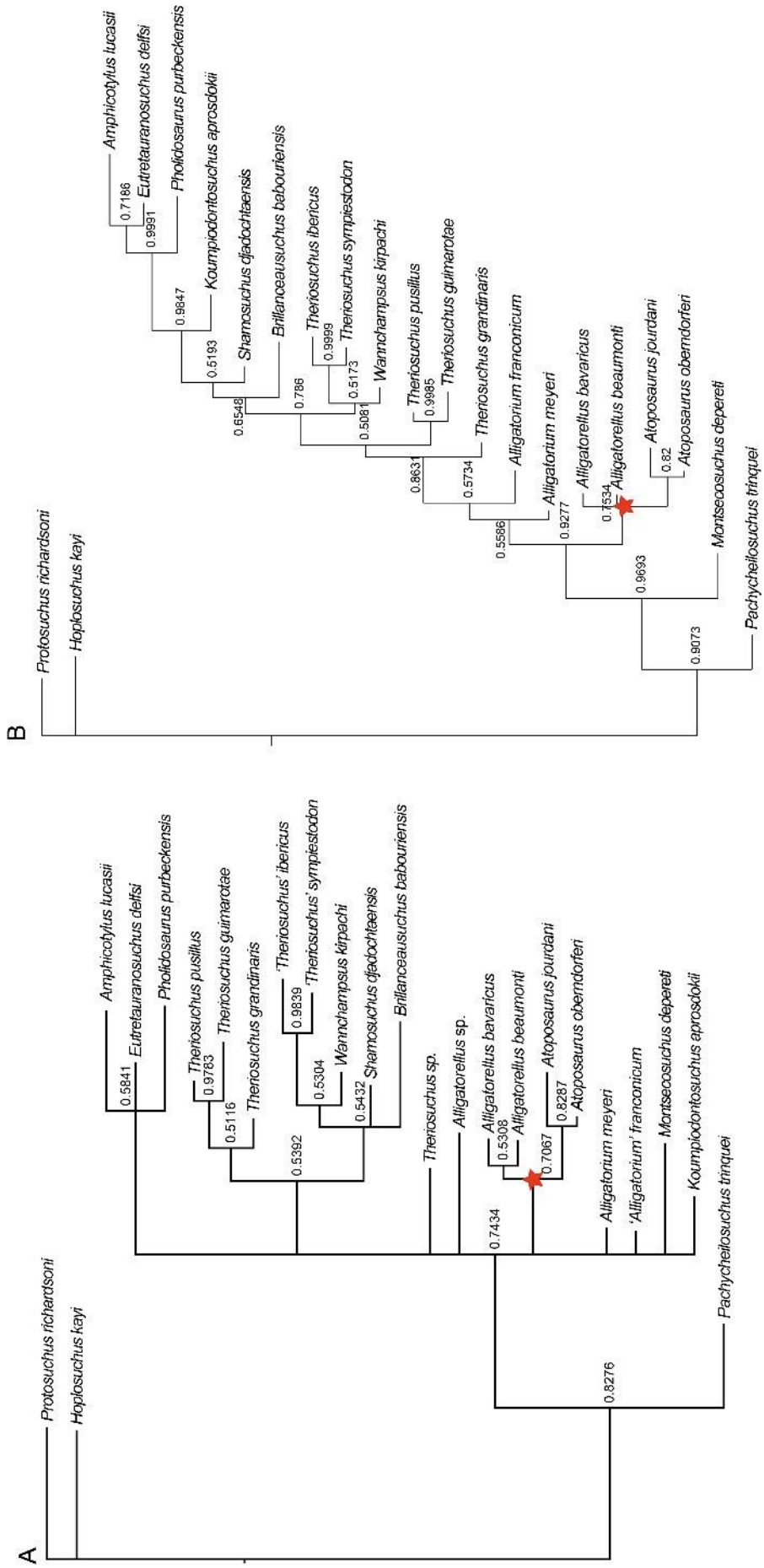
Figure 44. Single most parsimonious tree for phylogenetic analysis when implied weighting is employed with a weighting exponent of k=3. Selected characters are considered to be ordered, and no taxa were excluded a priori. Absolute Bremer support values are provided adjacent to nodes.

5.2.2 Bayesian analyses

When all taxa are included, the results of the Bayesian analysis produces a largely unresolved topology (Figure 45). *Protosuchus* and *Hoplosuchus* are basal crocodyliforms, and *Pachycheilosuchus* retains a position basal to all other remaining taxa. The interrelationships of MB.R.3632 ('*Alligatorellus*' sp.), NMS G. 2014.52.1 (*Theriosuchus* sp.), *Alligatorium*, *Montsecosuchus* and *Koumpiodontosuchus* are all unresolved. Only *Alligatorellus* and *Atoposaurus* are definitely members of Atoposauridae, with a posterior node support value of 0.71. *Theriosuchus* is polyphyletic, as before in the parsimony results, with one group within Paralligatoridae, and the other group just outside of this clade. These groups are the most strongly supported nodes across the tree, with the clades *Theriosuchus sympiestodon* + *T. ibericus* and *Theriosuchus guimarotae* + *T. pusillus* each having a posterior node support value of 0.98.

When MB.R.3632 and NMS G. 2014.52.1 are both excluded *a priori* from analyses, then the topology changes, with *Koumpiodontosuchus* + coelognathosuchians nested within Paralligatoridae (Figure 43), a result not supported by any previous crocodyliform analysis. *Alligatorium meyeri* is excluded from Atoposauridae, in a slightly more crownward position at the base of *Theriosuchus* + all other higher neosuchians. *Pachycheilosuchus* and *Montsecosuchus* retain their basal positions.

Figure 45 (A) Results of phylogenetic analysis using Bayesian inference, when all OTUs are active and selected characters are considered to be ordered. (B) Results of phylogenetic analysis using Bayesian inference, when '*Alligatorellus*' sp. (MB.R.3632) and *Theriosuchus* sp. (NMS G. 2014.52.1 and selected characters are considered to be ordered (see Appendix 6).


A
Protosuchus richardsoni
Hoplosuchus kayi
Amphicotylus lucasii
0.5841
Eutretauranosuchus delfsi
Pholidosaurus purbeckensis
Theriosuchus pusillus
0.9783
Theriosuchus guimarotae
0.5116
Theriosuchus grandinaris
0.5392
'Theriosuchus' ibericus
0.9839
'Theriosuchus' sympiestodon
0.5304
Wannchampsus kirpachi
0.5432
Shamosuchus djadochtaensis
Brillanceausuchus babouriensis
Theriosuchus sp.
Alligatorellus sp.
Alligatorellus bavaricus
0.5308
Alligatorellus beaumonti
0.7434
0.7067
Atoposaurus jourdani
0.8287
Atoposaurus oberndorferi
Alligatorium meyeri
'Alligatorium' franconicum
Montsecosuchus depereti
Koumpiodontosuchus aprosdokii
Pachycheilosuchus trinquei
0.8276
B
Protosuchus richardsoni
Hoplosuchus kayi
Amphicotylus lucasii
0.7186
Eutretauranosuchus delfsi
0.9991
Pholidosaurus purbeckensis
0.9847
Koumpiodontosuchus aprosdokii
0.5193
Shamosuchus djadochtaensis
0.6548
Brillanceausuchus babouriensis
0.786
Theriosuchus ibericus
0.9999
Theriosuchus sympiestodon
0.5173
Wannchampsus kirpachi
0.5081
Theriosuchus pusillus
0.9985
Theriosuchus guimarotae
0.8631
Theriosuchus grandinaris
0.5734
Alligatorium meyeri
0.5586
Alligatorellus bavaricus
0.9277
Alligatorellus beaumonti
0.7534
Atoposaurus jourdani
0.82
Atoposaurus oberndorferi
0.9693
Montsecosuchus depereti
0.9073
Pachycheilosuchus trinquei

5.2.3 Branch lengths and stratigraphic ranges

Based on the phylogenetic analyses presented, two different sets of 'branch lengths' are output. One of these is from the Bayesian analyses, which outputs branch lengths as a measure of the amount of evolution that has occurred along a lineage, based on the proportion of site changes over a given amount of time. This method is commonly used to calculate branch lengths using phylogenetic analysis, and they can also be output from standard parsimony analysis through different modes of character optimisation (Pierce *et al.*, 2009b). The second, using the *strap* package for R (which has *geoscale* inbuilt) (Bell and Lloyd, 2015) calculates branch lengths based on the interplay between phylogeny and stratigraphy, and calibrates branch lengths according to taxon age. This is essentially conducted by time-scaling cladograms, where branches of trees are scaled to time based on a combination of first- and last-appearances of taxa, and the hierarchy of relationships implied by the cladogram. Resulting time-scaled trees provide branch lengths that are reported as durations in millions of years (Bell and Lloyd, 2015), and have been widely used for the basis of exploring macroevolutionary patterns in Mesozoic tetrapods (Irmis, 2010; Close and Rayfield, 2012; Benson and Choiniere, 2013; Wang and Lloyd, 2016). However, rather than representing the true duration of a lineage, this method relies on tip dating based on the stratigraphic ages for associated sediments that taxa are found in, and therefore it is best that this method be regarded as using stratigraphic uncertainty as a proxy for taxonomic durations. One issue that might arise is that both of these are differing interpretations of branch lengths, but can both be utilised to the same effect for additional studies, particularly those in macroevolution regarding the tempo and mode of evolution. To date, I am not aware of any direct comparison between these two different ways of measuring something that is often treated in the same manner. To test this, I plotted the stratigraphic ranges (in millions of years) obtained from time-scaling the atoposaurid cladogram (Figure 62) resulting from the parsimony analysis when '*Alligatorium*' *franconicum* and '*Alligatorellus*' sp. are excluded *a priori*, and the terminal branch lengths obtained using the equivalent Bayesian analysis. When all OTUs are considered, there

is no relationship found between terminal branch lengths and inferred stratigraphic ranges, based on this diverse but small sample (Figure 46). This lack of relationship remains if the data are constrained to exclude coelognathosuchian outgroups (Figure 47). Based on these preliminary results, it suggests that branch lengths obtained from phylogenetic analysis based on substitution rates are not equivalent to those obtained by time-scaling cladograms, and therefore care should be taken in employing both of these for similar macroevolutionary analyses. These results are based on an extremely small sample size, however, and require further investigation in future on more comprehensively sampled datasets. This is especially pertinent in light of studies showing that different branch length calculation methods can lead to different interpretation of macroevolutionary hypotheses (Pierce *et al.*, 2009b).

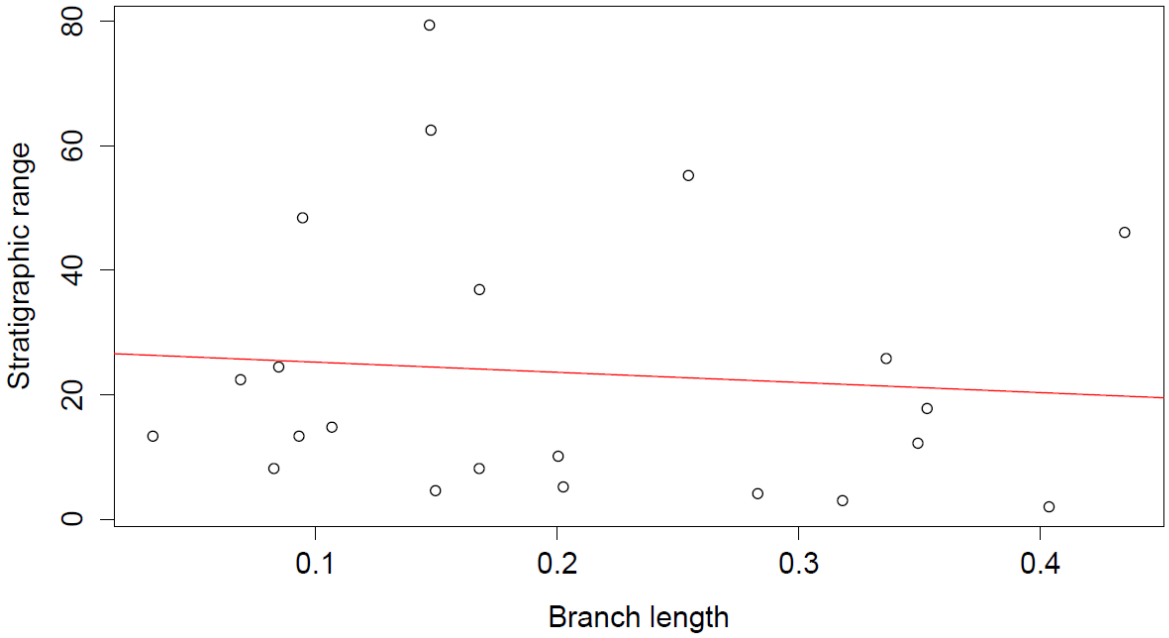


Figure 46. Relationship between branch lengths resulting from Bayesian phylogenetic analysis and total stratigraphic range implied from time-scaling analyses (see Figure 62) for all analysed OTUs. Pearson's p = 0.694, r = -0.089.

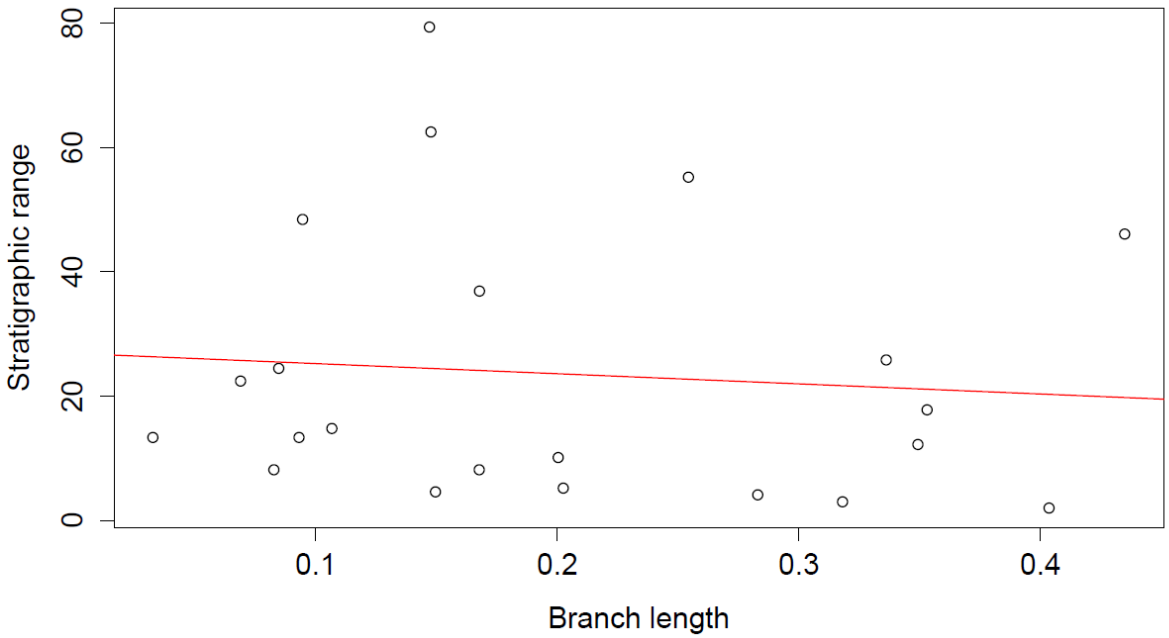


Figure 47. Relationship between branch lengths resulting from Bayesian phylogenetic analysis and total stratigraphic range implied from time-scaling analyses (see Figure 62) for all analysed OTUs excluding protosuchian and coelognathosuchian outgroups. Pearson's p = 0.834, r = -0.057.

5.2.4 Results summary

This suite of analyses demonstrates that Atoposauridae is a much more restricted clade than previously considered, comprising only *Alligatorellus bavaricus*, *Alligatorellus beaumonti*, *Atoposaurus jourdani*, *Atoposaurus oberndorferi*, and *Alligatorium meyeri*. However, this inclusion of *Alligatorium meyeri* is not supported by the Bayesian results. Based on this restricted taxonomic inclusion, Atoposauridae is recovered in a basal position within Neosuchia. *Theriosuchus* is consistently shown to be a polyphyletic taxon, comprising one set of species (*T. guimarotae* + (*T. pusillus* + *T. grandinaris*)) closely related to paralligatorids, and one clade (*T. ibericus* + *T. sympiestodon*) within Paralligatoridae. NMS G. 2014.52.1 (*Theriosuchus* sp.) is likely to be referable to the more basal group of *Theriosuchus* species. The position of MB.R.3632 (*Alligatorellus* sp.) cannot be conclusively determined, with an atoposaurid and a basal neosuchian placement supported in different analyses. *Montsecosuchus* is recovered outside of Atoposauridae in almost all of the analyses, and might be more closely related to *Pachycheilosuchus* and other hylaeochampsids, although the position of these

taxa cannot be conclusively determined. *Alligatorium franconicum* is shown to be a non-atoposaurid taxon that is more closely related to bernissartiids and coelognathosuchians. *Brillanceausuchus* occupies a position within Paralligatoridae. Below, revised diagnoses are provided for each of these taxa, along with a discussion of the character states that support the revised systematic positions for all atoposaurid and non-atoposaurid taxa which were analysed.

Table 78. All OTUs analysed in the present analysis, including data regarding their geographic range, temporal duration, source publications, and status following phylogenetic and systematic analysis.

Taxon	Age	Numerical age (Ma)	Distribution	Reference/source	Personally observed	This thesis	Parent taxon
Ingroups							
Alligatorium meyeri	Kimmeridgian	157.3-152.1	Cerin, France	Wellnhofer (1971)	Yes	*Alligatorium meyeri*	Atoposauridae
Alligatorium franconicum	Late Kimmeridgian	154.75-152.1	Kelheim, Germany	Wellnhofer (1971)	No	*"Alligatorium" franconicum*	Neosuchia
Atoposaurus jourdani	Kimmeridgian	157.3-152.1	Cerin, France	Wellnhofer (1971)	Yes	*Atoposaurus jourdani*	Atoposauridae
Atoposaurus oberndorferi	Early Tithonian	152.1-148.55	Kelheim, Germany	Wellnhofer (1971)	Yes	*Atoposaurus oberndorferi*	Atoposauridae
Alligatorellus bavaricus	Early Tithonian	152.1-148.55	Eichstätt, Germany	Wellnhofer (1971); Tennant & Mannion (2014)	Yes	*Alligatorellus bavaricus*	Atoposauridae
Alligatorellus beamonti	Kimmeridgian	157.3-152.1	Cerin, France	Wellnhofer (1971); Tennant & Mannion (2014)	Yes	*Alligatorellus beamonti*	Atoposauridae
Alligatorellus sp.	Early Tithonian	152.1-148.55	Kelheim, Germany	Schwarz-Wings *et al*. (2011)	Yes	*Alligatorellus* sp.	Atoposauridae
Montsecosuchus depereti	Late Berriasian–Early Valanginian	142.4-136.35	Montsec, Spain	Buscalioni & Sanz (1990a)	Yes	*Montsecosuchus depereti*	Neosuchia
Theriosuchus pusillus	Berriasian	145-139.8	Dorset, England	Owen (1879); Clark (1986)	Yes	*Theriosuchus pusillus*	Neosuchia
Theriosuchus guimarotae	Kimmeridgian	157.3-152.1	Guimarota, Portugal	Schwarz & Salisbury (2005)	No	*Theriosuchus guimarotae*	Neosuchia
Theriosuchus grandinaris	Early Aptian	125-118	Sakon Nakhon, Thailand	Lauprasert *et al*. (2011)	No	*Theriosuchus grandinaris*	Neosuchia
Theriosuchus ibericus	Barremian	129.4-125	Serrania de Cuenca, Spain	Brinkman (1989, 1992)	Yes	*Sabresuchus ibericus*	Paralligatoridae
Theriosuchus sympiestodon	Maastrichtian	72.1-66	Haţeg, Romania	Martin *et al*. (2010, 2014)	Yes	*Sabresuchus sympiestodon*	Paralligatoridae
Theriosuchus sp.	Late Bajocian–Bathonian	169.3-166.1	Isle of Skye, Scotland	Young *et al*. (in press)	No	*Theriosuchus* sp.	Neosuchia
Brillanceausuchus babouriensis	Barremian	145-139.8	Babouri-Figuil, Cameroon	Michard *et al*. (1990)	Yes	*Brillanceausuchus babouriensis*	Paralligatoridae
Outgroups							
Pachycheilosuchus trinquei	Early Albian	113-106.75	Texas, USA	Rogers (2003)	Yes	*Pachycheilosuchus trinquei*	Hylaeochampsidae
Wannchampsus kirpachi	Aptian	125-114	Texas, USA	Adams (2014)	Yes	*Wannchampsus kirpachi*	Paralligatoridae
Karatausuchus sharovi	Oxfordian	163.5-157.3	Karatau, Kazakhstan	Storrs & Efimov (2000)	No	*Karatausuchus sharovi*	Neosuchia
Hoplosuchus kayi	Early Tithonian	152.1-148.55	Utah, USA	Gilmore (1926)	Yes	*Hoplosuchus kayi*	Protosuchia
Koumpiodontosuchus aprosdokiti	Barremian	129.4-125	Isle of Wight, England	Sweetman *et al*. (2015)	No	*Koumpiodontosuchus aprosdokiti*	Bernissartiidae
Eutretauronosuchus delfsi	Kimmeridgian–Early Tithonian	157.3-148.55	Colorado and Wyoming, USA	Smith and Pritchard (2010)	No	*Eutretauronosuchus delfsi*	Goniopholididae
Amphicotylus lucasii	Kimmeridgian	157.3-152.1	Colorado, USA	Mook (1942)	Yes	*Amphicotylus lucasii*	Goniopholididae
Protosuchus richardsoni	Hettangian	201.3-199.3	Arizona, USA	Colbert & Mook (1952)	Yes	*Protosuchus richardsoni*	Protosuchia
Pholidosaurus purbeckensis	Berriasian	145-139.8	Swanage, England	Salisbury (2002)	No	*Pholidosaurus purbeckensis*	Pholidosauridae
Shamosuchus djadochtaensis	Late Campanian	77.85-72.1	Omnogov, Mongolia	Pol *et al*. (2009)	No	*Shamosuchus djadochtaensis*	Paralligatoridae

5.3 Systematic Palaeontology

Crocodylomorpha (Walker, 1970)

Crocodyliformes (Hay, 1930)

Neosuchia (Benton and Clark, 1988)

Atoposauridae (Gervais, 1871)

Previous diagnoses and comments: Atoposauridae was originally named as 'Atoposauridés' (Gervais, 1871). Since its genesis, there have been few attempts at providing a group diagnosis based on morphology and, to my knowledge, no phylogenetic definition has ever been proposed.

The first morphological definition for Atoposauridae was not proposed until the middle of the 20th Century (Romer, 1956): (1) small, with a broad head and short, pointed snout; (2) external nares sometimes divided; (3) postorbital bar moderately inwardly displaced; (4) large orbits and small supratemporal fenestrae; (5) two rows of flattened dorsal osteoderms; (6) long and slender limbs; and (7) platycoelous vertebrae. However, this assessment was based exclusively on taxa known at the time from the Late Jurassic, comprising *Atoposaurus*, *Alligatorellus* and *Alligatorium*, as well as *Hoplosuchus*. Subsequent researchers largely followed this diagnosis (Kuhn, 1960), but omitted several characteristics, whereas others subsequently re-incorporated them (Steel, 1973), and noted that there were at least some cases of atoposaurids with procoelous vertebrae, presumably referring to their inferred presence in *Theriosuchus pusillus* (Joffe, 1967). Although some of these characteristics, such as the relative sizes of the orbit and supratemporal fenestra, are known to occur in juvenile crocodyliform specimens (Joffe, 1967; Schwarz and Salisbury, 2005), it is noteworthy that even specimens of adult atoposaurids possess this feature. Therefore, this condition indicates that atoposaurids might consistently retain paedomorphic characteristics into adulthood, a factor that has likely contributed to difficulties in resolving their phylogenetic affinities.

The first phylogenetic analysis of atoposaurids presented several hypotheses of their inter-relationships by treating cranial, postcranial and metric characters independently (Buscalioni and Sanz, 1988). They regarded several taxa as *nomina dubia*, including '*Alligatorium*' *franconicum* and '*Alligatorium paintenense*' and/or as non-atoposaurids, including *Karatausuchus*, *Shantungosuchus*, and *Hoplosuchus*, but without explicit statements regarding their morphology to support these taxonomic opinions. The conclusion was that Atoposauridae could be diagnosed based on: (1) enlarged anterior maxillary teeth; (2) loss of the external mandibular fenestra; (3) reduction or loss of the antorbital fenestra; (4) squamosals not ventrally depressed; and (5) lack of dental hypertrophy (Buscalioni and Sanz, 1988). These authors also considered the possession of five premaxillary teeth and between 12–18 maxillary teeth as additional ambiguous synapomorphies for Atoposauridae, as these characteristics are not visible in either *Atoposaurus* or *Alligatorium*. However, almost all of these characteristics are more widespread in Neosuchia, or variably present within *Theriosuchus* and other putative atoposaurids. Furthermore, their recovery as atoposaurid synapomorphies might largely have been a product of limited sampling of outgroups, and as such it remains unclear which morphological characteristics help to diagnose Atoposauridae and any included taxa.

The most recent diagnosis for Atoposauridae was conducted based on the discovery of a new species, *Theriosuchus sympiestodon* (Martin *et al.*, 2010), based largely upon a previously published data matrix (Pol *et al.*, 2009), which focussed on early eusuchian relationships and their morphological transformation from Neosuchia. This revised diagnosis of Atoposauridae consisted of the following synapomorphies: (1) external nares facing dorsally and not separated by a premaxillary bar from anterior edge of rostrum; (2) antorbital fenestra much smaller than the orbit; (3) five premaxillary teeth; (4) basioccipital and ventral part of otoccipital facing posteriorly; (5) unsculpted region in the dentary below the tooth row absent; and (6) lateral surface of dentaries below alveolar margins at middle to posterior region of tooth row vertically oriented, continuous with rest of lateral surface of

dentaries (Martin *et al.*, 2010). However, this diagnosis was based only on information provided by three species of *Theriosuchus* and *Alligatorium*.

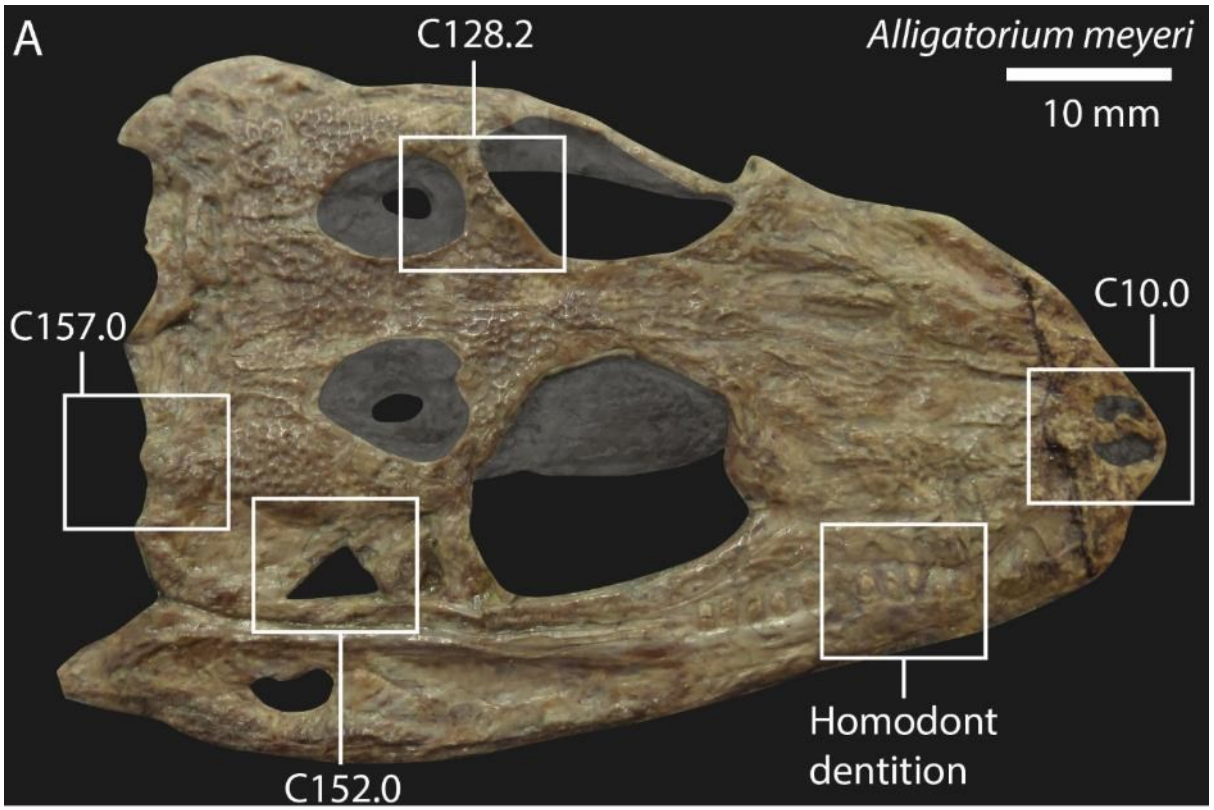
All of these aforementioned putative synapomorphies are included as characters in the new data matrix and below a revised diagnosis is presented for Atoposauridae, as well as a definition of the group as a phylogenetic clade for the first time. Numbers in parentheses refer to characters and states (e.g. C159.1 means character 159, state 1).

Phylogenetic definition: Atoposauridae is a stem-based clade comprising all taxa more closely related to *Atoposaurus jourdani* (Meyer, 1850) than to *Crocodylus* (Laurenti, 1768).

Included taxa: *Alligatorium meyeri* (Vidal, 1915), *Alligatorellus beaumonti* (Gervais, 1871), *Alligatorellus bavaricus* (Wellnhofer, 1971), *Atoposaurus jourdani* (Meyer, 1850), *Atoposaurus oberndorferi* (Meyer, 1850).

Distribution: Late Jurassic of France and Germany.

Revised diagnosis and discussion: Many of the synapomorphies below represent the quantification and demarcation of state boundaries from previously proposed characters. They also diagnose a more exclusive set of taxa, as features shared between *Theriosuchus* and definitive atoposaurids are no longer considered to be diagnostic for a united clade. Measurements and ratios pertaining to synapomorphies for taxa are provided in Table 16, Table 18, Table 19 and Table 20, respectively. Atoposauridae can be diagnosed based on the following unique combination of character states (synapomorphies, S) (Figure 48,Figure 50Figure 50).


A
C128.2
Alligatorium meyeri
10 mm
C157.0
C10.0
Homodont
dentition
C152.0

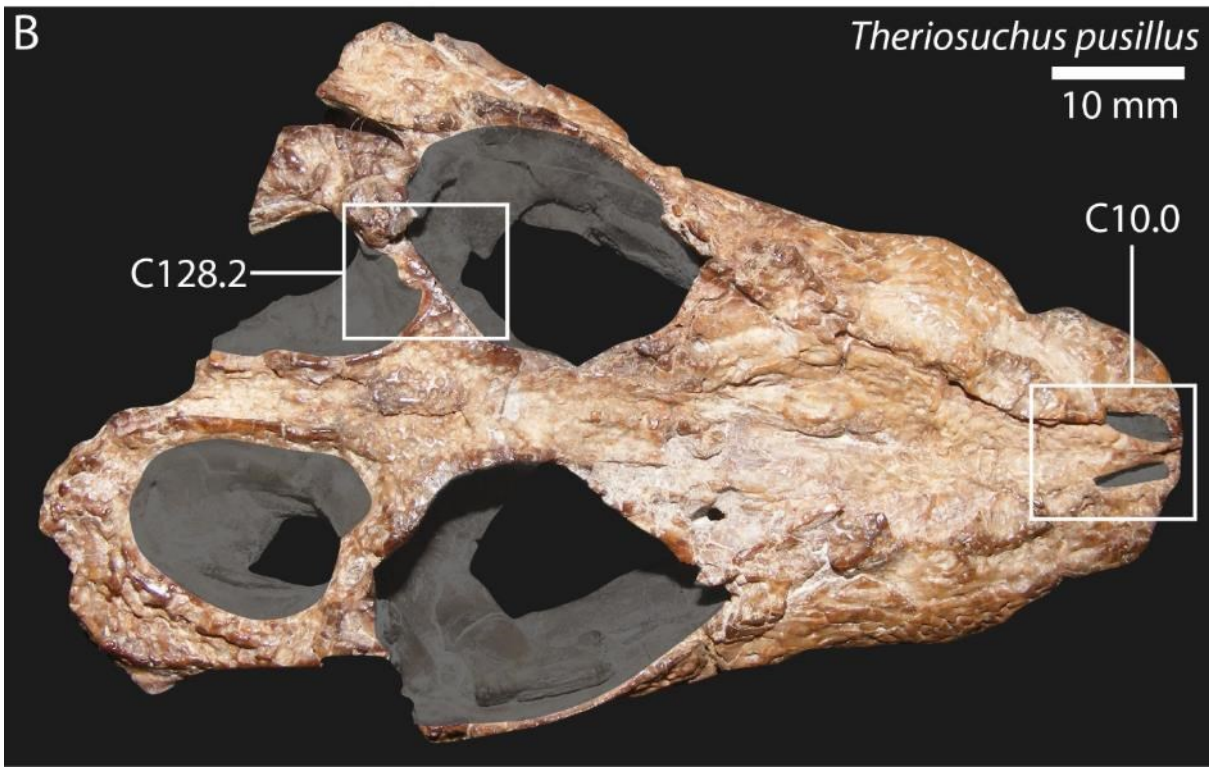

B
Theriosuchus pusillus
10 mm
C10.0
C128.2

Figure 48. A. Skull of the holotype of *Alligatorium meyeri* (MNHL 15646) in dorsal view. Synapomorphies for Atoposauridae are indicated (see text for details) B. Skull of the paratype of *Theriosuchus pusillus* (NHMUK PV R48330) in dorsal view. Shared characteristics with atoposaurids are indicated (see text for details).

(S1) Complete division of the external nares dorsally by anterior projection of the nasals (C10.0). This feature is only known for Atoposauridae (Figure 48, Figure 50), *Theriosuchus guimarotae* and *T. pusillus* (Figure 48B). In '*Alligatorium*' *franconicum*, the external nares are completely opened and undivided, based on the only known reconstruction of this taxon (Wellnhofer, 1971), and similar to *Theriosuchus grandinaris* (Lauprasert *et al.*, 2011), *Amphicotylus* (Mook, 1942), *Brillanceausuchus*, and some notosuchians, including the baurusuchid *Campinasuchus dinizi* (Carvalho *et al.*, 2011). This division of the external nares by the anterior-most extent of the nasals was thought previously to be diagnostic for *Theriosuchus* (Salisbury and Naish, 2011), but it was more likely independently acquired in this genus and atoposaurids. Some other species, such as the notosuchian *Araripesuchus*, also share this division, but the external nares are more anteriorly placed and face anteriorly (Buffetaut, 1981a).

(S2) Skull anteroposterior length to orbit length ratio less than 4.0 (C27.0-1). This synapomorphy is also shared by other neosuchian taxa, including *Theriosuchus pusillus*, *Wannchampsus* (Adams, 2014), the 'protosuchian' *Hoplosuchus* (Gilmore, 1926), and possibly *Karatausuchus* (Efimov, 1976). *Atoposaurus* displays an extreme version of this morphology, possessing a relatively longer orbit, giving a ratio of less than 3.0 for both species. *Montsecosuchus* falls just outside of this range, with a ratio of 4.05. Although the latter value is similar in orbital dimensions to atoposaurids, the state boundaries for this character were set at regular intervals, as opposed to selecting them towards creating inclusive groupings *a priori*, and therefore *Montsecosuchus* is distinct from atoposaurids in this respect. Longirostrine taxa, as expected, have a much higher ratio, with *Amphicotylus* possessing an extreme of this with a value of 10.0. *Shamosuchus* and *Brillanceausuchus*, although brevirostrine, have intermediate ratio values (6.1 and 6.8, respectively), reflecting the smaller dimensions of the orbits.

(S3) Skull mediolateral width to orbit width ratio of less than 2.5 (C28.0). Among atoposaurids, only *Atoposaurus jourdani* differs in having a smaller orbital width, giving a ratio of 2.69. '*Alligatorium*' *franconicum* is also just outside this state boundary with a value of 2.53. This ratio is unknown for most specimens attributed to *Theriosuchus*, but the ratios are 3.0 and 3.46 for *T. guimarotae* and *T. pusillus*, respectively. *Montsecosuchus* falls between these two species, with a ratio of 3.19. The relatively large size of the orbits in atoposaurids, as quantified here, might relate to retention of the paedomorphic state, as it appears to also be possessed by mature representatives of species (e.g., *Theriosuchus*).

(S4) Skull mediolateral width to external supratemporal fenestra width between 3.0 and 5.0 (C30.1). This feature, similar to the proportionally large orbits, also possibly relates to the relatively small body sizes of these taxa. This state is unknown in *Atoposaurus* because it is not possible to assess the morphology of the supratemporal fenestrae due to their preservation. Both *Theriosuchus guimarotae* and *T. pusillus* share this character state with atoposaurids, with ratios of 4.64 and 4.8, respectively. The only taxon in the data matrix that has a proportionally larger supratemporal fenestra is *Pholidosaurus* (Salisbury, 2002), which has a ratio of 2.81. Both '*Alligatorium*' *franconicum* and *Montsecosuchus* have proportionally smaller supratemporal fenestrae, with ratio values of 5.15 and 5.21, respectively.

(S5) Dorsal surface of the premaxilla internarial bar projects anteriorly to main body of premaxilla (C35.1). This feature is diagnostic for atoposaurids, and possibly only shared outside with '*Alligatorium*' *franconicum* (Wellnhofer, 1971). In all other sampled taxa, the internarial bar of the premaxilla does not project anteriorly to the main body of the premaxilla and the external nares. This morphology is also different to that seen in goniopholidids, in which there is a distinct mediolateral constriction and an anteriorly spatulate morphology.

(S6) Ventral depression on dorsal margin of postorbital, sometimes developing into a shallow sulcus (C128.2). Previously, the inwardly displaced (ventrally depressed) postorbital bar between the supratemporal fenestra has been considered to be diagnostic for *Theriosuchus* (Wu *et al.*, 1996b), but this appears to be absent in *T. pusillus* and its presence is questionable in *T. guimarotae*. It is clearly present in *Alligatorellus* (Figure 50, Figure 51, Figure 52, Figure 53, Figure 54, Figure 55), and perhaps *Alligatorium meyeri* too, and therefore it is considered here to be diagnostic for Atoposauridae. However, this feature might have also been acquired by the 'Glen Rose Form' ((Turner, 2015), a specimen that is probably referable to *Wannchampsus* (Adams, 2014), and is similar to the condition observed in more basal crocodyliforms, including the shartgeosuchid *Fruitachampsa callisoni* (Clark, 2011), in which the postorbital bar is relatively poorly developed. *Paralligator gradilifrons* (Turner, 2015) also possesses this supratemporal-orbital groove, but the postorbital bar is well-developed and robust, distinct from *Alligatorellus*.

(S7) Quadratojugal contributes extensively to the ventral and posterior margins of the lateral temporal (infratemporal) fenestra (C152.0). This feature is present in all atoposaurids (Figs. 8, 9A), but cannot be assessed in *Atoposaurus* due to the preservation of the skull. It is also shared by *Theriosuchus pusillus*. In some crocodyliforms, including goniopholidids, *Protosuchus*, and *Theriosuchus guimarotae* (Schwarz and Salisbury, 2005), the quadratojugal only contributes to the posterior margin. In *Montsecosuchus*, *Brillanceausuchus*, *Araripesuchus patagonicus* (Ortega *et al.*, 2000), *Allodaposuchus precedens* (Delfino *et al.*, 2008a), and eusuchians including *Wannchampsus* (Adams, 2014), *Acynodon iberoccitanus* (Martin, 2007), and *Shamosuchus* (Pol *et al.*, 2009), the quadratojugal participates extensively in the dorsal and posterior margins of the lateral temporal fenestra.

(**S8) Otic aperture between squamosal and quadrate posteriorly open, not closed by the quadrate and otoccipital (C157.0).** This character state appears to be shared by *Alligatorium* and *Alligatorellus*, but cannot be assessed for *Atoposaurus* due to the preservation of the skull. It is also shared with

several other neosuchian taxa, including *Goniopholis simus* (Salisbury *et al.*, 2006), *Pholidosaurus* (Salisbury, 2002), *Amphicotylus* (Mook, 1942), *Allodaposuchus precedens* (Delfino *et al.*, 2008a), and *Shamosuchus* (Turner, 2015) although this aperture appears to be closed in *Shamosuchus djadochtaensis* (Pol *et al.*, 2009). In these taxa, the cranioquadrate passage lacks a lateral wall, forming a sulcus or *canalis quadratosquamosoexoccipitalis* (Salisbury *et al.*, 1999). This feature is distinct from most mesoeucrocodylians, including *Susisuchus* and *Isisfordia*, as well as modern crocodylians, in which there is a sharp posterior rim and the passage is enclosed by the otoccipital and quadrate (Salisbury *et al.*, 2006; Pol *et al.*, 2009).

(S9) Homodont pseudocaniniform dentition (combination of C253.1, C254.1, C255.0 and C258.0). Although difficult to evaluate due to the dorsal flattening of specimens, this type of dentition appears to be present for all specimens of *Alligatorellus* in which teeth are visible (Figure 50), *Alligatorium meyeri* (Figure 48), and synapomorphic among all putative atoposaurids (although see below). All species of *Theriosuchus* are clearly distinct from *Alligatorellus*, with their characteristic combinations of heterodont morphologies. The teeth of *Atoposaurus* are poorly known due to preservation, although several damaged teeth preserved in the type specimen of *Atoposaurus oberndorferi* also appear to be pseudocaniniform. In *Alligatorium meyeri*, the tooth row is exposed in lateral view, but only one or two of these appear to actually be from the maxillary arcade, with the rest from the dentary, against which the maxilla is apressed. All of these exposed teeth appear to be pseudocaniniform in morphology, and of a similar conical shape to *Alligatorellus*. Therefore, here this feature is tentatively regarded as being diagnostic for Atoposauridae, pending the further discovery and analysis of teeth in atoposaurids.

Below, revised diagnoses and discussions for all definitive atoposaurid taxa are presented, and those previously regarded as putative atoposaurids. These are based on the character state distributions from the results of the parsimony-based phylogenetic analyses, and supplemented with details from

original descriptions and personal observations where possible. Autapomorphies in the diagnoses are highlighted with an asterisk (S*).

5.4 Definitive atoposaurid taxa

5.4.1 Alligatorium Jourdan 1862

Included species: *Alligatorium meyeri* (type species)

Previous diagnoses and comments: *Alligatorium* was erected based on an incomplete skeleton from the lithographic limestones of Cerin, France (Jourdan, 1862), and described and figured in a subsequent publication (Lortet, 1892). This genus has also been reported from the Upper Jurassic of Bavaria, Germany (von Zittel, 1890; Kuhn, 1961), and identified as *Alligatorium franconicum* and *Alligatorium paintenense* (all specimens of both lost or destroyed during World War II (Wellnhofer, 1971)), but here the latter species is considered to be a junior synonym of the former (Tennant and Mannion, 2014), and regard '*Alligatorium*' *franconicum* as representing a non-atoposaurid taxon (see below). A further specimen from the Early Cretaceous of Spain was described as *Alligatorium depereti* (Vidal, 1915), and later recombined as *Montsecosuchus depereti* (Buscalioni and Sanz, 1988; Buscalioni and Sanz, 1990b).

Revised diagnosis: as for the type and only species

Distribution: Late Jurassic of southern France.

5.4.1.1 *Alligatorium meyeri* (Jourdan, 1862) (type species)

Type locality and horizon: Unknown bed, Kimmeridgian (Late Jurassic); Cerin, Ain, France.

Type specimen: MNHL 15646, partial skeleton and skull, with counterpart slab MNHL 15462.

Previous diagnoses and comments: Previous authors have considered *Alligatorium meyeri* to be an immature specimen (Joffe, 1967) based on: (1) the visibility of cranial sutures; (2) the lack of thickening of the cranial table; (3) the slight skull ossification; and (4) the internal supratemporal fenestrae being small and anteroposteriorly slit-like, in contrast to the relatively large orbits. However, others have considered *Alligatorium* to represent the most mature specimen of a lineage in which *Atoposaurus* and *Alligatorellus* represented younger growth stages (Clark, 1986; Benton and Clark, 1988). The most recent analysis of these taxa was unable to confirm this ontogenetic sequence based on the few specimens available for allometric analysis (Tennant and Mannion, 2014), and instead noted several morphological distinctions between the three putative genera. The phylogenetic results presented here are distinct from those which investigated Atoposauridae within a broad Crocodylomorpha framework (Clark, 1986; Benton and Clark, 1988), as well as those which investigate the relationships within Atoposauridae in more detail (Buscalioni and Sanz, 1988; Buscalioni and Sanz, 1990b; Karl *et al.*, 2006), with these latter studies instead finding a sister relationship between *Alligatorium* and *Theriosuchus*. This discrepancy in the results is likely due to increased sampling of paralligatorids, and generally broader sampling of basal neosuchian taxa. In addition, the analysis presented here is the first to treat individual species as distinct OTUs, which helps to clarify character distributions, as well as whether or not previously assigned genera form truly monophyletic groupings. *Alligatorium meyeri* is recovered at the base of Atoposauridae. However, it should be noted that the Bayesian analysis did not recover *Alligatorium meyeri* within a monophyletic Atoposauridae, and its position was unable to be resolved more precisely using this analytical approach.

Revised diagnosis and discussion: **(S1) Paired and unfused nasals (C65.0).** The presence of 'paired' nasal bones has been widely used in diagnoses of atoposaurids, and noted in other mesoeucrocodylians, including the notosuchian *Simosuchus* (Buckley *et al.*, 2000) and the neosuchian *Paluxysuchus* (Adams, 2013). However, it is not entirely clear what this means, as the nasal bones are always paired. Therefore, this character is considered to refer to whether or not the paired nasals are

fused, and as such constitute a 'single' element, or are unfused. In *Alligatorium meyeri*, the nasals are fused along the midline, similar to *Wannchampsus*, *Theriosuchus guimarotae*, *T. grandinaris* and *T. pusillus*. In *Alligatorellus*, the nasals are only weakly fused or contact one another along the midline, comparable to goniopholidids, *Montsecosuchus* and *Shamosuchus* (Pol *et al.*, 2009).

(S2) Lateral edges of the nasals sub-parallel to one another (C67.0). This morphology occurs anterior to the nasal contact with the periorbital elements, and is similar to *Montsecosuchus*, *Brillanceausuchus*, *Allodaposuchus precedens* (Delfino *et al.*, 2008a), and possibly *Araripesuchus patagonicus* (Ortega *et al.*, 2000). *Alligatorellus* is distinct among atoposaurids in that the edges are oblique to one another and converge anteriorly (Tennant and Mannion, 2014), similar to *Bernissartia* (Buscalioni and Sanz, 1984; Norell and Clark, 1990). They are laterally flared posteriorly in *Theriosuchus pusillus*.

(S3) Jugal and lacrimal with confluent anterior margins (C78.0). The jugal and lacrimal have confluent anterior contacts, instead of a discrete convexity in which a notch develops and is filled by the maxilla. This morphology is also seen in '*Theriosuchus*' *sympiestodon* (Martin *et al.*, 2010; Martin *et al.*, 2014c), as well as *Protosuchus* (Colbert *et al.*, 1951), *Amphicotylus* (Mook, 1942), and *Pholidosaurus* (Salisbury, 2002).

(S4) Frontal with single longitudinal ridge along midline suture (C100.1). The presence of a midline ridge on the frontal suture has often been considered diagnostic for *Theriosuchus* (Schwarz and Salisbury, 2005; Salisbury and Naish, 2011), being present on all specimens attributed to *Theriosuchus* in which the interorbital region is preserved. However, this ridge is also present in *Shamosuchus djadochtaensis* (Pol *et al.*, 2009) and *Wannchampsus* (Adams, 2014). It is likely that the presence of this character is related to ontogeny because in *Theriosuchus guimarotae* this frontal ridge is only developed in more mature individuals (Schwarz and Salisbury, 2005). *Alligatorellus* and *Atoposaurus* do not show any evidence of this ridge, despite appearing to have completely fused frontals.

(S5) Anterior portion of frontal mediolaterally constricted, with convergent lateral margins (C109.1). This feature is tentatively considered to be diagnostic for *Alligatorium meyeri*, although it might also be present in '*Alligatorium*' *franconicum* (Wellnhofer, 1971), *Theriosuchus guimarotae* (Schwarz and Salisbury, 2005), and *Amphicotylus* (Mook, 1942). This morphology is distinct from notosuchians in which the frontal is slightly mediolaterally constricted, but remains broad between the prefrontals (Gomani, 1997; Buckley *et al.*, 2000), the goniopholidid *Calsoyasuchus* in which the frontal-nasal suture forms a 'valley' on the dorsal surface (Tykoski *et al.*, 2002), the neosuchian *Khoratosuchus* with a non-constricted and bifurcated frontal anterior process (Lauprasert *et al.*, 2009), and eusuchians such as *Aegisuchus* in which the frontals are constant in width anterior to the orbits (Holliday and Gardner, 2012).

(S6) Supratemporal rims developed along entire medial margin (C119.2). *Alligatorium meyeri* possesses well-developed supratemporal rims along the entire medial border of each external fenestra, similar to *Wannchampsus* and *Theriosuchus pusillus*, *T. guimarotae*, '*T.*' *ibericus* and '*T.*' *sympiestodon*. This morphology is distinct from that in *Alligatorellus beaumonti* and *Brillanceausuchus*, in which this ridge is only developed posteriorly, and from that in *Alligatorellus bavaricus* and *Montsecosuchus* in which the medial edges are flat (Tennant and Mannion, 2014). *Pachycheilosuchus*, coelognathosuchians, and *Shamosuchus* (Pol *et al.*, 2009) do not appear to possess supratemporal rims.

(S7) Dorsal margin groove for dorsal ear lid with a medial curvature (C137.1). This character state appears to be unique for *Alligatorium meyeri* within atoposaurids, but is also present in more advanced neosuchians, including '*Theriosuchus*' *ibericus*, *Wannchampsus*, and *Brillanceausuchus*. In other atoposaurids, this margin, comprising the lateral edge of the postorbital and squamosal, is straight, similar to *Theriosuchus guimarotae* (Schwarz and Salisbury, 2005) and *T. pusillus*.

(S8) External mandibular fenestra present (C207.1) and oval-shaped with anteroposteriorly-oriented long axis (C210.0). The presence of an external mandibular fenestra is also shared with *Theriosuchus guimarotae* (Schwarz and Salisbury, 2005) amongst those taxa included in the analysis as putative atoposaurids, but also represents the plesiomorphic crocodyliform condition, being present in goniopholidids (Halliday *et al.*, 2015), *Protosuchus* (Colbert *et al.*, 1951), as well as in notosuchians such as *Baurusuchus* (Nascimento and Zaher, 2011) and *Labidiosuchus* (Kellner *et al.*, 2011), in which the opening is enlarged. This fenestra is lost in some advanced neosuchians, including paralligatorids (Montefeltro *et al.*, 2013), but is present in most eusuchians and Crocodylia (Brochu, 2004; Salisbury *et al.*, 2006; Pol *et al.*, 2009), although in some cases it is strongly reduced (Brochu *et al.*, 2012).

(S9*) Individual dorsal and caudal osteoderms with unsculpted edges (C304.1), square-shaped (C308.3), and lacking a dorsal keel anteriorly (C311.0) and posteriorly (C312.0). The individual osteoderms preserved in *Alligatorium meyeri* have unsculpted edges on all but the nuchalmost elements, a feature that cannot be due to preservation as the cranial table remains sculpted, and the centre of each osteoderm remains relatively lightly sculpted. Although this feature might be present in '*Alligatorium*' *franconicum* based on the only published figures of this taxon (Wellnhofer, 1971), this cannot be assessed this first-hand. Furthermore, *Hoplosuchus* (Gilmore, 1926) also possesses unsculpted osteoderms, although it is likely that this species represents a protosuchian-grade taxon. Therefore, this feature is considered to be autapomorphic for *Alligatorium meyeri*, pending future discoveries of '*Alligatorium*' *franconicum*. The dorsal osteoderms of *Alligatorium meyeri* are also square-shaped in dorsal view, a feature shared with *Theriosuchus pusillus*, *Pachycheilosuchus* (Rogers, 2003), and some of the osteoderms of *Protosuchus* (Colbert *et al.*, 1951). The overall morphology of the osteoderm shield closely resembles that of the neosuchian *Araripesuchus patagonicus* (Ortega *et al.*, 2000). In addition, the osteoderms of *Alligatorium meyeri* lack any presence of a dorsal keel, a

feature shared with a range of neosuchian taxa, but that is distinct from *Alligatorellus*, in which the presence and morphology of this keel varies longitudinally axially (Tennant and Mannion, 2014).

5.4.2 Unnamed clade: Atoposaurus + Alligatorellus

Alligatorellus is united with *Atoposaurus* within all of the analyses (Figure 42, Figure 43, Figure 44, Figure 45). This is based on a range of character states, including: (1) a slit-like (i.e., mediolaterally narrow and anteroposteriorly elongated) external supratemporal fenestra (not visible in *Atoposaurus oberndorferi* due to preservation) (C17.2); (2) smooth lateral surface of anterior jugal process near maxillary contact, not stippled or striated (C51; note that this was not coded this as a separate character state due to potential duplication, as in *Atoposaurus*, the entire external surface of the skull is smooth and unsculpted); (3) straight ventral edge of maxilla in lateral view (C52.0), similar to protosuchians (not sinusoidal or convex as in other neosuchians); (4) minimum mediolateral width between supratemporal fenestrae more than one third of total width of cranial table (C126.1), acquired in parallel with *Montsecosuchus*, *Brillanceausuchus*, *Theriosuchus pusillus*, and '*T.*' *sympiestodon*; and (5) postorbital bar between orbit and supratemporal fenestra very narrow (with respect to lateral edge of postorbital lateral to supratemporal fenestra) and unsculpted, with superficial furrow on dorsal surface of postorbital connecting anterior edge of supratemporal fenestra to the posterior edge of and orbital (C128.2).

5.4.3 Atoposaurus von Meyer 1850

Included species: *A. jourdani* (type species, based on it being named first in the paper identifying both species (Meyer, 1850)) and *A. oberndorferi*

Distribution: Late Jurassic of southern France and southeast Germany.

Previous diagnoses and comments: Both species of *Atoposaurus* were named in a single publication (Meyer, 1850), with *A. jourdani* receiving a full description subsequently by the same author (Meyer, 1851). However, the first study to present a diagnosis for *Atoposaurus* based on the specimens from France and Germany was not until over a century later (Wellnhofer, 1971). In this analysis, the lack of dermal armour was noted, and subsequently identified as a feature that could be related to either ontogeny or taphonomy (Schwarz and Salisbury, 2005). Subsequently, *Atoposaurus* and its constituent species have largely been considered to be *nomina dubia*, and often regarded as juvenile representatives of *Alligatorellus* and/or *Alligatorium* (Clark, 1986; Buscalioni and Sanz, 1988). Furthermore, one view is that *Alligatorellus*, *Alligatorium* and *Atoposaurus* are all the same taxon represented by different growth stages (Clark, 1986; Benton and Clark, 1988). If this were the case, then *Atoposaurus* (Meyer, 1850) would retain priority, and *Alligatorium* (Jourdan, 1862), along with *Alligatorellus* (Gervais, 1871), would be synonymised with *Atoposaurus*. Almost all subsequent phylogenetic analyses have included just *Alligatorium* based on this conclusion, without consideration of the other taxa. The present analysis is the first to consider both potential species of *Atoposaurus* as independent OTUs, and finds them to be sister taxa in all cases (Figure 42, Figure 43, Figure 44, Figure 45), thus supporting their generic assignment.

Despite noting the same features in *Alligatorellus*, several authors have stated that the presence of large orbits, a closed internal supratemporal fenestra, and a divided external nares were all features defining *Atoposaurus* (Wellnhofer, 1971; Steel, 1973). The presence of an inwardly displaced postorbital bar (Steel, 1973) is not clear due to the preservation of available specimens of *Atoposaurus oberndorferi*, but does appear to be a feature of *Atoposaurus jourdani*. Four of the five synapomorphies identified for *Atoposaurus* (S1-3, S5) are contentious as they could be indicative of a juvenile phase of growth (Joffe, 1967), but equally probably they could represent the retention of juvenile characteristics through paedomorphism related to the relatively small body size of

Atoposaurus. Unfortunately, based on currently available specimens, it is impossible to distinguish between these two hypotheses (Tennant and Mannion, 2014).

Revised diagnosis and discussion: (S1) Dorsal cranial bones comprising the skull roof unsculpted (C1.0). This lack of dermal sculpting, combined with their overall diminutive size, indicates that *Atoposaurus* specimens might be represented by juveniles. However, it cannot be definitively confirmed that *Atoposaurus* is a juvenile representative of other contemporaneous atoposaurids based on allometric growth patterns alone (Tennant and Mannion, 2014), and it is likely that *Atoposaurus*, *Alligatorellus*, and *Alligatorium* represent three distinct genera, as the results indicate (Figure 42, Figure 43, Figure 44, Figure 45).

(S2) External surface of snout unsculpted (C3.0). This is considered here to be a distinct feature from S1, as in *Alligatorellus* there is a different pattern of sculpting between the cranial table and the rostrum. *Atoposaurus* is similar to *Alligatorellus* in this respect, completely lacking any evidence of cranial ornamentation, although this cannot be assessed properly in *Atoposaurus oberndorferi* due to the mode of preservation of the holotype specimen. As with S1, this character is likely to be highly influenced by either ontogeny or paedomorphism (Joffe, 1967).

(S3) Skull anteroposterior length to orbit length ratio less than 3.0 (C27.0). This feature is unique to *Atoposaurus*, and represents the characteristic proportionally large orbits and short snout of this taxon, noted to be indicative of a juvenile status (Joffe, 1967). Other atoposaurids have a ratio of between 3.0 and 4.0. *Karatausuchus* has a ratio of 3.36, slightly higher than *Alligatorellus bavaricus* (3.12), which approaches the state boundary for *Atoposaurus*, but it is likely that *Karatausuchus* represents a juvenile specimen of a (probably non-atoposaurid) crocodyliform (Storrs and Efimov, 2000) (see Section 5.6.8).

(S4) 50 or more caudal vertebrae (C276.1). Complete axial columns are rarely preserved in specimens previously assigned to Atoposauridae, and the proportional numbers of cervical, dorsal, sacral and

caudal vertebrae remain poorly known, especially for *Theriosuchus*. Both species of *Alligatorellus* preserve complete and articulated caudal vertebral series, and have 40 vertebrae each. *Montsecosuchus* appears to only have 21 caudal vertebrae, and *Pachycheilosuchus* has just 18 (Rogers, 2003). *Protosuchus richardsoni* has 39 caudal vertebrae, and *Karatausuchus* has 46 (Storrs and Efimov, 2000), approaching the number for *Atoposaurus*, but no other crocodyliform taxon has 50 vertebrae. The presence of 50 or more caudal vertebrae, in all specimens of *Atoposaurus* in which this feature can be measured, is not known in any other mesoeucrocodylian taxon, and cannot be explained by ontogeny (Tennant and Mannion, 2014); therefore, it is regarded here as a diagnostic feature for *Atoposaurus*, irrespective of the ontogenetic stage of the specimens, and therefore consider *Atoposaurus* to be a valid taxon.

(S5) Osteoderms absent. The lack of osteoderms is unlikely to be a taphonomic artefact (Schwarz-Wings *et al.*, 2011), and is either a feature associated with extreme dwarfism in *Atoposaurus*, or relates to their lack of development in juvenile individuals. The only other putative atoposaurid that is similar in this respect is *Karatausuchus*, which has been described as having reduced dermal ossicles (Storrs and Efimov, 2000).

5.4.3.1 *Atoposaurus jourdani* (Meyer, 1850) (type species)

Type locality and horizon: Unknown bed, Kimmeridgian (Late Jurassic); Cerin, Ain, France.

Type specimen: MHNL 15679, articulated partial skeleton comprising dorsally flattened skeleton and skull, missing the posteriormost caudal vertebrae, with distal hindlimbs and distal left forearm preserved as impressions.

Referred specimen: MHNL 15680 (same locality as type specimen), posterior half of articulated skeleton, including trunk vertebrae and forearms.

Previous diagnoses and comments: *Atoposaurus jourdani* was first identified more than a century ago (Meyer, 1850) and described in a second publication shortly thereafter (Meyer, 1851). Conversely to almost all previous examinations of this taxon, the analysis presented here shows that a unique combination of metric characters, almost exclusively regarding the relative proportions of the forelimb and hindlimb elements, can be used to distinguish *Atoposaurus jourdani* from *Atoposaurus oberndorferi*, along with a single autapomorphy.

Revised diagnosis and discussion: (S1) Skull mediolateral width to orbit width ratio of 1.80 (C28.0). This represents the lowest ratio for all atoposaurids, demonstrating that the orbits comprise almost the entire mediolateral width of the skull, separated by the narrow frontals. This is similar to *Alligatorellus bavaricus*, which also has enlarged orbits, but slightly mediolaterally wider frontals between the orbits (Tennant and Mannion, 2014).

(S2*) 6 cervical vertebrae (C266.0). This character state is unique among all putative atoposaurids, with all others possessing 7 cervical vertebrae. I was unable to determine this character state for any specimens assigned to *Theriosuchus* due to their preservation and/or incompleteness. This cervical count is distinct from *Protosuchus richardsoni* (9), *Hoplosuchus* (11), as well as *Karatausuchus* (8) (Storrs and Efimov, 2000) (Table 18).

(S3) Forelimb length to hindlimb length ratio of 0.63 (C285.0). This character state is similar to *Protosuchus richardsoni* (0.65) and *Montsecosuchus* (0.63). *Atoposaurus jourdani* is distinct in this respect from other atoposaurids, including *Alligatorellus beaumonti* which has a ratio of 0.81, and *Atoposaurus oberndorferi* which has a ratio of 0.78. *Alligatorellus bavaricus* has an intermediate ratio of 0.76 (Table 20).

(S4) Humerus length to femur length ratio of 0.67. This feature is similar to *Protosuchus richardsoni* (0.66) and *Montsecosuchus* (0.70). *Alligatorellus beaumonti* is similar, with a ratio of 0.75, but *Alligatorellus bavaricus* is quite distinct, with a ratio of 0.89, similar to *Atoposaurus oberndorferi* (0.89).

Karatausuchus also has similar limb proportions, with a ratio of 0.73. *Theriosuchus pusillus* falls within the range for atoposaurids, with a ratio of 0.76, but *T. guimarotae* is distinct with a ratio of 0.98, approaching that for *Pachycheilosuchus* (1.09) and *Brillanceausuchus* (1.11) (Table 20).

(S5) Radius to tibia length of 0.61 (C286.0). This character state is similar to *Protosuchus richardsoni* (0.63) and *Montsecosuchus* (0.64), along with *Pachycheilosuchus* (0.64). *Theriosuchus pusillus* has a proportionally long radius to tibia ratio (0.55), with this value only being exceeded by *Karatausuchus* (0.47). Based on Wellnhofer (1971), '*Alligatorium*' *franconicum* has the most extreme value, with a ratio of 0.89, reflecting a proportionally long radius. This value is similar to *Brillanceausuchus* (0.88). *Atoposaurus oberndorferi* and *Alligatorium meyeri* each have a ratio of 0.74, similar to *Shamosuchus* (0.72) and *Hoplosuchus* (0.76) (Table 20).

(S6) Metatarsals longitudinally grooved (C302.0). This feature also characterises *Alligatorellus beaumonti* and *Montsecosuchus* (Tennant and Mannion, 2014), in contrast to the smooth and flat metatarsals that characterise most other mesoeucrocodylians. However, caution is advised in interpretation of this feature, as there remains the possibility that it could represent post-mortem crushing of the delicate long bones in the tarsus.

5.4.3.2 *Atoposaurus oberndorferi* (Meyer, 1850)

Type locality and horizon: Solnhofen Formation, early Tithonian (Late Jurassic, *Hybonoticeras hybonotum* ammonoid zone); Kelheim, Eichstätt, Bavaria, Germany.

Type specimen: TM 3956, near-complete skeleton, missing only the dorsal part of the skull and posterior portion of the tail.

Referred specimen: BSPG 1901 I 12, a counterpart specimen of a different individual comprising the impression of the complete skull and skeleton in lateral view.

Previous diagnoses and comments: The first formal diagnosis for *Atoposaurus oberndorferi* was based primarily on several size-based characteristics (Wellnhofer, 1971), but these are unlikely to represent diagnostic morphological characters. He also noted the presence of 5 premaxillary and 8 maxillary teeth, but this could not be confirmed via observation of the type specimen due to the way in which it is preserved, and was not illustrated in the only published figure of the referred specimen (Wellnhofer, 1971). This first diagnosis was copied shortly after in a second review of crocodyliforms (Steel, 1973), which further suggested that the inwardly displaced postorbital bar was diagnostic of *Atoposaurus oberndorferi*; however, this feature is now recognised as characterising Atoposauridae (see above). Furthermore, because of the lateral compression of the type specimen, it was not possible to directly confirm the presence of this feature in *Atoposaurus oberndorferi*, and it is not figured in previous publications (Wellnhofer, 1971), and therefore cannot be supported. Here, a revised diagnosis is presented based on examination of the type specimen for *Atoposaurus oberndorferi*, and it is tentatively considered to be a valid taxon based on three ambiguous autapomorphies.

Revised diagnosis and discussion: **(S1) Skull anteroposterior length to width ratio ~2.00 (1.98) (C25.0).** This feature is tentatively considered to be diagnostic for *Atoposaurus oberndorferi*, as the skull is highly incomplete and preserved only in ventrolateral aspect. This estimated skull length to width ratio is high, similar to *Eutretauranosuchus* (1.97), *Montsecosuchus* (1.80), which is represented by a mature specimen (Buscalioni and Sanz, 1990b), and *Theriosuchus guimarotae* (1.82) (Schwarz and Salisbury, 2005). *Atoposaurus jourdani* has a much lower ratio (1.28), more similar to *Protosuchus* (1.31) and *Hoplosuchus* (1.35). The only taxa which have higher ratios are *Alligatorellus* (2.06-2.21), *Alligatorium meyeri* (2.26), '*Alligatorium*' *franconicum* (2.77) and K*oumpiodontosuchus* (2.04) (Table 20).

(S2) Skull anteroposterior length to orbit length ratio <3.00 (2.86) (C27.0). As with (S1), caution is urged in the interpretation of this character state based on the way in which the observed type specimen of *Atoposaurus oberndorferi* is preserved, exposing the enlarged orbit only in ventral aspect. The only taxon with a lower ratio is *Atoposaurus jourdani* (2.33), with *Alligatorellus* and *Alligatorium* possessing ratio values between 3.0 and 4.0. *Protosuchus* has a ratio of 4.52 (Table 20), an intermediate value between atoposaurids and higher neosuchians.

(S3) Inwardly (dorsally) displaced splenial on the ventral mandibular surface (C234.1). In all other taxa analysed in which the ventral surface of the mandible was exposed, the anterior portion of the splenial is confluent ventrally with the posterior cavity that is formed from the two posteriorly divergent mandibular rami. In *Atoposaurus oberndorferi*, the splenial is slightly inset at its contact with the dentary, a feature shared only with *Theriosuchus pusillus*. The ventral side of the skull and mandibular region is not preserved in *Atoposaurus jourdani*, and this character state might also be present in that taxon too. Therefore, caution is advised in the retention of *Atoposaurus oberndorferi* as a distinct, second species of *Atoposaurus*.

5.4.4 Alligatorellus Gervais 1871

Included species: *Alligatorellus beaumonti* (Gervais, 1871), *Alligatorellus bavaricus* (Wellnhofer, 1971; Tennant and Mannion, 2014).

Distribution: Late Jurassic of southern France and southeast Germany.

Previous diagnoses and comments: *Alligatorellus* was originally diagnosed based on its overall size, the shape of its skull, and its relatively large orbits (Wellnhofer, 1971), features which are all more widespread among atoposaurids and other small-bodied neosuchians. Originally two subspecies of *Alligatorellus beaumonti* were described (Wellnhofer, 1971), based on relative sizes and differences

and geographical distribution. Most recently, a revision of specimens assigned to *Alligatorellus* documented a number of distinguishing characters between *Alligatorellus beaumonti beaumonti* from France and *Alligatorellus beaumonti bavaricus* from Germany (Tennant and Mannion, 2014), and reranked the latter to its own species, *Alligatorellus bavaricus*. Several of the diagnostic synapomorphies for *Alligatorellus*, presented below, might be related to ontogenetic factors, such as the heterogeneity of the cranial sculpting and the closed internal supratemporal fenestra (Joffe, 1967). However, these features could also be related to the proposed 'dwarfism' for atoposaurids, and there are other indicators that the available specimens of *Alligatorellus* represent a reasonably mature state of growth, such as neurocentral fusion and the degree of fusion of the cranial bones (Joffe, 1967; Tennant and Mannion, 2014).



Figure 49. (a) Geographic distribution of Late Jurassic atoposaurid specimen localities. (b) Approximate palaeogeographic distribution of Late Jurassic atoposaurids. 1: Cerin; 2: Kelheim; 3: Painten; 4: Solnhofen; 5: Guimarota; 6: Andrès; 7: Langenberg; 8: Uppen. Note that those localities not mentioned in the text all include occurrences of indeterminate remains of Theriosuchus. Palaeomap reconstruction from Ron Blakey, Colorado Plateau Geosystems, Arizona USA (http://cpgeosystems.com/paleomaps.html).

More recently, a partial skeleton, MB.R.3632, from the early Tithonian of Franconia, Germany (*Gravesia gigas* ammonoid zone) has been identified as *Alligatorellus* sp. (Schwarz-Wings *et al.*, 2011), but a subsequent revision of *Alligatorellus* noted that this specimen could only be referred to as Atoposauridae indet. (Tennant and Mannion, 2014). In most of the analyses, this specimen is recovered as an indeterminate non-atoposaurid taxon (Figure 42, Figure 46). However, when implied weighting was used, this specimen groups with the other species of *Alligatorellus* within Atoposauridae (Figure 44). Therefore, retaining its status as *Alligatorellus* sp. as valid is very tentative, with the caveat that implied weighting might perform quite poorly for relatively small character sets (O'Reilly *et al.*, 2016), and pending future discoveries of related material.

Revised diagnosis and discussion: **(S1) Cranial table sculpting composed of homogeneous, sub-circular shallow pits (C2.2).** The cranial sculpting pattern for *Alligatorellus* is distinct from that of *Atoposaurus*, which has a smooth dorsal surface, and from *Alligatorium* and *Theriosuchus* in which the sculpting is much more prominent. It is similar to *Wannchampsus*, which is also lightly sculpted. The reduction or lack of sculpting has been noted in smaller specimens of the basal mesoeucrocodylian *Zosuchus* (Pol and Norell, 2004a), as well as the protosuchian *Gobiosuchus* (Osmólska *et al.*, 1997).

(S2) Rostrum unsculpted or relatively less than the cranial table (C3.1). Similar to (S1), the sculpting of the rostrum is relatively light compared to *Alligatorium meyeri*, *Theriosuchus pusillus*, and *Wannchampsus*. Distinct from these taxa, however, is how the degree of sculpting appears to decrease anteriorly for *Alligatorellus*, with a more prominent pattern on the cranial table, and almost no sculpting on the dorsal surface of the rostrum. This morphology is similar to that seen in the paratype of *Isisfordia*, which is represented by an adult specimen (Salisbury *et al.*, 2006), and *Pachycheilosuchus*, which is known from mature individuals (Rogers, 2003). In other taxa represented by mature specimens, such as *Theriosuchus pusillus* and *Rugosuchus* (Wu *et al.*, 2001a), sculpting patterns are homogeneous across the entire dorsal surface of the skull. *Alligatorium meyeri* is unusual

in that the degree of sculpting remains the same between the rostrum and cranial table, but anteriorly the sub-circular pits become more elongated, a feature visible in the counterpart to its holotype specimen (MNHL 15462), and which helps to distinguish it from *Alligatorellus*.

(S3) Closed internal supratemporal fenestra (C16.1). This feature refers to the lack of opening of the internal supratemporal fenestra, as noted previously (Wellnhofer, 1971). In all other specimens observed, the internal supratemporal fenestra is completely open. Others have described the opening as 'slit-like' for *Theriosuchus pusillus*, and regarded it as indicative of an immature individual (Joffe, 1967). However, personal observations of the paratype specimen (NHMUK PV OR48330) did not confirm this, and the internal fenestrae appear to be fully open. Because of poor preservation, I was unable to determine whether the morphology of the internal supratemporal fenestra was open or closed in any specimen of *Atoposaurus*.

(S4) Frontal maximal mediolateral width between the orbits narrower than maximal width of nasals (C97.1). This character state relates to the proportionally large size of the orbits, which occupy the majority of the mediolateral width of the dorsal surface of the skull, with a proportionally narrow interorbital region composed of the fused frontals. Although this feature is shared by many other neosuchians, including *Theriosuchus* and *Wannchampsus*, the frontals are distinctly narrower in *Alligatorellus*. In protosuchians, such as *Protosuchus* and *Hoplosuchus*, the mediolateral width of the frontal is broader than the nasal, because in these taxa the orbit is more laterally facing, and therefore does not occupy as much of the mediolateral width of the skull in dorsal view.

(S5) Broad frontal anterior process with parallel lateral margins, not constricted (C109.0). This feature is distinct from the morphology described in (S4), and relates exclusively to the development of the frontals anteriorly to the anterior margin of the orbits, excluding the morphology of any frontal anterior process where present. The broad anterior edge of the frontal with parallel lateral edges in *Alligatorellus* is similar to paralligatorids, *Theriosuchus pusillus*, and *Montsecosuchus*, but contrast

with *T. guimarotae* in which the mediolaterally constricted anterior portions of the frontals distinctly underlap the nasals (Schwarz and Salisbury, 2005).

(S6) Flat and unsculpted anterior supratemporal margins (C119.0). In *Alligatorellus bavaricus*, the supratemporal rims are flat and unsculpted along their entire medial edge, similar to protosuchians, *Pachycheilosuchus*, coelognathosuchians, *Montsecosuchus* and *Koumpiodontosuchus*. However, in *Alligatorellus beaumonti*, there is a slight posterior development of the supratemporal margins, similar to *Brillanceausuchus* (specimen UP BBR 203). This is distinct from *Alligatorium meyeri*, *Wannchampsus*, and all species referred to *Theriosuchus*, in which the supratemporal rims are consistently well-developed along their entire medial margin.

(S7*) Anterior process of squamosal extends to the posterior orbital margin (C144.0). This character state appears to be diagnostic for *Alligatorellus*, although caution should be taken with this assignment, as the postorbital region is poorly preserved, and the exact morphology of the postorbital with respect to the other posterior periorbital elements is difficult to assess. However, in the holotypes of *Alligatorellus beaumonti* and *Alligatorellus bavaricus*, there is no notable suture on the dorsal surface of the skull table, lateral to the supratemporal fenestra, which would represent the suture between the posterior process of the postorbital and the anterior process of the squamosal. I therefore infer that the anterior process of the squamosal reached the posterior orbital margin.

(S8) Posterodorsal margin of parietals and squamosals completely covers posterodorsal occipital region, excluding the supraoccipital from the dorsal surface of the skull (C197.1). This feature was proposed to be autapomorphic for *Alligatorellus* (Tennant and Mannion, 2014), but also appears to be present in a range of neosuchian taxa (e.g., *Acynodon adriaticus* (Delfino *et al.*, 2008b)) in which the supraoccipital is excluded from the posterodorsal surface of the skull roof. I therefore consider it to only be locally diagnostic for *Alligatorellus*. In other mesoeucrocodylians, such as *Mahajangasuchus*

(Turner and Buckley, 2008), the supraoccipital is broadly visible in the midline portion of the posterodorsal region of the skull, contacting the parietals.

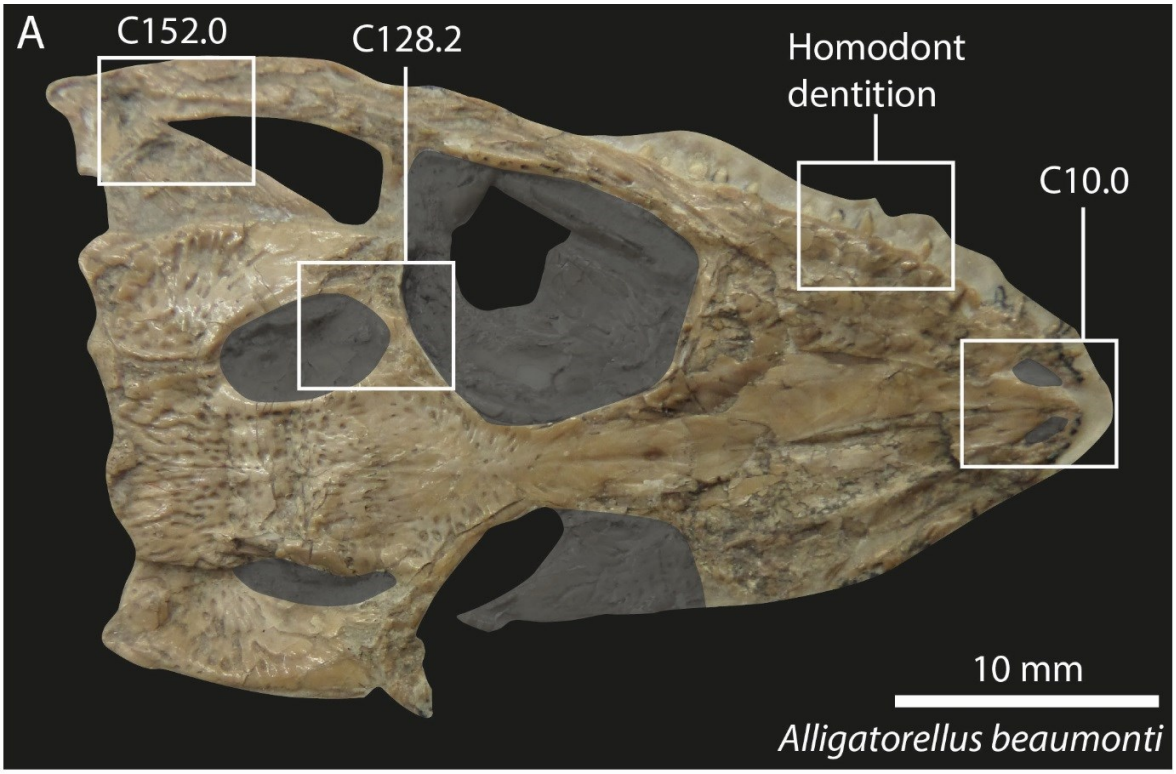
(S9) Smooth mandibular external surface, lacking sculpting (C201.0). This feature is difficult to observe in *Alligatorellus bavaricus* due to the dorsal flattening of the holotype specimen, although what is visible indicates that the mandible, much like the anterior portion of the skull, lacked any sculpting pattern, unlike the dorsal surface of the cranial table. This is distinct from *Theriosuchus* and *Wannchampsus*, in which the sculpting pattern on the external surface of the dentaries and posterior mandibular elements is similar to that of the dorsal surface of the skull.

(S10) Proximal end of the radiale 'hatchet-shaped' (C290.1). This feature also characterises MB.R.3632, and was used to refer this specimen to *Alligatorellus* (Schwarz-Wings *et al.*, 2011). However, this morphology is also shared by *Wannchampsus* (Adams, 2014), but is not known in *Theriosuchus* specimens, due to lack of preservation of the radiales. In other atoposaurids, the proximal end of the radiale is more expanded equidimensionally, lacking the asymmetry observed in *Alligatorellus*.

(S11) Proportionally short metatarsal I relative to metatarsals II–IV (C303.1). In other atoposaurids, metatarsals I–IV are almost equidimensional, possibly reflecting different locomotor adaptations in *Alligatorellus*.

(S12*) Dorsal surface of dorsal osteoderms completely sculpted (C304.0), with parallel and straight anterior and posterior margins (C308.1), and a longitudinal ridge along entire lateral margin (C311.1 and C312.1). The utility of osteoderms in atoposaurid systematics, particularly regarding *Alligatorellus*, was discussed in a recent publication (Tennant and Mannion, 2014). These authors noted that the mediolateral position and anteroposterior extent of the dorsal keel, and its serial variation along the axial column, are diagnostic for *Alligatorellus*, as well as for other crocodyliforms (e.g. teleosauroids, eusuchians) that preserve a dorsal series of paravertebral osteoderms.

(S13) Caudal osteoderms with smooth, non-serrated edges (C327.1). This morphology is similar to the osteoderms preserved for *Theriosuchus guimarotae* and *T. pusillus*, but distinct from *Brillanceausuchus* and *Montsecosuchus* in which the margins of the caudal osteoderms are serrated. Serrated edges might also be present in caudal osteoderms of MB.R.3632, based on at least three caudal osteoderms disassociated from the main osteoderm shield preserved on the specimen slab. However, the possibility that these elements are accessory dorsal osteoderms cannot be discounted, as found in *Montsecosuchus* and in the proximal caudal series of *Alligatorellus beaumonti*.


A
C152.0
C128.2
Homodont
dentition
C10.0
10 mm
Alligatorellus beaumonti

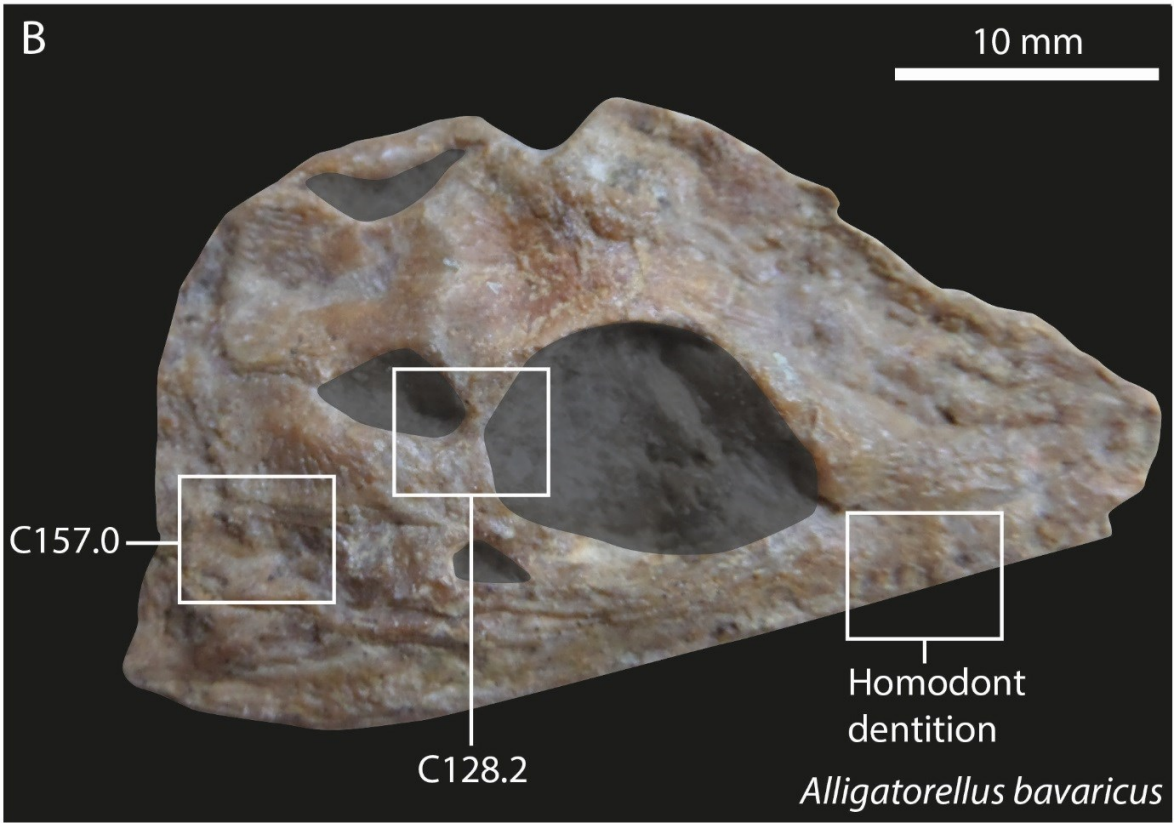

B
10 mm
C157.0
C128.2
Homodont
dentition
Alligatorellus bavaricus

Figure 50. A. Skull of the holotype of *Alligatorellus beaumonti* (MNHL 15639) in dorsal view. See text for details. B. Skull of the holotype of *Alligatorellus bavaricus* (BSPG 1937 I 26) in dorsolateral view. Synapomorphies for Atoposauridae indicated (see text for details). *Alligatorellus beaumonti* (Gervais, 1871) (type species).

5.4.4.1 *Alligatorellus beaumonti beaumonti* (Wellnhofer, 1971)

Type locality and horizon: Unknown bed, Kimmeridgian (Late Jurassic); Cerin, Ain, France.

Type specimen: MNHL 15639, part and counterpart slabs comprising a near-complete and articulated skeleton, missing the distal-most caudal vertebrae (preserved as impressions) and part of the left forelimb (Figure 52). Parts of the skull roof and a large portion of the right maxilla, along with several axial fragments, are embedded into the counterpart slab.

Referred specimen: MNHL 15638, part slab comprising a near-complete and articulated skull and skeleton, missing just the distal-most caudal vertebrae, the right forelimb, and the distal left forelimb, all of which are preserved as impressions (Figure 53). The skull is exposed in ventrolateral aspect.

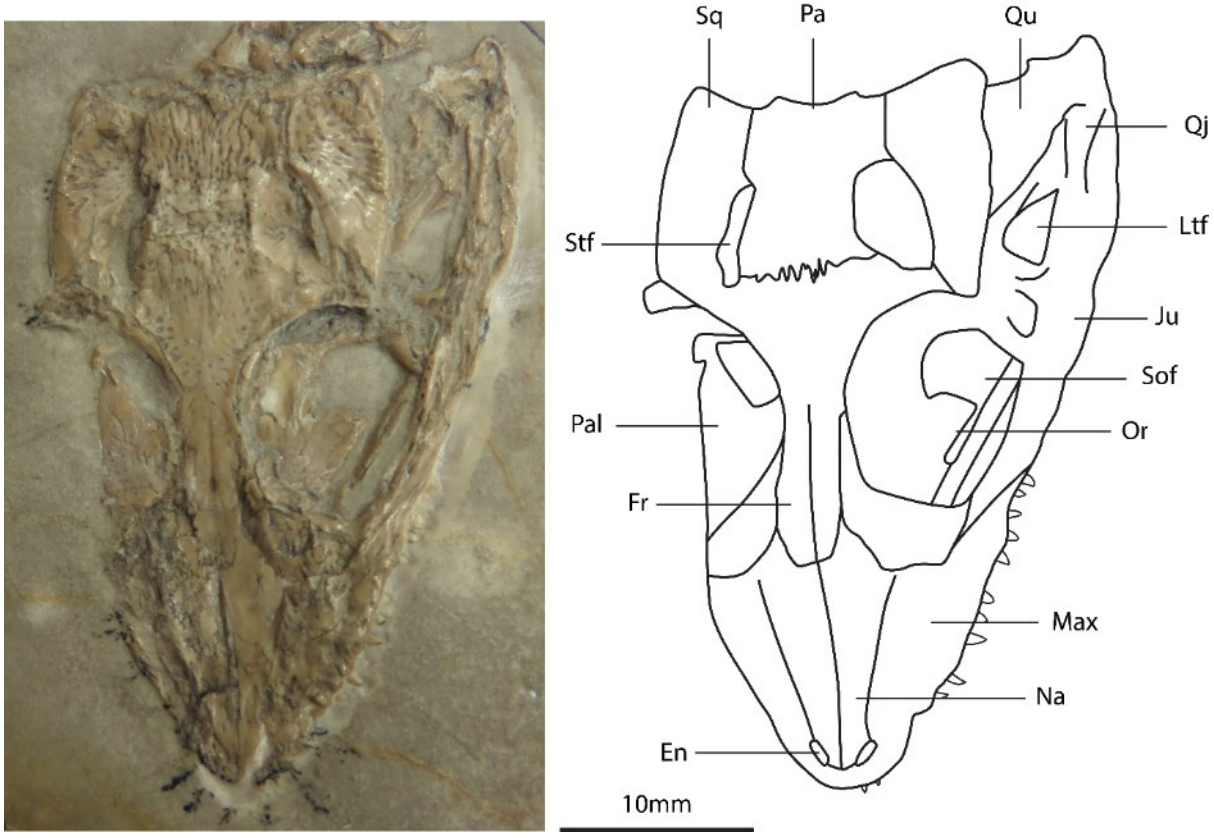


Figure 51. Photograph and line drawing of the skull of the holotype specimen of *Alligatorellus beaumonti* (MNHN 15639) in dorsal aspect.

Previous diagnoses and comments: *Alligatorellus beaumonti* was originally named for two specimens from the Late Jurassic of Cerin, eastern France (Gervais, 1871). Subsequently, these were identified as the subspecies *Alligatorellus beaumonti beaumonti* (Wellnhofer, 1971). This was based largely on size differences between these and additional coeval specimens from Eichstätt, southeast Germany, for which the subspecies *Alligatorellus beaumonti bavaricus* was erected (see Section 5.5.4.2) (Wellnhofer, 1971). Together these specimens have largely been regarded as representing a single taxon, *Alligatorellus beaumonti*, by subsequent workers (Buscalioni and Sanz, 1988; Schwarz-Wings *et al.*, 2011). However, following a redescription of the German remains, a number of morphological differences with the French material were noted (Tennant and Mannion, 2014), and a revised diagnosis for *Alligatorellus beaumonti* was formally presented, along with a re-ranking for the German material as *Alligatorellus bavaricus*.

Previously it has been noted that as in *Theriosuchus*, the external nares in *Alligatorellus beaumonti* are divided by an anterior projection of the nasals (Wellnhofer, 1971), a feature that also appears to be shared by *Alligatorium meyeri* and possibly *Alligatorellus bavaricus*, although the anteriormost portion of the snout in the holotype of the latter is damaged. *Alligatorellus beaumonti* is similar to *Alligatorium meyeri* in the presence of an unsculpted posterolateral 'lobe' of the squamosal, differing from *Alligatorellus bavaricus* in which the posterolateral corner of the squamosal instead displays orthogonal posterior and lateral edges. Subsequently it was suggested that another distinguishing feature between *Alligatorellus beaumonti* and *Alligatorium meyeri* is the contribution of the frontal to the supratemporal fenestra in the former (Buscalioni and Sanz, 1988); however, this feature is clearly also present in *Alligatorium meyeri*, and therefore cannot be used to distinguish the two taxa. The presence of a biserial osteoderm shield comprising singular sculpted osteoderms is not diagnostic for *Alligatorellus* (contra (Wellnhofer, 1971)), as it also characterises both *Theriosuchus pusillus* and

Alligatorium meyeri. In a previous publication, it was proposed that the frontal width between the orbits being mediolaterally narrower than the nasals is an autapomorphy of *Alligatorellus beaumonti* based on comparative anatomy (Tennant and Mannion, 2014); however, this condition is not considered to be diagnostic here following formal phylogenetic analysis, as it is also known in a wide range of neosuchian taxa, and the width of the paired nasals in *Alligatorellus bavaricus* might have been underestimated. *Alligatorellus beaumonti* also has the reversed condition to *Alligatorellus bavaricus*, in that the anterior extension of the frontal exceeds the anterior margin of the orbits, similar to almost all other neosuchian taxa.

Revised diagnosis and discussion: (S1*) Frontal with unsculpted anterior and posterior portions, and sculpted medial surface (Figure 51). I elected not to code this as a distinct character state from that of S3 in the matrix in order to avoid duplication of character states. Nonetheless, subsequent work identified this heterogeneity in sculpting pattern as distinct from other atoposaurids and *Theriosuchus*, and considered it to be autapomorphic of *Alligatorellus beaumonti* (Tennant and Mannion, 2014).

(S2) Surface of rostrum notably less sculpted than cranial table (C4.1). See S2 for *Alligatorellus* for discussion of this character state.

(S3) Relatively large lateral temporal fenestra, approximately 30% the size of the orbit (C20.1). A lateral temporal fenestra of this size with respect to the orbit represents the intermediate condition in the analyses. This relatively large size is unique among atoposaurids, but is also shared with *T. pusillus*, *Koumpiodontosuchus* (Sweetman *et al.*, 2015), protosuchians, as well as the advanced neosuchians *Shamosuchus* (Pol *et al.*, 2009), *Isisfordia* (Salisbury *et al.*, 2006), and *Brillanceausuchus*. In other taxa, such as *Allodaposuchus precedens*, the lateral temporal fenestra approaches the size of the orbit (Buscalioni *et al.*, 2001).

(**S4) Smooth contact between maxilla and jugal (C51.2).** As noted above, the pattern of sculpting on the anterior portion of the dorsal surface of the skull is diagnostic for the different species of

Alligatorellus. In *Alligatorellus bavaricus*, the entire dorsal surface is lightly sculpted, but *Alligatorellus beaumonti* has a smooth contact between the maxilla and jugal, similar to *Atoposaurus* and *Hoplosuchus*, although in both of these taxa the entire external surface of the skull is not ornamented. This is distinct from *Theriosuchus guimarotae* and *T. pusillus*, which both have a contact in which the external surface is sculpted to the same degree as the rest of the cranial table, and from *Brillanceausuchus*, '*Theriosuchus*' *ibericus*, '*Theriosuchus*' *sympiestodon*, and *Montsecosuchus*, in which the contact is heavily striated.

(S5*) Medial longitudinal depression on posterior portion of nasal and anterior portion of frontal (C74.1). This is diagnostic of *Alligatorellus beaumonti* as a local autapomorphy, but is also present in the goniopholidid *Amphicotylus* (Mook, 1942). This condition differs from that in *Theriosuchus* and a range of paralligatorids, including *Brillanceausuchus*, in which a distinct midline longitudinal crest develops.

(**S6*) Posteromedial border of supratemporal fenestra forms a low sagittal rim (C119.1).** This feature is considered to be locally autapomorphic, as it is also present in *Brillanceausuchus*. *Alligatorellus bavaricus* and *Atoposaurus* have no supratemporal rim development, and the rims are strongly developed along the whole medial edge of the external supratemporal fenestra in *Alligatorium meyeri*, *Theriosuchus pusillus* and *Wannchampsus* (Adams, 2014).

(S7*) Smooth and unsculpted region on anterior portion of squamosal nearing orbit and posterolateral process of squamosal (C148.1). This feature appears to be locally diagnostic, but is also shared by *Khoratosuchus* (Lauprasert *et al.*, 2009). For all other OTUs for which this feature could be scored, the pattern of sculpting did not change between the main body of the squamosal and the immediate postorbital region.

(S8*) Ratio of forelimb to hindlimb length high (0.8) (C180.2). This feature is diagnostic for *Alligatorellus beaumonti* among all OTUs for which this character could be scored. *Atoposaurus*

oberndorferi and *Alligatorellus bavaricus* both have similar ratios, 0.78 and 0.76, respectively, but *Atoposaurus jourdani* is distinct, with a ratio of 0.63 (Table 20). However, this character state could not be scored for *Theriosuchus*, or the majority of the outgroup taxa, because of the relative rarity with which these specimens preserve associated and complete limb material. Therefore, although these unusual ratios are diagnostic among atoposaurids, it cannot be determined whether they are unique or only local autapomorphies.

(S9) Ratio of tibia to femur length low (0.9) (C300.0). The relative dimensions of the tibia and femur are a feature that is closely shared with MB.R.3632 (0.91), *Hoplosuchus* (0.92), *Alligatorium meyeri* (0.93), and *Atoposaurus jourdani* (0.94). This ratio far exceeds that for '*Alligatorium*' *franconicum* (0.64), and is distinct from *Alligatorellus bavaricus* (0.96) (Table 3). This feature was also noted previously (Tennant and Mannion, 2014), but these authors used a ratio of femur to tibia length.

(S10*) Nuchal osteoderms reduced, less than 50% of the size of the dorsal osteoderms (C307.1). This feature is distinct from the condition in *Alligatorellus bavaricus*, *Alligatorium meyeri*, *Montsecosuchus*, and *Protosuchus*, in which the preserved nuchal osteoderms retain the same size and morphology as the dorsal series, or only decrease slightly.

(S11*) Dorsal keel in dorsal osteoderms shifts laterally in more posterior dorsal osteoderms (C317.1). The position of the dorsal keel on the dorsal osteoderm series is distinct from that in *Alligatorellus bavaricus*, in which the morphology is more consistent along the axial column (Tennant and Mannion, 2014). This feature is not present in any of the other OTUs which were sampled, and therefore it is here considered to be diagnostic for *Alligatorellus beaumonti*.

(S12*) Lateral ridge on sacral osteoderms forms an incipient posterior projection. The posterior development of the lateral keel (as noted in S9) into an incipient lateral projection among the more sacrally-positioned osteoderms, is diagnostic for *Alligatorellus beaumonti*. In *Alligatorellus bavaricus*, the morphology of the keel does not change anteroposteriorly (Tennant and Mannion, 2014), and

Theriosuchus, *Alligatorium meyeri*, and higher neosuchians do not seem to possess this keel at all. '*Alligatorium*' *franconicum* and *Hoplosuchus* are convergently similar, in that the lateral keel appears to form an anterolateral process, distinct from the 'peg and socket' articulation described for goniopholidids and *T. guimarotae* (Schwarz and Salisbury, 2005). This character was not incorporated in order to avoid duplication and over-weighting of the observation that the morphology of the dorsal keel changes axially in *Alligatorellus beaumonti* (S11).

(S13*) Secondary osteoderms present in caudal series (C328.0). This feature does not appear to be present in any other atoposaurid that preserves caudal osteoderms.

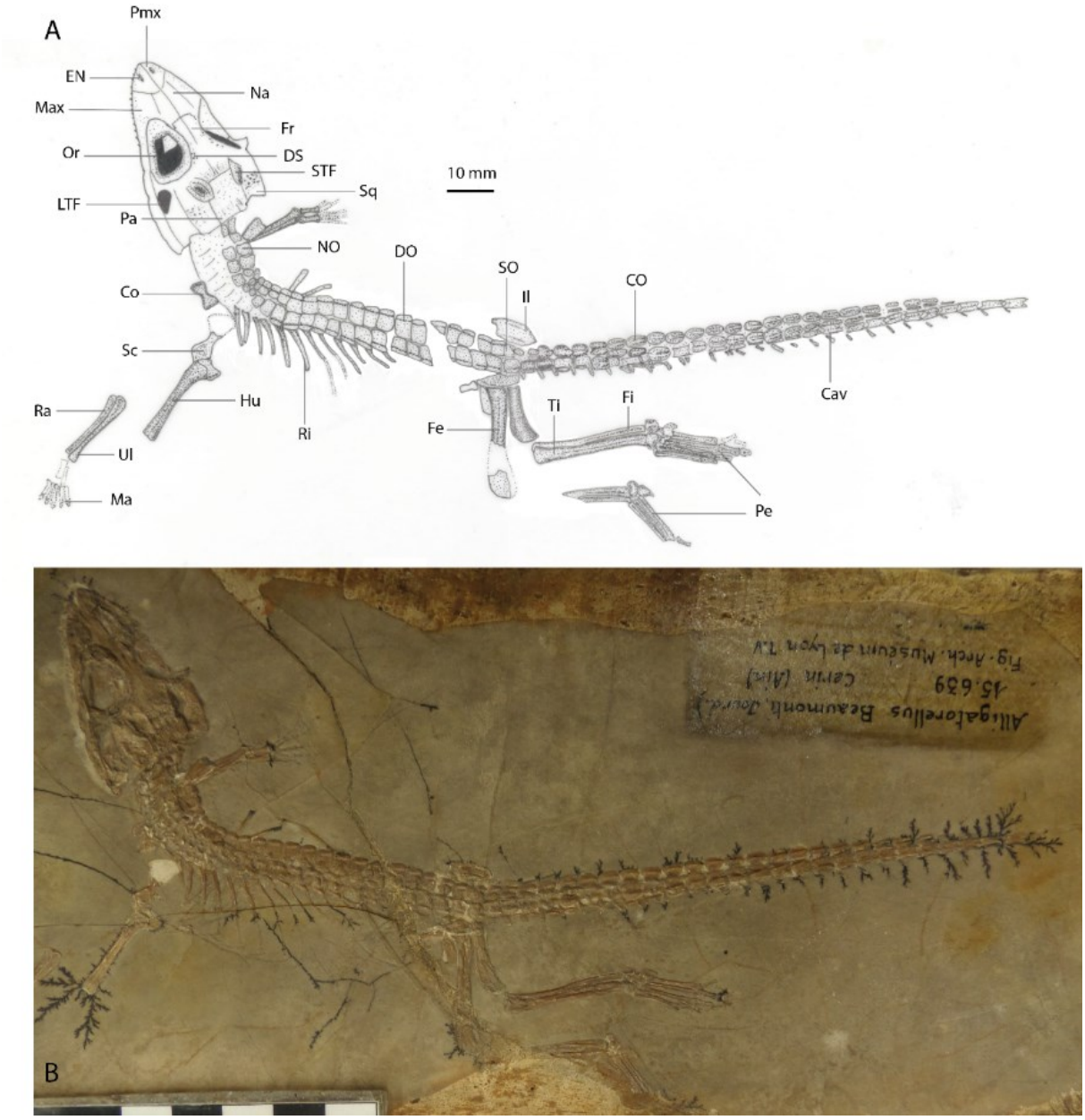


Figure 52. (a) Line drawing of holotype specimen of *Alligatorellus beaumonti* (MNHN 15639); (b) photograph of holotype specimen. Abbreviations: AF, antorbital fenestra; Cav, caudal vertebra; Cev, cervical vertebra; Ch, chevron; Co, coracoid; CO, caudal osteoderm; DO, dorsal osteoderm; Dov, dorsal vertebra; DR, dorsal ridge; DS, dermal sculpting; EN, external nares; Fi, fibula; Fr, frontal; Hu, humerus; Il, ilium; Is, ischium; LTF, lateral temporal fenestra; Ma, manus; Man, mandible; Max, maxilla; MC, metacarpal; MP, manual phalanx; MT, metatarsal; Na, nasal; NO, nuchal osteoderm; Or, orbit; Pa, parietal; Pal, palatine; Pe, pes; PMn, premaxilla-maxilla notch; Pmx, premaxilla; PP, pedal phalanx; Pu, pubis; Ra, radius; Rad, radiale; Ri, rib; Sc, scapula; SO, sacral osteoderm; Sq, squamosal; STF, supratemporal fenestra; Sym, symphysis; Ti, tibia; Ul, ulna; Uln, ulnare; UP, ungual phalanx.

Additional comments: In the holotype specimen of *Alligatorellus beaumonti*, the posteriormost maxillary teeth have a more labiolingually compressed, apically pointed morphology than the remaining teeth, similar to the 'lanceolate' morphology exhibited by several species of *Theriosuchus* (Schwarz and Salisbury, 2005; Lauprasert *et al.*, 2011), *Brillanceausuchus*, as well as the bernissartiid *Koumpiodontosuchus* (Sweetman *et al.*, 2015). This is different to the homodont dentition typically reported for *Alligatorellus*, which is usually described as possessing simple pseudocaniniform teeth that are smooth and lack ridges or carinae (Wellnhofer, 1971; Buscalioni and Sanz, 1990b; Thies *et al.*, 1997). However, this is not assigned as a local autapomorphy of *Alligatorellus beaumonti* as it is only visible for one or two teeth in a specimen that shows strong evidence of dorsal compression. Its validity therefore requires further investigation pending the discovery of more specimens of *Alligatorellus*. Although this more lanceolate morphology has also been figured for the posterior teeth of *Alligatorellus bavaricus* (Wellnhofer, 1971), I have been unable to personally validate this on the figured specimen, and it is not visible on the holotype. Therefore, caution is urged in interpreting *Alligatorellus* as possessing lanceolate posterior teeth that are homologous to those found in *Theriosuchus*. Re-running phylogenetic analysis (excluding '*Alligatorellus*' sp. [MB.R.3632] and *Pachycheilosuchus* as before) with *Alligatorellus* scored as possessing lanceolate posterior teeth, a single MPT is achieved with a length of 793 steps with an unchanged topology. However, the presence of a lanceolate dentition instead becomes the basal condition in the clade containing atoposaurids and higher neosuchians, secondarily lost in *Alligatorium meyeri*, *Brillanceausuchus*, '*Theriosuchus*' *ibericus*, '*Theriosuchus*' *sympiestodon*, and the clade containing *Koumpiodontosuchus* and coelognathosuchians.



Figure 53. (A) Line drawing of referred specimen of *Alligatorellus beaumonti* (MNHN 15638) in dorsoventral view; (B) photograph of referred specimen.

5.4.4.2 *Alligatorellus bavaricus* Wellnhofer 1971 (re-ranked; (Tennant and Mannion, 2014))

Alligatorellus beaumonti bavaricus Wellnhofer 1971

Type locality and horizon: Solnhofen Formation, early Tithonian (Late Jurassic, *Hybonoticeras hybonotum* zone); Eichstätt, southeast Germany.

Type specimen: BSPG 1937 I 26, a near-complete skeleton including the skull, lacking only the left forelimb, compressed onto a slab of lithographic limestone (Figure 54). Note that Tennant and Mannion (2014) incorrectly stated that the specimen number was LMU 1937 I 26.

Referred specimen: A specimen held in the private collection of E. Schöpfel was described and referred to *Alligatorellus bavaricus* (Wellnhofer, 1971), from the Wintershof Quarry (Solnhofen Formation, Eichstätt, southeast Germany).

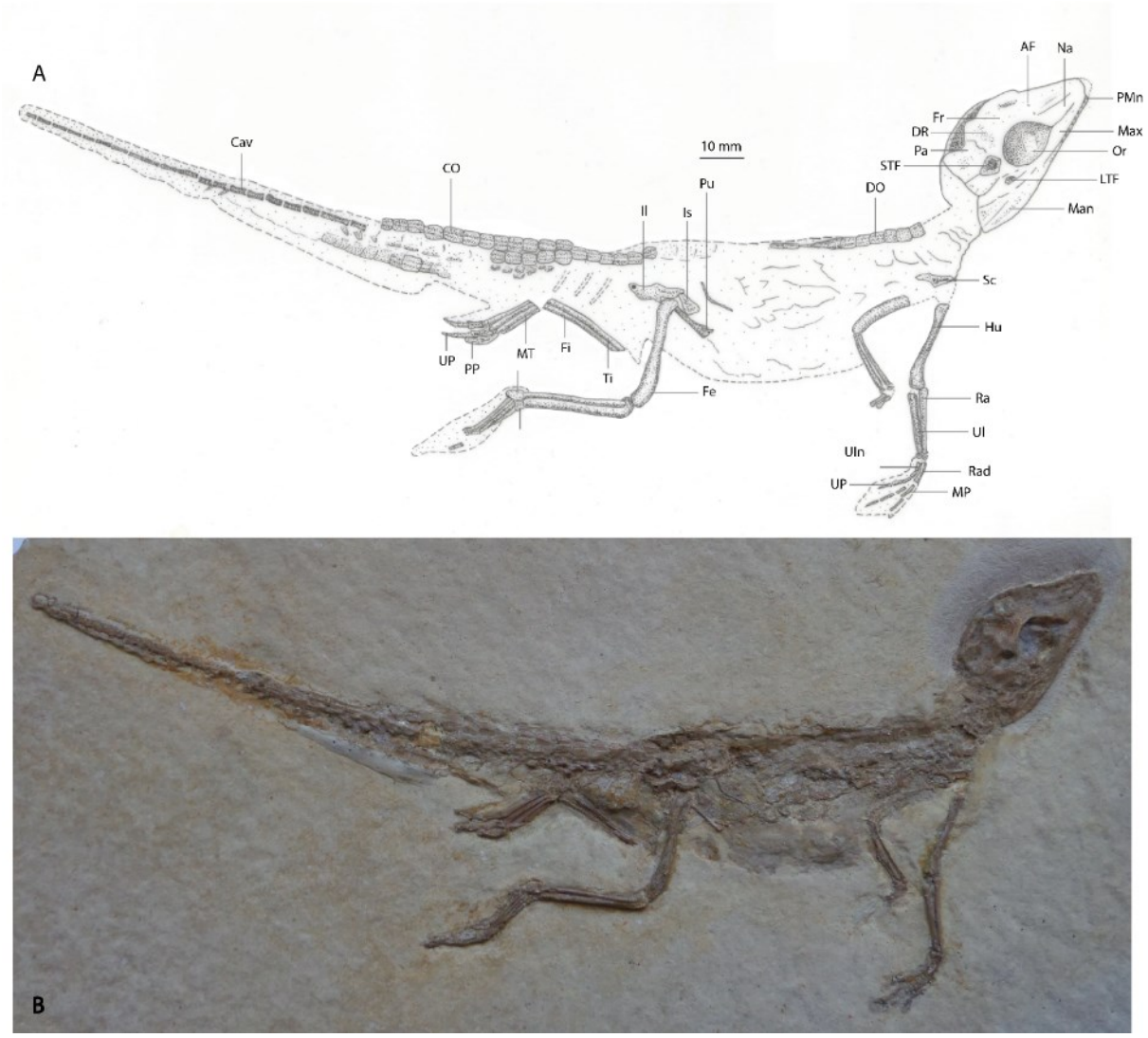


Figure 54. (A) Line drawing of holotype specimen of *Alligatorellus bavaricus* (BSPG 1937 I 26) in dorsolateral view; (B) photograph of holotype specimen.

Revised diagnosis and discussion: (S1) Concave profile of dorsal surface of snout in lateral view (C8.0)

This feature represents a reversion back to the plesiomorphic state known for *Protosuchus* (Colbert *et al.*, 1951) and *Hoplosuchus* (Gilmore, 1926), with other atoposaurids and neosuchians usually

presenting a straight profile in lateral aspect; with exceptions such as the longirostrine goniopholidid *Amphicotylus* (Mook, 1942).

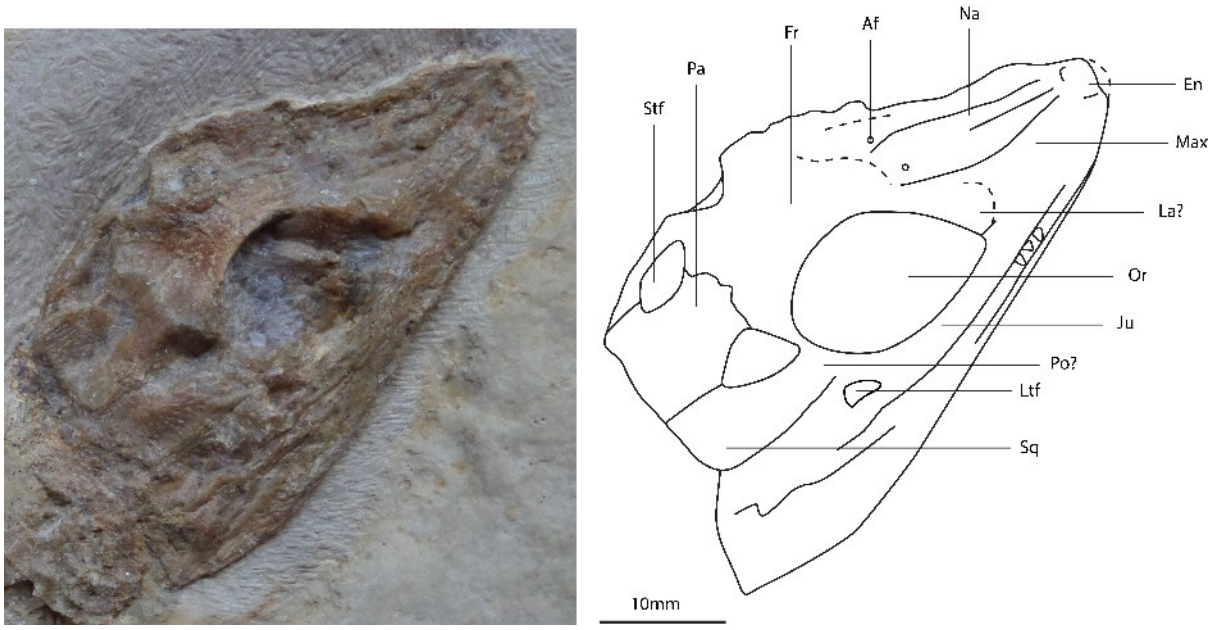


Figure 55. Photograph and line drawing of the skull of the holotype specimen of Alligatorellus bavaricus (LMU 1937 I 26) in dorsolateral aspect.

(S2) Small, slit-shaped antorbital fenestra, enclosed by nasals (C13.0 and C14.1). *Alligatorellus bavaricus* appears to possess a small, slit-like antorbital fenestra, similar to the notosuchians *Gondwanasuchus* (da Silva Marinho *et al.*, 2013) and *Malawisuchus* (Gomani, 1997). In other taxa with an antorbital fenestra, including *Theriosuchus guimarotae* (Schwarz and Salisbury, 2005), *T. pusillus* and '*T.*' *ibericus*, it is proportionally larger and rounded. *Alligatorellus beaumonti* does not appear to possess an antorbital fenestra, although part of the snout is embedded in the counterpart slab, with a small opening observable near the posterior margin of the nasals, which could be a diminutive fenestra. The presence of an antorbital fenestra is documented in basal crocodyliforms, including the protosuchians *Hoplosuchus* (Gilmore, 1926) and *Protosuchus haughtoni* (Gow, 2000), *Zosuchus* (Pol and Norell, 2004a), and thalattosuchians (Leardi *et al.*, 2012), but becomes closed in shartegosuchids,

including *Fruitachampsa* (Clark, 2011). *Pachycheilosuchus* might have also possessed an antorbital fenestra (Rogers, 2003).

(S3*) Extremely narrow and short skull, with a low skull width to orbit width ratio (<2.0) (C28.0). This character state is the lowest value for all atoposaurids, and much lower than all other OTUs in which this character was measurable. For other atoposaurids, this ratio is between 2.15 (*Alligatorellus beaumonti*) and 2.69 (*Atoposaurus jourdani*), and the only other taxon that comes close to this range is *Wannchampsus* (2.77). *Brillanceausuchus*, *Montsecosuchus* and *Theriosuchus* species all have ratios between 3.0 and 3.5, with the ratio being considerably greater in longirostrine taxa and protosuchians (Table 3). It is likely that this character state is influenced by ontogeny (Joffe, 1967), but the broad distribution of ratios among the sampled OTUs, which possess a range of body sizes and ontogenetic states, means that ontogeny is unlikely to entirely control this feature.

(S4) Skull anteroposterior length to supratemporal fenestra length ratio ~7.2 (7.18) (C29.2). The proportional length of the external supratemporal fenestra is similar to *Wannchampsus kirpachi* (7.53), but distinct from *Alligatorium meyeri* (6.43) and *Alligatorellus beaumonti* (6.23), which have proportionally larger external supratemporal fenestrae. Consequently, the proportionally short anteroposterior length of the supratemporal fenestra to skull length is considered to be diagnostic for *Alligatorellus bavaricus*, because in *Montsecosuchus* this ratio is considerably higher (8.9) (Table 20), with a much smaller supratemporal fenestra.

(S5*) Posterior surface of nasals longitudinally crenulated (C69.0). The longitudinal crenulations on the dorsal surface of the nasals are not known in any other crocodyliform, in which the nasals are dorsally flat and sculpted like the rest of the cranial dorsal surface.

(S6*) Smooth anterior region of parietal dorsal surface with a transverse frontal-parietal ridge, and shallow emargination at the posterior parietal-squamosal contact (C117.1) that develops into a thin dorsal groove connected to the supratemporal fenestra (C147.1). The morphology of the parietal is

diagnostic, with a small anterior concavity at the posterodorsal suture contact between the parietal and squamosal, leading to a shallow sulcus along this contact into the posterior margin of the supratemporal fenestra, and a smooth anterior dorsal surface. This is distinct from the condition observed in *Theriosuchus* in which this contact is deep and expands mediolaterally towards the supratemporal fenestra border, and from *Alligatorellus beaumonti* and *Alligatorium meyeri* in which the grooved contact is bordered by raised crests. The presence of a transverse ridge at the parietal-frontal suture distinguishes *Alligatorellus bavaricus* from all other species, in which this suture is flat.

(S7) Squamosal posterolateral lobe absent (C139.1). The squamosal posterolateral lobe is completely absent in *Alligatorellus bavaricus*, a feature considered to be diagnostic among all atoposaurids.

(S8*) Distinct ridge on proximodorsal edge of scapula (C280.1). The scapula of *Alligatorellus bavaricus* can be distinguished from *Alligatorellus beaumonti* and other atoposaurids based on the presence of a distinct ridge on the proximodorsal surface. In other specimens analysed, the proximodorsal edge of the scapula is flat in lateral view, and confluent with the scapular shaft.

(S9) Extremely low radius proximodistal length to humerus length ratio (0.69) (C288.1). The radius to humerus ratio is extremely low, distinct from other atoposaurids in which the value is closer to 1.0. This low ratio is identical to that for '*Alligatorium*' *franconicum* and *Karatausuchus* (Storrs and Efimov, 2000), but higher than in *Pachycheilosuchus* (0.58).

(S10*) Low radius proximodistal length to tibia length ratio (0.64) (C289.1). This value is almost identical to that for *Montsecosuchus*, *Pachycheilosuchus*, *Atoposaurus jourdani* (0.61), and *Protosuchus richardsoni* (0.63), but much higher than that for *Karatausuchus* (0.47) and *T. pusillus* (0.55). Other taxa have proportionally long radii, including *Alligatorium meyeri* (0.74), *Alligatorellus beaumonti* (0.71), '*Alligatorium*' *franconicum* (0.89), and *Brillanceausuchus* (0.88).

(S11*) Dorsal osteoderms with longitudinal medial ridge, becoming more laterally placed anteriorly (C311.1 and C312.1). This feature pertains to the morphology of the dorsal osteoderm series, which are distinct from those in *Alligatorellus beaumonti* (Tennant and Mannion, 2014), as well as MB.R.3632 (Schwarz-Wings *et al.*, 2011). In *Alligatorium meyeri* and *Theriosuchus pusillus*, there is no evidence of a lateral keel.

5.5 Osteoderm morphology in atoposaurid systematics

The morphology of the parasagittally-arranged postcranial osteoderms, or dermal scutes, of atoposaurids has not previously been regarded as an important characteristic in atoposaurid taxonomy, generally due to their relatively rare preservation in situ (Buscalioni and Sanz, 1990b; Michard *et al.*, 1990; Wu *et al.*, 1996b). The exception to this is a study of exclusively western European atoposaurids (Schwarz-Wings *et al.*, 2011). However, as noted here for specimens referred to *Alligatorellus*, subtle differences in osteoderm morphologies, particularly the extent, position, and continuity of the longitudinal keels on the dorsal surfaces, can prove to be diagnostic at the species level.

The pattern of ornamentation on the osteoderms of atoposaurids, as with other osteoderm-bearing crocodylomorphs (Vickaryous and Hall, 2008), is similar to the sculpting seen in the dermatocranial ornamentation, particularly with respect to the dorsal surface of the skull table. The exception to this appears to be for *Atoposaurus*, as well as the putative atoposaurid *Karatausuchus*, in which there is no evidence of cranial sculpting, and no preserved osteoderms (Wellnhofer, 1971). There is the possibility that the morphology of osteoderms varies intraspecifically, with multiple morphotypes represented within a population, as is the case in some other archosaurs (e.g., ankylosaurs (Burns, 2008)), but sample sizes are currently too small to ascertain if this might be the case in atoposaurids. The overall distribution of osteoderms in *Alligatorellus* is similar to that of basal crocodylomorphs such

as sphenosuchians and protosuchians, which have biserial rows of imbricated, rectangular dorsal osteoderms that might have served in a more functional support role than that proposed for atoposaurids (Clark and Sues, 2002; Pol *et al.*, 2004). Certainly, intrageneric variation in osteoderm morphology is present between *Alligatorium* and *Theriosuchus* species (Owen, 1879; Wellnhofer, 1971; Wu *et al.*, 1996b), and therefore prompts a discussion of its systematic utility for *Alligatorellus*.

Establishing the positional homology of osteoderms is important for evaluating taxonomic status in many tetrapod groups, including crocodylians (Ross and Mayer, 1983), aetosaurians (Parker, 2007; Parker *et al.*, 2008), and chroniosuchians (Buchwitz *et al.*, 2012). This is difficult with less complete or disarticulated specimens, such as the specimen of *Alligatorellus* sp., MB. R. 4317.1-12, in which it is postulated that articulated and disarticulated elements represent a single specimen with heterogeneous osteoderm morphology (Schwarz-Wings *et al.*, 2011). In *Alligatorellus*, both the positional homology and the differences in morphology in the discrete axial regions are diagnostic at the species level. There are four regions: cervical (or nuchal), dorsal, sacral, and caudal. These regions typically comprise continuous rows of anteroposteriorly arranged (paramedian or paravertebral) osteoderms. Below, the three different morphotype series found in the various specimens ascribed to *Alligatorellus* are discussed. *Alligatorellus* is distinguished from *Theriosuchus pusillus* and advanced eusuchians such as *Leidyosuchus* which have a ventral body encased within an articulating (but not overlapping or imbricating) shield of parasagittal rows of singular osteoderms (Owen, 1879; Brochu, 1997); from *Alligatorium* which has no dorsal keel; and from *Montsecosuchus* which has two to three rows of non-imbricating, and longitudinally oval dorsal osteoderms.

5.5.1 Alligatorellus bavaricus morphotype

The dorsal keel in osteoderms of *A. bavaricus* is in a more medial position nuchally, gradually migrating laterally along the dorsal series before becoming medially placed in the sacral and caudal series (Figure

56). Throughout this gradation, individual osteoderms are similarly robust, but adopt an increasingly more sub-rectangular to elliptical morphology posteriorly. Whereas they imbricate in the dorsal series, this change in shape leads to them abutting one another longitudinally, with no overlap. The longitudinal keel always occupies the entire length of the dorsal surface, and becomes more prominent posteriorly. There may have been a caudal ventral series of secondary osteoderms, but these are few in number and do not extend beyond the anterior half of the tail. This is similar to the condition in *Montsecosuchus depereti* (Buscalioni and Sanz, 1990b), but contrasts with *Theriosuchus*, in which they extend to the end of the caudal series. In the sacral and anterior caudal osteoderms of *A. bavaricus*, the dorsal keel never develops an incipient posterior projection, unlike in *A. beaumonti*. It is likely that the 'accessory osteoderms' described in *Alligatorellus bavaricus* (Wellnhofer, 1971) are the result of incomplete osteoderm development. The evidence for this is that they appear to be mostly comprised of the longitudinal keel, which forms as part of the earliest phase of development in osteoderms (Vickaryous and Hall, 2008).

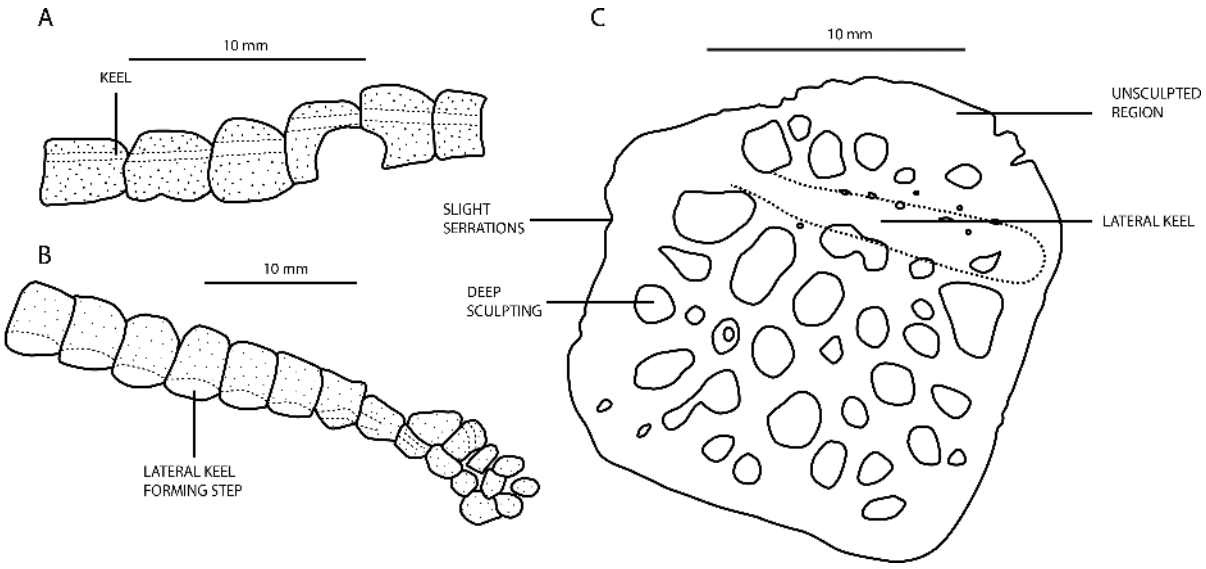


Figure 56. (A) Line drawings of the dorsal osteoderms of *A. bavaricus*; (B) line drawings of the cervical and dorsal osteoderm series of *A. beaumonti*; (C) Line drawing of a dorsal osteoderm of the specimen described as *Alligatorellus* sp. (MfN MB. R. 4317.1-12) (Schwarz-Wings et al., 2011).

5.5.2 Alligatorellus beaumonti morphotype

The biserially arranged osteoderms of *A. beaumonti* form a continuous dorsal shield, similar to *Theriosuchus pusillus* and other atoposaurids (Figure 56). Their longitudinally imbricating structure is comparable to extant alligatoroid species like *Caiman crocodilus* and *Alligator mississippiensis* (Burns *et al.*, 2013), but with fewer paramedian dorsal series. The extent of the caudal ventral series is much greater than in *A. bavaricus*, forming a complete dermal coating. The distal-most osteoderms are small, seemingly under-developed, sculpted elements. In the caudal series, the longitudinal ridges are pronounced, longitudinally extensive, and medially placed, similar to *A. bavaricus*. The more sacrally placed caudal elements have less pronounced keels, unlike *A. bavaricus*, becoming smaller and more ovate, with the ridges gradually almost disappearing and only occupying the posterior portion of each element, while sculpting remains the same. This skewing of the keels is seen most heavily in the dorsal and sacral osteoderms, where they form rounded protrusions on the dorsal side and become laterally displaced on the ventral series. This unusual shift develops into the dorsal series as a prominent lateral keel, becoming more anteroposteriorly extensive and forming a distinct step from the main body of each osteoderm. The ventral and dorsal morphology is quite similar, with the ventral keels almost seeming to diverge ventrally with each accompanying rib. The sacral and anteriormost caudal osteoderms develop an incipient lateral projection, almost appearing to diverge into two individual elements medial to this. The ventral series either terminates around the position of the third dorsal rib or is not preserved from this point onwards. The dorsal series adopts a heterogeneous range of morphologies, with some elements reducing to around one-sixth the size of the other osteoderms more nuchally, and with all losing the presence of the keel. This contrasts with *Alligatorium meyeri* and *Theriosuchus pusillus*, where they are morphologically continuous.

5.5.3 MfN MB. R. 4317.1-12 ('Alligatorellus sp.') morphotype

The deeper sculpting present in this specimen was previously ascribed to ontogenetic variation (Schwarz-Wings *et al.*, 2011), based on its larger size compared to other specimens of *Alligatorellus*. Maturity of the type specimens of both species of *Alligatorellus* is discussed elsewhere in this thesis (Section 5.5.4), and differences in the morphology suggest that this specimen is distinct from others of *Alligatorellus*, including the more medial position of the keel in *Alligatorellus* sp., and the lateral deflection of the body of the osteoderms adjacent to this. The keel is also not as longitudinally continuous in MfN MB. R. 4317.1-12 as it is in *A. beaumonti* and *A. bavaricus*. Additionally, the lateral edge is serrated, and there are unsculpted areas on the dorsal surface. Moreover, they are less robust overall than the other specimens of *Alligatorellus* in spite of their greater size, and overall appear similar to the osteoderm ascribed to *Theriosuchus* sp. (Wu *et al.*, 1996b). Together, these differences imply that the specimen represents a distinct morphotype. These lines of evidence lead us to conclude that this specimen does not represent *Alligatorellus*, and instead belongs to a distinct and poorly known atoposaurid taxon. Future histological analyses may prove useful in increasing our understanding of the taxonomic utility of atoposaurid, and more broadly crocodyliform, osteoderms (Burns, 2008; Burns *et al.*, 2013).

5.6 The taxonomic validity of Atoposaurus and Alligatorium

Alligatorellus beaumonti coexisted with *Atoposaurus jourdani* and *Alligatorium meyeri* in eastern France, while *Alligatorellus bavaricus* lived alongside *Atoposaurus oberndorferi* (as well as possibly *Alligatorium paintenense* and *Alligatorium franconicum*) in south-eastern Germany (Wellnhofer, 1971) (Figure 49). This high diversity of atoposaurids in the Late Jurassic of Germany and France, combined with potential juvenile features in *Atoposaurus*, has led to suggestions that *Atoposaurus* might characterise a juvenile specimen of one of the other sympatric atoposaurid species (Buscalioni and

Sanz, 1988), with others suggesting that *Atoposaurus*, *Alligatorellus* and *Alligatorium* might represent a single growth series (Benton and Clark, 1988).

Ontogenetic allometric variation has received considerable attention in extant crocodylians, particularly in population-level studies (Dodson, 1975). Through crocodylian ontogeny, several allometric relationships have been recognised in different taxa: (1) the skull lengthens, and becomes more dorsoventrally flattened and laterally compressed in *Caiman* (Monteiro *et al.*, 1997; Monteiro and Soares, 1997); (2) the skull lengthens and widens in *Alligator sinensis* (Wu *et al.*, 2006), *Crocodylus moreletii* (Platt *et al.*, 2009) and *Crocodylus siamensis* (Chentanez *et al.*, 1983), as does the snout in *Alligator sinensis*; (3) reduction in relative orbit size to the skull occurs in *Crocodylus acutus*, *Gavialis gangeticus*, *Mecistops cataphractus* and *Tomistoma schlegelii* (Piras *et al.*, 2010); and (4) the orbit, snout and skull shape changes through ontogeny in *Caiman latirostris* (Verdade, 2000). However, as Verdade (2000) noted, many of these allometric factors covary with both size and ontogenetic stage, and therefore it is often difficult to interpolate from these allometric relationships to determine an ontogenetic stage in fossil taxa.

To test the hypothesis that *Alligatorellus*, *Alligatorium* and *Atoposaurus* represent a single ontogenetic series (Benton and Clark, 1988), or that *Atoposaurus* is a juvenile of at least one of the other taxa, a number of anatomical measurements (skull width, snout length, and orbit length) were plotted for each of the species against skull length, and also carried out a covariance-based Principal Components Analysis (PCA) (Figure 57).

An increase in skull width and snout length relative to skull length is seen in both the French and German atoposaurid groups, although this is much more pronounced in the German specimens as a result of the longirostrine form of *Alligatorium franconicum* (Figure 57A, B). However, this trend is not entirely linear, with *Alligatorellus beaumonti* having a distinctly longer, but almost equally wide, skull relative to *Atoposaurus jourdani*. A similar pattern is recorded for orbit length relative to skull length,

although this trend is considerably less pronounced in the German taxa, and there is little difference between *Atoposaurus jourdani* and *Alligatorellus beaumonti*, despite an almost doubling of skull length (Figure 57C). If *Atoposaurus*, *Alligatorellus*, and *Alligatorium* were part of the same growth series, one would expect a consistent relationship between the two geographic groups in each of these aspects, a pattern not produced here.

The PCA of six primary measurements (skull length, skull width, orbit length, ulna length, femur length and tibia length) shows a distinct pattern, with the three genera separated in morphospace, especially along PC-1 (Figure 57D). Furthermore, neither the French or German specimens show equivalent distributions to each other, which might be expected if each basin records the same taxon along one growth series. The two Atoposaurus species are distinguished by the PC-1 (94.1% variance). *Alligatorellus* species are weakly distinguished from each other by PC-2 (2.8% variance), but show almost no variation in PC-1. Whereas the two *Alligatorium* species are strongly distinguished from each other on PC-2, they are closely united by PC-1 (Figure 57D). As such, there is little convincing uni-directional evidence that *Atoposaurus*, Alligatorellus, and *Alligatorium* form a single growth series of one species. Although the possibility cannot be fully excluded that *Atoposaurus* represents an immature specimen of either *Alligatorellus* or *Alligatorium*, below other anatomical features that support its taxonomic validity are discussed.

Atoposaurus is unique among all definite atoposaurids in lacking osteodermal armour. It has previously been suggested that this might merely be a taphonomic artefact (Schwarz-Wings *et al.*, 2011); however this mode of preservation selectivity seems unlikely given that there is no clear reason why similarly ossified parts of the skeleton would undergo differential preservation. When combined with their diminutive size, and the absence of any cranial sculpting of calcified palpebrals, this line of evidence appears to be indicative of a juvenile status. In fact, *Atoposaurus* looks superficially similar to the alligatoroid *Diplocynodon* from the Eocene-aged Messel deposits (Delfino and Sánchez-Villagra,

2010), in terms of the relatively long caudal vertebral series, large orbits, lack of ossification of the dermal armour, and proportionally short skull. As such, *Atoposaurus* superficially takes on the appearance of more advanced eusuchians, while retaining paedomorphic characteristics (e.g., the proportionally large orbits). In crocodylians, the initiation of osteoderm ossification is usually substantially delayed relative to skeletal ossification (Vickaryous and Hall, 2008), so it is difficult to infer a more accurate ontogenetic age for *Atoposaurus* specimens. However, there are additional morphological aspects that demonstrate that *Atoposaurus* might not be a juvenile.

Similar to most other atoposaurids, *Atoposaurus* has a relatively short, low, acute, triangular-shaped skull. However, as with some theropod dinosaurs, the extant crocodylian *Osteolaemus*, and perhaps even the extant alligatoroid *Alligator*, this shortening of the rostral region may be a paedomorphic characteristic, with the morphology similar to juveniles and sub-adult specimens of *Melanosuchus* (the black caiman) (Foth *et al.*, 2015). A platyrostral skull is also known in basal eusuchians such as *Iharkutosuchus makadii* (Ősi *et al.*, 2007; Ősi, 2008), and is distinct from the majority of contemporaneous crocodylomorphs, including goniopholidids and thalattosuchians. Heterochrony in crocodylomorphs may be directly related to body size or diet, as atoposaurid species and *Osteolaemus* are relatively small forms and occupy distinctive ecologies. However, patterns of heterochrony, particularly relating to paedomorphosis, in 'dwarfed' specimens are currently poorly understood in crocodylomorphs, but could be responsible, at least in part, for the lack of osteoderm ossification in *Atoposaurus*.

The degree of suturing between the vertebral centrum and neural arch provides ontogenetic information (Mook, 1933; Brochu, 1996). Closure of cervical sutures is a consistent indicator of morphological maturity, and is known in more basal crocodylomorphs (e.g. thalattosuchians) (Delfino and Dal Sasso, 2006) and advanced eusuchians (Brochu, 1996). In *Atoposaurus jourdani*, the neural arches are fused to the centra (MNHN 15680), which implies that these specimens are not juveniles,

and despite their size represent a more mature growth stage. As such, I suggest that *Atoposaurus* represents an extreme case of dwarfism, and it is interesting to note that other putative atoposaurids of diminutive size, such as the 160 mm long *Karatausuchus* (Efimov, 1976) also lack osteoderms, suggesting the possibility that osteoderm development might be positively correlated with body size in atoposaurids.

Alligatorium is currently composed of three species: *A. meyeri* from Cerin, France (Jourdan, 1862), "*Alligatorium*" *franconicum* (Ammon, 1906) and "*Alligatorium*" *paintenense* (Kuhn, 1961) from Painten, central Bavaria, Germany. However, based on the figures and descriptions provided in the only known publication of these specimens (Wellnhofer, 1971), *A. franconicum* (based on an articulated hindlimb and pelvic girdle) cannot be distinguished from *A. paintenense* (a near-complete, articulated skeleton), aside from slight differences in femur-to-tibia length proportions. Given that both specimens are from the same locality, it is most probable that they do not represent distinct species, and regard *A. paintenense* (Kuhn, 1961) as synonymous with *A. franconicum* (Ammon, 1906), pending the relocation of the type material and/or discovery of new material. The type specimen of *A. paintenense* is clearly distinct from *A. meyeri* and both species of *Alligatorellus*, based on its more longirostrine snout, and dorsal osteoderms which each possess a longitudinal keel and an anterolateral hook (Wellnhofer, 1971). *A. meyeri* can be distinguished from *Alligatorellus* based on the absence of a longitudinal keel on all osteoderms in the latter taxon, as well as disparity in the cranial sculpting between the two taxa (see Section 5.5).

The French specimens of *Alligatorellus* and *Atoposaurus* both are proportionally smaller with respect to their total length to skull length (ratios of 5.4-5.59) compared to their generic German equivalents (6.73-6.78), and members of both genera are smaller still than *Alligatorium* (6.88-7.15). However, the skull length to orbit length ratio is 2.5 in *Atoposaurus jourdani* and 4.0 in *A. beaumonti*, with both *A. bavaricus* and *A. oberndorferi* having a ratio of approximately 3.2. *Alligatorellus* has a relatively longer

skull to width ratio than *Atoposaurus* (*A. beaumonti* = 1.8; *A. bavaricus* = 1.5; *Atoposaurus jourdani* = 1.38). A further difference between the two genera is the larger humerus to femur ratio in *Alligatorellus*. If *Atoposaurus* was indeed a juvenile of *Alligatorellus*, then we would expect the same scaling relationships between the geographically different taxa. Furthermore, if *Atoposaurus*, *Alligatorellus*, and *Alligatorium* all represented a single growth series, we might expect a linear growth series between the two geographic clusters. As such, there is little convincing unidirectional evidence to consider *Atoposaurus* as a juvenile of a contemporaneous atoposaurid. This taxonomic reappraisal suggests that there were three sympatric atoposaurid taxa – *Alligatorellus*, *Alligatorium*, and *Atoposaurus* – in each of the Late Jurassic French and German basins.

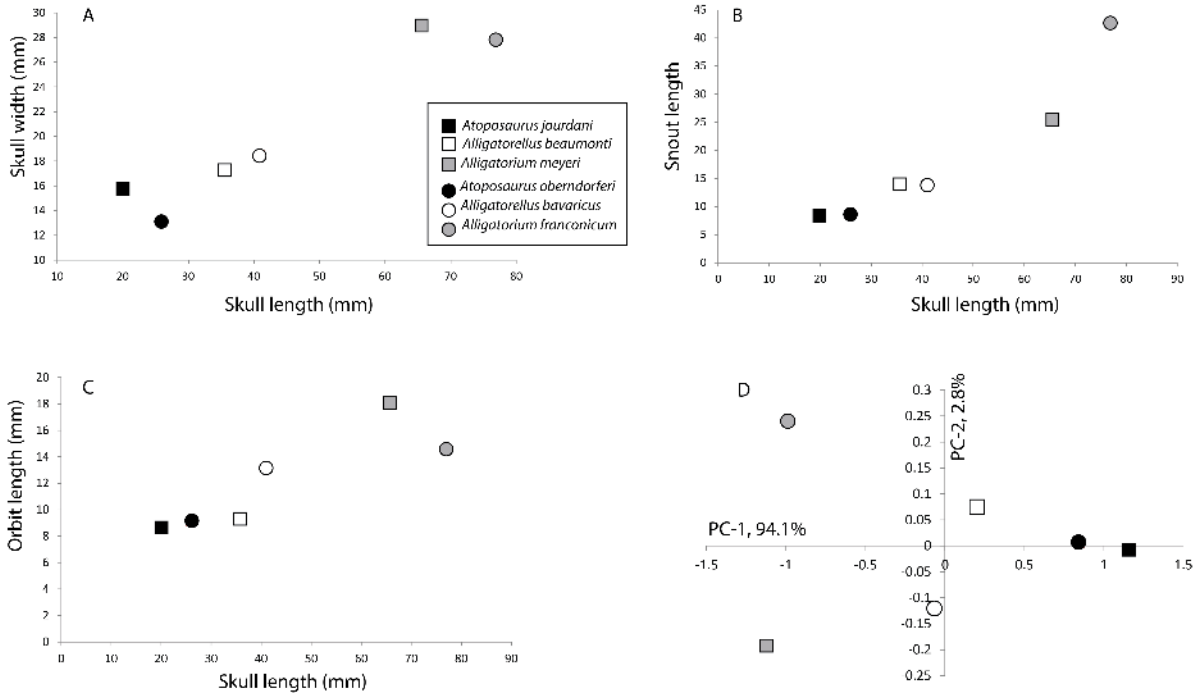


Figure 57. Morphometric plots of the holotype specimens of the Late Jurassic atoposaurids *Alligatorellus*, *Alligatorium*, and *Atoposaurus*. (A) Skull length versus skull width; (B) skull length versus snout length; (C) skull length versus orbit length; and (D) PCA plot for all specimens based on six primary measurements. Squares represent French taxa, and circles represent German taxa.

5.7 Putative atoposaurid taxa

In this section, comments and discussion are provided on the systematic position of taxa that historically have been attributed to Atoposauridae, but are here recovered as non-atoposaurids. Here, emended diagnoses are provided for *Montsecosuchus*, '*Alligatorium*' *franconicum*, *Theriosuchus*, '*Theriosuchus*' *ibericus*, '*Theriosuchus*' *sympiestodon*, and *Brillanceausuchus*, for which a non-atoposaurid position is novel to this study, and thetaxonomic affinities of taxa that have previously been recognised as non-atoposaurids (e.g. *Hoplosuchus*) are discussed.

Neosuchia (Benton, 1986)

5.7.1 Montsecosuchus (Buscalioni and Sanz, 1988)

Included species: *Montsecosuchus depereti*

Revised diagnosis: as for the type and only species

Distribution: Early Cretaceous of Spain.

Previous diagnoses and comments: Originally described as a species belonging to *Alligatorium* (Vidal, 1915), the differences with *Alligatorium* were first noted but not formally acted upon through changes in taxonomy (Buffetaut, 1981a). Subsequently, such variation led to the erection of the new genus, *Montsecosuchus* (Buscalioni and Sanz, 1988; Buscalioni and Sanz, 1990b). *Montsecosuchus* is an unusual crocodyliform in its relatively robust and shortened forelimbs with respect to its hindlimbs, including a large, transversely expanded distal humerus and proportionally small manus (Buscalioni and Sanz, 1988; Buscalioni and Sanz, 1990b). It was originally assigned to Atoposauridae based on its overall small size, and is similar to other atoposaurids in the 'hatchet shaped' radiale morphology (Buscalioni and Sanz, 1988; Buscalioni and Sanz, 1990b), but distinct from *Atoposaurus* and *Alligatorellus* in the absence of a reduced fifth metatarsal (Buscalioni and Sanz, 1988; Buscalioni and Sanz, 1990b).

The first phylogenetic analysis of Atoposauridae found *Montsecosuchus* to be either the sister taxon to *Theriosuchus*, or to *Alligatorium* + *Alligatorellus*, with this uncertainty reflecting the unusual morphology of *Montsecosuchus* (Buscalioni and Sanz, 1988). Many of the autapomorphies defined within this study are metric character states (Buscalioni and Sanz, 1988), and therefore might not be solely reliable in generic-level diagnoses within a group in which there is much uncertainty over ontogenetic allometry and potential dwarfism (Joffe, 1967; Schwarz and Salisbury, 2005; Martin *et al.*, 2010; Schwarz-Wings *et al.*, 2011; Tennant and Mannion, 2014). The only recent formal phylogenetic analysis to include *Montsecosuchus* found it to be the sister taxon to *T. guimarotae*, to the exclusion of *T. pusillus* (Figueiredo *et al.*, 2011), although this analysis was not designed to assess the relationships between putative atoposaurids. The only other analysis to include *Montsecosuchus* was that involving the construction of a crocodyliform supertree, so did not formally assess the position of this taxon (Bronzati *et al.*, 2012). The phylogenetic results mostly recover *Montsecosuchus* as a non-atoposaurid taxon, but also outside of Paralligatoridae, in an uncertain position along with *Pachycheilosuchus*. This analysis was not designed to constrain the phylogenetic position of non-atoposaurids, but to recover the composition and relative position of Atoposauridae, and *Montsecosuchus* is considered to be Neosuchia *incertae sedis*. However, in the results of the analysis using implied weights, *Montsecosuchus* nestles within Atoposauridae (Figure 44). However, while this result might seem more favourable based on previous interpretations of atoposaurid relationships, it has been found that implied weighting has a tendency to propagate errors by inconsistently and incorrectly resolving nodes (Congreve and Lamsdell, 2016), and therefore caution should be applied when interpreting the results of this analysis and the systematic placement of *Montsecouchus*. These inconclusive results warrant further comparison between *Montsecosuchus* and other neosuchians, to determine its affinities. Therefore, I await the inclusion of *Montsecosuchus* into analyses covering broader neosuchian relationships (Adams, 2014; Turner, 2015) to resolve its phylogenetic relationships.

A further specimen has been identified as *Montsecosuchus* sp. from the late Barremian Huérgina Formation of Cuenca, Spain (Sanz *et al.*, 2014), but I have not observed this specimen directly, and there is not enough information in that publication, so cannot comment on this further. Examination of this material, and further discoveries of additional material - particularly of the basicranial region - will be important in determining the relationships of this enigmatic taxon.

5.7.1.1 *Montsecosuchus depereti* (Buscalioni and Sanz, 1988)

Alligatorium depereti (Vidal, 1915)

Type locality and horizon: Le Pedrera de Rubies Formation, late Berriasian–early Barremian (Early Cretaceous); Sierra del Montsec, Lérida Province, Spain.

Type specimen: MGB 512, near-complete skeleton and skull, and counterpart MGB 597.

Revised diagnosis and discussion: **(S1) Intertemporal mediolateral width greater than interorbital width (C19.1).** The relatively high proportion of the interorbital relative to intertemporal region is a feature shared with '*Alligatorium*' *franconicum*, *Alligatorellus beaumonti* (Wellnhofer, 1971; Tennant and Mannion, 2014) and *Pachycheilosuchus* (Rogers, 2003). In protosuchians, coelognathosuchians, paralligatorids, *Alligatorium meyeri*, and *Theriosuchus pusillus*, the interorbital width exceeds the width of the intertemporal region. It is unlikely that variation in this feature is exclusively due to relative growth differences through ontogeny in all of these species, as there are multiple additional lines of evidence that indicate that many specimens had reached skeletal maturity (e.g., neurocentral fusion).

(S2*) Intermandibular angle 61° (C24.3). *Montsecosuchus* has an extremely anteroposteriorly short and mediolaterally wide skull for its body size, as previously noted (Buscalioni and Sanz, 1990b). The only other taxon to come close to this characteristically wide intermandibular angle is *Atoposaurus*

jourdani (55°), in which this state could be due to an allometric growth factor (Schwarz-Wings *et al.*, 2011; Tennant and Mannion, 2014). Other brevirostrine taxa, including *Wannchampsus*, *Brillanceausuchus*, *Shamosuchus*, and *Theriosuchus pusillus* have intermandibular angles in the range of 40–45°. Longirostrine taxa, including *Koumpiodontosuchus* and *Amphicotylus*, have a much lower intermandibular angle of 32–34° (Table 16).

(S3) Skull anteroposterior length to supratemporal fenestra length ratio 8.9 (C29.3). This dimension reflects the extremely small external supratemporal fenestra of *Montsecosuchus* despite its small skull size, and is similar to *Amphicotylus* (8.57) and *Koumpiodontosuchus* (8.0), as well as possibly *Karatausuchus* (8.41). *Brillanceausuchus* represents the opposite end of the spectrum, with a proportionally longer supratemporal fenestra (ratio of 5.36) (Table 20). Atoposaurids, *T. guimarotae*, *T. pusillus*, and *Protosuchus richardsoni* fall within a range of around 6–7.5.

(S4) Longitudinal ridge on the jugal below lateral temporal fenestra (C87.1). The presence of a longitudinal ridge on the lateral surface of the jugal, just below the lateral temporal fenestra, is shared with *Theriosuchus guimarotae* (Schwarz and Salisbury, 2005), and '*T.*' *ibericus*. In atoposaurids, the lateral margin of the jugal is smooth, although this cannot be observed in the holotypes of *Alligatorellus beaumonti* or *Atoposaurus jourdani* due to the dorsal flattening of these specimens.

(S5*) Lateral border of the skull roof terminates immediately dorsal to the medial-most point of contact with the quadrate (C118.1). *Montsecosuchus* possesses a very mediolaterally narrow dorsal skull roof compared to the infratemporal region, similar to the eusuchians *Acynodon* (Delfino *et al.*, 2008b), and possibly *Hylaeochampsa* (Clark and Norell, 1992). The lateral extent of the skull roof with respect to the contact with the quadrate is a feature that here is considered to be locally diagnostic for *Montsecosuchus*.

(S6*) Flat and ungrooved parietal-squamosal suture (147.0). The lack of a parietal-squamosal sutural groove is distinct for *Montsecosuchus* among all specimens scored, similar to *Hylaeochampsa* (Clark

and Norell, 1992). In atoposaurids, there is a thin groove occupying the suture, flanked by slightly raised ridges, and in *Theriosuchus* the groove is deeper and expands anteriorly towards the posterior border of the supratemporal fenestra.

(S7) Supraoccipital exposed medially in posterodorsal surface of skull roof (C197.0). The dorsal exposure of the supraoccipital in the posterior margin of the skull roof is a feature shared with *T. pusillus*, *T. guimarotae* (Schwarz and Salisbury, 2005), *Wannchampsus* (Adams, 2014) and *Brillanceausuchus*. However, in these latter two taxa, the supraoccipital is restricted to a thin surface attached to the posteriormost portion of the parietal and squamosal, and is not as well exposed as it is in *Montsecosuchus*, *Theriosuchus*, and *Mahajangasuchus* (Turner and Buckley, 2008). In *Shamosuchus* (Pol *et al.*, 2009), protosuchians, goniopholidids, atoposaurids, and *Hylaeochampsa* (Clark and Norell, 1992), the supraoccipital is not exposed dorsally in the posterior margin of the skull roof.

(S8) Posteriorly domed occipital surface comprising the medial portion of the exoccipitals. The posteriorly domed occipital region is autapomorphic for *Montsecosuchus* (the 'dolichocephalous' condition) (Buscalioni and Sanz, 1990b), whereas in other taxa this surface is flat and faces posteriorly or posteroventrally. However, caution is urged in the interpretation of this character state as autapomorphic as others have (Buscalioni and Sanz, 1990b), because it is clear that this specimen has undergone a degree of dorsoventral flattening, and therefore a component of this character could pertain to the displacement of the exoccipitals.

(S9*) Posteriorly projecting and dorsally recurved retroarticular process (C242.3). This morphology is shared only with *Brillanceausuchus*, and here it is considered to be a local autapomorphy for *Montsecosuchus*. The morphology of the retroarticular process appears to be highly phylogenetically informative, with taxa such as *Alligatorellus* having a posteriorly projecting but ventrally recurved form, similar to *Simosuchus* (Buckley *et al.*, 2000) and *Stolokrosuchus* (Sereno *et al.*, 2003), whereas in

Theriosuchus pusillus and *T. guimarotae* the process projects posteroventrally and is 'paddle-shaped' (Schwarz and Salisbury, 2005; Pol *et al.*, 2009), similar to *Rugosuchus* (Wu *et al.*, 2001a) and notosuchians (Gomani, 1997). More advanced neosuchians appear to have an extremely reduced, or completely absent, retroarticular process (e.g., *Wannchampsus* and *Shamosuchus*) (Pol *et al.*, 2009), a condition similar to *Protosuchus* (Colbert *et al.*, 1951) and the notosuchian *Yacarerani boliviensis* (Novas *et al.*, 2009).

(S10*) Preacetabular (anterior) process of the ilium absent (C291.2). The absence of the preacetabular process on the ilium is a feature that is shared with '*Alligatorium*' *franconicum* (Wellnhofer, 1971). This process is extremely reduced in *Theriosuchus guimarotae* (Schwarz and Salisbury, 2005), *Pachycheilosuchus* (Rogers, 2003), a specimen described as *Theriosuchus* sp. (IVPP V10613) (Wu *et al.*, 1996b), as well as the giant crocodyliform *Sarcosuchus imperator* (Sereno *et al.*, 2001), being 75% or less of the length of the postacetabular process. The reduction of the iliac anterior process is also the condition for notosuchians (Buckley and Brochu, 1999; Pol and Apesteguía, 2005; Turner, 2006; Pol, 2013).

(**S11) Three sacral vertebrae (C274.1).** *Montsecosuchus* is unusual in that it appears to have three sacral vertebrae, a feature that seems to be shared exclusively with *Alligatorellus* (Buscalioni and Sanz, 1990b) within Neosuchia (Table 18), and could relate to reconfiguration of the pelvic girdle (also see S10) due to mechanical requirements for adaptation to a more terrestrial mode of life. Other occurrences of a third sacral vertebra among crocodyliforms are documented in notosuchians (Riff and Kellner, 2011; Pol, 2013).

(S12*) Dorsal osteoderms not imbricated (C313.1) or sutured (C314.1), oval-shaped, and with medially-placed anteroposterior keel on dorsal surface (C311.1 and C312.1). The osteoderms of *Montsecosuchus* are distinct from those assigned to *Theriosuchus* and atoposaurids, in that they appear not to contact each other, forming two evenly spaced rows. The shape and spacing is

somewhat similar to some of the dorsal osteoderms observed in *Brillanceausuchus*. Cervical osteoderms are not preserved, and there is no evidence of an anterolateral process. In *Alligatorellus*, *Alligatorium*, *Pachycheilosuchus* and *Theriosuchus*, the osteoderms are sub-rectangular to square shaped, and form a distinct dorsal shield. Similar to *Alligatorellus* is the presence of the anteroposterior dorsal keel (Tennant and Mannion, 2014), but this appears to have a uniform morphology anteroposteriorly along the axial column in *Montsecosuchus*.

(S13*) Accessory osteoderms present in dorsal series (C316.1). *Montsecosuchus* also possesses accessory osteoderms that do not contribute to the main dorsal dermal shield. The presence of accessory osteoderms is also known in a range of mesoeucrocodylians, including dyrosaurids (Schwarz-Wings *et al.*, 2009a), the hylaeochampsid *Pietraroiasuchus ormezzanoi* (Buscalioni *et al.*, 2011), the advanced neosuchians *Susisuchus anatoceps* (Figueiredo *et al.*, 2011) and *Isisfordia* (Salisbury *et al.*, 2006), and the eusuchian *Acynodon adriaticus* (Delfino *et al.*, 2008b).

(S14*) Caudal osteoderms oval-shaped (C326.0) with serrated lateral edges (C327.0). The caudal osteoderms have an oval profile in dorsal view, a feature not known in any atoposaurid or *Theriosuchus*. The serration of the lateral edges of each caudal osteoderm is also diagnostic when combined with the overall morphology of the caudal series, but is a feature shared with *Brillanceausuchus* and *Pachycheilosuchus* (Rogers, 2003).

Neosuchia (Benton and Clark, 1988)

5.7.2 Theriosuchus Owen 1878a

Included species: *Theriosuchus guimarotae* (Schwarz and Salisbury, 2005), *Theriosuchus grandinaris* (Lauprasert *et al.*, 2011), *Theriosuchus pusillus* (Owen, 1878a; 1879). '*Theriosuchus*' *ibericus*

(Brinkmann, 1989; 1992) and '*Theriosuchus*' *sympiestodon* (Martin *et al.*, 2010; Martin *et al.*, 2014c) are excluded from this genus (see below).

Distribution: Late Bajocian/Bathonian (Middle Jurassic) to Cenomanian (early Late Cretaceous) of Western Europe; Bathonian (Middle Jurassic) of Morocco; Early Cretaceous (possibly latest Jurassic too) of Asia.

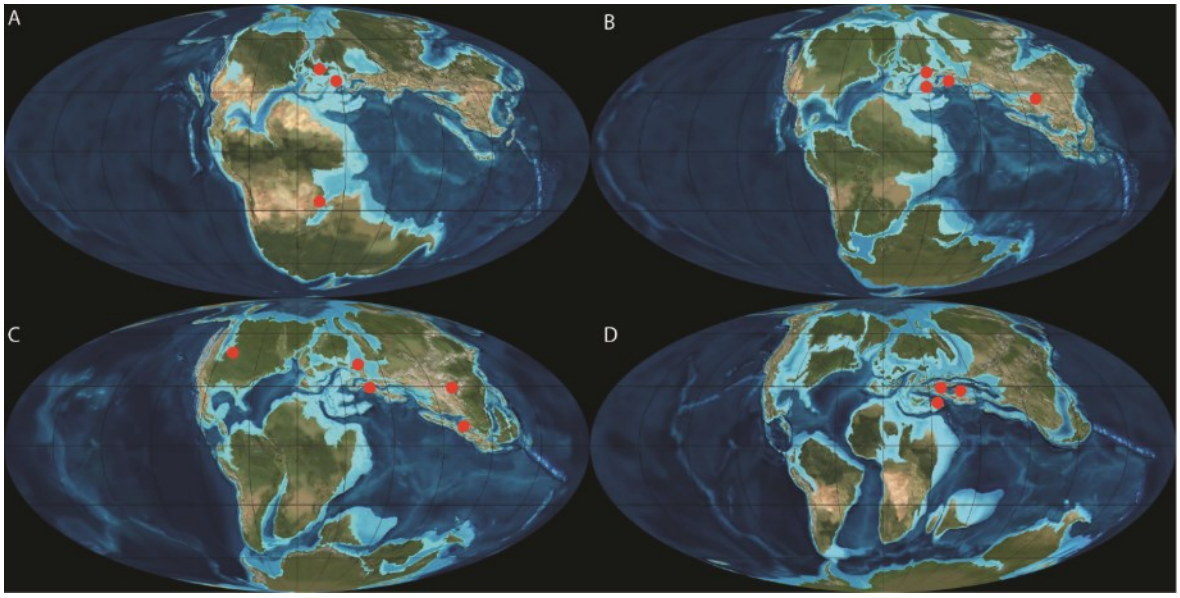


Figure 58. Map of *Theriosuchus* and *Theriosuchus*-like specimens from the (a) Middle Jurassic, (b) Upper Jurassic, and (c) Lower Cretaceous and (d) Upper Cretaceous. See the discussion for the relevant references. Palaeomaps were modified version of high-resolution versions kindly provided by Ron Blakey (http://cpgeosystems.com/).

Note on taxonomy: The identification of the genus *Theriosuchus* has been generally attributed to an incorrect publication (Owen, 1879), and was actually first named one year prior to this (Owen, 1878b) – see discussion of the type species below. In all of the analyses, *Theriosuchus* is found to be polyphyletic within Neosuchia. *T. pusillus* + *T. guimarotae* are sister taxa, and form a clade with *T. grandinaris* (Lauprasert *et al*., 2011) + *Theriosuchus* sp. (NMS G. 2014.52.1) (Young *et al.*, 2016). The most surprising result is that *Theriosuchus* does not group with other atoposaurids, and is more closely related to more crownwardly placed neosuchians (i.e., paralligatorids). '*T.*' *ibericus* + '*T.*' *sympiestodon*

form a clade that is separated from the other species, and which occupies a position nested within paralligatorids. *T. pusillus* was the first named species of this genus (Owen, 1878b; a; 1879), and therefore retains taxonomic priority for the genus name. Consequently, a new genus name is erected for '*Theriosuchus*' *ibericus* and '*Theriosuchus*' *sympiestodon* (see below), and the revised diagnosis presented below is exclusively for *Theriosuchus*, comprising *T. grandinaris*, *T. guimarotae*, and *T. pusillus* (as well as remains attributed to *Theriosuchus* sp.) (Young *et al.*, 2016).

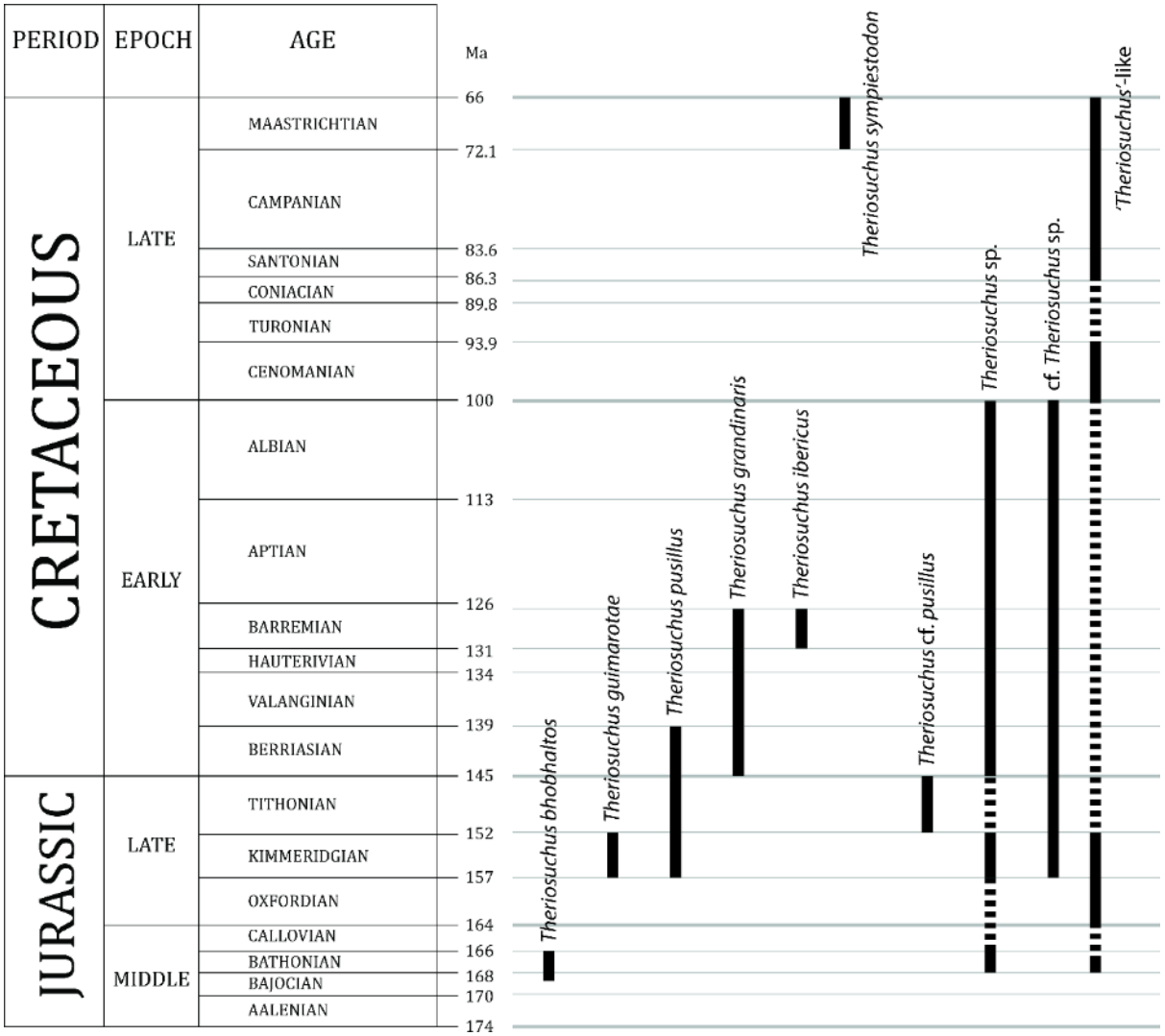


Figure 59. Chronostratigraphic chart of the *Theriosuchus* species, cf. *Theriosuchus* specimens and *Theriosuchus*-like specimens. See the Discussion for the relevant references.

Previous diagnoses and comments: *Theriosuchus* was first identified by the biologist, comparative anatomist and palaeontologist Richard Owen in a series of monographic publications (Owen, 1878b; a; 1879), based on several specimens from the Purbeck beds of England. The genus was first referred to Atoposauridae some years later (Joffe, 1967) in a study which noted numerous similarities between *Theriosuchus pusillus* and atoposaurids from western Europe. Since then, its position has varied within Neosuchia, being positioned either as one of the basal-most taxa within Atoposauridae, or more recently in a much more advanced position as the sister taxon to Paralligatoridae, within Eusuchia (Turner, 2015; Turner & Pritchard, 2015). Jouve *et al*. (2006) also noted the similarities between *Theriosuchus* and other 'advanced' neosuchians, including *Rugosuchus* and *Shamosuchus*, finding them to be closely related to a clade comprising bernissartiids, hylaeochampsids, and crocodylians. Although there are five named species of *Theriosuchus*, typically only *T. pusillus* (Owen, 1878b; a; 1879) has been included in phylogenetic analyses involving Neosuchia, sometimes with *Alligatorium meyeri* as a further representative of Atoposauridae. Exceptions to this comprise several more recent analyses (Martin *et al.*, 2010; Turner, 2015; Turner and Pritchard, 2015), which also included *T. guimarotae* and '*T.*' *sympiestodon*. Whereas the first of these analyses resulted in a monophyletic *Theriosuchus* (Martin *et al.*, 2010), both of the most recent studies recovered *Theriosuchus* as paraphyletic with respect to *Alligatorium meyeri* (Turner, 2015; Turner and Pritchard, 2015), when a series of alternate palatal character state scores for *Isisfordia duncani* (Salisbury *et al.*, 2006) (a possible non-eusuchian susisuchian; (Turner and Pritchard, 2015)) were applied. To my knowledge, neither '*Theriosuchus*' *ibericus* nor *T. grandinaris* have ever been included in a formal phylogenetic analysis. Therefore, the monophyly of *Theriosuchus* has never been fully examined or confirmed, and nor have the character states that support this been tested within a formal phylogenetic framework.

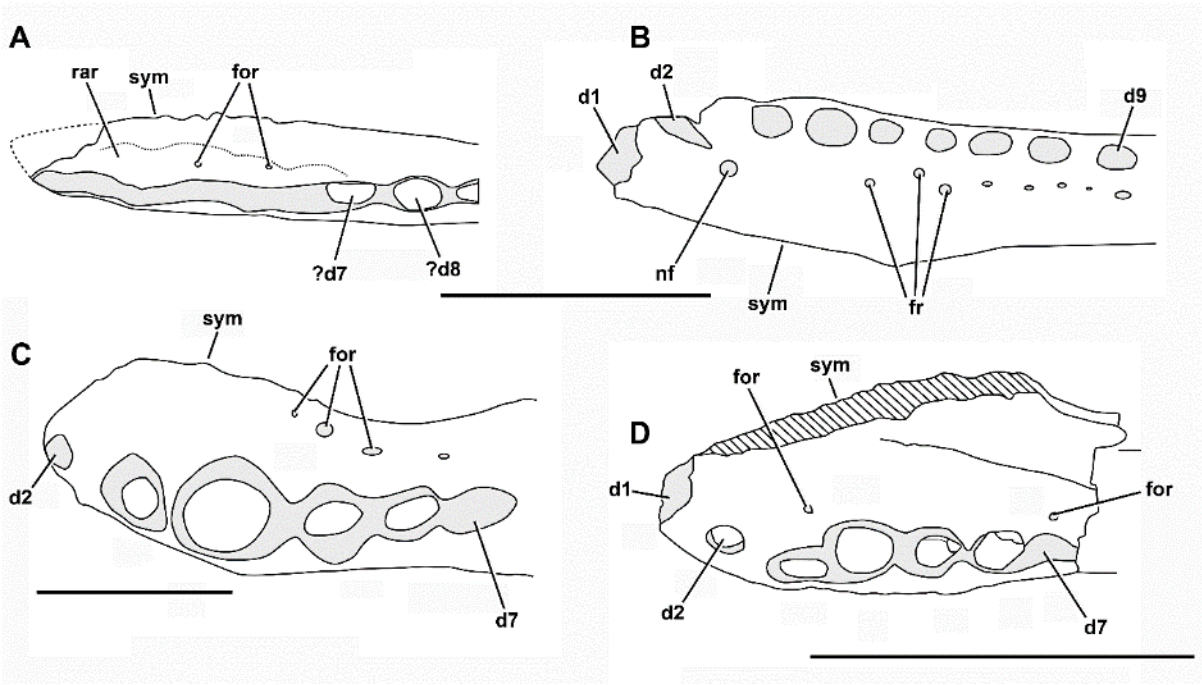


Figure 60. Line drawings of the dentaries of *Theriosuchus* species in dorsal aspect. A, '*T.*' *ibericus*; B, *T. guimarotae*; C, '*T.*' *sympiestodon*; D, *T. pusillus*. Abbreviations: for, nutrient foramina; d, dentary tooth positions; fr, foramen row; nf, nutrient foramen; rar, raised alveolar rims; sym, symphysis. Scale bars represent 10mm.

Diagnoses of *Theriosuchus* have varied since the original description (Owen, 1879). In an unpublished thesis (Clark, 1986), a comprehensive redescription of *Theriosuchus pusillus* was provided, as well as an emended diagnosis. However, these works are yet to be formally published. Subsequently, a diagnosis for *Theriosuchus* was provided but based only on '*T.*' *ibericus* and *T. pusillus* (Brinkmann, 1992). A diagnosis of *Theriosuchus* was included in the description and naming of *T. guimarotae* (Schwarz and Salisbury, 2005), which was repeated subsequently in the description of a poorly known skull and partial skeleton from Germany (Karl *et al.*, 2006), which was cautiously attributed to *T. pusillus*. However, these publications did not discuss '*T.*' *ibericus* in detail (Brinkmann, 1989; 1992), and this was prior to the identification of *T. grandinaris* (Lauprasert *et al.*, 2011) and '*T.*' *sympiestodon* (Martin *et al.*, 2010; Martin *et al.*, 2014c). The most comprehensive recent diagnosis of *Theriosuchus* was provided in a review of crocodyliforms from the Wealden of the UK (Salisbury and Naish, 2011), and which listed the following diagnostic character states: (1) proportionately short and broad

rostrum, with the maxillary rostrum forming between 40–45% of the total skull length; (2) proportionately small antorbital fenestra; (3) slit-like, horizontally orientated and rostrally pointed external nares, separated from each other by the rostral-most extent of the nasals; (4) shallow sulcus on the dorsal surface of the maxillary rostrum, immediately posterior to the junction between the maxilla, premaxilla and nasal; (5) proportionally long jugal; (6) medial base of the postorbital process formed by the ectopterygoid; (7) median crest on the frontal and the parietal in later ontogenetic stages; (8) frontal and parietal partially unfused in early ontogenetic stages; (9) dorsal margin of the supratemporal fenestra smaller than the orbit throughout ontogeny; (10) lateral margin of the squamosal bevelled ventrally; (11) proportionally narrow quadrate with a concave mandibular articular surface; (12) secondary choanae bounded by the palatines rostrally and separated by a median septum of the pterygoids; (13) mandibular symphysis that does not extend posteriorly beyond a point level with the sixth dentary tooth; (14) ilium with short preacetabular process and long postacetabular process; and (15) biserial dorsal shield comprising parasagittal osteoderms. However, it was not clear how all of these character states are distributed across the five named species of *Theriosuchus*. Furthermore, many of these characters can be demonstrated to be more broadly present in Atoposauridae, or characterise smaller sub-groups within *Theriosuchus*. For example, feature 1 is consistently present in all small, brevirostrine crocodyliforms. The presence of an antorbital fenestra is variable (feature 2), with *T. guimarotae* clearly possessing a large fenestra, '*T.*' *sympiestodon* and '*T.*' *ibericus* possibly retaining one, and *T. pusillus* having a pinhole and dorsally placed antorbital fenestra. The presence of an antorbital fenestra is further documented for *Pachycheilosuchus* (Rogers, 2003), and possibly *Alligatorellus bavaricus* (Tennant and Mannion, 2014). The division of the external nares by an anterior projection of the nasals (feature 3) appears to be the condition for *Alligatorium meyeri* and '*Alligatorium*' *franconicum*, as well as *Alligatorellus* (Tennant and Mannion, 2014) and *Wannchampsus* (Adams, 2014). Feature 4 might be diagnostic for *Theriosuchus*, as it was also documented for *T. guimarotae* (Schwarz and Salisbury, 2005), and for '*T.*'

sympiestodon (Martin *et al.*, 2010; Martin *et al.*, 2014c), with this sulcus in a position posterior to the maxilla-nasal-premaxilla triple junction; however, despite first-hand examination of the type specimens, I have been unable to locate this sulcus on *T. pusillus*, '*T.*' *sympiestodon*, or '*T.*' *ibericus*. Therefore, this feature might be diagnostic only for *T. guimarotae*. These characters are discussed in more detail for each taxon below. These features have all been incorporated into the present analysis to test whether they are more broadly present in crocodyliforms, or can be used to diagnose *Theriosuchus* or a sub-set of species within *Theriosuchus*.

5.7.2.1 The dentition of *Theriosuchus*

Species previously assigned to *Theriosuchus* have four dentition-based morphotypes (Owen, 1879; Joffe, 1967; Brinkmann, 1992; Salisbury, 2002; Schwarz and Salisbury, 2005; Schwarz-Wings *et al.*, 2009b; Lauprasert *et al.*, 2011; Salisbury and Naish, 2011), which are typically structured from an anteriorly to more posteriorly position in the following sequence: (1) slender and conical teeth with apicobasally aligned striations that are largely restricted to the lingual face of the crown, located in the premaxilla, and the rostralmost maxilla and dentary (pseudocaniniform morphotype); (2) lanceolate morphotype, moderately labiolingually compressed, with a radial distribution of the marginal lingual striations and mesial and distal carinae, situated in the middle and posterior portions of the maxilla and dentary; (3) labiolingually compressed morphotype, in which teeth are broad and strongly labiolingually compressed, with both the lingual and labial surfaces covered with vertical, straight, and sub-parallel striations (although fan-shaped striations are present only on the lingual face) (Thies *et al.*, 1997); and (4) a 'low-crowned' tooth morphotype that is characterised by the apical margins being oriented at less than 45° from the horizontal, forming a crown that is as mesiodistally broad (or broader) than it is apicobasally tall, and more posteriorly placed in the dental arcade.

In all of these morphotypes, there is variation within the profile shape, size, striation development and strength of carinae, degree of lingual curvature through asymmetrical compression, and shape of

the transverse section (Thies *et al.*, 1997). *Theriosuchus guimarotae* possesses pseudocaniniform and lanceolate tooth morphotypes, all of which exhibit mesial and distal carinae (Schwarz and Salisbury, 2005). *T. grandinaris* possesses a combination of pseudocaniniform, lanceolate-shaped, and labiolingually flattened teeth with faintly crenulated mesial and distal carinae (Lauprasert *et al.*, 2011). The strongly labiolingually compressed morphotype appears to be restricted to *T. pusillus* and '*T.*' *ibericus*. The low-crowned morphotype is only known in '*T.*' *ibericus*, *T. pusillus and* '*T.*' *sympiestodon* (Martin *et al.*, 2010; Martin *et al.*, 2014c).

This 'low-crowned' morphology is distinct from the 'low-crowned' tribodont dentition of *Bernissartia* and *Koumpiodontosuchus* (Buffetaut and Ford, 1979; Norell and Clark, 1990; Schwarz-Wings *et al.*, 2009b; Sweetman *et al.*, 2015), in which the teeth are multi-cusped. However, both morphologies probably had a similar function in crushing harder prey items (e.g., molluscs). This niche specialisation fits in with the ecology and geographic distribution of bernissartiids and *Theriosuchus*, as these taxa represent crocodylomorphs of reduced body size constrained to island environments. In all four dental morphotypes, the apical edges range from smooth, to faintly crenulated or serrated, to possessing well-developed carinae. Ornamentation varies, but includes apicobasally oriented longitudinal ridges on the labial and lingual surfaces of the crown, sometimes more developed on the labial side, and with variation in the regularity of spacing between ridges. It is the presence of crenulations, formed from the faint ridges on the crown, which has been used to ascribe atoposaurids and *Theriosuchus* with their characteristic 'pseudoziphodont' morphology (Prasad and de Broin, 2002). '*Theriosuchus*' *ibericus* is distinct in possessing more prominent serrations on the mesial and distal tooth margins, approaching the fully ziphodont condition. The close packing of the maxillary and dentary alveoli in *Theriosuchus* is similar to a range of neosuchian taxa, including goniopholidids, *Bernissartia* (Buffetaut and Ford, 1979), *Wannchampsus* (Adams, 2014), and *Shamosuchus* (Pol *et al.*, 2009), but is distinct from *Pachycheilosuchus*, *Rugosuchus*, and crocodylians, in which the alveoli are consistently well-separated by interalveolar septae (Wu *et al.*, 2001a; Rogers, 2003; Pol *et al.*, 2009).

This dental variation has led to several differing hypotheses as to the diet of *Theriosuchus*, including the consumption of small mammals (Owen, 1879) or insects (Buscalioni and Sanz, 1988), to herbivory (Brinkmann, 1992), ovivory (Kirkland, 1994), or piscivory (Thies *et al.*, 1997), all based around a semi-aquatic or amphibious mode of life. There is sufficient evidence to accept all of these as valid hypotheses, suggesting that *Theriosuchus* was adept at adapting to take advantage of whichever trophic style fitted its ecological position. However, it is likely that, based on these results, such a morphological or dietary plasticity evolved at least twice independently within advanced neosuchian lineages, or represents a highly adaptive continuum. Finally, it is worth noting that among definitive atoposaurids, *Alligatorium* and *Alligatorellus* both exclusively have smooth-surfaced teeth lacking ridges (Wellnhofer, 1971; Tennant and Mannion, 2014), and the teeth of *Atoposaurus* and *Montsecosuchus* are still unknown (Buscalioni and Sanz, 1988; Buscalioni and Sanz, 1990b; Thies *et al.*, 1997).

Recently, some of the oldest known diagnosable remains of *Theriosuchus* have been identified from the Middle Jurassic of Europe (Young *et al.*, 2016), and those authors provided a list of dentary synapomorphies that might diagnose *Theriosuchus*. This included the presence of a heterodont dentition, with a combination of pseudocaniniform, labiolingually compressed and lanceolate (or 'leaf-shaped') tooth crown morphotypes (Schwarz and Salisbury, 2005; Lauprasert *et al.*, 2011), which have never previously been incorporated within a phylogenetic analysis that includes atoposaurids, despite their clear importance in diagnosing species of *Theriosuchus*. The more posteriorly placed teeth in *Theriosuchus* possess 'false denticles' (Prasad and de Broin, 2002), accompanied by a progressive reduction in alveolus size from the fourth-to-sixth dentary alveoli. Some of these dentary alveoli form a confluent chain, with the dental arcade occupying an anteroposterior sulcus. Most recently, it has been noted that there are additional features that might be characteristic of less-inclusive sub-groups within the *Theriosuchus* species complex (Young *et al.*, 2016), including: (1) a non-spatulate anterior dentary in lateral view (i.e., straight or slightly convex in dorsoventral profile); (2) a dual pair of

foramina medial to the dental arcade on the occlusal dental surface, the position of which may vary intraspecifically; (3) vertically festooned external alveolar margins; (4) raised internal alveolar margins; and (5) a symphyseal suture extending to the D5-D7 alveoli. The features that unite the clades *T. pusillus* + *T. guimarotae*, and '*T.*' *ibericus* + '*T.*' *sympiestodon* are discussed below.

Revised diagnosis of *Theriosuchus* and discussion: (S1) Premaxilla-maxilla suture aligned posteromedially in dorsal view (C47.1). The posteromedial alignment of the premaxilla-maxilla suture was originally regarded as an autapomorphy of *T. grandinaris* (Lauprasert *et al.*, 2011), but it also characterises *T. guimarotae* and *T. pusillus*, and therefore it is considered to be diagnostic for *Theriosuchus*. This feature cannot be assessed in '*T.*' *sympiestodon*, but might be present in '*T.*' *ibericus* (specimen PIFUB 102/21.43), although the posterior end of this premaxilla is broken, and I cannot be certain of the nature of the contact with the maxilla.

(S2) Absence of a maxillary occlusal pit for reception of an enlarged dentary tooth, anterior to maxillary dental arcade (C54.0). The absence of a maxillary occlusal pit is shared with *Pachycheilosuchus* (Rogers, 2003). There is an occlusal pit present in both '*Theriosuchus*' *sympiestodon*, for which a referred specimen (MCDRD 134) has an associated enlarged dentary tooth (Martin *et al.*, 2014c), and '*Theriosuchus*' *ibericus*, anterior to the hypertrophied fifth maxillary tooth. The goniopholidid *Amphicotylus* also appears to possess this occlusal pit, visible in lateral view (Mook, 1942).

(S3) Lacrimal tapers posteroventrally, not contacting jugal or only forming a point contact (C77.1). The morphology of the lacrimal is not known in '*T.*' *ibericus* or '*T.*' *sympiestodon*, but the morphology exhibited by *Theriosuchus* is distinct from atoposaurids, *Wannchampsus* (Adams, 2014), *Brillanceausuchus*, and *Koumpiodontosuchus* (Sweetman *et al.*, 2015), in which the lacrimal extends posteroventrally and broadly contacts the jugal.

(S4) External surface of the dentary (C201.1) and splenial (C202.1) sculpted, including grooved or rugose patterning posteriorly. The morphology of the dentary is poorly known among atoposaurids due to poor preservation (Wellnhofer, 1971; Tennant and Mannion, 2014), but all species herein assigned to *Theriosuchus* exhibit strong ornamentation on the external surface of the dentaries, and sometimes on the splenial when preserved (Lauprasert *et al.*, 2011; Young *et al.*, 2016). This sculpting pattern is shared with *Shamosuchus* (Pol *et al.*, 2009) and *Hsisosuchus chowi* (Peng and Shu, 2004), but is distinct from *Montsecosuchus*, *Wannchampsus* (Adams, 2014), *Pachycheilosuchus* (Rogers, 2003), and *Brillanceausuchus* (Michard *et al.*, 1990), in which only the dentary is sculpted, and the external surface of the splenial is smooth and lacks ornamentation.

(S5) Presence of a combination of pseudocaniniform and lanceolate (C253.0), pseudoziphodont maxillary teeth. *Theriosuchus pusillus* also possesses two additional 'low-crowned' and labiolingually-compressed tooth morphotypes. Labiolingually compressed teeth are absent in *Theriosuchus guimarotae* (Schwarz and Salisbury, 2005), and this combination of dental morphologies is unique amongst other heterodont crocodyliforms (e.g., bernissartiids, notosuchians). Low-crowned teeth are also absent in *T. guimarotae and T. grandinaris* (Schwarz and Salisbury, 2005; Lauprasert *et al.*, 2011). '*Theriosuchus*' *ibericus* and '*T.*' *sympiestodon* also possess an enlarged fifth maxillary tooth, typically with a corresponding notch on the dentary, whereas this tooth is not present in *T. grandinaris*, and remains only moderately enlarged in *T. guimarotae* and *T. pusillus*.

5.7.2.2 Unnamed clade: *Theriosuchus pusillus* + *Theriosuchus guimarotae*

There is strong evidence for a sister taxon relationship between *Theriosuchus guimarotae* and *T. pusillus*, with this topology recovered in all resulting trees, and possessing a Bremer support value of 4 and posterior node probability of 0.99. Synapomorphies uniting these two species include: (1) a posteriorly divided and dorsally facing external naris, similar to atoposaurids (Wellnhofer, 1971;

Tennant and Mannion, 2014); (2) a proportionally small antorbital fenestra, less than half of the size of the orbit, similar to *Alligatorellus bavaricus* (Tennant and Mannion, 2014), *Pachycheilosuchus* (Rogers, 2003), and *Hoplosuchus* (Gilmore, 1926); (3) middle maxillary teeth implanted within single, confluent dental groove, similar to '*Theriosuchus*' *ibericus*, in which all maxillary teeth occupy a single groove; (4) frontal with bifurcated anterior process, penetrating the posterior border of the nasals; (5) lateral dentary surface with concavity for reception of enlarged maxillary tooth, a feature also present in '*T.*' *ibericus*, '*T.*' *sympiestodon*, and *Brillanceausuchus*; (6) transitional dentary tooth morphology posteriorly from the 5th alveolus; (7) distinct foramina on the dentary occlusal surface lingual to the 2nd and 3rd dentary alveoli.

5.7.2.3 *Theriosuchus pusillus* (Owen, 1878b) (type species)

Brachydectes minor (Owen, 1879)

Oweniasuchus minor (Woodward, 1885)

Type locality and horizon: Beccles' residuary marls (Salisbury, 2002) Lulworth Beds, Purbeck Group, Berriasian (Early Cretaceous); Durlston Bay, Swanage, Dorset, England.

Lectotype: NHMUK PV OR48216, a near-complete partially articulated skeleton with skull.

Paratype: NHMUK PV OR48330, a near-complete articulated and three-dimensionally preserved skull.

Referred specimens: NHMUK PV OR48328 (holotype of '*Brachydetes minor*'), left mandibular ramus; NHMUK PV OR48244, an articulated lower jaw preserved in dorsal aspect and NHMUK PV OR48262, a well-preserved dentary and teeth, all from the same locality as the type series.

Previous diagnoses and comments: This species name was originally erected based upon seven paravertebral osteoderms figured in a publication by Richard Owen (Owen, 1878b), which are no

longer within the NHMUK collections (Salisbury, 2002). These specimens were figured again in a subsequent publication by the same author (Owen, 1879), but this time they were listed as belonging to an *incertae sedis* crocodyliform. In the same paper, a near-complete skull (NHMUK PV OR48330) and a near-complete skeleton (NHMUK PV OR48216) were also figured and described as *Theriosuchus pusillus* (Owen, 1879; Salisbury, 2002). Alongside this, several additional craniomandibular elements were figured as *Theriosuchus pusillus* (Owen, 1879); however, until further analysis of this material and a census of all Wealden crocodyliform material ascribed to *Theriosuchus*, it cannot be considered to be directly referable to *Theriosuchus pusillus*. In an unpublished thesis (Clark, 1986), NHMUK PV OR48330 was regarded to be the holotype specimen of *Theriosuchus pusillus*, but a subsequent publication designated NHMUK PV OR48216 and NHMUK PV OR48330 as the lectotype and paratype (Salisbury, 2002), respectively, which is followed here. Until a revision of the type species is conducted, including the referral of other putative specimens, the *T. pusillus* OTU is restricted to the lectotype and paratype, as well as NHMUK PV OR48244 and NHMUK PV OR48262, following the most recent analysis of *Theriosuchus* specimens (Young *et al.*, 2016). All current authors regard '*Oweniasuchus* ('*Brachydectes*') *minor*' (Owen, 1879; Woodward, 1885) as a junior synonym of *T. pusillus* (Clark, 1986; Brinkmann, 1992; Salisbury, 2002; Schwarz and Salisbury, 2005), an interpretation which is followed here pending further analysis of the Purbeck crocodyliform material.

Theriosuchus pusillus possesses an unusual combination of derived and plesiomorphic character states, the latter of which might be related to the retention of paedomorphic features associated with its small body size, although both of the specimens belonging to the type series are skeletally mature (Martin *et al.*, 2014c). This heterogeneity is emphasised by the equivocal phylogenetic positions recovered for this taxon (and Atoposauridae), possibly exacerbated by the representation of the '*Theriosuchus* complex' often as a single taxon (i.e., *Theriosuchus pusillus*), and the lack of use of appropriately sampled character matrices to resolve its phylogenetic position. Features that might be driving the uncertainty in the phylogenetic position of *Theriosuchus* include:

(1) The presence of a longitudinal ridge on the external surface of the angular, which is shared with the paralligatorids *Rugosuchus*, *Shamosuchus* and *Wannchampsus* (Wu *et al.*, 2001a; Pol *et al.*, 2009) and is a feature uniting *Theriosuchus* + Paralligatoridae according to the most recent analyses (Turner, 2015). However, the presence of this feature on the type specimen of *T. pusillus* could not be confirmed, or on any other specimen assigned to *Theriosuchus*.

(2) In *T. pusillus*, the splenial contributes significantly to the dorsal surface of the mandibular symphysis (Lauprasert *et al.*, 2011; Young *et al.*, 2016), similar to basal crocodylians and a range of basal mesoeucrocodylians (Buffetaut, 1981a; Ortega *et al.*, 1996a; Pol *et al.*, 2009). However, I was unable to observe this feature in definitive atoposaurids, because of the manner in which they are preserved.

(3) The presence of a raised supraorbital ridge in *T. pusillus* is similar to a range of neosuchians, including *Trematochampsa* (Buffetaut, 1976), *Bernissartia* (Buffetaut, 1975; Buffetaut and Ford, 1979; Norell and Clark, 1990), *Hylaeochampsa* (Clark and Norell, 1992), *Shamosuchus*, and several crocodylians (Pol *et al.*, 2009). This feature is absent in definitive atoposaurids, goniopholidids, dyrosaurids, and pholidosaurids, and secondarily lost among most crocodylians (Pol *et al.*, 2009).

(4) A preorbital lacrimal-prefrontal sutural crest might be present in *Theriosuchus pusillus*, a feature that was recently stated as common for *Theriosuchus* (Turner, 2015), and shared with more advanced neosuchians including *Shamosuchus*, *Rugosuchus*, *Wannchampsus*, and some goniopholidids. There does appear to be a slight longitudinal crest on the paratype specimen of *Theriosuchus pusillus*, although it cannot be ruled out that this is due to taphonomic distortion, as the skull shows evidence of dorsoventral compression.

(5) The morphology of the retroarticular process in *T. pusillus*, as well as in *Alligatorellus* and *Alligatorium*, is similar to goniopholidids, *Shamosuchus*, and other advanced neosuchians (Pol *et al.*, 2009) in being reduced and ‘paddle-shaped’, and projects posteriorly or posteroventrally. This is

distinct from crocodylians in which the dorsally facing retroarticular process is more anteroposteriorly elongated and sub-triangular (Pol *et al.*, 2009).

(6) The anterior ends of the palatine bar between the suborbital fenestrae are subparallel in *Theriosuchus pusillus*, similar to some members of Eusuchia, dyrosaurids, and the pholidosaurid *Terminonaris robusta* (Wu *et al.*, 2001b), and not laterally flared as in other advanced neosuchians, such as *Shamosuchus* (Pol *et al.*, 2009) and *Wannchampsus* (Adams, 2014). Additionally, the expansion of the posterior ends of the palatines, just anterior to the choana and pterygoid contact, is similar to *Shamosuchus* (Pol *et al.*, 2009), *Batrachomimus pastosbonensis*, *Rugosuchus*, and *Paralligator gradilifrons* (Turner and Pritchard, 2015), but is distinct from *Wannchampsus* in which the posterior ends remain narrow and parallel (Adams, 2014).

(7) *Theriosuchus pusillus* shares a single appendicular plesiomorphic feature with *Alligatorium meyeri* in that the coracoid is sub-equal in length to the scapula. This is distinct from paralligatorids and hylaeochampsids, in which the coracoid is proportionally smaller (Turner, 2015) (note that the coracoid is about two-thirds the length of the scapula in *Pachycheilosuchus*, not sub-equal as others have stated (Turner, 2015)).

(8) It has previously been stated that goniopholidids and *Theriosuchus pusillus* share a well-developed anterolateral articular peg on the dorsal osteoderms (i.e., a 'peg and socket' articulation) (Pol *et al.*, 2009), a feature also noted for *T. guimarotae* (Schwarz and Salisbury, 2005) and *Theriosuchus* sp. from China (Wu *et al.*, 1996b). However, this comparison was based on a figured osteoderm (now lost) (Owen, 1878b), and I agree with others (Joffe, 1967; Salisbury, 2002) that this feature is not visible in any of the osteoderms preserved on the paratype specimen of *T. pusillus* (NHMUK PV OR 48216), or any other specimens definitively attributable to *T. pusillus*. Rare (Salisbury and Frey, 2001). Goniopholidids are commonly found alongside specimens of *Theriosuchus* isolated and disassociated instances of osteoderms attributed to *Theriosuchus* (Wu *et al.*, 1996b; Schwarz and Salisbury, 2005)

with this articular morphology are more likely to be referable to a small goniopholidid, and therefore the presence of this articular peg should not be used to unite *Theriosuchus* with goniopholidids until it can be shown that a specimen that definitively belongs to *Theriosuchus* possesses this morphology.

Revised diagnosis of *Theriosuchus pusillus* and discussion: (S1) Skull anteroposterior length to orbit length ratio between 3.5 and 4.0 (3.83 [NHMUK PV OR48330]) (C27.1). This feature illustrates the characteristically large orbits that *Theriosuchus pusillus* possesses, and has often been used to support the referral of this taxon to Atoposauridae. This ratio is similar to *Wannchampsus* (3.72) and *Alligatorellus beaumonti* (3.86), but is higher than *Atoposaurus* (2.33–2.86), *Alligatorellus bavaricus* (3.12), *Alligatorium meyeri* (3.64), *Karatausuchus* (3.36) (Storrs and Efimov, 2000), and *Hoplosuchus* (3.10) (Gilmore, 1926). The relative sizes of the orbit and supratemporal fenestra do not appear to decrease through ontogeny in *Theriosuchus*, and the retention of this feature is therefore likely to be a paedomorphic state related to the generally small body size of *Theriosuchus* (Schwarz and Salisbury, 2005).

(S2) Abrupt mediolateral expansion of the nasals adjacent to the maxilla anterior to the lacrimals and prefrontals (C70.0). This feature is also present in *Koumpiodontosuchus* (Sweetman *et al.*, 2015) and *Brillanceausuchus*, but is distinct from the condition in *Theriosuchus guimarotae*, in which the lateral margins of the nasals are parallel throughout their length (Schwarz and Salisbury, 2005). In atoposaurids, *Wannchampsus*, *Shamosuchus* (Pol *et al.*, 2009), *Theriosuchus grandinaris*, protosuchians, and goniopholidids, the nasals gradually widen posteriorly.

(S3) Posterior tips of nasals perforated by an anterior, sagittal projection of the frontals (C73.1). This contact between the frontals and the nasals is similar to *Shamosuchus* (Pol *et al.*, 2009), *Brillanceausuchus*, and goniopholidids (Mook, 1942; Salisbury *et al.*, 1999; Smith *et al.*, 2010; de Andrade *et al.*, 2011b; Pritchard *et al.*, 2012), contrasting with the transverse suture that characterises *Alligatorellus* and other neosuchians (e.g. *Gilchristosuchus*) (Wu and Brinkman, 1993). Notosuchians

are similar in possessing a transversely oriented suture, but this is distinct from the simple sutures seen in some neosuchians because it displays a complex interdigitation between the frontals and nasals (Ortega *et al.*, 2000; Turner, 2006). Goniopholidids, including *Eutretauranosuchus* (Smith *et al.*, 2010) and *Amphicotylus* (Mook, 1942), possess an anterior projection of the frontals, which is sometimes anteriorly bifurcated. More advanced eusuchians, including *Acynodon iberoccitanus*, have a posteriorly convex frontal-nasal suture, although smaller individuals of this taxon have transversely oriented sutures (Martin, 2007).

(S4) Minimum intertemporal width more than one third of total width of cranial table. This feature describes a proportionally broad parietal-frontal region between the supratemporal fenestrae on the dorsal skull roof, and is a feature shared by a range of taxa, including atoposaurids (Wellnhofer, 1971; Tennant and Mannion, 2014), *Montsecosuchus* (Buscalioni and Sanz, 1990b), '*Theriosuchus*' *sympiestodon* (estimated based on an incomplete skull table) (Martin *et al.*, 2010; Martin *et al.*, 2014c), and *Brillanceausuchus*. A new character was not created to describe this feature, because of probable non-independence with C19, which describes the relative width of the interorbital and intertemporal regions.

(S5*) Palatines laterally diverge posteriorly, forming palatine bars around choanal groove (C176.1). The palatines of *T. pusillus* form the anterior and lateral borders of the choana, and laterally diverge posteriorly between the suborbital fenestrae, becoming thickened and rod-like lateral to the choana, where they overlap the anterior portion of the pterygoids that contributes to the lateral margins of the choana. *Wannchampsus* has a similar morphology, but possesses a deeper choanal groove, which is slightly more posteriorly placed (Adams, 2014). This is distinct from some notosuchians, in which the palatine rods are more laterally directed around the choanal groove (Godoy *et al.*, 2014), and from bernissartiids in which the bars are formed from the anterior extension of the pterygoids.

(S6*) Choana with anterior border mid-way anteroposteriorly between suborbital fenestrae (C181.0), with a V-shaped palatine-pterygoid contact defining anterior edge, and divided anteriorly by a pterygoidean choanal septum (C183.1). The choanal morphology of *T. pusillus* is distinct in that the anterior edge of the choanal groove is situated relatively anteriorly between the suborbital fenestrae, compared to more advanced neosuchians (e.g., bernissartiids and paralligatorids). The choana in *T. pusillus* also receives an anterior and lateral contribution from the palatine, with a V-shaped contact similar to *Rugosuchus* (Wu *et al.*, 2001a), representing an intermediate morphology between basal neosuchians and eusuchians. The groove is divided by a choanal septum of the pterygoid, similar to *Theriosuchus guimarotae* (Schwarz and Salisbury, 2005), *Araripesuchus* (Ortega *et al.*, 2000; Turner, 2006), *Hsisosuchus* (Peng, 1996), and paralligatorids such as *Batrachomimus* (Montefeltro *et al.*, 2013) and *Paralligator* (Turner, 2015).

(S7) Absence of external mandibular fenestra (C207.0). *Theriosuchus pusillus* completely lacks an external mandibular fenestra, as is also the case in *Shamosuchus* (Pol *et al.*, 2009), *Wannchampsus* (Adams, 2014), *Goniopholis* (Salisbury *et al.*, 1999), and *Bernissartia* (Buffetaut, 1975; Buffetaut and Ford, 1979; Norell and Clark, 1990). This is distinct from most eusuchians and crocodylians, in which the external mandibular fenestra is secondarily well developed (Salisbury *et al.*, 2006), or reduced to a slit-like opening (Brochu, 2004).

(S8) Dorsolateral edge of dentary presenting two concave 'waves' (dorsal expansions) (C232.1). The dorsolateral edge of the dentary in *T. pusillus* is similar to *Wannchampsus* (Adams, 2014), *Koumpiodontosuchus* (Sweetman *et al.*, 2015), as well as '*T.*' *ibericus* and '*T.*' *sympiestodon*. In *Alligatorium meyeri* and *Theriosuchus guimarotae*, the dentary is straight, closer to the condition in *Shamosuchus* (Pol *et al.*, 2009) and *Brillanceausuchus*.

(S9*) Splenial dorsally inset into symphysis in ventral view (C234.1). Where the splenial of *T. pusillus* enters into the symphysis, it is dorsally inset with respect to the ventral surface of the mandible, and

slopes posterodorsally. This is a feature otherwise only observed in *Atoposaurus oberndorferi* and therefore it is considered here to be locally autapomorphic. In other taxa in which the ventral surface of the mandible can be observed, the contact between the splenial and dentary portion of the symphysis is ventrally confluent.

(S10*) Heterodont dentition, possessing a combination of anteriorly positioned pseudocaniniform teeth, intermediately positioned labiolingually compressed 'lanceolate' teeth (C253.0), and posteriorly placed 'low-crowned' teeth (C254.0). This unique combination of the three dental morphotypes in *T. pusillus* is diagnostic among all known species of *Theriosuchus* and all other known heterodont crocodylomorphs. The low-crowned morphotype is not known in either *T. guimarotae* or *T. grandinaris* (Schwarz and Salisbury, 2005; Lauprasert *et al.*, 2011).

(S11) Biconvex first caudal vertebra (C278.1). This is an unusual feature of the axial bracing system in crocodylomorphs (Salisbury and Frey, 2001), and related to the development of procoely throughout the axial series in neosuchians, which has a complicated and unresolved evolutionary history (Salisbury and Frey, 2001). The presence of a biconvex first caudal vertebra is also shared with *Pachycheilosuchus* (Rogers, 2003), *Bernissartia* (Buffetaut, 1975; Buffetaut and Ford, 1979; Norell and Clark, 1990), as well as possibly *Brillanceausuchus* (Michard *et al.*, 1990), and characterises all eusuchians (Salisbury *et al.*, 2006; Blanco *et al.*, 2014), including marine forms (Brochu, 2004).

(S12*) Posterior surface of tibial shaft curved, leaving a void between the tibia and fibula (C299.1). The tibia and fibula of *T. pusillus* are unusual in that they are not confluent, as in other crocodylomorph taxa. Similar to *Montsecosuchus* (Buscalioni and Sanz, 1988; Buscalioni and Sanz, 1990b), the tibial shaft is curved, which leaves a void between the tibia and fibula, the mechanical implications of which are unclear.

(S13) Square-shaped dorsal osteoderms (in dorsoventral view) (C308.3). The square-shaped osteoderms of *T. pusillus* form a well-developed biserial shield, and retain a similar outline shape to

Pachycheilosuchus (Rogers, 2003) and *Alligatorium meyeri* (Wellnhofer, 1971). This is distinct from the oval-shaped dorsal osteoderms of *Montsecosuchus*, and those of *Alligatorellus*, in which they are sub-rectangular.

5.7.2.4 *Theriosuchus guimarotae* (Schwarz and Salisbury, 2005)

Type locality and horizon: Alcobaça Formation (lower "Fundschichten" and upper "Ruafolge" lignite coal layer), Kimmeridgian, (Late Jurassic); Guimarota Coal Mine, Guimarota, Portugal.

Type specimen: IPFUB Gui Croc 7308, partial skull and mandible, with partial isolated surangular, sacral vertebra II, and two partial osteoderms.

Referred specimens (Schwarz and Salisbury, 2005): IPFUB Gui Croc 7309, 7403-1, 7709 (partial skulls); IPFUB Gui Croc 73187, 7520, 8240 (premaxillae); IFPUB Gui Croc 7311, 7319, 7320, 7330, 7415-1, 7503, 7528, 75100, 7606, 7608, 7611, 7612, 7701, 7702, 7713, 7719, 8001, 8101, 8102 (maxillae); IPFUB Gui Croc 7333, 7338, 7405, 7591, 75101, 75102, 7708, 7806, 8106 (palpebrals); IPFUB Gui Croc 8008 (lacrimal); IPFUB Gui Croc 7304, 7406, 7414, 7601, 7602, 7630, 7705, 7717, 7807, 8238 (frontals); IPFUB Gui Croc 73120, 7410, 7456, 7506, 7508, 7511, 7613, 7712, 7903, 8004, 8108 (jugals); IPFUB Gui Croc 7326, 7339, 73121, 7519, 7902 (postorbitals); IPFUB Gui Croc 7343, 73103, 73106, 7703, 8043 (squamosals); IPFUB Gui Croc 7510, 7595, 7732, 7802, 7805, 8003, 8239 (parietals); IPFUB Gui Croc 7455, 8202 (supraoccipitals); IPFUB Gui Croc 7340, 7371, 73107, 73108, 73122, 7578 (ectopterygoids); IPFUB Gui Croc 7501, 7593 (pterygoids); IPFUB Gui Croc 7402, 8204, 8207 (basioccipitals); IPFUB Gui Croc 7447, 7539. 7710 (quadrates); IPFUBGui Croc 7306, 7310, 7316, 73124, 7404, 7411, 7413, 7513, 7518, 7521, 7525, 7530, 7531, 7533, 7534, 7592, 7607, 7704, 7716, 7733, 7737, 7901, 7904, 8005, 8007, 8045, 8105, 8109, 8110 (dentaries); IPFUB Gui Croc 8103, 8201 (splenials); IPFUB Gui Croc 7318, 7331, 7337, 73125, 73186, 7415-2, 7507, 7512, 7524, 7536, 7706, 7707 (angulars); IFPUB Gui Croc

7322, 7328, 73123, 7454, 7587, 7588, 7589, 8042, 8044 (surangulars), IPFUB Gui Croc 7327, 7344 7345, 7347, 7407, 7408, 7412, 7538, 75103, 7605, 7905, 8006, 8046, 8215 (isolated teeth); IPFUB Gui Croc 7352 (caudal vertebrae, right femur, caudal osteoderms); IPFUB Gui Croc 7441 (caudal osteoderms and left ulna); IPFUB Gui Croc 7545 (three articulated dorsal vertebrae, right and left ischium, paravertebral and caudal osteoderms); Gui Croc 7564 (left femur, left humerus, paravertebral osteoderm); Gui Croc 7634 thoracic and lumbar vertebrae, cervical rib, caudal osteoderms); IPFUB Gui Croc 8037 (cervical and dorsal vertebra and osteoderms); IPFUB Gui Croc 7349 (proatlas); IPFUB Gui Croc 7550, 7555 (axis); IPFUB Gui Croc 7381, 7394, 73133 73134, 73135, 7475, 7614, 8138, 8148 (cervical vertebrae); IPFUB Gui Croc 7351, 7360, 7426, 7429, 7560, 75108, 7526, 7743, 7809, 7910, 8033, 8111, 8132 (dorsal vertebrae); IPFUB Gui Croc 7472, 8028 (first sacral vertebrae); IPFUB Gui Croc 7423 (second sacral vertebra); IPFUB Gui Croc 7584 (centrum of sacral vertebra); IPFUB Gui Croc 7363, 7388, 7395, 73137, 73138, 73139, 7422, 7478, 7552, 7575, 75109, 75110, 7633, 7654, 7658, 7682, 7725, 7744, 7811, 7906, 7913, 8024, 8047, 8052, 8114, 8133, 8136, 8218, 8248 (caudal vertebrae); IPFUB Gui Croc 7369, 7629, 7727, 7810, 8123 (cervical ribs); IPFUB Gui Croc 7480, 7570, 8017, 8217 (dorsal ribs); IFPUB Gui Croc 7548, 7549, 8116 (coracoids); IPFUB Gui Croc 7420, 7542, 7661, 7674, 7675, 7908, 8142, 8230 (humeri); IPFUB Gui Croc 7391, 7457, 7641, 7668 (ilia); IPFUB Gui Croc 7580, 7678, 7680, 8130 (ischia); IPFUB Gui Croc 7350, 7366, 7389, 7396, 73140, 73141, 73142, 7428, 7839, 7482, 7543, 7544, 7553, 7564, 7568, 7577, 7585, 7599, 75112, 75113, 75127, 7617, 7618, 7621, 7624, 7625, 7643, 7722, 7723, 7728, 7909, 8010, 8016, 8135, 8139, 8210, 8212 (femora); IPFUB Gui Croc 7348, 7397, 7562, 8025, 8039, 8053, 8221, 8231 (tibiae); IPFUB Gui Croc 73125, 7659, 8141, 8232 (metatarsals); IPFUB Gui Croc 75104, 7579, 8245 (phalanges); IPFUB 7301, 7352, 7355, 7357, 7359, 7374, 7375, 7376, 7377, 7379, 7380, 7383, 7385, 7392, 73101, 73128, 73129, 73130, 73131, 73132, 7415-3, 7416, 7417, 7419, 7421, 7424, 7425, 7430, 7431, 7432, 7434, 7437, 7438, 7441-1-6, 7442, 7458, 7459, 7461, 7462, 7463, 7464, 7465, 7466, 7467, 7468, 7469, 7470, 7471, 7472, 7473, 7474, 7496, 74108, 7563, 7565, 7566, 7572, 7583, 75105, 75106, 75107, 75118, 75134, 75135, 7623, 7627,

7650, 7685, 7729, 7730, 7912, 8012, 8014, 8015, 8019, 8026, 8031, 8037, 8041, 8057, 8058, 8113, 8118, 8125, 8137, 8146, 8147, 8159, 8160, 8216, 8226, 8227, 8228, 8236, 8246, 8247 (osteoderms). All referred specimens are from the same locality as the holotype specimen. The majority are disarticulated, and were collected from at least two different horizons – the upper and lower lignite coal layers (Schwarz and Salisbury, 2005).

Previous diagnoses and comments: A range of diagnostic cranial and axial characteristics for *T. guimarotae* have previously been documented in the original description of this taxon (Schwarz and Salisbury, 2005), and included a detailed comparative discussion of this taxon and other specimens assigned to *Theriosuchus*. However, a number of these features are more widespread among neosuchians. For example, it has been previously noted that the squamosal of *T. guimarotae* is bevelled ventrally, and possesses a notch anteriorly on the lateral surface, both features that were regarded as autapomorphic (Schwarz and Salisbury, 2005). However, these features are also visible in *Theriosuchus pusillus* (NHMUK PV OR48216) and *Brillanceausuchus*. Additionally, the morphology of the posterolateral corner of the squamosal was considered to be diagnostic (Schwarz and Salisbury, 2005), in that it forms a rounded 'lobe', which projects posteriorly and is similarly sculpted to the rest of the cranial table. Although distinct from *T. pusillus* and '*T.*' *ibericus*, which both possess an unsculpted lobe, this overall morphology is similar to *Rugosuchus* (Wu *et al.*, 2001a), *Alligatorium meyeri* and *Alligatorellus beaumonti*. Furthermore, an unsculpted posterolateral lobe is present in *Shamosuchus* (Pol *et al.*, 2009; Turner, 2015), *Sunosuchus* (Wu *et al.*, 1996a) and *Goniopholis* (Salisbury *et al.*, 1999), but might be an ontogenetic feature that occurs in younger individuals. Furthermore, others have considered this feature to be synapomorphic for Atoposauridae (Clark, 1986), but here the presence of this lobe is considered to be a synapomorphy that unites *Theriosuchus* and Paralligatoridae in agreement with more recent analyses (Turner, 2015), and consequently a feature that was acquired independently in some atoposaurids.

Revised diagnosis and discussion: **(S1) Sub-rectangular shaped external supratemporal fenestra, in dorsal view (C17.0).** The shape of the supratemporal fenestra is distinct from that of other species of *Theriosuchus* and advanced neosuchians (Schwarz and Salisbury, 2005), which have a circular or sub-circular outline. The subrectangular morphology in *T. guimarotae* is similar to that of pholidosaurids, such as *Pholidosaurus* (Salisbury, 2002), *Sarcosuchus* (Sereno *et al.*, 2001) and *Chalawan thailandicus* (Martin *et al.*, 2014b), dyrosaurids (Jouve *et al.*, 2005), as well as *Protosuchus richardsoni* (Colbert *et al.*, 1951).

(S2) Proportionally large lateral temporal fenestra, with an area greater than 50% the area of the orbit (C20.2). The lateral temporal fenestra is relatively larger than that of *Theriosuchus pusillus*, *Isisfordia* (Salisbury *et al.*, 2006), and notosuchians (Buckley *et al.*, 2000; Novas *et al.*, 2009). Goniopholidids, *Rugosuchus* (Wu *et al.*, 2001a), *Wannchampsus* (Adams, 2014), and the eusuchians *Allodaposuchus precedens* (Buscalioni *et al.*, 2001) and *Iharkutosuchus makadii* (Ősi *et al.*, 2007; Ősi, 2008), are similar to *T. guimarotae* in the large proportional size of the lateral temporal fenestra to the orbit. In dyrosaurids, the fenestra becomes approximately the same size as the supratemporal fenestra, and proportionally larger than the orbit (Jouve *et al.*, 2005).

(S3) Notch on the posterolateral surface of the premaxilla within the dorsal margin of the external nares (C39.1). Similar to the goniopholidid *Amphicotylus* (Mook, 1942), *T. guimarotae* possesses a shallow fossa, or notch, on the dorsolateral surface of the premaxilla, immediately adjacent to the external nares (Schwarz and Salisbury, 2005), and this feature is considered to be a local autapomorphy for this taxon.

(S4) Nasal-lacrimal contact absent on dorsal surface (C71.1). The lacrimal does not contact the nasal (Schwarz and Salisbury, 2005), instead being medially restricted and only contacting the prefrontal. This contact is also absent in *Protosuchus richardsoni* (Colbert *et al.*, 1951), *Shamosuchus* (Pol *et al.*, 2009), *Hylaeochampsa* (Clark and Norell, 1992), and *Iharkutosuchus* (Turner, 2015), but is present in

the notosuchian *Araripesuchus gomesii* (Turner, 2006) and atoposaurids (Wellnhofer, 1971), and represents a series of reconfigurations of the periorbital elements with respect to the remainder of the rostrum in advanced neosuchians.

(S5) Jugal with posteriorly directed (C83.0), anteriorly placed (C84.0) and ventromedially displaced (C85.1) postorbital process (C83.0). The jugal postorbital process is slightly anteriorly placed, instead of being medially placed, as in other species of *Theriosuchus*, which have equally long anterior and posterior processes of the jugal. This process also has a dorsally directed base similar to *Montsecosuchus* and *Brillanceausuchus*, instead of the posterodorsal orientation that characterises atoposaurids, *T. pusillus* and '*T.*' *ibericus*.

(S6) Anterior process of frontal constricted between the prefrontals (C109.0). This feature excludes the sagittal projection of the frontals into the nasals anterior to the orbits, which some crocodyliforms possess, and refers to the convergence between the lateral margins of the anterior portion of the frontals. This feature is shared with *Alligatorium meyeri*, '*Alligatorium*' *franconicum*, and *Amphicotylus* (Mook, 1942). In other crocodyliforms, including *Alligatorellus* and other species of *Theriosuchus*, the lateral edges of the nasal are not mediolaterally constricted and remain sub-parallel.

(S7*) Ectopterygoid with well-developed anterior process, reaching the posteriormost two maxillary teeth (C170.0). The anterior process of the ectopterygoid is extremely well-developed, reaching a point level with the anterior margin of the sub-orbital fenestra and the posteriormost maxillary teeth. In *Theriosuchus pusillus*, goniopholidids, and paralligatorids, this process is short and poorly developed in ventral aspect.

(S8) Anterior margin of palatines anteriorly pointed (C173.1). The maxilla-palatine suture is posteroventrally directed towards the anterior margin of the suborbital fenestra along the midline, level with the sixth maxillary tooth (Schwarz and Salisbury, 2005). In *T. pusillus*, this contact is gently rounded anteriorly, similar to *Koumpiodontosuchus* (Sweetman *et al.*, 2015). However, this region of

the palate is not preserved in many of the specimens included in the analysis – especially atoposaurids – and therefore this is tentatively considered to be an autapomorphy at present.

(S9) Parallel posterolateral margins of interfenestral bar between suborbital fenestrae (C175.1). The interfenestral bar of *T. guimarotae* is formed entirely from the paired and fused palatines, and the lateral margins of the posterior portion nearing the paired choanae run parallel to one another. This is distinct from *Brillanceausuchus*, in which the lateral margins converge posteriorly, and *Theriosuchus pusillus*, *Wannchampsus*, and *Shamosuchus*, in which the lateral margins flare posterolaterally.

(S10*) Pterygoids excluded from the posterior margin of suborbital fenestra by ectopterygoid-palatine contact (C180.1). The exclusion of the pterygoid ventral lamina from the posterior margin of the suborbital fenestra is unique in *Theriosuchus guimarotae*. In all other specimens analysed, for which the presence or absence of this feature can be assessed (including *T. pusillus*, '*T.*' *sympiestodon*, protosuchians, goniopholidids, and paralligatorids), the pterygoids contribute to the posterior margin of the suborbital fenestra.

(S11*) Completely septated choanal groove (C183.2). The choanae of *T. guimarotae* are completely septated, formed anteriorly by the palatines and posteriorly by the pterygoids, similar to the goniopholidids *Amphicotylus* (Mook, 1942) and *Eutretauranosuchus* (Smith *et al.*, 2010; Pritchard *et al.*, 2012). This morphology is distinct from that in *Theriosuchus pusillus*, in which the choanal groove is partially septated, and '*Theriosuchus*' *sympiestodon* (Martin *et al.*, 2010; Martin *et al.*, 2014c) and other paralligatorids, in which the groove is open and undivided.

(S12) Basisphenoid ventrally exposed anteriorly to the basioccipital (C188.0), and ventral surface continuous with surrounding cranial elements (C190.0). The conformation of the basisphenoid to the remainder of the occipital plane is distinct from that in *Theriosuchus pusillus* and other advanced neosuchians in which the main body of the basisphenoid is separated by a sulcus and posteroventral step.

(S13) Mandibular symphysis of moderate posterior length, posteriorly reaching the 5th-6th dentary tooth position (C204.1). The relative length of the symphysis to the dental arcade is highly variable within species currently and previously assigned to *Theriosuchus*, being short up to the 5th alveolus in '*T.*' *ibericus* (also shared with *Brillanceausuchus*), terminating medial to the 5th and 6th alveolus in *T. guimarotae*, medial to the 6th in '*T.*' *sympiestodon*, and medial to the 7th alveolus in *T. pusillus*, *T. grandinaris*, and *Theriosuchus* sp. (NMS G. 2014.52.1) (Young *et al.*, 2016).

(S14*) External mandibular fenestra present (C207.1). *Theriosuchus guimarotae* possesses the plesiomorphic condition in the retention of a triangular-shaped external mandibular fenestra, as also occurs in *Alligatorium meyeri*, *Protosuchus richardsoni* (Colbert *et al.*, 1951), and *Eutretauranosuchus* (Smith *et al.*, 2010; Pritchard *et al.*, 2012). This morphology is not known in any atoposaurid specimen, although the posterior portion of the dentaries of *Alligatorellus*, *Atoposaurus*, *Montsecosuchus*, and *T. grandinaris* are partially obscured or unknown.

5.7.2.5 *Theriosuchus grandinaris* (Lauprasert *et al.*, 2011)

Type locality and horizon: Sao Khua Formation, Khorat Group, early Aptian (Early Cretaceous); Phu Phok, Kok Prasil Sub-district, Phu Phan District, Sakon Nakhon Province, northwestern Thailand.

Type specimen: PRC-2, fused anterior rostrum and mandible (note that the specimen ID is stated as 'PPC' in the original publication of this taxon (Lauprasert *et al.*, 2011), but the institutional abbreviation is given as PRC).

Previous diagnoses and comments: *T. grandinaris* was originally assigned to *Theriosuchus* (and therefore to Atoposauridae) based on the possession of a brevirostrine skull with the maxilla transversely flattened, symmetrical and pointed at the apex (Lauprasert *et al.*, 2011), which is a feature common in numerous small neosuchian crocodyliforms. The premaxilla-maxilla suture of *T.*

grandinaris is aligned posteromedially in dorsal view, deemed to be diagnostic (Lauprasert *et al.*, 2011), but this feature is also present in *T. guimarotae* (Schwarz and Salisbury, 2005) and *T. pusillus*, and is more likely to characterise the genus *Theriosuchus* (see above). It is not entirely clear what is meant by the 'weak notch' described as present at the premaxilla-maxilla suture (Lauprasert *et al.*, 2011), although such a potential notch is present ventrally in this suture in *T. pusillus* and possibly *T. guimarotae* (Schwarz and Salisbury, 2005), which is for the enlarged dentary tooth. This feature is different from '*T.*' *ibericus* and '*T.*' *sympiestodon*, in which there is a distinct occlusal pit within the dental arcade to accommodate the enlarged dental tooth. The relatively long mandibular symphysis terminating posteriorly medial to the D7 alveolus is a feature shared with *T. pusillus*, but not unique within *Theriosuchus* as previously asserted (Lauprasert *et al.*, 2011), and might be a diagnostic feature for sub-groups within the *Theriosuchus* cluster (Young *et al.*, 2016). The presence of an anteriorly tapering and slender prefrontal was also stated as diagnostic for *T. grandinaris* (Lauprasert *et al.*, 2011) but this morphology is present in both *T. pusillus* and *T. guimarotae*, as well as *Alligatorellus* and paralligatorids.

Revised diagnosis and discussion: **(S1) Fully divided external nares (C10.0).** The presence of paired external nares (i.e., divided by either the premaxilla or an anterior extension of the nasals) might be synapomorphic for Atoposauridae (see above), but is clearly present in *T. grandinaris* too.

(S2) Premaxilla-maxilla suture ventrally confluent (C42.0), with ventral diastema at the contact suture. In the original description of *T. grandinaris* it was stated that there is a diastema at the premaxilla-maxilla suture (Lauprasert *et al.*, 2011), not a lateral concavity as in *T. pusillus* and *T. guimarotae*, which might be diagnostic for this species.

(S3) Nasals gradually widen adjacent to the maxilla (C70.1). The gradual widening of the nasal bones posteriorly is distinct from the condition in *T. pusillus*, in which the lateral margins expand rapidly adjacent to the maxilla and anterior to the periorbital elements, and *T. guimarotae* in which the nasals

are consistently narrow (Schwarz and Salisbury, 2005). This gradual widening of the nasals is reminiscent of longirostrine neosuchians, such as *Rugosuchus* (Wu *et al.*, 2001a).

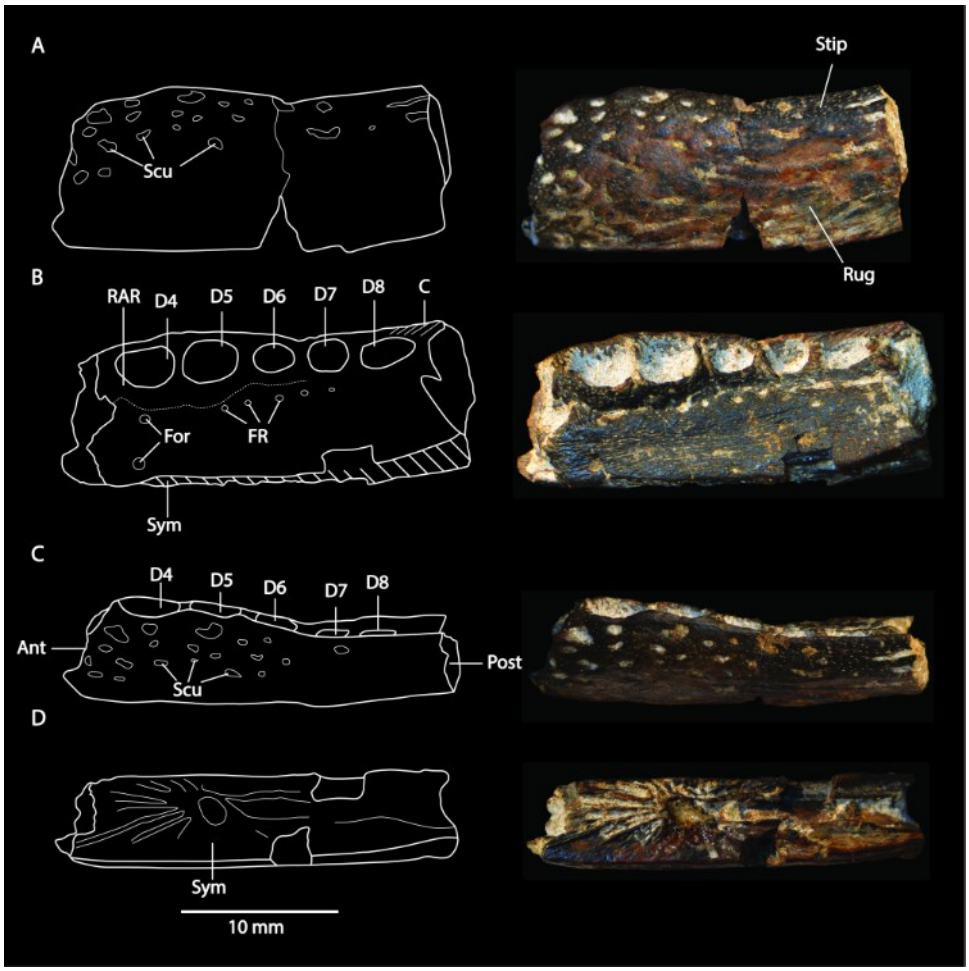
(S4*) Unique combination of pseudocaniniform, lanceolate-shaped (C253.0) and labiolingually flattened (C354.0) teeth with faintly crenulated mesial and distal carinae (C245.0). The heterodont dentition of species attributed to *Theriosuchus* has long been recognised as diagnostic. Heterodonty is not exclusive to *Theriosuchus*, also being known in bernissartiids, notosuchians and a range of other neosuchian taxa (Ősi, 2014). However, variation in dentition differentiates the species of *Theriosuchus* from one another (see above).

Additional comment: *Theriosuchus grandinaris* shares many similarities with a fragmentary specimen described as *Theriosuchus* sp. (NMS G. 2014.52.1) from the Isle of Skye, UK, known solely from the anterior portion of a right dentary (Young *et al.*, 2016). The two are recovered as sister taxa in these analyses, and shared features include: (1) a straight lateral margin of the dentary in dorsolateral view; and (2) a parallel dentary symphysis to the dental arcade. Although this might indicate that *Theriosuchus* sp. is referable to *Theriosuchus grandinaris*, they are widely separated from one another spatiotemporally, and other features allow us to distinguish the two taxa (Young *et al.*, 2016).

5.7.2.6 *Theriosuchus* sp.

European occurrences:

Figure 61. Photographs and line drawings of *Theriosuchus* sp. from the late Bajocian-Bathonian Valtos Sandstone Formation of Skye, Scotland. A, ventral view; B, dorsal view; C, lateral view; D, medial view. Abbreviations: ant, anterior edge; for, nutrient foramina; c, crenulations; d, dentary tooth positions; fr, foramen row; rar, raised alveolar rims; rug, rugose texture; scu, sculpting; stip, stippled texture; sym, symphysis. Scale bar represents 10 mm.



Additional material referred to *Theriosuchus* has been described from a host of other continental European localities, but is typically fragmentary or isolated in nature, and therefore difficult to assign to a particular species. The majority of these have been assigned to *Theriosuchus* based on its highly diagnostic tooth morphotypes, as discussed above. These teeth are usually small, no more then 2–3mm in either dimension. The bases of the crowns are always mesiodistally constricted, and there are varying degrees of labiolingual compression, which can be asymmetrical, leading to a convex labial face and a flat lingual face. A lanceolate tooth morphology is also diagnostic for *Theriosuchus* (see Section 5.7.2.1) (Schwarz and Salisbury, 2005). These occurrences include, in stratigraphic order from oldest to youngest:

(1) *Theriosuchus* sp. is known from a dentary from the late Bajocian–Bathonian of the Isle of Skye, UK (Young *et al.*, 2016). This specimen (NMS G. 2014.52.1), although based on highly fragmentary material, appears to have several unique dental characteristics that distinguish it from *T. grandinaris* and other species of *Theriosuchus*, including: (1) posterolaterally oriented crenulations on the posterior end of the dental arcade; (2) a longitudinally crenulated occlusal surface; and (3) the symphysis not contributing to the splenial (Young *et al*., 2016). Although additional crocodyliform material is in preparation from the Isle of Skye that might be referable to this taxon (Brusatte, S., pers. comm., 2015), the currently available material appears to possess a unique combination of character states among *Theriosuchus* species. Despite this, it was not referred to a new species, because of the fragmentary nature of the remains (Young *et al.*, 2016).

(2) Isolated tooth crowns from the late Bathonian Forest Marble microvertebrate horizon of the UK were referred to Atoposauridae, but described as '*Theriosuchus*'-like (Evans *et al.*, 1994). Based on the information provided (figure 18.6e, p.315) (Evans *et al.*, 1994), at least one of these teeth possesses a pseudoziphodont morphology, and characteristic labiolingually compressed and lanceolate morphology. These specimens are therefore tentatively regarded as cf. *Theriosuchus* sp.

(3) 59 variably worn or abraded teeth, from the Oker and Uppen sections of the Kimmeridgian of northwest Germany, assigned to cf. *Theriosuchus* sp. (Thies *et al.*, 1997). These teeth possess the characteristic lanceolate morphology of *Theriosuchus pusillus* and *T. guimarotae*, and therefore they are considered to represent *Theriosuchus* sp.

(4) Another specimen (DFMMh 200, the anterior part of a crushed skeleton) from the Kimmeridgian of northern Germany was tentatively referred to *Theriosuchus pusillus* (Karl *et al.*, 2006), although it is probably of a different ontogenetic age to the type material. This specimen has a posterior maxillary dental arcade situated within a confluent dental groove, similar to the feature which is identified as synapomorphic for *T. pusillus* + *T. guimarotae* (see above). The teeth of DFMMh 200 are

morphologically similar to *Theriosuchus pusillus* (Karl *et al.*, 2006), due to the presence of faint carinae, a slightly labiolingually compressed and lanceolate morphology, an enlarged fourth maxillary tooth, and caniniform 3rd and 4th dentary teeth. However, the external nares are almost completely divided by an anterior projection of the nasals, a feature that is considered to be diagnostic of Atoposauridae, to the exclusion of *Theriosuchus*. Despite this latter feature, DFMMh 200 is tentatively referred to *Theriosuchus* cf. *pusillus*, pending a more detailed description of this potentially important specimen.

Additional material referable to *Theriosuchus* sp. comes from the same region as DFMMh 200, including DFMMh 605 (a partial and damaged skull, probably of a hatchling); DFMMh 325 (4 ventral osteoderms, 2 ribs and a fragment of a dorsal vertebra; DFMMh 236 (numerous dorsal osteoderms); DFMMh 279 (single femur); and DFMMh 507 (a solitary tooth) (Karl *et al.*, 2006). However, the dorsal osteoderms possess an anterior process, a feature that is here not considered to be present in *Theriosuchus*, and therefore at least some of the osteoderms comprising DFMMH 236 are more likely to belong to a goniopholidid. The femur and axial material cannot be definitively attributed to *Theriosuchus* based on the revised understanding of this genus, and it is here considered to belong to an indeterminate mesoeucrocodylian. The partial skull and the single tooth are tentatively considered to be referable to cf. *Theriosuchus* sp., due to the dental similarities they possess.

(5) Isolated teeth from two localities in the Tithonian of north-eastern France were referred to cf. *Theriosuchus* sp. (Cuny *et al.*, 1991). One of the figured teeth (PMC MO2.15) appears to possess a lanceolate and pseudoziphodont morphology. I therefore designate the specimen as *Theriosuchus* sp.

(6) Isolated teeth (MO-CHA-30, 31, 32) from the Tithonian of western France were referred to *Theriosuchus* cf. *pusillus* (Vullo *et al.*, 2014). These teeth possess a lanceolate morphology, as well as carinae that are 'festooned' on the apical margins of each tooth, giving a pseudoziphodont appearance. This morphology is characteristic of *Theriosuchus pusillus*, and therefore I agree with their original

assessment (Vullo *et al.*, 2014) in referencing to *Theriosuchus* cf. *pusillus*, pending the discovery of more complete material.

(7) *Theriosuchus* sp. was described based on teeth from the Berriasian of southwest France (Pouech *et al*., 2006, 2014)(Pouech and Mazin, 2006; Pouech *et al.*, 2014). A single anterior tooth is figured in lingual view (CHEm03.506) (Pouech and Mazin, 2006), and possesses faint apicobasal striations, a mesiodistally compressed crown base, and a pointed apex, giving it a lanceolate morphology. This is characteristic of *Theriosuchus*, and therefore the status of these specimens as *Theriosuchus* sp. is retained, noting that these are of the same age as *Theriosuchus pusillus* from the UK (Owen, 1878b; 1879; Salisbury, 2002).

(8) 284 teeth have been referred to *Theriosuchus* sp. from the Berriasian of southern Scandinavia (Skyttegård Member, Rabekke Formation of Bornholm, Denmark, and Annero Formation, Vitaback Clays, of Skåne, Sweden (Schwarz-Wings *et al.*, 2009b). These teeth possess the labiolingually compressed and lanceolate morphologies characteristic of *Theriosuchus pusillus* and *T. guimarotae* (Schwarz and Salisbury, 2005), and also the broader 'low-crowned' morphotype. This third morphotype is also known in '*Theriosuchus*' *ibericus*, and therefore these teeth as a whole are considered to represent cf. *Theriosuchus* sp., but in recognition that more than one heterodont species, including one closely related to *Theriosuchus pusillus*, might be present.

(9) A partial left mandible (GZG.BA.0139) was described, but not figured, from the Bückeberg Formation (Berriasian–Valanginian) of northern Germany (Old comital quarry, Harrl Hill, approximately 1.7 km SE of Bückeberg) in an as of yet unpublished PhD thesis (Hornung, 2013). The specimen was assigned to *Theriosuchus* sp. based on the presence of a ridge on the ventrolateral surface of the angular, a posteriorly-directed retroarticular process, and the absence of the external mandibular fenestra. The absence of the latter feature suggests that it is not referable to *Theriosuchus guimarotae* (see above). This specimen is about three times the size of the holotype of *T. pusillus*, and

might therefore represent one of the largest known individuals of *Theriosuchus*. The presence of a distinct knob-like lateral swelling on the anterior end of the lateral shelf of the angular was also noted (Hornung, 2013). Combined with its relatively large size, GZG.BA.0139 might therefore represent a novel species of *Theriosuchus*, but it is here referred to cf. *Theriosuchus* sp., pending examination of this material. Several osteoderms were also briefly mentioned (Hornung, 2013) from an unspecified locality near Sehnde (Lower Saxony) as resembling *Theriosuchus*, including one (GZG.STR.50293) that was identified as closely reminiscent of *Theriosuchus pusillus*. In that thesis, it was also noted that complete 'atoposaurid' skeletons are preserved in the Cherves-de-Cognac region in south-western France (Berriasian), and remain undescribed (Hornung, 2013).

(10) *Theriosuchus* sp. has been identified from multiple localities in the Early Cretaceous (early Berriasian to early Barremian) Teruel region of eastern Spain (Ruiz-Omeñaca *et al.*, 2004). However, these occurrences were only documented as part of faunal lists, and no further details are given. Therefore, I consider these occurrences to represent aff. *Theriosuchus* sp., pending examination of the identified material.

(11) *Theriosuchus*-like teeth have been described from the Cenomanian of south-western France, and assigned to Atoposauridae (Vullo and Neraudeau, 2008). Based on the figured specimen, these teeth possess a pseudoziphodont morphology, formed by the apical extension of the lingual carinae. Although the only tooth figure has a worn apex, it is clear that these teeth possess a lanceolate morphology, with evidence of labiolingual compression. I therefore assign these specimens to *Theriosuchus* sp., pending further examination.

Non-European occurrences: Outside of Europe, reports of *Theriosuchus* are less frequent, but provide further evidence that this genus was a common component of Cretaceous Asian semi-aquatic ecosystems. These occurrences comprise:

(1) A recent publication documented the occurrence of numerous small teeth from the Bathonian of eastern Morocco, and ascribed them to cf. *Theriosuchus* sp. based on their lanceolate crown morphology and pseudoziphodont carinae (Haddoumi *et al.*, 2016). As a consequence of the revision of Atoposauridae and *Theriosuchus*, these teeth are referred to *Theriosuchus* sp. These specimens currently represent the only confirmed occurrences of *Theriosuchus* from Gondwana.

(2) In the same publication that identified *Theriosuchus grandinaris* (Lauprasert *et al.*, 2011), the authors also assigned a partial left dentary (PRCMR CCC-1) and a single tooth (PRCMR 283) to cf. *Theriosuchus* sp. from the Phu Kradung Formation (latest Jurassic to Early Cretaceous) of the Nong Bua Lum Phu Province in Thailand. This dentary clearly belongs to a heterodont crocodyliform with a combination of pseudocaniniform and lanceolate teeth that display the presence of festooned crenulations, formed by anastomosing and irregular ridges on the crown (the characteristic pseudoziphodont apical morphology). Furthermore, the presence of interalveolar septae and dental teeth occupying a single groove (Lauprasert *et al.*, 2011) can be used to assign this specimen to *Theriosuchus* (Young *et al.*, 2016).

(3) A single tooth was ascribed (PRCMR 218) to cf. *Theriosuchus* sp. from the Early Cretaceous of Thailand (Cuny *et al.*, 2010). This tooth has a similar morphology to other teeth assigned to *Theriosuchus* from Thailand (Lauprasert *et al.*, 2011), and therefore the assignment to *Theriosuchus* sp. is supported. It might be that these teeth represent isolated occurrences of *Theriosuchus grandinaris* based on their near-identical morphologies.

(4) Recently a single tooth was identified as cf. *Theriosuchus* from the Aptian of southern China (Mo *et al.*, 2016). This tooth is similar to the Asian occurrences of *Theriosuchus*, and therefore I agree with the original identification (Mo *et al.*, 2016), retaining its status as cf. *Theriosuchus* sp.

Neosuchia (Benton and Clark, 1988)

5.7.3 ‘Alligatorium’ franconicum (Ammon, 1906)

Alligatorium paintenense (Kuhn, 1961)

Type locality and horizon: Unknown bed, late Kimmeridgian (Late Jurassic); Painten, 10km north of Kelheim, southeast Germany.

Type specimen: BSPG specimen (number unknown): destroyed or lost; articulated hindlimb and pelvic girdle.

Referred specimen: BSPG specimen (number unknown): destroyed or lost; type of *Alligatorium paintenense*, a skull and near-complete skeleton missing most of the tail and the right hindlimb.

Previous diagnoses and comments: *Alligatorium franconicum* was originally named based on an articulated right hindlimb from the Late Jurassic of Painten, Bavaria (Ammon, 1906). Subsequently, a partial skeleton from the same locality was tentatively referred to this species (Broili, 1931). Following this, the latter skeleton was referred to a new species, *Alligatorium paintenense*, without detailed discussion (Kuhn, 1961), an interpretation which remained in subsequent publications by the same author (Kuhn, 1966; Kuhn, 1971; Kuhn, 1977). The first formal and emended diagnoses for both species were published in a review of European atoposaurids (Wellnhofer, 1971), and both *Alligatorium franconicum* and *Alligatorium paintenense* were considered to be valid, along with *Montsecosuchus* (‘*Alligatorium*’) *depereti* (Vidal, 1915) and *Alligatorium meyeri* (Gervais, 1871). Most recently, a review of European atoposaurids concluded that the differences in limb proportions were not enough to distinguish ‘*Alligatorium paintenense*’ from ‘*Alligatorium*’ *franconicum* (Tennant and Mannion, 2014), and synonymised the former with the latter, an interpretation which is followed here.

As well as the holotype specimen of ’*Alligatorium*‘ *paintenense*, a small brevirostrine skull has been described from the Late Jurassic of Brauvilliers, Meuse, France,(Buffetaut, 1981b), and assigned to

Alligatorium cf. *paintenense*. This assignment was based on the significantly longer and pointed rostrum compared to other atoposaurids, the posteriorly placed orbits, a mediolaterally narrow interorbital region, and the dense external surface sculpting. Some differences were also noted (Buffetaut, 1981b), including the overall larger size and moderate development of the posterolateral squamosal 'lobe', as described for *Alligatorium meyeri*, *Alligatorellus beaumonti*, and *Theriosuchus pusillus*. Unfortunately, I have been unable to examine this specimen first-hand and, based on the figures (Buffetaut, 1981b) which are sadly of low quality simply due to the age of the publication, I cannot determine its relationship to the now lost German specimens of '*Alligatorium*' *franconicum* (Wellnhofer, 1971).

The skull of '*Alligatorium*' *franconicum* has been described as strongly sculpted and more longirostrine than the typically brevirostrine atoposaurids (Wellnhofer, 1971), and that the external nares were fully open and not divided by a septum, the presence of which is a feature that is considered to be diagnostic for atoposaurids, but also possessed by *T. pusillus* (Owen, 1879). Additionally, '*Alligatorium*' *franconicum* possesses a biserial paravertebral rows of sculpted dorsal osteoderms, similar to atoposaurids and *Theriosuchus pusillus*, but with a central keel that diminishes anteriorly.

Most of the analyses found '*Alligatorium*' *franconicum* to be united within a clade comprising *Pholidosaurus* (Salisbury, 2002), *Eutretauranosuchus* (Smith *et al.*, 2010; Pritchard *et al.*, 2012), *Amphicotylus* (Mook, 1942) and *Koumpiodontosuchus* (Sweetman *et al.*, 2015), representing Bernissartiidae, Goniopholididae, and Pholidosauridae. However, resolving the position of these groups within Neosuchia is not the focus of this study, although it is noteworthy that they were found to be more closely related to paralligatorids than atoposaurids. The characters uniting '*Alligatorium*' *franconicum* with these non-atoposaurid taxa include: (1) an intermandibular angle of less than 40° (36°); (2) a total anteroposterior skull length to snout length (measured from the anterior margin of the orbit to the anterior edge of the premaxilla in dorsal view) ratio of less than 2.0 (1.81); (3) a skull

anteroposterior length to orbit length ratio of greater than 5.0 (5.27), a feature also shared with *Brillanceausuchus* and *Shamosuchus* (Pol *et al.*, 2009); (4) a nasal that only participates posteriorly in the margin of the external nares, a feature that appears to only be shared with *Amphicotylus* (Mook, 1942), and distinct from atoposaurids and *Theriosuchus* in which the nasal participates posteriorly and medially, often projecting anteriorly into and dividing the external nares; and (5) asymmetrical dorsal osteoderms in dorsal aspect (excluding any anterolateral peg articulation), a feature more widespread across Neosuchia, including *Alligatorellus* (Tennant and Mannion, 2014), *Pachycheilosuchus* (Rogers, 2003) and *Wannchampsus* (Adams, 2014).

'*Alligatorium*' *franconicum* was originally found to be closely related to goniopholidids, bernissartiids, and paralligatorids (Buscalioni, 1986), based on a combination of factors including longer rostral length, undivided external nares, proportionally broad supratemporal fenestra, and transversely broad osteoderms. However, subsequent revisions to this preliminary analysis (Buscalioni and Sanz, 1988; Buscalioni and Sanz, 1990b) considered it to be a *nomen dubium*, due to the fact that the specimen is lost, and because the single autapomorphy originally proposed (a reduced anterior process of the ilium) (Wellnhofer, 1971) is present in *Montsecosuchus* and atoposaurids, and more broadly within Neosuchia. I regard '*Alligatorium*' *franconicum* as a potentially diagnostic non-atoposaurid taxon, but refrain from erecting a new genus name because all specimens are lost/destroyed and the proposed autapomorphies are tentative pending the discovery of additional material. Future discoveries referable to '*Alligatorium*' *franconicum* should shed light on the taxonomy of specimens attributed to *Alligatorium*, the evolution of the biserial osteoderm shield in Neosuchia, as well as the early development of a longirostrine cranial morphology in non-thalattosuchian Jurassic taxa.

Revised diagnosis and discussion: (S1) Minimum mediolateral width between supratemporal fenestrae broader than minimum mediolateral width between orbits (C19.0). This feature describes

the relatively high intertemporal mediolateral width compared to the interorbital region, a feature which '*Alligatorium*' *franconicum* shares with some atoposaurids, but also *Montsecosuchus* (Buscalioni and Sanz, 1990b) and *Pachycheilosuchus* (Rogers, 2003).

(S2) Skull length to width ratio greater than 2.5 (2.77) (C25.2). The skull length to width ratio reported here is diagnostic only in the sense that not many fully longirostrine taxa were sampled, with the exception of *Pholidosaurus* (Salisbury, 2002), with which it also shares this character state. *Koumpiodontosuchus* (Sweetman *et al.*, 2015) and the two goniopholidid taxa are semi-longirostrine, but not to the extent of pholidosaurids and fully marine crocodyliforms. As such, '*Alligatorium*' *franconicum* might represent a transitional form towards a more aquatic lifestyle, but this requires much more detailed investigation pending the discovery of new remains.

(S3) Presence of a lateral keel on posterior part of dorsal osteoderms (C312.1). This character state is shared with *Alligatorellus*, but the morphology of the osteoderms of '*Alligatorium*' *franconicum* appears to be distinct, with a central longitudinal keel, and a lateral sulcus with an anterolateral projection, similar to the 'peg and socket' morphology described for *Theriosuchus guimarotae* (Schwarz and Salisbury, 2005) and goniopholidids (Salisbury and Frey, 2001). This overall geometry appears to be different from the dorsal osteoderm shield for any known atoposaurid (Tennant and Mannion, 2014), and from any goniopholidid, and identifies '*Alligatorium*' *franconicum* as a distinct neosuchian taxon.

Neosuchia (Benton and Clark, 1988)

Paralligatoridae (Konzhukova, 1954) *sensu* (Turner, 2015)

5.7.4 Sabresuchus nov. gen.

Zoobank LSID: zoobank.org:act:35B479C6-7620-428A-92A7-F613B43FEC24.

Etymology: 'Sabre' in reference to the enlarged and curved 5th maxillary tooth, and 'suchus' from the Ancient Greek, *soûkhos*, for crocodile.

Included species: *Sabresuchus ibericus* (type species) and *Sabresuchus sympiestodon*.

Distribution: Cretaceous of Europe.

Comments: '*Theriosuchus*' *sympiestodon* shares a number of features with '*Theriosuchus*' *ibericus*, and these two taxa form a sister taxon relationship in all analyses, distantly related to other species definitively ascribed to *Theriosuchus*. These taxa have never been directly compared or included together in a phylogenetic analysis, and based on this novel finding here I erect the name *Sabresuchus* gen. nov. to include them both. The name refers to the hypertrophied 5th maxillary tooth, which is at least four times the size of adjacent teeth in both species, and is the most striking feature of this genus.

The phylogenetic analyses place *Sabresuchus sympiestodon* and S. *ibericus* within Paralligatoridae. The Bremer support uniting these two species is 3-4 (Figure 42, Figure 43, Figure 44), with a posterior node probability of nearly 1 (Figure 45), providing strong support for their sister taxon relationship. *Sabresuchus* is the sister taxon to *Wannchampsus* (Adams, 2014), a taxon comprising several specimens that have often been cited alongside *Theriosuchus pusillus* as an important transitional form on the lineage leading to Eusuchia (Langston Jr, 1974; Adams, 2014; Turner, 2015). A number of dental features characterise this relationship with *Wannchampsus*, including the maxillary teeth with denticulate carinae on the mesiodistal margins, and ridged ornamentation on the enamel surface in middle to posterior teeth. However, the instability of this relationship with *Wannchampsus* is highlighted by the fact that if *Pachycheilosuchus* (Rogers, 2003) is retained in phylogenetic analyses *a priori*, then *Brillanceausuchus* and *Shamosuchus* instead form a polytomy with *Wannchampsus*, with *Sabresuchus* as the sister taxon to that clade (Figure 42, Figure 43) However, these analyses were not designed to resolve paralligatorid relationships and, irrespective of this lack of consensus, the sister taxon relationship is still found between *S. ibericus* + *S. sympiestodon* that is nestled within this

paralligatorid assemblage, in a more crownward position than *Theriosuchus*. This relationship between *Sabresuchus* and other paralligatorids is further supported by a number of unequivocal synapomorphies, including: (1) a striated external surface of the posterior portion of the maxilla (C51.0); (2) an anteroposterior ridge occupying the entire length of the frontal dorsal surface (restricted to the median portion of this surface in *S. sympiestodon*) (C101.3); and (3) the presence of an obliquely oriented ridge on the dorsal surface of the squamosal (C145.0).

Diagnosis and discussion: (S1) Ventral edge of the groove for the upper ear lid positioned directly ventral to dorsal edge (C136.1). This morphology is distinct from *Theriosuchus guimarotae* (Schwarz and Salisbury, 2005) and *T. pusillus*, in which the ventral edge of the ear lid is laterally displaced with respect to the dorsal edge. However, it is similar to a range of neosuchians, including *Brillanceausuchus*, *Wannchampsus*, and *Koumpiodontosuchus* (Sweetman *et al.*, 2015), *Alligatorellus*, *Pholidosaurus* (Salisbury, 2002), *Eutretauranosuchus* (Smith *et al.*, 2010; Pritchard *et al.*, 2012), *Mahajangasuchus* (Turner and Buckley, 2008), and *Shamosuchus* (Pol *et al.*, 2009; Turner, 2015), as well as *Protosuchus richardsoni* (Colbert *et al.*, 1951).

(S2) Squamosal posterolateral process ('lobe') offset from the dorsally flat skull table (C140.1). The depression of the squamosal posterolateral lobe and its confluence with the paroccipital process is similar to the condition seen in the paralligatorids *Brillanceausuchus* and *Shamosuchus* (Pol *et al.*, 2009; Turner, 2015), the eusuchian *Allodaposuchus precedens* (Buscalioni *et al.*, 2001), as well as the crocodyliform *Zosuchus* (Pol and Norell, 2004a).

(S3) Squamosal with an oblique ridge on the dorsal surface (C145.0), posterior to the posterior margin of the supratemporal fenestra (C146.0). This morphology of the dorsal surface of the squamosal is distinct from *Brillanceausuchus*, *Shamosuchus*, *and Wannchampsus*, in which the ridge is positioned laterally to the external supratemporal fenestra. In protosuchians, coelognathosuchians, atoposaurids, bernissartiids, *Montsecosuchus*, '*Alligatorium*' *franconicum*, and *Theriosuchus pusillus*,

there does not appear to be any ridge. *Theriosuchus guimarotae* is distinct from *Sabresuchus* in possessing a rounded and longitudinally oriented crest that occupies the whole of the anteroposterior length of the flat dorsal surface, separating it from the bevelled lateral portion (Schwarz and Salisbury, 2005).

(S4) Lateral surface of dentary with concavity for reception of enlarged maxillary tooth (C212.1). The presence of this lateral concavity is similar to *Brillanceausuchus*, *T. pusillus* and *T. guimarotae*, which all possess either an individual enlarged maxillary tooth, or a wave of enlarged teeth. To accommodate this, the lateral surface of the dentary becomes invaginated, with the maxillary teeth occluding laterally to this surface. In protosuchians, and all other neosuchians which were observed, the lateral surface of the dentary is smooth and confluent with the rest of the external surface of the dentary at the position where the anterior maxillary teeth occlude.

(S5) At least some medially-positioned confluent maxillary teeth, implanted in a dental groove (C217.1 and C217.2). In both species of *Sabresuchus*, at least some of the maxillary teeth are implanted in a confluent dental groove, instead of individual alveoli. This is shared by *Theriosuchus guimarotae* (Schwarz and Salisbury, 2005), *Eutretauranosuchus* (Smith *et al.*, 2010; Pritchard *et al.*, 2012) and *Koumpiodontosuchus* (Sweetman *et al.*, 2015), as well as by some notosuchians, in which an 'alveolar trough' develops (Gomani, 1997; Turner and Buckley, 2008; O'Connor *et al.*, 2010). This feature is distinct from the condition in thalattosuchians (Gasparini *et al.*, 2006; Pierce *et al.*, 2009b; Pol and Gasparini, 2009; Young and de Andrade, 2009; de Andrade *et al.*, 2010b; Young *et al.*, 2011a; Herrera *et al.*, 2013; Young *et al.*, 2013a; Young *et al.*, 2014b), goniopholidids (Salisbury *et al.*, 1999; Tykoski *et al.*, 2002; de Andrade *et al.*, 2011b; Pritchard *et al.*, 2012), and eusuchians (Buscalioni *et al.*, 2001; Salisbury *et al.*, 2006; Delfino *et al.*, 2008a; Ősi, 2008; Pol *et al.*, 2009; Puértolas-Pascual *et al.*, 2014), in which individual teeth are differentially spaced, and occupy isolated alveoli, separated by interalveolar septae.

(S6) Maxillary teeth with low-crowned and strongly labiolingually compressed morphotype (C254.0). The presence of a 'low-crowned' dental morphology has been observed and used as a defining feature for some *Theriosuchus* species, without ever giving a precise definition of what this characterises. I consider this morphology to describe a dental crown that is mesiodistally broader than it is apicobasally tall, and with apical margins oriented at less than 45° from the horizontal. This dental morphotype is diagnostic for *Sabresuchus*, but also shared with *T. pusillus*.

(S7) Maxillary tooth 5 hypertrophied, at least 4.0 times the size of adjacent maxillary teeth (C258.1). In all other specimens observed (including *Theriosuchus pusillus* and atoposaurids), the maxillary teeth were sub-equal in size or developed one or two enlarged 'waves' (e.g., goniopholidids). In protosuchians, maxillary teeth 1–3 are proportionally and variably the largest (Wu *et al.*, 1997; Gow, 2000; Pol *et al.*, 2004), and in notosuchians there is a progressive reduction in size posteriorly from the enlarged second maxillary tooth (Ortega *et al.*, 2000; Carvalho *et al.*, 2005; Pol and Apesteguía, 2005; Zaher *et al.*, 2006; Campos *et al.*, 2011; Kellner *et al.*, 2011; Nascimento and Zaher, 2011; Pol *et al.*, 2014). In *Sabresuchus*, the 5th maxillary tooth is larger than the 4th, which is in turn larger than the 3rd tooth.

5.7.4.1 *Sabresuchus ibericus* nov. comb.

Theriosuchus ibericus (Brinkmann, 1989; 1992)

Type locality and horizon: Lowest horizon of an abandoned lignite mine, La Huérgina (or 'Uña') Formation, Barremian (Early Cretaceous); southwest of the eastern edge of Uña, Serranía de Cuenca, eastern Spain.

Type specimen: MfN MB.R IPFUB 102/21.2, partial right maxilla with *in situ* teeth.

Referred material (specimens housed at the MfN MB.R, unless stated): IPFUB 102/11.2 (incomplete left maxilla); IPFUB 102/11.3 (incomplete right maxilla); IPFUB 102/11.5 (frontal); IPFUB 102/11.6 (incomplete mandible); IPFUB 102/11.7 (cranial fragments); IPFUB 102/12.1 (incomplete left dentary); IPFUB 102/12.2 (incomplete right dentary); IPFUB 102/21.1 (left maxilla fragment with a tooth); IPFUB 102/21.3 (incomplete frontals); IPFUB 102.21.4 (parietal); IPFUB 102/21.5 (incomplete left jugal); IPFUB 102/21.6 (incomplete right jugal); IPFUB 102/21.7 (incomplete right squamosal); IPFUB 102/21.8 (left quadrate fragment with incomplete left squamosal and left quadratojugal); IPFUB 102/21.9 (right quadrate fragment); IPFUB 102/21.10 (near-incomplete pterygoid and basisphenoid); IPFUB 102/21.18 (basioccipital fragment); IPFUB 102/21.11 (left incomplete dentary); IPFUB 102/21.12 (left splenial fragment); IPFUB 102/21.13 (left angular fragment); IPFUB 102/21.14 (left fractured surangular); IPFUB 102/21.15 (incomplete right angular with right surangular fragment and right coronoid); IPFUB 102/21.16 (incomplete left articular); IPFUB 102/21.17 (right articular); IPFUB 102/21.19 (24 teeth, representing three different morphotypes); IPFUB 102/21.43 (right premaxilla); IPFUB 102/21.44 (caudal vertebra); IPFUB 102/21.45 (anterior caudal vertebrae, and various other cranial bones); IPFUB 102/22.1 (two teeth and roots, one incomplete tooth crown); IPFUB 102/22.2 (two teeth and roots, one fragmentary tooth crown); IPFUB 102/22.3 (angular fragment); IPFUB 102/22.4 (incomplete left dentary); IPFUB 102/22.5 (one caudal and two dorsal vertebrae); IPFUB 102/22.6 (proximal left femur fragment). This material is likely to all be from the same individual, and Brinkmann (1989, 1992) regarded all of the referred material as belonging to the holotype individual, a view which is followed here.

Tentatively referred material: BUE4-NT2#25 (teeth) (La Huérgina Limestone Formation, late Barremian (Early Cretaceous); El Inglés Quarry, Serranía de Cuenca, eastern Spain); provisionally housed in the Unidad de Paleontología, Universidad Autónoma de Madrid, and will be eventually stored in the Museo de Ciencias de Castilla-La Mancha in Cuenca, Spain, at which point permanent catalogue numbers will be assigned (Buscalioni *et al.*, 2008).

Previous diagnoses and comments: Two studies from the same author both referred to *Theriosuchus ibericus* as a new species (Brinkmann, 1989; 1992), and therefore the oldest of these has taxonomic priority (Brinkmann, 1989). The original specific designation was based on a range of features, including variation in tooth morphology and the width of the internal choanae, as well as the presence of procoelous caudal vertebrae. However, subsequent work on this taxon has regarded this species to be of questionable validity (Schwarz and Salisbury, 2005; Martin *et al.*, 2010), and it remains poorly understood. Here, I demonstrate that '*Theriosuchus*' *ibericus* is a valid taxon, and distinct enough to warrant erection of the new combination *Sabresuchus ibericus*.

In spite of the differences recovered here, and the novel phylogenetic position for *Sabresuchus ibericus*, this taxon retains some morphological similarities to *T. pusillus*, observations that resulted in its original generic assignment to *Theriosuchus*. Similar to *T. pusillus*, *S. ibericus* possesses a longitudinal median ridge on the parietal and frontal, and a deep groove between the squamosal and parietal on the dorsal surface of the skull table (Brinkmann, 1989; 1992). However, these features have since been found to be more widespread within crownward neosuchians, including Paralligatoridae (Turner, 2015; Turner and Pritchard, 2015), and cannot be used to unambiguously unite *Sabresuchus ibericus* with *Theriosuchus*.

Sabresuchus ibericus retains several of the diagnostic dental morphotypes of *Theriosuchus*, possessing labiolingually compressed pseudocaniniform, and low-crowned teeth, but these teeth are fully ziphodont (i.e., with denticulate carinae) in *S. ibericus*. There is a third morphotype figured in the original publication of these specimens (Brinkmann, 1989), where the labial surface of one of the teeth from the middle of the tooth rows is punctured by a series of small pits, which might prove to be an additional dental morphotype. The bases of the middle to posterior tooth crowns are mesiodistally constricted and, despite an overall labiolingual compression, contain a thicker central core to each

tooth. The pseudocaniniform teeth of *S. ibericus* show evidence of apicobasal striations on the labial sides of the teeth, which terminate 40% of the way towards the tip of the crown (Brinkmann, 1989).

Teeth that might be referable to *Sabresuchus ibericus* (BUE4-NT2#25) have also been reported from a second locality in the Barremian of eastern Spain (Buscalioni *et al.*, 2008). Here, this referral is tentatively, pending their further study.

Diagnosis and discussion: (S1) Palatal surface of maxilla sculpted throughout by ridged ornamentation (C57.2). The palatal surface of *Sabresuchus ibericus* (IPFUB 102/21.2) is sculpted with longitudinal ridges, a feature otherwise found only in *Amphicotylus* (Mook, 1942). This is distinct from the condition seen in notosuchians (Pol and Powell, 2011) and other advanced neosuchians (Salisbury *et al.*, 2006; Ősi *et al.*, 2007; Adams, 2013), as well as *Theriosuchus* and *Sabresuchus sympiestodon* (Martin *et al.*, 2010), in which the maxillary palatal surface is flat and smooth. The posterior palatal surface of the maxilla is slightly crenulated in the mesoeucrocodylian *Mahajangasuchus* (Turner and Buckley, 2008), but this is not the same as the marked sculpting seen in *S. ibericus*.

(S2*) Dorsal surface of the parietal depressed relative to the squamosal (C115.2). This depression might be partially explained by mediolateral compression of this element. However, for taphonomic processes to fully explain this dorsal concavity, it would be expected for this degree of compression to be visible on other specimens from the type locality, which is not the case. In other mesoeucrocodylians, including *Sabresuchus sympiestodon* (Martin *et al.*, 2010; Martin *et al.*, 2014c), the posterior portion of the dorsal surface of the skull table is horizontal and flat (Sereno *et al.*, 2003; Ősi *et al.*, 2007; Adams, 2013).

(S3) Proportionally short mandibular symphysis, extending posteriorly medial to the 5th dentary alveolus (C205.0). The posterior extension of the symphysis in *Sabresuchus ibericus* is proportionally shorter than in *Theriosuchus* (Young *et al.*, 2016) and notosuchians (Pol and Apesteguía, 2005), terminating medial to the D5 alveolus. This condition is only found in other brevirostrine taxa, such as

Brillanceausuchus, *Pachycheilosuchus* (Rogers, 2003), and possibly *Ilharkutosuchus* (Ősi *et al.*, 2007; Ősi, 2008). In *Sabresuchus sympiestodon*, the symphysis extends posteriorly to the 6th dentary alveolus (based on specimen MCDRD 134) (Martin *et al.*, 2014c).

(S4*) All dentary teeth occupy single, continuous, longitudinal groove (C217.2). In *Theriosuchus*, at least some of the dentary alveoli are independent from one another, with each tooth occupying a single alveolus and separated by interalveolar septae of varying thickness. However, *Sabresuchus ibericus* is unique in that all of its dentary teeth appear to occupy a single continuous alveolar groove, along a mediolaterally narrow dentary occlusal surface. This feature is considered to be locally autapomorphic for *S*. *ibericus*, as it has also been documented in basal notosuchians (Pol and Apesteguía, 2005), the hylaeochampsid *Ilharkutosuchus* (Ősi *et al.*, 2007; Ősi, 2008), and the posterior dentary teeth of *Isisfordia* (Salisbury *et al.*, 2006).

(S5) Occlusal dentary surface strongly mediolaterally compressed and devoid of nutrient foramina (C220.0). *Sabresuchus ibericus* does not appear to possess any distinctive foramina on the dorsal surface of the dentary, lingual to the mediolaterally compressed dental arcade (Young *et al.*, 2016). In contrast, *Theriosuchus*, *Sabresuchus sympiestodon* (Martin *et al.*, 2014c), and notosuchians (e.g., *Araripesuchus*) have a mediolaterally broad dentary occlusal surface, pierced by at least one foramen (Pol and Apesteguía, 2005; Young *et al.*, 2016). The overall morphology of the dentary of *Sabresuchus ibericus* is similar to that of *Pachycheilosuchus*, but the latter has a medially curved anterior end, giving a 'scimitar-shaped' profile in dorsal aspect.

(S6) Grooved ornamentation (rugose patterning) present posteriorly on the external surface of the dentary (C227.1). The presence of a grooved ornamentation on the external surface of the dentary is similar to the condition observed in *Theriosuchus*, as well as *Pachycheilosuchus* (Rogers, 2003), *Brillanceausuchus*, and notosuchians (Ortega *et al.*, 2000; Pol and Apesteguía, 2005), but distinguishes

S. ibericus from *S. sympiestodon* (Martin *et al.*, 2014c). In basal crocodyliforms, sculpture patterns consist exclusively of evenly spaced sub-circular pits (Pol *et al.*, 2004).

(S7*) Hypertrophied 5th maxillary tooth with fully caniniform morphology (C257.1), directed posteroventrally with respect to rest of maxillary tooth row (C259.0). The enlarged maxillary tooth is at least 4 times the total size of the adjacent teeth, possesses growth rings of varying colouration, and is posteroventrally recurved. In *S. sympiestodon*, an enlarged tooth is also present at this position, but is directed ventrally, and not as proportionally enlarged with respect to the adjacent maxillary teeth. This level of heterodonty is not seen in *Theriosuchus*.

(S8) Tooth crowns with denticulate carinae (fully ziphodont condition) (C245.1). Ziphodonty is known in a range of mesoeucrocodylians, including notosuchians (Pol and Powell, 2011). The difference between the heterodont morphologies of the maxillary tooth crowns of *Theriosuchus pusillus* and *Sabresuchus ibericus* is that whereas the former have slightly crenulated enamel surfaces leading to 'false' ziphodonty (pseudoziphodonty) (Prasad and de Broin, 2002), the latter have 'true' serrations on the apical surfaces of the teeth, giving a fully ziphodont morphology. The 'false' ziphodont condition forms via the apical prolongation of the enamel ridges on the labial and lingual enamel surfaces (Prasad and de Broin, 2002), rather than through the development of an incisive and serrated texture.

5.7.4.2 *Sabresuchus sympiestodon* nov. comb.

Theriosuchus sympiestodon (Martin *et al.*, 2010)

Type locality and horizon: Densuş-Ciula Formation (upper part of unnamed middle member), Maastrichtian (Late Cretaceous); Oltoane Hill, Tuştea, Haţeg Basin, western Southern Carpathians, Romania.

Type specimen: FGGUB R.1782, a right maxilla with *in situ* teeth.

Paratype: FGGUB R.1781, skull roof that might belong to the holotype individual.

Referred material: MCDRD 134, anterior portion of a right dentary from the Sânpetru Formation (Maastrichtian) at Cioaca Târnovului, Sânpetru, Romania; MCDRD 793, a maxilla with teeth from the Sânpetru Formation (Maastrichtian) at La Cărare, Sânpetru, Romania; LPB (FGGUB) R.1945, a fragmentary maxilla from the Densuş-Ciula Formation (Maastrichtian), Valioara-Fântânele, in the Haţeg Basin, Romania.

Previous diagnoses and comments: A series of fragmentary mesoeucrocodylian remains were assigned to *Theriosuchus* (Martin *et al.*, 2010), erecting the new species *T. sympiestodon*. Additional material was subsequently referred to this taxon from nearby localities of approximately the same age (Martin *et al.*, 2014c). A dentary (MCDRD 134) from a different provenance was referred to '*T.*' *sympiestodon* based on the similarity of its tooth morphology with *Theriosuchus pusillus*. However, this specimen is poorly preserved and does not share any clear features to unite it with the type specimen of '*T.*', *sympiestodon*, although I have followed its referral here. The original referral of '*T.*' *sympiestodon* to *Theriosuchus* was based on: (1) the presence of a transversely (or ventrolaterally) directed groove on the anterolateral side of the maxilla; (2) a longitudinal crest on the frontal; and (3) the presence of low-crowned, labiolingually compressed, pseudoziphodont posterior maxillary teeth. However, the presence of this maxillary groove could not be confirmed via personal examination of the type specimen, nor was it observed in *S. ibericus* or *T. pusillus*. The presence of this groove was noted for *T. guimarotae* (Schwarz and Salisbury, 2005) and possibly *S. ibericus*, and was also reported to be visible on the paratype specimen of *Theriosuchus pusillus* (Turner, 2015). On NHMUK PV OR48330 (*Theriosuchus pusillus*), the left maxilla does exhibit a longitudinal mark, but this is parallel to the nasal-maxilla suture, almost orthogonal to that figured for '*T.*' *sympiestodon* (Martin *et al.*, 2010; Martin *et al.*, 2014c) and does not appear to occur on any of the other specimens referred to

Theriosuchus in the NHMUK collections. A referred specimen of *S. sympiestodon* (MCDRD 793) has a depression of some description in this area (Martin *et al.*, 2014c), at an oblique orientation to that of the holotype specimen, although I was not able to examine this specimen first hand, and so cannot comment on whether it is a groove, bite mark, post-mortem artefact or a pathology. Therefore, the presence and orientation of any potential maxillary groove, and indeed its functional significance, remains uncertain, especially given that almost all specimens assigned to *Theriosuchus* have undergone taphonomic distortion or damage. I do not consider it to be diagnostic for '*T.*' *sympiestodon*, or the genus *Theriosuchus*, although it might be autapomorphic for *Theriosuchus guimarotae* (Schwarz and Salisbury, 2005). In the original description, it was concluded that '*T.*' *sympiestodon* lies outside of Eusuchia due to the anterior contribution of the palatine to the 'internal nares' (which here is assumed to mean choana, due to the progressive posterior migration of this feature from the anterior rostrum in Crocodyliformes) (Martin *et al.*, 2010), a feature which is not actually visible in the holotype specimen. The entire basioccipital region around the choana is poorly preserved, and it is difficult to assess whether the choana was fully pterygoidean or bound anteriorly by the posterior palatines. However, it does seem to be situated close to the posterior margin of the suborbital fenestra, similar to paralligatorids and *T. pusillus*. Here, it is demonstrated that '*Theriosuchus*' *sympiestodon* is a valid taxon, with the new combination *Sabresuchus sympiestodon*.

Revised diagnosis and discussion: (S1*) Longitudinal ridge on dorsal surface of frontal restricted to median portion (C101.1). The presence of a midline frontal crest is likely to be related to ontogeny and the fusion of the frontals, as small individuals of *T. guimarotae* lack this crest (Schwarz and Salisbury, 2005). *Alligatorium meyeri* also possesses this feature, as well as a range of non-atoposaurid neosuchians, including *Wannchampsus* (Adams, 2014), *Shamosuchus* (Pol *et al.*, 2009; Turner, 2015) and *Isisfordia* (Salisbury *et al.*, 2006). However, the position of the ridge and its continuation on the parietal appears to be phylogenetically informative; in *Sabresuchus sympiestodon*, this ridge is restricted to the middle portion of the frontal, whereas in *T. guimarotae* and *T. pusillus* it is restricted

to the posterior portion (Schwarz and Salisbury, 2005). In *Sabresuchus ibericus*, *Wannchampsus*, and *Shamosuchus* (Pol *et al.*, 2009; Turner, 2015), this ridge occupies the entire length of the frontal, and therefore it is likely that this heterogeneity in anteroposterior extent is taxonomically informative.

(S2) Dentary internal alveolar margins not raised, but flat and confluent with remainder of dentary occlusal surface (C22.1). The lack of raised internal alveolar rims in *Sabresuchus sympiestodon* distinguishes it from *Theriosuchus* and *S. ibericus*, which have raised rims at least in the anterior alveoli (Young *et al.*, 2016). Eusuchians (Salisbury *et al.*, 2006), thalattosuchians and tethysuchians also lack raised alveolar rims (Young *et al.*, 2014c), whereas they appear to be raised in notosuchians (Campos *et al.*, 2011). This feature is not observable in atoposaurids because of the nature of their preservation.

(S3*) Diastema present on dentary between D7 and D8 alveoli (C225.0). *Sabresuchus sympiestodon* possesses a diastema between the D7 and D8 alveoli, in contrast with *Theriosuchus*, as well as *Pachycheilosuchus* and *Wannchampsus*. I therefore consider this feature to be locally diagnostic for *S. sympiestodon*. However, as a result of the lack of anatomical overlap between this dentary and the type material of *S. sympiestodon*, caution is advised in recognition of this feature as diagnostic for the species.

(S4*) Maxillary teeth lacking striae on the labial and lingual surfaces (C250.0), with hypertrophied (C258.0) and ventrally directed 5th maxillary tooth (C259.1). Originally, '*Theriosuchus*' *sympiestodon* was distinguished from other species of *Theriosuchus* based on the presence of a single, enlarged maxillary caniniform tooth, and the anterior maxillary teeth lacking striae on labial and lingual faces (Martin *et al.*, 2010), a conclusion with which I agree. *Sabresuchus ibericus* also possesses this enlarged maxillary tooth, although in the one available specimen this tooth is strongly posteriorly recurved, and not directed ventrally as in *S. sympiestodon*. In *Shamosuchus*, the 5th maxillary tooth is also the largest, whereas in *Theriosuchus pusillus* and *Allodaposuchus* the 4th tooth is the largest (Delfino *et al.*, 2008a), but in none of these cases does the proportional size difference come close to that for either *S.*

sympiestodon or *S*. *ibericus*. Therefore, this combination of maxillary dental character states is considered to be diagnostic for *S*. *sympiestodon*.

5.7.5 Brillanceausuchus babouriensis (Michard et al., 1990)

Type locality and horizon: Unnamed bed, ?Barremian (Early Cretaceous), Babouri-Figuil Basin, north Cameroon.

Type specimen: UP BBR 201, skull and partial skeleton.

Previous diagnoses and comments: Despite there being numerous similarities with atoposaurids originally, *Brillanceausuchus* was initially assigned to its own family, Brillanceausuchidae (Michard *et al.*, 1990), within Neosuchia. However, a monogeneric family has no systematic purpose, and Brillanceausuchidae has not been used by subsequent workers, and nor have any subsequent taxa been referred to this group. Pending the recovery of closely related taxa that do not already form a named clade, I recommend disuse of Brillanceausuchidae. *Brillanceausuchus* has remained a neglected taxon in phylogenetic and comparative analyses, despite its apparent important morphology in possessing a number of 'primitive' character states (e.g., possession of a partially septated external nares and presence of a biserial osteoderm shield) alongside more 'transitional' morphologies between advanced neosuchians and eusuchians (e.g., reduced ventral exposure of the basisphenoid and procoelous presacral vertebrae) (Michard *et al.*, 1990). It has been differentially regarded as an atoposaurid (Salisbury and Frey, 2001; Salisbury *et al.*, 2006), or as an 'advanced neosuchian' by others (Turner, 2015), but without additional comment in either case. To my knowledge, only one phylogenetic analysis to date has elected to include *Brillanceausuchus* (Ősi *et al.*, 2007), who commented that its inclusion "gave much less resolution inside Eusuchia due to its incompleteness" (p. 174), and therefore did not report the results. Such a conclusion is counter-

intuitive, as this taxon is actually represented by several partial skeletons and skulls, but with the published literature regarding it being relatively deficient in anatomical detail (Michard *et al.*, 1990).

Discussion: *Brillanceausuchus* possesses procoelous cervical and dorsal vertebrae (Michard *et al.*, 1990), as well as fully pterygoidean choanae that are situated posteriorly to the posterior edge of the suborbital fenestrae, as in eusuchians (Buscalioni *et al.*, 2001; Pol *et al.*, 2009). Many authors have considered the presence of this combination of vertebral and palatal morphologies to imply that the eusuchian condition has evolved in parallel in several different neosuchian lineages, based on the underlying assumption that *Brillanceausuchus* is an atoposaurid, and therefore more basally positioned within Neosuchia (Brochu, 1999; Buscalioni *et al.*, 2001; Salisbury *et al.*, 2006). However, these preliminary results indicate that *Brillanceausuchus* belongs to Paralligatoridae (Figure 42, Figure 43, Figure 44, Figure 45), a clade most recently placed within Eusuchia (Turner, 2015; Turner and Pritchard, 2015), which together with Atoposauridae form the most basal group according to these studies (both based on the same source dataset). If such a topology is correct, this implies that the eusuchian condition might not be as homoplasious as previously regarded. Additional material assigned to *Brillanceausuchus* is currently being prepared, and comprises numerous skeletons (including skulls) preserved in three-dimensions (J. Martin, pers. comm., 2015). I await the full description of this material before a comprehensive taxonomic assessment of *Brillanceausuchus* can be made, and preliminarily assign it to Paralligatoridae.

Preliminary emended diagnosis: (S1) proportionally long supratemporal fenestra, with anteroposterior length exceeding that of the orbit, and a skull length to supratemporal fenestra length ratio of less than 6.0 (5.36) (C29.0), and a skull width to supratemporal fenestra width ratio of 7.0 (C30.3); (S2) sinusoidal lateral nasal borders oblique to one another (C66.3), with abrupt widening adjacent to maxilla (C70.1); (S3) base of jugal postorbital process directed dorsally (C83.1); (S4) flat frontal dorsal surface (no longitudinal crest or periorbital rims) (C100.0); (S5) parietal-postorbital

suture visible on the dorsal surface of the skull roof (C112.1) and within the supratemporal fenestra (C113.1); (S6) concavity at posterodorsal edge of squamosal-parietal contact (C117.1); (S7) lateral margins of squamosal and postorbital medially concave in dorsal view (C134.2), and dorsal surface of squamosal bevelled ventrally (C138.1), becoming unsculpted anteriorly (C148.1); (S8) squamosal posterolateral process elongate, distally tapered (C143.0) and depressed from skull table (C140.1); (S9) basisphenoid ventral surface mediolaterally narrower than basioccipital (C191.0), and basioccipital with large, well-developed bilateral tuberosities (C192.1); (S10) ventrolateral surface of anterior portion of dentary strongly mediolaterally compressed and flat (C215.0), with grooved ornamentation on external surface (C227.1); (S11) retroarticular process projects posteriorly and dorsally recurved (C242.3); (S12) posterior dentary teeth occlude medial to opposing maxillary teeth (C263.0); (S13) rounded and ovate dorsal osteoderm shape (C308.0).

5.7.6 Pachycheilosuchus trinquei (Rogers, 2003)

Pachycheilosuchus trinquei is known from a near-complete, disarticulated skeleton and partial skull from the Albian (Early Cretaceous) Glen Rose Formation of Erath County, Texas, USA. Initially described as a possible atoposaurid (Rogers, 2003), a position at the base of Atoposauridae was subsequently demonstrated in several phylogenetic analyses (Turner and Buckley, 2008; Pol *et al.*, 2009). However, more recent analyses have placed *Pachycheilosuchus* outside of Atoposauridae, either within the basal eusuchian clade Hylaeochampsidae (Buscalioni *et al.*, 2011) (though note that this study used *Theriosuchus* as an outgroup, and included no definite atoposaurids) (Turner, 2015; Turner and Pritchard, 2015), or just outside the eusuchian radiation (Adams, 2013). The most recent analyses add further confusion, with the same authors finding it to be either included as the basalmost eusuchian besides *Shamosuchus* (Narváez *et al.*, 2016), or outside Eusuchia with both *Shamosuchus* and *Pietraroiasuchus*, with instead *Hylaeochampsa* as the basalmost eusuchian (Narváez *et al.*, 2015);

note that this discrepancy is partially due to inconsistent treatment of the phylogenetic definition of Eusuchia. The original assignment to Atoposauridae was primarily based on the presence of a jugal with equally broad anterior and posterior processes, and the possession of procoelous presacral vertebrae (Rogers, 2003). However, this jugal morphology is known in other neosuchians, including *Paluxysuchus*, as well as thalattosuchians (Adams, 2013). The presence of procoelous vertebrae could be more broadly distributed among non-neosuchian eusuchians than previously recognised, and full procoely is not definitively known among any atoposaurid species (Salisbury and Frey, 2001). Hylaeochampsid affinities are supported by the reinterpretation of a defining character state for Atoposauridae, pertaining to whether the bar between the orbit and supratemporal fenestra is narrow, with sculpting restricted to the anterior surface (Clark *et al.*, 1994). Others have regarded this feature to be associated more broadly with 'dwarfism' (as initially proposed for *Pachycheilosuchus*) or immature specimens, and not a synapomorphy of Atoposauridae (Buscalioni *et al.*, 2011). *Pachycheilosuchus* is additionally unusual in the retention of an antorbital fenestra, to which the maxilla contributes (Rogers, 2003), which is similar to *Theriosuchus guimarotae* (Schwarz and Salisbury, 2005) and *Alligatorellus bavaricus (Tennant and Mannion, 2014)*.

The present study was not designed to resolve the phylogenetic placement of *Pachycheilosuchus*, except whether or not to include it within Atoposauridae. Its exclusion from Atoposauridae is supported, but here cannot provide further comment on its placement within Hylaeochampsidae (Buscalioni *et al.*, 2011). It is unusual in that *Pachycheilosuchus* is recovered in a more stemward position than Atoposauridae. I anticipate that inclusion of a broader range of atoposaurid specimens, *Theriosuchus* species, hylaeochampsids (including *Pietraroiasuchus ormezzanoi*) (Buscalioni *et al.*, 2011), and additional paralligatorids within a larger Neosuchia-focussed data matrix, will help to resolve the position of *Pachycheilosuchus* and its clearly important role in the ascent of advanced neosuchians and Eusuchia.

5.7.7 Wannchampsus kirpachi (Adams, 2014)

The 'Glen Rose Form' has been commonly referred to in neosuchian systematics since it was first briefly mentioned and figured (Langston Jr, 1974). Comprising a skull and lower jaw from the Early Cretaceous (late Aptian) Antlers Formation of Montague County, Texas, USA, it was described as resembling the extant dwarfed crocodile *Osteolaemus tetraspis*, and also similarities to *Theriosuchus pusillus* were noted (Langston Jr, 1974). Subsequently, *Wannchampsus kirpachi* was erected for two skulls and postcranial material from the late Aptian (Early Cretaceous) Twin Mountains Formation of Comanche County (Texas, USA) (Adams, 2014), and the 'Glen Rose Form' was assigned to this taxon. In this study, it was noted that the skull of *Wannchampsus* was similar to that of *Theriosuchus pusillus* (Adams, 2014), sharing features such as medial supraorbital rims, and therefore prompting its inclusion in the present analysis and discussion here. However, *Wannchampsus* is distinct from *T. pusillus* in: (1) the possession of an enlarged 3rd maxillary tooth (instead present at the 4th position in *T. pusillus*); (2) the absence of an antorbital fenestra; (3) choanae with an anterior margin close to the posterior edge of the suborbital fenestra (whereas it is more anteriorly placed in *T. pusillus*); and (4) the definitive presence of procoelous dorsal and caudal vertebrae. *Wannchampsus* is recovered in a position close to *Shamosuchus* as others have recently (Pol *et al.*, 2009; Adams, 2014; Turner, 2015), forming a paralligatorid clade with *Sabresuchus* and *Brillanceausuchus*.

5.7.8 Karatausuchus sharovi (Efimov, 1976)

Karatausuchus sharovi is known only from a single skeleton of a juvenile individual from the Late Jurassic (Oxfordian–Kimmeridgian) Karabastau Formation in southern Kazakhstan. It was originally considered to be an atoposaurid (Efimov, 1976; 1988), but subsequently thought to be more closely

related to paralligatorids by the same author (Efimov, 1996). The most recent analysis involving this taxon argued that it was a relatively basal crocodyliform due to the possession of amphiplatyan vertebral centra, and designated it as a questionable atoposaurid (Storrs and Efimov, 2000). It is generally similar to atoposaurids in being small, at only 160 mm in total anteroposterior body length, but possesses reduced dermal osteoderms, suggestive of a juvenile phase of growth. Intriguingly, over 90 small, labiolingually compressed teeth have been observed within the jaws (Storrs and Efimov, 2000), a striking feature that is unique among crocodyliforms. It also possesses 46 caudal vertebrae, approaching the condition known for *Atoposaurus*. However, it has 8 cervical vertebrae, placing it intermediate to *Protosuchus* (9 cervical vertebrae) and the majority of other atoposaurids (7 cervical vertebrae, with the exception of *Atoposaurus jourdani* which appears to have 6). *Karatausuchus* is similar to atoposaurids in that its skull length to orbit length ratio is relatively low, between 3.0 and 4.0 (3.37), but the other diagnostic features presented in this study for Atoposauridae cannot be assessed in the single known specimen. Therefore, I agree with other studies (Buscalioni and Sanz, 1988) that *Karatausuchus sharovi* is currently too poorly known to be assigned to any family, including Atoposauridae, and regard it as an indeterminately positioned crocodyliform. However, here it is still tentatively regarded as a valid taxon, due to the high number of cervical and caudal vertebrae, and the possession of an anomalously high number of teeth.

5.7.9 Hoplosuchus kayi (Gilmore, 1926)

Hoplosuchus was originally recognised based on a near-complete and articulated skeleton from the Late Jurassic Morrison Formation at Dinosaur National Monument (Utah, USA), as a pseudosuchian archosaur (aetosaurian) (Gilmore, 1926). Subsequently, several authors assigned *Hoplosuchus kayi* to Atoposauridae (Romer, 1956; Kuhn, 1960; Steel, 1973), based on its overall size, and the possession of relatively large, posteriorly placed and anterolaterally-facing orbits. Several ensuing studies

regarded *Hoplosuchus* as more similar to protosuchians, but noted its phylogenetic affinities remained uncertain (Buffetaut, 1982; Osmólska *et al.*, 1997). In the most recent review of Atoposauridae, it was concluded that *Hoplosuchus* represents a poorly known 'protosuchian-grade' crocodyliform (Buscalioni and Sanz, 1988).

Examination of the holotype specimen of this taxon could not confirm any definitive atoposaurid affinities. *Hoplosuchus* retains features present in basal crocodyliforms, including a small and circular antorbital fenestra, and a triangular lateral temporal fenestra that is nearly as large as the orbit. Potential autapomorphies for *Hoplosuchus* include: (1) a steeply posteriorly inclined quadrate; (2) the pterygoid bearing a descending process that is extensively conjoined in the mid-line anterior to the basisphenoid; and (3) a lower jaw lacking the external mandibular fenestra (Steel, 1973). *Hoplosuchus* has slender limbs, the dorsal armour is composed of paired oblong plates, and the caudal region is completely enclosed by dermal ossifications. A full revision of protosuchian crocodyliforms is currently underway (A. Buscalioni, pers. comm., 2014), and I await this before drawing any conclusions about the affinities of *Hoplosuchus*. Nonetheless, *Hoplosuchus* is still excluded from Atoposauridae.

5.7.10 Shantungosuchus chuhsienensis (Young, 1961)

Shantungosuchus chuhsienensis was originally named based on a near-complete skeleton and skull from the Early Cretaceous Mengyin Formation of Shandong Province, China, and identified as an atoposaurid (Young, 1961). This referral was subsequently supported by Steel (1973), who provided an emended diagnosis in his discussion of Atoposauridae. This included: (1) a triangular-shaped skull; (2) closely set teeth deeply implanted in independent alveoli; (3) seven cervical and eighteen dorsal vertebrae; (4) short cervical vertebral centra; (5) relatively long dorsal vertebral centra; (6) a slightly shorter ulna than humerus; (7) the tibia significantly exceeding the femur in length; and (8) the forelimbs being proportionally long. However, almost all subsequent work that has included

Shantungosuchus has excluded this taxon from Atoposauridae (Buffetaut, 1981b; Buscalioni and Sanz, 1988). In addition to this, some authors (Wu *et al.*, 1994) 994) have regarded much of the original interpretation (Young, 1961) as incorrect. These authors presented a revision of the multiple species assigned to *Shantungosuchus*, finding them to be more closely related to protosuchians than to atoposaurids (Wu *et al.*, 1994). I concur with this conclusion and exclude *Shantungosuchus chuhsienensis* from Atoposauridae, supporting a basal position within Crocodyliformes. However, it should be noted that atoposaurids do share numerous metric features with protosuchians, reflecting their small body size and paedomorphic retention of basal morphologies.

5.7.11 Indeterminate remains previously attributed to Atoposauridae

Alongside these named taxa, numerous additional remains (primarily teeth) have been referred to Atoposauridae. These referrals have generally been based on the dental morphotypes that have been regarded as characteristic of *Theriosuchus* and, in stratigraphic order, comprise:

(1) A partial skeleton from the Lower Toarcian Toyora Group of Japan, tentatively regarded as an atoposaurid due to its similarity with *Alligatorellus* (Manabe and Hasegawa, 1998). Unfortunately, the images and description are either of too poor quality or too brief for a meaningful comparison with more well-known atoposaurids, and therefore it is best that this specimen be regarded as Crocodyliformes indet. pending further detailed investigation. Howevr, it should be noted that if this is indeed an atoposaurid then it extends the lineage of this group back into the Early Jurassic.

(1) Teeth comparable to those of *Theriosuchus* were described from two localities from the early Bathonian of southern France (Kriwet *et al.*, 1997). Their referral to Atoposauridae was based on the presence of different morphotypes, and the teeth were thought to represent two distinct species. The first of these ‘species’ includes several dozen teeth (Larnagol, IPFUB Lar-Cr 1-20, and Gardies, IPFUB

Gar-Cr 1-20). Among this set of teeth, four gradational morphotypes were identified based on their inferred positions in the dental arcade (Kriwet *et al.*, 1997). However, their referral to Atoposauridae is based mainly upon them being heterodont, a feature that is not exclusive to either Atoposauridae or *Theriosuchus*. The second 'species' (Larnagol, IPFUB Lar-Cr 21-40) differs in possessing more prominent ridges on the crown surfaces (Kriwet *et al.*, 1997). These were referred to Atoposauridae based on their inferred heterodonty (Kriwet *et al.*, 1997); however, it cannot be determined whether or not all of these morphotypes belong to the same heterodont taxon, or two or more homodont or heterodont taxa. As atoposaurids are now considered to have a homodont (pseudocaniniform) dental morphology, these teeth cannot be referred to this group. They might represent at least one (and probably more) small-bodied heterodont taxon, and therefore I consider them to be only referable to Mesoeucrocodylia indet. at present.

(2) Small crocodyliform teeth were noted from the Bathonian 'stipite' layers of the Grand Causses (France) (Knoll *et al.*, 2013; Knoll and López-Antoñanzas, 2014), and referred to an indeterminate atoposaurid. No further details were given, and therefore they are regarded here as representing indeterminate crocodyliforms pending further description of this material.

(3) 1,391 specimens comprising teeth, osteoderms, a jaw fragment with teeth, as well as undescribed cranial and postcranial specimens, from the Bathonian of Madagascar were referred to Atoposauridae (Flynn *et al.*, 2006). Based on the description and figures provided, these teeth appear to be pseudocaniniform in morphology, with well-developed mesial and distal carinae and a ridged enamel surface. Although they vary in shape and size (up to 10 mm in apicobasal length), none can be defined as pseudoziphodont, ziphodont, lanceolate, labiolingually compressed, or low-crowned. Based on the brief description, it cannot be concluded that these teeth belonged to an atoposaurid, and therefore regard them as Mesoeucrocodylia indet., pending further description. Further examination of this material, along with remains identified as *Theriosuchus* sp. from the Bathonian of Morocco (Haddoumi

et al., 2016), will be important in evaluating evidence for the presence of atoposaurids and *Theriosuchus* in the Middle Jurassic of Gondwana.

(4) Teeth from the Kimmeridgian of northern Germany have been described as '*Theriosuchus*-like', but only identified as belonging to a small-bodied mesosuchian (Thies and Broschinski, 2001). These teeth were provisionally referred to Mesoeucrocodylia indet. (Karl *et al.*, 2006), with these authors stating that their morphology is not known for any other crocodylomorph. I follow this decision pending the direct comparison of this material with *Theriosuchus* and other small-bodied crocodyliforms.

(5) A fragmentary set of specimens (IVPP V10613) from the Early Cretaceous of Inner Mongolia, including cranial and mandibular elements, were assigned to cf. *Theriosuchus* sp. (Wu *et al.*, 1996b). However, the material might not be referable to a single individual or even taxon, as it was collected from across an extensive outcrop. The figured osteoderm (Wu *et al.*, 1996b) is almost identical in overall morphology to *Alligatorellus* sp. (MB.R.3632) (Schwarz-Wings *et al.*, 2011), including the position and extent of the lateral keel, and the near-absence of the anterior process of the ilium is similar to that of *Montsecosuchus*. The dorsal vertebrae possess the 'semi-procoelous' condition, similar to *Pachycheilosuchus*. The cranio-quadrate canal is closed, and therefore IVPP V10613 can be excluded from Atoposauridae. The external mandibular fenestra is absent, similar to paralligatorids and *Theriosuchus pusillus*. Additionally, the parietals bear a longitudinal median ridge on the dorsal surface, a feature which was used to link IVPP V10613 with *Theriosuchus* (Wu *et al.*, 1996b), although this feature is herein shown to be more widespread throughout Neosuchia. Furthermore, IVPP V10613 was assigned to *Theriosuchus* based on the broad intertemporal region, raised supratemporal rims, and elevated medial orbital margin (Wu *et al.*, 1996b), but such features are found in numerous other taxa. Based on this combination of unusual characteristics, it is likely that IVPP V10613 comprises more than one taxon, including at least one non-atoposaurid, non-*Theriosuchus* taxon, and one

Theriosuchus-like taxon. Therefore IVPP V10613 is best regarded as representing Neosuchia indet. pending further study of this material.

(6) A skull fragment (NHMUK PV OR176) was assigned to *Theriosuchus* sp. from the Berriasian–Barremian of the Isle of Wight, UK (Buffetaut, 1983; Salisbury and Naish, 2011). Originally, the posterior portion of a skull was assigned to *Theriosuchus* sp. based on comparison with the lectotype specimen of *Theriosuchus pusillus* (NHMUK PV OR48216) (Buffetaut, 1983). It has a median longitudinal ridge on the parietal, similar to all specimens assigned to *Theriosuchus*, but also to *Alligatorium meyeri* and paralligatorids. The otoccipitals also meet dorsal to the foramen magnum, separating it from the supraoccipitals, a feature shared with *Theriosuchus pusillus*, *T. guimarotae*, and paralligatorids. The contact between the parietal and the squamosal on the dorsal surface, posterior to the external supratemporal fenestra, is also weakly developed, not forming the deep groove that characterises *Theriosuchus pusillus*. Therefore, it cannot be determined whether this specimen represents *Theriosuchus* or another advanced neosuchian, and thus this specimen here is considered to represent Neosuchia indet., pending its comparison to a broader set of neosuchians. In addition, some procoelous vertebrae (the type of '*Heterosuchus valdensis*') from the Early Cretaceous of the UK were assigned to *Theriosuchus* (Buffetaut, 1983). The presence of procoely indicates that it is not referable to *Theriosuchus* (see Section 5.8.3.4), and it is instead regarded as an indeterminate neosuchian.

(7) Indeterminate remains (primarily teeth) attributed to atoposaurids, usually referred to *Theriosuchus* based on heterodont tooth morphotypes, have been identified from numerous microvertebrate sites in the Aptian–Albian (late Early Cretaceous) of North America (Pomes, 1990; Winkler *et al.*, 1990; Cifelli *et al.*, 1999; Eaton *et al.*, 1999; Fiorelli, 1999; Garrison *et al.*, 2007; Oreska *et al.*, 2013). However, because of the removal of *Theriosuchus* from Atoposauridae, it is more likely

that these 'atoposaurids' remains represent other small-bodied taxa. Therefore, they are tentatively considered to each represent Mesoeucrocodylia indet., pending further study.

(8) *Theriosuchus*-like teeth (MTM V 2010.243.1) were described from the Santonian of western Hungary (Iharkút), but conservatively referred to Mesoeucrocodylia indet. (Ösi *et al.*, 2012). These teeth are lanceolate in crown morphology, and possess pseudoziphodont carinae. Two additional undescribed maxillae from the same locality have also been briefly mentioned before (Martin *et al.*, 2014c), which together with the teeth might be referable to *Theriosuchus*. As the Maastrichtian occurrences of '*Theriosuchus*' have been recombined into a new taxon, *Sabresuchus sympiestodon*, it is best that these teeth be regarded as Neosuchia indet., pending further analysis of this material and the possibly associated maxillae.

(9) A *Theriosuchus*-like tooth has been described from the Campanian–Maastrichtian of Portugal (Galton, 1996). This tooth is distinct from *Theriosuchus*, possessing a fully ziphodont morphology, and was suggested to instead belong to *Bernissartia* (Lauprasert *et al.*, 2011). However, here it is considered to belong to an indeterminate neosuchian based on the more widespread distribution of ziphodont dentition in this group.

(10) The stratigraphically youngest material assigned to Atoposauridae comes from the middle Eocene Kaninah Formation of Yemen (Stevens *et al.*, 2013). This fragmentary material was tentatively designated as an atoposaurid, based on the presence of a ziphodont tooth crown, a procoelous caudal vertebral centrum, a biserial osteoderm shield (though see below), and polygonal gastral osteoderms. However, none of these characteristics are unambiguously diagnostic under the revised definition of Atoposauridae, and this material likely comprises a small, advanced eusuchian, based on the presence of procoelous caudal vertebrae. The presence of a biserial osteoderm shield is usually considered diagnostic for Atoposauridae; however, the analyses here demonstrate that this feature is more widespread among small-bodied neosuchians. Furthermore, the material from Yemen is too

fragmentary to confidently infer that the osteoderm shield was biserial. Therefore, this material is regarded as an indeterminate eusuchian pending the discovery of more complete and better preserved specimens.

5.8 Discussion

5.8.1 Western European Late Jurassic to Early Cretaceous Atoposaurid Diversity

The Late Jurassic–Early Cretaceous of Europe records high atoposaurid diversity, comprising the multispecific genera *Alligatorellus*, *Alligatorium*, *Atoposaurus* (Gervais, 1871; Wellnhofer, 1971; Buscalioni and Sanz, 1988; Buscalioni and Sanz, 1990a; Buscalioni and Sanz, 1990b; Tennant and Mannion, 2014). Both *Theriosuchus* spp. and *Montsecosuchus depereti* are now excluded from Atoposauridae, so do not contribute to their diversity (Owen, 1878b; 1879; Buffetaut, 1983; Schwarz and Salisbury, 2005; Martin *et al.*, 2010; Martin *et al.*, 2014c; Young *et al.*, 2016). Currently valid European species of *Theriosuchus* include*: T. guimarotae* from the Kimmeridgian of Portugal (Schwarz and Salisbury, 2005) and *T. pusillus* from the Early Cretaceous of England (Owen, 1879; Joffe, 1967; Buffetaut, 1983; Salisbury, 2002; Salisbury and Naish, 2011). Based on the suite of analyses here, both '*Theriosuchus*' *ibericus* from the Barremian of Spain (Brinkmann, 1989; 1992) and '*Theriosuchus*' *sympiestodon* from the Maastrichtian of Romania (Martin *et al.*, 2010; Martin *et al.*, 2014c) have been transferred to a new genus, decreasing the overall diversity and distribution of *Theriosuchus*. Along with the removal of *Theriosuchus* from Atoposauridae, this drastically reduces the spatiotemporal distribution of atoposaurids, which are now exclusively confined to the Late Jurassic of western Europe (pending the status of *Montsecosuchus*).

Late Jurassic outcrops of the Eichstätt-Solnhofen region of Bavaria, south-eastern Germany, have now yielded *Alligatorellus bavaricus*, as well as up to three additional atoposaurid species: *Atoposaurus*

oberndorferi, *Alligatorium franconicum* (including *Alligatorium paintenense*; see Section 5.7.3), and the atoposaurid previously identified as *Alligatorellus* sp. ((Schwarz-Wings *et al.*, 2011), which is either an indeterminate neosuchian (Tennant and Mannion, 2014) or a poorly known atoposaurid taxon closely related to *Alligatorellus* (see Section 5.5.4). The Late Jurassic limestones of Cerin, eastern France, have yielded *Alligatorellus beaumonti*, *Alligatorium meyeri*, and *Atoposaurus jourdani* (Wellnhofer, 1971; Tennant and Mannion, 2014). From Montsec in Spain, only the late Berriasian–early Valanginian *Montsecosuchus* (‘*Alligatorium’*) *depereti* is known (Vidal, 1915; Peybernes and Oertli, 1972; Buscalioni and Sanz, 1990b), which is unable to be confirmed as a definitive atoposaurid (Section 5.7.1). Along with these, there is a host of European material that has previously been ascribed to *Theriosuchus* sp., which consequently has been used to imply a high Late Jurassic–Early Cretaceous diversity of atoposaurids (Buffetaut, 1981b; 1983; Thies *et al.*, 1997; Thies and Broschinski, 2001; Ruiz-Omeñaca *et al.*, 2004; Schwarz and Salisbury, 2005; Karl *et al.*, 2006; Schwarz-Wings *et al.*, 2009b; Canudo *et al.*, 2010; Schwarz-Wings *et al.*, 2011; Hornung, 2013; Vullo *et al.*, 2014). However, with the removal of *Theriosuchus* from Atoposauridae, and subsequent revision of this genus (see Section 5.7.2) and all referred material, these previous statements about atoposaurid diversity cannot be supported.

The taxonomic restriction of Atoposauridae also implies that previously associated remains from the Cenomanian of France (Vullo and Neraudeau, 2008), mid-Cretaceous deposits from the USA (Cifelli *et al.*, 1999; Eaton *et al.*, 1999), the Santonian of Hungary (Ösi *et al.*, 2012) and the Upper Campanian-Maastrichtian of Portugal (Galton, 1996), cannot be referred to this clade, and instead represent either a range of *Theriosuchus*-like taxa or other indeterminate neosuchians (see Section 5.7.11). Previously, these remains were used to provide evidence for bridging the temporal gap between the definitive Late Jurassic atoposaurids (Tennant and Mannion, 2014), putative Early Cretaceous remains and *Theriosuchus sympiestodon* from the latest Cretaceous of Romania (Martin *et al.*, 2010; Martin *et al.*, 2014c), a conclusion which can no longer be supported based on the results of the phylogenetic

analyses presented here. Rather, these specimens hint at a high cryptic diversity of mid-Late Cretaceous small-bodied advanced neosuchian taxa in both Europe and North America.

It is possible that the high diversity of Late Jurassic to Early Cretaceous European atoposaurids is related to the island archipelago system that existed during this time, with epicontinental seas driven by fluctuating highstand sea levels (Hallam, 1986; Ziegler, 1988; Hallam and Cohen, 1989; Miller *et al.*, 2005; Schwarz and Salisbury, 2005). The separation of areas (e.g., basins in present day Cerin and Bavaria) might have led to allopatric speciation, evidenced by closely related species found in each region (i.e., *Alligatorellus beaumonti*, *Alligatorium meyeri* and *Atoposaurus jourdani* in Cerin, and *Alligatorellus bavaricus*, *Alligatorium franconicum* and *Atoposaurus oberndorferi* in Bavaria). The small body size of atoposaurids in general might also be explained by these environmental conditions, with insular dwarfism driven by the reduction in range size, as also proposed for the contemporaneous Late Jurassic German sauropod *Europasaurus* (Sander *et al.*, 2006; Carballido and Sander, 2014; Marpmann *et al.*, 2015). This reasoning is also supported by the persistence of other small-bodied crocodyliforms into the Maastrichtian (i.e., *Sabresuchus sympiestodon*) as part of an assemblage of insular island dwarfs in a range of environments and localities including the Haţeg Basin of Romania (Grigorescu *et al.*, 1999; Martin *et al.*, 2006; Benton *et al.*, 2010; Csiki *et al.*, 2010; Martin *et al.*, 2010; Weishampel *et al.*, 2010; Martin *et al.*, 2014c). Dwarf crocodiles are also known from the Quaternary of the Aldabara Atoll (western Indian Ocean), with *Aldabrachampsus dilophus* (Brochu, 2006) indicating that island dwarfism in crocodyliforms might not be an uncommon feature. Multiple contemporaneous dwarf species within a similar geographic region is analogous to that of the extant African dwarf crocodile, *Osteolaemus*, which is divided into a Congo Basin form (*O. osborni*), a West African form (*O. tetraspis*), and possibly a third distinct lineage within West Africa (Eaton *et al.*, 2009; Franke *et al.*, 2013; Shirley *et al.*, 2014; Velo-Antón *et al.*, 2014; Smolensky *et al.*, 2015), as well as other extant crocodilians (Marioni *et al.*, 2008; Weaver *et al.*, 2008; Milián‐García *et al.*, 2011; Villamarín *et al.*, 2011; Velo-Antón *et al.*, 2014). This modern day sympatry supports the idea that atoposaurids could

similarly have had multiple co-existing lineages, such as that seen in the French and German basins, and additional, indeterminate material from other European localities might represent further, cryptic diversity of atoposaurid dwarf crocodylomorphs. Recognition of additional fossil species might be made even more difficult in that modern dwarf crocodiles are morphologically conservative, with cryptic species only recognised through molecular sequencing analyses (Eaton *et al.*, 2009).

Currently, testing of these hypotheses is limited as a result of the small number of localities preserving definitive atoposaurids. To support the hypothesis of insular dwarfism, basal members of Atoposauridae should be expected to be much larger than these Late Jurassic European forms; however, this will only be able to be demonstrated with the discovery of additional well preserved, stratigraphically older forms, from non-island archipelago settings. Previously described but poorly understood specimens referred to Atoposauridae (Buffetaut, 1981b; Hornung, 2013; Young *et al.*, 2016) should prove pivotal in our understanding of this group and their role in Late Cretaceous semi-aquatic ecosystems.

5.8.2 Phylogenetic relationships and systematic implications

In all of the analyses here, Atoposauridae is recovered in a basal position within Neosuchia, supporting several recent analyses (Figueiredo *et al.*, 2011; Adams, 2014). Atoposauridae is a much more restricted clade than previously recognised, comprising *Atoposaurus* (*A*. *jourdani* and *A*. *oberndorferi*), *Alligatorellus* (*A*. *bavaricus* and *A*. *beaumonti*), and *Alligatorium meyeri*, and excluding *Theriosuchus*, *Montsecosuchus*, *Brillanceausuchus*, and '*Alligatorium*' *franconicum* (as well as taxa previously demonstrated to lie outside Atoposauridae, e.g. *Hoplosuchus*).

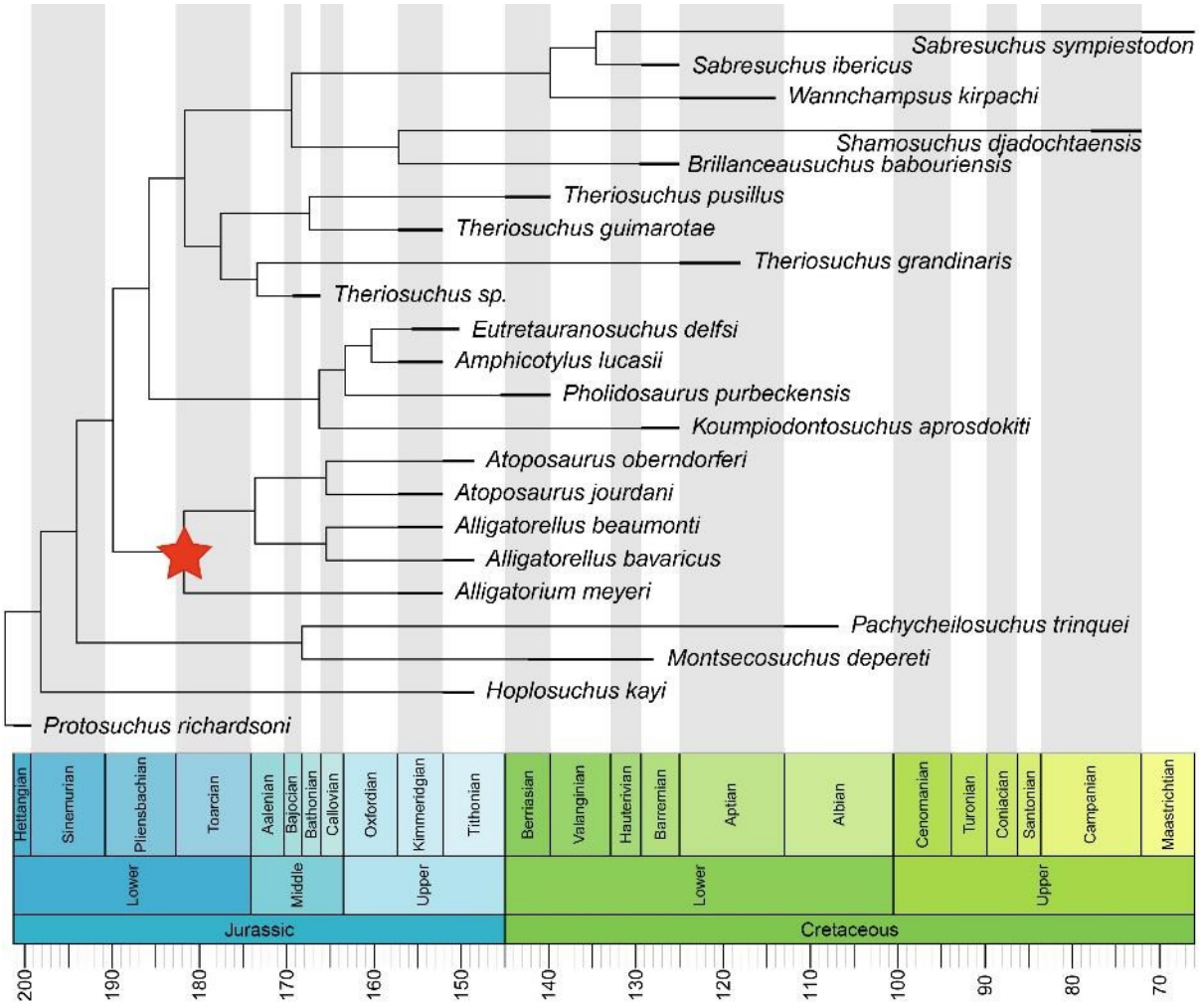


Figure 62. Time-scaled phylogeny showing the relationships of Atoposauridae to the other taxa analysed in the present study (based on the topology provided in Figure 42). Atoposauridae is marked with a red star. Created using the strap package (Bell & Lloyd, 2015), using the geoscalePhylo() function and an 'equal' time-scaling method.

The majority of previous phylogenetic analyses focused on crocodyliforms or basal neosuchians have generally only incorporated *Theriosuchus* (usually *T. pusillus*) and *Alligatorium meyeri*, with other atoposaurid taxa rarely included (Pol *et al.*, 2009; Adams, 2014). It is likely that this taxonomic under-sampling is at least partly responsible for the conflicting systematic positions previously recovered for Atoposauridae (Figure 40, Figure 41). *Alligatorium meyeri* does not display any clear derived eusuchian features, whereas *Theriosuchus* has an unusual combination of derived, plesiomorphic, and 'transitional' character states. This is the most likely explanation for the results recovered here, in

which specimens traditionally assigned to Atoposauridae are 'split', representing clusters of basal neosuchians (i.e., 'true' atoposaurids), advanced non-paralligatorid neosuchians (i.e., *Theriosuchus*), and paralligatorids (i.e., *Sabresuchus*: see below). These results further demonstrate that *Theriosuchus* had become a taxonomic 'waste-basket', to which discoveries of teeth representing small-bodied heterodont crocodyliforms were consistently attributed. It is likely that some of these teeth (and other fragmentary remains) from the northern hemisphere instead represent a much more taxonomically diverse group of neosuchians, including paralligatorids.

5.8.3 Evolutionary history of Atoposauridae, Theriosuchus and Sabresuchus

As a result of the systematic revision, Atoposauridae is now restricted to the Late Jurassic of Western Europe. Specimens previously assigned to Atoposauridae from the Middle Jurassic of Europe and Gondwana cannot be assigned to this clade, and most likely represent taxa closely related to *Theriosuchus*, or other small-bodied mesoeucrocodylian forms. This more restricted view demonstrates that atoposaurids were highly specialised, with a small body size, semi-aquatic lifestyle, and unusual limb proportions. They also possessed a biserial dorsal osteoderm shield, and their dentition was homodont. Atoposauridae appears to have gone extinct at the Jurassic/Cretaceous (J/K) boundary (Figure 56), as part of an overall drop in biodiversity in both marine and terrestrial crocodyliform groups (Mannion *et al.*, 2015), an event that might be related to a major regression and the closing off of shallow marine basins in Europe across the J/K boundary (Hallam, 1986; Miller *et al.*, 2005; Smith and McGowan, 2007).

The implications for the removal of *Theriosuchus* from Atoposauridae, and restriction of this genus to include just *T. guimarotae*, *T. grandinaris* and *T. pusillus*, are complicated by the numerous referrals of teeth and poorly preserved fossils to *Theriosuchus* from across Laurasia (as well as less common referrals from Africa and North America). Therefore, although *Theriosuchus* appears to have been

highly successful, spanning the Middle Jurassic–early Late Cretaceous, it was more temporally restricted than previously regarded, and did not persist into the latest Cretaceous, counter to previous assertions (Martin *et al.*, 2010; Martin *et al.*, 2014c). Based on our current understanding, *Theriosuchus* was present in the Middle Jurassic to early Late Cretaceous of Europe, the Middle Jurassic of North Africa, and the Early Cretaceous of Asia. The unequivocal presence of *Theriosuchus* in the Cretaceous of Asia supports the hypothesis of intermittent connections between western Europe and Asia through part of the Early Cretaceous (Baraboshkin *et al.*, 2003; Lauprasert *et al.*, 2011). Despite the taxonomic revisions here, *Theriosuchus* remains one of the most temporally long-lived archosaurian lineages of all time, which could be attributed to its small body size, its flexible morphology and ecology, or indicate that further splitting is required, pending the discovery of additional, well-preserved and complete specimens. The results here have recognised two separate and distinct clusters within *Theriosuchus*, possibly based on the more comprehensive sampling of definitive and putative atoposaurids, resulting in the erection of the new genus *Sabresuchus*. Given the temporal distance between the two species of *Sabresuchus*, it would not be a surprise if new material of either species (especially the fragmentary *S. sympiestodon*) led to the recognition of two distinct genera.

5.8.4 The transition to Eusuchia

5.8.4.1 Background

In this section, I follow the phylogenetic definition of Eusuchia previously established and traditionally followed (Brochu, 1999): the last common ancestor of *Hylaeochampsa vectiana* and Crocodylia and all of its descendants. Along with *Wannchampsus* (including the 'Glen Rose Form' (Adams, 2014)), *Theriosuchus* (and by association, atoposaurids) has been considered to be an important taxon in understanding the transition to Eusuchia, because of the relatively advanced development of their

secondary palates (Joffe, 1967; Clark and Norell, 1992; Brochu, 1999; Buscalioni *et al.*, 2001; Salisbury *et al.*, 2006; Ősi, 2008; Turner and Buckley, 2008; Pol *et al.*, 2009; Martin and Delfino, 2010; Turner, 2015). A close relationship between *Theriosuchus* and Eusuchia is based on a number of features that are evident primarily in the type species *T. pusillus*, including: (1) an undivided external nares; (2) sub-dermal post-orbital bars; (3) a lack of contribution from the frontals to the supratemporal fenestra; (4) relatively small internal supratemporal fenestrae; (5) development of the squamosal posterolateral process; (6) fully pterygoidean choanae within the secondary palate; (7) an enclosed eustachian canal; (8) procoelous vertebrae; and (9) a biconvex first caudal vertebra (Joffe, 1967; Buscalioni *et al.*, 2001; Rogers, 2003; Pol *et al.*, 2009; Adams, 2014; Turner, 2015; Turner and Pritchard, 2015). *Theriosuchus* shares combinations of these features with a range of more advanced neosuchians, particularly those assigned to Paralligatoridae (Turner, 2015). In addition, *T. guimarotae* shares a posteriorly opened cranioquadrate canal with *Sabresuchus sympiestodon*, comparable to the paralligatorid *Shamosuchus* (Turner, 2015). As is also the case in the paralligatorids *Sabresuchus*, *Shamosuchus* and *Wannchampsus*, the parietal of *T. pusillus* has a longitudinal midline ridge along its dorsal surface. Unfortunately, no specimens of *Alligatorellus*, *Alligatorium*, or *Atoposaurus* are preserved in a manner that would allow us to assess features such as the morphology of the choanae or the nature of presacral vertebral articulations, and we must await future examination of these specimens using 3D scanning techniques, or the discovery of new specimens that expose this morphology. Below, I discuss the evolution of several 'key' anatomical features that have played a significant role in discussions of the transition from basal neosuchians to Eusuchia.

5.8.4.2 Development of the squamosal posterolateral process

Basal crocodyliforms and mesoeucrocodylians do not possess a posterolateral process (or 'lobe') on the squamosal (Clark and Sues, 2002; Pol *et al.*, 2004; Pol and Norell, 2004a). Atoposaurids and other

basal neosuchians, such as *Paluxysuchus*, have a posterolateral lobe that is in the same horizontal plane as the dorsal surface of the skull table, with this lobe sculpted in the latter taxon (Adams, 2013). In goniopholidids, the process is short, narrow, and typically unsculpted (Ortega *et al.*, 1996b; Salisbury *et al.*, 1999; Averianov, 2001; Smith *et al.*, 2010; de Andrade *et al.*, 2011b; Pritchard *et al.*, 2012), and in notosuchians it is proportionally longer and rhombohedral-shaped (Buckley and Brochu, 1999; Buckley *et al.*, 2000; Sereno *et al.*, 2003; Zaher *et al.*, 2006; Novas *et al.*, 2009; Kellner *et al.*, 2011; Pol *et al.*, 2014), distinct from atoposaurids, *Theriosuchus*, or eusuchians. *Theriosuchus pusillus* and *T*. *guimarotae* possess this posterolateral process, but it is ventrally deflected and unsculpted in these taxa, similar to that of *Rugosuchus* and *Shamosuchus* (although in the latter taxon the 'lobe' is sculpted as in the rest of the dorsal surface of the cranial table) (Turner, 2015). In paralligatorids (e.g., *Sabresuchus ibericus*) (Turner, 2015) and eusuchians (e.g., *Allodaposuchus*) (Buscalioni *et al.*, 2001) the posterolateral process is posteroventrally confluent with the paroccipital process, enclosing the otic aperture, and in most Brevirostres the posterior margin of the otic aperture is invaginated (Brochu, 1999). *Sabresuchus ibericus* is also similar to the peirosaurid *Pepehsuchus* (Campos *et al.*, 2011) and to *Rugosuchus* (Wu *et al.*, 2001a) in that the 'lobe' is separated by a step from the main body of the squamosal, and remains unsculpted compared to the skull roof. The ventral deflection of the posterolateral process from the plesiomorphic horizontally oriented state seems to have been an important stage in the acquisition of this eusuchian morphology. In dyrosaurids (Jouve *et al.*, 2005) and gavialoids (Jouve *et al.*, 2008), this process is ventrally directed and blade-like, forming the anterior face of the paroccipital process, and possibly relates to the transition to an aquatic lifestyle.

5.8.4.3 Development of the secondary choanae

In crocodyliforms, the paired secondary choanae have migrated from an anterior position within the primary palate (as in protosuchians), posteriorly through the ventral interorbital bar in neosuchians,

and are positioned posteriorly within the pterygoids in eusuchians (Pol *et al.*, 2009; Turner, 2015). This posterior positioning of the choanae, with respect to the suborbital fenestrae, coupled with the complete ventral enclosure by the pterygoids, has long been regarded as diagnostic for Eusuchia (Benton and Clark, 1988; Norell and Clark, 1990; Clark and Norell, 1992; Buscalioni *et al.*, 2001; Salisbury *et al.*, 2006; Pol *et al.*, 2009; Turner, 2015)(Benton & Clark, 1988; Norell & Clark, 1990; Clark & Norell, 1992; Buscalioni *et al*., 2001; Salisbury *et al*., 2006; Pol *et al*., 2009).

Basal neosuchians, such as the goniopholidids *Amphicotylus* (Mook, 1942), *Eutretauranosuchus* (Smith *et al.*, 2010; Pritchard *et al.*, 2012) (Figure 63A) and *Sunosuchus* (Wu *et al.*, 1996a), possess the plesiomorphic choanal condition, with the anterior portion of the choanae receiving a significant contribution from the palatines. In the original reconstruction of *Theriosuchus guimarotae* (fig. 5B) (Schwarz and Salisbury, 2005), the anterior border of the choanae was placed in a more posterior position than that of *T. pusillus*, closer to the posterior border of the suborbital fenestra. However, based on the specimens figured, the anterior edge of the choanae and the pterygoid flanges appear to be broken (fig. 4I) (Schwarz and Salisbury, 2005), and it seems more likely that the choanae extended anteriorly to a position similar to *T. pusillus* (see reconstruction in Figure 63B). *Theriosuchus pusillus* possesses an intermediate choanal morphology, with the anterior border of the choanae placed anteriorly with respect to the posterior border of the suborbital fenestra (Figure 63C). The paired choanae in *T. guimarotae* appear to be mediolaterally narrower than those of *T. pusillus*, and seem to be fully bifurcated by a midline pterygoidean septum, closer to the general morphology seen in goniopholidids (Mook, 1942; Wu *et al.*, 1996a; Smith *et al.*, 2010; Pritchard *et al.*, 2012) and notosuchians (Ortega *et al.*, 2000; Apesteguía *et al.*, 2005). However, in *T. pusillus* only the anterior portion of the choanal groove appears to be septated. In *Sabresuchus sympiestodon* (Martin *et al.*, 2010; Martin *et al.*, 2014c) (Figure 63D) and other paralligatorids (e.g. *Rugosuchus*) (Wu *et al.*, 2001a) (Figure 63E-G), the choanal groove is fully open and undivided, similar to *Hylaeochampsa* (Clark and Norell, 1992) (Figure 63H).

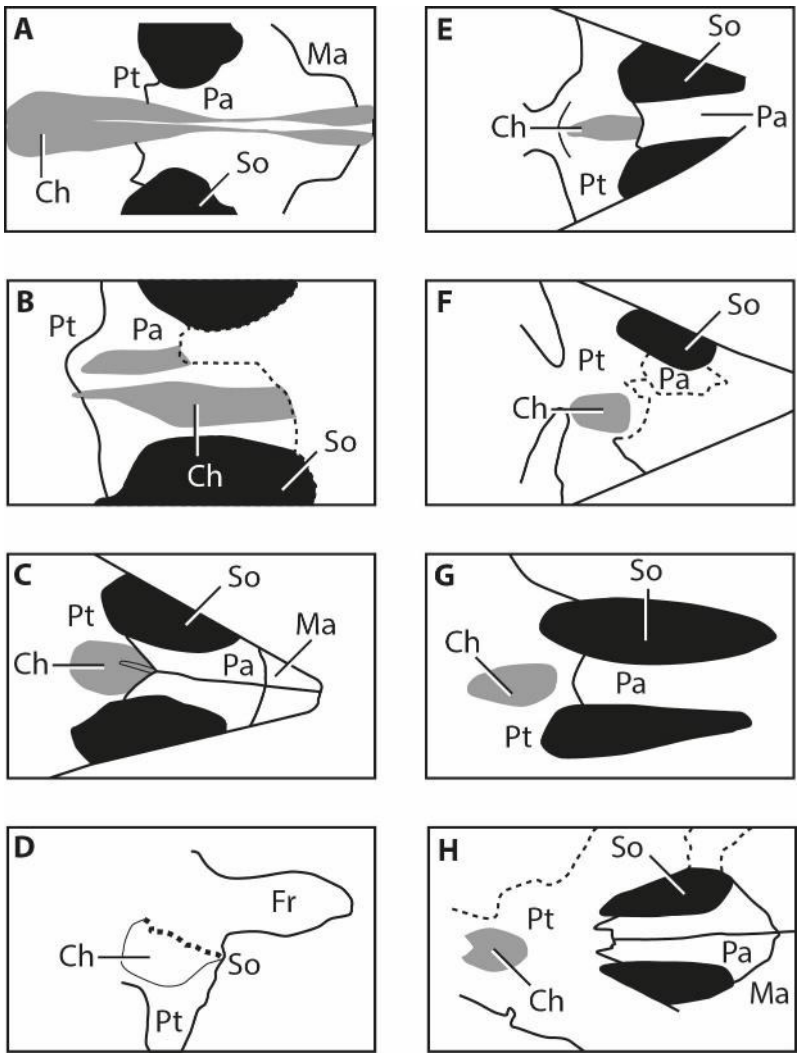


Figure 63. Relative positions of the choanae with respect to the main palatal bones in a range of neosuchian taxa. Citations are given were these reconstructions are based on in-text illustrations. (A) *Eutretauranosuchus delfsi* (Smith *et al.*, 2010; Pritchard *et al.*, 2012); (B) *Theriosuchus guimarotae* (Schwarz and Salisbury, 2005); (C) *Theriosuchus pusillus*; (D) *Sabresuchus sympiestodon*; (E) *Wannchampsus kirpachi*; (F) *Shamosuchus djadochtaensis* (Pol *et al.*, 2009); (G) *Koumpiodontosuchus aprosdokiti* (Sweetman *et al.*, 2015); (H) *Hylaeochampsa vectiana* (Clark and Norell, 1992).

In both *Theriosuchus guimarotae* and *T. pusillus*, the anterior edge of the choanae is formed by the posterior portion of the palatines, similar to *Rugosuchus* (Wu *et al.*, 2001a). However, in *T. guimarotae* the choanae enter into the ventral lamina of the palatines (Schwarz and Salisbury, 2005), rather than just being bordered by it as in *T. pusillus*. In this respect, *T. pusillus* is similar to the advanced neosuchian *Khoratosuchus*, in which the palatines form only a point contact with the anterior margin of the fully open choanae (Lauprasert *et al.*, 2009). Furthermore, the palatines contribute to the lateral

margins of the choanal opening in *Theriosuchus pusillus*, forming a bar-like, overlapping contact with the pterygoids. This morphology in *T. pusillus* is distinct from more crownward taxa (e.g., *Brillanceausuchus* (Michard *et al.*, 1990), *Gilchristosuchus* (Wu and Brinkman, 1993), *Pietraroiasuchus* (Buscalioni *et al.*, 2011), *Shamosuchus* (Pol *et al.*, 2009; Turner, 2015), and *Wannchampsus (Adams, 2014)*), in which the choanae are almost entirely enclosed by the pterygoids. The fact that this range of basal eusuchians (Turner, 2015; Turner and Pritchard, 2015) therefore appears to retain a palatine contribution to the anterior edge of the choana raises doubt over whether or not a fully pterygoidean choana is a synapomorphy for Eusuchia, rather than for a slightly more inclusive grouping. *Theriosuchus*, as the sister taxon to Paralligatoridae, exhibits a possible transitional morphology leading to the development of fully pterygoidean choanae. The sequence appears to involve the posterolateral widening of the choanal groove, coincident with migration to a point level with the posterior border of the suborbital fenestra, and reduction and eventual loss of the pterygoidean septum. This transition might have occurred in several lineages of advanced neosuchians (e.g., Susisuchidae, *Theriosuchus*), and it is possible that additional features of *Theriosuchus*, such as the relatively anterior positions of the mandibular tooth rows (distinct from eusuchians, dyrosaurids, and *Susisuchus*, in which the tooth rows extend posteriorly), are related to the formation of the eusuchian palatal morphology (Salisbury *et al.*, 2006).

Our collective understanding of the development of this morphology is potentially complicated by taxa such as *Isisfordia*, considered originally to be a basal eusuchian (Salisbury *et al.*, 2006), but placed outside of Eusuchia in many subsequent analyses (Turner, 2015; Turner and Pritchard, 2015). In this taxon, the choanae appear to have become fully enclosed by the pterygoids, with the anterior border located at the same level as the posterior edge of the suborbital fenestra (Salisbury *et al.*, 2006), which would indicate that the 'eusuchian' condition had evolved independently in at least one other lineage. However, this morphology was re-assessed recently (Turner and Pritchard, 2015), and instead

Isisfordia has been re-interpreted as possessing a palatine-pterygoid contact within the choanae, and therefore lacking completely pterygoidean choanae.

The neosuchian *Bernissartia* was also originally reported to have fully pterygoidean choanae based on its holotype (Buffetaut, 1975), but this specimen is poorly preserved, and it was subsequently argued that it is unlikely that the choanae receive a pterygoidean contribution (Norell and Clark, 1990). However, the bernissartiid *Koumpiodontosuchus* does have a fully pterygoidean choana (Sweetman *et al.*, 2015) (Figure 63G). Although the position of *Bernissartia* within Neosuchia is unstable, with the latest analysis finding both a eusuchian and non-eusuchian placement (Turner, 2015), the presence of fully pterygoidean choanae in its sister taxon *Koumpiodontosuchus* (Sweetman *et al.*, 2015) indicates that either: (1) it was secondarily lost in *Bernissartia*, or (2) that its presence in *Koumpiodontosuchus* represents an independent acquisition.

Regardless of whether the 'eusuchian' condition evolved more than once, it appears that the existing terminology does not describe the condition in basal eusuchians. As such, a more appropriately worded synapomorphy for Eusuchia could be the possession of posteriorly placed choanae, with an anterior margin medial to the posterior edge of the suborbital fenestra, often with a posterior contribution from the pterygoids and the complete loss of any sagittal pterygoidean septum.

5.8.4.4 Development of vertebral procoely

The presence of procoelous presacral vertebrae was first considered to be diagnostic for Eusuchia based on a re-analysis of *Bernissartia* that identified its importance as a transitional taxon between Neosuchia and Eusuchia (Norell and Clark, 1990). Based on a damaged anterior cervical vertebra referred to *Theriosuchus pusillus* (NHMUK PV OR48723), it was stated that *Theriosuchus* must have evolved procoely convergently (Norell and Clark, 1990; Clark and Norell, 1992), due to the

phylogenetic distance between *Theriosuchus* and Eusuchia. Both *Pachycheilosuchus* and *Theriosuchus pusillus* have been described as possessing 'semi-procoelous' dorsal centra, in which there is a convex posterior condyle, with a central depression sometimes filled by a plug. This intermediate morphology between amphicoely and procoely has been hypothesised as an alternative 'route' to the fully procoelous condition (Rogers, 2003). The degree of procoely decreases posteriorly along the axial column in *Pachycheilosuchus*, with the posterior caudal vertebrae possessing thickened centrum margins, which might represent the development of an incipient articular condyle, inferred as the possible origin of caudal procoely (Rogers, 2003). The paratype of *T. pusillus* has previously been examined using X-ray scanning (Salisbury and Frey, 2001), and it was found that all presacral vertebrae are gently amphicoelous, contrary to previous assertions (Norell and Clark, 1990), and as is also the case for *T. guimarotae* (Schwarz and Salisbury, 2005). Despite this, it was tentatively concluded that at least some of the cervical vertebrae of *T. pusillus* were procoelous (Salisbury and Frey, 2001), based on NHMUK PV OR48273, an interpretation followed in the scoring of this taxon in at least some more recent data matrices (Turner, 2015; Turner and Pritchard, 2015). However, NHMUK PV OR48273 is embedded in a block comprising several fragments (including a poorly-preserved mandibular ramus) that was not found in association with the type specimen, and it does not preserve diagnostic features that would allow it to be unequivocally assigned to *Theriosuchus pusillus*. Furthermore, examination of this specimen could not confirm the presence of procoely, with the vertebra instead being amphicoelous, with thickened rims along the centrum articular surfaces. Therefore I reject the hypothesis that this specimen, and thus *Theriosuchus pusillus*, possessed any procoelous vertebrae.

In contrast, the presacral vertebrae are procoelous in the paralligatorids *Wannchampsus* (Adams, 2014) and *Shamosuchus* (Pol *et al.*, 2009; Turner, 2015). *Pachycheilosuchus* appears to possess a vertebral morphology more similar to paralligatorids than *Theriosuchus*, and therefore more likely to be representative of a transitional morphology between the neosuchian and eusuchian conditions. *Isisfordia* and *Susisuchus* both possess weakly or 'incipiently' procoelous vertebrae (Salisbury *et al.*,

2006; Figueiredo *et al.*, 2011), which has been suggested to also represent a transitional morphology from the plesiomorphic amphicoelous condition (Turner and Pritchard, 2015).

A series of fully procoelous caudal vertebrae were described from the Early Cretaceous of Spain (Brinkmann, 1989; 1992), and others with a central depression (i.e., the 'semi-procoelous' condition), along with the material of *Sabresuchus ibericus* and *Bernissartia* reported from the Uña locality. Although the direct association of the procoelous caudal vertebrae with either of these taxa cannot be confirmed (Salisbury and Frey, 2001), it was claimed in the original publications that this vertebral series was found alongside the skull elements referred to *S*. ('*Theriosuchus*') *ibericus* (Brinkmann, 1989; 1992). Based on the size of these vertebrae and the purported presence of a form of procoely in *Theriosuchus pusillus* (Clark, 1986; Salisbury and Frey, 2001), coupled with the absence of this condition in *Bernissartia* (although some specimens of *Bernissartia* might have procoelous caudal vertebrae) (Norell and Clark, 1990), others also deemed it more probable that the fully procoelous vertebrae belong to *S*. *ibericus* (Brinkmann, 1989; Rogers, 2003). However, their argument relies on the congeneric status between *T. pusillus* and *S*. *ibericus*, which is not supported here. Goniopholidids, also known from the Uña region, can be excluded from 'ownership' of these vertebrae, because they have exclusively amphicoelous vertebrae (Brinkmann, 1989). *Unasuchus reginae*, also found at the Uña locality, is only known from fragmentary cranial and mandibular material, and its affinities are uncertain within Neosuchia (Brinkmann, 1992). The semi-procoelous vertebrae are from a larger individual than that of the type of *Sabresuchus*, and might be referable to *Unasuchus* or an additional taxon. I have incorporated this uncertainty over the vertebral morphology of *S*. *ibericus* into the data matrix, electing not to code this taxon for the presence of procoely or a biconvex first caudal vertebra (see below). Nonetheless, this taxon groups with paralligatorids (which all show a degree of procoely), and therefore is the most likely candidate taxon at Uña for the series of procoelous vertebrae. If this is correct, the entire vertebral column of *S*. *ibericus* would appear to show some form of procoely, and supports the findings of this study that *Sabresuchus* is closely related to eusuchians.

Pending the discovery of associated remains, I agree with several authors (Brinkmann, 1989; Salisbury and Frey, 2001) that procoely, including semi-procoely, cannot currently be determined for *Sabresuchus*. Nevertheless, it seems likely that well-developed vertebral procoely only evolved once within the lineage leading to Eusuchia. However, the presence of weak procoely in the vertebrae of Susisuchidae (*Isisfordia* + *Susisuchus*) (Turner and Pritchard, 2015) and semi-procoely in *Pachycheilosuchus* indicates that a number of neosuchian lineages developed some form of incipient procoely.

5.8.4.5 Biconvex first caudal vertebra

The first caudal vertebra of *Pachycheilosuchus* is biconvex (Rogers, 2003), a feature also proposed for *Brillanceausuchus* (Michard *et al.*, 1990), but not confirmed through direct observation of the holotype specimen. A biconvex first caudal vertebra has also been documented for *Theriosuchus guimarotae* (Schwarz and Salisbury, 2005), *Theriosuchus pusillus* (Salisbury and Frey, 2001), and probably *Sabresuchus ibericus* (Brinkmann, 1989; 1992; Salisbury and Frey, 2001) (though see above regarding specimen association). Moreover, a biconvex first caudal vertebra is a feature of all eusuchians (Salisbury and Frey, 2001), and its development is likely an important morphological aspect of the neosuchian–eusuchian transition. Whether I code a biconvex first caudal vertebra as present or absent for *Sabresuchus ibericus* has no effect on the topology of each tree, irrespective of whether or not *Pachycheilosuchus* is excluded *a priori*. This indicates that if a biconvex first caudal vertebra is indeed present in *Brillanceausuchus*, along with *Pachycheilosuchus* (Rogers, 2003) and *Theriosuchus* (Salisbury and Frey, 2001; Schwarz and Salisbury, 2005), then it is likely to have been independently acquired at least twice. The acquisition of this biconvex first caudal vertebra in *Theriosuchus* and other taxa close to the eusuchian radiation might have been important in the initiation of procoely in

advanced neosuchians, and the differential acquisition of a concave posterior centrum condyle in different regions of the axial column.

5.9 Summary

Atoposauridae is now considered to be a much more restrictive clade of basal neosuchians, comprising only *Atoposaurus jourdani*, *Atoposaurus oberndorferi*, *Alligatorellus beaumonti*, *Alligatorellus bavaricus*, and *Alligatorium meyeri*. Based on this more exclusive taxonomic grouping, atoposaurids were restricted to the Late Jurassic of Western Europe, and went extinct at the J/K boundary. *Theriosuchus* is excluded from Atoposauridae, recovering this genus as polyphyletic. *Theriosuchus* is a more crownward neosuchian than atoposaurids, and is here restricted to *T. pusillus* (the type species), *T. guimarotae* (Schwarz and Salisbury, 2005), and *T. grandinaris* (Lauprasert *et al.*, 2011). In addition, a specimen described from the Middle Jurassic of the UK might represent a distinct species of *Theriosuchus* (Young *et al.*, 2016). *Theriosuchus* is known from the Middle Jurassic–early Late Cretaceous, with occurrences from Europe, Asia and North Africa. '*Theriosuchus*' *ibericus* and '*Theriosuchus*' *sympiestodon* are recombined under the new genus denomination, *Sabresuchus* gen. nov. Along with *Brillanceausuchus*, *Sabresuchus* is recovered as a paralligatorid.

'*Alligatorium*' *franconicum* is recovered outside of Atoposauridae, and is not referable to *Alligatorium*, but instead appears to be more closely related to longirostrine forms, such as bernissartiids and coelognathosuchians. As the only specimens referable to this taxon are lost or destroyed (Wellnhofer, 1971), a new genus name is not given here, pending the discovery of new material. *Montsecosuchus* cannot be unequivocally confirmed to be an atoposaurid, and in the majority of the analyses it clusters with *Pachycheilosuchus*.

The revised placements of Atoposauridae and *Theriosuchus* have important implications for the transition from Neosuchia to Eusuchia. *Theriosuchus* exhibits one possible transitional route to the development of a pterygoidean-bound choana, involving the posterior migration and posterolateral widening of the choanal groove, with the reduction of the pterygoidean septum. No definitive atoposaurid possesses procoelous vertebral centra, and no specimen ascribed to *Theriosuchus* can be demonstrated to possess this feature. Therefore, current evidence suggests that full vertebral procoely only evolved once within the lineage leading to Eusuchia.

Future research on the systematic placement of Atoposauridae, *Theriosuchus* and Paralligatoridae within Neosuchia will need to incorporate a wider set of taxa into phylogenetic analysis, such as the basal neosuchian *Stolokrosuchus lapparenti* (Larsson and Gado, 2000), hylaeochampsids including *Paluxysuchus newmani* (Adams, 2013), *Hylaeochampsa vectiana* (Clark and Norell, 1992), and *Pietraroiasuchus ormezzanoi* (Buscalioni *et al.*, 2011), *Bernissartia fagesii*, and additional paralligatorids including *Batrachomimus pastosbonensis* (Montefeltro *et al.*, 2013) and *Rugosuchus nonganensis* (Wu *et al.*, 2001a). These additions should help to develop a clearer understanding of the Neosuchia–Eusuchia transition.

Disclosure: Much of this Chapter is drawn from text in Tennant *et al*. (2016). While the primary author wrote the majority of this text and performed all analyses, parts of it have been contributed to by all other authors, as well as receiving input from the peer review process.

Tennant, J. P., Mannion, P. D. and Upchurch, P. (2016) Evolutionary relationships and systematics of Atoposauridae (Crocodylomorpha: Neosuchia): implications for the rise of Eusuchia, *Zoological Journal of the Linnean Society*, **177**, 854-936.

6 Discussion and Conclusions

This thesis set out to explore four fundamental questions regarding the extinction status of tetrapods across the Jurassic/Cretaceous boundary. To explore this issue, I investigated their evolutionary dynamics at several different levels, using a suite of complimentary methodologies. What this has enabled, rather than providing a simple magnitude of extinction, is a multi-dimensional perspective into the dynamics of different tetrapod groups at different scales, and constraints on our understanding based on how the available data are analysed and interpreted.

6.1 What was the scale of any extinction across the Jurassic/Cretaceous boundary?

This first query asks broadly whether or not a putative mass extinction (Raup and Sepkoski Jr, 1982; 1984), minor extinction (Hallam, 1986; Bambach, 2006), or faunal turnover (Benson and Druckenmiller, 2014) occurred at the J/K boundary. As has been documented throughout this thesis, the answer to this is dependent on how the fossil record is interpreted. Numerous studies have demonstrated that a literal, raw reading of the fossil record is complicated by heterogeneous sampling, which has led to much disagreement and uncertainty in interpreting the J/K boundary. Despite this issue being quantitatively and qualitatively investigated in detail, there is currently little consensus as to what the optimal methods for compensating for such variation, or sampling biases, are (Alroy *et al.*, 2001; Alroy, 2010a; Benton *et al.*, 2013a; Dunhill *et al.*, 2013; Alroy, 2014; Dunhill *et al.*, 2014b; Alroy, 2015; Benton, 2015; Benson *et al.*, 2016). This has direct consequences on our interpretation of the scale of biotic changes through time, and in particular at the J/K boundary where there are radically different sampling regimes within a disparate spatiotemporal context.

To address this problem, two different scales were analysed: taxonomic, and geographical, with the temporal scale automatically implied by investigation of the J/K boundary. There seemed little point in asking simply about the clade Tetrapoda, which in itself is an enormous and hyperdiverse group comprising a massive variation in body sizes, ecologies, and modes of life. Therefore, Tetrapoda was broken down into its constitutent subclades, representing major higher level taxa. Unfortunately, for some important but poorly known Jurassic/Cretaceous groups such as Aves, Chelonioidea, or Choristodera, their fossil records during this interval are either non-existent or too poorly sampled through time to determine anything quantitatively rigorous about their dynamics. For all remaining groups, assessment of diversity changes required three components: standing diversity, extinction rates, and origination rates. The latter of these two contribute in different ways to diversity; for example, low diversity can be caused by low origination rates or high extinction rates, and therefore all three components require analysis in order to understand why we see resulting patterns in diversity. The issue of sampling adds an extra dimension of complexity to this (Alroy *et al.*, 2001; Alroy, 2010b; Upchurch *et al.*, 2011b; Benton *et al.*, 2013a; Benton, 2015). To counteract this problem, three main modes of analysis were selected to assess changes in diversity: raw, empirical diversity; subsampled diversity (through SQS), and phylogenetic diversity, the latter exclusively for Crocodyliformes. While each of these has benefits and drawbacks, the opportunity presented by analysing different methods in concert is to test for congruence between resulting patterns (Smith *et al.*, 2012; Brocklehurst, 2015). Such comparison then provides the basis for understanding the constraints on diversity patterns, and which methods might be more appropriate in terms of accuracy and precision.

6.1.1 The influene of different measures of diversity

Raw, taxonomic or empirical diversity, in almost all cases, is strongly influenced by sampling bias, based on both geological and anthropogenic sampling proxies. While the appropriateness of these

sampling proxies has been questioned at different levels (Butler *et al.*, 2009c; Peters and Heim, 2010; Benton *et al.*, 2011; Butler *et al.*, 2011; Mannion and Upchurch, 2011; Mannion *et al.*, 2011; Peters and Heim, 2011; Upchurch *et al.*, 2011b; Dunhill *et al.*, 2012; Benton *et al.*, 2013a; Dunhill *et al.*, 2013; Dunhill *et al.*, 2014a; Dunhill *et al.*, 2014b; Newham *et al.*, 2014; Benton, 2015), and in some cases seemingly used with little regard or justification as to their suitability, quality, or basis, the seemingly broad relationship between sampling proxies of different levels and types and taxonomic diversity suggests that generally raw diversity does capture a genuine sampling signal. Therefore this suggests that it is inappropriate to firstly use raw diversity as an estimate for true diversity, and secondly as the basis for investigating the parameters that shape diversity through time. On the other hand, subsampled diversity appears to be independent of these confounding biases at different levels (i.e., per taxonomic group, and at a higher tetrapod level) and for every higher taxonomic unit in Tetrapoda in which there was sufficient data to assess the relationship. Combined with a strong correlation between PDE and subsampled diversity, the results presented here suggest that SQS is an appropriate method for reconstructing diversity (although see Starrfelt and Liow (2016) and Hannisdal *et al.* (2016)), and therefore can be used to assess the relative magnitude of diversity changes across the J/K boundary.

6.1.2 Global versus regional patterns of diversity and extinction

Overall, the analyses presented provide strong evidence for an extinction event of intermediate magnitude at the end of the Jurassic (see point 2 below for discussion of this). Interpreting the pattern of extinction in terms of stratigraphy is complicated by an incredibly heterogeneous stratigraphical architecture. It is unfortunate that continuous sequences that span the J/K boundary are extremely rare, seemingly confined to marine groups in South America, and terrestrial units in southern Africa and Europe, with an overall very patchy earliest Cretaceous record (Benson *et al.*, 2013; Fanti *et al.*,

2016b; McPhee *et al.*, 2016). Combined with this is a series of diachronous unconformities which are variably correlated with the tetrapod fossil record, which makes detecting the scale of any potential single, global event difficult to pin down (Michalík *et al.*, 2009; Pruner *et al.*, 2010; Grabowski, 2011; Michalík and Reháková, 2011; Wimbledon *et al.*, 2011; Žák *et al.*, 2011). Such a problem is alleviated in part by exploration of regional diversity patterns, which are based on fossil collections in an explicit spatiotemporal and stratigraphical context, and regional-level analyses are now becoming more commonplace in investigations of Mesozoic tetrapod diversity in order to compensate for spatial biases and incomplete sampling (Upchurch *et al.*, 2011b; Mannion *et al.*, 2015; Nicholson *et al.*, 2015). By combining occurrence records with their macrostratigraphic context, some of the complications of using global range through data are avoided, and thus the risk of oversimplifying the temporal and geographic context of taxonomic occurrences is negated. The reason why this is of such importance is that of almost all purported extinction boundaries, the J/K boundary completely lacks either a globally trackable sequence-bounding subaerial unconformity (Wimbledon *et al.*, 2011; Vennari *et al.*, 2014; Schnabl *et al.*, 2015), a basal surface representing a forced regression, or a major flooding surface as part of a transgressive systems tract (Holland and Patzkowsky, 2015), or isotopic anomaly (Kudielka *et al.*, 2002; Schulte *et al.*, 2010). However, individual local surveys by Kudielka *et al.* (2002), Grabowski *et al.* (2010b), Lipinski *et al.* (2003), Michalík and Reháková (2011), Price *et al.* (2016) and Žák *et al.* (2011), combined with evidence for regional level extra-terrestrial material input (McDonald *et al.*, 2001; McDonald *et al.*, 2006). suggest that there is much progress to be made in using geochemistry to define the J/K boundary. The result of this stratigraphic incompleteness and geographic heterogeneity is an almost total absence of tetrapod fossils in North America and Africa during the earliest Cretaceous, and those that exist in South America and Asia are often too poorly constrained, or cross multiple time bins, to draw definitive quantitative conclusions about continent-level changes in these regions. As such, the geographic scale of any J/K boundary event appears to be largely constrained to Europe, and with differential contributions from Asia and South America, which is

largely reflected in the overall similarity between superficially 'global' patterns, and those recorded on a European level. One of the issues that was considered in depth in this thesis is that of relative abundances (i.e., changes in the taxon-abundance curve), and a generally poor earliest Cretaceous fossil record. It has been argued, however, that rarity of fossils based on their abundance distribution, might be a characteristic of mass extinctions, as these represent breakdowns in functional ecological networks (Hull *et al.*, 2015). At the present, it is difficult to distinguish between this hypothesis, that of a taphonomic filter (see below), or a generally poor tetrapod fossil record. Use of a fair subsampling protocol eliminates this final alternative as a possibility, as well as explicitly defining constraints on the strength of possible interpretations. Therefore, the results here are more indicative of elevated extinction rates leading to a diversity decline, and a breakdown of European ecosystems across the J/K boundary. This is reflected in elevated extinction rates at the end of the Jurassic, and suppressed origination rates during the earliest Cretaceous, which is overall evidence for a moderate-level extinction, protracted over several million years and leading to suppressed biological recovery.

6.2 How did the timing, magnitude, and tempo of the J/K boundary extinction vary between different groups?

Across the Tithonian–Berriasian (Jurassic/Cretaceous) boundary, stage-level diversity patterns are distinct between different higher tetrapod clades. In dinosaurs, the dominant terrestrial group throughout the Jurassic and Cretaceous, the magnitude of the diversity decline based on estimates of subsampled diversity varies from 75% in theropods, to 33% in ornithischians, and 63% in sauropods, although in the latter, the timing of this decline is masked by a failure to adequately sample this group in the Berriasian. Non-marine crocodyliforms declined by around 50%, and pterosaurs show a similar pattern to sauropods, in failing to recover a signal in the Berriasian but having a subsequent Hauterivian diversity of 80% lower than that of Tithonian levels. Non-marine turtles also declined by

33% of their diversity, and mammals declined by 69%, but from the Kimmeridgian to the Valanginian. Finally, the only other group for which a constant subsampled diversity estimate through the J/K interval could be recovered, lepidosauromorphs (excluding aquatic mosasauroids), show a decline of 48% across the boundary. Therefore, in the non-marine realm, a total mean estimate of diversity decline across the J/K boundary is between 48% and 56% of tetrapod genera, depending on the timing of decline in those groups, for which this is difficult to determine. The precise magnitude of this decline varies depending on how we treat coverage and set the quorum level with SQS, but this resolution provides a good compromise between being able to extract a signal from the data, and that signal being a reliable representation of underlying patterns. In the marine realm, the scale of diversity decline is more difficult to determine. Due to a poor earliest Cretaceous fossil record, the maximum decline can be approximated at 50%, although this is very tentative as the signal is very patchy.

As suggested by the differences in when the greatest diversity decline occurred in time, extinction and origination rates also are not supportive of a temporally synchronous event across all clades. Sauropods, theropods, pterosaurs, non-marine turtles, crocodyliforms (marine and non-marine), ichthyosaurs and sauropterygians all have their highest Jurassic and Cretaceous extinction levels at the end of the Tithonian, indicated by instantaneous rates that account for artificial clustering through alleviation of the Signor-Lipps effect. Groups which suffered the highest diversity losses (marine crocodyliforms, theropods, and pterosaurs) all show sustained elevated extinction rates even in the Berriasian, indicative of high levels of protracted extinction. Therefore, while the greatest overall extinction was at the end of the Jurassic, we see a continuous knock-on effect of this extinction into the onset of the Cretaceous in some groups.

Elevated origination rates and high diversity in some groups did not seem to confer any advantage in survivorship through the J/K boundary extinction. Thalattosuchian crocodylomorphs diversified during the Oxfordian (de Andrade *et al.*, 2010b; Young *et al.*, 2011b; Young *et al.*, 2014a), and all other

archosaur lineages reached a peak of diversification subsequently in the Kimmeridgian (Barrett *et al.*, 2009; Upchurch *et al.*, 2011b; Butler *et al.*, 2013). Ichthyosaurs also rapidly diversified in the Kimmeridgian and Tithonian, with the radiation of Platypterygiinae and Xenoparsia, altogether indicating that the Late Jurassic was generally a highly productive time for tetrapods. In some cases, figures are suggestive of adaptive radiation rates, with 5 times Jurassic background rates in theropods, and equally high rates in sauropods and ornithischians. Pterosaur origination rates continued to be high in the Tithonian unlike the other archosaur groups. In fact, the only time such high rates are seen again in any group is in the Turonian and Campanian (Late Cretaceous) for lissamphibians, the Albian for mammals, and the Albian and Campanian for ornithischians. The synchronicity of this event in the Kimmeridgian across dinosaurs, non-marine crocodyliforms, and pterosaurs, suggests that terrestrial archosaurs were experiencing extremely distinct, and advantageous, macroevolutionary processes at this time, and at a global extent. However, in spite of this, these groups experienced the highest rates of extinction at the J/K boundary. This suggests that high rates of speciation prior to an extinction event do not confer a survivorship advantage on those clades, and in fact might have been responsible for elevated extinction rates and high levels of faunal turnover.

This provides further evidence that the diversity declines recorded in these groups are genuine biological signals, and not the product of a taphonomic regime shift across the J/K boundary, or indicative of a sampling failure. The combination of dual methods that account for these possibilities in different ways on largely independent datasets is supportive of this conclusion. As such, this raises a further question about the earliest Cretaceous fossil record. Is the fossil record ‘poorer’ because of a change in sampling, which is reflected in overall lower abundances, or is it because elevated extinctions have made taxa rarer, and decreased the probability of fossil preservation. This final option would seem to be the most favoured based on the currently available data, but again there is the problem that this might be over-interpreting what is still a very poor Berriasian fossil record, with very few fossil-bearing sites.

6.3 What was the ecological response of different tetrapod groups to the J/K boundary extinction?

One thing all of the 'Big Five' mass extinctions have in common are profound losses of taxonomic diversity, coupled with prolonged episodes of ecological change. The most notable aspect of them, perhaps, is that animals or groups which enjoyed ecological dominance prior to a mass extinction either went completely extinct or survived, but only as relatively minor components of ecosystems. This aspect of taxonomic and ecological reorganisation is characteristic of all mass extinctions, and the two are not always linearly correlated (Benton, 1994; McGhee *et al.*, 2004; Twitchett, 2006; McGhee *et al.*, 2012).

In the case of the Jurassic/Cretaceous boundary, there is evidence for ecological remodelling both coupled with, and resulting from, substantial diversity loss. This can be tracked on a complete ecosystem level, with evidence for disruption in vertebrates (Benson and Druckenmiller, 2014), invertebrates (Kiessling, 2008; Kiessling, 2009; Alroy, 2010a; b), micro-organisms (Bralower *et al.*, 1989; Danelian and Johnson, 2001; Kiessling, 2002; Bornemann *et al.*, 2003), and the biophysical environment in which they form interactive networks. What is distinct from mass extinction intervals is that we do not see the widespread loss of higher groups that were dominant prior to the extinction event at the J/K boundary. With this extinction are a series of radiations that do not appear to have supplanted previously dominant groups, as with mass extinctions. Rather, we see within-group re-organisation, with selective extinctions paving the way for subsequent opportunistic radiations. This is most clearly emphasised in groups such as crocodyliforms, sauropods, and pterosaurs. In each of these, the more basal members appear to have become extinct at the J/K boundary, followed by the subsequent radiation of new groups in the earliest Cretaceous. In almost all cases though, these radiations do not occur instantaneously after the extinction. They occur in a staggered fashion,

reflected by a combination of clade origination times and high origination rates, but with a period of quiescence in the earliest Cretaceous.

6.3.1 Marine and semi-aquatic groups

A faunal turnover is documented in sauropterygian taxa, along with the extinction of shallow marine and semi-aquatic crocodylomorphs and testudines at the J/K boundary (Benson *et al.*, 2010; Benson and Butler, 2011; Benson and Druckenmiller, 2014; Martin *et al.*, 2014a). The staggered Late Jurassic decline in thalattosuchians, along with semi-aquatic crocodylomorphs, might be related to the closing off of shallow marine basins during this global sea level regression (Hallam, 1988; Hallam, 1992; Hallam, 2001; Miller *et al.*, 2005; Pierce *et al.*, 2009b; a). It might be that among marine tetrapods, those fully adapted to a free-swimming lifestyle (such as ichthyosaurs and some metriorhynchid crocodylomorphs) were more resistant to regional sea-level changes occurring over the J/K boundary by exploiting new dispersal pathways (Zammit, 2012; Stinnesbeck *et al.*, 2014), and therefore did not experience elevated extinction rates. Furthermore, a recent study of marine tetrapods shows that they exhibited their greatest Mesozoic decline in morphological disparity across the J/K transition, although statistical support for this is generally weak, and it appears that no major functional morphotypes went extinct at the boundary (Stubbs and Benton, 2016). The timing of these declines and radiations coincides with the diversification of pancryptodiran and pleurodiran turtles (Hirayama *et al.*, 2000; Bardet *et al.*, 2014). The radiation of these clades suggests that there might have been broader ecological shifts occurring in semi-aquatic to shallow marine reptile faunas. The occupation of high tier predatory niches by new groups was likely an important factor in suppressing the recovery of marine crocodyliforms, which throughout the Cretaceous never recovered to their pre-J/K boundary diversity levels. This marine pattern is distinct from that observed in continental crocodyliform ecosystems: there we see a drop in diversity followed by a rapid recovery and

subsequent radiations (Eusuchia and Notosuchia) during the Early Cretaceous (Carvalho *et al.*, 2010; Bronzati *et al.*, 2015), representing a faunal turnover in non-marine crocodyliform faunas as ecological pressure was released following the J/K boundary decline. This pattern is emphasised by the taxonomic revision of Atoposauridae presented here, with the new view of this clade indicating that they went extinct at the J/K boundary along with numerous other shallow marine groups in Europe.

Thalattoschian crocodylomorphs suffered a staggered decline through the J/K boundary, but marine groups did not recover, instead being opportunistically replaced as apex predators by elasmosaurid and leptocleidid sauropterygians (Benson and Druckenmiller, 2014), all major extant shark lineages (Sorenson *et al.*, 2014), and also allowing for the ecological release of marine turtles (Cadena and Parham, 2015). The decline and final extinction of marine thalattosuchian crocodylomorphs is synchronous with the loss of multiple non-marine turtle groups (e.g., basal eucryptodirans, eurysternids and plesiochelyids) in Europe at the J/K boundary (Pérez-García *et al.*, 2011). Non-marine crocodyliforms suffered, with atoposaurids becoming extinct, prior to the origination of notosuchians and eusuchians (Bronzati *et al.*, 2015), the latter of which led to the origin of crown group crocodylians. Coastal turtle faunas in Europe also suffered, with eurysternids and thalassemydids being replaced by more advanced eucryptodirans and paracryptodirans, although much of this faunal turnover again appears to have been focussed in Europe. With this, there is also evidence for a degree of facies- or environmentally-oriented selectivity in turtles during the Late Jurassic and Early Cretaceous. Only a single freshwater taxon is currently known to have survived the J/K boundary among an assortment of European coastal and semi-aquatic plesiochelyids, eurysternids, and thalassemydids (Pérez-García and Ortega, 2014), although xinjiangchelyids might have persisted in a European Cretaceous refugium (Pérez-García *et al.*, 2014). Similarly in Asia, it is likely that palaeoenvironmental preferences and seasonal climatic variations controlled turtle distributions through the J/K boundary and until the late Early Cretaceous (Rabi *et al.*, 2010).

The low ecological diversity of plesiosaurians and testudines might have been a distinct contributing factor to their decline and turnover at the J/K boundary (Benson *et al*., 2010; Benson and Druckenmiller, 2014; Rabi *et al*., 2014). At the J/K boundary, numerous semi-aquatic to shallow-marine basal forms went extinct, including eucryptodirans, plesiochelyids, and eurysternids. This was followed by the subsequent diversification of pancryptodirans and pleurodirans in a geographically structured manner (Hirayama *et al*., 2000; Cadena *et al*., 2013; Bardet *et al*., 2014; Püntener *et al*., 2014; Nicholson et al., 2015). The radiation of new plesiosaurian lineages immediately after the J/K boundary (i.e., Elasmosauridae and Leptocleididae) is clear evidence for a within-group faunal turnover, and conceivably related to the easing of ecological pressure following the gradual extinction of thalattosuchian crocodylomorphs in the Late Jurassic and Early Cretaceous (Young *et al*., 2010; Mannion et al., 2015; Chiarenza et al., 2015). Although metriorhynchids exhibited a range of ecologies in the Late Jurassic, their diversity and disparity declined in the earliest Cretaceous (Young *et al*., 2010). Ecological plasticity might have been important for ichthyopterygians, with high overall ecological diversity of platypterygiines contributing to their persistence through the J/K boundary (Fischer *et al*., 2013b), although this is masked by a very poor earliest Cretaceous fossil record.

6.3.2 Terrestrial groups

In dinosaur faunas, non-neosauropods appear to have been replaced by titanosauriforms, medium-bodied theropods were replaced by a suite of smaller-bodied maniraptorans and larger-bodied carcharodontosaurids and spinosaurids, and stegosaurs declined to pave the way for the ankylosaurian radiation. There is a seemingly selective extinction of medium and larger-sized dinosaurs (sauropods and theropods) at the J/K boundary (Upchurch *et al.*, 2011b; Carballido *et al.*, 2012; Upchurch and Mannion, 2012; Zanno and Makovicky, 2013; Cobos *et al.*, 2014; Souza and Santucci, 2014). In sauropods, this extinction is focused on broad-toothed non-neosauropod

eusauropods and narrow-toothed diplodocid species (Barrett and Upchurch, 2005), with just two occurrences of the latter known from the Cretaceous (Gallina *et al.*, 2014; McPhee *et al.*, 2016), and is followed by the subsequent diversification of rebbachisaurids and titanosauriforms (Upchurch and Mannion, 2012; Gorscak and O'Connor, 2016). This pattern is also repeated in Asia, with the replacement of mamenchisaurid non-neosauropods by titanosauriforms across the J/K boundary (Wilson, 2005; Wilson *et al.*, 2012; Mannion *et al.*, 2013), and in South America there do not appear to have been any titanosaurs until the Cenomanian (Gallina, 2016), although Titanosaurifomes were present from the Barremian onwards, which is contemporaneous with the Asian sauropod record.

Evidence of a combined ecological and taxonomic focus of extinction in saurischian dinosaurs, to the exclusion of ornithischians, combined with environmental preferences between different sauropod groups (Mannion and Upchurch, 2010b), suggests that a combination of factors were acting upon dinosaurs at the J/K boundary (Upchurch *et al.*, 2011b; Upchurch and Mannion, 2012). These differences between the major herbivorous dinosaur groups potentially relate to different requirements for forage consumption; however, there is little evidence for any major floral perturbations at the J/K boundary (Barrett, 2014), except for a tentative coupling between the decline of cycadophytes and stegosaurs during the earliest Cretaceous (Butler *et al.*, 2009a; Butler *et al.*, 2009b). The only known herbivorous tetanuran theropod lineage in the Jurassic, *Chilesaurus*, has no known Cretaceous representative (Novas *et al.*, 2015). It has been suggested that medium-sized theropods underwent a substantial decline across the J/K boundary, and were replaced by larger-bodied carcharodontosaurids and spinosaurids (Novas *et al.*, 2013; Tortosa *et al.*, 2014). Whereas a literal reading of the fossil record might indicate an Early Cretaceous diversification of smaller-bodied coelurosaurian theropods (Zanno and Makovicky, 2013; Tortosa *et al.*, 2014; Wang *et al.*, 2014), at least a portion of this is undoubtedly an artefact of variation in the degree of Early Cretaceous preservation and the discovery of numerous new species in the Jehol Biota. Furthermore, at least some medium-sized basal theropod clades persisted into the Early Cretaceous (Sánchez-Hernández

and Benton, 2012), which suggests that part of this extinction selectivity signal might be a product of our poor sampling of earliest Cretaceous terrestrial deposits (Benson *et al.*, 2013).

This evidence points towards the J/K boundary representing a period of ecophysiologically-driven faunal turnover in dinosaurs. Whether or not this was due to competitive displacement or opportunistic replacement, as some groups declined followed by the radiation of new groups, is currently unknown. It is noteworthy that herbivorous groups including diplodocids and stegosaurs show evidence of a decline, followed by the subsequent diversification of other herbivorous lineages, including ankylosaurs, basal ceratopsians, and iguanodontians, which does not appear to be related to major changes in floral patterns (Butler *et al.*, 2009a; Butler *et al.*, 2009b). This lends support to the opportunistic replacement hypothesis, whereby extinction creates vacant ecospace, which subsequently becomes occupied by newly radiating groups (Benton, 1987; 1996; Harries *et al.*, 1996).

The apparent Early Cretaceous radiation of diverse groups of avialans, including Enantiornithes and Ornithuromorpha (O'Connor *et al.*, 2011a; Wang *et al.*, 2013; Lee *et al.*, 2014; Wang *et al.*, 2016b), might have been caused by the release of ecological pressure from the decimation of non-pterodactyloid faunas at the J/K boundary (Butler *et al.*, 2009c; Butler *et al.*, 2013), although the timing of these events might be distorted by taphonomic artefacts. This timing comes from evidence of increased diversification rates in pygostylian theropods in the latest Jurassic and earliest Cretaceous (Benson and Choiniere, 2013), combined with sustained decreases in body size (Benson *et al.*, 2014; Brusatte *et al.*, 2014), broader occupation of ecological roles (Mitchell and Makovicky, 2014; Huang *et al.*, 2016; Wang *et al.*, 2016b), positive phenotypic selection rates (Baker *et al.*, 2016), and increasing rates of morphological change (Wang and Lloyd, 2016), although these diversification studies cannot account for heterogeneous sampling of the fossil record. Additionally, pterosaurs began to occupy increasingly terrestrial environments in the Cretaceous (Butler *et al.*, 2013; Andres *et al.*, 2014), which might represent an ecological reorganisation of flight-capable faunas at this time. This is supported by

evidence for sustained constraint on pterosaur body sizes through the Late Jurassic, potentially through competitive interaction with increasingly diverse avialan faunas (Benson *et al.*, 2014). The remaining pterosaur lineages after the J/K boundary experienced an increase in morphological disparity, synchronous with that for birds (Wang *et al.*, 2016a), suggesting a form of competitive interaction to fill ecological morphospace subsequent to the boundary extinctions (Butler *et al.*, 2009c; Butler *et al.*, 2013). This ecological expansion is most discernible in groups such as azhdarchoids, which adopted novel aerial morphologies leading to enhanced maneuverability (Frey *et al.*, 2011).

Rhamphorynchid pterosaurs went extinct, becoming replaced by increasingly diverse ornithocheiroideans (Andres *et al.*, 2014; Upchurch *et al.*, 2014), and paving the way for the paravian radiation in the Early Cretaceous. Major extant squamate lineages including Lacertoidea, Scincoidea, Acrodonta and Pleurodonta diversified close to the J/K boundary (Pyron and Burbrink, 2012; Jones *et al.*, 2013), coincident with the diversification of multiple lineages of anurans (Marjanovic and Laurin, 2013). Mammal faunas appear to have undergone a faunal turnover prior to the J/K boundary, with dryolestids and docodonts being replaced by multituberculates and eutriconodonts, but the diversifications in these groups did not take place until the earliest Cretaceous, in the wake of the J/K boundary extinction.

6.3.3 Broader ecological implications

This discovery of a wide-scale faunal and ecological turnover is congruent with previous studies that have shown that low-latitude, shallow marine and sessile epifauna were the most severely hit across the J/K boundary, including articulate brachiopods, gastropods, crustaceans, cemented bivalves and some ammonites (Alroy, 2010b; Rogov *et al.*, 2010; Klompmaker *et al.*, 2013), with the latter two groups showing evidence for regional selectivity during the transition (Alroy, 2010b; Rogov *et al.*, 2010), alongside a higher extinction intensity in northern hemisphere taxa (Alroy, 2010c). Additionally,

these groups exhibited latitudinal constraints on diversity, possibly driven by large-scale changes in global climate regimes at the J/K boundary (Anderson *et al.*, 1999; Scotese *et al.*, 1999; Bergman *et al.*, 2004; Meyers, 2014). Such constraints might be responsible for global declines in diversity (Peters and Foote, 2001; Jablonski *et al.*, 2003; Lu *et al.*, 2006; Smith and McGowan, 2007; McGowan and Smith, 2008; Alroy, 2010c; Rogov *et al.*, 2010; Smith *et al.*, 2012), and the reorganisation of marine ecosystems through the J/K boundary. In particular, reef-dwelling taxa including some corals and arthropods seem to have been the worst affected (Kiessling, 2008; Kiessling, 2009; Ruban, 2011; Foote, 2014), with a turnover from rudist to scleractinian-dominated reefs being one major consequence of this (Aberhan *et al.*, 2006). It has previously been suggested that the cause of this was an ecological shift from shallow shelf-dwelling communities to deeper-water ecosystems (Aberhan and Kiessling, 2012; Klompmaker *et al.*, 2013), which is fully congruent with the results here documenting sea level as the principle factor driving changes across the J/K boundary. Additionally, foraminiferans and calcareous phytoplankton all declined in diversity at this time (Danelian and Johnson, 2001), indicative of broader scale changes in the marine realm, such as a shift from calcitic to aragonitic organisms (Kiessling *et al.*, 2008), and climatic disruption influencing oceanic productivity and nutrient cycles.

The decline of reefs over the J/K boundary was probably also tied to changes in global temperatures (Anderson *et al.*, 1999; Scotese *et al.*, 1999; Bergman *et al.*, 2004; Martin-Garin *et al.*, 2012). Additionally, it is likely that factors relating to sea-level changes, including declining salinity and shifts in nutrient flux systems, constrained organisms to increasingly rare shallower shelf systems over the J/K boundary and until the middle Cretaceous (Hay *et al.*, 2006). The core driver for these changes in sea level and marine productivity (Danelian and Johnson, 2001) potentially relates to the connection between the Atlantic and the Pacific (Panthalassa) oceans during the J/K interval, with shorter term variation driven by fluctuations in the extent of polar ice caps (Haq, 2014). Large-scale tectonic processes at this time, particularly regarding the break-up of Pangaea, must have been important in

controlling the biogeography of marine and terrestrial taxa (Galton, 1982; Scotese *et al.*, 1988; Scotese, 1991; Pérez-Moreno *et al.*, 1999; Escaso *et al.*, 2007; Jordan *et al.*, 2016).

However, the impact of these apparently global changes appears to have been biotically confined to Europe or the northern hemisphere, congruent with previous results in marine invertebrates (Smith and McGowan, 2007; Alroy, 2010b). Therefore, the J/K boundary event can only be interpreted in the context of regional, not global, ecological changes. This conclusion for tetrapods is congruent with previous studies of marine invertebrates that showed that any J/K boundary event was confined to Europe (Hallam, 1986).

6.4 To what extent do abiotic factors correlate with biological changes through the Jurassic/Cretaceous boundary?

The best-documented decline in tetrapod faunas is in Europe. Here, we see the extinction of localised coastal-dwelling faunas, including thalassemydid, eurysternid and plesiochelyid turtles, and semi to fully aquatic groups of crocodyliforms. Of the diverse Late Jurassic European turtle faunas, only a single lineage is known to have survived the J/K boundary (Pérez-García and Ortega, 2014; Cadena and Parham, 2015). That sea level then seems to act as the primary driver controlling diversity is perhaps no surprise, as the habitability of coastal environments will be entirely dependent on regional sea-level fluctuations. This is coincident with other recent studies that noted that shallow marine and semi-aquatic crocodyliform and turtle faunas were particularly affected by J/K boundary events (Benson *et al.*, 2010; Benson and Butler, 2011; Martin *et al.*, 2014a), leading to an overall faunal turnover in marine tetrapods (Benson and Druckenmiller, 2014). Previously it was suggested that sea level change was the primary cause for localised extinctions in Europe in both vertebrates and invertebrates, but this was never documented quantatively and after accounting for sampling bias (Hallam, 1986; Hallam, 1988; Hallam, 1992; Hallam, 2001; Miller *et al.*, 2005; Pierce *et al.*, 2009a).

Importantly, it seems that despite high origination rates in groups such as ichthyosaurs and a potential to exploit marine dispersal corridors (Zammit, 2012; Stinnesbeck *et al.*, 2014; Zverkov *et al.*, 2015), this conferred little survival advantage during the J/K boundary regression. This broad correlation between sea level and diversity fits in well with a range of previous studies at a variety of different scales and scopes that have noted that sea level controls the architecture and structure of near-shore ecosystems (Valentine and Moores, 1970; Haq *et al.*, 1987; Hallam, 1988; Hallam and Cohen, 1989; Hallam, 1992; Hallam, 2001; Smith *et al.*, 2001; Miller *et al.*, 2005; Peters, 2005; Bambach, 2006; Smith and McGowan, 2007; Purdy, 2008).

The fact that sea level appears to be the primary agent driving changes in tetrapods suggests that eustatic sea level is the principal force controlling the structure and diversity of marine ecosystems on a larger scale. The knock on effects of sea level change, including variation in salinity and nutrient fluxes, cannot be ignored, and it is likely that these factors, combined with increasingly constrained reef and shelf systems over the J/K boundary, led to more widespread ecosystem changes (Hay *et al.*, 2006). The causes of such large scale changes could be due to the changing tectonic configurations occurring across the J/K interval (Scotese *et al.*, 1988; Scotese, 1991; Scotese *et al.*, 1999), including the connecting of the Atlantic and Panthalassa oceans, as well as oscilations in the extent of polar ice (Haq, 2014), both factors which would influence sea level.

Although eustatic sea level has been identified as the principle driver behind these patterns, the wider implications within a total ecosystem context need to be considered. The J/K boundary also wtinessed a major revolution in marine micro-organism communities that has been attributed to increasing global aridity and continental weathering (Weissert and Channell, 1989; Hallam *et al.*, 1991), culminating in increasingly oligotrophic conditions in the marine realm (Danelian and Johnson, 2001; Tremolada *et al.*, 2006). It is likely that such environmental changes were primarily related to the sea-level regression that occurred across the J/K boundary, which together impacted upon global

ecosystems. Additional evidence suggests that climate strongly influenced oceanic productivity and nutrient cycles at the J/K boundary (Danelian and Johnson, 2001), which, combined with a eustatic lowstand (Miller *et al.*, 2005), would have strongly impacted upon marine life. This could have provided a mechanism for the different patterns exhibited by shallow- and deep-water invertebrate taxa.

Evidence for a 'common cause' driving both sampling and diversity is also variable. We would expect two things to have occurred as a result of the J/K boundary regression. The first of these is enhanced extinction through contraction or elimination of shallow marine ecosystems, which also can create anoxic bottom waters, both of which are found at the J/K boundary (McGowan and Smith, 2008; Pyenson *et al.*, 2014). Secondly, decreasing sea level also leads to lower preservation rates for sedimentary rocks, which therefore negatively influences our ability to sample. In North America, it seems that sea level influences both the marine and sedimentary rock record to a degree that diversity, sea level and sampling are all cross correlated. However, this pattern is not reflected in either Europe or on a global scale, which suggests that different regional sampling regimes strongly influence our ability to adequately interpret diversity patterns.

While sea level appears to exert overall control on tetrapod diversity, other secondary factors cannot be ruled out. The carbon cycle appears to be an important factor in biological events throughout the Mesozoic, indicative of major biological changes, and with additional consequences as organic matter fluxes change (Weissert and Erba, 2004; Bambach, 2006; Bodin *et al.*, 2015; Birch *et al.*, 2016; Naafs *et al.*, 2016; Price *et al.*, 2016). This case is most clearly emphasised in marine thalattosuchian crocodyliforms, which in the earliest Cretaceous became confined to increasingly rarer and uninhabitable shallow marine basins and shelf environments (Hay *et al.*, 2006), until their apparent geographic isolation and extinction in the late Early Cretaceous (Fanti *et al.*, 2016b). While there is some evidence for a minor oceanic anoxic event at the J/K boundary (Pyenson *et al.*, 2014), this

appears to have had little direct effect on marine faunas, or if it did then the effects are masked by an overwhelming regulating signal from changes in sea level.

Palaeotemperature also appears to have played an important role in regulating the diversity in some ectothermic groups, including testudines and lepidosaurians, which suggests that these organisms responded differently to abiotic changes than other groups such as archosaurs. Global palaeotemperatures changed dramatically over the J/K boundary (Anderson *et al.*, 1999; Scotese *et al.*, 1999), including several episodic 'cold snaps' (Jenkyns *et al.*, 2012) which could have been the main reason for the J/K boundary declines in these tetrapod groups. There is further evidence for rapid sea surface temperature cooling from the Tithonian and across the J/K boundary (Weissert and Channell, 1989; Bice *et al.*, 2003; Price and Rogov, 2009; Jenkyns *et al.*, 2011; 2012), which might have also played a role in the diversity crash witnessed in testudines and lepidosaurs (if marine temperatures can be used as a proxy for terrestrial temperatures), with their recovery in the earliest Cretaceous due to an increasingly warmer climatic regime (Hay, 2008; Littler *et al.*, 2011; Pouech *et al.*, 2014).

6.5 Future directions of research

6.5.1 Global correlation of the J/K boundary

One principal issue which remains unresolved is the timing of any extinction event through the J/K boundary. While it has been demonstrated that there was a phase of extinction between the Tithonian and the Berriasian, this period still covers several million years. Extinctions are usually brief, and instantaneous in geological terms. They are also spatially heterogeneous, a factor which is exacerbated by the spatial distribution of sampling across extinction intervals. This makes discerning the tempo of tetrapod extinctions extremely difficult to measure, and therefore the corresponding processes behind them challenging to distinguish. Part of this problem stems from the simple fact that

tetrapod species cannot be given actual biological durations, but the rocks which they are found in are used as proxies to provide stratigraphic ranges, and therefore the durations of lineages are constrained simply based on the macrostratigraphic resolution. One of the advantages of analysing tetrapods through the J/K boundary extinction is that the interval has typically been characterised by invertebrates and microfossil taxa (Wimbledon *et al.*, 2011; Schnabl *et al.*, 2015), and therefore is relatively free from the biases associated with opinions over which taxonomic groups should be used to characterise the identity of the boundary. The best current evidence for the age of the J/K boundary comes from the numerous biotic markers in the Tethys (Riccardi, 1991; Adatte *et al.*, 1996; Grabowski, 2011; Michalík and Reháková, 2011; Li *et al.*, 2013). However, there is still an issue with geographic correlation between different potential J/K boundary stratigraphic sections, particularly between the condensed Boreal sites and Austral regions (Houša *et al.*, 2007; Žák *et al.*, 2011; Dzyuba *et al.*, 2013). Appropriate refinement of these stratigraphic correlations will be important in determining the absolute date of the J/K boundary, which despite still being debated, seems to be homing in on around 145.5 Ma and the middle of the M19n magnetostratigraphic chron. This correlates well with calpionellids biostratigraphy, and in particular the base of the Alpina Subzone, but lies above the historical base for the Berriasian (i.e., the *Berriasella jacobi* Subzone), and is more consistent than previously used ammonite subzone stratigraphy (W. Wimbledon, pers. comm. 2016). The problem with suggestions for the base of the M18r chron is that this is not supported by any biomarkers, which makes temporal calibration more difficult. Future work cross-correlating between Tethyan, austral, boreal and terrestrial biozones, including those which preserve vertebrate fossils, will be important for refining our view of the J/K boundary, and the timing and structure of any biotic events through this interval. Future investigations of biotic changes through the J/K transition must take this regional heterogeneity and temporal uncertainty into account.

6.5.2 Paying homage to the Red Queen

The majority of this thesis investigated the abioic factors that regulated tetrapod diversity through the J/K interval, be they sampling related or some extrinsic environmental factor. However, I did not explore the biotic processes that could potentially govern these diversity patterns in more detail beyond the relative timings between groups of extinctions and radiations, and as such have almost fallen into the 'Red Queen versus Court Jester' dichotomy that seeks to explain the variable processes regulating diversity through time (Benton, 2009; 2010; Voje *et al.*, 2015). The interactions between species and groups of species is an important biological process, and includes ecological or physiological factors such as competition, opportunism, community structure, body size and metabolic rate, resource availability, mutualism, predator-prey relationships, feeding strategies, and others that create the biotic system that underpins diversity within ecological networks. However, such processes can be difficult to measure in tetrapod groups when often, as we have seen, the fossil record is so patchy and incomplete as to be poorly reflective of underlying ecosystems. This leads to macroevolutionary investigations using the fossil record to be at a supra-ecoystem level (Marshall and Quental, 2016), which is necessitated simply due to the overall incompleteness of the fossil record. As such, it is not so much that biological processes are ignored and the Red Queen dismissed, but more a case of what is feasible based on the underlying data.

That is not to say that measuring biotic interactions is impossible. For example, by examining rates of change in functional features (such as those related to feeding) in concert with changes to abiotic processes, we might be able to expose the interaction between organisms, their environment, and macroevolutionary patterns on a broader scale. While an overall strong signal is recovered for a regulating effect of sea level on diversity based on a maximum likelihood modelling approach, that often also recover low correlation scores based on pairwise comparisons between the two strongly suggests that no single factor can be claimed to completely regulate diversity, and further work

undoubtedly needs to investigate this issue within a multivariate framework. Future work on the J/K boundary should focus on estimating temporal shifts in morphological diversity and disparity (Pierce *et al.*, 2009a; Brusatte *et al.*, 2010; Young *et al.*, 2011a; Young *et al.*, 2011b; Butler *et al.*, 2013; Baker *et al.*, 2016; Hopkins, 2016; Lloyd, 2016), and the tempo, magnitude, and mode of phenotypic change that corresponds with the macroevolutionary dynamics recovered here. For example, the crocodyliform supertree constructed here could be used to infer the phenotypic macroevolutionary changes occurring to clades around the J/K transition, and integrate the important additional dimension of phylogeny. This will feed into suggestions that higher ecological diversity or plasticity was responsible for differential survival rates in many animal groups across the J/K boundary (Baumeister and Leinfelder, 1998; Young *et al.*, 2010; Fischer *et al.*, 2012; Rauhut *et al.*, 2012; Fischer *et al.*, 2013; Rabi *et al.*, 2014).

6.5.3 Macroevolutionary changes across the J/K transition

Additional insight into macroevolutionary changes around the J/K transition has been yielded through examination of clades in the context of dating using molecular or morphological clock techniques. For example, molecular analysis of extant sharks (Sorenson *et al.*, 2014) and monocots (Eguchi and Tamura, 2016), both non-tetrapod groups, reveals that almost all extant lineages in these groups diverged and diversified in the Early Cretaceous. Similar results have also been documented in various lepidosaur clades (Marjanović and Laurin, 2007; Marjanovic and Laurin, 2013), and suggest a major global ecological release of modern clades subsequent to the J/K boundary. Future investigations combining the fossil record with molecular and morphological clock analyses in extant clades will undoubtedly clarify this emerging picture of extinction and radiation across the J/K interval. Furthermore, there is some evidence that pterosaurs and paravian theropods rapidly diversified and adopted new ecomorphotypes in the Early Cretaceous, including the explosive radiation of the most

successful extant tetrapod group, birds (O'Connor *et al.*, 2011a; Brusatte *et al.*, 2014; Mayr, 2014; O'Connor and Zhou, 2015; Huang *et al.*, 2016; Wang *et al.*, 2016a; Wang *et al.*, 2016b). However, the precise timing of these events is obscured by varying spatiotemporal sampling of these clades, and could be illuminated through combined morphological and molecular clock analyses. Refining the timing of these diversification events will be important in distinguishing between hypotheses of opportunistic replacement or competitive displacement between different groups.

Recently, a new method of accounting for sampling probability heterogeneity through time was implemented using Mesozoic dinosaurs as a case study (Starrfelt and Liow, 2016). In some ways, this method might be superior to SQS, in that the sampling probability is an explicit function of the observation of occurrences as a rate, and estimations of diversity are calculated within a maximum likelihood framework with confidence intervals. Extension of this methodology to other tetrapod groups is the next clear step, and will provide a solid baseline for comparing between these two methods, as they both calculate and treat 'evenness' (i.e., fossil record sampling heterogeneity) in different ways. Additional estimates of extinction and origination rates beyond the 3T and BC methods used here will also be critical in capturing the full extent of any J/K boundary extinction. For example, 'gap filler' methods have been shown to be more precise than 3T estimates using Phanerozoic invertebrates (Alroy, 2014; Alroy, 2015), and could be used to refine the estimates provided here.

Geographic selectivity might have played a role in the diversification of plants, with the development of endemism in some groups, followed by dispersal-induced cosmopolitanism, a pattern that might be characteristic of both floras and faunas through the progressive break-up of Pangaea (Martín-Closas *et al.*, 2013). It is likely that shifting climates strongly influenced floral diversity on a regional scale in the Late Jurassic (Dettmann, 1989; Rees *et al.*, 2000; Parrish *et al.*, 2004), but diversity patterns for major groups across the J/K boundary remain unknown.

The J/K boundary represents an opportunity to investigate the environmental and ecological factors governing recovery. Distinct extinction and diversification patterns are clearly recorded in different groups, with a range of potential extrinsic abiotic controls. Additionally, the fact that a faunal turnover at the J/K boundary appears to be coupled with an ecological turnover in many groups, suggests that intrinsic biological parameters, principally regarding acquisition of key ecological characteristics and morphological plasticity and disparity, require further investigation in terms of the effects that these might have had on survivability.

6.5.4 Taphonomic distortion of the J/K boundary extinction

It is presently unclear whether, as with other major extinctions, the J/K boundary extinction selectively targeted larger-bodied taxa. For example, larger-sized sauropods and theropod megapredators superficially appear to disappear or become drastically reduced in numbers across the J/K boundary (Upchurch *et al.*, 2011b; Upchurch and Mannion, 2012; Zanno and Makovicky, 2013; Cobos *et al.*, 2014; Souza and Santucci, 2014; Carballido *et al.*, 2015). At extinction events, we expect to see larger-bodied taxa become extinct, or shift evolutionary trajectory to become dwarfed or replaced with smaller-bodied variants. The reason for this lack of clarity is that the issue of taphonomic filtering cannot be accounted for in the earliest Cretaceous. The majority of the earliest Cretaceous (Berriasian) record is known exclusively from microsite localities (Sigogneau-Russell *et al.*, 1998; Sigogneau-Russell *et al.*, 2001; Pouech and Mazin, 2006), in which the preservation or identification of larger-bodied taxa is negatively biased. Therefore, at the present it cannot be distinguished between whether larger-bodied taxa were selectively targeted by extinction at the J/K boundary, or are just rarely sampled among earliest Cretaceous tetrapod faunas. However, such a scenario where the preservation of large-bodied taxa is selected against is unlikely, as preservability generally favours larger-bodied organisms (Plotnick *et al.*, 2016) and we expect that larger-bodied taxa are represented in the fossil

record to a greater extent than smaller bodied taxa. It is also generally unclear what the lithofacies controls on diversity through the J/K transition were. While several key trends have been identified that might have influenced tetrapod diversity through this interval, the relationship between lithofacies preservation and occupation and diversity remains a potentially fruitful avenue for future research. As well as this, future work in the earliest Cretaceous should focus on distinguishing the following hypotheses: Fossil record absences are due to: (1) true localised taxon absence; (2) absence due to taxon extinction or local extirpation; (3) failure to sample a taxon; and (4) failure of the method to sample the taxon from the underlying population pool, including due to time averaging issues (Kosnik and Kowalewski, 2016). This will require greater collaboration between taphonomists, palaeoecologists, stratigraphers, and vertebrate and invertebrate palaeontologists to differentiate between these competing hypotheses .

6.5.5 Catastrophism and the J/K boundary extinction

The Late Jurassic–Early Cretaceous transition was a period of major environmental perturbations that have largely been ignored or overlooked in historical analyses of Mesozoic diversity dynamics, in favour of more 'exotic' extinction intervals. A range of evidence indicates the following major changes: (i) at least three large bolide impacts in the latest Jurassic, Tithonian (Milton *et al.*, 1972; Dypvik *et al.*, 1996; Corner *et al.*, 1997), including one which might have been greater in diameter than the Chicxulub impact at the K/Pg boundary (Misra *et al.*, 2014); (ii) the emplacement of the Paraná and Etendeka (late Valanginian–Hauterivian) and Ontong Java Plateau (Barremian–early Aptian) flood basalts, the latter of which might have been three times as voluminous as the end-Cretaceous Deccan volcanism; and (iii) some of the largest volcanic episodes in the history of the Earth, following the emplacement of the Shatsky Rise supervolcano at the J/K boundary. Interestingly, no correlation between any of these bolide impact impacts and any 3-phase extinction event during the Tithonian

has ever been thoroughly investigated (Walliser, 1996; Bambach, 2006), although it was briefly highlighted by Barnes *et al.* (1996) and Upchurch and Mannion (2012), and associations with this large-scale volcanism have also been largely overlooked (Dodd *et al.*, 2015). The problem is that, as singular events, it is very difficult to tie these to changes identified in time series beyond temporal association (i.e., the association cannot be identified statistically). Despite both of the Paraná and Etendeka and Ontong Java Plateau existing for longer time-scales and being of considerably more volume than the end-Cretaceous Deccan volcanism, their potential biotic impacts have never been investigated. With the exception of the Mjølnir impact, these bolide and volcanic episodes were focussed exclusively in Gondwana or the Tethys and Panthalassa oceans (Figure 1). The environmental impacts of these events are mostly well understood (Bralower *et al.*, 1994; Wignall, 2001; Weissert and Erba, 2004), although how they relate to the patterns of biotic extinction and diversity we see from the Tithonian–Barremian is less clear. This series of environmental perturbations undoubtedly warrants further investigation in the context of our revised understanding of biotic changes over the Jurassic/Cretaceous boundary.

Bibliography

Abbink, O., Targarona, J., Brinkhuis, H. and Visscher, H. (2001). Late Jurassic to earliest Cretaceous palaeoclimatic evolution of the southern North Sea. *Global and Planetary Change* **30**(3): 231-256.

Aberhan, M. and Kiessling, W. (2012). Phanerozoic marine biodiversity: a fresh look at data, methods, patterns and processes. *Earth and Life*. J. A. Talent, Springer Netherlands. **1:** 3-22.

Aberhan, M. and Kiessling, W. (2014). Rebuilding biodiversity of Patagonian marine molluscs after the end-Cretaceous mass extinction. *PLOS ONE* **9**(7): e102629.

Aberhan, M., Kiessling, W. and Fürsich, F. T. (2006). Testing the role of biological interactions in the evolution of mid-Mesozoic marine benthic ecosystems. *Paleobiology* **32**(2): 259-277.

Aberhan, M., Nürnberg, S. and Kiessling, W. (2012). Vision and the diversification of Phanerozoic marine invertebrates. *Paleobiology* **38**(2): 187-204.

Adams, T. L. (2013). A new neosuchian crocodyliform from the Lower Cretaceous (late Aptian) Twin Mountains Formation of north-central Texas. *Journal of Vertebrate Paleontology* **33**(1): 85-101.

Adams, T. L. (2014). Small crocodyliform from the Lower Cretaceous (late Aptian) of central Texas and its systematic relationship to the evolution of Eusuchia. *Journal of Paleontology* **88**(5): 1031-1049.

Adatte, T., Stinnesbeck, W., Remane, J. and Hubberten, H. (1996). Paleoceanographic changes at the Jurassic–Cretaceous boundary in the Western Tethys, northeastern Mexico. *Cretaceous Research* **17**(6): 671-689.

Ager, D. (1975). Brachiopods at the Jurassic-Cretaceous boundary. *Mémoires du Bureau de Recherches Géologiques et Minieres* **86**: 150-162.

Ager, D. and Walley, C. (1977). Mesozoic brachiopod migrations and the opening of the North Atlantic. *Palaeogeography, Palaeoclimatology, Palaeoecology* **21**(2): 85-99.

Alroy, J. (2000). New methods for quantifying macroevolutionary patterns and processes. *Paleobiology* **26**: 707-733.

Alroy, J. (2003). Global databases will yield reliable measures of global biodiversity. *Paleobiology* **29**: 26-29.

Alroy, J. (2008). Dynamics of origination and extinction in the marine fossil record. *Proceedings of the National Academy of Sciences of the United States of America* **105**: 11536-11542.

Alroy, J. (2010a). Fair sampling of taxonomic richness and unbiased estimation of origination and extinction rates. *Quantitative Methods in Paleobiology*. G. H. J. Alroy, The Paleontological Society. **16:** 55-80.

Alroy, J. (2010b). Geographical, environmental and intrinsic biotic controls on Phanerozoic marine diversification. *Palaeontology* **53**: 1211-1235.

Alroy, J. (2010c). The shifting balance of diversity among major marine animal groups. *Science* **329**: 1191-1194.

Alroy, J. (2014). Accurate and precise estimates of origination and extinction rates. *Paleobiology* **40**(3): 374-397.

Alroy, J. (2015). A more precise speciation and extinction rate estimator. *Paleobiology* **41**(04): 633-639.

Alroy, J., Aberhan, M., Bottjer, D. J., Foote, M., Fursich, F. T., Harries, P. J., Hendy, A. J. W., Holland, S. M., Ivany, L. C., Kiessling, W., Kosnik, M. A., Marshall, C. R., McGowan, A. J., Miller, A. I., Olszewski, T. D., Patzkowsky, M. E., Peters, S. E., Villier, L., Wagner, P. J., Bonuso, N., Borkow, P. S., Brenneis, B., Clapham, M. E., Fall, L. M., Ferguson, C. A., Hanson, V. L., Krug, A. Z., Layou, K. M., Leckey, E. H., Nurnberg, S., Powers, C. M., Sessa, J. A., Simpson, C., Tomasovych, A. and Visaggi, C. C. (2008). Phanerozoic trends in the global diversity of marine invertebrates. *Science* **321**(5885): 97-100.

Alroy, J., Marshall, C. R., Bambach, R. K., Bezusko, K., Foote, M., Fürsich, F. T., Hansen, T. A., Holland, S. M., Ivany, L. C., Jablonski, D., Jacobs, D. K., Jones, D. C., Kosnik, M. A., Lidgard, S., Low, S., Miller, A. I., Novack-Gottshall, P. M., Olszewski, T. D., Patzkowsky, M. E., Raup, D. M., Roy, K., Sepkoski Jr., J. J., Sommers, M. G., Wagner, P. J. and Webber, A. (2001). Effects of a sampling standardization on estimates of Phanerozoic marine diversification. *Proceedings of the National Academy of Sciences of the United States of America* **98**: 6261-6266.

Alvarez, L. W., Alvarez, W., Asaro, F. and Michel, H. V. (1980). Extraterrestrial cause for the Cretaceous-Tertiary extinction. *Science* **208**(4448): 1095-1108.

Amiot, R., Wang, X., Zhou, Z. H., Wang, X. L., Buffetaut, E., Lecuyer, C., Ding, Z. L., Fluteau, F., Hibino, T., Kusuhashi, N., Mo, J. Y., Suteethorn, V., Wang, Y. Q., Xu, X. and Zhang, F. S. (2011). Oxygen isotopes of East Asian dinosaurs reveal exceptionally cold Early Cretaceous climates. *Proceedings of the National Academy of Sciences of the United States of America* **108**(13): 5179-5183.

Ammon, L. V. (1906). Über Jurassische krokodile aus Bayern. *Geognostische Jahresheften* **18**: 56-71.

Anderson, J. M., Anderson, H., Archangelsky, S., Bamford, M., Chandra, S., Dettmann, M., Hill, R., McLoughlin, S. and Rösler, O. (1999). Patterns of Gondwana plant colonisation and diversification. *Journal of African Earth Sciences* **28**(1): 145-167.

Anderson, P. E., Benton, M. J., Trueman, C. N., Paterson, B. A. and Cuny, G. (2007). Palaeoenvironments of vertebrates on the southern shore of Tethys: The nonmarine Early Cretaceous of Tunisia. *Palaeogeography, Palaeoclimatology, Palaeoecology* **243**(1): 118-131.

Andres, B., Clark, J. and Xu, X. (2014). The earliest pterodactyloid and the origin of the group. *Current Biology* **24**(9): 1011-1016.

Anquetin, J. and Chapman, S. D. (2016). First report of *Plesiochelys etalloni* and *Tropidemys langii* from the Late Jurassic of the UK and the palaeobiogeography of plesiochelyid turtles. *Royal Society Open Science* **3**(1): 150470.

Anquetin, J. and Joyce, W. G. (2014). A reassessment of the Late Jurassic turtle *Eurysternum wagleri* (Eucryptodira, Eurysternidae). *Journal of Vertebrate Paleontology* **34**(6): 1317-1328.

Apesteguía, S., Agnolin, F. L. and Lio, G. L. (2005). An early Late Cretaceous lizard from Patagonia, Argentina. *Comptes Rendus Palevol* **4**(4): 311-315.

Apesteguia, S. and Carballido, J. L. (2014). A new eilenodontine (Lepidosauria, Sphenodontidae) from the Lower Cretaceous of central Patagonia. *Journal of Vertebrate Paleontology* **34**(2): 303-317.

Arbour, V. M. and Currie, P. J. (2015). Systematics, phylogeny and palaeobiogeography of the ankylosaurid dinosaurs. *Journal of Systematic Palaeontology*, http://dx.doi.org/10.1080/14772019.2015.1059985: 1-60.

Arbour, V. M., Zanno, L. E. and Gates, T. (2016). Ankylosaurian dinosaur palaeoenvironmental associations were influenced by extirpation, sea-level fluctuation, and geodispersal. *Palaeogeography, Palaeoclimatology, Palaeoecology* **449**: 289-299.

Arkhangelsky, M. and Zverkov, N. (2014). On a new ichthyosaur of the genus *Undorosaurus*. *Proceedings of the Zoological Institute RAS* **318**(3): 187-196.

Averianov, A. and Lopatin, A. (2015). Mammal remains from the Lower Cretaceous Bol'shoi Terekhtyul' locality in West Siberia, Russia. *Cretaceous Research* **54**: 145-153.

Averianov, A. O. (2001). *Sunosuchus* sp. (Crocodylomorpha, Goniopholididae) from the Middle Jurassic of Kirghisia. *Journal of Vertebrate Paleontology* **20**(4): 776-779.

Averianov, A. O., Martin, T., Evans, S. E. and Bakirov, A. A. (2006). First Jurassic Choristodera from Asia. *Naturwissenschaften* **93**(1): 46-50.

Baker, J., Meader, A., Pagel, M. and Venditti, C. (2016). Positive phenotypic selection inferred from phylogenies. *Biological Journal of the Linnean Society* **118**: 95-115.

Bakker, R. T. (1978). Dinosaur feeding behaviour and the origin of flowering plants. *Nature* **274**: 661-663.

Bakker, R. T. (1993). Plesiosaur extinction cycles—events that mark the beginning, middle and end of the Cretaceous. *Evolution of the western interior basin. Geological Association of Canada, Special Paper* **39**: 641-664.

Baksi, A. K. and Archibald, D. (1997). Mesozoic igneous activity in the Maranhão province, northern Brazil: $^{4}0Ar/^{39}$ Ar evidence for separate episodes of basaltic magmatism. *Earth and Planetary Science Letters* **151**(3): 139-153.

Bambach, R. K. (2006). Phanerozoic biodiversity mass extinctions. *Annual Review of Earth and Planetary Sciences* **34**: 127-155.

Bambach, R. K., Knoll, A. H. and Sepkoski, J. J. (2002). Anatomical and ecological constraints on Phanerozoic animal diversity in the marine realm. *Proceedings of the National Academy of Sciences of the United States of America* **99**(10): 6854-6859.

Bambach, R. K., Knoll, A. H. and Wang, S. C. (2004). Origination, extinction, and mass depletions of marine diversity. *Paleobiology* **30**(4): 522-542.

Bapst, D. W. (2012). paleotree: an R package for paleontological and phylogenetic analyses of evolution. *Methods in Ecology and Evolution* **3**(5): 803-807.

Baraboshkin, E. Y., Alekseev, A. S. and Kopaevich, L. F. (2003). Cretaceous palaeogeography of the north-eastern Peri-Tethys. *Palaeogeography, Palaeoclimatology, Palaeoecology* **196**(1): 177-208.

Barale, G. and Ouaja, M. (2002). La biodiversité végétale des gisements d'âge Jurassique supérieur–Crétacé inférieur de Merbah El Asfer (Sud-Tunisien). *Cretaceous Research* **23**(6): 707-737.

Bardet, N. (1994). Extinction events among Mesozoic marine reptiles. *Historical Biology* **7**(4): 313-324.

Bardet, N., Falconnet, J., Fischer, V., Houssaye, A., Jouve, S., Suberbiola, X. P., Perez-Garcia, A., Rage, J. C. and Vincent, P. (2014). Mesozoic marine reptile palaeobiogeography in response to drifting plates. *Gondwana Research* **26**(3-4): 869-887.

Bardet, N., Mazin, J.-M., Cariou, E., Enay, R. and Krishna, J. (1991). Les Plesiosauria du Jurassique supérieur de la province de Kachchh (Inde). *Comptes rendus de l'Académie des sciences. Série 2, Mécanique, Physique, Chimie, Sciences de l'univers, Sciences de la Terre* **313**(11): 1343-1347.

Bardhan, S., Shome, S., Bose, P. and Ghosh, G. (1989). Faunal crisis and marine regression across the Jurassic-Cretaceous boundary in Kutch, India. *Mesozoic Research* **2**(1): 1-10.

Bardhan, S., Shome, S. and Roy, P. (2007). Biogeography of Kutch ammonites during the latest Jurassic (Tithonian) and a global paleobiogeographic overview. *Cephalopods Present and Past: New Insights and Fresh Perspectives*. N. H. Landman, R. A. Davis and R. H. Mapes. Netherlands, Springer**:** 375-395.

Barnes, C. R., Hallam, A., Kaljo, D., Kauffman, E. G. and Walliser, O. H. (1996). Global event stratigraphy. *Global Events and Event Stratigraphy in the Phanerozoic*. O. H. Walliser, Springer-Verlag Berlin Heidelberg. **3:** 319-333.

Barrett, P. M. (2014). Paleobiology of herbivorous dinosaurs. *Annual Review of Earth and Planetary Sciences* **42**: 207-230.

Barrett, P. M., Butler, R. J., Edwards, N. P. and Milner, A. R. (2008). Pterosaur distribution in time and space: an atlas. *Zitteliana, An International Journal of Palaeontology and Geobiology, Series B/Reihe B* **28**: 61-107.

Barrett, P. M., McGowan, A. J. and Page, V. (2009). Dinosaur diversity and the rock record. *Proceedings of the Royal Society Series B: Biological Sciences* **276**(1667): 2667-2674.

Barrett, P. M. and Upchurch, P. (2005). Sauropodomorph diversity through time: possible macroevolutionary and palaeoecological implications. *The Sauropods: Evolution and Paleobiology*. K. C. Rogers and J. A. Wilson. Berkeley, California, University of California Press**:** 125-156.

Barrett, P. M. and Willis, K. J. (2001). Did dinosaurs invent flowers? Dinosaur—angiosperm coevolution revisited. *Biological Reviews* **76**(3): 411-447.

Baumeister, J. G. and Leinfelder, R. R. (1998). Constructional morphology and palaeoecological significance of three Late Jurassic regular echinoids. *Palaeontology* **41**(2): 203-219.

Baumgartner, P. O. (1987). Age and genesis of Tethyan Jurassic radiolarites. *Eclogae Geologicae Helvetiae* **80**(3): 831-879.

Bell, M. A. and Lloyd, G. T. (2015). strap: an R package for plotting phylogenies against stratigraphy and assessing their stratigraphic congruence. *Palaeontology* **58**(2): 379-389.

Benjamini, Y. and Hochberg, Y. (1995). Controlling the false discovery rate: a practical and powerful approach to multiple testing. *Journal of the Royal Statistical Society. Series B (Methodological)* **57**(1): 289-300.

Benson, R. B. and Bowdler, T. (2014). Anatomy of *Colymbosaurus megadeirus* (Reptilia, Plesiosauria) from the Kimmeridge Clay Formation of the UK, and high diversity among Late Jurassic plesiosauroids. *Journal of Vertebrate Paleontology* **34**(5): 1053-1071.

Benson, R. B., Butler, R. J., Carrano, M. T. and O'Connor, P. M. (2012). Air‐filled postcranial bones in theropod dinosaurs: physiological implications and the 'reptile'‐bird transition. *Biological Reviews* **87**(1): 168-193.

Benson, R. B., Campione, N. E., Carrano, M. T., Mannion, P. D., Sullivan, C., Upchurch, P. and Evans, D. C. (2014). Rates of dinosaur body mass evolution indicate 170 million years of sustained ecological innovation on the avian stem lineage. *PLOS Biology* **12**(6): e1001853.

Benson, R. B. and Choiniere, J. N. (2013). Rates of dinosaur limb evolution provide evidence for exceptional radiation in Mesozoic birds. *Proceedings of the Royal Society Series B: Biological Sciences* **280**(1768): 20131780.

Benson, R. B. and Mannion, P. D. (2011). Multi-variate models are essential for understanding vertebrate diversification in deep time. *Biology Letters* **8**(1): 127-130.

Benson, R. B. J. and Butler, R. J. (2011). Uncovering the diversification history of marine tetrapods: ecology influences the effect of geological sampling biases. *Comparing the Geological and Fossil Records: Implications for Biodiversity Studies*. A. J. McGowan and A. B. Smith, Geological Society of London, Special Publications. **358:** 191-208.

Benson, R. B. J., Butler, R. J., Alroy, J., Mannion, P. D., Carrano, M. T. and Lloyd, G. T. (2016). Near-stasis in the long-term diversification of Mesozoic tetrapods. *PLOS Biology* **14**(1): e1002359.

Benson, R. B. J., Butler, R. J., Lindgren, J. and Smith, A. S. (2010). Mesozoic marine tetrapod diversity: mass extinctions and temporal heterogeneity in geological megabiases affecting vertebrates. *Proceedings of the Royal Society Series B: Biological Sciences* **277**(1683): 829-834.

Benson, R. B. J. and Druckenmiller, P. S. (2014). Faunal turnover of marine tetrapods during the Jurassic-Cretaceous transition. *Biological Reviews* **89**(1): 1-23.

Benson, R. B. J., Mannion, P. D., Butler, R. J., Upchurch, P., Goswami, A. and Evans, S. E. (2013). Cretaceous tetrapod fossil record sampling and faunal turnover: Implications for biogeography and the rise of modern clades. *Palaeogeography, Palaeoclimatology, Palaeoecology* **372**: 88-107.

Benson, R. B. J. and Upchurch, P. (2012). Diversity trends in the establishment of terrestrial vertebrate ecosystems: Interactions between spatial and temporal sampling biases. *Geology* **41**(1): 43-46.

Benton, M., J. and Clark, J. (1988). Archosaur phylogeny and the relationships of the Crocodylia. *The Phylogeny and Classification of Tetrapods, Volume 1: Amphibians, Reptiles, Birds*. M. J. Benton. Oxford, Clarendon Press. **1:** 295-338.

Benton, M., J. and Spencer, P. S. (1995). Fossil Reptiles of Great Britain. London, Chapman and Hall.

Benton, M. J. (1986). Paleobiology: Phanerozoic diversity patterns. *Science* **233**(4769): 1207-1208.

Benton, M. J. (1987). Progress and competition in macroevolution. *Biological Reviews* **62**(3): 305-338.

Benton, M. J. (1994). Palaeontological data and identifying mass extinctions. *Trends in Ecology and Evolution* **9**(5): 181-185.

Benton, M. J. (1996). Testing the roles of competition and expansion in tetrapod evolution. *Proceedings of the Royal Society of London Series B: Biological Sciences* **263**(1370): 641-646.

Benton, M. J. (2001). Biodiversity on land and in the sea. *Geological Journal* **36**(3 - 4): 211-230.

Benton, M. J. (2009). The Red Queen and the Court Jester: species diversity and the role of biotic and abiotic factors through time. *Science* **323**(5915): 728-732.

Benton, M. J. (2010). Evolutionary biology: new take on the Red Queen. *Nature* **463**(7279): 306-307.

Benton, M. J. (2015). Palaeodiversity and formation counts: redundancy or bias? *Palaeontology* **58**(6): 1003-1029.

Benton, M. J., Bouaziz, S., Buffetaut, E., Martill, D., Ouaja, M., Soussi, M. and Trueman, C. (2000). Dinosaurs and other fossil vertebrates from fluvial deposits in the Lower Cretaceous of southern Tunisia. *Palaeogeography, Palaeoclimatology, Palaeoecology* **157**(3): 227-246.

Benton, M. J., Csiki, Z., Grigorescu, D., Redelstorff, R., Sander, P. M., Stein, K. and Weishampel, D. B. (2010). Dinosaurs and the island rule: The dwarfed dinosaurs from Haţeg Island. *Palaeogeography, Palaeoclimatology, Palaeoecology* **293**(3): 438-454.

Benton, M. J., Dunhill, A. M., Lloyd, G. T. and Marx, F. G. (2011). Assessing the quality of the fossil record: insights from vertebrates. *Comparing the Geological and Fossil Records: Implications for*

Biodiversity Studies. A. J. McGowan and A. B. Smith. London, Geological Society of London. **358:** 63-94.

Benton, M. J., Minter, N. J. and Posmosanu, E. (2006). Dwarfing in ornithopod dinosaurs from the Early Cretaceous of Romania. *Mesozoic and Cenozoic vertebrates and paleoenvironments; tributes to the career of Prof Dan Grigorescu, Ars Docendi, Bucharest*: 79-87.

Benton, M. J., Ruta, M., Dunhill, A. M. and Sakamoto, M. (2013a). The first half of tetrapod evolution, sampling proxies, and fossil record quality. *Palaeogeography, Palaeoclimatology, Palaeoecology* **372**: 18-41.

Benton, M. J., Ruta, M., Dunhill, A. M. and Sakamoto, M. (2013b). The first half of tetrapod evolution, sampling proxies, and fossil record quality. *Palaeogeography Palaeoclimatology Palaeoecology* **372**: 18-41.

Benton, M. J. and Walker, R. J. (1993). The Fossil Record 2, Springer Netherlands.

Bergman, N. M., Lenton, T. M. and Watson, A. J. (2004). COPSE: a new model of biogeochemical cycling over Phanerozoic time. *American Journal of Science* **304**(5): 397-437.

Berner, R. A. (1994). GEOCARB II: A revised model of atmospheric CO_2 over Phanerozoic time. *American Journal of Science* **294**(1): 56-91.

Berner, R. A. (2001). Modeling atmospheric O_2 over Phanerozoic time. *Geochimica et Cosmochimica Acta* **65**(5): 685-694.

Berner, R. A. (2006). GEOCARBSULF: a combined model for Phanerozoic atmospheric O_2 and CO_2. *Geochimica et Cosmochimica Acta* **70**(23): 5653-5664.

Berner, R. A. (2009). Phanerozoic atmospheric oxygen: New results using the GEOCARBSULF model. *American Journal of Science* **309**(7): 603-606.

Berner, R. A. and Kothavala, Z. (2001). GEOCARB III: a revised model of atmospheric CO2 over Phanerozoic time. *American Journal of Science* **301**(2): 182-204.

Bice, K. L., Huber, B. T. and Norris, R. D. (2003). Extreme polar warmth during the Cretaceous greenhouse? Paradox of the late Turonian delta O-18 record at Deep Sea Drilling Project Site 511. *Paleoceanography* **18**(2): 1031.

Bininda-Emonds, O. R. (2004). The evolution of supertrees. *Trends in Ecology and Evolution* **19**(6): 315-322.

Birch, H. S., Coxall, H. K., Pearson, P. N., Kroon, D. and Schmidt, D. N. (2016). Partial collapse of the marine carbon pump after the Cretaceous-Paleogene boundary. *Geology* **44**(4): 287-290.

Blackburn, T. J., Olsen, P. E., Bowring, S. A., McLean, N. M., Kent, D. V., Puffer, J., McHone, G., Rasbury, E. T. and Et-Touhami, M. (2013). Zircon U-Pb geochronology links the end-Triassic extinction with the Central Atlantic Magmatic Province. *Science* **340**(6135): 941-945.

Blanco, A., Puértolas-Pascual, E., Marmi, J., Vila, B. and Sellés, A. G. (2014). *Allodaposuchus palustris* sp. nov. from the upper Cretaceous of Fumanya (south-eastern Pyrenees, Iberian Peninsula): systematics, palaeoecology and palaeobiogeography of the enigmatic allodaposuchian crocodylians. *PLOS ONE* **9**(12): e115837.

Blau, J. and Grün, B. (1997). Late Jurassic/Early Cretaceous revised calpionellid zonal and subzonal division and correlation with ammonite and absolute time scales. *Mineralia slovaca* **29**(4-5): 297-300.

Blum, M. D. and Törnqvist, T. E. (2000). Fluvial responses to climate and sea‐level change: a review and look forward. *Sedimentology* **47**(s1): 2-48.

Bluth, G. J. S., Schnetzer, C. C., Krueger, A. J. and Walter, L. S. (1993). The contribution of explosive volcanism to global atmospheric sulphur dioxide concentrations. *Nature* **366**: 327-329.

Bodin, S., Meissner, P., Janssen, N. M., Steuber, T. and Mutterlose, J. (2015). Large igneous provinces and organic carbon burial: Controls on global temperature and continental weathering during the Early Cretaceous. *Global and Planetary Change* **133**: 238-253.

Bornemann, A., Aschwer, U. and Mutterlose, J. (2003). The impact of calcareous nannofossils on the pelagic carbonate accumulation across the Jurassic–Cretaceous boundary. *Palaeogeography, Palaeoclimatology, Palaeoecology* **199**(3): 187-228.

Bown, P. (1992). New calcareous nannofossil taxa from the Jurassic/Cretaceous boundary interval of Sites 765 and 261, Argo Abyssal Plain. *Proc., scientific results, ODP, Leg 123, Argo Abyssal Plain/Exmouth Plateau* **123**: 369-380.

Bown, P. R., Lees, J. A. and Young, J. R. (2004). Calcareous nannoplankton evolution and diversity through time. *Coccolithophores: From Molecular Processes to Global Impact*. D. H. R. Thierstein and J. R. Young. Berlin Heidelberg, Springer. **4:** 481-508.

Box, G. E. and Jenkins, G. M. (1976). Time Series Analysis: Forecasting and Control. San Francisco, Holden-Day.

Bragin, V. Y., Dzyuba, O., Kazansky, A. Y. and Shurygin, B. (2013). New data on the magnetostratigraphy of the Jurassic–Cretaceous boundary interval, Nordvik Peninsula (northern East Siberia). *Russian Geology and Geophysics* **54**(3): 335-348.

Bralower, T. J., Arthur, M. A., Leckie, R. M., Sliter, W. V., Allard, D. J. and Schlanger, S. O. (1994). Timing and paleoceanography of oceanic dysoxia/anoxia in the Late Barremian to Early Aptian (Early Cretaceous). *Palaios* **9**(4): 335-369.

Bralower, T. J., Monechi, S. and Thierstein, H. R. (1989). Calcareous nannofossil zonation of the Jurassic-Cretaceous boundary interval and correlation with the geomagnetic polarity timescale. *Marine Micropaleontology* **14**(1): 153-235.

Brass, G., Southam, J. and Peterson, W. (1982). Warm saline bottom water in the ancient ocean. *Nature* **296**: 620-623.

Brazeau, M. D. (2011). Problematic character coding methods in morphology and their effects. *Biological Journal of the Linnean Society* **104**(3): 489-498.

Bremer, K. (1994). Branch support and tree stability. *Cladistics* **10**(3): 295-304.

Brikiatis, L. (2016a). Late Mesozoic North Atlantic land bridges. *Earth-Science Reviews* **159**: 47-57.

Brikiatis, L. (2016b). Late Mesozoic North Atlantic land bridges. *Earth-Science Reviews*, 10.1016/j.earscirev.2016.05.002.

Brinkmann, W. (1989). Vorläufige Mitteilung über die Krokodilier-Faunen aus dem Ober-Jura (Kimmeridgium) der Kohlegrube Guimarota, bei Leiria (Portugal) und der Unter-Kreide (Barremium) von Uña (Provinz Cuenca, Spanien). *Documenta Naturae* **56**: 1-28.

Brinkmann, W. (1992). Die krokodilier-fauna aus der Unter-Kreide (Ober-Barremium) von Uña (Provinz Cuenca, Spanien). *Berliner Geowissenschaftliche Abhandlungen* **5**: 1-123.

Britt, B. B., Scheetz, R. D., Brinkman, D. B. and Eberth, D. A. (2006). A Barremian neochoristodere from the Cedar Mountain Formation, Utah, USA. *Journal of Vertebrate Paleontology* **26**(4): 1005-1008.

Brochu, C. A. (1996). Closure of neurocentral sutures during crocodilian ontogeny: implications for maturity assessment in fossil archosaurs. *Journal of Vertebrate Paleontology* **16**(1): 49-62.

Brochu, C. A. (1997). A review of "*Leidyosuchus*"(Crocodyliformes, Eusuchia) from the Cretaceous through Eocene of North America. *Journal of Vertebrate Paleontology* **17**(4): 679-697.

Brochu, C. A. (1999). Phylogenetics, taxonomy, and historical biogeography of Alligatoroidea. *Journal of Vertebrate Paleontology* **19**(S2): 9-100.

Brochu, C. A. (2003). Phylogenetic approaches toward crocodylian history. *Annual Review of Earth and Planetary Sciences* **31**: 357-397.

Brochu, C. A. (2004). A new Late Cretaceous gavialoid crocodylian from eastern North America and the phylogenetic relationships of thoracosaurs. *Journal of Vertebrate Paleontology* **24**(3): 610-633.

Brochu, C. A. (2006). A new miniature horned crocodile from the Quaternary of Aldabra Atoll, western Indian Ocean. *Copeia* **2006**(2): 149-158.

Brochu, C. A., Parris, D. C., Grandstaff, B. S., Denton Jr, R. K. and Gallagher, W. B. (2012). A new species of *Borealosuchus* (Crocodyliformes, Eusuchia) from the Late Cretaceous–early Paleogene of New Jersey. *Journal of Vertebrate Paleontology* **32**(1): 105-116.

Brochu, C. A., Wagner, J. R., Jouve, S., Sumrall, C. D. and Densmore, L. D. (2009). A correction corrected: consensus over the meaning of Crocodylia and why it matters. *Systematic Biology* **58**: 537-543.

Brocklehurst, N. (2015). A simulation-based examination of residual diversity estimates as a method of correcting for sampling bias. *Palaeontologia Electronica* **18**(3): 1-15.

Brocklehurst, N., Kammerer, C. F. and Frobisch, J. (2013). The early evolution of synapsids, and the influence of sampling on their fossil record. *Paleobiology* **39**(3): 470-490.

Brocklehurst, N., Upchurch, P., Mannion, P. D. and O'Connor, J. (2012). The completeness of the fossil record of Mesozoic birds: implications for early avian evolution. *PLOS ONE* **7**(E39056).

Broili, F. (1931). *Alligatorium* im oberen Jura von Franken. *Sitzungsberichte der Bayer Akadamie der Wissenschaften.Munich: Mathematika und Naturwissenschaften, Abteilung*: 63-74.

Bron, K. A. and Gostin, V. (2012). The Tookoonooka marine impact horizon, Australia: Sedimentary and petrologic evidence. *Meteoritics and Planetary Science* **47**(2): 296-318.

Bronzati, M., Montefeltro, F. C. and Langer, M. C. (2012). A species-level supertree of Crocodyliformes. *Historical Biology* **24**(6): 598-606.

Bronzati, M., Montefeltro, F. C. and Langer, M. C. (2015). Diversification events and the effects of mass extinctions on Crocodyliformes evolutionary history. *Royal Society Open Science* **2**(5): 140385.

Broschinski, A. (1999). Ein Lacertilier (Scincomorpha, Paramacellodidae) aus dem Oberen Jura von Tendaguru (Tansania). *Fossil Record* **2**(1): 155-158.

Brusatte, S. L., Averianov, A., Sues, H.-D., Muir, A. and Butler, I. B. (2016). New tyrannosaur from the mid-Cretaceous of Uzbekistan clarifies evolution of giant body sizes and advanced senses in tyrant dinosaurs. *Proceedings of the National Academy of Sciences of the United States of America* **113**(13): 3447-3452.

Brusatte, S. L., Benton, M. J., Lloyd, G. T., Ruta, M. and Wang, S. C. (2010). Macroevolutionary patterns in the evolutionary radiation of archosaurs (Tetrapoda: Diapsida). *Earth and Environmental Science Transactions of the Royal Society of Edinburgh* **101**: 367-382.

Brusatte, S. L., Benton, M. J., Ruta, M. and Lloyd, G. T. (2008). Superiority, competition, and opportunism in the evolutionary radiation of dinosaurs. *Science* **321**(5895): 1485-1488.

Brusatte, S. L., Butler, R. J., Barrett, P. M., Carrano, M. T., Evans, D. C., Lloyd, G. T., Mannion, P. D., Norell, M. A., Peppe, D. J. and Upchurch, P. (2015). The extinction of the dinosaurs. *Biological Reviews* **90**(2): 628-642.

Brusatte, S. L. and Carr, T. D. (2016). The phylogeny and evolutionary history of tyrannosauroid dinosaurs. *Scientific Reports* **6**: 20252.

Brusatte, S. L., Lloyd, G. T., Wang, S. C. and Norell, M. A. (2014). Gradual assembly of avian body plan culminated in rapid rates of evolution across the dinosaur-bird transition. *Current Biology* **24**(20): 2386-2392.

Brusatte, S. L. and Sereno, P. C. (2007). A new species of *Carcharodontosaurus* (Dinosauria: Theropoda) from the Cenomanian of Niger and a revision of the genus. *Journal of Vertebrate Paleontology* **27**(4): 902-916.

Bryan, S., Constantine, A., Stephens, C., Ewart, A., Schön, R. and Parianos, J. (1997). Early Cretaceous volcano-sedimentary successions along the eastern Australian continental margin: implications for the break-up of eastern Gondwana. *Earth and Planetary Science Letters* **153**(1): 85-102.

Buchwitz, M., Foth, C., Kogan, I. and Voigt, S. (2012). On the use of osteoderm features in a phylogenetic approach on the internal relationships of the Chroniosuchia (Tetrapoda: Reptiliomorpha). *Palaeontology* **55**(3): 623-640.

Buchy, M.-C., Young, M. T. and Andrade, M. (2013). A new specimen of *Cricosaurus saltillensis* (Crocodylomorpha: Metriorhynchidae) from the Upper Jurassic of Mexico: evidence for craniofacial convergence within Metriorhynchidae. *Oryctos* **10**: 9-21.

Buckley, G. and Brochu, C. (1999). An enigmatic new crocodile from the Upper Cretaceous of Madagascar. *Cretaceous Fossil Vertebrates* **60**: 149-175.

Buckley, G. A., Brochu, C. A., Krause, D. W. and Pol, D. (2000). A pug-nosed crocodyliform from the Late Cretaceous of Madagascar. *Nature* **405**(6789): 941-944.

Budyko, M. I., Ronov, A. B. and Yanshin, A. L. (1987). History of the Earth's Atmosphere. Berlin, Springer-Verlag, Berlin.

Buffetaut, E. (1975). Sur l'anatomie et la position systématique de *Bernissartia fagesii* Dollo, L., 1883, crocodilien du Wealdien de Bernissart, Belgique. *Bulletin de l'Institut Royal des Sciences Naturelles de Belgique (sci. Terre)* **51**: 1-20.

Buffetaut, E. (1976). Ostéologie et affinités de *Trematochampsa taqueti* (Crocodylia, Mesosuchia) du Sénonien Inférieur d'In Beceten (République du Niger). *Geobios* **9**(2): 143-198.

Buffetaut, E. (1981a). Die biogeographische Geschichte der Krokodilier, mit Beschreibung einer neuen Art, *Araripesuchus wegeneri*. *Geologische Rundschau* **70**(2): 611-624.

Buffetaut, E. (1981b). Un Atoposauridé (Crocodylia, Mesosuchia) du Portlandien de la Meuse (Est de la France). *Geobios* **14**(6): 815-819.

Buffetaut, E. (1982). Radiation évolutive, paléoécologie et biogéographie des crocodiliens mésosuchiens. *Mémoires de la Société Géologique de France* **60**(142): 1-88.

Buffetaut, E. (1983). The crocodilian *Theriosuchus* Owen, 1879 in the Wealden of England. *Bulletin of the British Museum, Natural History. Geology* **37**(3): 93-97.

Buffetaut, E. and Ford, R. (1979). The crocodilian *Bernissartia* in the Wealden of the Isle of Wight. *Palaeontology* **22**(4): 905-912.

Burgess, P. M. and Hovius, N. (1998). Rates of delta progradation during highstands: consequences for timing of deposition in deep-marine systems. *Journal of the Geological Society* **155**(2): 217-222.

Burns, M. E. (2008). Taxonomic utility of ankylosaur (Dinosauria, Ornithischia) osteoderms: *Glyptodontopelta mimus* Ford, 2000: a test case. *Journal of Vertebrate Paleontology* **28**(4): 1102-1109.

Burns, M. E., Vickaryous, M. K. and Currie, P. J. (2013). Histological variability in fossil and recent alligatoroid osteoderms: systematic and functional implications. *Journal of morphology* **274**(6): 676-686.

Buscalioni, A. (1986). Cocodrilos Fossiles del Registro Español. Anáilisis Filogenético y Sistemático de la Familia Atoposauridae (Reptilia, Crocodylia). PhD, Universidad Autónoma de Madrid.

Buscalioni, A., Fregenal, M., Bravo, A., Poyato-Ariza, F., Sanchíz, B., Báez, A., Moo, O. C., Closas, C. M., Evans, S. and Lobón, J. M. (2008). The vertebrate assemblage of Buenache de la Sierra (Upper Barremian of Serrania de Cuenca, Spain) with insights into its taphonomy and palaeoecology. *Cretaceous Research* **29**(4): 687-710.

Buscalioni, A., Ortega, F., Weishampel, D. and Jianu, C. (2001). A revision of the crocodyliform *Allodaposuchus precedens* from the Upper Cretaceous of the Hateg Basin, Romania. Its relevance in the phylogeny of Eusuchia. *Journal of Vertebrate Paleontology* **21**(1): 74-86.

Buscalioni, A. and Sanz, J. (1984). Los Arcosaurios (Reptilia) del Jurásico Superior - Cretácico Inferior de Galve (Teruel, España). *Separata de la Revista Teruel* **71**: 9-28.

Buscalioni, A. and Sanz, J. (1987a). Cocodrilos del Cretácico inferior de Galve (Teruel, España). *Estudios geológicos* **43**(Extra): 23-43.

Buscalioni, A. and Sanz, J. (1987b). Lista faunistica de los Vertebrados de Galve (Teruel). *Estudios Geologicos, Vol. Extraord, Galve-Tremp* **43**: 65-67.

Buscalioni, A. and Sanz, J. (1990a). La familia Atoposauridae: una approximación a la historia de los cocodrilos enanos. *Treballs del Museu de Geología de Barcelona* **1**: 77-89.

Buscalioni, A. and Sanz, J. L. (1990b). *Montsecosuchus depereti* (Crocodylomorpha, Atoposauridae), new denomination for *Alligatorium depereti* Vidal, 1915 (Early Cretaceous, Spain): redescription and phylogenetic relationships. *Journal of Vertebrate Paleontology* **10**(2): 244-254.

Buscalioni, A. D., Piras, P., Vullo, R., Signore, M. and Barbera, C. (2011). Early Eusuchia Crocodylomorpha from the vertebrate ‐ rich Plattenkalk of Pietraroia (Lower Albian, southern Apennines, Italy). *Zoological Journal of the Linnean Society* **163**(s1): S199-S227.

Buscalioni, A. D. and Sanz, J. L. (1988). Phylogenetic relationships of the Atoposauridae (Archosauria, Crocodylomorpha). *Historical Biology* **1**(3): 233-250.

Bush, A. M. and Bambach, R. K. (2004). Did alpha diversity increase during the Phanerozoic? Lifting the veils of taphonomic, latitudinal, and environmental biases. *The Journal of Geology* **112**(6): 625-642.

Bush, A. M., Markey, M. J. and Marshall, C. R. (2004). Removing bias from diversity curves: the effects of spatially organized biodiversity on sampling-standardization. *Paleobiology* **30**(4): 666-686.

Butler, R., Barrett, P., Kenrick, P. and Penn, M. (2009a). Diversity patterns amongst herbivorous dinosaurs and plants during the Cretaceous: implications for hypotheses of dinosaur/angiosperm co ‐ evolution. *Journal of Evolutionary Biology* **22**(3): 446-459.

Butler, R. J., Barrett, P. M., Kenrick, P. and Penn, M. G. (2009b). Testing co ‐ evolutionary hypotheses over geological timescales: interactions between Mesozoic non ‐ avian dinosaurs and cycads. *Biological Reviews* **84**(1): 73-89.

Butler, R. J., Barrett, P. M., Nowbath, S. and Upchurch, P. (2009c). Estimating the effects of sampling biases on pterosaur diversity patterns: implications for hypotheses of bird/pterosaur competitive replacement. *Paleobiology* **35**(3): 432-446.

Butler, R. J., Benson, R. B. J. and Barrett, P. M. (2013). Pterosaur diversity: Untangling the influence of sampling biases, Lagerstatten, and genuine biodiversity signals. *Palaeogeography, Palaeoclimatology, Palaeoecology* **372**: 78-87.

Butler, R. J., Benson, R. B. J., Carrano, M. T., Mannion, P. D. and Upchurch, P. (2011). Sea level, dinosaur diversity and sampling biases: investigating the 'common cause' hypothesis in the terrestrial realm. *Proceedings of the Royal Society of London Series B: Biological Sciences* **278**(1709): 1165-1170.

Butler, R. J., Brusatte, S. L., Andres, B. and Benson, R. B. (2012). How do geological sampling biases affect studies of morphological evolution in deep time? A case study of pterosaur (Reptilia: Archosauria) disparity. *Evolution* **66**(1): 147-162.

Cadena, E. A., Jaramillo, C. A. and Bloch, J. I. (2013). New material of the Platychelyid Turtle *Notoemys zapatocaensis* from the Early Cretaceous of Colombia; Implications for Understanding Pleurodira Evolution. *Morphology and Evolution of Turtles*. D. B. Brinkman, P. A. Holroyd and J. D. Gardner, Springer Netherlands**:** 105-120.

Cadena, E. A. and Parham, J. F. (2015). Oldest known marine turtle? A new protostegid from the Lower Cretaceous of Colombia. *PaleoBios* **32**(1): 1-42.

Caldwell, M. W., Nydam, R. L., Palci, A. and Apesteguía, S. (2015). The oldest known snakes from the Middle Jurassic-Lower Cretaceous provide insights on snake evolution. *Nature Communications* **6**: e5996.

Campos, D. A., Oliveira, G. R., Figueiredo, R. G., Riff, D., Azevedo, S. A., Carvalho, L. B. and Kellner, A. W. (2011). On a new peirosaurid crocodyliform from the Upper Cretaceous, Bauru Group, southeastern Brazil. *Anais da Academia Brasileira de Ciências* **83**(1): 317-327.

Canudo, J., Gasca, J., Aurell, M., Badiola, A., Blain, H., Cruzado-Caballero, P., Gómez-Fernández, D., Moreno-Azanza, M., Parrilla, J. and Rabal-Garcés, R. (2010). La Cantalera: an exceptional window onto the vertebrate biodiversity of the Hauterivian-Barremian transition in the Iberian Peninsula/La Cantalera: una excepcional ventana a la biodiversidad del tránsito Hauteriviense-Barremiense en la Península Ibérica. *Journal of Iberian Geology* **36**(2): 205.

Carballido, J. L., Pol, D., Parra Ruge, M. L., Padilla Bernal, S., Páramo-Fonseca, M. E. and Etayo-Serna, F. (2015). A new Early Cretaceous brachiosaurid (Dinosauria, Neosauropoda) from northwestern Gondwana (Villa de Leiva, Colombia). *Journal of Vertebrate Paleontology* **35**(5): e980505.

Carballido, J. L., Salgado, L., Pol, D., Canudo, J. I. and Garrido, A. (2012). A new basal rebbachisaurid (Sauropoda, Diplodocoidea) from the Early Cretaceous of the Neuquén Basin; evolution and biogeography of the group. *Historical Biology* **24**(6): 631-654.

Carballido, J. L. and Sander, P. M. (2014). Postcranial axial skeleton of *Europasaurus holgeri* (Dinosauria, Sauropoda) from the Upper Jurassic of Germany: implications for sauropod ontogeny and phylogenetic relationships of basal Macronaria. *Journal of Systematic Palaeontology* **12**(3): 335-387.

Carrano, M., Mannion, P. and Alroy, J. (2015a). Taxonomic occurrences of Jurassic to Cretaceous Crocodyliformes recorded in Fossilworks, the Evolution of Terrestrial Ecosystems database, and the Paleobiology Database, https://paleobiodb.org/.

Carrano, M. T., Alroy, J., Mannion, P. D., Benson, R. and Butler, R. J. (2015b). Taxonomic occurrences of Jurassic to Cretaceous Tetrapoda recorded in , Fossilworks, the Evolution of Terrestrial Ecosystems database, and the Paleobiology Database, https://paleobiodb.org/.

Carrano, M. T., Benson, R. B. and Sampson, S. D. (2012). The phylogeny of Tetanurae (Dinosauria: Theropoda). *Journal of Systematic Palaeontology* **10**(2): 211-300.

Carroll, R. L. (1988). Vertebrate Paleontology and Evolution. New York, W. H. Freeman and Company.

Carvalho, I., Teixeira, V., Ferraz, M., Ribeiro, L. C. B., Martinelli, A. G., Neto, F., Sertich, J. J., Cunha, G. C., Cunha, I. C. and Ferraz, P. F. (2011). *Campinasuchus dinizi* gen. *et* sp. *nov*., a new Late Cretaceous baurusuchid (Crocodyliformes) from the Bauru Basin, Brazil. *Zootaxa* **2871**(2011): 19-42.

Carvalho, I. D., Campos, A. D. A. and Nobre, P. H. (2005). *Baurusuchus salgadoensis*, a new crocodylomorpha from the Bauru Basin (Cretaceous), Brazil. *Gondwana Research* **8**(1): 11-30.

Carvalho, I. D., de Gasparini, Z. B., Salgado, L., de Vasconcellos, F. M. and Marinho, T. D. (2010). Climate's role in the distribution of the Cretaceous terrestrial Crocodyliformes throughout Gondwana. *Palaeogeography Palaeoclimatology Palaeoecology* **297**(2): 252-262.

Cascales-Miñana, B. and Cleal, C. J. (2014). The plant fossil record reflects just two great extinction events. *Terra Nova* **26**(3): 195-200.

Cascales-Miñana, B., Cleal, C. J. and Diez, J. B. (2013). What is the best way to measure extinction? A reflection from the palaeobotanical record. *Earth-Science Reviews* **124**: 126-147.

Casellato, C. E. (2010). Calcareous nannofossil biostratigraphy of Upper Callovian–Lower Berriasian successions from the southern alps, North Italy. *Rivista Italiana di Paleontologia e Stratigrafia* **116**(3): 357-404.

Cau, A. and Fanti, F. (2011). The oldest known metriorhynchid crocodylian from the Middle Jurassic of North-eastern Italy: *Neptunidraco ammoniticus* gen. *et* sp. *nov*. *Gondwana Research* **19**(2): 550-565.

Cavin, L. (2010). The Late Jurassic ray-finned fish peak of diversity: biological radiation or preservational bias. *Origin and Phylogenetic Interrelationships of Teleosts. Honoring Gloria Arratia*. J. Nelson, H.-P. Schultze and M. Wilson. München, Germany, Verlag Dr. Friedrich Pfeil**:** 111-121.

Cavin, L. and Forey, P. L. (2007). Using ghost lineages to identify diversification events in the fossil record. *Biology Letters* **3**(2): 201-204.

Cavin, L., Forey, P. L. and Lécuyer, C. (2007). Correlation between environment and Late Mesozoic ray-finned fish evolution. *Palaeogeography, Palaeoclimatology, Palaeoecology* **245**(3): 353-367.

Cecca, F. (1997). Late Jurassic and Early Cretaceous uncoiled ammonites: Trophism-related evolutionary processes. *Comptes Rendus de l'Académie des Sciences-Series IIA - Earth and Planetary Science* **325**(8): 629-634.

Cecca, F. (1998). Early Cretaceous (pre-Aptian) ammonites of the Mediterranean Tethys: palaeoecology and palaeobiogeography. *Palaeogeography, Palaeoclimatology, Palaeoecology* **138**(1): 305-323.

Cecca, F. (1999). Palaeobiogeography of Tethyan ammonites during the Tithonian (latest Jurassic). *Palaeogeography, Palaeoclimatology, Palaeoecology* **147**(1): 1-37.

Cecca, F., Vrielynck, B., Lavoyer, T. and Gaget, H. (2005). Changes in the ammonite taxonomical diversity gradient during the Late Jurassic–Early Cretaceous. *Journal of Biogeography* **32**(3): 535-547.

Cermeño, P., Falkowski, P. G., Romero, O. E., Schaller, M. F. and Vallina, S. M. (2015). Continental erosion and the Cenozoic rise of marine diatoms. *Proceedings of the National Academy of Sciences of the United States of America* **112**(14): 4239-4244.

Cermeño, P., Rodríguez-Ramos, T., Dornelas, M., Figueiras, F. G., Marañón, E., Teixeira, I. G. and Vallina, S. M. (2013). Species richness in marine phytoplankton communities is not correlated to ecosystem productivity. *Marine Ecology Progress Series* **488**: 1-9.

Chaboureau, A.-C., Sepulchre, P., Donnadieu, Y. and Franc, A. (2014). Tectonic-driven climate change and the diversification of angiosperms. *Proceedings of the National Academy of Sciences of the United States of America* **111**(39): 14066-14070.

Chao, A., Colwell, R. K., Lin, C.-W. and Gotelli, N. J. (2009). Sufficient sampling for asymptotic minimum species richness estimators. *Ecology* **90**(4): 1125-1133.

Chao, A. and Jost, L. (2012). Coverage-based rarefaction and extrapolation: standardizing samples by completeness rather than size. *Ecology* **93**(12): 2533-2547.

Chatalov, A., Bonev, N. and Ivanova, D. (2015). Depositional characteristics and constraints on the mid-Valanginian demise of a carbonate platform in the intra-Tethyan domain, Circum-Rhodope Belt, northern Greece. *Cretaceous Research* **55**: 84-115.

Chentanez, T., Hggins, S. E. and Chentanez, V. (1983). Allometric relationships of the Siamese crocodiles, *Crocodylus siamensis*. *Journal of the Science Society of Thailand* **9**: 5-26.

Chiappe, L., Rivarola, D., Romero, E., Dávila, S. and Codorniú, L. (1998). Recent advances in the paleontology of the Lower Cretaceous Lagarcito Formation (Parque Nacional Sierra de Las Quijadas, San Luis; Argentina). *New Mexico Museum of Natural History and Science Bulletin* **14**: 187-192.

Chiarenza, A. A., Foffa, D., Young, M. T., Insacco, G., Cau, A., Carnevale, G. and Catanzariti, R. (2015). The youngest record of metriorhynchid crocodylomorphs, with implications for the extinction of Thalattosuchia. *Cretaceous Research* **56**: 608-616.

Cifelli, R. L. and Davis, B. M. (2015). Tribosphenic mammals from the Lower Cretaceous Cloverly Formation of Montana and Wyoming. *Journal of Vertebrate Paleontology* **35**(3): e920848.

Cifelli, R. L., Davis, B. M. and Sames, B. (2012). Earliest Cretaceous mammals from the western United States. *Acta Palaeontologica Polonica* **59**(1): 31-52.

Cifelli, R. L., Gardner, J. D., Nydam, R. L. and Brinkman, D. L. (1997). Additions to the vertebrate fauna of the Antlers Formation (Lower Cretaceous), southeastern Oklahoma. *Oklahoma Geology Notes* **57**(4): 124-131.

Cifelli, R. L., Nydam, R. L., Gardner, J. D., Weil, A., Eaton, J. G., Kirkland, J. I. and Madsen, S. K. (1999). Medial Cretaceous vertebrates from the Cedar Mountain Formation, Emery County, Utah: the Mussentuchit local fauna. *Vertebrate paleontology in Utah* **99**(1): 219-242.

Clapham, M. E., Karr, J. A., Nicholson, D. B., Ross, A. J. and Mayhew, P. J. (2016). Ancient origin of high taxonomic richness among insects. *Proceedings of the Royal Society of London B: Biological Sciences* **283**(1824): 20152476.

Clark, J. M. (1986). Phylogenetic relationships of the crocodylomorph archosaurs. PhD, University of Chicago.

Clark, J. M. (2011). A new shartegosuchid crocodyliform from the Upper Jurassic Morrison Formation of western Colorado. *Zoological Journal of the Linnean Society* **163**(s1): S152-S172.

Clark, J. M., Fraser, N. and Sues, H. (1994). Patterns of evolution in Mesozoic Crocodyliformes. *In the shadow of the dinosaurs: Early Mesozoic tetrapods*. N. Fraser and H.-D. Sues, Cambridge University Press**:** 84-97.

Clark, J. M. and Norell, M. A. (1992). The Early Cretaceous crocodylomorph *Hylaeochampsa vectiana* from the Wealden of the Isle of Wight. *American Museum Novitates* **3032**: 1-19.

Clark, J. M. and Sues, H. D. (2002). Two new basal crocodylomorph archosaurs from the Lower Jurassic and the monophyly of the Sphenosuchia. *Zoological Journal of the Linnean Society* **136**(1): 77-95.

Cleary, T. J., Moon, B. C., Dunhill, A. M. and Benton, M. J. (2015). The fossil record of ichthyosaurs, completeness metrics and sampling biases. *Palaeontology* **58**(3): 521-536.

Close, R. A., Friedman, M., Lloyd, G. T. and Benson, R. B. (2015). Evidence for a mid-Jurassic adaptive radiation in mammals. *Current Biology* **25**(16): 2137-2142.

Close, R. A. and Rayfield, E. J. (2012). Functional morphometric analysis of the furcula in Mesozoic birds. *PLOS ONE* **7**(5): e36664.

Cobos, A., Lockley, M. G., Gascó, F., Royo–Torres, R. and Alcalá, L. (2014). Megatheropods as apex predators in the typically Jurassic ecosystems of the Villar del Arzobispo Formation (Iberian Range, Spain). *Palaeogeography, Palaeoclimatology, Palaeoecology* **399**: 31-41.

Codorniú, L. and Gasparini, Z. (2013). The Late Jurassic pterosaurs from northern Patagonia, Argentina. *Earth and Environmental Science Transactions of the Royal Society of Edinburgh* **103**(3-4): 399-408.

Coffin, M. F. and Eldholm, O. (1994). Large Igneous Provinces - crustal structure, dimensions, and external consequences. *Reviews of Geophysics* **32**(1): 1-36.

Cohen, K., Finney, S., Gibbard, P. and Fan, J.-X. (2013). The ICS International Chronostratigraphic Chart. *Episodes* **36**(3): 199-204.

Coiffard, C., Gomez, B., Daviero-Gomez, V. and Dilcher, D. L. (2012). Rise to dominance of angiosperm pioneers in European Cretaceous environments. *Proceedings of the National Academy of Sciences of the United States of America* **109**(51): 20955-20959.

Colbert, E. H., Mook, C. C. and Brown, B. (1951). The ancestral crocodilian *Protosuchus*. *Bulletin of the American Museum of Natural History* **97**(3): 147-182.

Company, J., Suberbiola, X. P., Ruiz-Omeñaca, J. I. and Buscalioni, A. D. (2005). A new species of *Doratodon* (Crocodyliformes: Ziphosuchia) from the Late Cretaceous of Spain. *Journal of Vertebrate Paleontology* **25**(2): 343-353.

Congreve, C. R. and Lamsdell, J. C. (2016). Implied weighting and its utility in palaeontological datasets: a study using modelled phylogenetic matrices. *Palaeontology*, 10.1111/pala.12236.

Connor, E. F. and Taverner, M. P. (1997). The evolution and adaptive significance of the leaf-mining habit. *Oikos* **79**: 6-25.

Conrad, J. L. (2008). Phylogeny and systematics of Squamata (Reptilia) based on morphology. *Bulletin of the American Museum of Natural History* **310**: 1-182.

Corner, B., Reimold, W., Brandt, D. and Koeberl, C. (1997). Morokweng impact structure, Northwest Province, South Africa: Geophysical imaging and shock petrographic studies. *Earth and Planetary Science Letters* **146**(1): 351-364.

Courtillot, V. and Olson, P. (2007). Mantle plumes link magnetic superchrons to phanerozoic mass depletion events. *Earth and Planetary Science Letters* **260**(3): 495-504.

Crame, J. A. (2002). Evolution of taxonomic diversity gradients in the marine realm: a comparison of Late Jurassic and Recent bivalve faunas. *Paleobiology* **28**(2): 184-207.

Crampton, J. S., Beu, A. G., Cooper, R. A., Jones, C. M., Marshall, B. and Maxwell, P. A. (2003). Estimating the rock volume bias in paleobiodiversity studies. *Science* **301**(5631): 358-360.

Csiki-Sava, Z., Brusatte, S. L. and Vasile, Ş. (2016). "*Megalosaurus* cf. *superbus*" from southeastern Romania: The oldest known Cretaceous carcharodontosaurid (Dinosauria: Theropoda) and its implications for earliest Cretaceous Europe-Gondwana connections. *Cretaceous Research* **60**: 221-238.

Csiki, Z., Grigorescu, D., Codrea, V. and Therrien, F. (2010). Taphonomic modes in the Maastrichtian continental deposits of the Haţeg Basin, Romania—Palaeoecological and palaeobiological inferences. *Palaeogeography, Palaeoclimatology, Palaeoecology* **293**(3): 375-390.

Cuny, G., Buffetaut, E., Cappetta, H., Martin, M., Mazin, J. and Rose, J. (1991). Nouveaux restes de Vertébrés du Jurassique terminal du Boulonnais (Nord de la France). *Neues Jahrbuch für Geologie und Paläontologie, Abhandlungen* **180**(3): 323-347.

Cuny, G., Laojumpon, C. and Lauprasert, K. (2010). Fossil vertebrate remains from Kut Island (Gulf of Thailand, Early Cretaceous). *Cretaceous Research* **31**(4): 415-423.

Curry, G. B. and Brunton, C. H. C. (2007). Stratigraphic distribution of Brachiopoda. *Treatise on Invertebrate Paleontology, Part H Brachiopoda Revised*. P. A. Selden. Boulder, Colorado, USA, The Geological Society of America and the University of Kansas**:** 2901–3081.

D'Emic, M. and Foster, J. (2016). The oldest Cretaceous North American sauropod dinosaur. *Historical Biology* **28**(4): 470-478.

D'emic, M. D. (2012). The early evolution of titanosauriform sauropod dinosaurs. *Zoological Journal of the Linnean Society* **166**(3): 624-671.

da Silva Marinho, T., Iori, F. V., de Souza Carvalho, I. and de Vasconcellos, F. M. (2013). *Gondwanasuchus scabrosus* gen. et sp. nov., a new terrestrial predatory crocodyliform (Mesoeucrocodylia: Baurusuchidae) from the Late Cretaceous Bauru Basin of Brazil. *Cretaceous Research* **44**: 104-111.

Damborenea, S. E. (2002). Jurassic evolution of Southern Hemisphere marine palaeobiogeographic units based on benthonic bivalves. *Geobios* **35**: 51-71.

Danelian, T. and Johnson, K. G. (2001). Patterns of biotic change in Middle Jurassic to Early Cretaceous Tethyan radiolaria. *Marine Micropaleontology* **43**(3): 239-260.

Danilov, I. G. and Parham, J. F. (2006). A redescription of '*Plesiochelys*' *tatsuensis* from the Late Jurassic of China, with comments on the antiquity of the crown clade Cryptodira. *Journal of Vertebrate Paleontology* **26**(3): 573-580.

Danilov, I. G. and Parham, J. F. (2008). A reassessment of some poorly known turtles from the Middle Jurassic of China, with comments on the antiquity of extant turtles. *Journal of Vertebrate Paleontology* **28**(2): 306-318.

Danilov, I. G. and Sukhanov, V. B. (2006). A basal eucryptodiran turtle "*Sinemys*" *efremovi* (=*Wuguia efremovi*) from the Early Cretaceous of China. *Acta Palaeontologica Polonica* **51**(1): 105.

de Andrade, M. B. and Bertini, R. J. (2008). A new *Sphagesaurus* (Mesoeucrocodylia: Notosuchia) from the Upper Cretaceous of Monte Alto City (Bauru Group, Brazil), and a revision of the Sphagesauridae. *Historical Biology* **20**(2): 101-136.

de Andrade, M. B., Edmonds, R., Benton, M. J. and Schouten, R. (2011a). A new Berriasian species of Goniopholis (Mesoeucrocodylia, Neosuchia) from England, and a review of the genus. *Zoological Journal of the Linnean Society* **163**(s1): S66-S108.

de Andrade, M. B., Edmonds, R., Benton, M. J. and Schouten, R. (2011b). A new Berriasian species of *Goniopholis* (Mesoeucrocodylia, Neosuchia) from England, and a review of the genus. *Zoological Journal of the Linnean Society* **163**: S66-S108.

de Andrade, M. B., Young, M. T., Desojo, J. B. and Brusatte, S. L. (2010a). The evolution of extreme hypercarnivory in Metriorhynchidae (Mesoeucrocodylia: Thalattosuchia) based on evidence from microscopic denticle morphology. *Journal of Vertebrate Paleontology* **30**(5): 1451-1465.

de Andrade, M. B., Young, M. T., Desojo, J. B. and Brusatte, S. L. (2010b). The evolution of extreme hypercarnivory in Metriorhynchidae (Mesoeucrocodylia: Thalattosuchia): evidence from microscopic denticle morphology and a new tri-faceted Kimmeridgian tooth from Germany. *Journal of Vertebrate Paleontology* **30**: 1451-1465.

de Lapparent de Broin, A. F. (2001). The European turtle fauna from the Triassic to the Present. *Dumerilia* **4**(3): 155-217.

Dean, C. D., Mannion, P. D. and Butler, R. J. (2016). Preservational bias controls the fossil record of pterosaurs. *Palaeontology* **59**(2): 225-247.

Debelmas, J. and Strannoloubsky, A. (1957). Découverte d'un crocodilien dans le Néocomien de La Martre (Var) *Dacosaurus lapparen*t n. sp. *Travaux Laboratoire de Géologie de l'université de Grenoble* **33**: 89-99.

DeCelles, P. G. (2004). Late Jurassic to Eocene evolution of the Cordilleran thrust belt and foreland basin system, western USA. *American Journal of Science* **304**(2): 105-168.

Delfino, M., Codrea, V., Folie, A., Dica, P., Godefroit, P. and Smith, T. (2008a). A complete skull of *Allodaposuchus precedens* Nopcsa, 1928 (Eusuchia) and a reassessment of the morphology of the taxon based on the Romanian remains. *Journal of Vertebrate Paleontology* **28**(1): 111-122.

Delfino, M. and Dal Sasso, C. (2006). Marine reptiles (Thalattosuchia) from the Early Jurassic of Lombardy (northern Italy). *Geobios* **39**(3): 346-354.

Delfino, M., Martin, J. E. and Buffetaut, E. (2008b). A new species of *Acynodon* (Crocodylia) from the Upper Cretaceous (Santonian–Campanian) of Villaggio del Pescatore, Italy. *Palaeontology* **51**(5): 1091-1106.

Delfino, M. and Sánchez-Villagra, M. R. (2010). A survey of the rock record of reptilian ontogeny. *Seminars in Cell & Developmental Biology* **21**(4): 432-440.

Dera, G., Brigaud, B., Monna, F., Laffont, R., Pucéat, E., Deconinck, J.-F., Pellenard, P., Joachimski, M. M. and Durlet, C. (2011). Climatic ups and downs in a disturbed Jurassic world. *Geology* **39**(3): 215-218.

Deroo, G., Herbin, J. and Roucaché, J. (1983). Organic geochemistry of Upper Jurassic-Cretaceous sediments from Site 511, Leg 71, western South Atlantic. *Initial Reports of the Deep Sea Drilling Project* **71**: 1001-1013.

Dettmann, M. E. (1989). Antarctica: Cretaceous cradle of austral temperate rainforests? *Geological Society, London, Special Publications* **47**(1): 89-105.

Dias-Brito, D., Musacchio, E., de Castro, J., Maranhão, M., Suárez, J. and Rodrigues, R. (2001). Grupo Bauru: uma unidade continental do Cretáceo no Brasil-concepções baseadas em dados micropaleontológicos, isotópicos e estratigráficos. *Revue de Paléobiologie* **20**(1): 245-304.

Dietrich, W. (1927). *Brancatherulum* n. g., ein Proplacentalier aus dem obersten Jura des Tendaguru in Deutsch-Ostafrika. *Centralblatt fur Mineralogie, Geologie, Palaeontologie Abteilung B* **10**: 423-426.

Dodd, S. C., Niocaill, C. M. and Muxworthy, A. R. (2015). Long duration (>4 Ma) and steady-state volcanic activity in the Early Cretaceous Paraná-Etendeka Large Igneous Province: new palaeomagnetic data from Namibia. *Earth and Planetary Science Letters* **414**: 16-29.

Dodson, P. (1975). Functional and ecological significance of relative growth in *Alligator*. *Journal of Zoology* **175**(3): 315-355.

Dodson, P. (1990). Counting dinosaurs: how many kinds were there? *Proceedings of the National Academy of Sciences of the United States of America* **87**(19): 7608-7612.

Douglas, J. and Williams, G. (1982). Southern polar forests: the Early Cretaceous floras of Victoria and their palaeoclimatic significance. *Palaeogeography, Palaeoclimatology, Palaeoecology* **39**(3): 171-185.

Dunhill, A. M. (2011). Using remote sensing and a geographic information system to quantify rock exposure area in England and Wales: Implications for paleodiversity studies. *Geology* **39**(2): 111-114.

Dunhill, A. M. (2012). Problems with using rock outcrop area as a paleontological sampling proxy: rock outcrop and exposure area compared with coastal proximity, topography, land use, and lithology. *Paleobiology* **38**(1): 126-143.

Dunhill, A. M., Benton, M. J., Newell, A. J. and Twitchett, R. J. (2013). Completeness of the fossil record and the validity of sampling proxies: a case study from the Triassic of England and Wales. *Journal of the Geological Society* **170**(2): 291-300.

Dunhill, A. M., Benton, M. J., Twitchett, R. J. and Newell, A. J. (2012). Completeness of the fossil record and the validity of sampling proxies at outcrop level. *Palaeontology* **55**(6): 1155-1175.

Dunhill, A. M., Benton, M. J., Twitchett, R. J. and Newell, A. J. (2014a). Testing the fossil record: Sampling proxies and scaling in the British Triassic–Jurassic. *Palaeogeography, Palaeoclimatology, Palaeoecology* **404**: 1-11.

Dunhill, A. M., Bestwick, J., Narey, H. and Sciberras, J. (2016). Dinosaur biogeographical structure and Mesozoic continental fragmentation: a network‐based approach. *Journal of Biogeography*.

Dunhill, A. M., Hannisdal, B. and Benton, M. J. (2014b). Disentangling rock record bias and common-cause from redundancy in the British fossil record. *Nature Communications* **5**: 4818.

Dunhill, A. M. and Wills, M. A. (2015). Geographic range did not confer resilience to extinction in terrestrial vertebrates at the end-Triassic crisis. *Nature Communications* **6**: 7980.

Dunlop, J. A. (2010). Geological history and phylogeny of Chelicerata. *Arthropod Structure and Development* **39**(2): 124-142.

Dupret, V. (2004). The pleurosaurs: anatomy and phylogeny. *Revue de Paléobiologie, Vol. Spéc.* **9**: 61-80.

Dyke, G. J., Benton, M. J., Posmosanu, E. and Naish, D. (2011). Early Cretaceous (Berriasian) birds and pterosaurs from the Cornet bauxite mine, Romania. *Palaeontology* **54**(1): 79-95.

Dyke, G. J., McGowan, A., Nudds, R. and Smith, D. (2009). The shape of pterosaur evolution: evidence from the fossil record. *Journal of Evolutionary Biology* **22**(4): 890-898.

Dypvik, H., Gudlaugsson, S. T., Tsikalas, F., Attrep, M., Ferrell, R. E., Krinsley, D. H., Mørk, A., Faleide, J. I. and Nagy, J. (1996). Mjølnir structure: An impact crater in the Barents Sea. *Geology* **24**(9): 779-782.

Dypvik, H., Smelror, M., Sandbakken, P. T., Salvigsen, O. and Kalleson, E. (2006). Traces of the marine Mjølnir impact event. *Palaeogeography, Palaeoclimatology, Palaeoecology* **241**(3): 621-636.

Dypvik, H. and Zakharov, V. (2012). Fine-grained epicontinental Arctic sedimentation–mineralogy and geochemistry of shales from the Late Jurassic-Early Cretaceous transition. *Norwegian Journal of Geology/Norsk Geologisk Forening* **92**(2-3): 65-87.

Dzyuba, O. S., Izokh, O. P. and Shurygin, B. N. (2013). Carbon isotope excursions in boreal Jurassic–Cretaceous boundary sections and their correlation potential. *Palaeogeography, Palaeoclimatology, Palaeoecology* **381**: 33-46.

Eaton, J. G., Cifelli, R. L., Hutchison, J. H., Kirkland, J. I. and Parrish, J. M. (1999). Cretaceous vertebrate faunas from the Kaiparowits Plateau, south-central Utah. *Vertebrate paleontology in Utah*. D. D. Gillette. Salt Lake City, Utah Geological Survey. **99:** 345.

Eaton, M. J., Martin, A., Thorbjarnarson, J. and Amato, G. (2009). Species-level diversification of African dwarf crocodiles (Genus *Osteolaemus*): a geographic and phylogenetic perspective. *Molecular Phylogenetics and Evolution* **50**(3): 496-506.

Eble, G. J. (2000). Contrasting evolutionary flexibility in sister groups: disparity and diversity in Mesozoic atelostomate echinoids. *Paleobiology* **26**(1): 56-79.

Efimov, M. (1976). The oldest crocodile on the territory of the USSR. *Paleontologicheskii Zhurnal* **10**: 115-117.

Efimov, M. (1988). Fossil crocodiles and champsosaurs of Mongolia and the USSR. *Trudy Sovmestnoi Sovetsko-Mongol'skoi Paleontologicheskoi Ekspeditsii* **36**: 1-108.

Efimov, M. (1996). The Jurassic crocodylomorphs of Inner Asia. *The continental Jurassic. Museum of Northern Arizona Bulletin* **60**: 305-309.

Eguchi, S. and Tamura, M. (2016). Evolutionary timescale of monocots determined by the fossilized birth-death model using a large number of fossil records. *Evolution*, 10.1111/evo.12911.

Erba, E. (2004). Calcareous nannofossils and Mesozoic oceanic anoxic events. *Marine Micropaleontology* **52**(1): 85-106.

Erba, E. (2006). The first 150 million years history of calcareous nannoplankton: biosphere–geosphere interactions. *Palaeogeography, Palaeoclimatology, Palaeoecology* **232**(2): 237-250.

Erba, E., Bartolini, A. and Larson, R. L. (2004). Valanginian Weissert oceanic anoxic event. *Geology* **32**(2): 149-152.

Erba, E. and Tremolada, F. (2004). Nannofossil carbonate fluxes during the Early Cretaceous: phytoplankton response to nutrification episodes, atmospheric CO_2, and anoxia. *Paleoceanography* **19**(1): 1-18.

Erickson, G. M. and Brochu, C. A. (1999). How the 'terror crocodile'grew so big. *Nature* **398**(6724): 205-206.

Escaso, F., Ortega, F., Dantas, P., Malafaia, E., Pimentel, N. L., Pereda-Suberbiola, X., Sanz, J. L., Kullberg, J. C., Kullberg, M. C. and Barriga, F. (2007). New evidence of shared dinosaur across Upper Jurassic proto-North Atlantic: *Stegosaurus* from Portugal. *Naturwissenschaften* **94**(5): 367-374.

Escaso, F., Ortega, F., Dantas, P., Malafaia, E., Silva, B., Gasulla, J. M., Mocho, P., Narváez, I. and Sanz, J. L. (2014). A new dryosaurid ornithopod (Dinosauria, Ornithischia) from the Late Jurassic of Portugal. *Journal of Vertebrate Paleontology* **34**(5): 1102-1112.

Etheridge, R. (1885). Manual of Geology: Theoretical and Practical. London, Charles Griffin and Company.

Evans, R. (1977). Origin and significance of evaporites in basins around the Atlantic Margin. *AAPG Bulletin* **61**(2): 223-234.

Evans, S. and Manabe, M. (1999a). A choristoderan reptile from the Lower Cretaceous of Japan. *Special Papers in Palaeontology*, (60): 101-119.

Evans, S. E. (2003). At the feet of the dinosaurs: the early history and radiation of lizards. *Biological Reviews* **78**(04): 513-551.

Evans, S. E. and Chure, D. J. (1999). Upper Jurassic lizards from the Morrison Formation of Dinosaur National Monument, Utah. *Vertebrate paleontology in Utah*. D. D. Gillette. Salt Lake City, Utah Geological Survey Miscellaneous Publication. **99:** 151-159.

Evans, S. E. and Jones, M. E. (2010). The origin, early history and diversification of lepidosauromorph reptiles. *New Aspects of Mesozoic Biodiversity*, Springer Berlin Heidelberg. **132:** 27-44.

Evans, S. E., Jones, M. E. and Matsumoto, R. (2012). A new lizard skull from the Purbeck Limestone Group (Lower Cretaceous) of England. *Bulletin de la Societe Geologique de France* **183**(6): 517-524.

Evans, S. E. and Klembara, J. (2005). A choristoderan reptile (Reptilia: Diapsida) from the lower miocene of northwest Bohemia (Czech republic). *Journal of Vertebrate Paleontology* **25**(1): 171-184.

Evans, S. E., Lally, C., Chure, D., Elder, A. and Maisano, J. (2005). A Late Jurassic salamander (Amphibia: Caudata) from the Morrison Formation of North America. *Zoological Journal of the Linnean Society* **143**(4): 599-616.

Evans, S. E. and Manabe, M. (1998). Early Cretaceous frog remains from the Okurodani Formation, Tetori Group, Japan. *Paleontological Research* **2**(4): 275-278.

Evans, S. E. and Manabe, M. (1999b). Early Cretaceous lizards from the Okurodani Formation of Japan. *Geobios* **32**(6): 889-899.

Evans, S. E. and Milner, A. R. (1993). Frogs and salamanders from the Upper Jurassic Morrison Formation (Quarry Nine, Como Bluff) of North America. *Journal of Vertebrate Paleontology* **13**(1): 24-30.

Evans, S. E., Milner, A. R., Fraser, N. and Sues, H. (1994). Middle Jurassic microvertebrate assemblages from the British Isles. *In the shadow of the dinosaurs: Early Mesozoic tetrapods*. N. C. Fraser and H.-D. Sues, Cambridge University Press**:** 303-321.

Evans, S. E., Prasad, G. and Manhas, B. (2002). Fossil lizards from the Jurassic Kota formation of India. *Journal of Vertebrate Paleontology* **22**(2): 299-312.

Evans, S. E. and Sigogneau-Russell, D. (1997). New sphenodontians (Diapsida: Lepidosauria: Rhynchocephalia) from the Early Cretaceous of North Africa. *Journal of Vertebrate Paleontology* **17**(1): 45-51.

Evans, S. E. and Sigogneau-Russell, D. (2001). A stem‐group caecilian (Lissamphibia: Gymnophiona) from the Lower Cretaceous of North Africa. *Palaeontology* **44**(2): 259-273.

Evers, S. W., Rauhut, O. W., Milner, A. C., McFeeters, B. and Allain, R. (2015). A reappraisal of the morphology and systematic position of the theropod dinosaur *Sigilmassasaurus* from the “middle” Cretaceous of Morocco. *PeerJ* **3**: e1323.

Falkowski, P. G., Katz, M. E., Knoll, A. H., Quigg, A., Raven, J. A., Schofield, O. and Taylor, F. (2004). The evolution of modern eukaryotic phytoplankton. *Science* **305**(5682): 354-360.

Fanti, F., Cau, A., Panzarin, L. and Cantelli, L. (2016a). Evidence of iguanodontian dinosaurs from the Lower Cretaceous of Tunisia. *Cretaceous Research* **60**: 267-274.

Fanti, F., Contessi, M. and Franchi, F. (2012). The “Continental Intercalaire” of southern Tunisia: stratigraphy, paleontology, and paleoecology. *Journal of African Earth Sciences* **73**: 1-23.

Fanti, F., Miyashita, T., Cantelli, L., Mnasri, F., Dridi, J., Contessi, M. and Cau, A. (2016b). The largest thalattosuchian (Crocodylomorpha) supports teleosaurid survival across the Jurassic-Cretaceous boundary. *Cretaceous Research* **61**: 263-274.

Fara, E. (2000). Diversity of Callovian-Ypresian (Middle Jurassic-Eocene) tetrapod families and selectivity of extinctions at the K/T boundary. *Geobios* **33**(3): 387-396.

Fara, E. (2004). Estimating minimum global species diversity for groups with a poor fossil record: a case study of Late Jurassic-Eocene lissamphibians. *Palaeogeography, Palaeoclimatology, Palaeoecology* **207**(1-2): 59-82.

Farke, A. A., Maxwell, W. D., Cifelli, R. L. and Wedel, M. J. (2014). A ceratopsian dinosaur from the Lower Cretaceous of Western North America, and the biogeography of Neoceratopsia. *PLOS ONE* **9**(12): e112055.

Féraud, G., Alric, V., Fornari, M., Bertrand, H. and Haller, M. (1999). $^{40}Ar/^{39}Ar$ dating of the Jurassic volcanic province of Patagonia: migrating magmatism related to Gondwana break-up and subduction. *Earth and Planetary Science Letters* **172**(1): 83-96.

Fernandes, L. A. and Coimbra, A. M. (2008). Revisão estratigráfica da parte oriental da Bacia Bauru (Neocretáceo). *Brazilian Journal of Geology* **30**(4): 717-728.

Fernandez, M. S. and Campos, L. (2015). Ophthalmosaurids (Ichthyosauria: Thunnosauria): Alpha taxonomy, clades and names. *Publicación Electrónica de la Asociación Paleontológica Argentina* **15**(1).

Figueiredo, R. G., Moreira, J. K., Saraiva, A. A. and Kellner, A. W. (2011). Description of a new specimen of *Susisuchus anatoceps* (Crocodylomorpha: Mesoeucrocodylia) from the Crato Formation (Santana Group) with comments on Neosuchia. *Zoological Journal of the Linnean Society* **163**(s1): S273-S288.

Finnegan, S., Heim, N. A., Peters, S. E. and Fischer, W. W. (2012). Climate change and the selective signature of the Late Ordovician mass extinction. *Proceedings of the National Academy of Sciences of the United States of America* **109**(18): 6829-6834.

Fiorelli, L. E. (1999). Non-mammalian microvertebrate remains from the Robison Eggshell Site, Cedar Mountain Formation (Lower Cretaceous), Emery County, Utah. *Vertebrate paleontology in Utah*. G. DD. Salt Lake City, Utha Geological Survey. **99:** 259-268.

Fischer, V., Appleby, R. M., Naish, D., Liston, J., Riding, J. B., Brindley, S. and Godefroit, P. (2013). A basal thunnosaurian from Iraq reveals disparate phylogenetic origins for Cretaceous ichthyosaurs. *Biology Letters* **9**(4): 20130021.

Fischer, V., Arkhangelsky, M. S., Stenshin, I. M., Uspensky, G. N., Zverkov, N. G. and Benson, R. B. J. (2015). Peculiar macrophagous adaptations in a new Cretaceous pliosaurid. *Royal Society Open Science* **2**(12).

Fischer, V., Arkhangelsky, M. S., Uspensky, G. N., Stenshin, I. M. and Godefroit, P. (2014). A new Lower Cretaceous ichthyosaur from Russia reveals skull shape conservatism within Ophthalmosaurinae. *Geological Magazine* **151**(01): 60-70.

Fischer, V., Bardet, N., Benson, R. B., Arkhangelsky, M. S. and Friedman, M. (2016). Extinction of fish-shaped marine reptiles associated with reduced evolutionary rates and global environmental volatility. *Nature Communications* **7**: 10825.

Fischer, V., Maisch, M. W., Naish, D., Kosma, R., Liston, J., Joger, U., Kruger, F. J., Perez, J. P., Tainsh, J. and Appleby, R. M. (2012). New ophthalmosaurid ichthyosaurs from the European Lower Cretaceous

demonstrate extensive ichthyosaur survival across the Jurassic-Cretaceous boundary. *PLOS ONE* **7**(1): e29234.

Flynn, J., Fox, S. R., Parrish, J. M., Ranivoharimanana, L. and Wyss, A. R. (2006). Assessing diversity and paleoecology of a Middle Jurassic microvertebrate assemblage from Madagascar. *New Mexico Museum of Natural History and Science Bulletin* **37**: 476-489.

Foffa, D. and Young, M. T. (2014). The cranial osteology of *Tyrannoneustes lythrodectikos* (Crocodylomorpha: Metriorhynchidae) from the Middle Jurassic of Europe. *PeerJ* **2**: e608.

Föllmi, K. (2012). Early Cretaceous life, climate and anoxia. *Cretaceous Research* **35**: 230-257.

Fonseca, M. E. P. (2015). Estado actual del conocimiento de los reptiles marinos Cretácicos de Colombia. *Publicación Electrónica de la Asociación Paleontológica Argentina* **15**(1).

Foote, M. (1996). On the probability of ancestors in the fossil record. *Paleobiology* **22**(02): 141-151.

Foote, M. (2000). Origination and extinction components of taxonomic diversity: general problems. *Paleobiology* **26**: 74-102.

Foote, M. (2003). Origination and extinction through the Phanerozoic: a new approach. *The Journal of Geology* **111**(2): 125-148.

Foote, M. (2005). Pulsed origination and extinction in the marine realm. *Paleobiology* **31**(1): 6-20.

Foote, M. (2014). Environmental controls on geographic range size in marine animal genera. *Paleobiology* **40**(3): 440-458.

Ford, D. and Golonka, J. (2003). Phanerozoic paleogeography, paleoenvironment and lithofacies maps of the circum-Atlantic margins. *Marine and Petroleum Geology* **20**(3): 249-285.

Förster, R. (1985). Evolutionary trends and ecology of Mesozoic decapod crustaceans. *Transactions of the Royal Society of Edinburgh: Earth Sciences* **76**(2-3): 299-304.

Fortier, D. C. and Schultz, C. L. (2009). A new neosuchian crocodylomorph (Crocodyliformes, Mesoeucrocodylia) from the Early Cretaceous of North-East Brazil. *Palaeontology* **52**: 991-1007.

Foth, C., Bona, P. and Desojo, J. B. (2015). Intraspecific variation in the skull morphology of the black caiman *Melanosuchus niger* (Alligatoridae, Caimaninae). *Acta Zoologica* **96**(1): 1-13.

Foth, C. and Rauhut, O. W. (2013). Macroevolutionary and morphofunctional patterns in theropod skulls: a morphometric approach. *Acta Palaeontologica Polonica* **58**(1): 1-16.

Franke, F. A., Schmidt, F., Borgwardt, C., Bernhard, D., Bleidorn, C., Engelmann, W.-E. and Schlegel, M. (2013). Genetic differentiation of the African dwarf crocodile *Osteolaemus tetraspis* Cope, 1861 (Crocodylia: Crocodylidae) and consequences for European zoos. *Organisms Diversity & Evolution* **13**(2): 255-266.

Frey, E., Meyer, C. A. and Tischlinger, H. (2011). The oldest azhdarchoid pterosaur from the Late Jurassic Solnhofen Limestone (early Tithonian) of southern Germany. *Swiss Journal of Geosciences* **104**(1): 35-55.

Friedman, M. and Sallan, L. C. (2012). Five hundred million years of extinction and recovery: a phanerozoic survey of large-scale diversity patterns in fishes. *Palaeontology* **55**: 707-742.

Fröbisch, J. (2013). Vertebrate diversity across the end-Permian mass extinction—Separating biological and geological signals. *Palaeogeography, Palaeoclimatology, Palaeoecology* **372**: 50-61.

Gallina, P. A. (2016). Reappraisal of the Early Cretaceous sauropod dinosaur *Amargatitanis macni* (Apesteguía, 2007), from northwestern Patagonia, Argentina. *Cretaceous Research* **64**: 79-87.

Gallina, P. A., Apesteguía, S., Haluza, A. and Canale, J. I. (2014). A diplodocid sauropod survivor from the Early Cretaceous of South America. *PLOS ONE* **9**(5): e97128.

Galton, P. (1996). Notes on Dinosauria from the Upper Cretaceous of Portugal. *Neues Jahrbuch fur Geologie und Palaontologie-Monatshefte* **2**: 83-90.

Galton, P. M. (1982). *Elaphrosaurus*, an ornithomimid dinosaur from the Upper Jurassic of North America and Africa. *Paläontologische Zeitschrift* **56**(3-4): 265-275.

Gao, K.-Q. and Shubin, N. H. (2003). Earliest known crown-group salamanders. *Nature* **422**(6930): 424-428.

Gao, K.-Q., Zhou, C.-F., Hou, L. and Fox, R. C. (2013). Osteology and ontogeny of Early Cretaceous *Philydrosaurus* (Diapsida: Choristodera) based on new specimens from Liaoning Province, China. *Cretaceous Research* **45**: 91-102.

Gao, K. and Cheng, Z. (1999). A new lizard from the Lower Cretaceous of Shandong, China. *Journal of Vertebrate Paleontology* **19**(3): 456-465.

Gao, K. Q. and Fox, R. C. (2005). A new choristodere (Reptilia: Diapsida) from the Lower Cretaceous of western Liaoning Province, China, and phylogenetic relationships of Monjurosuchidae. *Zoological Journal of the Linnean Society* **145**(3): 427-444.

Gardner, G., Harvey, A. and Phillips, G. (1980). Algorithm AS 154: An algorithm for exact maximum likelihood estimation of autoregressive-moving average models by means of Kalman filtering. *Journal of the Royal Statistical Society. Series C (Applied Statistics)* **29**(3): 311-322.

Gardner, J. D. (1999). New albanerpetontid amphibians from the Albian to Coniacian of Utah, USA—bridging the gap. *Journal of Vertebrate Paleontology* **19**(4): 632-638.

Gardner, J. D. and DeMar Jr, D. G. (2013). Mesozoic and Palaeocene lissamphibian assemblages of North America: a comprehensive review. *Palaeobiodiversity and Palaeoenvironments* **93**(4): 459-515.

Gardner, J. D., Evans, S. E. and Sigogneau-Russell, D. (2003). New albanerpetontid amphibians from the Early Cretaceous of Morocco and Middle Jurassic of England. *Acta Palaeontologica Polonica* **48**(2): 301-319.

Gardner, J. D. and Rage, J.-C. (2016). The fossil record of lissamphibians from Africa, Madagascar, and the Arabian Plate. *Palaeobiodiversity and Palaeoenvironments* **96**(1): 169-220.

Garfunkel, Z. (1998). Constrains on the origin and history of the Eastern Mediterranean basin. *Tectonophysics* **298**(1): 5-35.

Garrison, J. R., Brinkman, D., Nichols, D. J., Layer, P., Burge, D. and Thayn, D. (2007). A multidisciplinary study of the Lower Cretaceous Cedar Mountain Formation, Mussentuchit Wash, Utah: a determination of the paleoenvironment and paleoecology of the *Eolambia caroljonesa* dinosaur quarry. *Cretaceous Research* **28**(3): 461-494.

Gasparini, Z. and Dellapé, D. (1976). Un nuevo cocodrilo marino (Thalattosuchia, Metriorhynchidae) de la Formación Vaca Muerta (Jurasico, Tithoniano) de la Provincia de Neuquén (República Argentina). Congreso Geológico Chileno.

Gasparini, Z. and Fernández, M. (1997). Tithonian marine reptiles of the Eastern Pacific. *Ancient Marine Reptiles*. San Diego, Academic Press**:** 435-450.

Gasparini, Z. and Fernández, M. (2005). Jurassic marine reptiles of the Neuquén Basin: records, faunas and their palaeobiogeographic significance. *The Neuquén Basin, Argentina: A Case Study in Sequence*

Stratigraphy and Basin Dynamics. G. D. Veiga, L. A. Spalletti, J. A. Howell and E. Schwarz. London, Geological Society of London. **252:** 279-294.

Gasparini, Z., Pol, D. and Spalletti, L. A. (2006). An unusual marine crocodyliform from the Jurassic-Cretaceous boundary of Patagonia. *Science* **311**(5757): 70-73.

Gatesy, J., Baker, R. H. and Hayashi, C. (2004). Inconsistencies in arguments for the supertree approach: supermatrices versus supertrees of Crocodylia. *Systematic Biology* **53**(2): 342-355.

Geldmacher, J., van den Bogaard, P., Heydolph, K. and Hoernle, K. (2014). The age of Earth's largest volcano: Tamu Massif on Shatsky Rise (northwest Pacific Ocean). *International Journal of Earth Sciences* **103**(8): 2351-2357.

Gervais, P. (1871). Remarques au sujet des Reptiles provenant des calcaires lithographiques de Cerin, dans le Bugey, qui sont conservés au Musée de Lyon. *Comptes Rendus des Séances de l'Academie de Sciences, Paris* **73**: 603-607.

Gilmore, C. (1926). A new aetosaurian reptile from the Morrison Formation of Utah. *Annals of Carnegie Museum* **16**: 325-348.

Gobbo-Rodrigues, S., Petri, S. and Bertini, R. (1999). Ocorrências de ostrácodes na Formação Adamantina do Grupo Bauru, Cretáceo Superior da Bacia do Paraná e possibilidades de correlação com depósitos isócronos argentinos. Parte I–Família Ilyocyprididae. *Acta Geológica Leopoldensia* **23**(49): 3-13.

Godefroit, P., Cau, A., Dong-Yu, H., Escuillié, F., Wenhao, W. and Dyke, G. (2013a). A Jurassic avialan dinosaur from China resolves the early phylogenetic history of birds. *Nature* **498**(7454): 359-362.

Godefroit, P., Demuynck, H., Dyke, G., Hu, D., Escuillié, F. and Claeys, P. (2013b). Reduced plumage and flight ability of a new Jurassic paravian theropod from China. *Nature Communications* **4**: 1394.

Godoy, P. L., Montefeltro, F. C., Norell, M. A. and Langer, M. C. (2014). An additional baurusuchid from the Cretaceous of Brazil with evidence of interspecific predation among Crocodyliformes. *PLOS ONE* **9**(5): e97138.

Goloboff, P., Farris, S. and Nixon, K. (2000). TNT (Tree analysis using New Technology).

Goloboff, P. A. (1993). Estimating character weights during tree search. *Cladistics* **9**(1): 83-91.

Goloboff, P. A., Farris, J. S., Källersjö, M., Oxelman, B. and Szumik, C. A. (2003). Improvements to resampling measures of group support. *Cladistics* **19**(4): 324-332.

Goloboff, P. A., Farris, J. S. and Nixon, K. C. (2008). TNT, a free program for phylogenetic analysis. *Cladistics* **24**(5): 774-786.

Gomani, E. M. (1997). A crocodyliform from the Early Cretaceous dinosaur beds, northern Malawi. *Journal of Vertebrate Paleontology* **17**(2): 280-294.

Good, I. J. (1953). The population frequencies of species and the estimation of population parameters. *Biometrika* **403**: 237-264.

Gorscak, E. and O'Connor, P. M. (2016). Time-calibrated models support congruency between Cretaceous continental rifting and titanosaurian evolutionary history. *Biology Letters* **12**: 20151047.

Gorzelak, P., Salamon, M. A., Trzęsiok, D., Lach, R. and Baumiller, T. K. (in press). Diversity dynamics of post‐Palaeozoic crinoids–in quest of the factors affecting crinoid macroevolution. *Lethaia* **49**(2): 231-244.

Götz, S., Löser, H. and Schmid, D. U. (2005). Reef development on a deepening platform: two Early Cretaceous coralgal patch reefs (Catí, Llàcova Formation, eastern Spain) compared. *Cretaceous Research* **26**(6): 864-881.

Gow, C. (2000). The skull of *Protosuchus haughtoni*, an Early Jurassic crocodyliform from southern Africa. *Journal of Vertebrate Paleontology* **20**(1): 49-56.

Grabowski, J. (2011). Magnetostratigraphy of the Jurassic/Cretaceous boundary interval in the Western Tethys and its correlations with other regions: a review. *Volumina Jurassica* **9**(9): 105-128.

Grabowski, J., Haas, J., Márton, E. and Pszczółkowski, A. (2010a). Magneto- and biostratigraphy of the Jurassic/Cretaceous boundary in the Lókút section (Transdanubian Range, Hungary). *Studia Geophysica et Geodaetica* **54**(1): 1-26.

Grabowski, J., Michalík, J., Pszczółkowski, A. and Lintnerová, O. (2010b). Magneto-, and isotope stratigraphy around the Jurassic/Cretaceous boundary in the Vysoká Unit (Malé Karpaty Mountains, Slovakia): correlations and tectonic implications. *Geologica Carpathica* **61**(4): 309-326.

Grabowski, J. and Pszczółkowski, A. (2006). Magneto- and biostratigraphy of the Tithonian–berriasian pelagic sediments in the Tatra Mountains (central western Carpathians, Poland): sedimentary and rock magnetic changes at the Jurassic/Cretaceous boundary. *Cretaceous Research* **27**(3): 398-417.

Grabowski, J., Schnyder, J., Sobień, K., Koptikova, L., Krzemiński, L., Pszczółkowski, A., Hejnar, J. and Schnabl, P. (2013). Magnetic susceptibility and spectral gamma logs in the Tithonian–Berriasian pelagic carbonates in the Tatra Mts (Western Carpathians, Poland): Palaeoenvironmental changes at the Jurassic/Cretaceous boundary. *Cretaceous Research* **43**: 1-17.

Gradstein, F., Huang, Z., Merrett, D. and Ogg, J. (1992). Probabilistic zonation of Early Cretaceous microfossil sequences, Atlantic and Indian Oceans, with special reference to ODP Leg 123. *Proceedings of the Ocean Drilling Program, Scientific Result* **123**: 759-777.

Gradstein, F. M., Ogg, J. G., Schmitz, M. and Ogg, G. (2012). The Geologic Time Scale 2012, Elsevier.

Green, J. P. and Lomax, D. R. (2014). An ichthyosaur (Reptilia: Ichthyosauria) specimen from the Lower Cretaceous (Berriasian) Spilsby Sandstone Formation of Nettleton, Lincolnshire, UK. *Proceedings of the Geologists' Association* **125**(4): 432-436.

Grigorescu, D., Venczel, M., Csiki, Z. and Limberea, R. (1999). New latest Cretaceous microvertebrate fossil assemblages from the Haţeg Basin (Romania). *Geologie en Mijnbouw* **78**(3-4): 301-314.

Grimaldi, D. A. (2010). 400 million years on six legs: on the origin and early evolution of Hexapoda. *Arthropod Structure and Development* **39**(2): 191-203.

Gröcke, D. R., Price, G. D., Ruffell, A. H., Mutterlose, J. and Baraboshkin, E. (2003). Isotopic evidence for late Jurassic–Early Cretaceous climate change. *Palaeogeography, Palaeoclimatology, Palaeoecology* **202**(1): 97-118.

Guinot, G., Adnet, S. and Cappetta, H. (2012). An analytical approach for estimating fossil record and diversification events in sharks, skates and rays. *PLOS ONE* **7**(9): e44632.

Haddoumi, H., Allain, R., Meslouh, S., Metais, G., Monbaron, M., Pons, D., Rage, J.-C., Vullo, R., Zouhri, S. and Gheerbrant, E. (2015). Guelb el Ahmar (Bathonian, Anoual Syncline, eastern Morocco): First continental flora and fauna including mammals from the Middle Jurassic of Africa. *Gondwana Research*.

Haddoumi, H., Allain, R., Meslouh, S., Metais, G., Monbaron, M., Pons, D., Rage, J.-C., Vullo, R., Zouhri, S. and Gheerbrant, E. (2016). Guelb el Ahmar (Bathonian, Anoual Syncline, eastern Morocco): First

continental flora and fauna including mammals from the Middle Jurassic of Africa. *Gondwana Research* **29**(1): 290-319.

Hallam, A. (1986). The Pliensbachian and Tithonian extinction events. *Nature* **319**(6056): 765-768.

Hallam, A. (1988). A re-evaluation of Jurassic eustacy in the light of new data and the revised Exxon curve. *Sea-level Changes - an Integrated Approach*. B. S. Hastings, C. G. S. C. Kendall, H. W. Posamentier, C. A. Ross and J. C. van Wagoner, The Society of Economic Paleontologists and Mineralogists. **SEPM Special Publication 42:** 261-274.

Hallam, A. (1992). Phanerozoic sea-level changes. New York, Columbia University Press.

Hallam, A. (1994). Jurassic climates as inferred from the sedimentary and fossil record. *Palaeoclimates and their Modelling, with Special Reference to the Mesozoic Era*. J. R. L. Allen, B. J. Hoskins, B. W. Sellwood, R. A. Spicer and P. J. Valdes. Amsterdam, Springer Netherlands**:** 79-88.

Hallam, A. (1998). Lyell's views on organic progression, evolution and extinction. *Lyell: the Past is the Key to the Present*. D. J. Blundell and A. C. Scott. London, Geological Society of London. **143:** 133-136.

Hallam, A. (2001). A review of the broad pattern of Jurassic sea-level changes and their possible causes in the light of current knowledge. *Palaeogeography, Palaeoclimatology, Palaeoecology* **167**(1-2): 23-37.

Hallam, A. (2002). How catastrophic was the end‐Triassic mass extinction? *Lethaia* **35**(2): 147-157.

Hallam, A. and Cohen, J. (1989). The case for sea-level change as a dominant causal factor in mass extinction of marine invertebrates [and discussion]. *Philosophical Transactions of the Royal Society of London Series B: Biological Sciences* **325**(1228): 437-455.

Hallam, A., Grose, J. and Ruffell, A. (1991). Palaeoclimatic significance of changes in clay mineralogy across the Jurassic-Cretaceous boundary in England and France. *Palaeogeography, Palaeoclimatology, Palaeoecology* **81**(3): 173-187.

Hallam, A. and Wignall, P. B. (1997). Mass Extinctions and their Aftermath. Oxford, Oxford University Press.

Halliday, T. J., de Andrade, M. B., Benton, M. J. and Efimov, M. B. (2015). A re-evaluation of goniopholidid crocodylomorph material from Central Asia: Biogeographic and phylogenetic implications. *Acta Palaeontologica Polonica* **60**(2): 291-312.

Han, F.-L., Barrett, P. M., Butler, R. J. and Xu, X. (2012). Postcranial anatomy of *Jeholosaurus shangyuanensis* (Dinosauria, Ornithischia) from the Lower Cretaceous Yixian Formation of China. *Journal of Vertebrate Paleontology* **32**(6): 1370-1395.

Hannisdal, B., Haaga, K. A., Reitan, T., Diego, D. and Liow, L. H. (2016). Common species link global ecosystems to climate change. *bioRxiv*: 043729.

Hannisdal, B. and Peters, S. E. (2011). Phanerozoic Earth system evolution and marine biodiversity. *Science* **334**(6059): 1121-1124.

Haq, B. U. (2014). Cretaceous eustasy revisited. *Global and Planetary Change* **113**: 44-58.

Haq, B. U., Hardenbol, J. and Vail, P. R. (1987). Chronology of fluctuating sea levels since the Triassic. *Science* **235**(4793): 1156-1167.

Harnik, P. G., Lotze, H. K., Anderson, S. C., Finkel, Z. V., Finnegan, S., Lindberg, D. R., Liow, L. H., Lockwood, R., McClain, C. R. and McGuire, J. L. (2012). Extinctions in ancient and modern seas. *Trends in Ecology and Evolution* **27**(11): 608-617.

Harries, P. J., Kauffman, E. G. and Hansen, T. A. (1996). Models for biotic survival following mass extinction. *Biotic Recovery from Mass Extinction Events*. M. B. Hart. London, Geological Society of London. **102:** 41-60.

Harry, D. L. and Sawyer, D. S. (1992). Basaltic volcanism, mantle plumes, and the mechanics of rifting - the Paraná flood-basalt province of South America. *Geology* **20**(3): 207-210.

Hart, M. B. (1999). The evolution and biodiversity of Cretaceous planktonic Foraminiferida. *Geobios* **32**(2): 247-255.

Hart, R. J., Andreoli, M. A., Tredoux, M., Moser, D., Ashwal, L. D., Eide, E. A., Webb, S. J. and Brandt, D. (1997). Late Jurassic age for the Morokweng impact structure, southern Africa. *Earth and Planetary Science Letters* **147**(1): 25-35.

Hathway, B. (2000). Continental rift to back ‐ arc basin: Jurassic ‐ Cretaceous stratigraphical and structural evolution of the Larsen Basin, Antarctic Peninsula. *Journal of the Geological Society* **157**(2): 417-432.

Haubold, H. (1990). Dinosaurs and fluctuating sea levels during the Mesozoic. *Historical Biology* **4**(2): 75-106.

Hay, O. (1930). Second Bibliography and Catalogue of the Fossil Vertebrata of North America. Washington DC, Carnegie Institute, Washington.

Hay, W. W. (2008). Evolving ideas about the Cretaceous climate and ocean circulation. *Cretaceous Research* **29**(5): 725-753.

Hay, W. W., Migdisov, A., Balukhovsky, A. N., Wold, C. N., Flögel, S. and Söding, E. (2006). Evaporites and the salinity of the ocean during the Phanerozoic: implications for climate, ocean circulation and life. *Palaeogeography, Palaeoclimatology, Palaeoecology* **240**(1): 3-46.

Head, J. J. (2015). Fossil calibration dates for molecular phylogenetic analysis of snakes 1: Serpentes, Alethinophidia, Boidae, Pythonidae. *Palaeontologia Electronica* **18**(1): 1-17.

Heim, N. A. and Peters, S. E. (2011a). Covariation in macrostratigraphic and macroevolutionary patterns in the marine record of North America. *Geological Society of America Bulletin* **123**(3-4): 620-630.

Heim, N. A. and Peters, S. E. (2011b). Regional environmental breadth predicts geographic range and longevity in fossil marine genera. *PLOS ONE* **6**(5): e18946.

Hendricks, J. R., Saupe, E. E., Myers, C. E., Hermsen, E. J. and Allmon, W. D. (2014). The Generification of the Fossil Record. *Paleobiology* **40**(4): 511-528.

Henkel, H., Reimold, W. U. and Koeberl, C. (2002). Magnetic and gravity model of the Morokweng impact structure. *Journal of Applied Geophysics* **49**(3): 129-147.

Henrici, A. C. (1998). A new pipoid anuran from the late Jurassic Morrison Formation at Dinosaur National Monument, Utah. *Journal of Vertebrate Paleontology* **18**(2): 321-332.

Herrera, Y. (2015). Metriorhynchidae (Crocodylomorpha: Thalattosuchia) from Upper Jurassic–Lower Cretaceous of Neuquén Basin (Argentina), with comments on the natural casts of the brain. *Publicación Electrónica de la Asociación Paleontológica Argentina* **15**(1): 159-171.

Herrera, Y., Gasparini, Z. and Fernandez, M. S. (2013). A new Patagonian species of *Cricosaurus* (Crocodyliformes, Thalattosuchia): first evidence of Cricosaurus in Middle–Upper Tithonian lithographic limestone from Gondwana. *Palaeontology* **56**(3): 663-678.

Hirayama, R. (1998). Oldest known sea turtle. *Nature* **392**(6677): 705-708.

Hirayama, R., Brinkman, D. B. and Danilov, I. G. (2000). Distribution and biogeography of non-marine Cretaceous turtles. *Russian Journal of Herpetology* **7**(3): 181-198.

Hoffman, A. (1985). Patterns of family extinction depend on definition and geological timescale. *Nature* **315**(6021): 659-662.

Höfling, R. and Scott, R. (2002). Early and mid-Cretaceous buildups *Phanerozoic Reef Patterns*. W. Kiessling, E. Flugel and J. Golonka. Tulsa, Society for Sedimentary Geology. **72:** 521-548.

Holland, S. M. (2000). The quality of the fossil record: a sequence stratigraphic perspective. *Paleobiology* **26**: 148-168.

Holland, S. M. and Patzkowsky, M. E. (2015). The stratigraphy of mass extinction. *Palaeontology* **58**(5): 903-924.

Holliday, C. M. and Gardner, N. M. (2012). A new eusuchian crocodyliform with novel cranial integument and its significance for the origin and evolution of Crocodylia. *PLOS ONE* **7**(1): e30471.

Hopkins, M. J. (2016). Magnitude versus direction of change and the contribution of macroevolutionary trends to morphological disparity. *Biological Journal of the Linnean Society* **118**: 116-130.

Hornung, J. (2013). Contributions to the Palaeobiology of the Archosaurs (Reptilia: Diapsida) from the Bückeberg Formation ('Northwest German Wealden'-Berriasian-Valanginian, Lower Cretaceous) of northern Germany. PhD, Georg-August-Universität Göttingen.

Houša, V., Pruner, P., Zakharov, V., Kostak, M., Chadima, M., Rogov, M., Šlechta, S. and Mazuch, M. (2007). Boreal-Tethyan correlation of the Jurassic-Cretaceous boundary interval by magneto- and biostratigraphy. *Stratigraphy and Geological Correlation* **15**(3): 297-309.

Hu, D., Hou, L., Zhang, L. and Xu, X. (2009). A pre-*Archaeopteryx* troodontid theropod from China with long feathers on the metatarsus. *Nature* **461**(7264): 640-643.

Hu, X. M., Wagreich, M. and Yilmaz, I. O. (2012). Marine rapid environmental/climatic change in the Cretaceous greenhouse world. *Cretaceous Research* **38**: 1-6.

Hua, S., Vignaud, P., Atrops, F. and Clément, A. (2000). *Enaliosuchus macrospondylus* (Crocodylia, Metriorhynchidae) du Valanginien de Barret-le-Bas (Hautes Alpes, France): Un cas unique de remontée des narines externes parmi les crocodiliens. *Geobios* **33**(4): 467-474.

Huang, J., Wang, X., Hu, Y., Liu, J., Peteya, J. A. and Clarke, J. A. (2016). A new ornithurine from the Early Cretaceous of China sheds light on the evolution of early ecological and cranial diversity in birds. *PeerJ* **4**: e1765.

Hull, P. M., Darroch, S. A. and Erwin, D. H. (2015). Rarity in mass extinctions and the future of ecosystems. *Nature* **528**(7582): 345-351.

Hunt, A. P. and Lockley, M. G. (1995). A nonmarine tetrapod from the Middle Jurassic of the United States: A primitive crocodyliform from the Entrada Sandstone of eastern Utah. *Journal of Vertebrate Paleontology* **15**(3): 554-560.

Hurvich, C. M. and Tsai, C. L. (1989). Regression and time-series model selection in small samples. *Biometrika* **76**(2): 297-307.

Hynes, A. (1990). Two-stage rifting of Pangea by two different mechanisms. *Geology* **18**(4): 323-326.

Irmis, R. B. (2010). Evaluating hypotheses for the early diversification of dinosaurs. *Earth and Environmental Science Transactions of the Royal Society of Edinburgh* **101**(3-4): 397-426.

Ivakhnenko, M. (1978). Caudates from the Triassic and Jurassic of Middle Asia. *Paleontologicheskii Zhurnal* **3**: 84-89.

Jablonski, D. and Chaloner, W. (1994). Extinctions in the fossil record [and discussion]. *Philosophical Transactions of the Royal Society of London Series B: Biological Sciences* **344**(1307): 11-17.

Jablonski, D. and Finarelli, J. A. (2009). Congruence of morphologically-defined genera with molecular phylogenies. *Proceedings of the National Academy of Sciences of the United States of America* **106**(20): 8262-8266.

Jablonski, D., Roy, K., Valentine, J. W., Price, R. M. and Anderson, P. S. (2003). The impact of the pull of the recent on the history of marine diversity. *Science* **300**(5622): 1133-1135.

Jackson, J. B. C. and Johnson, K. G. (2001). Measuring past biodiversity. *Science* **293**: 2401-2404.

Jacobs, L., Winkler, D., Kaufulu, Z. and Downs, W. (1990). The dinosaur beds of northern Malawi, Africa. *National Geographic Research* **6**(2): 196-204.

Jansen, M. and Klein, N. (2014). A juvenile turtle (Testudines, Eucryptodira) from the Upper Jurassic of Langenberg Quarry, Oker, Northern Germany. *Palaeontology* **57**(4): 743-756.

Jenkins, P. A. and Walsh, D. M. (1993). An Early Jurassic caecilian with limbs. *Nature* **365**: 246-250.

Jenkyns, H., Schouten-Huibers, L., Schouten, S. and Sinninghe Damsté, J. (2011). Middle Jurassic-Early Cretaceous high-latitude sea-surface temperatures from the Southern Ocean. *Climate of the Past Discussions* **7**: 1339-1361.

Jenkyns, H., Schouten-Huibers, L., Schouten, S. and Sinninghe Damsté, J. (2012). Warm Middle Jurassic–Early Cretaceous high-latitude sea-surface temperatures from the Southern Ocean. *Climate of the Past* **8**(1): 215-226.

Jerram, D., Mountney, N., Holzforster, F. and Stollhofen, H. (1999). Internal stratigraphic relationships in the Etendeka Group in the Huab Basin, NW Namibia: understanding the onset of flood volcanism. *Journal of Geodynamics* **28**(4-5): 393-418.

Jha, N., Prakash, N. and Joshi, H. (2016). Integrated palaeobotanical and palynological analysis of subsurface Gondwana sedimentary succession (Jurassic–Cretaceous) in Jangareddygudem area, Chintalapudi Sub-basin, South India: Stratigraphical and phytogeographical implications. *Palaeoworld*, 10.1016/j.palwor.2016.03.002.

Ji, C., Jiang, D.-Y., Motani, R., Rieppel, O., Hao, W.-C. and Sun, Z.-Y. (in press). Phylogeny of the Ichthyopterygia incorporating recent discoveries from South China. *Journal of Vertebrate Paleontology* **36**(1): e1025956.

Ji, Q., Luo, Z.-X., Yuan, C.-X., Wible, J. R., Zhang, J.-P. and Georgi, J. A. (2002). The earliest known eutherian mammal. *Nature* **416**(6883): 816-822.

Ji, S.-A., Ji, Q. and Padian, K. (1999). Biostratigraphy of new pterosaurs from China. *Nature* **398**(6728): 573-573.

Joachimski, M. M. and Buggisch, W. (2002). Conodont apatite $\delta_{18}O$ signatures indicate climatic cooling as a trigger of the Late Devonian mass extinction. *Geology* **30**(8): 711-714.

Joffe, J. (1967). The 'dwarf'crocodiles of the Purbeck Formation, Dorset: a reappraisal. *Palaeontology* **10**(4): 629-639.

Jones, C. E. and Jenkyns, H. C. (2001). Seawater strontium isotopes, oceanic anoxic events, and seafloor hydrothermal activity in the Jurassic and Cretaceous. *American Journal of Science* **301**(2): 112-149.

Jones, C. E., Jenkyns, H. C., Coe, A. L. and Stephen, H. P. (1994). Strontium isotopic variations in Jurassic and Cretaceous seawater. *Geochimica et Cosmochimica Acta* **58**(14): 3061-3074.

Jones, M. E., Anderson, C. L., Hipsley, C. A., Müller, J., Evans, S. E. and Schoch, R. R. (2013). Integration of molecules and new fossils supports a Triassic origin for Lepidosauria (lizards, snakes, and tuatara). *BMC Evolutionary biology* **13**(1): 208.

Jones, R. H. (1980). Maximum likelihood fitting of ARMA models to time series with missing observations. *Technometrics* **22**(3): 389-395.

Jordan, S. M., Barraclough, T. G. and Rosindell, J. (2016). Quantifying the effects of the break up of Pangaea on global terrestrial diversification with neutral theory. *Philosophical Transactions of the Royal Society B: Biological Sciences* **371**(1691): 20150221.

Jourdan, C. (1862). Des terrains sidérolitiques. *Revue des sociétés savantes. Sciences Mathématiques, Physiques et Naturelles Paris* **1**: 130-133.

Jouve, S. (2004). Etude des Crocodyliformes fini Crétacé-Paléogène du Bassin des Oulad Abdoun (Maroc) et comparaison avec les faunes africaines contemporaines: systématique, phylogénie et paléobiogéographie. DPhil, Muséum National d'Histoire Naturelle.

Jouve, S. (2009). The skull of *Teleosaurus cadomensis* (Crocodylomorpha; Thalattosuchia), and phylogenetic analysis of Thalattosuchia. *Journal of Vertebrate Paleontology* **29**(1): 88-102.

Jouve, S., Bardet, N., Jalil, N.-E., Suberbiola, X. P., Bouya, B. and Amaghzaz, M. (2008). The oldest African crocodylian: phylogeny, paleobiogeography, and differential survivorship of marine reptiles through the Cretaceous-Tertiary boundary. *Journal of Vertebrate Paleontology* **28**(2): 409-421.

Jouve, S., Iarochene, M., Bouya, B. and Amaghzaz, M. (2005). A new dyrosaurid crocodyliform from the Palaeocene of Morocco and a phylogenetic analysis of Dyrosauridae. *Acta Palaeontologica Polonica* **50**(3): 581.

Joyce, W. G. (2007). Phylogenetic relationships of Mesozoic turtles. *Bulletin of the Peabody Museum of Natural History* **48**(1): 3-102.

Joyce, W. G., Chapman, S. D., Moody, R. T. and Walker, C. A. (2011). The skull of the solemydid turtle *Helochelydra nopcsai* from the Early Cretaceous of the Isle of Wight (UK) and a review of Solemydidae. *Special Papers in Palaeontology* **86**: 75-97.

Joyce, W. G., Parham, J. F. and Gauthier, J. A. (2004). Developing a protocol for the conversion of rank-based taxon names to phylogenetically defined clade names, as exemplified by turtles. *Journal of Paleontology* **78**(5): 989-1013.

Kaiho, K., Kajiwara, Y., Nakano, T., Miura, Y., Kawahata, H., Tazaki, K., Ueshima, M., Chen, Z. and Shi, G. R. (2001). End-Permian catastrophe by a bolide impact: evidence of a gigantic release of sulfur from the mantle. *Geology* **29**(9): 815-818.

Kakizaki, Y., Weissert, H., Hasegawa, T., Ishikawa, T., Matsuoka, J. and Kano, A. (2013). Strontium and carbon isotope stratigraphy of the Late Jurassic shallow marine limestone in western Palaeo-Pacific, northwest Borneo. *Journal of Asian Earth Sciences* **73**: 57-67.

Kälin, J. A. (1955). Crocodilia. *Traite de Palaeontologie*. J. Piveteau. Paris, Masson et Cie. **5:** 695-784.

Kaminski, M. A., Gradstein, F. M. and Geroch, S. (1992). Uppermost Jurassic to Lower Cretaceous benthic foraminiferal biostratigraphy at ODP Site 765 on the Argo Abyssal Plain. *Proceedings of the Ocean Drilling Program: Scientific Results* **123**: 239-269.

Kaminski, M. A., Setoyama, E. and Cetean, C. G. (2010). The Phanerozoic diversity of agglutinated foraminifera: origination and extinction rates. *Acta Palaeontologica Polonica* **55**(3): 529-539.

Kampschulte, A. and Strauss, H. (2004). The sulfur isotopic evolution of Phanerozoic seawater based on the analysis of structurally substituted sulfate in carbonates. *Chemical Geology* **204**(3): 255-286.

Karl, H.-V., Gröning, E., Brauckmann, C., Schwarz, D. and Knötschke, N. (2006). The Late Jurassic crocodiles of the Langenberg near Oker, Lower Saxony (Germany), and description of related materials (with remarks on the history of quarrying the "Langenberg Limestone" and "Obernkirchen Sandstone"). *Clausthaler Geowissenschaften* **5**: 59-77.

Karr, J. A. and Clapham, M. E. (2015). Taphonomic biases in the insect fossil record: shifts in articulation over geologic time. *Paleobiology* **41**(01): 16-32.

Kauffman, E. G. (1973). Cretaceous Bivalvia. *Atlas of Palaeobiogeography*. A. Hallam. Amsterdam, Elsevier**:** 353-383.

Kellner, A. W. A., Campos, D. A., Riff, D. and De Andrade, M. B. (2011). A new crocodylomorph (Sphagesauridae, Notosuchia) with horn-like tubercles from Brazil. *Zoological Journal of the Linnean Society* **163**: S57-S65.

Kessels, K., Mutterlose, J. and Ruffell, A. (2003). Calcareous nannofossils from late Jurassic sediments of the Volga Basin (Russian Platform): evidence for productivity-controlled black shale deposition. *International Journal of Earth Sciences* **92**(5): 743-757.

Ketchum, H. F. and Benson, R. B. (2010). Global interrelationships of Plesiosauria (Reptilia, Sauropterygia) and the pivotal role of taxon sampling in determining the outcome of phylogenetic analyses. *Biological Reviews* **85**(2): 361-392.

Kielan-Jaworowska, Z., Cifelli, R. and Luo, Z. (2004). Mammals from the age of dinosaurs: structure, relationships, and paleobiology. New York, Columbia University Press.

Kiessling, W. (2002). Radiolarian diversity patterns in the latest Jurassic–earliest Cretaceous. *Palaeogeography, Palaeoclimatology, Palaeoecology* **187**(1): 179-206.

Kiessling, W. (2008). Sampling-standardized expansion and collapse of reef building in the Phanerozoic. *Fossil Record* **11**(1): 7-18.

Kiessling, W. (2009). Geologic and biologic controls on the evolution of reefs. *Annual Review of Ecology, Evolution, and Systematics* **40**: 173-192.

Kiessling, W. and Aberhan, M. (2007). Geographical distribution and extinction risk: lessons from Triassic–Jurassic marine benthic organisms. *Journal of Biogeography* **34**(9): 1473-1489.

Kiessling, W., Aberhan, M. and Villier, L. (2008). Phanerozoic trends in skeletal mineralogy driven by mass extinctions. *Nature Geoscience* **1**(8): 527-530.

Kirkland, J. I. (1994). Predation of dinosaur nests by terrestrial crocodilians. *Dinosaur eggs and babies*. K. Carpenter, K. Hirsch and J. Horner. Cambridge, Cambridge University Press**:** 124-133.

Klompmaker, A. A., Schweitzer, C. E., Feldmann, R. M. and Kowalewski, M. (2013). The influence of reefs on the rise of Mesozoic marine crustaceans. *Geology* **41**(11): 1179-1182.

Klug, S. and Kriwet, J. (2013). Node age estimations and the origin of angel sharks, Squatiniformes (Neoselachii, Squalomorphii). *Journal of Systematic Palaeontology* **11**(1): 91-110.

Knoll, F., Cuny, G., Mojon, P.-O., López-Antoñanzas, R. and Huguet, D. (2013). A new vertebrate-, ostracod-, and charophyte-bearing locality in the Middle Jurassic of the Grands Causses (southern France). *Proceedings of the Geologists' Association* **124**(3): 525-529.

Knoll, F. and López-Antoñanzas, R. (2014). The vertebrate fauna from the “stipite” layers of the Grands Causses (Middle Jurassic, France). *Frontiers in Ecology and Evolution* **2**: 48.

Kocsis, Á. T., Kiessling, W. and Pálfy, J. (2014). Radiolarian biodiversity dynamics through the Triassic and Jurassic: implications for proximate causes of the end-Triassic mass extinction. *Paleobiology* **40**(4): 625-639.

Koeberl, C., Armstrong, R. A. and Reimold, W. U. (1997). Morokweng, South Africa: A large impact structure of Jurassic-Cretaceous boundary age. *Geology* **25**(8): 731-734.

Konzhukova, E. (1954). Newly discovered crocodiles from Mongolia. *Trudy Paleontologicheskii Institut Akademia Nauk SSSR* **48**: 171-194.

Kosnik, M. A. and Kowalewski, M. (2016). Understanding modern extinctions in marine ecosystems: the role of palaeoecological data. *Biology Letters* **12**: 20150951.

Kotova, I. (1983). Palynological study of Upper Jurassic and Lower Cretaceous sediments, site 511, Deep Sea Drilling Project leg 71 (Falkland Plateau). *Initial Reports of the Deep Sea Drilling Project* **71**: 879-906.

Kowalewski, M., Kiessling, W., Aberhan, M., Fürsich, F. T., Scarponi, D., Wood, S. L. B. and Hoffmeister, A. P. (2006). Ecological, taxonomic, and taphonomic components of the post-Paleozoic increase in sample-level species diversity of marine benthos. *Paleobiology* **32**(4): 533-561.

Krassilo.Va (1973). Climatic Changes in Eastern Asia as Indicated by Fossil Floras .1. Early Cretaceous. *Palaeogeography, Palaeoclimatology, Palaeoecology* **13**(4): 261-273.

Krause, D. W., Hoffmann, S., Wible, J. R., Kirk, E. C., Schultz, J. A., von Koenigswald, W., Groenke, J. R., Rossie, J. B., O’Connor, P. M. and Seiffert, E. R. (2014). First cranial remains of a gondwanatherian mammal reveal remarkable mosaicism. *Nature* **515**(7528): 512-517.

Kristensen, N. and Skalski, A. (1998). Palaeontology and phylogeny. *Lepidoptera, Moths and Butterflies. Volume 1: Evolution, Systematics, and Biogeography*. M. Fischer. Berlin, Germany, Walter de Gruyter. **1:** 7-25.

Kriwet, J. (2003). Neoselachian remains (Chondrichthyes, Elasmobranchii) from the Middle Jurassic of SW Germany and NW Poland. *Acta Palaeontologica Polonica* **48**(4): 583-594.

Kriwet, J., Kiessling, W. and Klug, S. (2009a). Diversification trajectories and evolutionary life-history traits in early sharks and batoids. *Proceedings of the Royal Society of London Series B: Biological Sciences* **276**(1658): 945-951.

Kriwet, J. and Klug, S. (2008). Diversity and biogeography patterns of Late Jurassic neoselachians (Chondrichthyes: Elasmobranchii). *Fishes and the Break-up of Pangaea*. L. Cavin, A. Longbottom and M. Richer. London, Geological Society of London. **295:** 55-70.

Kriwet, J., Nunn, E. V. and Klug, S. (2009b). Neoselachians (Chondrichthyes, Elasmobranchii) from the Lower and lower Upper Cretaceous of north‐eastern Spain. *Zoological Journal of the Linnean Society* **155**(2): 316-347.

Kriwet, J., Rauhut, O. W. and Gloy, U. (1997). Microvertebrate remains (Pisces, Archosauria) from the Middle Jurassic (Bathonian) of southern France. *Neues Jahrbuch für Geologie und Paläontologie - Abhandlungen* **206**(1): 1-28.

Krobicki, M. and Zatoń, M. (2008). Middle and Late Jurassic roots of brachyuran crabs: palaeoenvironmental distribution during their early evolution. *Palaeogeography, Palaeoclimatology, Palaeoecology* **263**(1): 30-43.

Kroh, A. and Smith, A. B. (2010). The phylogeny and classification of post-Palaeozoic echinoids. *Journal of Systematic Palaeontology* **8**(2): 147-212.

Ksepka, D. T., Gao, K.-Q. and Norell, M. A. (2005). A new choristodere from the Cretaceous of Mongolia. *American Museum Novitates* **3468**: 1-22.

Kudielka, G., Koeberl, C., Montanari, A., Newton, J. and Reimold, W. U. (2002). Stable-isotope and trace element stratigraphy of the Jurassic/Cretaceous boundary, Bosso River Gorge, Italy. *Geological and Biological Effects of Impact Events*. E. Buffetaut and C. Koeberl, Springer Berlin Heidelberg**:** 25-68.

Kuhn, O. (1960). Die familien der fossilen amphibien und reptilian. *Berichte der Naturforschenden Gesellschaft Bamberg* **37**: 20-52.

Kuhn, O. (1961). Die Tierwelt des Solnhofener Schiefers. Wittenberg, Ziemsen.

Kuhn, O. (1966). Die Tierwelt des Solnhofer Schiefers. *Auflage Neue Brehmbücherei* **40S**: 144.

Kuhn, O. (1971). Die Tierwelt des Solnhofener Schiefers, Ziemsen.

Kuhn, O. (1977). Die Tierwelt des Solnhofener Schiefers. Wittenberg Lutherstadt, Ziemsen Verlag.

Kujau, A., Heimhofer, U., Ostertag-Henning, C., Gréselle, B. and Mutterlose, J. (2012). No evidence for anoxia during the Valanginian carbon isotope event—an organic-geochemical study from the Vocontian Basin, SE France. *Global and Planetary Change* **92**: 92-104.

Kusuhashi, N., Matsumoto, A., Murakami, M., Tagami, T., Hirata, T., Iizuka, T., Handa, T. and Matsuoka, H. (2006). Zircon U–Pb ages from tuff beds of the upper Mesozoic Tetori Group in the Shokawa district, Gifu Prefecture, central Japan. *Island Arc* **15**(3): 378-390.

Labandeira, C. C. (2005). The fossil record of insect extinction: new approaches and future directions. *American Entomologist* **51**(1): 14-29.

Labandeira, C. C. and Currano, E. D. (2013). The fossil record of plant-insect dynamics. *Annual Review of Earth and Planetary Sciences* **41**: 287-311.

Labandeira, C. C. and Eble, G. J. (2000). The fossil record of insect diversity and disparity. *Gondwana Alive: Biodiversity and the Evolving Biosphere* J. Anderson, F. Thackeray, B. V. Wyk and M. D. Wit. Johanesburg, Witwaterstrand University Press**:** 55.

Labandeira, C. C. and Sepkoski, J. J. (1993). Insect diversity in the fossil record. *Science* **261**(5119): 310-315.

Lane, A., Janis, C. M. and Sepkoski, J. J. (2005). Estimating paleodiversities: a test of the taxic and phylogenetic methods. *Paleobiology* **31**(1): 21-34.

Langston Jr, W. (1974). Nonmammalian comanchean tetrapods. *Geoscience and Man* **8**: 77-102.

Larsson, H. C. and Gado, B. (2000). A new Early Cretaceous crocodyliform from Niger. *Neues Jahrbuch fur Geologie und Palaontologie-Abhandlungen* **217**(1): 131-142.

Larsson, H. C. and Sues, H. D. (2007). Cranial osteology and phylogenetic relationships of *Hamadasuchus rebouli* (Crocodyliformes: Mesoeucrocodylia) from the Cretaceous of Morocco. *Zoological Journal of the Linnean Society* **149**(4): 533-567.

Lauprasert, K., Cuny, G., Thirakhupt, K. and Suteethorn, V. (2009). *Khoratosuchus jintasakuli* gen. *et* sp. *nov*., an advanced neosuchian crocodyliform from the Early Cretaceous (Aptian-Albian) of NE Thailand. *Late Palaeozoic and Mesozoic Ecosystems in SE Asia*. E. Buffetaut, G. Cuny, J. Le Loeuff and V. Suteethorn. London, Geological Society of London. **315:** 175-187.

Lauprasert, K., Laojumpon, C., Saenphala, W., Cuny, G., Thirakhupt, K. and Suteethorn, V. (2011). Atoposaurid crocodyliforms from the Khorat Group of Thailand: first record of *Theriosuchus* from Southeast Asia. *Paläontologische Zeitschrift* **85**(1): 37-47.

Laurenti, J. N. (1768). Specimen medicum, exhibens synopsin reptilium emendatam cum experimentis circa venena et antidota reptilium austracorum, quod authoritate et consensu. Vienna, Joan Thomae.

Leardi, J. M., Fiorelli, L. E. and Gasparini, Z. (2015). Redescription and reevaluation of the taxonomical status of *Microsuchus schilleri* (Crocodyliformes: Mesoeucrocodylia) from the Upper Cretaceous of Neuquén, Argentina. *Cretaceous Research* **52**: 153-166.

Leardi, J. M., Pol, D. and Fernández, M. S. (2012). The antorbital fenestra of Metriorhynchidae (Crocodyliformes, Thalattosuchia): testing its homology within a phylogenetic framework. *Journal of Vertebrate Paleontology* **32**(2): 490-494.

Lee, M. S., Cau, A., Naish, D. and Dyke, G. J. (2014). Morphological clocks in paleontology, and a mid-Cretaceous origin of crown Aves. *Systematic Biology* **63**(3): 442-449.

Lee, Y.-N. (1997). The Archosauria from the Woodbine Formation (Cenomanian) in Texas. *Journal of Paleontology* **71**(6): 1147-1156.

Leinfelder, R. R. (1993). Upper Jurassic reef types and controlling factors. A preliminary report. *Profil* **5**: 1-45.

Leinfelder, R. R. (2001). Jurassic reef ecosystems. *The History and Sedimentology of ancient Reef Systems*. S. J. G. D., Springer US. **17:** 251-309.

Lewis, P. O. (2001). A likelihood approach to estimating phylogeny from discrete morphological character data. *Systematic Biology* **50**(6): 913-925.

Li, J. (1993). A new specimen of *Peipehsuchus teleorhinus* from Ziliujing formation of Daxian, Sichuan. *Vertebrata PalAsiatica* **31**: 92-97.

Li, J., Peng, J. and Batten, D. J. (2013). Palynostratigraphy of a Jurassic–Cretaceous transitional succession in the Himalayan Tethys, southern Xizang (Tibet), China. *Cretaceous Research* **46**: 123-135.

Li, P.-P., Gao, K.-Q., Hou, L.-H. and Xu, X. (2007). A gliding lizard from the Early Cretaceous of China. *Proceedings of the National Academy of Sciences of the United States of America* **104**(13): 5507-5509.

Liow, L. H. (2007). Lineages with long durations are old and morphologically average: An analysis using multiple datasets. *Evolution* **61**(4): 885-901.

Liow, L. H. (2013). Simultaneous estimation of occupancy and detection probabilities: an illustration using Cincinnatian brachiopods. *Paleobiology* **39**(2): 193-213.

Liow, L. H. and Finarelli, J. A. (2014). A dynamic global equilibrium in carnivoran diversification over 20 million years. *Proceedings of the Royal Society of London Series B: Biological Sciences* **281**(1778): 20132312.

Liow, L. H., Fortelius, M., Bingham, E., Lintulaakso, K., Mannila, H., Flynn, L. and Stenseth, N. C. (2008). Higher origination and extinction rates in larger mammals. *Proceedings of the National Academy of Sciences of the United States of America* **105**(16): 6097-6102.

Liow, L. H. and Nichols, J. D. (2010). Estimating rates and probabilities of origination and extinctionusing taxonomic occurrence data: capture-mark-recapture (CMR) approaches. *Quantitative Methods in Paleobiology*. J. Alroy and G. Hunt, The Paleontological Society**:** 81-94.

Liow, L. H. and Stenseth, N. C. (2007). The rise and fall of species: implications for macroevolutionary and macroecological studies. *Proceedings of the Royal Society of London B: Biological Sciences* **274**(1626): 2745-2752.

Lipinski, M., Warning, B. and Brumsack, H.-J. (2003). Trace metal signatures of Jurassic/Cretaceous black shales from the Norwegian Shelf and the Barents Sea. *Palaeogeography, Palaeoclimatology, Palaeoecology* **190**: 459-475.

Lipka, T. R., Therrien, F., Weishampel, D. B., Jamniczky, H. A., Joyce, W. G., Colbert, M. W. and Brinkman, D. B. (2006). A new turtle from the Arundel Clay facies (Potomac Formation, Early Cretaceous) of Maryland, USA. *Journal of Vertebrate Paleontology* **26**(2): 300-307.

Littler, K., Robinson, S. A., Bown, P. R., Nederbragt, A. J. and Pancost, R. D. (2011). High sea-surface temperatures during the Early Cretaceous Epoch. *Nature Geoscience* **4**(3): 169-172.

Liu, Y.-Q., Kuang, H.-W., Jiang, X.-J., Peng, N., Xu, H. and Sun, H.-Y. (2012). Timing of the earliest known feathered dinosaurs and transitional pterosaurs older than the Jehol Biota. *Palaeogeography, Palaeoclimatology, Palaeoecology* **323**: 1-12.

Lloyd, G. T. (2012). A refined modelling approach to assess the influence of sampling on palaeobiodiversity curves: new support for declining Cretaceous dinosaur richness. *Biology Letters* **8**(1): 123-126.

Lloyd, G. T. (2016). Estimating morphological diversity and tempo with discrete character-taxon matrices: implementation, challenges, progress, and future directions. *Biological Journal of the Linnean Society* **118**: 131-151.

Lloyd, G. T., Davis, K. E., Pisani, D., Tarver, J. E., Ruta, M., Sakamoto, M., Hone, D. W. E., Jennings, R. and Benton, M. J. (2008). Dinosaurs and the Cretaceous Terrestrial Revolution. *Proceedings of the Royal Society of London Series B: Biological Sciences* **275**(1650): 2483-2490.

Lloyd, G. T. and Friedman, M. (2013). A survey of palaeontological sampling biases in fishes based on the Phanerozoic record of Great Britain. *Palaeogeography, Palaeoclimatology, Palaeoecology* **372**: 5-17.

Lloyd, G. T., Young, J. R. and Smith, A. B. (2012). Comparative quality and fidelity of deep-sea and land-based nannofossil records. *Geology* **40**(2): 155-158.

Longrich, N. R., Vinther, J., Pyron, R. A., Pisani, D. and Gauthier, J. A. (2015). Biogeography of worm lizards (Amphisbaenia) driven by end-Cretaceous mass extinction. *Proceedings of the Royal Society of London Series B: Biological Sciences* **282**(1806): 20143034.

Lortet, L. (1892). Les Reptiles fossiles du bassin du Rhone. *Archives du Muséum d'Histoire naturelle de Lyon*: 3-139.

Lu, P. J., Yogo, M. and Marshall, C. R. (2006). Phanerozoic marine biodiversity dynamics in light of the incompleteness of the fossil record. *Proceedings of the National Academy of Sciences of the United States of America* **103**(8): 2736-2739.

Lucas, S. G. and Estep, J. W. (1998). Vertebrate biostratigraphy and biochronology of the Cretaceous of China. *New Mexico Museum of Natural History and Science Bulletin* **14**: 1-20.

Lukeneder, A., Halásová, E., Kroh, A., Mayrhofer, S., Pruner, P., Reháková, D., Schnabl, P., Sprovieri, M. and Wagreich, M. (2010). High resolution stratigraphy of the Jurassic-Cretaceous boundary interval in the Gresten Klippenbelt (Austria). *Geologica Carpathica* **61**(5): 365-381.

Luo, Z.-X. (2007). Transformation and diversification in early mammal evolution. *Nature* **450**(7172): 1011-1019.

Luo, Z.-X., Ji, Q., Wible, J. R. and Yuan, C.-X. (2003). An Early Cretaceous tribosphenic mammal and metatherian evolution. *Science* **302**(5652): 1934-1940.

Luo, Z.-X. and Wible, J. R. (2005). A Late Jurassic digging mammal and early mammalian diversification. *Science* **308**(5718): 103-107.

Luo, Z.-X., Yuan, C.-X., Meng, Q.-J. and Ji, Q. (2011). A Jurassic eutherian mammal and divergence of marsupials and placentals. *Nature* **476**(7361): 442-445.

Luque, J. (2015). The oldest higher true crabs (Crustacea: Decapoda: Brachyura): insights from the Early Cretaceous of the Americas. *Palaeontology* **58**(2): 251-263.

Mahoney, J., Duncan, R., Tejada, M., Sager, W. and Bralower, T. (2005). Jurassic-Cretaceous boundary age and mid-ocean-ridge–type mantle source for Shatsky Rise. *Geology* **33**(3): 185-188.

Maidment, S. C., Norman, D. B., Barrett, P. M. and Upchurch, P. (2008). Systematics and phylogeny of Stegosauria (Dinosauria: Ornithischia). *Journal of Systematic Palaeontology* **6**(04): 367-407.

Maier, W. D., Andreoli, M., McDonald, I., Higgins, M., Boyce, A., Shukolyukov, A., Lugmair, G., Ashwal, L., Gräser, P. and Ripley, E. (2006). Discovery of a 25-cm asteroid clast in the giant Morokweng impact crater, South Africa. *Nature* **441**(7090): 203-206.

Maluski, H., Coulon, C., Popoff, M. and Baudin, P. (1995). $^{40}Ar/^{39}Ar$ chronology, petrology and geodynamic setting of Mesozoic to early Cenozoic magmatism from the Benue Trough, Nigeria. *Journal of the Geological Society* **152**(2): 311-326.

Manabe, M. and Hasegawa, Y. (1998). A Crocodile from the Early Jurassic Toyora Group, Yamaguchi, Japan. *Memoirs of the National Science Museum, Tokyo* **31**: 73-77.

Mannion, P. D. and Barrett, P. M. (2013). Additions to the sauropod dinosaur fauna of the Cenomanian (early Late Cretaceous) Kem Kem beds of Morocco: Palaeobiogeographical implications of the mid-Cretaceous African sauropod fossil record. *Cretaceous Research* **45**: 49-59.

Mannion, P. D., Benson, R. B., Upchurch, P., Butler, R. J., Carrano, M. T. and Barrett, P. M. (2012). A temperate palaeodiversity peak in Mesozoic dinosaurs and evidence for Late Cretaceous geographical partitioning. *Global Ecology and Biogeography* **21**(9): 898-908.

Mannion, P. D., Benson, R. B. J., Carrano, M. T., Tennant, J. P., Judd, J. and Butler, R. J. (2015). Climate constrains the evolutionary history and biodiversity of crocodylians. *Nature Communications* **6**: 8438.

Mannion, P. D. and Upchurch, P. (2010a). Completeness metrics and the quality of the sauropodomorph fossil record through geological and historical time. *Paleobiology* **36**(2): 283-302.

Mannion, P. D. and Upchurch, P. (2010b). A quantitative analysis of environmental associations in sauropod dinosaurs. *Paleobiology* **36**(2): 253-282.

Mannion, P. D. and Upchurch, P. (2011). A re-evaluation of the 'mid-Cretaceous sauropod hiatus' and the impact of uneven sampling of the fossil record on patterns of regional dinosaur extinction. *Palaeogeography, Palaeoclimatology, Palaeoecology* **299**(3): 529-540.

Mannion, P. D., Upchurch, P., Barnes, R. N. and Mateus, O. (2013). Osteology of the Late Jurassic Portuguese sauropod dinosaur *Lusotitan atalaiensis* (Macronaria) and the evolutionary history of basal titanosauriforms. *Zoological Journal of the Linnean Society* **168**(1): 98-206.

Mannion, P. D., Upchurch, P., Benson, R. B. and Goswami, A. (2014). The latitudinal biodiversity gradient through deep time. *Trends in Ecology & Evolution* **29**(1): 42-50.

Mannion, P. D., Upchurch, P., Carrano, M. T. and Barrett, P. M. (2011). Testing the effect of the rock record on diversity: a multidisciplinary approach to elucidating the generic richness of sauropodomorph dinosaurs through time. *Biological Reviews* **86**(1): 157-181.

Marinho, T. S. and Carvalho, I. S. (2009). An armadillo-like sphagesaurid crocodyliform from the Late Cretaceous of Brazil. *Journal of South American Earth Sciences* **27**(1): 36-41.

Marioni, B., Da Silveira, R., Magnusson, W. E. and Thorbjarnarson, J. (2008). Feeding behavior of two sympatric caiman species, *Melanosuchus niger* and *Caiman crocodilus*, in the Brazilian Amazon. *Journal of Herpetology* **42**(4): 768-772.

Marjanovic, D. and Laurin, M. (2013). The origin(s) of extant amphibians: a review with emphasis on the "lepospondyl hypothesis". *Geodiversitas* **35**(1): 207-272.

Marjanović, D. and Laurin, M. (2007). Fossils, molecules, divergence times, and the origin of lissamphibians. *Systematic Biology* **56**(3): 369-388.

Markov, A., Bondarev, A. and Vinarsky, M. (2012). Diversity dynamics of echinoderms and evolution of marine communities. *Paleontological Journal* **46**(8): 865-876.

Markwick, P. J. (1998). Crocodilian diversity in space and time: the role of climate in paleoecology and its implication for understanding K/T extinctions. *Paleobiology* **24**(4): 470-497.

Marpmann, J. S., Carballido, J. L., Sander, P. M. and Knötschke, N. (2015). Cranial anatomy of the Late Jurassic dwarf sauropod *Europasaurus holgeri* (Dinosauria, Camarasauromorpha): ontogenetic changes and size dimorphism. *Journal of Systematic Palaeontology* **13**(3): 221-263.

Marshall, C. R. and Quental, T. B. (2016). The uncertain role of diversity dependence in species diversification and the need to incorporate time-varying carrying capacities. *Philosophical Transactions of the Royal Society B: Biological Sciences* **371**(1691): 20150217.

Martill, D. M., Tischlinger, H. and Longrich, N. R. (2015). A four-legged snake from the Early Cretaceous of Gondwana. *Science* **349**(6246): 416-419.

Martín-Closas, C., Sames, B. and Schudack, M. E. (2013). Charophytes from the upper Berriasian of the Western Interior Basin of the United States. *Cretaceous Research* **46**: 11-23.

Martin-Garin, B., Lathuilière, B. and Geister, J. (2012). The shifting biogeography of reef corals during the Oxfordian (Late Jurassic). A climatic control? *Palaeogeography, Palaeoclimatology, Palaeoecology* **365**: 136-153.

Martin, J. E. (2007). New material of the Late Cretaceous globidontan *Acynodon iberoccitanus* (Crocodylia) from southern France. *Journal of Vertebrate Paleontology* **27**(2): 362-372.

Martin, J. E., Amiot, R., Lecuyer, C. and Benton, M. J. (2014a). Sea surface temperature contributes to marine crocodylomorph evolution. *Nature Communications* **5**: 4658.

Martin, J. E. and Buffetaut, E. (2008). *Crocodilus affuvelensis* Matheron, 1869 from the Late Cretaceous of southern France: a reassessment. *Zoological Journal of the Linnean Society* **152**(3): 567-580.

Martin, J. E., Csiki, Z., Grigorescu, D. and Buffetaut, E. (2006). Late Cretaceous crocodilian diversity in Haţeg Basin, Romania. *Hantkeniana* **5**: 31-37.

Martin, J. E., Deesri, U., Liard, R., Wattanapituksakul, A., Suteethorn, S., Lauprasert, K., Tong, H., Buffetaut, E., Suteethorn, V. and Suan, G. (2015a). Strontium isotopes and the long-term residency of thalattosuchians in the freshwater environment. *Paleobiology*: 1-14.

Martin, J. E. and Delfino, M. (2010). Recent advances in the comprehension of the biogeography of Cretaceous European eusuchians. *Palaeogeography, Palaeoclimatology, Palaeoecology* **293**(3): 406-418.

Martin, J. E., Lauprasert, K., Buffetaut, E., Liard, R. and Suteethorn, V. (2014b). A large pholidosaurid in the Phu Kradung Formation of north‐eastern Thailand. *Palaeontology* **57**(4): 757-769.

Martin, J. E., Rabi, M., Csiki-Sava, Z. and Vasile, S. (2014c). Cranial morphology of *Theriosuchus sympiestodon* (Mesoeucrocodylia, Atoposauridae) and the widespread occurrence of *Theriosuchus* in the Late Cretaceous of Europe. *Journal of Paleontology* **88**(3): 444-456.

Martin, J. E., Rabi, M. and Csiki, Z. (2010). Survival of *Theriosuchus* (Mesoeucrocodylia: Atoposauridae) in a Late Cretaceous archipelago: a new species from the Maastrichtian of Romania. *Naturwissenschaften* **97**(9): 845-854.

Martin, J. E., Vincent, P. and Falconnet, J. (2015b). The taxonomic content of *Machimosaurus* (Crocodylomorpha, Thalattosuchia). *Comptes Rendus Palevol* **14**(4): 305-310.

Martinelli, A. G. (2003). New cranial remains of the bizarre notosuchid *Comahuesuchus brachybuccalis* (Archosauria, Crocodyliformes) from the Late Cretaceous of Río Negro Province (Argentina). *Ameghiniana* **40**(4): 559-572.

Martinelli, A. G., Sertich, J. J., Garrido, A. C. and Praderio, Á. M. (2012). A new peirosaurid from the Upper Cretaceous of Argentina: Implications for specimens referred to *Peirosaurus torminni* Price (Crocodyliformes: Peirosauridae). *Cretaceous Research* **37**: 191-200.

Martinez, M., Deconinck, J.-F., Pellenard, P., Reboulet, S. and Riquier, L. (2013). Astrochronology of the Valanginian Stage from reference sections (Vocontian Basin, France) and palaeoenvironmental implications for the Weissert Event. *Palaeogeography, Palaeoclimatology, Palaeoecology* **376**: 91-102.

Martinez, M., Deconinck, J.-F., Pellenard, P., Riquier, L., Company, M., Reboulet, S. and Moiroud, M. (2015). Astrochronology of the Valanginian–Hauterivian stages (Early Cretaceous): Chronological relationships between the Paraná–Etendeka large igneous province and the Weissert and the Faraoni events. *Global and Planetary Change* **131**: 158-173.

Martinez, M. and Dera, G. (2015). Orbital pacing of carbon fluxes by a ∼9-My eccentricity cycle during the Mesozoic. *Proceedings of the National Academy of Sciences of the United States of America* **112**(41): 12604-12609.

Matsukawa, M., Ito, M., Nishida, N., Koarai, K., Lockley, M. G. and Nichols, D. J. (2006). The Cretaceous Tetori biota in Japan and its evolutionary significance for terrestrial ecosystems in Asia. *Cretaceous Research* **27**(2): 199-225.

Matsumoto, R. and Evans, S. (2010). Choristoderes and the freshwater assemblages of Laurasia. *Journal of Iberian Geology* **36**(2): 253-274.

Matsumoto, R., Manabe, M. and Evans, S. E. (2015). The first record of a long-snouted choristodere (Reptilia, Diapsida) from the Early Cretaceous of Ishikawa Prefecture, Japan. *Historical Biology* **27**(5): 583-594.

Matsumoto, R., Suzuki, S., Tsogtbaatar, K. and Evans, S. E. (2009). New material of the enigmatic reptile *Khurendukhosaurus* (Diapsida: Choristodera) from Mongolia. *Naturwissenschaften* **96**(2): 233-242.

Matsuoka, A. (1992). Jurassic and Early Cretaceous radiolarians from Leg 129, Sites 800 and 801, western Pacific Ocean. *Proceedings of the Ocean Drilling Program, Scientific Results* **129**: 203-220.

Mattioli, E., Pittet, B., Riquier, L. and Grossi, V. (2014). The mid-Valanginian Weissert Event as recorded by calcareous nannoplankton in the Vocontian Basin. *Palaeogeography Palaeoclimatology Palaeoecology* **414**: 472-485.

Mayhew, P. J., Bell, M. A., Benton, T. G. and McGowan, A. J. (2012). Biodiversity tracks temperature over time. *Proceedings of the National Academy of Sciences of the United States of America* **109**(38): 15141-15145.

Mayr, G. (2014). The origins of crown group birds: molecules and fossils. *Palaeontology* **57**(2): 231-242.

McAnena, A., Flögel, S., Hofmann, P., Herrle, J., Griesand, A., Pross, J., Talbot, H., Rethemeyer, J., Wallmann, K. and Wagner, T. (2013). Atlantic cooling associated with a marine biotic crisis during the mid-Cretaceous period. *Nature Geoscience* **6**(7): 558-561.

McArthur, J., Howarth, R. and Bailey, T. (2001). Strontium isotope stratigraphy: LOWESS version 3: best fit to the marine Sr‐isotope curve for 0‐509 Ma and accompanying look‐up table for deriving numerical age. *The Journal of Geology* **109**(2): 155-170.

McDonald, I., Andreoli, M., Hart, R. and Tredoux, M. (2001). Platinum-group elements in the Morokweng impact structure, South Africa: Evidence for the impact of a large ordinary chondrite projectile at the Jurassic-Cretaceous boundary. *Geochimica et Cosmochimica Acta* **65**(2): 299-309.

McDonald, I., Irvine, G. J., de Vos, E., Gale, A. S. and Reimold, W. U. (2006). Geochemical search for impact signatures in possible impact-generated units associated with the Jurassic-Cretaceous Boundary in southern England and northern France. *Biological Processes Associated with Impact Events*. C. Cockell, I. Gilmour and C. Koeberl, Springer Berlin Heidelberg**:** 257-286.

McElwain, J. C. and Punyasena, S. W. (2007). Mass extinction events and the plant fossil record. *Trends in Ecology and Evolution* **22**(10): 548-557.

McGhee, G. R., Sheehan, P. M., Bottjer, D. J. and Droser, M. L. (2004). Ecological ranking of Phanerozoic biodiversity crises: ecological and taxonomic severities are decoupled. *Palaeogeography, Palaeoclimatology, Palaeoecology* **211**(3): 289-297.

McGhee, G. R., Sheehan, P. M., Bottjer, D. J. and Droser, M. L. (2012). Ecological ranking of Phanerozoic biodiversity crises: The Serpukhovian (early Carboniferous) crisis had a greater ecological impact than the end-Ordovician. *Geology* **40**(2): 147-150.

McGowan, A. J. and Smith, A. B. (2008). Are global Phanerozoic marine diversity curves truly global? A study of the relationship between regional rock records and global Phanerozoic marine diversity. *Paleobiology* **34**(1): 80-103.

McLoughlin, S. (2001). The breakup history of Gondwana and its impact on pre-Cenozoic floristic provincialism. *Australian Journal of Botany* **49**(3): 271-300.

McPhee, B. W., Mannion, P. D., de Klerk, W. J. and Choiniere, J. N. (2016). High diversity in the sauropod dinosaur fauna of the Lower Cretaceous Kirkwood Formation of South Africa: Implications for the Jurassic–Cretaceous transition. *Cretaceous Research* **59**: 228-248.

Melott, A. L. and Bambach, R. K. (2011). A ubiquitous ~62-Myr periodic fluctuation superimposed on general trends in fossil biodiversity. I. Documentation. *Paleobiology* **37**(1): 92-112.

Meyer, H. (1850). Mittheilungen an Professor Bronn gerichtet. *Neues Jahrbuch für Mineralogie, Geognosie, Geologie und Petrefaktenkunde*: 195-204.

Meyer, H. (1851). Description de l'*Atoposaurus jourdani* et du *Sapheosaurus thiollierei*, reptiles fossiles des calcaires lithographiques du Bugey. Annales des Sciences Physiques et Naturelles, d'Agriculture et d'Industrie.

Meyers, P. A. (2014). Why are the δ_{13}Corg values in Phanerozoic black shales more negative than in modern marine organic matter? *Geochemistry, Geophysics, Geosystems* **15**(7): 3085-3106.

Michalík, J. and Reháková, D. (2011). Possible markers of the Jurassic/Cretaceous boundary in the Mediterranean Tethys: A review and state of art. *Geoscience Frontiers* **2**(4): 475-490.

Michalík, J., Reháková, D., Halásová, E. and Lintnerová, O. (2009). The Brodno section—a potential regional stratotype of the Jurassic/Cretaceous boundary (Western Carpathians). *Geologica Carpathica* **60**(3): 213-232.

Michard, J.-G., De Broin, F., Brunet, M. and Hell, J. (1990). Le plus ancien crocodilien néosuchien spécialisée à caractères eusuchiens du continent africain (Crétacé Inférieur Cameroun). *Comptes rendus de l'Académie des sciences. Série 2, Mécanique, Physique, Chimie, Sciences de l'univers, Sciences de la Terre* **311**(2): 365-371.

Milián ‐ García, Y., Venegas ‐ Anaya, M., Frias ‐ Soler, R., Crawford, A. J., Ramos ‐ Targarona, R., Rodríguez ‐ Soberón, R., Alonso ‐ Tabet, M., Thorbjarnarson, J., Sanjur, O. I. and Espinosa ‐ López, G. (2011). Evolutionary history of Cuban crocodiles *Crocodylus rhombifer* and *Crocodylus acutus* inferred from multilocus markers. *Journal of Experimental Zoology Part A: Ecological Genetics and Physiology* **315**(6): 358-375.

Miller, K. G., Kominz, M. A., Browning, J. V., Wright, J. D., Mountain, G. S., Katz, M. E., Sugarman, P. J., Cramer, B. S., Christie-Blick, N. and Pekar, S. F. (2005). The Phanerozoic record of global sea-level change. *Science* **310**(5752): 1293-1298.

Milton, D., Glikson, A., Manwaring, E., Moss, F., Sedmik, E., Van Son, J., Barlow, B., Brett, R. and Young, G. (1972). Gosses Bluff impact structure, Australia. *Science* **175**(4027): 1199-1207.

Milton, D. J. and Sutter, J. F. (1987). Revised age for the Gosses Bluff impact structure, Northern Territory, Australia, based on $^{40}Ar/^{39}Ar$ dating. *Meteoritics* **22**(3): 281-289.

Misof, B., Liu, S., Meusemann, K., Peters, R. S., Donath, A., Mayer, C., Frandsen, P. B., Ware, J., Flouri, T. and Beutel, R. G. (2014). Phylogenomics resolves the timing and pattern of insect evolution. *Science* **346**(6210): 763-767.

Misra, S., Mazumder, A., Andreoli, M. A. G. and Ray, D. (2014). Large meteorite impacts, volcanism and possible environmental disruption at the Jurassic-Cretaceous boundary. Lunar and Planetary Science Conference.

Mitchell, J. S. and Makovicky, P. J. (2014). Low ecological disparity in Early Cretaceous birds. *Proceedings of the Royal Society of London Series B: Biological Sciences* **281**(1787): 20140608.

Mizera, J., Řanda, Z. and Košťák, M. (2010). Neutron activation analysis in geochemical characterization of Jurassic–Cretaceous sedimentary rocks from the Nordvik Peninsula. *Journal of radioanalytical and nuclear chemistry* **284**(1): 211-219.

Mo, J., Buffetaut, E., Tong, H., Amiot, R., Cavin, L., Cuny, G., Suteethorn, V., Suteethorn, S. and Jiang, S. (2016). Early Cretaceous vertebrates from the Xinlong Formation of Guangxi (southern China): a review. *Geological Magazine* **153**(01): 143-159.

Mondal, S. and Harries, P. J. (2015). The effect of taxonomic corrections on Phanerozoic generic richness trends in marine bivalves with a discussion on the clade's overall history. *Paleobiology* **42**(1): 1-15.

Monger, J., Van Der Heyden, P., Journeay, J., Evenchick, C. and Mahoney, J. (1994). Jurassic-Cretaceous basins along the Canadian Coast Belt: Their bearing on pre-mid-Cretaceous sinistral displacements. *Geology* **22**(2): 175-178.

Montefeltro, F. C., Larsson, H. C., de França, M. A. and Langer, M. C. (2013). A new neosuchian with Asian affinities from the Jurassic of northeastern Brazil. *Naturwissenschaften* **100**(9): 835-841.

Montefeltro, F. C., Larsson, H. C. and Langer, M. C. (2011). A new baurusuchid (Crocodyliformes, Mesoeucrocodylia) from the Late Cretaceous of Brazil and the phylogeny of Baurusuchidae. *PLOS ONE* **6**(7): e21916.

Monteiro, L., Cavalcanti, M. and Sommer III, H. (1997). Comparative ontogenetic shape changes in the skull of *Caiman* species (Crocodylia, Alligatoridae). *Journal of morphology* **231**(1): 53-62.

Monteiro, L. R. and Soares, M. (1997). Allometric analysis of the ontogenetic variation and evolution of the skull in *Caiman* Spix, 1825 (Crocodylia: Alligatoridae). *Herpetologica* **53**(1): 62-69.

Mook, C. C. (1933). A crocodilian skeleton from the Morrison Formation at Canyon City, Colorado. *American Museum Novitates* **671**(Contributions to the Osteology, Affinities, and Distribution of the Crocodilia, 26): 1-8.

Mook, C. C. (1942). Skull characters of *Amphicotylus lucasii* Cope. *American Museum Novitates* **1165**: 1-8.

Müller, J. and Reisz, R. R. (2006). The phylogeny of early eureptiles: comparing parsimony and Bayesian approaches in the investigation of a basal fossil clade. *Systematic Biology* **55**(3): 503-511.

Na, L. and Kiessling, W. (2015). Diversity partitioning during the Cambrian radiation. *Proceedings of the National Academy of Sciences of the United States of America* **112**(15): 4702-4706.

Naafs, B., Castro, J., De Gea, G., Quijano, M., Schmidt, D. and Pancost, R. (2016). Gradual and sustained carbon dioxide release during Aptian Oceanic Anoxic Event 1a. *Nature Geoscience* **9**: 135-139.

Naimark, E. and Markov, A. (2011). Northward shift in faunal diversity: a general pattern of evolution of Phanerozoic marine biota. *Biology Bulletin Reviews* **1**(1): 71-81.

Naipauer, M., Tunik, M., Marques, J. C., Vera, E. A. R., Vujovich, G. I., Pimentel, M. M. and Ramos, V. A. (2015). U–Pb detrital zircon ages of Upper Jurassic continental successions: implications for the provenance and absolute age of the Jurassic–Cretaceous boundary in the Neuquén Basin. *Geodynamic Processes in the Andes of Central Chile and Argentina*. S. A. Sepúlveda, L. B. Giambiagi, S. M. Moreiras et al. London, Geological Society of London. **399:** 131-154.

Narváez, I., Brochu, C., Escaso, F., Pérez-García, A. and Ortega, F. (2016). New Spanish Late Cretaceous eusuchian reveals the synchronic and sympatric presence of two allodaposuchids. *Cretaceous Research*, 10.1016/j.cretres.2016.04.018.

Narváez, I., Brochu, C. A., Escaso, F., Pérez-García, A. and Ortega, F. (2015). New crocodyliforms from southwestern Europe and definition of a diverse clade of European Late Cretaceous basal eusuchians. *PLOS ONE* **10**(11): e0140679.

Nascimento, P. M. and Zaher, H. (2011). The skull of the Upper Cretaceous baurusuchid crocodile *Baurusuchus albertoi* Nascimento & Zaher 2010, and its phylogenetic affinities. *Zoological Journal of the Linnean Society* **163**(s1): S116-S131.

Nesbitt, S. J. (2011). The early evolution of archosaurs: Relationships and the origin of major clades. *Bulletin of the American Museum of Natural History* **352**: 1-288.

Newell, N. D. (1952). Periodicity in invertebrate evolution. *Journal of Paleontology* **26**(3): 371-385.

Newell, N. D. (1963). Crises in the history of life. *Scientific American* **208**: 76-93.

Newell, N. D. (1967). Revolutions in the history of life. *Geological Society of America Special Papers* **89**: 63-92.

Newham, E., Benson, R., Upchurch, P. and Goswami, A. (2014). Mesozoic mammaliaform diversity: The effect of sampling corrections on reconstructions of evolutionary dynamics. *Palaeogeography, Palaeoclimatology, Palaeoecology* **412**: 32-44.

Nichols, J. D. and Pollock, K. H. (1983). Estimating taxonomic diversity, extinction rates, and speciation rates from fossil data using capture-recapture models. *Paleobiology* **9**(2): 150-163.

Nicholson, D. B., Holroyd, P. A., Benson, R. B. and Barrett, P. M. (2015). Climate-mediated diversification of turtles in the Cretaceous. *Nature Communications* **6**(7848): 1-8.

Nicholson, D. B., Ross, A. J. and Mayhew, P. J. (2014). Fossil evidence for key innovations in the evolution of insect diversity. *Proceedings of the Royal Society of London Series B: Biological Sciences* **281**(1793): 20141823.

Niklas, K. J. (1988). Patterns of vascular plant diversification in the fossil record: proof and conjecture. *Annals of the Missouri Botanical Garden* **75**(1): 35-54.

Niklas, K. J. and Tiffney, B. H. (1994). The quantification of plant biodiversity through time. *Philosophical Transactions of the Royal Society B: Biological Sciences* **345**(1311): 35-44.

Nobre, P. H., Carvalho, I. D., de Vasconcellos, F. M. and Souto, P. R. (2008). Feeding behavior of the gondwanic Crocodylomorpha *Mariliasuchus amarali* from the upper cretaceous Bauru Basin, Brazil. *Gondwana Research* **13**(1): 139-145.

Norell, M., Clark, J. M. and Hutchison, J. H. (1994). The Late Cretaceous alligatoroid *Brachychampsa montana* (Crocodylia): new material and putative relationships. *American Museum Novitates* **3116**: 1-26.

Norell, M. and Gao, K. (1997). Braincase and phylogenetic relationships of *Estesia mongoliensis* from the Late Cretaceous of the Gobi Desert and the recognition of a new clade of lizards. *American Museum Novitates* **3211**: 1-28.

Norell, M. A. (1988). Cladistic approaches to paleobiology as applied to the phylogeny of alligatorids. PhD, Yale University.

Norell, M. A. (1993). Tree-based approaches to understanding history - comments on ranks, rules, and the quality of the fossil record. *American Journal of Science* **293A**: 407-417.

Norell, M. A. and Clark, J. (1990). A reanalysis of *Bernissartia fagesii*, with comments on its phylogenetic position and its bearing on the origin and diagnosis of the Eusuchia. *Bulletin-Institut royal des sciences naturelles de Belgique. Sciences de la terre* **60**: 115-128.

Novas, F. E., Agnolín, F. L., Ezcurra, M. D., Porfiri, J. and Canale, J. I. (2013). Evolution of the carnivorous dinosaurs during the Cretaceous: the evidence from Patagonia. *Cretaceous Research* **45**: 174-215.

Novas, F. E., de Valais, S., Vickers-Rich, P. and Rich, T. (2005). A large Cretaceous theropod from Patagonia, Argentina, and the evolution of carcharodontosaurids. *Naturwissenschaften* **92**(5): 226-230.

Novas, F. E., Pais, D. F., Pol, D., Carvalho, I. D. S., Scanferla, A., Mones, A. and Riglos, M. S. (2009). Bizarre notosuchian crocodyliform with associated eggs from the Upper Cretaceous of Bolivia. *Journal of Vertebrate Paleontology* **29**(4): 1316-1320.

Novas, F. E., Salgado, L., Suarez, M., Agnolin, F. L., Ezcurra, M. D., Chimento, N. R., de la Cruz, R., Isasi, M. P., Vargas, A. O. and Rubilar-Rogers, D. (2015). An enigmatic plant-eating theropod from the Late Jurassic period of Chile. *Nature* **522**: 331-334.

Nürnberg, D. and Müller, R. D. (1991). The tectonic evolution of the South Atlantic from Late Jurassic to present. *Tectonophysics* **191**(1): 27-53.

Nydam, R. L. (2013). Squamates from the Jurassic and Cretaceous of North America. *Palaeobiodiversity and Palaeoenvironments* **93**(4): 535-565.

Nydam, R. L. and Cifelli, R. L. (2002). Lizards from the Lower Cretaceous (Aptian–Albian) Antlers and Cloverly Formations. *Journal of Vertebrate Paleontology* **22**(2): 286-298.

O'Dogherty, L., Carter, E. S., Dumitrica, P., Goriččan, Š., Wever, P. D., Bandini, A. N., Baumgartner, P. O. and Matsuoka, A. (2009). Catalogue of Mesozoic radiolarian genera. Part 2: Jurassic-Cretaceous. *Geodiversitas* **31**(2): 271-356.

O'Keefe, J. D. and Ahrens, T. J. (1989). Impact production of CO_2 by the Cretaceous/Tertiary extinction bolide and the resultant heating of the Earth. *Nature* **338**: 247-249.

O'Reilly, J. E., Puttick, M. N., Parry, L., Tanner, A. R., Tarver, J. E., Fleming, J., Pisani, D. and Donoghue, P. C. (2016). Bayesian methods outperform parsimony but at the expense of precision in the estimation of phylogeny from discrete morphological data. *Biology Letters* **12**(4): 20160081.

O'Connor, J., Chiappe, L. M. and Bell, A. (2011a). Pre-modern birds: avian divergences in the Mesozoic. *Living Dinosaurs: The Evolutionary History of Birds*. G. Dyke and G. Kaiser. Chichester, UK, J. Wiley & Sons. **3:** 39-114.

O'Connor, J. and Zhou, Z. (2015). Early evolution of the biological bird: perspectives from new fossil discoveries in China. *Journal of Ornithology* **156**(1): 333-342.

O'Connor, J. K., Zhou, Z. and Zhang, F. (2011b). A reappraisal of *Boluochia zhengi* (Aves: Enantiornithes) and a discussion of intraclade diversity in the Jehol avifauna, China. *Journal of Systematic Palaeontology* **9**(1): 51-63.

O'Connor, P. M., Sertich, J. J., Stevens, N. J., Roberts, E. M., Gottfried, M. D., Hieronymus, T. L., Jinnah, Z. A., Ridgely, R., Ngasala, S. E. and Temba, J. (2010). The evolution of mammal-like crocodyliforms in the Cretaceous Period of Gondwana. *Nature* **466**(7307): 748-751.

Ogg, J., Karl, S. and Behl, R. (1992). Jurassic through Early Cretaceous sedimentation history of the Central Equatorial Pacific and of Sites 800 and 801. *Proceedings of the Ocean Drilling Program, Scientific Results* **129**: 571-614.

Ogg, J. G., Hasenyager, R. W., Wimbledon, W. A., Channell, J. E. and Bralower, T. J. (1991). Magnetostratigraphy of the Jurassic-Cretaceous boundary interval—Tethyan and English faunal realms. *Cretaceous Research* **12**(5): 455-482.

Ogg, J. G. and Lowrie, W. (1986). Magnetostratigraphy of the Jurassic/Cretaceous boundary. *Geology* **14**(7): 547-550.

Olivier, N., Martin-Garin, B., Colombié, C., Cornée, J.-J., Giraud, F., Schnyder, J., Kabbachi, B. and Ezaidi, K. (2012). Ecological succession evidence in an Upper Jurassic coral reef system (Izwarn Section, High Atlas, Morocco). *Geobios* **45**(6): 555-572.

Oreska, M. P., Carrano, M. T. and Dzikiewicz, K. M. (2013). Vertebrate paleontology of the Cloverly Formation (Lower Cretaceous), I: faunal composition, biogeographic relationships, and sampling. *Journal of Vertebrate Paleontology* **33**(2): 264-292.

Ortega, F., Buscalioni, A. D. and Gasparini, Z. (1996a). Reinterpretation and new denomination of *Atacisaurus crassiproratus* (Middle Eocene; Issel, France) as cf. *Iberosuchus* (Crocodylomorpha, Metasuchia). *Geobios* **29**(3): 353-364.

Ortega, F., García, J. J. M., García, J. L. S., Buscalioni, Á. D., Valbuena, J. and Jiménez, S. (1996b). Sobre la presencia de un cocodrilo fósil (Crocodylomorpha: Neosuchia:" *Goniopholis*" sp.) en la Cuenca de Cameros (Cretácico inferior: Vadillos-San Román de Cameros, La Rioja). *Zubía* **14**: 113-120.

Ortega, F., Gasparini, Z., Buscalioni, A. and Calvo, J. (2000). A new species of *Araripesuchus* (Crocodylomorpha, Mesoeucrocodylia) from the Lower Cretaceous of Patagonia (Argentina). *Journal of Vertebrate Paleontology* **20**(1): 57-76.

Ősi, A. (2008). Cranial osteology of *Iharkutosuchus makadii*, a Late Cretaceous basal eusuchian crocodyliform from Hungary. *Neues Jahrbuch fur Geologie und Palaontologie-Abhandlungen* **248**(3): 279-299.

Ősi, A. (2014). The evolution of jaw mechanism and dental function in heterodont crocodyliforms. *Historical Biology* **26**(3): 279-414.

Ősi, A., Clark, J. M. and Weishampel, D. B. (2007). First report on a new basal eusuchian crocodyliform with multicusped teeth from the Upper Cretaceous (Santonian) of Hungary. *Neues Jahrbuch fur Geologie und Palaontologie-Abhandlungen* **243**(2): 169-177.

Ösi, A., Rabi, M., Makádi, L., Szentesi, Z., Botfalvai, G., Gulyás, P. and Godefroit, P. (2012). The Late Cretaceous continental vertebrate fauna from Iharkút (Western Hungary, Central Europe): a review. *Tribute to Charles Darwin and the Bemissart Iguanodons: New Perspectives of Vertebrate Evolution and Early Cretaceous Ecosystems*. P. Godefroit. Bloomington, Indiana, Indiana University Press**:** 533-570.

Osmólska, H., Hua, S. and Buffetaut, E. (1997). *Gobiosuchus kielanae* [Protosuchia] from the Late Cretaceous of Mongolia: anatomy and relationships. *Acta Palaeontologica Polonica* **42**(2): 257-289.

Owen, R. (1878a). Monograph on the fossil Reptilia of the Wealden and Purbeck formations. Supplement No. IX. Crocodilia (*Goniopholis*, *Petrosuchus* abd *Suchosaurus*). *Monograph of the Palaeontographical Society* **32**: 1-15.

Owen, R. (1878b). On the fossils called 'granicones': being a contribution to the histology of the exoskeleton in 'Reptilia'. *Journal of the Royal Microscopical Society* **1**: 222-236.

Owen, R. (1879). Monograph on the Reptilia of the Wealden and Purbeck formations. 18 Supplement No. IX. Crocodilia (*Goniopholis*, *Brachydectes*, *Nannosuchus*, *Theriosuchus* and *Nuthetes*. *Monograph of the Palaeontographical Society* **33**: 1-15.

Pan, Y., Sha, J., Zhou, Z. and Fürsich, F. T. (2013). The Jehol Biota: definition and distribution of exceptionally preserved relicts of a continental Early Cretaceous ecosystem. *Cretaceous Research* **44**: 30-38.

Paradis, E., Claude, J. and Strimmer, K. (2004). APE: Analyses of Phylogenetics and Evolution in R language. *Bioinformatics* **20**(2): 289-290.

Parker, W. G. (2007). Reassessment of the aetosaur '*Desmatosuchus*' *chamaensis* with a reanalysis of the phylogeny of the Aetosauria (Archosauria: Pseudosuchia). *Journal of Systematic Palaeontology* **5**(1): 41-68.

Parker, W. G., Stocker, M. R. and Irmis, R. B. (2008). A new desmatosuchine aetosaur (Archosauria: Suchia) from the Upper Triassic Tecovas Formation (Dockum Group) of Texas. *Journal of Vertebrate Paleontology* **28**(3): 692-701.

Parrilla-Bel, J., Young, M. T., Moreno-Azanza, M. and Canudo, J. I. (2013). The first metriorhynchid crocodylomorph from the Middle Jurassic of Spain, with implications for evolution of the subclade Rhacheosaurini. *PLOS ONE* **8**(1): e54275.

Parrish, J. T., Peterson, F. and Turner, C. E. (2004). Jurassic "savannah"—plant taphonomy and climate of the Morrison Formation (Upper Jurassic, Western USA). *Sedimentary Geology* **167**(3): 137-162.

Payne, J. L. and Clapham, M. E. (2012). End-Permian mass extinction in the oceans: an ancient analog for the twenty-first century? *Annual Review of Earth and Planetary Sciences* **40**: 89-111.

Peng, G. (1996). A Late Jurassic protosuchian *Sichuanosuchus huidongensis* from Zigong, Sichuan Province. *Vertebrata PalAsiatica* **34**(4): 269-278.

Peng, G. and Shu, C. (2004). A new species of *Hsisosuchus* from the Late Jurassic of Zigong, Sichuan, China. *Vertebrata PalAsiatica* **43**(4): 312-324.

Penney, D. (2003). Does the fossil record of spiders track that of their principal prey, the insects? *Transactions of the Royal Society of Edinburgh: Earth Sciences* **94**(03): 275-281.

Perea, D., Soto, M., Sterli, J., Mesa, V., Toriño, P., Roland, G. and Da Silva, J. (2014). *Tacuarembemys kusterae*, gen. *et* sp. *nov*., a new Late Jurassic–? earliest Cretaceous continental turtle from western Gondwana. *Journal of Vertebrate Paleontology* **34**(6): 1329-1341.

Pérez-García, A. (2012). High diversity of pancryptodiran turtles in the Lower Cretaceous of Europe. *Cretaceous Research* **36**: 67-82.

Pérez-García, A. (2014a). A new interpretation of the holotype of "*Hispaniachelys prebetica*", a plesiochelyid turtle (Testudines, Pan-Cryptodira) from the Late Jurassic of Spain. *Acta Palaeontologica Polonica* **59**: 879-885.

Pérez-García, A. (2014b). Revision of the poorly known *Dorsetochelys typocardium*, a relatively abundant pleurosternid turtle (Paracryptodira) in the Early Cretaceous of Europe. *Cretaceous Research* **49**: 152-162.

Pérez-García, A., Fuente, M. S. d. l. and Ortega, F. (2011). A new freshwater basal eucryptodiran turtle from the Early Cretaceous of Spain. *Acta Palaeontologica Polonica* **57**(2): 285-298.

Pérez-García, A., Gasulla, J. M. and Ortega, F. (2014). A new turtle species of *Brodiechelys* from the Early Cretaceous of Spain: Systematic and palaeobiogeographic implications. *Acta Palaeontologica Polonica* **59**(2): 333-342.

Pérez-García, A., Murelaga, X. and Gasulla, J. (2008). Una nueva tortuga (Chelonii, Eucryptodira) del Cretácico Inferior (Aptiense) de Morella (Castellón). *Libro de Resúmenes de las XXIV Jornadas de la Sociedad Española de Paleontología*: 175-176.

Pérez-García, A. and Ortega, F. (2014). A new species of the turtle *Hylaeochelys* (Eucryptodira) outside its known geographic and stratigraphic ranges of distribution. *Comptes Rendus Palevol* **13**(3): 183-188.

Pérez-García, A., Scheyer, T. and Murelaga, X. (2012). New interpretations of *Dortoka vasconica* Lapparent de Broin and Murelaga, a freshwater turtle with an unusual carapace. *Cretaceous Research* **36**: 151-161.

Pérez-Moreno, B., Chure, D., Pires, C., Da Silva, C. M., Dos Santos, V., Dantas, P., Póvoas, L., Cachão, M., Sanz, J. and De Carvalho, A. G. (1999). On the presence of *Allosaurus fragilis* (Theropoda: Carnosauria) in the Upper Jurassic of Portugal: first evidence of an intercontinental dinosaur species. *Journal of the Geological Society* **156**(3): 449-452.

Peters, S. E. (2005). Geologic constraints on the macroevolutionary history of marine animals. *Proceedings of the National Academy of Sciences of the United States of America* **102**(35): 12326-12331.

Peters, S. E. (2006). Genus extinction, origination, and the durations of sedimentary hiatuses. *Paleobiology* **32**(03): 387-407.

Peters, S. E. and Foote, M. (2001). Biodiversity in the Phanerozoic: a reinterpretation. *Paleobiology* **27**(4): 583-601.

Peters, S. E. and Foote, M. (2002). Determinants of extinction in the fossil record. *Nature* **416**(6879): 420-424.

Peters, S. E. and Heim, N. A. (2010). The geological completeness of paleontological sampling in North America. *Paleobiology* **36**(1): 61-79.

Peters, S. E. and Heim, N. A. (2011). Macrostratigraphy and macroevolution in marine environments: testing the common-cause hypothesis. *Comparing the Geological and Fossil Records: Implications for Biodiversity Studies*. A. J. McGowan and A. B. Smith. London, Geological Society of London. **358:** 95-104.

Peybernes, B. and Oertli, H. (1972). La série de passage du Jurassique au Crétacé dans le Bassin sud-pyrénéen (Espagne). *Comptes Rendus des Séances de l'Academie de Sciences, Paris* **276**: 2501-2504.

Philippe, M., Gomez, B., Girard, V., Coiffard, C., Daviero-Gomez, V., Thevenard, F., Billon-Bruyat, J.-P., Guiomar, M., Latil, J.-L. and Néraudeau, D. (2008). Woody or not woody? Evidence for early angiosperm habit from the Early Cretaceous fossil wood record of Europe. *Palaeoworld* **17**(2): 142-152.

Pielou, E. C. (1975). Ecological Diversity. New York, John Wiley and Sons.

Pierce, S. E., Angielczyk, K. D. and Rayfield, E. J. (2009a). Morphospace occupation in thalattosuchian crocodylomorphs: Skull shape variation, species delineation and temporal patterns. *Palaeontology* **52**: 1057-1097.

Pierce, S. E., Angielczyk, K. D. and Rayfield, E. J. (2009b). Shape and mechanics in thalattosuchian (Crocodylomorpha) skulls: implications for feeding behaviour and niche partitioning. *Journal of Anatomy* **215**(5): 555-576.

Pindell, J. L. and Kennan, L. (2009). Tectonic evolution of the Gulf of Mexico, Caribbean and northern South America in the mantle reference frame: an update. *The Origin and Evolution of the Caribbean Plate*. K. H. James, M. A. Lorente and J. L. Pindell. **328:** 1-55.

Piras, P., Colangelo, P., Adams, D. C., Buscalioni, A., Cubo, J., Kotsakis, T., Meloro, C. and Raia, P. (2010). The *Gavialis–Tomistoma* debate: the contribution of skull ontogenetic allometry and growth trajectories to the study of crocodylian relationships. *Evolution & development* **12**(6): 568-579.

Piveteau, J. (1928). Etudes sur quelques Amphibiens et Reptiles fossiles: Le reptile de Gigondas et l'évolution des Métriorhynchidés. *Annales De Paleontologie* **17**: 30-47.

Platt, S. G., Rainwater, T. R., Thorbjarnarson, J. B., Finger, A. G., Anderson, T. A. and McMurry, S. T. (2009). Size estimation, morphometrics, sex ratio, sexual size dimorphism, and biomass of Morelet's crocodile in northern Belize. *Caribbean Journal of Science* **45**(1): 80-93.

Plotnick, R. E., Smith, F. A. and Lyons, S. K. (2016). The fossil record of the sixth extinction. *Ecology letters* **19**(5): 546-553.

Pol, D. (1999). El esqueleto postcraneano de *Notosuchus terrestris* (Archosauria: Crocodyliformes) del Cretácico Superior de la Cuenca Neuquina y su información fi logenética. PhD, Universidad de Buenos Aires.

Pol, D. (2013). Postcranial remains of *Notosuchus terrestris* Woodward (Archosauria: Crocodyliformes) from the Upper Cretaceous of Patagonia, Argentina. *Ameghiniana* **42**(1): 21-38.

Pol, D. and Apesteguía, S. (2005). New *Araripesuchus* remains from the early Late Cretaceous (Cenomanian-Turonian) of Patagonia. *American Museum Novitates* **3490**: 1-38.

Pol, D. and Escapa, I. H. (2009). Unstable taxa in cladistic analysis: identification and the assessment of relevant characters. *Cladistics* **25**(5): 515-527.

Pol, D. and Gasparini, Z. (2009). Skull anatomy of *Dakosaurus andiniensis* (Thalattosuchia: Crocodylomorpha) and the phylogenetic position of Thalattosuchia. *Journal of Systematic Palaeontology* **7**(2): 163-197.

Pol, D., Ji, S.-a., Clark, J. M. and Chiappe, L. M. (2004). Basal crocodyliforms from the Lower Cretaceous Tugulu Group (Xinjiang, China), and the phylogenetic position of *Edentosuchus*. *Cretaceous Research* **25**(4): 603-622.

Pol, D. and Leardi, J. M. (2015). Diversity patterns of Notosuchia (Crocodyliformes, Mesoeucrocodylia) during the Cretaceous of Gondwana. *Publicación Electrónica de la Asociación Paleontológica Argentina* **15**(1).

Pol, D., Leardi, J. M., Lecuona, A. and Krause, M. (2012). Postcranial anatomy of *Sebecus icaeorhinus* (Crocodyliformes, Sebecidae) from the Eocene of Patagonia. *Journal of Vertebrate Paleontology* **32**(2): 328-354.

Pol, D., Nascimento, P. M., Carvalho, A. B., Riccomini, C., Pires-Domingues, R. A. and Zaher, H. (2014). A new notosuchian from the Late Cretaceous of Brazil and the phylogeny of advanced notosuchians. *PLOS ONE* **9**(4): e93105.

Pol, D. and Norell, M. A. (2004a). A new crocodyliform from Zos Canyon, Mongolia. *American Museum Novitates* **3445**: 1-36.

Pol, D. and Norell, M. A. (2004b). A new gobiosuchid crocodyliform taxon from the Cretaceous of Mongolia. *American Museum Novitates* **3458**: 1-31.

Pol, D. and Powell, J. E. (2011). A new sebecid mesoeucrocodylian from the Rio Loro Formation (Palaeocene) of north ‐ western Argentina. *Zoological Journal of the Linnean Society* **163**(s1): S7-S36.

Pol, D., Turner, A. H. and Norell, M. A. (2009). Morphology of the Late Cretaceous crocodylomorph *Shamosuchus djadochtaensis* and a discussion of neosuchian phylogeny as related to the origin of Eusuchia. *Bulletin of the American Museum of Natural History* **324**: 1-103.

Pomes, M. L. (1990). Morphotype of Lower Cretaceous crocodilian teeth (Archosauria) from the Cedar Mountain Formation of Utah and the Antlers formation of Texas. *Journal of Vertebrate Paleontology* **10**(3): 38.

Ponomarenko, A. (1988). New Mesozoic insects. *Trudy Sovmestnaya Sovetsko-Mongol'skaya Paleontologicheskaya Ekspeditsiya* **33**: 71-80.

Pouech, J., Amiot, R., Lécuyer, C., Mazin, J.-M., Martineau, F. and Fourel, F. (2014). Oxygen isotope composition of vertebrate phosphates from Cherves-de-Cognac (Berriasian, France): Environmental and ecological significance. *Palaeogeography, Palaeoclimatology, Palaeoecology* **410**: 290-299.

Pouech, J. and Mazin, J.-M. (2006). Microvertebrate biodiversity from Cherves-de-Cognac (Lower Cretaceous, Berriasian: Charente, France). 9th [Ninth] Symposium on Mesozoic Terrestrial Ecosystems: short papers.

Powell, M. G. (2009). The latitudinal diversity gradient of brachiopods over the past 530 million years. *The Journal of Geology* **117**(6): 585-594.

Prasad, G. V. and de Broin, F. d. L. (2002). Late Cretaceous crocodile remains from Naskal (India): comparisons and biogeographic affinities. Annales De Paleontologie, Elsevier.

Price, G. and Mutterlose, J. (2004). Isotopic signals from late Jurassic–early Cretaceous (Volgian–Valanginian) sub-Arctic belemnites, Yatria River, Western Siberia. *Journal of the Geological Society* **161**(6): 959-968.

Price, G. D., Főzy, I. and Pálfy, J. (2016). Carbon cycle history through the Jurassic–Cretaceous boundary: A new global $\delta_{13}C$ stack. *Palaeogeography, Palaeoclimatology, Palaeoecology*, 10.1016/j.palaeo.2016.03.016.

Price, G. D. and Gröcke, D. R. (2002). Strontium-isotope stratigraphy and oxygen-and carbon-isotope variation during the Middle Jurassic–Early Cretaceous of the Falkland Plateau, South Atlantic. *Palaeogeography, Palaeoclimatology, Palaeoecology* **183**(3): 209-222.

Price, G. D. and Passey, B. H. (2013). Dynamic polar climates in a greenhouse world: Evidence from clumped isotope thermometry of Early Cretaceous belemnites. *Geology* **41**(8): 923-926.

Price, G. D. and Rogov, M. A. (2009). An isotopic appraisal of the Late Jurassic greenhouse phase in the Russian Platform. *Palaeogeography, Palaeoclimatology, Palaeoecology* **273**(1): 41-49.

Price, G. D., Twitchett, R. J., Wheeley, J. R. and Buono, G. (2013). Isotopic evidence for long term warmth in the Mesozoic. *Scientific Reports* **3**(1438).

Prieto-Márquez, A. (2010). Global phylogeny of Hadrosauridae (Dinosauria: Ornithopoda) using parsimony and Bayesian methods. *Zoological Journal of the Linnean Society* **159**(2): 435-502.

Pritchard, A. C., Turner, A. H., Allen, E. R. and Norell, M. A. (2012). Osteology of a North American goniopholidid (*Eutretauranosuchus delfsi*) and palate evolution in Neosuchia. *American Museum Novitates* **3783**: 1-56.

Prokoph, A., Shields, G. A. and Veizer, J. (2008). Compilation and time-series analysis of a marine carbonate $\delta_{18}O$, $\delta_{13}C$, $^{87}Sr/^{86}Sr$ and $\delta^{34}S$ database through Earth history. *Earth-Science Reviews* **87**(3–4): 113-133.

Prosorovskaya, E., Pálfy, J. and Vörös, A. (1993). Brachiopods at the Jurassic–Cretaceous boundary from the Ukrainian Carpathians, Crimea, Caucasus, and Transcaspian Region. *Mesozoic Brachiopods of Alpine Europe*. J. Pálfy and A. Vörös. Budapest, Hungarian Geological Society**:** 109-112.

Pruner, P., Houša, V., Olóriz, F., Košťák, M., Krs, M., Man, O., Schnabl, P., Venhodová, D., Tavera, J. and Mazuch, M. (2010). High-resolution magnetostratigraphy and biostratigraphic zonation of the Jurassic/Cretaceous boundary strata in the Puerto Escaño section (southern Spain). *Cretaceous Research* **31**(2): 192-206.

Puértolas-Pascual, E., Canudo, J. and Moreno-Azanza, M. (2014). The eusuchian crocodylomorph *Allodaposuchus subjuniperus* sp. *nov*., a new species from the latest Cretaceous (upper Maastrichtian) of Spain. *Historical Biology* **26**(1): 91-109.

Puértolas, E., Canudo, J. I. and Cruzado-Caballero, P. (2011). A new crocodylian from the Late Maastrichtian of Spain: implications for the initial radiation of crocodyloids. *PLOS ONE* **6**(6): e20011.

Püntener, C., Billon-Bruyat, J.-P., Bocat, L., Berger, J.-P. and Joyce, W. G. (2014). Taxonomy and phylogeny of the turtle *Tropidemys langii* Rütimeyer, 1873, based on new specimens from the Kimmeridgian of the Swiss Jura Mountains. *Journal of Vertebrate Paleontology* **34**(2): 353-374.

Purdy, E. G. (2008). Comparison of taxonomic diversity, strontium isotope and sea-level patterns. *International Journal of Earth Sciences* **97**(3): 651-664.

Pyenson, N. D., Kelley, N. P. and Parham, J. F. (2014). Marine tetrapod macroevolution: Physical and biological drivers on 250Ma of invasions and evolution in ocean ecosystems. *Palaeogeography, Palaeoclimatology, Palaeoecology* **400**: 1-8.

Pyron, R. A. and Burbrink, F. T. (2012). Extinction, ecological opportunity, and the origins of global snake diversity. *Evolution* **66**(1): 163-178.

R Development Core Team (2013). R: A language and environment for statistical computing. R Foundation for Statistical Computing. Vienna, Austria.

Rabi, M., Joyce, W. G. and Wings, O. (2010). A review of the Mesozoic turtles of the Junggar Basin (Xinjiang, Northwest China) and the paleobiogeography of Jurassic to Early Cretaceous Asian testudinates. *Palaeobiodiversity and Palaeoenvironments* **90**(3): 259-273.

Rabi, M., Sukhanov, V. B., Egorova, V. N., Danilov, I. and Joyce, W. G. (2014). Osteology, relationships, and ecology of *Annemys* (Testudines, Eucryptodira) from the Late Jurassic of Shar Teg, Mongolia, and phylogenetic definitions for Xinjiangchelyidae, Sinemydidae, and Macrobaenidae. *Journal of Vertebrate Paleontology* **34**(2): 327-352.

Racey, A. (2009). Mesozoic red bed sequences from SE Asia and the significance of the Khorat Group of NE Thailand. *Late Palaeozoic and Mesozoic Ecosystems in SE Asia*. E. Buffetaut, G. Cuny, J. Le Loeuff and V. Suteethorn. London, Geological Society of London. **315:** 41-67.

Racey, A. and Goodall, J. G. (2009). Palynology and stratigraphy of the Mesozoic Khorat Group red bed sequences from Thailand. *Late Palaeozoic and Mesozoic Ecosystems in SE Asia*. E. Buffetaut, G. Cuny, J. Le Loeuff and V. Suteethorn. London, Geological Society of London. **315:** 69-83.

Rage, J.-C. (2013). Mesozoic and Cenozoic squamates of Europe. *Palaeobiodiversity and Palaeoenvironments* **93**(4): 517-534.

Rainford, J. L., Hofreiter, M., Nicholson, D. B. and Mayhew, P. J. (2014). Phylogenetic distribution of extant richness suggests metamorphosis is a key innovation driving diversification in insects. *PLOS ONE* **9**(10): e109085.

Rampino, M. R. and Haggerty, B. M. (1996). Impact crises and mass extinctions: a working hypothesis. *The Cretaceous Tertiary Event and Other Catastrophes in Earth History*. G. Ryder, D. Fastovsky and S. Gartner, Geological Society of America. **Special Paper 307:** 11-30.

Raspail, E. (1842). Observations sur un nouveau genre de Saurien fossile, le *Neustosaurus gigondarum*. University of Lausanne, Paris, Meilhac.

Rauhut, O. W., Heyng, A. M., López-Arbarello, A. and Hecker, A. (2012). A new rhynchocephalian from the Late Jurassic of Germany with a dentition that is unique amongst tetrapods. *PLOS ONE* **7**(10): e46839.

Rauhut, O. W., Milner, A. C. and Moore‐Fay, S. (2010). Cranial osteology and phylogenetic position of the theropod dinosaur *Proceratosaurus bradleyi* (Woodward, 1910) from the Middle Jurassic of England. *Zoological Journal of the Linnean Society* **158**(1): 155-195.

Raup, D. M. (1972). Taxonomic diversity during the Phanerozoic. *Science* **177**(4054): 1065-1071.

Raup, D. M. (1975). Taxonomic diversity estimation using rarefaction. *Paleobiology* **1**(4): 333-342.

Raup, D. M. and Boyajian, G. E. (1988). Patterns of generic extinction in the fossil record. *Paleobiology* **14**(2): 109-125.

Raup, D. M. and Sepkoski Jr, J. J. (1982). Mass extinctions in the marine fossil record. *Science* **215**(4539): 1501-1503.

Raup, D. M. and Sepkoski Jr, J. J. (1984). Periodicity of extinctions in the geologic past. *Proceedings of the National Academy of Sciences of the United States of America* **81**(3): 801-805.

Rayfield, E. J. and Milner, A. C. (2008). Establishing a framework for archosaur cranial mechanics. *Paleobiology* **34**(04): 494-515.

Rees, J. (2005). Neoselachian shark and ray teeth from the Valanginian, Lower Cretaceous, of Wąwał, Central Poland. *Palaeontology* **48**(2): 209-221.

Rees, P., Ziegler, A. and Valdes, P. (2000). Jurassic phytogeography and climates: new data and model comparisons. Cambridge, Cambridge University Press.

Reimold, W. U., Armstrong, R. A. and Koeberl, C. (2002). A deep drillcore from the Morokweng impact structure, South Africa: petrography, geochemistry, and constraints on the crater size. *Earth and Planetary Science Letters* **201**(1): 221-232.

Renne, P. R., Ernesto, M., Pacca, I. G., Coe, R. S., Glen, J. M., Prévot, M. and Perrin, M. (1992). The age of Paraná flood volcanism, rifting of Gondwanaland, and the Jurassic-Cretaceous boundary. *Science* **258**(5084): 975-979.

Reynoso, V. (2000). An unusual aquatic sphenodontian (Reptilia: Diapsida) from the Tlayua Formation (Albian), central Mexico. *Journal of Paleontology* **74**(1): 133-148.

Riccardi, A. (1991). Jurassic and Cretaceous marine connections between the Southeast Pacific and Tethys. *Palaeogeography, Palaeoclimatology, Palaeoecology* **87**(1): 155-189.

Ricci, J., Quidelleur, X., Pavlov, V., Orlov, S., Shatsillo, A. and Courtillot, V. (2013). New $^{40}Ar/^{39}Ar$ and K–Ar ages of the Viluy traps (Eastern Siberia): Further evidence for a relationship with the Frasnian–Famennian mass extinction. *Palaeogeography, Palaeoclimatology, Palaeoecology* **386**: 531-540.

Richter, A. (1994). Lacertilia aus der Unteren Kreide von Uña und Galve (Spanien) und Anoual (Marokko). *Berliner Geowissenschaftliche Abhandlungen* **14**: 1-147.

Richter, A., Wings, O., Pfretzschner, H.-U. and Martin, T. (2010). Late Jurassic Squamata and possible Choristodera from the Junggar Basin, Xinjiang, Northwest China. *Palaeobiodiversity and Palaeoenvironments* **90**(3): 275-282.

Riff, D. and Kellner, A. W. A. (2011). Baurusuchid crocodyliforms as theropod mimics: clues from the skull and appendicular morphology of *Stratiotosuchus maxhechti* (Upper Cretaceous of Brazil). *Zoological Journal of the Linnean Society* **163**(s1): S37-S56.

Robeck, H. E., Maley, C. C. and Donoghue, M. J. (2000). Taxonomy and temporal diversity patterns. *Paleobiology* **26**(2): 171-187.

Roberts, A. J., Druckenmiller, P. S., Sætre, G.-P. and Hurum, J. H. (2014). A new Upper Jurassic ophthalmosaurid ichthyosaur from the Slottsmøya Member, Agardhfjellet Formation of Central Spitsbergen. *PLOS ONE* **9**(8): e103152.

Robock, A. (2002). Volcanic eruptions and climate. *Reviews of Geophysics* **38**(2): 191-219.

Rogers, J. V. (2003). *Pachycheilosuchus trinquei*, a new procoelous crocodyliform from the Lower Cretaceous (Albian) Glen Rose Formation of Texas. *Journal of Vertebrate Paleontology* **23**(1): 128-145.

Rogov, M. A., Zakharov, V. A. and Nikitenko, B. L. (2010). The Jurassic–Cretaceous boundary problem and the myth on J/K boundary extinction. *Earth Science Frontiers* **17**: 13-14.

Romer, A. S. (1956). Osteology of the Reptiles. Chicago, Chicago University Press.

Ronov, A., Khain, V., Balukhovsky, A. and Seslavinsky, K. (1980). Quantitative analysis of Phanerozoic sedimentation. *Sedimentary Geology* **25**(4): 311-325.

Ronquist, F. and Huelsenbeck, J. P. (2003). MrBayes 3: Bayesian phylogenetic inference under mixed models. *Bioinformatics* **19**(12): 1572-1574.

Ross, F. D. and Mayer, G. C. (1983). On the dorsal armor of the Crocodilia. *Advances in herpetology and evolutionary biology*. A. Rhodin and K. Mityata. Cambridge, Massachusetts, Museum of Comparative Zoology**:** 305-331.

Roth, P. H. (1989). Ocean circulation and calcareous nannoplankton evolution during the Jurassic and Cretaceous. *Palaeogeography, Palaeoclimatology, Palaeoecology* **74**(1): 111-126.

Roy, K., Hunt, G. and Jablonski, D. (2009). Phylogenetic conservatism of extinctions in marine bivalves. *Science* **325**(5941): 733-737.

Royo-Torres, R., Upchurch, P., Mannion, P. D., Mas, R., Cobos, A., Gascó, F., Alcalá, L. and Sanz, J. L. (2014). The anatomy, phylogenetic relationships, and stratigraphic position of the Tithonian–Berriasian Spanish sauropod dinosaur *Aragosaurus ischiaticus*. *Zoological Journal of the Linnean Society* **171**(3): 623-655.

Royo y Gómez, J. (1927). Sur le faciès Wealdien d'Espagne. *Compte Rendu sommaire des Séances de la Société géologique de France* **11**: 125-128.

Ruban, D. (2005). Mesozoic marine fossil diversity and mass extinctions: an experience with the middle XIX century paleontological data. *Revue de Paléobiologie* **24**(1): 287.

Ruban, D. A. (2006). Taxonomic diversity dynamics of the Jurassic bivalves in the Caucasus: Regional trends and recognition of global patterns. *Palaeogeography, Palaeoclimatology, Palaeoecology* **239**(1): 63-74.

Ruban, D. A. (2010). Do new reconstructions clarify the relationships between the Phanerozoic diversity dynamics of marine invertebrates and long-term eustatic trends? *Annales De Paleontologie* **96**(2): 51-59.

Ruban, D. A. (2011). Diversity dynamics of Callovian-Albian brachiopods in the Northern Caucasus (northern Neo-Tethys) and a Jurassic/Cretaceous mass extinction. *Paleontological Research* **15**(3): 154-167.

Ruffell, A. H. and Batten, D. J. (1990). The Barremian-Aptian arid phase in western Europe. *Palaeogeography, Palaeoclimatology, Palaeoecology* **80**(3): 197-212.

Ruiz-Omeñaca, J. I., Canudo, J., Aurell, M., Bádenas, B., Barco, J., Cuenca-Bescós, G. and Ipas, J. (2004). Estado de las investigaciones sobre los vertebrados del Jurásico Superior y Cretácico Inferior de Galve (Teruel). *Estudios geológicos* **60**(3-6): 179-202.

Sager, W. W., Zhang, J. C., Korenaga, J., Sano, T., Koppers, A. A. P., Widdowson, M. and Mahoney, J. J. (2013). An immense shield volcano within the Shatsky Rise oceanic plateau, northwest Pacific Ocean. *Nature Geoscience* **6**(11): 976-981.

Sahagian, D., Pinous, O., Olferiev, A. and Zakharov, V. (1996). Eustatic curve for the Middle Jurassic-Cretaceous based on Russian Platform and Siberian stratigraphy: Zonal resolution. *AAPG Bulletin* **80**(9): 1433-1458.

Sajadi, F. and Playford, G. (2002). Systematic and stratigraphic palynology of Late Jurassic-earliest Cretaceous strata of the Eromanga Basin, Queensland, Australia: Part one. *Palaeontographica Abteilung B-Palaophytologie* **261**: 1-112.

Sakamoto, M., Benton, M. J. and Venditti, C. (2016). Dinosaurs in decline tens of millions of years before their final extinction. *Proceedings of the National Academy of Sciences of the United States of America* **113**(18): 5036-5040.

Salgado, L. and Bonaparte, J. F. (1991). Un nuevo saurópodo Dicraeosauridae, *Amargasurus cazaui* gen. *et* sp. *nov*., de la Formación La Amarga, Neocomiano de la provincia del Neuquén, Argentina. *Ameghiniana* **28**: 333-346.

Salisbury, S. W. (2002). Crocodilians from the Lower Cretaceous (Berriasian) Purbeck Limestone Group of Dorset, southern England. *Special Papers in Palaeontology* **68**: 121-144.

Salisbury, S. W. and Frey, E. (2001). A biomechanical transformation model for the evolution of semi-spheroidal articulations between adjoining vertebral bodies in crocodilians. *Crocodilian biology and evolution*. G. C. Grigg, F. Seebacher and C. E. Franklin. Chipping Norton, Surrey Beatty**:** 85-134.

Salisbury, S. W., Molnar, R. E., Frey, E. and Willis, P. M. (2006). The origin of modern crocodyliforms: new evidence from the Cretaceous of Australia. *Proceedings of the Royal Society of London B: Biological Sciences* **273**(1600): 2439-2448.

Salisbury, S. W. and Naish, D. (2011). Crocodilians. *English Wealden Fossils*. D. Batten and P. D. Lane. Aberystwyth, Wales, U.K., Paleontological Association. **14:** 305-369.

Salisbury, S. W., Willis, P. M., Peitz, S. and Sander, P. M. (1999). The crocodilian *Goniopholis simus* from the Lower Cretaceous of north-western Germany. *Special Papers in Palaeontology* **60**: 121-148.

Sames, B., Wagreich, M., Wendler, J. E., Haq, B. U., Conrad, C. P., Melinte-Dobrinescu, M. C., Hu, X., Wendler, I., Wolfgring, E., Yilmaz, I. Ö. and Zorina, S. O. (2016). Review: Short-term sea-level changes in a greenhouse world — A view from the Cretaceous. *Palaeogeography, Palaeoclimatology, Palaeoecology* **441**(3): 393-411.

Sánchez-Hernández, B. and Benton, M. J. (2012). Filling the ceratosaur gap: A new ceratosaurian theropod from the Early Cretaceous of Spain. *Acta Palaeontologica Polonica* **59**(3): 581-600.

Sander, P. M. (2000). Ichthyosauria: their diversity, distribution, and phylogeny. *Paläontologische Zeitschrift* **74**(1-2): 1-35.

Sander, P. M., Mateus, O., Laven, T. and Knötschke, N. (2006). Bone histology indicates insular dwarfism in a new Late Jurassic sauropod dinosaur. *Nature* **441**(7094): 739-741.

Sandoval, J., O'Dogherty, L. and Guex, J. (2001). Evolutionary rates of Jurassic ammonites in relation to sea-level fluctuations. *Palaios* **16**(4): 311-335.

Sanford, W. E., Doughten, M. W., Coplen, T. B., Hunt, A. G. and Bullen, T. D. (2013). Evidence for high salinity of Early Cretaceous sea water from the Chesapeake Bay crater. *Nature* **503**(7475): 252-256.

Sanz, J. L., Ortega, F. and Shibata, M. (2014). Dinosaurios Maravillosos de España. Cuenca, Spain, Diputacion Provincial de Cuenca.

Săsăran, E., Bucur, I. I., Pleş, G. and Riding, R. (2014). Late Jurassic Epiphyton-like cyanobacteria: Indicators of long-term episodic variation in marine bioinduced microbial calcification? *Palaeogeography, Palaeoclimatology, Palaeoecology* **401**: 122-131.

Sauvage, H.-É. (1874). Mémoire sur les dinosauriens et les crocodiliens des terrains Jurassiques de Boulogne-sur-Mer. *Memoirs de la Société Géologique de France* **2**: 1-57.

Schaller, M. F., Wright, J. D. and Kent, D. V. (2011). Atmospheric pCO_2 perturbations associated with the Central Atlantic magmatic province. *Science* **331**(6023): 1404-1409.

Schlüter, T. and Schwarzhans, W. (1978). Eine Bonebed-Lagerstätte aus dem Wealden Süd-Tunesiens (Umgebung Ksar Krerachfa). *Berliner Geowissenschaftliche Abhandlungen A* **8**: 53-65.

Schnabl, P., Pruner, P. and Wimbledon, W. A. P. (2015). A review of magnetostratigraphic results from the Tithonian–Berriasian of Nordvik (Siberia) and possible biostratigraphic constraints. *Geologica Carpathica* **66**(6): 489-498.

Schneider, C. A., Rasband, W. S. and Eliceiri, K. W. (2012). NIH Image to ImageJ: 25 years of image analysis. *Nature Methods* **9**(7): 671-675.

Schnyder, J., Deconinck, J.-F., Baudin, F., Colombié, C., Du Chêne, R. J., Gardin, S., Galbrun, B. and De Rafélis, M. (2012). Purbeck beds (Late Jurassic) in the Phare de Chassiron section (Île d'Oléron, NW Aquitaine Basin, France): Refined age-assignment and long-term depositional sequences. *Geobios* **45**(5): 485-499.

Schulte, P., Alegret, L., Arenillas, I., Arz, J. A., Barton, P. J., Bown, P. R., Bralower, T. J., Christeson, G. L., Claeys, P. and Cockell, C. S. (2010). The Chicxulub asteroid impact and mass extinction at the Cretaceous-Paleogene boundary. *Science* **327**(5970): 1214-1218.

Schwarz-Wings, D., Frey, E. and Martin, T. (2009a). Reconstruction of the bracing system of the trunk and tail in hyposaurine dyrosaurids (Crocodylomorpha; Mesoeucrocodylia). *Journal of Vertebrate Paleontology* **29**(2): 453-472.

Schwarz-Wings, D., Klein, N., Neumann, C. and Resch, U. (2011). A new partial skeleton of *Alligatorellus* (Crocodyliformes) associated with echinoids from the Late Jurassic (Tithonian) lithographic limestone of Kelheim, S‐Germany. *Fossil Record* **14**(2): 195-205.

Schwarz-Wings, D., Rees, J. and Lindgren, J. (2009b). Lower cretaceous mesoeucrocodylians from Scandinavia (Denmark and Sweden). *Cretaceous Research* **30**(5): 1345-1355.

Schwarz, D. and Salisbury, S. W. (2005). A new species of *Theriosuchus* (Atoposauridae, Crocodylomorpha) from the Late Jurassic (Kimmeridgian) of Guimarota, Portugal. *Geobios* **38**(6): 779-802.

Scotese, C., Boucot, A. and McKerrow, W. (1999). Gondwanan palaeogeography and paleoclimatology. *Journal of African Earth Sciences* **28**(1): 99-114.

Scotese, C. R. (1991). Jurassic and Cretaceous plate tectonic reconstructions. *Palaeogeography, Palaeoclimatology, Palaeoecology* **87**(1): 493-501.

Scotese, C. R., Gahagan, L. M. and Larson, R. L. (1988). Plate tectonic reconstructions of the Cretaceous and Cenozoic ocean basins. *Tectonophysics* **155**(1): 27-48.

Scott, R. W. (1988). Evolution of Late Jurassic and Early Cretaceous reef biotas. *Palaios* **3**(2): 184-193.

Scott, R. W. (1995). Global environmental controls on Cretaceous reefal ecosystems. *Palaeogeography, Palaeoclimatology, Palaeoecology* **119**(1): 187-199.

Segev, A. (2002). Flood basalts, continental breakup and the dispersal of Gondwana: evidence for periodic migration of upwelling mantle flows (plumes). *EGU Stephan Mueller Special Publication Series* **2**: 171-191.

Segev, A. (2009). $^{40}Ar/^{39}Ar$ and K–Ar geochronology of Berriasian–Hauterivian and Cenomanian tectonomagmatic events in northern Israel: implications for regional stratigraphy. *Cretaceous Research* **30**(3): 810-828.

Sellwood, B. W. and Valdes, P. J. (2006). Mesozoic climates: General circulation models and the rock record. *Sedimentary Geology* **190**(1): 269-287.

Sepkoski Jr, J. J. (1982). Mass extinctions in the Phanerozoic oceans: a review. *Geological Society of America Special Papers* **190**: 283-290.

Sepkoski Jr, J. J. (1984). A kinetic-model of Phanerozoic taxonomic diversity. 3. Post-Paleozoic families and mass extinctions. *Paleobiology* **10**(2): 246-267.

Sepkoski Jr, J. J. (1986). Phanerozoic overview of mass extinction. *Patterns and Processes in the History of Life*, Springer**:** 277-295.

Sepkoski Jr, J. J. (1992). A compendium of fossil marine animal families. *Contributions in Biology and Geology. Milwaukee Public Museum* **83**: 1-156.

Sepkoski Jr, J. J. (1993). Ten years in the library: new data confirm paleontological patterns. *Paleobiology* **19**(1): 43-51.

Sepkoski Jr, J. J., Bambach, R. K., Raup, D. M. and Valentine, J. W. (1981). Phanerozoic marine diversity and the fossil record. *Nature* **293**(5832): 435-437.

Sepkoski Jr, J. J., Jablonski, D. and Foote, M. (2002). A compendium of fossil marine animal genera. *Bulletins of American Paleontology* **363**: 1-563.

Sereno, P. and Larsson, H. (2009). Cretaceous crocodyliforms from the Sahara. *ZooKeys* **28**: 1-143.

Sereno, P., Sidor, C., Larsson, H. and Gado, B. (2003). A new notosuchian from the Early Cretaceous of Niger. *Journal of Vertebrate Paleontology* **23**(2): 477-482.

Sereno, P. C., Dutheil, D. B., Iarochene, M., Larsson, H. C., Lyon, G. H., Magwene, P. M., Sidor, C. A., Varricchio, D. J. and Wilson, J. A. (1996). Predatory dinosaurs from the Sahara and Late Cretaceous faunal differentiation. *Science* **272**(5264): 986-991.

Sereno, P. C., Larsson, H. C., Sidor, C. A. and Gado, B. (2001). The giant crocodyliform *Sarcosuchus* from the Cretaceous of Africa. *Science* **294**(5546): 1516-1519.

Sertich, J. J. and O'Connor, P. M. (2014). A new crocodyliform from the middle Cretaceous Galula Formation, southwestern Tanzania. *Journal of Vertebrate Paleontology* **34**(3): 576-596.

Seton, M., Müller, R., Zahirovic, S., Gaina, C., Torsvik, T., Shephard, G., Talsma, A., Gurnis, M., Turner, M. and Maus, S. (2012). Global continental and ocean basin reconstructions since 200Ma. *Earth-Science Reviews* **113**(3): 212-270.

Shear, W. A. and Edgecombe, G. D. (2010). The geological record and phylogeny of the Myriapoda. *Arthropod Structure and Development* **39**(2): 174-190.

Shirley, M. H., Vliet, K. A., Carr, A. N. and Austin, J. D. (2014). Rigorous approaches to species delimitation have significant implications for African crocodilian systematics and conservation. *Proceedings of the Royal Society of London B: Biological Sciences* **281**(1776): 20132483.

Shome, S. and Bardhan, S. (2009). A new Late Tithonian ammonite assemblage from Kutch, western India. *Journal of the Palaeontological Society of India* **54**(1): 1.

Signor, P. W. and Lipps, L. H. (1982). Sampling bias, gradual extinction patterns and catastrophes in the fossil record. *Geological Society of America Special Papers* **190**: 351-367.

Sigogneau-Russell, D. (1998). Discovery of a Late Jurassic Chinese mammal in the upper Bathonian of England. *Comptes Rendus de l'Académie des Sciences-Series IIA - Earth and Planetary Science* **327**(8): 571-576.

Sigogneau-Russell, D., Evans, S., Levine, J. and Russell, D. (1998). The Early Cretaceous microvertebrate locality of Anoual, Morocco: a glimpse at the small vertebrate assemblages of Africa. *New Mexico Museum of Natural History and Science Bulletin* **14**: 177-181.

Sigogneau-Russell, D., Hooker, J. J. and Ensom, P. C. (2001). The oldest tribosphenic mammal from Laurasia (Purbeck Limestone Group, Berriasian, Cretaceous, UK) and its bearing on the 'dual origin' of Tribosphenida. *Comptes Rendus de l'Académie des Sciences-Series IIA - Earth and Planetary Science* **333**(2): 141-147.

Simpson, C., Kiessling, W., Mewis, H., Baron‐Szabo, R. C. and Müller, J. (2011). Evolutionary diversification of reef corals: a comparison of the molecular and fossil records. *Evolution* **65**(11): 3274-3284.

Skelton, P., Crame, J., Morris, N. and Harper, E. (1990). Adaptive divergence and taxonomic radiation in post-Palaeozoic bivalves. *Systematics Association Special Volume* **42**: 91-117.

Skutschas, P. P. (2013). Mesozoic salamanders and albanerpetontids of Middle Asia, Kazakhstan, and Siberia. *Palaeobiodiversity and Palaeoenvironments* **93**(4): 441-457.

Skutschas, P. P. (2016). A relict stem salamander: Evidence from the Early Cretaceous of Siberia. *Acta Palaeontologica Polonica* **61**(1): 119-123.

Slack, K. E., Jones, C. M., Ando, T., Harrison, G. A., Fordyce, R. E., Arnason, U. and Penny, D. (2006). Early penguin fossils, plus mitochondrial genomes, calibrate avian evolution. *Molecular Biology and Evolution* **23**(6): 1144-1155.

Slater, B. J., Reolid, M., Schouten, R. and Benton, M. J. (2011). A new Late Jurassic turtle from Spain: phylogenetic implications, taphonomy and palaeoecology. *Palaeontology* **54**(6): 1393-1414.

Slater, G. J. (2013). Phylogenetic evidence for a shift in the mode of mammalian body size evolution at the Cretaceous‐Palaeogene boundary. *Methods in Ecology and Evolution* **4**(8): 734-744.

Smith, A. B. (2001). Large-scale heterogeneity of the fossil record: implications for Phanerozoic biodiversity studies. *Philosophical Transactions of the Royal Society of London Series B: Biological Sciences* **356**(1407): 351-367.

Smith, A. B. (2007). Marine diversity through the Phanerozoic: problems and prospects. *Journal of the Geological Society* **164**: 731-745.

Smith, A. B. and Benson, R. B. J. (2013). Marine diversity in the geological record and its relationship to surviving bedrock area, lithofacies diversity, and original marine shelf area. *Geology* **41**(2): 171-174.

Smith, A. B., Gale, A. S. and Monks, N. E. (2001). Sea-level change and rock-record bias in the Cretaceous: a problem for extinction and biodiversity studies. *Paleobiology* **27**(2): 241-253.

Smith, A. B., Lloyd, G. T. and McGowan, A. J. (2012). Phanerozoic marine diversity: rock record modelling provides an independent test of large-scale trends. *Proceedings of the Royal Society of London Series B: Biological Sciences* **279**(1746): 4489-4495.

Smith, A. B. and McGowan, A. (2008). Temporal patterns of barren intervals in the Phanerozoic. *Paleobiology* **34**(1): 155-161.

Smith, A. B. and McGowan, A. J. (2005). Cyclicity in the fossil record mirrors rock outcrop area. *Biology Letters* **1**(4): 443-445.

Smith, A. B. and McGowan, A. J. (2007). The shape of the Phanerozoic marine palaeodiversity curve: How much can be predicted from the sedimentary rock record of western Europe? *Palaeontology* **50**: 765-774.

Smith, D. K., Allen, E. R., Sanders, R. K. and Stadtman, K. L. (2010). A new specimen of *Eutretauranosuchus* (Crocodyliformes; Goniopholididae) from Dry Mesa, Colorado. *Journal of Vertebrate Paleontology* **30**(5): 1466-1477.

Smolensky, N. L., Hurtado, L. A. and Fitzgerald, L. A. (2015). DNA barcoding of Cameroon samples enhances our knowledge on the distributional limits of putative species of *Osteolaemus* (African dwarf crocodiles). *Conservation Genetics* **16**(1): 235-240.

Sookias, R. B. (2016). The relationships of the Euparkeriidae and the rise of Archosauria. *Royal Society Open Science* **3**(3).

Sookias, R. B., Benson, R. B. J. and Butler, R. J. (2012a). Biology, not environment, drives major patterns in maximum tetrapod body size through time. *Biology Letters* **8**(4): 674-677.

Sookias, R. B., Butler, R. J. and Benson, R. B. (2012b). Rise of dinosaurs reveals major body-size transitions are driven by passive processes of trait evolution. *Proceedings of the Royal Society of London B: Biological Sciences* **279**: 2180-2187.

Sorenson, L., Santini, F. and Alrfaro, M. E. (2014). The effect of habitat on modern shark diversification. *Journal of Evolutionary Biology* **27**: 1536-1548.

Souza, L. and Santucci, R. (2014). Body size evolution in Titanosauriformes (Sauropoda, Macronaria). *Journal of Evolutionary Biology* **27**(9): 2001-2012.

Spicer, R. A. and Parrish, J. T. (1990). Late Cretaceous–early Tertiary palaeoclimates of northern high latitudes: a quantitative view. *Journal of the Geological Society* **147**(2): 329-341.

Starrfelt, J. and Liow, L. H. (2016). How many dinosaur species were there? Fossil bias and true richness estimated using a Poisson sampling model. *Philosophical Transactions of the Royal Society B: Biological Sciences* **371**(1691): 20150219.

Steel, R. (1973). Crocodylia, Stuttgart; Portland USA: Gustav Fischer.

Sterli, J., Marcelo, S. and Umazano, A. M. (2013a). New remains and new insights on the Gondwanan meiolaniform turtle *Chubutemys copelloi* from the Lower Cretaceous of Patagonia, Argentina. *Gondwana Research* **27**(3): 978–994.

Sterli, J., Pol, D. and Laurin, M. (2013b). Incorporating phylogenetic uncertainty on phylogeny‐based palaeontological dating and the timing of turtle diversification. *Cladistics* **29**(3): 233-246.

Stevens, N. J., Hill, R. V., Al-Wosabi, M., Schulp, A., As-Saruri, M., Al-Nimey, F., Jolley, L. A., Schulp-Stuip, Y. and O'Connor, P. (2013). A middle Eocene mesoeucrocodylian (Crocodyliformes) from the Kaninah Formation, Republic of Yemen. *Geologos* **19**(3): 175-183.

Stinnesbeck, W., Frey, E., Rivas, L., Pérez, J. P., Cartes, M. L., Soto, C. S. and Lobos, P. Z. (2014). A Lower Cretaceous ichthyosaur graveyard in deep marine slope channel deposits at Torres del Paine National Park, southern Chile. *Geological Society of America Bulletin* **126**(9-10): 1317-1339.

Storrs, G. W. and Efimov, M. B. (2000). Mesozoic crocodyliforms of north-central Eurasia. *The Age of Dinosaurs in Russia and Mongolia*. M. J. Benton, M. A. Shishkin, D. M. Unwin and E. N. Kurochkin. Cambridge, UK, Cambridge University Press**:** 402-419.

Strong, E. E. and Lipscomb, D. (1999). Character coding and inapplicable data. *Cladistics* **15**(4): 363-371.

Stubbs, T. L. and Benton, M. J. (2016). Ecomorphological diversifications of Mesozoic marine reptiles: the roles of ecological opportunity and extinction. *Paleobiology*, 10.1017/pab.2016.15: 1-27.

Sullivan, C., Wang, Y., Hone, D. W., Wang, Y., Xu, X. and Zhang, F. (2014). The vertebrates of the Jurassic Daohugou Biota of northeastern China. *Journal of Vertebrate Paleontology* **34**(2): 243-280.

Sutcliffe, O. E., Dowdeswell, J. A., Whittington, R. J., Theron, J. N. and Craig, J. (2000). Calibrating the Late Ordovician glaciation and mass extinction by the eccentricity cycles of Earth's orbit. *Geology* **28**(11): 967-970.

Sweetman, S. C., Pedreira-Segade, U. and Vidovic, S. U. (2015). A new bernissartiid crocodyliform from the Lower Cretaceous Wessex Formation (Wealden Group, Barremian) of the Isle of Wight, southern England. *Acta Palaeontologica Polonica* **60**(2): 257-268.

Tardy, Y., Nkounkou, R.-R. and Probst, J.-L. (1989). The global water cycle and continental erosion during Phanerozoic time (570 my). *American Journal of Science* **289**: 455-483.

Taylor, A. M., Gowland, S., Leary, S. and Martinius, A. W. (2014). Stratigraphical correlation of the Late Jurassic Lourinhã Formation in the Consolação Sub‐basin (Lusitanian Basin), Portugal. *Geological Journal* **49**(2): 143-162.

Taylor, P. (1994). An early cheilosteme bryozoan from the Upper Jurassic of Yemen. *Neues Jahrbuch fur Geologie und Palaontologie-Abhandlungen* **191**(3): 331-344.

Taylor, P. D. and Ernst, A. (2008). Bryozoans in transition: the depauperate and patchy Jurassic biota. *Palaeogeography, Palaeoclimatology, Palaeoecology* **263**(1): 9-23.

Taylor, P. D. and Waeschenbach, A. (2015). Phylogeny and diversification of bryozoans. *Palaeontology* **58**(4): 585-599.

Tennant, J. P. and Mannion, P. D. (2014). Revision of the Late Jurassic crocodyliform *Alligatorellus*, and evidence for allopatric speciation driving high diversity in western European atoposaurids. *PeerJ* **2**: e599.

Tennant, J. P., Mannion, P. D. and Upchurch, P. (2016). Environmental drivers of crocodyliform extinction across the Jurassic/Cretaceous transition. *Proceedings of the Royal Society of London B: Biological Sciences* **283**(1826).

Thies, D. and Broschinski, A. (2001). Teeth of a small durophagous crocodiles from the Late Jurassic (Kimmeridgian) of North Germany. *Geologische Beiträge Hannover* **2**: 65-70.

Thies, D., Windolf, R. and Mudroch, A. (1997). First record of Atoposauridae (Crocodylia: Metamesosuchia) in the Upper Jurassic (Kimmeridgian) of northwest Germany. *Neues Jahrbuch für Geologie und Paläontologie* **205**: 393-411.

Tong, H., Claude, J., Suteethorn, V., Naksri, W. and Buffetaut, E. (2009). Turtle assemblages of the Khorat Group (Late Jurassic-Early Cretaceous) of NE Thailand and their palaeobiogeographical significance. *Late Palaeozoic and Mesozoic Ecosystems in SE Asia*. E. Buffetaut, G. Cuny, J. Le Loeuff and V. Suteethorn. London, Geological Society of London. **315:** 141-152.

Toon, O. B., Zahnle, K., Morrison, D., Turco, R. P. and Covey, C. (1997). Environmental perturbations caused by the impacts of asteroids and comets. *Reviews of Geophysics* **35**(1): 41-78.

Tortosa, T., Buffetaut, E., Vialle, N., Dutour, Y., Turini, E. and Cheylan, G. (2014). A new abelisaurid dinosaur from the Late Cretaceous of southern France: Palaeobiogeographical implications. *Annales De Paleontologie* **100**(1): 63-86.

Tremolada, F., Bornemann, A., Bralower, T. J., Koeberl, C. and van de Schootbrugge, B. (2006). Paleoceanographic changes across the Jurassic/Cretaceous boundary: The calcareous phytoplankton response. *Earth and Planetary Science Letters* **241**(3): 361-371.

Turner, A. H. (2006). Osteology and phylogeny of a new species of *Araripesuchus* (Crocodyliformes: Mesoeucrocodylia) from the Late Cretaceous of Madagascar. *Historical Biology* **18**(3): 255-369.

Turner, A. H. (2015). A Review of *Shamosuchus* and *Paralligator* (Crocodyliformes, Neosuchia) from the Cretaceous of Asia. *PLOS ONE* **10**(2): e0118116.

Turner, A. H. and Buckley, G. A. (2008). *Mahajangasuchus insignis* (Crocodyliformes: Mesoeucrocodylia) cranial anatomy and new data on the origin of the eusuchian-style palate. *Journal of Vertebrate Paleontology* **28**(2): 382-408.

Turner, A. H. and Calvo, J. O. (2005). A new sebecosuchian crocodyliform from the Late Cretaceous of Patagonia. *Journal of Vertebrate Paleontology* **25**(1): 87-98.

Turner, A. H. and Pritchard, A. C. (2015). The monophyly of Susisuchidae (Crocodyliformes) and its phylogenetic placement in Neosuchia. *PeerJ* **3**: e759.

Turner, A. H. and Sertich, J. J. (2010). Phylogenetic history of *Simosuchus clarki* (Crocodyliformes: Notosuchia) from the Late Cretaceous of Madagascar. *Journal of Vertebrate Paleontology* **30**(sup1): 177-236.

Twitchett, R. J. (2006). The palaeoclimatology, palaeoecology and palaeoenvironmental analysis of mass extinction events. *Palaeogeography, Palaeoclimatology, Palaeoecology* **232**(2): 190-213.

Tykoski, R. S., Rowe, T. B., Ketcham, R. A. and Colbert, M. W. (2002). *Calsoyasuchus valliceps*, a new crocodyliform from the Early Jurassic Kayenta Formation of Arizona. *Journal of Vertebrate Paleontology* **22**(3): 593-611.

Underwood, C. J. (2006). Diversification of the Neoselachii (Chondrichthyes) during the Jurassic and Cretaceous. *Paleobiology* **32**(2): 215-235.

Unwin, D. and Martill, D. (2007). Pterosaurs of the Crato Formation. *The Crato Fossil Beds of Brazil: Window into an Ancient World*. D. Martill, G. Bechly and B. Loveridge. Cambridge, Cambridge University Press**:** 475-524.

Unwin, D. M. (2003). On the phylogeny and evolutionary history of pterosaurs. *Evolution and Palaeobiology of Pterosaurs*. E. Buffetaut and J.-M. Mazin. London, Geological Society of London. **217:** 139-190.

Upchurch, P., Andres, B., Butler, R. J. and Barrett, P. M. (2014). An analysis of pterosaurian biogeography: implications for the evolutionary history and fossil record quality of the first flying vertebrates. *Historical Biology* **27**(6): 697-717.

Upchurch, P. and Barrett, P. M. (2005). Phylogenetic and taxic perspectives on sauropod diversity. *The Sauropods: Evolution and Paleobiology*. K. A. Curry Rogers and J. A. Wilson. Berkeley, University of California Press**:** 104-124.

Upchurch, P., Mannion, P., Benson, R., Butler, R. and Carrano, M. (2011a). Geological and anthropogenic controls on the sampling of the terrestrial fossil record: a case study from the Dinosauria. *Geological Society, London, Special Publications* **358**(1): 209-240.

Upchurch, P., Mannion, P., Benson, R., Butler, R. and Carrano, M. (2011b). Geological and anthropogenic controls on the sampling of the terrestrial fossil record: a case study from the Dinosauria. *Comparing the Geological and Fossil Records: Implications for Biodiversity Studies*. A. J. McGowan and A. B. Smith. London, Geological Society of London. **358:** 209-240.

Upchurch, P. and Mannion, P. D. (2012). Dinosaur evolution and extinction across the Jurassic/Cretaceous boundary. *Actas de V Jornadas Internacionales sobre Paleontología de Dinosaurios y su Entorno, Salas de los Infantes, Burgos*: 135-155.

Upchurch, P., Mannion, P. D. and Taylor, M. P. (2015). The Anatomy and phylogenetic relationships of "*Pelorosaurus*" *becklesii* (Neosauropoda, Macronaria) from the Early Cretaceous of England. *PLOS ONE* **10**(6): e0125819.

Valentine, J. and Moores, E. (1970). Plate-tectonic regulation of faunal diversity and sea level: a model. *Nature* **228**: 657-669.

Valentine, J. W. (1971). Plate tetonics and shallow marine diversity and endemism, an actualistic model. *Systematic Biology* **20**(3): 253-264.

Valentine, J. W. and Moores, E. M. (1972). Global tectonics and the fossil record. *The Journal of Geology* **80**(2): 167-184.

Valentine, J. W. and Moores, E. M. (1974). Plate tectonics and the history of life in the oceans. *Scientific American* **230**: 80-89.

Vaughan, A., Wareham, C., Johnson, A. and Kelley, S. (1998). A Lower Cretaceous, syn-extensional magmatic source for a linear belt of positive magnetic anomalies: the Pacific Margin Anomaly (PMA), western Palmer Land, Antarctica. *Earth and Planetary Science Letters* **158**(3): 143-155.

Vaughan, A. P. and Pankhurst, R. J. (2008). Tectonic overview of the West Gondwana margin. *Gondwana Research* **13**(2): 150-162.

Veevers, J., Powell, C. M. and Roots, S. (1991). Review of seafloor spreading around Australia. I. Synthesis of the patterns of spreading. *Australian journal of earth sciences* **38**(4): 373-389.

Velo-Antón, G., Godinho, R., Campos, J. C. and Brito, J. C. (2014). Should I stay or should I go? Dispersal and population structure in small, isolated desert populations of West African crocodiles. *PLOS ONE* **9**(4): e94626.

Vennari, V. V., Lescano, M., Naipauer, M., Aguirre-Urreta, B., Concheyro, A., Schaltegger, U., Armstrong, R., Pimentel, M. and Ramos, V. A. (2014). New constraints on the Jurassic–Cretaceous boundary in the High Andes using high-precision U–Pb data. *Gondwana Research* **26**(1): 374-385.

Verdade, L. (2000). Regression equations between body and head measurements in the broad-snouted caiman (*Caiman latirostris*). *Revista Brasileira de Biologia* **60**(3): 469-482.

Vergara, M., Levi, B., Nyström, J. O. and Cancino, A. (1995). Jurassic and Early Cretaceous island arc volcanism, extension, and subsidence in the Coast Range of central Chile. *Geological Society of America Bulletin* **107**(12): 1427-1440.

Vickaryous, M. K. and Hall, B. K. (2008). Development of the dermal skeleton in *Alligator mississippiensis* (Archosauria, Crocodylia) with comments on the homology of osteoderms. *Journal of morphology* **269**(4): 398-422.

Vidal, L. M. (1915). Nota geologica y paleontologica sobre e Jurasico Superior de la Provincia de Lérida. *Boliten del Instetuto Geológico de Espana* **16**: 17-55.

Vilhena, D. A. and Smith, A. B. (2013). Spatial bias in the marine fossil record. *PLOS ONE* **8**(10): e74470.

Villamarín, F., Marioni, B., Thorbjarnarson, J. B., Nelson, B. W., Botero-Arias, R. and Magnusson, W. E. (2011). Conservation and management implications of nest-site selection of the sympatric crocodilians *Melanosuchus niger* and *Caiman crocodilus* in Central Amazonia, Brazil. *Biological Conservation* **144**(2): 913-919.

Vinarski, M., Bondarev, A. and Markov, A. (2011). Mollusks in Phanerozoic marine communities: Implications from the analysis of global paleontological databases. *Paleontological Journal* **45**(4): 358-369.

Voje, K. L., Holen, Ø. H., Liow, L. H. and Stenseth, N. C. (2015). The role of biotic forces in driving macroevolution: beyond the Red Queen. *Proceedings of the Royal Society of London B: Biological Sciences* **282**(1808): 20150186.

von Huene, F. (1931). Verschiedene Mesozoische Wirbeltierreste aus Südamerika. *Neues Jahrbuch für Mineralogie, Geologie, Paläontologie Monastshefte* **66**: 181-198.

von Zittel, K. A. (1890). Palaeozoologie: Vertebrata (Pisces, Amphibia, Reptilia, Aves). München and Leipzig, R. Oldenbourg.

Vörös, A. (2010). Escalation reflected in ornamentation and diversity history of brachiopod clades during the Mesozoic marine revolution. *Palaeogeography, Palaeoclimatology, Palaeoecology* **291**(3): 474-480.

Vullo, R., Abit, D., Ballèvre, M., Billon-Bruyat, J.-P., Bourgeais, R., Buffetaut, É., Daviero-Gomez, V., Garcia, G., Gomez, B. and Mazin, J.-M. (2014). Palaeontology of the Purbeck-type (Tithonian, Late Jurassic) bonebeds of Chassiron (Oléron Island, western France). *Comptes Rendus Palevol* **13**(5): 421-441.

Vullo, R. and Neraudeau, D. (2008). Cenomanian vertebrate assemblages from southwestern France: a new insight into the European mid-Cretaceous continental fauna. *Cretaceous Research* **29**(5): 930-935.

Wagner, P. J. (2000). The quality of the fossil record and the accuracy of phylogenetic inferences about sampling and diversity. *Systematic Biology* **49**(1): 65-86.

Walker, A. D. (1970). A revision of the Jurassic reptile Hallopus victor (Marsh), with remarks on the classification of crocodiles. *Philosophical Transactions of the Royal Society of London B: Biological Sciences* **257**(816): 323-372.

Wall, P. D., Ivany, L. C. and Wilkinson, B. H. (2009). Revisiting Raup: exploring the influence of outcrop area on diversity in light of modern sample-standardization techniques. *Paleobiology* **35**(1): 146-167.

Wall, P. D., Ivany, L. C. and Wilkinson, B. H. (2011). Impact of outcrop area on estimates of Phanerozoic terrestrial biodiversity trends. *Comparing the Geological and Fossil Records: Implications for Biodiversity Studies*. A. B. Smith and A. J. McGowan. London, Geological Society of London. **358:** 43-62.

Walliser, O. (1996). Global Events and Event Stratigraphy in the Phanerozoic. Berlin, Heidelberg, Springer.

Wang, F., Zhou, X.-H., Zhang, L.-C., Ying, J.-F., Zhang, Y.-T., Wu, F.-Y. and Zhu, R.-X. (2006). Late Mesozoic volcanism in the Great Xing'an Range (NE China): timing and implications for the dynamic setting of NE Asia. *Earth and Planetary Science Letters* **251**(1): 179-198.

Wang, M. and Lloyd, G. T. (2016). Rates of morphological evolution are heterogeneous in Early Cretaceous birds. *Proceedings of the Royal Society of London B: Biological Sciences* **283**: 20160214.

Wang, M., Wang, X., Wang, Y. and Zhou, Z. (2016a). A new basal bird from China with implications for morphological diversity in early birds. *Scientific Reports* **6**.

Wang, M., Zhou, Z. and Zhou, S. (2016b). A new basal ornithuromorph bird (Aves: Ornithothoraces) from the Early Cretaceous of China with implication for morphology of early Ornithuromorpha. *Zoological Journal of the Linnean Society* **176**(1): 207-223.

Wang, X., Kellner, A. W., Jiang, S. and Meng, X. (2009). An unusual long-tailed pterosaur with elongated neck from western Liaoning of China. *Anais da Academia Brasileira de Ciências* **81**(4): 793-812.

Wang, X., O'Connor, J. K., Zheng, X., Wang, M., Hu, H. and Zhou, Z. (2014). Insights into the evolution of rachis dominated tail feathers from a new basal enantiornithine (Aves: Ornithothoraces). *Biological Journal of the Linnean Society* **113**(3): 805-819.

Wang, Y.-M., O'Connor, J. K., Li, D.-Q. and You, H.-L. (2013). Previously unrecognized ornithuromorph bird diversity in the Early Cretaceous Changma Basin, Gansu Province, northwestern China. *PLOS ONE* **8**(10): e77693.

Wang, Y. and Evans, S. E. (2006). A new short-bodied salamander from the Upper Jurassic/Lower Cretaceous of China. *Acta Palaeontologica Polonica* **51**(1): 127.

Weaver, J. P., Rodriguez, D., Venegas‐Anaya, M., Cedeño‐Vázquez, J. R., Forstner, M. R. and Densmore, L. D. (2008). Genetic characterization of captive Cuban crocodiles (*Crocodylus rhombifer*) and evidence of hybridization with the American crocodile (*Crocodylus acutus*). *Journal of Experimental Zoology Part A: Ecological Genetics and Physiology* **309**(10): 649-660.

Wei, W. W.-S. (1994). Time Series Analysis: Univariate and Multivariate Methods. Redwood City, California, Addison-Wesley.

Weishampel, D. B., Csiki, Z., Benton, M. J., Grigorescu, D. and Codrea, V. (2010). Palaeobiogeographic relationships of the Haţeg biota—Between isolation and innovation. *Palaeogeography, Palaeoclimatology, Palaeoecology* **293**(3): 419-437.

Weissert, H. and Channell, J. (1989). Tethyan carbonate carbon isotope stratigraphy across the Jurassic‐Cretaceous boundary: An indicator of decelerated global carbon cycling? *Paleoceanography* **4**(4): 483-494.

Weissert, H. and Erba, E. (2004). Volcanism, CO_2 and palaeoclimate: a Late Jurassic-Early Cretaceous carbon and oxygen isotope record. *Journal of the Geological Society* **161**: 695-702.

Weissert, H., Lini, A., Föllmi, K. B. and Kuhn, O. (1998). Correlation of Early Cretaceous carbon isotope stratigraphy and platform drowning events: a possible link? *Palaeogeography, Palaeoclimatology, Palaeoecology* **137**(3): 189-203.

Weissert, H. and Mohr, H. (1996). Late Jurassic climate and its impact on carbon cycling. *Palaeogeography, Palaeoclimatology, Palaeoecology* **122**(1): 27-43.

Wellnhofer, P. (1970). Die Pterodactyloidea (Pterosauria) der Oberjura-Plattenkalke Suddeutschlands. *Bayerische Akademie der Wissenschaften, Mathematisch-Wissenschaftlichen Klasse, Abhandlungen* **141**: 1-133.

Wellnhofer, P. (1971). Die Atoposauridae (Crocodylia, Mesosuchia) der Oberjura-Plattenkalke Bayerns. *Palaeontographica Abteilung A* **138**(5-6): 133-165.

Werner, C. (1994). Die kontinentale Wirbeltierfauna aus der unteren Oberkreide des Sudan (Wadi Milk Formation). *Berliner Geowissenschaftliche Abhandlungen (E)* **13**: 221-249.

Wignall, P. (2001). Large igneous provinces and mass extinctions. *Earth-Science Reviews* **53**(1): 1-33.

Wignall, P. B. and Hallam, A. (1991). Biofacies, stratigraphic distribution and depositional models of British onshore Jurassic black shales. *Modern and Ancient Continental Shelf Anoxia*. R. V. Tyson and T. H. Pearson. London, Geological Society of London. **58:** 291-309.

Wignall, P. B. and Twitchett, R. J. (1996). Oceanic anoxia and the end Permian mass extinction. *Science* **272**(5265): 1155.

Wilberg, E. W. (2015). What's in an outgroup? The impact of outgroup choice on the phylogenetic position of Thalattosuchia (Crocodylomorpha) and the origin of Crocodyliformes. *Systematic Biology* **64**(4): 621-637.

Wilkinson, L. E., Young, M. T. and Benton, M. J. (2008). A new metriorhynchid crocodilian (Mesoeucrocodylia: Thalattosuchia) from the Kimmeridgian (Upper Jurassic) of Wiltshire, UK. *Palaeontology* **51**(6): 1307-1333.

Williamson, T. E., Brusatte, S. L. and Wilson, G. P. (2014). The origin and early evolution of metatherian mammals: the Cretaceous record. *ZooKeys* **465**: 1-76.

Williston, S. W. (1906). American amphicoelian crocodiles. *The Journal of Geology* **14**(1): 1-17.

Wilson, G. P., Evans, A. R., Corfe, I. J., Smits, P. D., Fortelius, M. and Jernvall, J. (2012). Adaptive radiation of multituberculate mammals before the extinction of dinosaurs. *Nature* **483**(7390): 457-460.

Wilson, J. A. (2005). Redescription of the Mongolian sauropod *Nemegtosaurus mongoliensis* Nowinski (Dinosauria: Saurischia) and comments on Late Cretaceous sauropod diversity. *Journal of Systematic Palaeontology* **3**(03): 283-318.

Wilson, J. A., Malkani, M. S. and Gingerich, P. D. (2001). New crocodyliform (Reptilia, Mesoeucrocodylia) from the Upper Cretaceous Pab Formation of Vitakri, Balochistan (Pakistan). *Contributions from the Museum of Paleontology, The University of Michigan* **30**(12): 321-336.

Wilson, M., Guiraud, R., Moreau, C. and Bellion, Y.-C. (1998). Late Permian to Recent magmatic activity on the African-Arabian margin of Tethys. *Petroleum Geology of North Africa*. D. S. MacGregor, R. T. J. Moody and D. D. Clark-Lowes. London, Geological Society of London. **132:** 231-263.

Wimbledon, W., Casellato, C. E., Reháková, D., Bulot, L. G., Erba, E., Gardin, S., Verreussel, R. M. C. H., Munsterman, D. K. and Hunt, C. O. (2011). Fixing a basal Berriasian and Jurassic/Cretaceous (J/K) boundary—is there perhaps some light at the end of the tunnel. *Rivista Italiana di Paleontologia e Stratigrafia* **117**(2): 295-307.

Winkler, D. A., Murry, P. A. and Jacobs, L. L. (1990). Early Cretaceous (Comanchean) vertebrates of central Texas. *Journal of Vertebrate Paleontology* **10**(1): 95-116.

Woodward, A. S. (1885). IV.—On the Literature and Nomenclature of British Fossil Crocodilia. *Geological Magazine (Decade III)* **2**(11): 496-510.

Wright, A. M., Lloyd, G. T. and Hillis, D. M. (2015). Modeling character change heterogeneity in phylogenetic analyses of morphology through the use of priors. *Systematic Biology*, 10.1093/sysbio/syv122.

Wu, X.-C. and Brinkman, D. B. (1993). A new crocodylomorph of “mesosuchian” grade from the Upper Cretaceous Upper Milk River Formation, southern Alberta. *Journal of Vertebrate Paleontology* **13**(2): 153-160.

Wu, X.-C., Brinkman, D. B. and Lu, J.-C. (1994). A new species of *Shantungosuchus* from the Lower Cretaceous of Inner Mongolia (China), with comments on *S. chuhsienensis* Young, 1961 and the phylogenetic position of the genus. *Journal of Vertebrate Paleontology* **14**(2): 210-229.

Wu, X.-C., Brinkman, D. B. and Russell, A. P. (1996a). *Sunosuchus junggarensis* sp. *nov*. (Archosauria: Crocodyliformes) from the Upper Jurassic of Xinjiang, People's Republic of China. *Canadian Journal of Earth Sciences* **33**(4): 606-630.

Wu, X.-C., Cheng, Z.-W. and Russell, A. P. (2001a). Cranial anatomy of a new crocodyliform (Archosauria: Crocodylomorpha) from the Lower Cretaceous of Song-Liao Plain, northeastern China. *Canadian Journal of Earth Sciences* **38**(12): 1653-1663.

Wu, X.-C., Russell, A. P. and Cumbaa, S. L. (2001b). *Terminonaris* (Archosauria: Crocodyliformes): new material from Saskatchewan, Canada, and comments on its phylogenetic relationships. *Journal of Vertebrate Paleontology* **21**(3): 492-514.

Wu, X.-C. and Sues, H.-D. (1996). Anatomy and phylogenetic relationships of *Chimaerasuchus paradoxus*, an unusual crocodyliform reptile from the Lower Cretaceous of Hubei, China. *Journal of Vertebrate Paleontology* **16**(4): 688-702.

Wu, X.-C., Sues, H.-D. and Brinkman, D. (1996b). An atoposaurid neosuchian (Archosauria: Crocodyliformes) from the Lower Cretaceous of Inner Mongolia (People's Republic of China). *Canadian Journal of Earth Sciences* **33**(4): 599-605.

Wu, X.-C., Sues, H.-D. and Dong, Z.-M. (1997). *Sichuanosuchus shuhanensis*, a new? Early Cretaceous protosuchian (Archosauria: Crocodyliformes) from Sichuan (China), and the monophyly of Protosuchia. *Journal of Vertebrate Paleontology* **17**(1): 89-103.

Wu, X., Xue, H., Wu, L., Zhu, J. and Wang, R. (2006). Regression analysis between body and head measurements of Chinese alligators (*Alligator sinensis*) in the captive population. *Animal biodiversity and conservation* **29**(1): 65-71.

Xiaolin, W. and Zhonghe, Z. (2006). Pterosaur assemblages of the Jehol Biota and their implication for the Early Cretaceous pterosaur radiation. *Geological Journal* **41**(3‐4): 405-418.

Xing, L., Lockley, M. G., Zhang, J., Klein, H., Persons, W. S. and Dai, H. (2014). Diverse sauropod-, theropod-, and ornithopod-track assemblages and a new ichnotaxon *Siamopodus xui* ichnosp. *nov*. from the Feitianshan Formation, Lower Cretaceous of Sichuan Province, southwest China. *Palaeogeography, Palaeoclimatology, Palaeoecology* **414**: 79-97.

Xu, X., Forster, C. A., Clark, J. M. and Mo, J. (2006). A basal ceratopsian with transitional features from the Late Jurassic of northwestern China. *Proceedings of the Royal Society of London Series B: Biological Sciences* **273**(1598): 2135-2140.

Xu, X., You, H., Du, K. and Han, F. (2011). An *Archaeopteryx*-like theropod from China and the origin of Avialae. *Nature* **475**(7357): 465-470.

Young, C. (1937). New Triassic and Cretaceous reptiles in China. *Bulletin of The Geological Society of China* **17**(1): 109-120.

Young, C. (1961). On a new crocodile from Chuhsien, E. Shantung. *Vertebrata PalAsiatica* **1**: 6-10.

Young, M. T. (2014). Filling the ‘Corallian Gap’: re-description of a metriorhynchid crocodylomorph from the Oxfordian (Late Jurassic) of Headington, England. *Historical Biology* **26**(1): 80-90.

Young, M. T., Bell, M. A. and Brusatte, S. L. (2011a). Craniofacial form and function in Metriorhynchidae (Crocodylomorpha: Thalattosuchia): modelling phenotypic evolution with maximum-likelihood methods. *Biology Letters* **7**(6): 913-916.

Young, M. T., Bell, M. A., De Andrade, M. B. and Brusatte, S. L. (2011b). Body size estimation and evolution in metriorhynchid crocodylomorphs: implications for species diversification and niche partitioning. *Zoological Journal of the Linnean Society* **163**(4): 1199-1216.

Young, M. T., Brusatte, S. L., De Andrade, M. B., Desojo, J. B., Beatty, B. L., Steel, L., Fernández, M. S., Sakamoto, M., Ruiz-Omeñaca, J. I. and Schoch, R. R. (2012). The cranial osteology and feeding ecology of the metriorhynchid crocodylomorph genera *Dakosaurus* and *Plesiosuchus* from the Late Jurassic of Europe. *PLOS ONE* **7**(9): e44985.

Young, M. T., Brusatte, S. L., Ruta, M. and de Andrade, M. B. (2010). The evolution of Metriorhynchoidea (Mesoeucrocodylia, Thalattosuchia): an integrated approach using geometric morphometrics, analysis of disparity, and biomechanics. *Zoological Journal of the Linnean Society* **158**(4): 801-859.

Young, M. T. and de Andrade, M. B. (2009). What is *Geosaurus*? Redescription of *Geosaurus giganteus* (Thalattosuchia: Metriorhynchidae) from the Upper Jurassic of Bayern, Germany. *Zoological Journal of the Linnean Society* **157**(3): 551-585.

Young, M. T., de Andrade, M. B., Brusatte, S. L., Sakamoto, M. and Liston, J. (2013a). The oldest known metriorhynchid super-predator: a new genus and species from the Middle Jurassic of England, with implications for serration and mandibular evolution in predacious clades. *Journal of Systematic Palaeontology* **11**(4): 475-513.

Young, M. T., de Andrade, M. B., Cornee, J. J., Steel, L. and Foffa, D. (2014a). Re-description of a putative Early Cretaceous "teleosaurid" from France, with implications for the survival of metriorhynchids and teleosaurids across the Jurassic-Cretaceous Boundary. *Annales De Paleontologie* **100**(2): 165-174.

Young, M. T., De Andrade, M. B., Etches, S. and Beatty, B. L. (2013b). A new metriorhynchid crocodylomorph from the Lower Kimmeridge Clay Formation (Late Jurassic) of England, with implications for the evolution of dermatocranium ornamentation in Geosaurini. *Zoological Journal of the Linnean Society* **169**(4): 820-848.

Young, M. T., Hua, S., Steel, L., Foffa, D., Brusatte, S. L., Thüring, S., Mateus, O., Ruiz-Omeñaca, J. I., Havlik, P. and Lepage, Y. (2014b). Revision of the Late Jurassic teleosaurid genus *Machimosaurus* (Crocodylomorpha, Thalattosuchia). *Royal Society Open Science* **1**(2): 140222.

Young, M. T., Steel, L., Foffa, D., Price, T., Naish, D. and Tennant, J. P. (2014c). Marine tethysuchian crocodyliform from the? Aptian - Albian (Lower Cretaceous) of the Isle of Wight, UK. *Biological Journal of the Linnean Society* **113**(3): 854-871.

Young, M. T., Tennant, J. P., Brusatte, S. L., Challands, T. J., Fraser, N. C., Clark, N. D. and Ross, D. A. (2016). The first definitive Middle Jurassic atoposaurid (Crocodylomorpha, Neosuchia), and a discussion on the genus *Theriosuchus*. *Zoological Journal of the Linnean Society* **176**(2): 443-462.

Yuan, C.-X., Ji, Q., Meng, Q.-J., Tabrum, A. R. and Luo, Z.-X. (2013). Earliest evolution of multituberculate mammals revealed by a new Jurassic fossil. *Science* **341**(6147): 779-783.

Yuan, W. (2000). A new salamander (Amphibia: Caudata) from the Early Cretaceous Jehol biota. *Vertebrata PalAsiatica* **2**: 002.

Zaher, H., Pol, D., Carvalho, A. B., Riccomini, C., Campos, D. and Nava, W. (2006). Redescription of the cranial morphology of *Mariliasuchus amarali*, and its phylogenetic affinities (Crocodyliformes, Notosuchia). *American Museum Novitates* **3512**: 1-40.

Žák, K., Košťák, M., Man, O., Zakharov, V. A., Rogov, M. A., Pruner, P., Rohovec, J., Dzyuba, O. S. and Mazuch, M. (2011). Comparison of carbonate C and O stable isotope records across the Jurassic/Cretaceous boundary in the Tethyan and Boreal Realms. *Palaeogeography, Palaeoclimatology, Palaeoecology* **299**(1): 83-96.

Zakharov, V., Lapukhov, A. and Shenfil, O. (1993). Iridium anomaly at the Jurassic–Cretaceous boundary in northern Siberia. *Russian Journal of Geology and Geophysics* **34**: 83-90.

Zakharov, V. and Yanine, B. (1975). Les bivalves á la fin du Jurassique et au début du Crétacé. *Mémoires du Bureau de Recherches Géologiques et Minieres* **86**: 221-228.

Zakharov, V. A., Bown, P. and Rawson, P. F. (1996). The Berriasian stage and the Jurassic-Cretaceous boundary. *Proceedings of the Second International Symposium on Cretaceous Stage Boundaries*. R. P.F., Dhondt A.V, H. J.M. and K. W.J, Bulletin de l'Institut Royal des Sciences Naturelles de Belgique, Sciences de la Terre. **66:** 7-10.

Zakharov, V. A., Rogov, M. A., Dzyuba, O. S., Žák, K., Košťák, M., Pruner, P., Skupien, P., Chadima, M., Mazuch, M. and Nikitenko, B. L. (2014). Palaeoenvironments and palaeoceanography changes across the Jurassic/Cretaceous boundary in the Arctic realm: case study of the Nordvik section (north Siberia, Russia). *Polar Research* **33**: 19714.

Zammit, M. (2012). Cretaceous ichthyosaurs: dwindling diversity, or the empire strikes back? *Geosciences* **2**(2): 11-24.

Zanno, L. E. and Makovicky, P. J. (2013). Neovenatorid theropods are apex predators in the Late Cretaceous of North America. *Nature Communications* **4**: 2827.

Zhang, G., Wang, Y., Jones, M. E. and Evans, S. E. (2009). A new Early Cretaceous salamander (*Regalerpeton weichangensis* gen. *et* sp. *nov*.) from the Huajiying Formation of northeastern China. *Cretaceous Research* **30**(3): 551-558.

Zhang, M., Dai, S., Heimhofer, U., Wu, M., Wang, Z. and Pan, B. (2014). Palynological records from two cores in the Gongpoquan Basin, central East Asia: Evidence for floristic and climatic change during the Late Jurassic to Early Cretaceous. *Review of Palaeobotany and Palynology* **204**: 1-17.

Zheng, X., Bi, S., Wang, X. and Meng, J. (2013). A new arboreal haramiyid shows the diversity of crown mammals in the Jurassic period. *Nature* **500**(7461): 199-202.

Zhou, C.-F. and Rabi, M. (2015). A sinemydid turtle from the Jehol Biota provides insights into the basal divergence of crown turtles. *Scientific Reports* **5**(16299).

Zhou, Z. and Wang, Y. (2010). Vertebrate diversity of the Jehol Biota as compared with other lagerstätten. *Science China Earth Sciences* **53**(12): 1894-1907.

Ziegler, P. A. (1988). Evolution of the Arctic-North Atlantic and Western Tethys - A visual presentation of a series of paleogegraphic-paleotectonic maps. *AAPG memoir* **43**: 164-196.

Zorina, S. O., Dzyuba, O. S., Shurygin, B. N. and Ruban, D. A. (2008). How global are the Jurassic–Cretaceous unconformities? *Terra Nova* **20**(5): 341-346.

Zverkov, N., Arkhangelsky, M., Pardo Pérez, J. and Beznosov, P. (2015). On the Upper Jurassic ichthyosaur remains from the Russian north. *Proceedings of the Zoological Institute RAS* **319**: 81-97.

Appendix 1 – Additional details regarding crocodyliform supertree construction. Note that these analyses were perform prior to the atoposaurid phylogenetic analyses in Chapter 5.

Higher Taxon	Species	Included in Supertree	Source	Notes
Aegyptosuchidae	*Aegisuchus witmeri*	Yes	Holliday and Gardner 2012	
Aegyptosuchidae	*Aegyptosuchus peyeri*	Yes	Holliday and Gardner 2012	
Atoposauridae	*Alligatorellus bavaricus*	Yes	Tennant and Mannion 2014	
Atoposauridae	*Alligatorellus beaumonti*	Yes	Tennant and Mannion 2014	
Atoposauridae	*Alligatorium franconicum*	Yes	Martin et al 2010	
Atoposauridae	*Alligatorium meyeri*	Yes	Martin et al 2010	
Atoposauridae	*Atoposaurus jourdani*	Yes	Tennant and Mannion 2014	
Atoposauridae	*Atoposaurus oberndorferi*	Yes	Tennant and Mannion 2014	
Atoposauridae	*Brillanceausuchus babouriensis*	No	Michard et al 1990	Uncertain phylogenetic affinities
Atoposauridae	*Karatausuchus sharovi*	No	Storrs and Efimov 1976	Uncertain phylogenetic affinities
Atoposauridae	*Montsecosuchus depereti*	Yes	Tennant and Mannion 2014	
Atoposauridae	*Theriosuchus grandinaris*	Yes	Tennant and Mannion 2014	
Atoposauridae	*Theriosuchus guimarotae*	Yes	Martin et al. 2010	
Atoposauridae	*Theriosuchus ibericus*	Yes	Tennant and Mannion 2014	
Atoposauridae	*Theriosuchus pusillus*	Yes	Martin et al. 2010	
Atoposauridae	*Theriosuchus sympiestodon*	Yes	Martin et al. 2010	
Baurusuchidae	*Aplestosuchus sordidus*	Yes	Godoy et al. 2014	
Baurusuchidae	*Baurusuchus albertoi*	Yes	Pol et al. 2014	
Baurusuchidae	*Baurusuchus pachecoi*	Yes	Pol et al. 2014	
Baurusuchidae	*Baurusuchus salgadoensis*	Yes	Pol et al. 2014	
Baurusuchidae	*Campinasuchus dinizi*	Yes	Pol et al. 2014	
Baurusuchidae	*Cynodontosuchus rothi*	Yes	Pol et al. 2014	

Baurusuchidae	*Gondwanasuchus scabrosus*	Yes	Godoy et al. 2014	
Baurusuchidae	*Pabwehshi pakistanensis*	Yes	Wilson et al. 2001	
Baurusuchidae	*Pissarrachampsa sera*	Yes	Pol et al. 2014	
Baurusuchidae	*Stratiotosuchus maxhechti*	Yes	Pol et al. 2014	
Baurusuchidae	*Wargosuchus australis*	Yes	Godoy et al. 2014	
Bernissartidae	*Bernissartia fagesii*	Yes	Adams 2014	
Bernissartidae	*Koumpiodontosuchus aprosdokiti*	Yes	Sweetman et al. In Press	
Brevirostres	*Deinosuchus riograndensis*	Yes	Erickson and Brochu 1999	
Brevirostres	*Deinosuchus rugosus*	Yes	Erickson and Brochu 1999	
Crocodylia	*Albertochampsa langstoni*	Yes	Norell et al. 1994	
Crocodylia	*Arenysuchus gascabadiolorum*	Yes	Puértolas et al. 2011	
Crocodylia	*Crocodylus blavieri*	No	Adams 2014	Invalid taxon
Crocodylia	*Crocodylus humilis*	No	Adams 2014	Invalid taxon
Crocodylia	*Crocodylus proavus*	No	Adams 2014	Invalid taxon
Crocodylia	*Crocodylus selaslophensis*	No	Adams 2014	Invalid taxon
Crocodylia	*Crocodylus vetustus*	No	Adams 2014	Invalid taxon
Crocodylia	*Tadzhikosuchus macrodentis*	No	NA	Uncertain phylogenetic affinities
Crocodylidae	*Bottosaurus harlani*	No	NA	Uncertain phylogenetic affinities
Crocodyliformes	*Artzosuchus brachicephalus*	No	NA	Uncertain phylogenetic affinities
Crocodyliformes	*Brachydectes major*	No	NA	Uncertain phylogenetic affinities
Crocodyliformes	*Brasileosaurus pachecoi*	No	NA	Uncertain phylogenetic affinities
Crocodyliformes	*Coringasuchus anisodontis*	No	NA	Uncertain phylogenetic affinities
Crocodyliformes	*Dakotasuchus kingi*	No	NA	Uncertain phylogenetic affinities
Crocodyliformes	*Edentosuchus tienshanensis*	Yes	Pol et al. 2004	

Crocodyliformes	*Entradasuchus spinosus*	Yes	Hunt and Lockley 1995	
Crocodyliformes	*Eopneumatosuchus colberti*	No	NA	Uncertain phylogenetic affinities
Crocodyliformes	*Gobiosuchus kielanae*	Yes	Pol et al. 2004	
Crocodyliformes	*Gobiosuchus parvus*	Yes	Pol et al. 2004	
Crocodyliformes	*Hoplosuchus kayi*	No	NA	Uncertain phylogenetic affinities
Crocodyliformes	*Kemkemia auditorei*	No	NA	Uncertain phylogenetic affinities
Crocodyliformes	*Megalosaurus mersensis*	No	NA	*Nomen dubium*, probably a theropod dinosaur
Crocodyliformes	*Neustosaurus gigondarum*	No	NA	Uncertain phylogenetic affinities
Crocodyliformes	*Orthosuchus stormbergi*	Yes	Pol et al. 2004	
Crocodyliformes	*Pinacosuchus mantiensis*	No	NA	Uncertain phylogenetic affinities
Crocodyliformes	*Prodiplocynodon langi*	No	NA	Uncertain phylogenetic affinities
Crocodyliformes	*Protosuchus haughtoni*	Yes	Pol et al. 2004	
Crocodyliformes	*Protosuchus micmac*	Yes	Pol et al. 2004	
Crocodyliformes	*Protosuchus richardsoni*	Yes	Pol et al. 2004	
Crocodyliformes	*Stromerosuchus aegyptiacus*	No	NA	
Crocodyliformes	*Zaraasuchus shepardi*	Yes	Pol and Norell 2004	
Crocodyliformes	*Zholsuchus procevus*	No	NA	Uncertain phylogenetic affinities
Crocodyliformes	*Zhyrasuchus angustifrons*	No	NA	Uncertain phylogenetic affinities
Dyrosauridae	*Chenanisuchus lateroculi*	Yes	Jouve et al. 2005	
Dyrosauridae	*Dyrosaurus phosphaticus*	Yes	Adams 2014	
Eusuchia	*Aigialosuchus villandensis*	Yes	Martin and Delfino 2010	

Eusuchia	*Allodaposuchus precedens*	Yes	Holliday and Gardner 2012	
Eusuchia	*Allodaposuchus subjuniperus*	Yes	Holliday and Gardner 2012	
Eusuchia	*Borealosuchus formidabilis*	Yes	Holliday and Gardner 2012	
Eusuchia	*Borealosuchus sternbergii*	Yes	Holliday and Gardner 2012	
Eusuchia	*Heterosuchus valdensis*	No	Clark and Norell 1992	Nomen dubium
Eusuchia	*Isisfordia duncani*	Yes	Holliday and Gardner 2012	
Eusuchia	*Leidyosuchus canadensis*	Yes	Holliday and Gardner 2012	
Eusuchia	*Massaliasuchus affuvelensis*	Yes	Martin and Buffetaut 2008	
Eusuchia	*Musturzabalsuchus buffetauti*	No	NA	Uncertain phylogenetic affinities
Gavialoidae	*Eothoracosaurus mississippiensis*	Yes	Holliday and Gardner 2012	
Gavialoidae	*Ocepesuchus eoafricanus*	Yes	Jouve et al. 2008	
Gavialoidae	*Thoracosaurus bahiensis*	Yes	Inferred	
Gavialoidae	*Thoracosaurus borissiaki*	Yes	Inferred	
Gavialoidae	*Thoracosaurus macrorhynchus*	Yes	Holliday and Gardner 2012	
Gavialoidae	*Thoracosaurus neocesariensis*	Yes	Inferred	
Geosaurinae	*Metriorhynchus brachyrhynchus*	Yes	Young et al. 2013	
Geosaurinae	*Metriorhynchus casamiquelai*	Yes	Young et al. 2013	
Geosaurinae	*Neptunidraco ammoniticus*	Yes	Young et al. 2013	
Geosaurinae	*Suchodus durobrivensis*	Yes	Young et al. 2009	
Geosaurinae	*Tyrannoneustes lythrodectikos*	Yes	Young et al. 2013	
Geosaurini	*Aggiosaurus nicaeensis*	Yes	Young et al. 2012	
Geosaurini	*Dakosaurus andiniensis*	Yes	Young et al. 2013	
Geosaurini	*Dakosaurus maximus*	Yes	Young et al. 2013	
Geosaurini	*Geosaurus araucaniensis*	Yes	Inferred	
Geosaurini	*Geosaurus giganteus*	Yes	Young et al. 2013	

Geosaurini	*Geosaurus grandis*	Yes	Young et al. 2013	
Geosaurini	*Geosaurus lapparenti*	Yes	Young et al. 2013	
Geosaurini	*Plesiosuchus manselii*	Yes	Young et al. 2013	
Geosaurini	*Torvoneustes carpenteri*	Yes	Young et al. 2013	
Geosaurini	*Torvoneustes coryphaeus*	Yes	Young et al. 2013	
Globidonta	*Brachychampsa montana*	Yes	Holliday and Gardner 2012	
Globidonta	*Stangerochampsa mccabei*	Yes	Holliday and Gardner 2012	
Goniopholididae	*Anteophthalmosuchus esuchae*	Yes	de Andrade et al 2011	
Goniopholididae	*Anteophthalmosuchus hooleyi*	Yes	de Andrade et al 2011	Hooley goniopholidid
Goniopholididae	*Calsoyasuchus valliceps*	Yes	de Andrade et al 2011	
Goniopholididae	*Coelosuchus reedii*	Yes	Williston 1906	
Goniopholididae	*Denazinosuchus kirtlandicus*	Yes	de Andrade et al 2011	
Goniopholididae	*Diplosaurus felix*	No	NA	Uncertain phylogenetic affinities
Goniopholididae	*Eutretauranosuchus delfsi*	Yes	de Andrade et al 2011	
Goniopholididae	*Goniopholis affinis*	Yes	Inferred	
Goniopholididae	*Goniopholis baryglyphaeus*	Yes	de Andrade et al 2011	
Goniopholididae	*Goniopholis brodiei*	Yes	Inferred	
Goniopholididae	*Goniopholis crassidens*	Yes	Inferred	
Goniopholididae	*Goniopholis felchi*	Yes	Inferred	
Goniopholididae	*Goniopholis kiplingi*	Yes	de Andrade et al 2011	
Goniopholididae	*Goniopholis lucasii*	Yes	Inferred	
Goniopholididae	*Goniopholis paulistanus*	No	de Andrade et al. 2011	Nomen dubium
Goniopholididae	*Goniopholis phuwiangensis*	Yes	Inferred	
Goniopholididae	*Goniopholis simus*	Yes	de Andrade et al 2011	
Goniopholididae	*Goniopholis stovalli*	Yes	Adams 2014	
Goniopholididae	*Goniopholis undidens*	Yes	Inferred	
Goniopholididae	*Hulkepholis plotos*	Yes	de Andrade et al 2011	
Goniopholididae	*Hulkepholis willetti*	Yes	de Andrade et al 2011	

Goniopholididae	*Nannosuchus gracilidens*	Yes	de Andrade et al 2011	
Goniopholididae	*Siamosuchus phuphokensis*	Yes	de Andrade et al 2011	
Goniopholididae	*Sunosuchus junggarensis*	Yes	de Andrade et al 2011	
Goniopholididae	*Sunosuchus miaoi*	Yes	de Andrade et al 2011	
Goniopholididae	*Sunosuchus shunanensis*	Yes	de Andrade et al 2011	
Goniopholididae	*Vectisuchus leptognathus*	Yes	Bronzati et al. 2012	
Goniopholididae	*Woodbinesuchus byersmauricei*	Yes	Lee 1997	
Hylaeochampsidae	*Acynodon adriaticus*	Yes	Puértolas-Pascual et al. 2014	
Hylaeochampsidae	*Acynodon iberoccitanus*	Yes	Puértolas-Pascual et al. 2014	
Hylaeochampsidae	*Acynodon lopezi*	Yes	Puértolas-Pascual et al. 2014	
Hylaeochampsidae	*Hylaeochampsa vectiana*	Yes	Puértolas-Pascual et al. 2014	
Hylaeochampsidae	*Iharkutosuchus makadii*	Yes	Puértolas-Pascual et al. 2014	
Hylaeochampsidae	*Pachycheilosuchus trinquei*	Yes	Puértolas-Pascual et al. 2014	
Hylaeochampsidae	*Pietraroiasuchus ormezzanoi*	Yes	Puértolas-Pascual et al. 2014	
Mahajangasuchidae	*Kaprosuchus saharicus*	Yes	Sertich and O'Connor 2014	
Mahajangasuchidae	*Mahajangasuchus insignis*	Yes	Sertich and O'Connor 2014	
Mesoeucrocodylia	*Dianchungosaurus lufengensis*	No	NA	Uncertain phylogenetic affinities
Mesoeucrocodylia	*Fruitachampsa callisoni*	Yes	Adams 2014	
Mesoeucrocodylia	*Hsisosuchus chowi*	Yes	Adams 2014	
Mesoeucrocodylia	*Hsisosuchus chungkingensis*	Yes	Adams 2014	
Mesoeucrocodylia	*Hsisosuchus dashanpuensis*	Yes	Adams 2014	
Mesoeucrocodylia	*Kansajsuchus extensus*	Yes	Halliday et al. 2015	
Mesoeucrocodylia	*Lisboasaurus estesi*	No	NA	Uncertain phylogenetic affinities

Mesoeucrocodylia	*Lusitanisuchus mitracostatus*	No	NA	Uncertain phylogenetic affinities
Mesoeucrocodylia	*Microsuchus schilleri*	Yes	Leadi et al. 2015	
Mesoeucrocodylia	*Shantungosuchus chuhsienensis*	Yes	Fiorillo and Calvo 2007	
Mesoeucrocodylia	*Shantungosuchus hangjinensis*	Yes	Fiorillo and Calvo 2007	
Mesoeucrocodylia	*Sichuanosuchus huidongensis*	Yes	Fiorillo and Calvo 2007	
Mesoeucrocodylia	*Sichuanosuchus shuhanensis*	Yes	Fiorillo and Calvo 2007	
Mesoeucrocodylia	*Turanosuchus aralensis*	No	Halliday et al. 2015	Nomen dubium
Mesoeucrocodylia	*Zosuchus davidsoni*	Yes	Fiorillo and Calvo 2007	
Metriorhynchidae	*Cricosaurus araucanensis*	Yes	Young et al. 2013	
Metriorhynchidae	*Cricosaurus elegans*	Yes	Young et al. 2013	
Metriorhynchidae	*Cricosaurus gracilis*	Yes	Inferred	
Metriorhynchidae	*Cricosaurus lithographicus*	Yes	Inferred	
Metriorhynchidae	*Cricosaurus macrospondylus*	Yes	Young et al. 2013	
Metriorhynchidae	*Cricosaurus saltillensis*	Yes	Young et al. 2013	
Metriorhynchidae	*Cricosaurus suevicus*	Yes	Young et al. 2013	
Metriorhynchidae	*Cricosaurus vignaudi*	Yes	Young et al. 2013	
Metriorhynchidae	*Gracilineustes acutus*	Yes	Young et al. 2013	
Metriorhynchidae	*Gracilineustes leedsi*	Yes	Young et al. 2013	
Metriorhynchidae	*Maledictosuchus riclaensis*	Yes	Parilla-Bel et al. 2013	
Metriorhynchidae	*Metriorhynchus geoffroyii*	Yes	Young et al. 2013	
Metriorhynchidae	*Metriorhynchus hastifer*	Yes	Young et al. 2013	
Metriorhynchidae	*Metriorhynchus littoreus*	Yes	Inferred	
Metriorhynchidae	*Metriorhynchus moreli*	Yes	Inferred	
Metriorhynchidae	*Metriorhynchus palpebosus*	Yes	Inferred	
Metriorhynchidae	*Metriorhynchus superciliosus*	Yes	Young et al. 2013	
Metriorhynchidae	*Metriorhynchus westermanni*	Yes	Young et al. 2013	
Metriorhynchidae	*Purranisaurus potens*	Yes	Cau and Fanti 2011	
Metriorhynchidae	*Rhacheosaurus gracilis*	Yes	Young et al. 2013	

Neosuchia	*Dolichochampsa minima*	No	NA	Uncertain phylogenetic affinities
Neosuchia	*Gilchristosuchus palatinus*	Yes	Wu and Brinkmann 1993	
Neosuchia	*Hyposaurus rogersii*	Yes	Adams 2014	
Neosuchia	*Khoratosuchus jintasakuli*	Yes	Lauprasert et al. 2009	
Neosuchia	*Laganosuchus maghrebensis*	Yes	Sereno and Larsson 2009	
Neosuchia	*Laganosuchus thaumastos*	Yes	Sereno and Larsson 2009	
Neosuchia	*Leiokarinosuchus brookensis*	No	NA	Uncertain phylogenetic affinities
Neosuchia	*Paluxysuchus newmani*	Yes	Adams 2014	
Neosuchia	*Pholidosaurus decipiens*	Yes	Adams 2014	
Neosuchia	*Pholidosaurus meyeri*	Yes	Adams 2014	
Neosuchia	*Pholidosaurus purbeckensis*	Yes	Adams 2014	
Neosuchia	*Pholidosaurus schaumburgensis*	Yes	Adams 2014	
Neosuchia	*Rhabdognathus keiniensis*	Yes	Adams 2014	
Neosuchia	*Sokotosuchus ianwilsoni*	Yes	Adams 2014	
Neosuchia	*Stomatosuchus inermis*	No	NA	Fossils destroyed
Neosuchia	*Susisuchus anatoceps*	Yes	Young et al. 2012	
Neosuchia	*Susisuchus jaguaribensis*	Yes	Young et al. 2012	
Neosuchia	*Unasuchus reginae*	No	NA	Uncertain phylogenetic affinities
Notosuchia	*Candidodon itapecuruense*	Yes	Pol et al. 2014	
Notosuchia	*Stolokrosuchus lapparenti*	Yes	Pol et al. 2014	
Paralligatoridae	*Batrachomimus pastosbonensis*	Yes	Adams 2014	
Paralligatoridae	*Rugosuchus nonganensis*	Yes	Adams 2014	
Paralligatoridae	*Shamosuchus ancestralis*	Yes	Adams 2014	
Paralligatoridae	*Shamosuchus borealis*	Yes	Adams 2014	
Paralligatoridae	*Shamosuchus djadochtaensis*	Yes	Adams 2014	

Paralligatoridae	*Shamosuchus gradilifrons*	Yes	Adams 2014	
Paralligatoridae	*Shamosuchus karakalpakensis*	Yes	Adams 2014	
Paralligatoridae	*Shamosuchus major*	Yes	Adams 2014	
Paralligatoridae	*Shamosuchus sungaricus*	Yes	Adams 2014	
Paralligatoridae	*Shamosuchus tersus*	Yes	Adams 2014	
Paralligatoridae	*Shamosuchus ulanicus*	Yes	Adams 2014	
Paralligatoridae	*Shamosuchus ulgicus*	Yes	Adams 2014	
Paralligatoridae	*Wannchampsus kirpachi*	Yes	Adams 2014	
Peirosauridae	*Barcinosuchus gradilis*	Yes	Martinelli et al. 2012	
Peirosauridae	*Gasparinisuchus peirosauroides*	Yes	Sertich and O'Connor 2014	
Peirosauridae	*Hamadasuchus rebouli*	Yes	Sertich and O'Connor 2014	
Peirosauridae	*Lomasuchus palpebrosus*	Yes	Sertich and O'Connor 2014	
Peirosauridae	*Montealtosuchus arrudacamposi*	Yes	Sertich and O'Connor 2014	
Peirosauridae	*Peirosaurus tormini*	Yes	Martinelli et al. 2012	
Peirosauridae	*Pepesuchus deiseae*	Yes	Campos et al. 2011	
Peirosauridae	*Rukwasuchus yajabalijekundu*	Yes	Sertich and O'Connor 2014	
Peirosauridae	*Trematochampsa taqueti*	Yes	Sertich and O'Connor 2014	
Peirosauridae	*Uberabasuchus terrificus*	Yes	Sertich and O'Connor 2014	
Pholidosauridae	*Chalawan thailandicus*	Yes	Martin et al. 2014	
Pholidosauridae	*Elosuchus cherifiensis*	Yes	Adams 2014	
Pholidosauridae	*Elosuchus felixi*	Yes	Adams 2014	
Pholidosauridae	*Meridiosaurus vallisparadisi*	Yes	Adams 2014	
Pholidosauridae	*Oceanosuchus boecensis*	Yes	Adams 2014	
Pholidosauridae	*Sarcosuchus hartti*	Yes	Adams 2014	
Pholidosauridae	*Sarcosuchus imperator*	Yes	Adams 2014	
Pholidosauridae	*Terminonaris browni*	Yes	Adams 2014	
Pholidosauridae	*Terminonaris robusta*	Yes	Adams 2014	
Protosuchia	*Dianosuchus changchiawaensis*	No	NA	Uncertain phylogenetic affinities

Protosuchia	*Hadongsuchus acerdentis*	No	NA	Uncertain phylogenetic affinities
Protosuchia	*Microchampsa scutata*	No	NA	Uncertain phylogenetic affinities
Protosuchia	*Notochampsa istedana*	No	NA	Uncertain phylogenetic affinities
Protosuchia	*Platyognathus hsui*	Yes	Wu and Sues 1996	
Protosuchia	*Stegomosuchus longipes*	No	NA	Uncertain phylogenetic affinities
Protosuchia	*Tagarosuchus kulemzini*	No	NA	Uncertain phylogenetic affinities
Sebecosuchia	*Pehuenchesuchus enderi*	Yes	Turner and Calvo 2005	
Shartegosuchidae	*Kyasuchus saevi*	Yes	Inferred	
Shartegosuchidae	*Nominosuchus matutinus*	Yes	Inferred	
Shartegosuchidae	*Shartegosuchus asperopalatum*	Yes	Clark 2011	
Sphagesauridae	*Adamantinasuchus navae*	Yes	Pol et al. 2014	
Sphagesauridae	*Armadillosuchus arrudai*	Yes	Pol et al. 2014	
Sphagesauridae	*Caipirasuchus paulistanus*	Yes	Pol et al. 2014	
Sphagesauridae	*Caipirasuchus stenognathus*	Yes	Pol et al. 2014	
Sphagesauridae	*Caryonosuchus pricei*	Yes	Pol et al. 2014	
Sphagesauridae	*Sphagesaurus huenei*	Yes	Pol et al. 2014	
Sphagesauridae	*Sphagesaurus montealtensis*	Yes	Pol et al. 2014	Caipirasuchus montealtensis
Sphagesauridae	*Yacarerani boliviensis*	Yes	Pol et al. 2014	
Stomatosuchidae	*Chiayusuchus cingulatus*	No	NA	Uncertain phylogenetic affinities
Teleosauridae	*Haematosaurus lanceolatus*	Yes	Sauvage 1874	
Teleosauridae	*Machimosaurus buffetauti*	No	Martin et al. 2015	
Teleosauridae	*Machimosaurus hugii*	Yes	Martin et al. 2015	
Teleosauridae	*Machimosaurus mosae*	No	Martin et al. 2015	
Teleosauridae	*Machimosaurus nowackianus*	No	Martin et al. 2015	

Teleosauridae	*Peipehsuchus teleorhinus*	Yes	Li 1993
Teleosauridae	*Platysuchus multiscrobiculatus*	Yes	Young 2014
Teleosauridae	*Steneosaurus bollensis*	Yes	Young 2014
Teleosauridae	*Steneosaurus boutilieri*	Yes	Inferred
Teleosauridae	*Steneosaurus brevidens*	Yes	Inferred
Teleosauridae	*Steneosaurus brevior*	Yes	Inferred
Teleosauridae	*Steneosaurus brevirostris*	Yes	Inferred
Teleosauridae	*Steneosaurus dasycephalus*	Yes	Inferred
Teleosauridae	*Steneosaurus durobrivensis*	Yes	Inferred
Teleosauridae	*Steneosaurus edwardsi*	Yes	Young 2014
Teleosauridae	*Steneosaurus gerthi*	Yes	Inferred
Teleosauridae	*Steneosaurus gracilirostris*	Yes	Inferred
Teleosauridae	*Steneosaurus heberti*	Yes	Inferred
Teleosauridae	*Steneosaurus intermedius*	Yes	Inferred
Teleosauridae	*Steneosaurus jugleri*	Yes	Inferred
Teleosauridae	*Steneosaurus larteti*	Yes	Inferred
Teleosauridae	*Steneosaurus leedsi*	Yes	Young 2014
Teleosauridae	*Steneosaurus megistorhynchus*	Yes	Young 2014
Teleosauridae	*Steneosaurus morinicus*	Yes	Inferred
Teleosauridae	*Steneosaurus pictaviensis*	Yes	Inferred
Teleosauridae	*Steneosaurus rudis*	Yes	Inferred
Teleosauridae	*Steneosaurus subulidens*	Yes	Inferred
Teleosauridae	*Teleosaurus cadomensis*	Yes	Young 2014
Teleosauridae	*Teleosaurus chapmani*	Yes	Inferred
Teleosauridae	*Teleosaurus geoffroyi*	Yes	Inferred
Teleosauridae	*Teleosaurus megarhinus*	Yes	Inferred
Teleosauridae	*Teleosaurus picteti*	Yes	Inferred
Teleosauridae	*Teleosaurus sublidens*	Yes	Inferred
Teleosauridae	*Teleosaurus temporalis*	Yes	Inferred
Thalattosuchia	*Eoneustes bathonicus*	Yes	Young et al. 2013

Thalattosuchia	*Eoneustes gaudryi*	Yes	Young et al. 2013	
Thalattosuchia	*Pelagosaurus brongniarti*	Yes	Inferred	
Thalattosuchia	*Pelagosaurus typus*	Yes	Young et al. 2013	
Thalattosuchia	*Teleidosaurus calvadosii*	Yes	Young et al. 2013	
Trematochampsidae	*Amargasuchus minor*	No	NA	Uncertain phylogenetic affinities
Trematochampsidae	*Baharijodon carnosauroides*	No	NA	Uncertain phylogenetic affinities
Trematochampsidae	*Barreirosuchus franciscoi*	No	NA	Uncertain phylogenetic affinities
Trematochampsidae	*Caririsuchus camposi*	No	NA	Uncertain phylogenetic affinities
Trematochampsidae	*Ischyrochampsa meridionalis*	No	NA	Uncertain phylogenetic affinities
Trematochampsidae	*Itasuchus jesuinoi*	No	NA	Uncertain phylogenetic affinities
Trematochampsidae	*Miadanasuchus oblita*	No	NA	Uncertain phylogenetic affinities
Uruguaysuchidae	*Anatosuchus minor*	Yes	Pol et al. 2014	
Uruguaysuchidae	*Araripesuchus buitreraensis*	Yes	Pol et al. 2014	
Uruguaysuchidae	*Araripesuchus gomesii*	Yes	Pol et al. 2014	
Uruguaysuchidae	*Araripesuchus patagonicus*	Yes	Pol et al. 2014	
Uruguaysuchidae	*Araripesuchus rattoides*	Yes	Sereno and Larsson 2009	
Uruguaysuchidae	*Araripesuchus tsangatsangana*	Yes	Pol et al. 2014	
Uruguaysuchidae	*Araripesuchus wegeneri*	Yes	Pol et al. 2014	
Uruguaysuchidae	*Uruguaysuchus aznarezi*	Yes	Pol et al. 2014	
Uruguaysuchidae	*Uruguaysuchus terrai*	Yes	Pol et al. 2014	
Ziphosuchia	*Chimaerasuchus paradoxus*	Yes	Pol et al. 2014	
Ziphosuchia	*Comahuesuchus brachybuccalis*	Yes	Pol et al. 2014	
Ziphosuchia	*Doratodon carcharidens*	Yes	Company et al. 2005	

Ziphosuchia	*Doratodon ibericus*	Yes	Company et al. 2005
Ziphosuchia	*Labidiosuchus amicum*	Yes	Pol et al. 2014
Ziphosuchia	*Libycosuchus brevirostris*	Yes	Pol et al. 2014
Ziphosuchia	*Malawisuchus mwakasyungutiensis*	Yes	Pol et al. 2014
Ziphosuchia	*Mariliasuchus amarali*	Yes	Pol et al. 2014
Ziphosuchia	*Mariliasuchus robustus*	Yes	Pol et al. 2014
Ziphosuchia	*Morrinhosuchus luziae*	Yes	Pol et al. 2014
Ziphosuchia	*Neuquensuchus universitas*	Yes	Leadi et al. 2015
Ziphosuchia	*Notosuchus terrestris*	Yes	Pol et al. 2014
Ziphosuchia	*Pakasuchus kapilimai*	Yes	Pol et al. 2014
Ziphosuchia	*Simosuchus clarki*	Yes	Pol et al. 2014

Appendix 2 – Mode of life for crocodyliform species used to construct supertree (see Section 2.6)

Higher Taxon	Species	Mode of Life
Aegyptosuchidae	*Aegisuchus witmeri*	Terrestrial
Aegyptosuchidae	*Aegyptosuchus peyeri*	Terrestrial
Atoposauridae	*Alligatorellus bavaricus*	Terrestrial
Atoposauridae	*Alligatorellus beaumonti*	Terrestrial
Atoposauridae	*Alligatorium franconicum*	Terrestrial
Atoposauridae	*Alligatorium meyeri*	Terrestrial
Atoposauridae	*Atoposaurus jourdani*	Terrestrial
Atoposauridae	*Atoposaurus oberndorferi*	Terrestrial
Atoposauridae	*Montsecosuchus depereti*	Terrestrial
Atoposauridae	*Theriosuchus grandinaris*	Terrestrial
Atoposauridae	*Theriosuchus guimarotae*	Terrestrial
Atoposauridae	*Theriosuchus ibericus*	Terrestrial
Atoposauridae	*Theriosuchus pusillus*	Terrestrial
Atoposauridae	*Theriosuchus sympiestodon*	Terrestrial
Baurusuchidae	*Aplestosuchus sordidus*	Terrestrial
Baurusuchidae	*Baurusuchus albertoi*	Terrestrial
Baurusuchidae	*Baurusuchus pachecoi*	Terrestrial
Baurusuchidae	*Baurusuchus salgadoensis*	Terrestrial
Baurusuchidae	*Campinasuchus dinizi*	Terrestrial
Baurusuchidae	*Cynodontosuchus rothi*	Terrestrial
Baurusuchidae	*Gondwanasuchus scabrosus*	Terrestrial
Baurusuchidae	*Pabwehshi pakistanensis*	Terrestrial
Baurusuchidae	*Pissarrachampsa sera*	Terrestrial
Baurusuchidae	*Stratiotosuchus maxhechti*	Terrestrial
Baurusuchidae	*Wargosuchus australis*	Terrestrial
Bernissartidae	*Bernissartia fagesii*	Terrestrial
Bernissartidae	*Koumpiodontosuchus aprosdokiti*	Terrestrial
Brevirostres	*Deinosuchus riograndensis*	Terrestrial
Brevirostres	*Deinosuchus rugosus*	Terrestrial
Crocodylia	*Albertochampsa langstoni*	Terrestrial
Crocodylia	*Arenysuchus gascabadiolorum*	Terrestrial
Crocodylia	*Laiyangpus liui*	Terrestrial
Crocodylia	*Tadzhikosuchus macrodentis*	Terrestrial
Crocodylidae	*Bottosaurus harlani*	Terrestrial
Crocodyliformes	*Artzosuchus brachicephalus*	Terrestrial
Crocodyliformes	*Brachydectes major*	Terrestrial
Crocodyliformes	*Brasileosaurus pachecoi*	Terrestrial
Crocodyliformes	*Coringasuchus anisodontis*	Terrestrial
Crocodyliformes	*Dakotasuchus kingi*	Terrestrial
Crocodyliformes	*Edentosuchus tienshanensis*	Terrestrial
Crocodyliformes	*Entradasuchus spinosus*	Terrestrial

Crocodyliformes	*Eopneumatosuchus colberti*	Terrestrial
Crocodyliformes	*Gobiosuchus kielanae*	Terrestrial
Crocodyliformes	*Gobiosuchus parvus*	Terrestrial
Crocodyliformes	*Hoplosuchus kayi*	Terrestrial
Crocodyliformes	*Kemkemia auditorei*	Terrestrial
Crocodyliformes	*Megalosaurus mersensis*	Terrestrial
Crocodyliformes	*Neustosaurus gigondarum*	Terrestrial
Crocodyliformes	*Orthosuchus stormbergi*	Terrestrial
Crocodyliformes	*Pinacosuchus mantiensis*	Terrestrial
Crocodyliformes	*Prodiplocynodon langi*	Terrestrial
Crocodyliformes	*Protosuchus haughtoni*	Terrestrial
Crocodyliformes	*Protosuchus micmac*	Terrestrial
Crocodyliformes	*Protosuchus richardsoni*	Terrestrial
Crocodyliformes	*Stromerosuchus aegyptiacus*	Terrestrial
Crocodyliformes	*Zaraasuchus shepardi*	Terrestrial
Crocodyliformes	*Zholsuchus procevus*	Terrestrial
Crocodyliformes	*Zhyrasuchus angustifrons*	Terrestrial
Dyrosauridae	*Chenanisuchus lateroculi*	Marine
Dyrosauridae	*Dyrosaurus phosphaticus*	Marine
Dyrosauridae	*Hyposaurus rogersii*	Marine
Dyrosauridae	*Rhabdognathus keiniensis*	Marine
Dyrosauridae	*Sokotosuchus ianwilsoni*	Marine
Eusuchia	*Aigialosuchus villandensis*	Terrestrial
Eusuchia	*Allodaposuchus precedens*	Terrestrial
Eusuchia	*Allodaposuchus subjuniperus*	Terrestrial
Eusuchia	*Borealosuchus formidabilis*	Terrestrial
Eusuchia	*Borealosuchus sternbergii*	Terrestrial
Eusuchia	*Heterosuchus valdensis*	Terrestrial
Eusuchia	*Isisfordia duncani*	Terrestrial
Eusuchia	*Leidyosuchus canadensis*	Terrestrial
Eusuchia	*Massaliasuchus affuvelensis*	Terrestrial
Eusuchia	*Musturzabalsuchus buffetauti*	Terrestrial
Gavialoidae	*Eothoracosaurus mississippiensis*	Marine
Gavialoidae	*Ocepesuchus eoafricanus*	Marine
Gavialoidae	*Thoracosaurus bahiensis*	Marine
Gavialoidae	*Thoracosaurus borissiaki*	Marine
Gavialoidae	*Thoracosaurus macrorhynchus*	Marine
Gavialoidae	*Thoracosaurus neocesariensis*	Marine
Geosaurinae	*Metriorhynchus brachyrhynchus*	Marine
Geosaurinae	*Metriorhynchus casamiquelai*	Marine
Geosaurinae	*Neptunidraco ammoniticus*	Marine
Geosaurinae	*Suchodus durobrivensis*	Marine
Geosaurinae	*Tyrannoneustes lythrodectikos*	Marine
Geosaurini	*Aggiosaurus nicaeensis*	Marine

Geosaurini	*Dakosaurus andiniensis*	Marine
Geosaurini	*Dakosaurus maximus*	Marine
Geosaurini	*Geosaurus araucaniensis*	Marine
Geosaurini	*Geosaurus giganteus*	Marine
Geosaurini	*Geosaurus grandis*	Marine
Geosaurini	*Geosaurus lapparenti*	Marine
Geosaurini	*Plesiosuchus manselii*	Marine
Geosaurini	*Torvoneustes carpenteri*	Marine
Geosaurini	*Torvoneustes coryphaeus*	Marine
Globidonta	*Brachychampsa montana*	Terrestrial
Globidonta	*Stangerochampsa mccabei*	Marine
Goniopholididae	*Anteophthalmosuchus esuchae*	Terrestrial
Goniopholididae	*Anteophthalmosuchus hooleyi*	Terrestrial
Goniopholididae	*Calsoyasuchus valliceps*	Terrestrial
Goniopholididae	*Coelosuchus reedii*	Terrestrial
Goniopholididae	*Denazinosuchus kirtlandicus*	Terrestrial
Goniopholididae	*Diplosaurus felix*	Terrestrial
Goniopholididae	*Eutretauranosuchus delfsi*	Terrestrial
Goniopholididae	*Goniopholis affinis*	Terrestrial
Goniopholididae	*Goniopholis baryglyphaeus*	Terrestrial
Goniopholididae	*Goniopholis brodiei*	Terrestrial
Goniopholididae	*Goniopholis crassidens*	Terrestrial
Goniopholididae	*Goniopholis felchi*	Terrestrial
Goniopholididae	*Goniopholis kiplingi*	Terrestrial
Goniopholididae	*Goniopholis lucasii*	Terrestrial
Goniopholididae	*Goniopholis paulistanus*	Terrestrial
Goniopholididae	*Goniopholis phuwiangensis*	Terrestrial
Goniopholididae	*Goniopholis simus*	Terrestrial
Goniopholididae	*Goniopholis stovalli*	Terrestrial
Goniopholididae	*Goniopholis undidens*	Terrestrial
Goniopholididae	*Hulkepholis plotos*	Terrestrial
Goniopholididae	*Hulkepholis willetti*	Terrestrial
Goniopholididae	*Nannosuchus gracilidens*	Terrestrial
Goniopholididae	*Siamosuchus phuphokensis*	Terrestrial
Goniopholididae	*Sunosuchus junggarensis*	Terrestrial
Goniopholididae	*Sunosuchus miaoi*	Terrestrial
Goniopholididae	*Sunosuchus shunanensis*	Terrestrial
Goniopholididae	*Vectisuchus leptognathus*	Terrestrial
Goniopholididae	*Woodbinesuchus byersmauricei*	Terrestrial
Hylaeochampsidae	*Acynodon adriaticus*	Terrestrial
Hylaeochampsidae	*Acynodon iberoccitanus*	Terrestrial
Hylaeochampsidae	*Acynodon lopezi*	Terrestrial
Hylaeochampsidae	*Hylaeochampsa vectiana*	Terrestrial
Hylaeochampsidae	*Iharkutosuchus makadii*	Terrestrial

Hylaeochampsidae	*Pachycheilosuchus trinquei*	Terrestrial
Hylaeochampsidae	*Pietraroiasuchus ormezzanoi*	Terrestrial
Mahajangasuchidae	*Kaprosuchus saharicus*	Terrestrial
Mahajangasuchidae	*Mahajangasuchus insignis*	Terrestrial
Mesoeucrocodylia	*Dianchungosaurus lufengensis*	Terrestrial
Mesoeucrocodylia	*Fruitachampsa callisoni*	Terrestrial
Mesoeucrocodylia	*Hsisosuchus chowi*	Terrestrial
Mesoeucrocodylia	*Hsisosuchus chungkingensis*	Terrestrial
Mesoeucrocodylia	*Hsisosuchus dashanpuensis*	Terrestrial
Mesoeucrocodylia	*Kansajsuchus extensus*	Terrestrial
Mesoeucrocodylia	*Lisboasaurus estesi*	Terrestrial
Mesoeucrocodylia	*Lusitanisuchus mitracostatus*	Terrestrial
Mesoeucrocodylia	*Microsuchus schilleri*	Terrestrial
Mesoeucrocodylia	*Shantungosuchus chuhsienensis*	Terrestrial
Mesoeucrocodylia	*Shantungosuchus hangjinensis*	Terrestrial
Mesoeucrocodylia	*Sichuanosuchus huidongensis*	Terrestrial
Mesoeucrocodylia	*Sichuanosuchus shuhanensis*	Terrestrial
Mesoeucrocodylia	*Turanosuchus aralensis*	Terrestrial
Mesoeucrocodylia	*Zosuchus davidsoni*	Terrestrial
Metriorhynchidae	*Cricosaurus araucanensis*	Marine
Metriorhynchidae	*Cricosaurus elegans*	Marine
Metriorhynchidae	*Cricosaurus gracilis*	Marine
Metriorhynchidae	*Cricosaurus lithographicus*	Marine
Metriorhynchidae	*Cricosaurus macrospondylus*	Marine
Metriorhynchidae	*Cricosaurus saltillensis*	Marine
Metriorhynchidae	*Cricosaurus suevicus*	Marine
Metriorhynchidae	*Cricosaurus vignaudi*	Marine
Metriorhynchidae	*Gracilineustes acutus*	Marine
Metriorhynchidae	*Gracilineustes leedsi*	Marine
Metriorhynchidae	*Maledictosuchus riclaensis*	Marine
Metriorhynchidae	*Metriorhynchus geoffroyii*	Marine
Metriorhynchidae	*Metriorhynchus hastifer*	Marine
Metriorhynchidae	*Metriorhynchus littoreus*	Marine
Metriorhynchidae	*Metriorhynchus moreli*	Marine
Metriorhynchidae	*Metriorhynchus palpebosus*	Marine
Metriorhynchidae	*Metriorhynchus superciliosus*	Marine
Metriorhynchidae	*Metriorhynchus westermanni*	Marine
Metriorhynchidae	*Purranisaurus potens*	Marine
Metriorhynchidae	*Rhacheosaurus gracilis*	Marine
Neosuchia	*Dolichochampsa minima*	Terrestrial
Neosuchia	*Gilchristosuchus palatinus*	Terrestrial
Neosuchia	*Khoratosuchus jintasakuli*	Terrestrial
Neosuchia	*Laganosuchus maghrebensis*	Terrestrial
Neosuchia	*Laganosuchus thaumastos*	Terrestrial

Neosuchia	*Leiokarinosuchus brookensis*	Terrestrial
Neosuchia	*Paluxysuchus newmani*	Terrestrial
Neosuchia	*Stomatosuchus inermis*	Terrestrial
Neosuchia	*Susisuchus anatoceps*	Terrestrial
Neosuchia	*Susisuchus jaguaribensis*	Terrestrial
Neosuchia	*Unasuchus reginae*	Terrestrial
Notosuchia	*Candidodon itapecuruense*	Terrestrial
Notosuchia	*Stolokrosuchus lapparenti*	Terrestrial
Paralligatoridae	*Batrachomimus pastosbonensis*	Terrestrial
Paralligatoridae	*Paralligator gradilifrons*	Terrestrial
Paralligatoridae	*Paralligator major*	Terrestrial
Paralligatoridae	*Rugosuchus nonganensis*	Terrestrial
Paralligatoridae	*Shamosuchus djadochtaensis*	Terrestrial
Paralligatoridae	*Wannchampsus kirpachi*	Terrestrial
Peirosauridae	*Barcinosuchus gradilis*	Terrestrial
Peirosauridae	*Gasparinisuchus peirosauroides*	Terrestrial
Peirosauridae	*Hamadasuchus rebouli*	Terrestrial
Peirosauridae	*Lomasuchus palpebrosus*	Terrestrial
Peirosauridae	*Montealtosuchus arrudacamposi*	Terrestrial
Peirosauridae	*Peirosaurus tormini*	Terrestrial
Peirosauridae	*Pepesuchus deiseae*	Terrestrial
Peirosauridae	*Rukwasuchus yajabalijekundu*	Terrestrial
Peirosauridae	*Trematochampsa taqueti*	Terrestrial
Peirosauridae	*Uberabasuchus terrificus*	Terrestrial
Pholidosauridae	*Chalawan thailandicus*	Terrestrial
Pholidosauridae	*Elosuchus cherifiensis*	Marine
Pholidosauridae	*Elosuchus felixi*	Marine
Pholidosauridae	*Meridiosaurus vallisparadisi*	Terrestrial
Pholidosauridae	*Oceanosuchus boecensis*	Marine
Pholidosauridae	*Pholidosaurus decipiens*	Terrestrial
Pholidosauridae	*Pholidosaurus meyeri*	Terrestrial
Pholidosauridae	*Pholidosaurus purbeckensis*	Terrestrial
Pholidosauridae	*Pholidosaurus schaumburgensis*	Terrestrial
Pholidosauridae	*Sarcosuchus hartti*	Terrestrial
Pholidosauridae	*Sarcosuchus imperator*	Terrestrial
Pholidosauridae	*Terminonaris browni*	Terrestrial
Pholidosauridae	*Terminonaris robusta*	Terrestrial
Protosuchia	*Dianosuchus changchiawaensis*	Terrestrial
Protosuchia	*Hadongsuchus acerdentis*	Terrestrial
Protosuchia	*Microchampsa scutata*	Terrestrial
Protosuchia	*Notochampsa istedana*	Terrestrial
Protosuchia	*Platyognathus hsui*	Terrestrial
Protosuchia	*Stegomosuchus longipes*	Terrestrial
Protosuchia	*Tagarosuchus kulemzini*	Terrestrial

Sebecosuchia	*Pehuenchesuchus enderi*	Terrestrial
Shartegosuchidae	*Kyasuchus saevi*	Terrestrial
Shartegosuchidae	*Nominosuchus matutinus*	Terrestrial
Shartegosuchidae	*Shartegosuchus asperopalatum*	Terrestrial
Sphagesauridae	*Adamantinasuchus navae*	Terrestrial
Sphagesauridae	*Armadillosuchus arrudai*	Terrestrial
Sphagesauridae	*Caipirasuchus paulistanus*	Terrestrial
Sphagesauridae	*Caipirasuchus stenognathus*	Terrestrial
Sphagesauridae	*Caryonosuchus pricei*	Terrestrial
Sphagesauridae	*Sphagesaurus huenei*	Terrestrial
Sphagesauridae	*Sphagesaurus montealtensis*	Terrestrial
Sphagesauridae	*Yacarerani boliviensis*	Terrestrial
Stomatosuchidae	*Chiayusuchus cingulatus*	Terrestrial
Teleosauridae	*Haematosaurus lanceolatus*	Marine
Teleosauridae	*Machimosaurus hugii*	Marine
Teleosauridae	*Peipehsuchus teleorhinus*	Marine
Teleosauridae	*Platysuchus multiscrobiculatus*	Marine
Teleosauridae	*Steneosaurus bollensis*	Marine
Teleosauridae	*Steneosaurus boutilieri*	Marine
Teleosauridae	*Steneosaurus brevidens*	Marine
Teleosauridae	*Steneosaurus brevior*	Marine
Teleosauridae	*Steneosaurus brevirostris*	Marine
Teleosauridae	*Steneosaurus dasycephalus*	Marine
Teleosauridae	*Steneosaurus durobrivensis*	Marine
Teleosauridae	*Steneosaurus edwardsi*	Marine
Teleosauridae	*Steneosaurus gerthi*	Marine
Teleosauridae	*Steneosaurus gracilirostris*	Marine
Teleosauridae	*Steneosaurus heberti*	Marine
Teleosauridae	*Steneosaurus intermedius*	Marine
Teleosauridae	*Steneosaurus jugleri*	Marine
Teleosauridae	*Steneosaurus larteti*	Marine
Teleosauridae	*Steneosaurus leedsi*	Marine
Teleosauridae	*Steneosaurus megistorhynchus*	Marine
Teleosauridae	*Steneosaurus morinicus*	Marine
Teleosauridae	*Steneosaurus pictaviensis*	Marine
Teleosauridae	*Steneosaurus rudis*	Marine
Teleosauridae	*Steneosaurus subulidens*	Marine
Teleosauridae	*Teleosaurus cadomensis*	Marine
Teleosauridae	*Teleosaurus chapmani*	Marine
Teleosauridae	*Teleosaurus geoffroyi*	Marine
Teleosauridae	*Teleosaurus megarhinus*	Marine
Teleosauridae	*Teleosaurus picteti*	Marine
Teleosauridae	*Teleosaurus sublidens*	Marine
Teleosauridae	*Teleosaurus temporalis*	Marine

Thalattosuchia	*Eoneustes bathonicus*	Marine
Thalattosuchia	*Eoneustes gaudryi*	Marine
Thalattosuchia	*Pelagosaurus brongniarti*	Marine
Thalattosuchia	*Pelagosaurus typus*	Marine
Thalattosuchia	*Teleidosaurus calvadosii*	Marine
Trematochampsidae	*Amargasuchus minor*	Terrestrial
Trematochampsidae	*Baharijodon carnosauroides*	Terrestrial
Trematochampsidae	*Barreirosuchus franciscoi*	Terrestrial
Trematochampsidae	*Caririsuchus camposi*	Terrestrial
Trematochampsidae	*Ischyrochampsa meridionalis*	Terrestrial
Trematochampsidae	*Itasuchus jesuinoi*	Terrestrial
Trematochampsidae	*Miadanasuchus oblita*	Terrestrial
Uruguaysuchidae	*Anatosuchus minor*	Terrestrial
Uruguaysuchidae	*Araripesuchus buitreraensis*	Terrestrial
Uruguaysuchidae	*Araripesuchus gomesii*	Terrestrial
Uruguaysuchidae	*Araripesuchus patagonicus*	Terrestrial
Uruguaysuchidae	*Araripesuchus rattoides*	Terrestrial
Uruguaysuchidae	*Araripesuchus tsangatsangana*	Terrestrial
Uruguaysuchidae	*Araripesuchus wegeneri*	Terrestrial
Uruguaysuchidae	*Uruguaysuchus aznarezi*	Terrestrial
Uruguaysuchidae	*Uruguaysuchus terrai*	Terrestrial
Ziphosuchia	*Chimaerasuchus paradoxus*	Terrestrial
Ziphosuchia	*Comahuesuchus brachybuccalis*	Terrestrial
Ziphosuchia	*Doratodon carcharidens*	Terrestrial
Ziphosuchia	*Doratodon ibericus*	Terrestrial
Ziphosuchia	*Labidiosuchus amicum*	Terrestrial
Ziphosuchia	*Libycosuchus brevirostris*	Terrestrial
Ziphosuchia	*Malawisuchus mwakasyungutiensis*	Terrestrial
Ziphosuchia	*Mariliasuchus amarali*	Terrestrial
Ziphosuchia	*Mariliasuchus robustus*	Terrestrial
Ziphosuchia	*Morrinhosuchus luziae*	Terrestrial
Ziphosuchia	*Neuquensuchus universitas*	Terrestrial
Ziphosuchia	*Notosuchus terrestris*	Terrestrial
Ziphosuchia	*Pakasuchus kapilimai*	Terrestrial
Ziphosuchia	*Simosuchus clarki*	Terrestrial

Appendix 3 – Mode of life and first and last appearance data occurrences for crocodyliform genera used for supertree construction (see Section 2.6).

Genus	FAD	LAD	Mode of Life
Aggiosaurus	161.2	155.7	Marine
Chenanisuchus	70.6	66.043	Marine
Cricosaurus	155.7	136.4	Marine
Dakosaurus	161.2	112.6	Marine
Dyrosaurus	112.6	66.043	Marine
Eoneustes	167.7	150.8	Marine
Eothoracosaurus	70.6	66.043	Marine
Geosaurus	161.2	130	Marine
Gracilineustes	164.7	150.8	Marine
Haematosaurus	155.7	150.8	Marine
Hyposaurus	84.9	66.043	Marine
Machimosaurus	164.7	145.5	Marine
Maledictosuchus	164.7	161.2	Marine
Metriorhynchus	171.6	145.5	Marine
Neptunidraco	171.6	164.7	Marine
Oceanosuchus	99.7	94.3	Marine
Peipehsuchus	164.7	99.7	Marine
Pelagosaurus	183	182	Marine
Platysuchus	183	182	Marine
Plesiosuchus	155.7	145.5	Marine
Purranisaurus	150.8	140.2	Marine
Rhabdognathus	70.6	66.043	Marine
Rhacheosaurus	150.8	145.5	Marine
Sokotosuchus	70.6	66.043	Marine
Steneosaurus	183	145.5	Marine
Suchodus	164.7	161.2	Marine
Teleidosaurus	171.6	164.7	Marine
Teleosaurus	183	145.5	Marine
Thoracosaurus	125.45	66.043	Marine
Torvoneustes	161.2	150.8	Marine
Tyrannoneustes	164.7	161.2	Marine
Acynodon	84.9	66.043	Terrestrial
Adamantinasuchus	94.3	84.9	Terrestrial
Aegisuchus	99.7	94.3	Terrestrial
Aegyptosuchus	99.7	94.3	Terrestrial
Aigialosuchus	84.9	70.6	Terrestrial
Albertochampsa	84.9	70.6	Terrestrial
Alligatorellus	155.7	145.5	Terrestrial
Alligatorium	155.7	150.8	Terrestrial

Allodaposuchus	84.9	66.043	Terrestrial
Anatosuchus	122.46	109	Terrestrial
Anteophthalmosuchus	130	109	Terrestrial
Aplestosuchus	99.7	66.043	Terrestrial
Araripesuchus	122.46	66.043	Terrestrial
Arenysuchus	70.6	66.043	Terrestrial
Armadillosuchus	94.3	84.9	Terrestrial
Atoposaurus	155.7	145.5	Terrestrial
Barcinosuchus	125.45	99.7	Terrestrial
Batrachomimus	161.2	145.5	Terrestrial
Baurusuchus	94.3	66.043	Terrestrial
Bernissartia	155.7	66.043	Terrestrial
Borealosuchus	84.9	66.043	Terrestrial
Brachychampsa	94.3	66.043	Terrestrial
Caipirasuchus	94.3	66.043	Terrestrial
Calsoyasuchus	196.5	183	Terrestrial
Campinasuchus	94.3	84.9	Terrestrial
Candidodon	112.6	99.7	Terrestrial
Caryonosuchus	94.3	84.9	Terrestrial
Chalawan	150.8	145.5	Terrestrial
Chimaerasuchus	125.45	99.7	Terrestrial
Coelosuchus	99.7	94.3	Terrestrial
Comahuesuchus	94.3	84.9	Terrestrial
Cynodontosuchus	85.8	84.9	Terrestrial
Deinosuchus	84.9	70.6	Terrestrial
Denazinosuchus	84.9	70.6	Terrestrial
Doratodon	85.8	66.043	Terrestrial
Edentosuchus	196.5	99.7	Terrestrial
Elosuchus	112.6	94.3	Terrestrial
Entradasuchus	164.7	161.2	Terrestrial
Eutretauranosuchus	155.7	150.2	Terrestrial
Fruitachampsa	150.8	145.5	Terrestrial
Gasparinisuchus	85.8	70.6	Terrestrial
Gilchristosuchus	85.8	84.9	Terrestrial
Gobiosuchus	84.9	70.6	Terrestrial
Gondwanasuchus	94.3	84.9	Terrestrial
Goniopholis	167.7	66.043	Terrestrial
Hamadasuchus	112.6	94.3	Terrestrial
Hsisosuchus	171.6	155.7	Terrestrial
Hulkepholis	140.2	109	Terrestrial
Hylaeochampsa	130	122.46	Terrestrial
Iharkutosuchus	85.8	84.9	Terrestrial
Isisfordia	105.3	94.3	Terrestrial
Kansajsuchus	85.8	84.9	Terrestrial

Kaprosuchus	99.7	94.3	Terrestrial
Khoratosuchus	130	112.6	Terrestrial
Koumpiodontosuchus	130	125.45	Terrestrial
Kyasuchus	130	112.6	Terrestrial
Labidiosuchus	70.6	66.043	Terrestrial
Laganosuchus	99.7	94.3	Terrestrial
Leidyosuchus	84.9	66.043	Terrestrial
Libycosuchus	99.7	84.9	Terrestrial
Lomasuchus	94.3	85.8	Terrestrial
Mahajangasuchus	70.6	66.043	Terrestrial
Malawisuchus	125.45	112.6	Terrestrial
Mariliasuchus	94.3	66.043	Terrestrial
Massaliasuchus	85.8	70.6	Terrestrial
Meridiosaurus	155.7	145.5	Terrestrial
Microsuchus	85.8	84.9	Terrestrial
Montealtosuchus	94.3	84.9	Terrestrial
Montsecosuchus	130	125.45	Terrestrial
Morrinhosuchus	94.3	84.9	Terrestrial
Nannosuchus	145.5	125.45	Terrestrial
Neuquensuchus	85.8	84.9	Terrestrial
Nominosuchus	161.2	145.5	Terrestrial
Notosuchus	85.8	84.9	Terrestrial
Ocepesuchus	70.6	66.043	Terrestrial
Orthosuchus	201.6	189.6	Terrestrial
Pabwehshi	70.6	66.043	Terrestrial
Pachycheilosuchus	112.6	109	Terrestrial
Pakasuchus	125.45	99.7	Terrestrial
Paluxysuchus	94.3	89.3	Terrestrial
Paralligator	122.46	112.6	Terrestrial
Pehuenchesuchus	89.3	84.9	Terrestrial
Peirosaurus	70.6	66.043	Terrestrial
Pepesuchus	84.9	66.043	Terrestrial
Pholidosaurus	150.8	140.2	Terrestrial
Pietraroiasuchus	112.6	109	Terrestrial
Pissarrachampsa	94.3	66.043	Terrestrial
Platyognathus	196.5	150.8	Terrestrial
Protosuchus	201.6	196.5	Terrestrial
Rugosuchus	94.3	84.9	Terrestrial
Rukwasuchus	125.45	94.3	Terrestrial
Sarcosuchus	125.45	94.3	Terrestrial
Shamosuchus	99.7	66.043	Terrestrial
Shantungosuchus	140.2	112.6	Terrestrial
Shartegosuchus	150.8	145.5	Terrestrial
Siamosuchus	130	112.6	Terrestrial

Sichuanosuchus	161.2	99.7	Terrestrial
Simosuchus	70.6	66.043	Terrestrial
Sphagesaurus	94.3	70.6	Terrestrial
Stangerochampsa	70.6	66.043	Terrestrial
Stolokrosuchus	125.45	99.7	Terrestrial
Stratiotosuchus	94.3	66.043	Terrestrial
Sunosuchus	201.6	145.5	Terrestrial
Susisuchus	145.5	99.7	Terrestrial
Terminonaris	99.7	89.3	Terrestrial
Theriosuchus	155.7	66.043	Terrestrial
Trematochampsa	89.3	66.043	Terrestrial
Uruguaysuchus	125.45	84.9	Terrestrial
Vectisuchus	130	122.46	Terrestrial
Wannchampsus	125.45	99.7	Terrestrial
Wargosuchus	85.8	84.9	Terrestrial
Woodbinesuchus	99.7	94.3	Terrestrial
Yacarerani	94.3	84.9	Terrestrial
Zaraasuchus	84.9	70.6	Terrestrial
Zosuchus	84.9	70.6	Terrestrial

Appendix 4 – Machine readable versions of crocodyliform supertrees

To read each one of these trees into R (or your program of choice), copy them into a new text file, and append the file extension to .tre. See main text for more details.

Genus-level supertree

((((((((((Shamosuchus,Paralligator),Wannchampsus),Batrachomimus),Rugosuchus)Paralligatoridae,(Gilchristosuchus,(Susisuchus,(((((((Eothoracosaurus,(Thoracosaurus,Ocepesuchus))Gavialoidea,Arenysuchus),(((Stangerochampsa,(Albertochampsa,Brachychampsa)),Deinosuchus),Massaliasuchus,Leidyosuchus)Brevirostres),((Aegyptosuchus,Aegisuchus)Aegyptosuchidae,Borealosuchus))Crocodylia,(Allodaposuchus,(((Pachycheilosuchus,Pietraroiasuchus),Iharkutosuchus),(Acynodon,Hylaeochampsa))Hylaeochampsidae)),Aigialosuchus),Isisfordia)Eusuchia))),(Laganosuchus,(Khoratosuchus,(Koumpiodontosuchus,Bernissartia)))),((Calsoyasuchus,(Eutretauranosuchus,Sunosuchus)),Denazinosuchus,Goniopholis,Woodbinesuchus,Coelosuchus,Vectisuchus,(Siamosuchus,(Nannosuchus,(Hulkepholis,Anteophthalmosuchus))))Goniopholididae),Paluxysuchus),((((((Dyrosaurus,Chenanisuchus),Rhabdognathus),Hyposaurus),Sokotosuchus),(Pholidosaurus,(Terminonaris,Sarcosuchus,Oceanosuchus,Elosuchus,Chalawan,Meridiosaurus))Pholidosauridae),((Pelagosaurus,(Teleidosaurus,(Eoneustes,((((((Geosaurus,Dakosaurus,Aggiosaurus,Plesiosuchus,(Tyrannoneustes,Torvoneustes))Geosaurini,Purranisaurus),Neptunidraco),Metriorhynchus),Suchodus)Geosaurinae,(Gracilineustes,(Maledictosuchus,(Cricosaurus,Rhacheosaurus))Rhacheosaurini))Metriorhynchidae))),((Teleosaurus,Platysuchus),Peipehsuchus,Steneosaurus,Haematosaurus,Machimosaurus)Teleosauridae)Thalattosuchia)),Microsuchus,(((((Alligatorium,Alligatorellus),Montsecosuchus),Atoposaurus),Theriosuchus)Atoposauridae,((Candidodon,(Libycosuchus,(Simosuchus,(Doratodon,((Malawisuchus,Pakasuchus,Neuquensuchus),(((((((((Baurusuchus,Aplestosuchus),Campinasuchus),Stratiotosuchus),(Wargosuchus,Pissarrachampsa)),Gondwanasuchus),Pehuenchesuchus,Pabwehshi,Cynodontosuchus)Baurusuchidae,Comahuesuchus),Chimaerasuchus),(Morrinhosuchus,(Notosuchus,((Mariliasuchus,Labidiosuchus),((Yacarerani,Adamantinasuchus),(Cai

pirasuchus,(Sphagesaurus,(Armadillosuchus,Caryonosuchus))))Sphagesauridae)))))))Ziphosuchia),(((Araripesuchus,Anatosuchus),Uruguaysuchus)Uruguaysuchidae,((Kaprosuchus,Mahajangasuchus),(Gasparinisuchus,Pepesuchus,Barcinosuchus,Peirosaurus,Lomasuchus,(Montealtosuchus,(Trematochampsa,(Hamadasuchus,Rukwasuchus,Stolokrosuchus))))Peirosauridae)))Notosuchia)Neosuchia)Mesoeucrocodylia,(((Protosuchus,Edentosuchus),Orthosuchus),Kansajsuchus,Platyognathus,Entradasuchus,((Gobiosuchus,Zaraasuchus),(((Shantungosuchus,Sichuanosuchus),Zosuchus),((Fruitachampsa,(Nominosuchus,Shartegosuchus,Kyasuchus)),Hsisosuchus)))))Crocodyliformes;

Species-level supertree

((((((((((Shamosuchus_djadochtaensis,Paralligator_gradilifrons,Paralligator_major),Wannchampsus_kirpachi),Batrachomimus_pastosbonensis),Rugosuchus_nonganensis)Paralligatoridae,(Gilchristosuchus_palatinus,((Susisuchus_jaguaribensis,Susisuchus_anatoceps),(((((((Eothoracosaurus_mississippiensis,((Thoracosaurus_neocesariensis,Thoracosaurus_bahiensis,Thoracosaurus_borissiaki,Thoracosaurus_macrorhynchus),Ocepesuchus_eoafricanus))Gavialoidea,Arenysuchus_gascabadiolorum),(((Stangerochampsa_mccabei,(Albertochampsa_langstoni,Brachychampsa_montana)),(Deinosuchus_riograndensis,Deinosuchus_rugosus)),Massaliasuchus_affuvelensis,Leidyosuchus_canadensis)Brevirostres),((Aegyptosuchus_peyeri,Aegisuchus_witmeri)Aegyptosuchidae,(Borealosuchus_formidabilis,Borealosuchus_sternbergii)))Crocodylia,((Allodaposuchus_subjuniperus,Allodaposuchus_precedens),(((Pachycheilosuchus_trinquei,Pietraroiasuchus_ormezzanoi),Iharkutosuchus_makadii),(Acynodon_lopezi,Acynodon_iberoccitanus,Acynodon_adriaticus,Hylaeochampsa_vectiana))Hylaeochampsidae)),Aigialosuchus_villandensis),Isisfordia_duncani)Eusuchia))),((Laganosuchus_thaumastos,Laganosuchus_maghrebensis),(Khoratosuchus_jintasakuli,(Koumpiodontosuchus_aprosdokiti,Bernissartia_fagesii)))),((Calsoyasuchus_valliceps,((Sunosuchus_junggarensis,Eutretauranosuchus_delfsi),Sunosuchus_miaoi,Sunosuchus_shunanensis)),Denazinosuchus_kirtlandicus,Goniopholis_felchi,Goniopholis_affinis,Goniop

holis_undidens,Goniopholis_lucasii,Woodbinesuchus_byersmauricei,Coelosuchus_reedii,Vectisuchus_leptognathus,Goniopholis_phuwiangensis,Goniopholis_brodiei,Goniopholis_crassidens,Goniopholis_stovalli,(Siamosuchus_phuphokensis,(Nannosuchus_gracilidens,(((Hulkepholis_plotos,Hulkepholis_willetti),(Anteophthalmosuchus_hooleyi,Anteophthalmosuchus_esuchae)),(Goniopholis_baryglyphaeus,(Goniopholis_kiplingi,Goniopholis_simus))))))Goniopholididae),Paluxysuchus_newmani),((((((Dyrosaurus_phosphaticus,Chenanisuchus_lateroculi),Rhabdognathus_keiniensis),Hyposaurus_rogersii),Sokotosuchus_ianwilsoni),((Pholidosaurus_decipiens,Pholidosaurus_meyeri,Pholidosaurus_purbeckensis,Pholidosaurus_schaumburgensis),((Terminonaris_browni,Terminonaris_robusta),(Sarcosuchus_hartti,Sarcosuchus_imperator),Oceanosuchus_boecensis,(Elosuchus_felixi,Elosuchus_cherifiensis),Chalawan_thailandicus,Meridiosaurus_vallisparadisi))Pholidosauridae),(((Pelagosaurus_typus,Pelagosaurus_brongniarti),(Teleidosaurus_calvadosii,((Eoneustes_bathonicus,Eoneustes_gaudryi),(((((((Geosaurus_grandis,Geosaurus_giganteus),Geosaurus_lapparenti),Geosaurus_araucaniensis,(Dakosaurus_andiniensis,Dakosaurus_maximus),Aggiosaurus_nicaeensis,Plesiosuchus_manselii,(Tyrannoneustes_lythrodectikos,(Torvoneustes_coryphaeus,Torvoneustes_carpenteri)))Geosaurini,Purranisaurus_potens),Metriorhynchus_brachyrhynchus,Neptunidraco_ammoniticus),(Metriorhynchus_casamiquelai,Metriorhynchus_westermanni)),Suchodus_durobrivensis)Geosaurinae,(Metriorhynchus_palpebosus,Metriorhynchus_littoreus,Metriorhynchus_moreli,(((Metriorhynchus_geoffroyii,Metriorhynchus_hastifer),Metriorhynchus_superciliosus),((Gracilineustes_acutus,Gracilineustes_leedsi),(Maledictosuchus_riclaensis,(((Cricosaurus_saltillensis,Cricosaurus_elegans,(Cricosaurus_gracilis,Cricosaurus_vignaudi,(Cricosaurus_araucanensis,Cricosaurus_macrospondylus,Cricosaurus_lithographicus))),Cricosaurus_suevicus),Rhacheosaurus_gracilis))Rhacheosaurini))))Metriorhynchidae))),(((Teleosaurus_cadomensis,Teleosaurus_chapmani,Teleosaurus_geoffroyi,Teleosaurus_sublidens,Teleosaurus_picteti,Teleosaurus_temporalis,Teleosaurus_megarhinus),Platysuchus_multiscrobiculatus),Peipehsuchus_teleorhinus,Steneosaurus_boutilieri,(Steneosaurus_brevidens,Steneosaurus_brevior,Steneosaurus_brevirostris,Steneosaurus_durobrivensis,Steneosaurus_larteti,Steneosaurus_morinicus,Steneosaurus_gerthi,S

teneosaurus_heberti,Steneosaurus_jugleri,Steneosaurus_pictaviensis,Steneosaurus_dasycephalus,St
eneosaurus_rudis,Steneosaurus_subulidens,Steneosaurus_gracilirostris,Steneosaurus_intermedius),
Haematosaurus_lanceolatus,(((Machimosaurus_hugii,Steneosaurus_edwardsi),(Steneosaurus_megis
torhynchus,Steneosaurus_leedsi)),Steneosaurus_bollensis))Teleosauridae)Thalattosuchia)),Microsuc
hus_schilleri,((((((Alligatorium_meyeri,Alligatorium_franconicum),(Alligatorellus_bavaricus,Alligatore
llus_beaumonti)),Montsecosuchus_depereti),(Atoposaurus_jourdani,Atoposaurus_oberndorferi)),((T
heriosuchus_ibericus,Theriosuchus_sympiestodon),(Theriosuchus_grandinaris,(Theriosuchus_pusillu
s,Theriosuchus_guimarotae))))Atoposauridae,((Candidodon_itapecuruense,(Libycosuchus_brevirostr
is,(Simosuchus_clarki,((Doratodon_carcharidens,Doratodon_ibericus),((Malawisuchus_mwakasyung
utiensis,Pakasuchus_kapilimai,Neuquensuchus_universitas),((((((((((Baurusuchus_albertoi,Aplestosu
chus_sordidus),(Baurusuchus_salgadoensis,Baurusuchus_pachecoi)),Campinasuchus_dinizi),Stratiot
osuchus_maxhechti),(Wargosuchus_australis,Pissarrachampsa_sera)),Gondwanasuchus_scabrosus),
Pehuenchesuchus_enderi,Pabwehshi_pakistanensis,Cynodontosuchus_rothi)Baurusuchidae,Comahu
esuchus_brachybuccalis),Chimaerasuchus_paradoxus),(Morrinhosuchus_luziae,(Notosuchus_terrest
ris,((Mariliasuchus_robustus,Mariliasuchus_amarali,Labidiosuchus_amicum),((Yacarerani_boliviensis
,Adamantinasuchus_navae),((Caipirasuchus_paulistanus,Caipirasuchus_stenognathus),((Sphagesaur
us_huenei,Sphagesaurus_montealtensis),(Armadillosuchus_arrudai,Caryonosuchus_pricei))))Sphage
sauridae)))))))Ziphosuchia),(((Araripesuchus_wegeneri,Araripesuchus_rattoides,Araripesuchus_tsan
gatsangana,Anatosuchus_minor),(((Araripesuchus_patagonicus,(Uruguaysuchus_aznarezi,Uruguaysu
chus_terrai)),Araripesuchus_gomesii),Araripesuchus_buitreraensis))Uruguaysuchidae,((Kaprosuchus
_saharicus,Mahajangasuchus_insignis),(Gasparinisuchus_peirosauroides,Pepesuchus_deiseae,Barcin
osuchus_gradilis,Peirosaurus_tormini,Lomasuchus_palpebrosus,((Montealtosuchus_arrudacamposi,
Uberabasuchus_terrificus),(Trematochampsa_taqueti,(Hamadasuchus_rebouli,Rukwasuchus_yajabal
ijekundu,Stolokrosuchus_lapparenti))))Peirosauridae)))Notosuchia)Neosuchia)Mesoeucrocodylia,((((
Protosuchus_haughtoni,Protosuchus_richardsoni,Protosuchus_micmac),Edentosuchus_tienshanensi

s),Orthosuchus_stormbergi),Kansajsuchus_extensus,Platyognathus_hsui,Entradasuchus_spinosus,(((Gobiosuchus_parvus,Gobiosuchus_kielanae),Zaraasuchus_shepardi),((((Shantungosuchus_chuhsienensis,Shantungosuchus_hangjinensis),(Sichuanosuchus_huidongensis,Sichuanosuchus_shuhanensis)),Zosuchus_davidsoni),((Fruitachampsa_callisoni,(Nominosuchus_matutinus,Shartegosuchus_asperopalatum,Kyasuchus_saevi)),(Hsisosuchus_chungkingensis,(Hsisosuchus_chowi,Hsisosuchus_dashanpuensis)))))))Crocodyliformes;

Appendix 5 – Age ranges for crocodyliform species used to construct supertree (see Section 2.6)

Species	FAD	LAD
Acynodon adriaticus	84.9	66.043
Acynodon iberoccitanus	84.9	66.043
Acynodon lopezi	70.6	66.043
Adamantinasuchus navae	94.3	84.9
Aegisuchus witmeri	99.7	94.3
Aegyptosuchus peyeri	99.7	94.3
Aggiosaurus nicaeensis	161.2	155.7
Aigialosuchus villandensis	84.9	70.6
Albertochampsa langstoni	84.9	70.6
Alligatorellus bavaricus	150.8	145.5
Alligatorellus beaumonti	155.7	150.8
Alligatorium franconicum	155.7	150.8
Alligatorium meyeri	155.7	150.8
Allodaposuchus precedens	84.9	66.043
Allodaposuchus subjuniperus	70.6	66.043
Anatosuchus minor	122.46	109
Anteophthalmosuchus esuchae	112.6	109
Anteophthalmosuchus hooleyi	130	125.45
Aplestosuchus sordidus	99.7	66.043
Araripesuchus buitreraensis	99.7	94.3
Araripesuchus gomesii	112.6	109
Araripesuchus patagonicus	99.7	94.3
Araripesuchus rattoides	99.7	94.3
Araripesuchus tsangatsangana	70.6	66.043
Araripesuchus wegeneri	122.46	99.7
Arenysuchus gascabadiolorum	70.6	66.043
Armadillosuchus arrudai	94.3	84.9
Atoposaurus jourdani	155.7	150.8
Atoposaurus oberndorferi	150.8	145.5
Barcinosuchus gradilis	125.45	99.7
Batrachomimus pastosbonensis	161.2	145.5
Baurusuchus albertoi	84.9	66.043
Baurusuchus pachecoi	94.3	84.9
Baurusuchus salgadoensis	94.3	84.9
Bernissartia fagesii	145.5	125.45
Borealosuchus formidabilis	84.9	70.6
Borealosuchus sternbergii	70.6	66.043
Brachychampsa montana	84.9	66.043
Caipirasuchus paulistanus	94.3	84.9

Caipirasuchus stenognathus	84.9	66.043
Calsoyasuchus valliceps	196.5	183
Campinasuchus dinizi	94.3	84.9
Candidodon itapecuruense	112.6	99.7
Caryonosuchus pricei	94.3	84.9
Chalawan thailandicus	150.8	145.5
Chenanisuchus lateroculi	70.6	66.043
Chimaerasuchus paradoxus	125.45	99.7
Coelosuchus reedii	99.7	94.3
Comahuesuchus brachybuccalis	85.8	84.9
Cricosaurus araucanensis	150.8	145.5
Cricosaurus elegans	150.8	145.5
Cricosaurus gracilis	150.8	145.5
Cricosaurus lithographicus	150.8	145.5
Cricosaurus macrospondylus	140.2	136.4
Cricosaurus saltillensis	150.8	145.5
Cricosaurus suevicus	155.7	150.8
Cricosaurus vignaudi	150.8	145.5
Cynodontosuchus rothi	85.8	84.9
Dakosaurus andiniensis	150.8	140.2
Dakosaurus maximus	155.7	145.5
Deinosuchus riograndensis	84.9	70.6
Deinosuchus rugosus	84.9	70.6
Denazinosuchus kirtlandicus	84.9	70.6
Doratodon carcharidens	84.9	70.6
Doratodon ibericus	84.9	66.043
Dyrosaurus phosphaticus	70.6	66.043
Edentosuchus tienshanensis	122.46	99.7
Elosuchus cherifiensis	112.6	94.3
Elosuchus felixi	112.6	94.3
Entradasuchus spinosus	164.7	161.2
Eoneustes bathonicus	155.7	150.8
Eoneustes gaudryi	167.7	164.7
Eothoracosaurus mississippiensis	70.6	66.043
Eutretauranosuchus delfsi	155.7	150.2
Fruitachampsa callisoni	155.7	145.5
Gasparinisuchus peirosauroides	85.8	70.6
Geosaurus araucaniensis	150.8	140.2
Geosaurus giganteus	150.8	145.5
Geosaurus grandis	150.8	145.5
Geosaurus lapparenti	140.2	130
Gilchristosuchus palatinus	85.8	84.9
Gobiosuchus kielanae	84.9	70.6
Gobiosuchus parvus	84.9	70.6

Gondwanasuchus scabrosus	94.3	84.9
Goniopholis affinis	125.45	112.6
Goniopholis baryglyphaeus	155.7	150.8
Goniopholis brodiei	155.7	140.2
Goniopholis crassidens	145.5	122.46
Goniopholis felchi	155.7	145.5
Goniopholis kiplingi	145.5	140.2
Goniopholis lucasii	155.7	145.5
Goniopholis phuwiangensis	130	112.6
Goniopholis simus	145.5	140.2
Goniopholis stovalli	155.7	145.5
Goniopholis undidens	150.8	145.5
Gracilineustes acutus	155.7	150.8
Gracilineustes leedsi	164.7	161.2
Haematosaurus lanceolatus	155.7	150.8
Hamadasuchus rebouli	105.3	94.3
Hsisosuchus chowi	161.2	155.7
Hsisosuchus chungkingensis	161.2	145.5
Hsisosuchus dashanpuensis	171.6	161.2
Hulkepholis plotos	112.6	109
Hulkepholis willetti	140.2	136.4
Hylaeochampsa vectiana	130	122.46
Hyposaurus rogersii	84.9	66.043
Iharkutosuchus makadii	85.8	84.9
Isisfordia duncani	105.3	94.3
Kansajsuchus extensus	85.8	84.9
Kaprosuchus saharicus	99.7	94.3
Khoratosuchus jintasakuli	130	112.6
Koumpiodontosuchus aprosdokiti	130	125.45
Kyasuchus saevi	125.45	112.6
Labidiosuchus amicum	70.6	66.043
Laganosuchus maghrebensis	99.7	94.3
Laganosuchus thaumastos	99.7	94.3
Leidyosuchus canadensis	84.9	70.6
Libycosuchus brevirostris	99.7	94.3
Lomasuchus palpebrosus	94.3	85.8
Machimosaurus hugii	164.7	130
Mahajangasuchus insignis	70.6	66.043
Malawisuchus mwakasyungutiensis	125.45	112.6
Maledictosuchus riclaensis	164.7	161.2
Mariliasuchus amarali	84.9	66.043
Mariliasuchus robustus	94.3	84.9
Massaliasuchus affuvelensis	85.8	70.6
Meridiosaurus vallisparadisi	155.7	145.5

Metriorhynchus brachyrhynchus	167.7	145.5
Metriorhynchus casamiquelai	164.7	161.2
Metriorhynchus geoffroyii	164.7	155.7
Metriorhynchus hastifer	155.7	150.8
Metriorhynchus littoreus	155.7	150.8
Metriorhynchus moreli	164.7	161.2
Metriorhynchus palpebosus	150.8	145.5
Metriorhynchus superciliosus	164.7	150.8
Metriorhynchus westermanni	164.7	155.7
Microsuchus schilleri	99.7	66.043
Montealtosuchus arrudacamposi	94.3	84.9
Montsecosuchus depereti	130	125.45
Morrinhosuchus luziae	94.3	84.9
Nannosuchus gracilidens	145.5	125.45
Neptunidraco ammoniticus	171.6	164.7
Neuquensuchus universitas	85.8	84.9
Nominosuchus matutinus	150.8	145.5
Notosuchus terrestris	85.8	84.9
Oceanosuchus boecensis	99.7	94.3
Ocepesuchus eoafricanus	70.6	66.043
Orthosuchus stormbergi	201.6	189.6
Pabwehshi pakistanensis	70.6	66.043
Pachycheilosuchus trinquei	112.6	109
Pakasuchus kapilimai	125.45	99.7
Paluxysuchus newmani	122.46	112.6
Pehuenchesuchus enderi	89.3	84.9
Peipehsuchus teleorhinus	145.5	99.7
Peirosaurus tormini	70.6	66.043
Pelagosaurus brongniarti	183	175.6
Pelagosaurus typus	183	182
Pepesuchus deiseae	84.9	66.043
Pholidosaurus decipiens	145.5	140.2
Pholidosaurus meyeri	145.5	140.2
Pholidosaurus purbeckensis	145.5	140.2
Pholidosaurus schaumburgensis	145.5	140.2
Pietraroiasuchus ormezzanoi	112.6	109
Pissarrachampsa sera	94.3	66.043
Platyognathus hsui	196.5	189.6
Platysuchus multiscrobiculatus	183	182
Plesiosuchus manselii	155.7	145.5
Protosuchus haughtoni	201.6	189.6
Protosuchus micmac	201.6	196.5
Protosuchus richardsoni	201.6	196.5
Purranisaurus potens	150.8	145.5

Rhabdognathus keiniensis	70.6	66.043
Rhacheosaurus gracilis	150.8	145.5
Rugosuchus nonganensis	94.3	84.9
Rukwasuchus yajabalijekundu	125.45	94.3
Sarcosuchus hartti	125.45	112.6
Sarcosuchus imperator	145.5	94.3
Shamosuchus djadochtaensis	84.9	70.6
Paralligator gradilifrons	99.7	89.3
Paralligator major	99.7	89.3
Shantungosuchus chuhsienensis	150.8	112.6
Shantungosuchus hangjinensis	145.5	99.7
Shartegosuchus asperopalatum	150.8	145.5
Siamosuchus phuphokensis	130	112.6
Sichuanosuchus huidongensis	161.2	155.7
Sichuanosuchus shuhanensis	145.5	99.7
Simosuchus clarki	70.6	66.043
Sokotosuchus ianwilsoni	70.6	66.043
Sphagesaurus huenei	84.9	70.6
Sphagesaurus montealtensis	84.9	66.043
Stangerochampsa mccabei	70.6	66.043
Steneosaurus bollensis	183	175.6
Steneosaurus boutilieri	167.7	161.2
Steneosaurus brevidens	167.7	164.7
Steneosaurus brevior	183	182
Steneosaurus brevirostris	155.7	150.8
Steneosaurus dasycephalus	164.7	161.2
Steneosaurus durobrivensis	164.7	161.2
Steneosaurus edwardsi	164.7	145.5
Steneosaurus gerthi	180.1	175.6
Steneosaurus gracilirostris	183	175.6
Steneosaurus heberti	167.7	155.7
Steneosaurus intermedius	164.7	155.7
Steneosaurus jugleri	161.2	155.7
Steneosaurus larteti	167.7	164.7
Steneosaurus leedsi	164.7	161.2
Steneosaurus megistorhynchus	167.7	164.7
Steneosaurus morinicus	155.7	150.8
Steneosaurus pictaviensis	161.2	145.5
Steneosaurus rudis	155.7	145.5
Steneosaurus subulidens	167.7	164.7
Stolokrosuchus lapparenti	125.45	99.7
Stratiotosuchus maxhechti	94.3	66.043
Suchodus durobrivensis	164.7	161.2
Sunosuchus junggarensis	161.2	155.7

Sunosuchus miaoi	201.6	145.5
Sunosuchus shunanensis	171.6	161.2
Susisuchus anatoceps	122.46	99.7
Susisuchus jaguaribensis	145.5	125.45
Teleidosaurus calvadosii	171.6	164.7
Teleosaurus cadomensis	167.7	150.8
Teleosaurus chapmani	183	182
Teleosaurus geoffroyi	167.7	164.7
Teleosaurus megarhinus	155.7	150.8
Teleosaurus picteti	155.7	150.8
Teleosaurus sublidens	167.7	164.7
Teleosaurus temporalis	155.7	150.8
Terminonaris browni	94.3	89.3
Terminonaris robusta	99.7	89.3
Theriosuchus grandinaris	130	112.6
Theriosuchus guimarotae	155.7	150.8
Theriosuchus ibericus	130	125.45
Theriosuchus pusillus	155.7	140.2
Theriosuchus sympiestodon	70.6	66.043
Thoracosaurus bahiensis	125.45	112.6
Thoracosaurus borissiaki	70.6	66.043
Thoracosaurus macrorhynchus	70.6	66.043
Thoracosaurus neocesariensis	84.9	66.043
Torvoneustes carpenteri	155.7	150.8
Torvoneustes coryphaeus	155.7	150.8
Trematochampsa taqueti	89.3	84.9
Tyrannoneustes lythrodectikos	164.7	161.2
Uberabasuchus terrificus	70.6	66.043
Uruguaysuchus aznarezi	125.45	84.9
Uruguaysuchus terrai	125.45	84.9
Vectisuchus leptognathus	130	122.46
Wannchampsus kirpachi	125.45	112.6
Wargosuchus australis	85.8	84.9
Woodbinesuchus byersmauricei	99.7	94.3
Yacarerani boliviensis	94.3	84.9
Zaraasuchus shepardi	84.9	70.6
Zosuchus davidsoni	84.9	70.6

Appendix 6 – Atoposaurid character list

Primary sources for characters are provided. Where characters have been modified, details are given at the end of the character statement. All characters have been reformatted to a standardised notation to be as explicit as possible about the morphology. New characters are indicated, although some of these are the product of splitting previously used characters, or modified from statements in previously published works.

The following 47 characters are **ordered**: 3, 7, 10, 13, 20, 23-30, 33, 37, 56, 58, 84, 89, 99, 100, 103, 115, 119, 128, 133, 150, 153, 175, 179, 183, 203, 204, 217, 246, 264-266, 272, 285, 288-291, 300, 305, 321.

Cranial Characters

1. Dorsal cranial bones (skull roof, cranial table), external surface: smooth (0); ornamented (1) (Clark *et al.*, 1994).
2. Dorsal cranial bones (skull roof, cranial table), external surface: slightly grooved (0); heavily ornamented with deep pits and/or grooves (1); with shallow pits (2) (Clark *et al.*, 1994) (character state 2 added here; added '/or' to state 1).
3. Snout, external surface, sculpting: absent (0); present but to a lesser degree than cranial table (1); present, as prominent as on cranial table (2) (Gasparini *et al.*, 2006) (character state 1 added here; added 'as prominent as on cranial table' to character state 2) [**ordered**].
4. Rostrum, dorsal projection posterior to the external nares, relative to remainder of rostrum: absent, rostrum straight or low (0); rostrum upturned (1) (de Andrade *et al.*, 2011b) (added 'posterior to the external nares, relative to remainder of rostrum').

5. Skull, lateral expansion at orbits relative to rostrum: gradual (0); abrupt (1) (Clark *et al.*, 1994) (added 'lateral' and 'relative to rostrum').

6. Snout, lateral contour, in dorsal view: straight (0); sinusoidal ('festooned') (1) (Ortega *et al.*, 2000).

7. Snout, overall proportions: narrow oreinirostral (tall and domed) (0); nearly tubular (1); platyrostral (broad and flat) (2) (Clark *et al.*, 1994) (terminology from (Rayfield and Milner, 2008)) [**ordered**].

8. Snout, profile of dorsal edge in lateral view (anterior to cranial table): concave (0); convex (1); approximately straight (2) (Sweetman *et al.*, 2015).

9. External nares, orientation: facing anterolaterally (0); facing dorsally (1); facing anterodorsally (2) (Clark *et al.*, 1994) (character state 2 added here).

10. External nares: completely divided by a septum (0); partially divided posteriorly (1); confluent, no indication of a septum (2) (Clark *et al.*, 1994) [**ordered**].

11. Orbit, orientation: facing anterolaterally (0); facing fully laterally (1) (Wilkinson *et al.*, 2008).

12. Orbit, anterolateral border: continuous margin (0); develops as a small groove into pre-orbital elements (1) (new character).

13. External antorbital fenestra: large, greater than 0.5 times the size of the orbit (0) small, less than or equal to 0.5 times the size of the orbit (1); absent (2) (de Andrade *et al.*, 2011b) (changed to a multistate, adding character states 0 and 1 to replace character state 'present') [**ordered**].

14. Antorbital fenestra, shape: rounded or dorsoventrally high (0); dorsoventrally low and anteroposteriorly elongate, slit-like (1) (2) (Gasparini *et al.*, 2006).

15. External supratemporal fenestra: present (0); absent (1) (Ortega *et al.*, 2000).

16. External supratemporal fenestra: perforated (0); imperforated (1) (new character (Joffe, 1967)).

17. External supratemporal fenestra, shape: square to sub-rectangular (0); circular to subcircular (1); mediolaterally narrow and slit-like (2) (de Andrade *et al.*, 2011b) (deleted character state 'triangular, converging medially'; added character state 2).

18. External supratemporal fenestra, maximum anteroposterior length: equal to or shorter than orbits (0); longer than orbits (1) (Clark *et al.*, 1994) (added 'maximum' to refine character).

19. Intertemporal mediolateral width (minimum between supratemporal fenestrae), relative to interorbital mediolateral width (minimum between orbits): intertemporal region broader (0); intertemporal region equal or narrower (1) (new character)

20. Lateral temporal fenestra in lateral view, size proportional to orbit in dorsal view: small to absent, no more than 20% of the area of the orbit (0); more than 20 to less than 50% of the area of the orbit (1); area is larger than 50% of the area of the orbit (2) (de Andrade *et al.*, 2011b) (character state 1 added here) [**ordered**].

21. Lateral temporal fenestra, orientation: faces laterally (0); faces dorsolaterally (1) (de Andrade *et al.*, 2011b).

22. Lateral temporal fenestra, shape: triangular (0); elliptical to subpolygonal (1) (Ortega *et al.*, 2000).

23. Suborbital fenestra: small, less than 50% of orbital area (0); between 50% and the same size as the orbit (1); larger than the orbit (2) (de Andrade *et al.*, 2011b) (quantified state 1) [**ordered**].

24. Intermandibular angle (degrees): lower than 40° (0); 40-45 (1); 46-50° (2); greater than 50° (3) (new character) [**ordered**].

25. Skull length: skull width, ratio: less than 2.0 (0); 2.0 to less than 2.5 (1); 2.5 or greater (2) (new character) [**ordered**].

26. Skull length: snout length, ratio: less than 2.0 (0); 2.0 to less than 2.5 (1); 2.5 to less than 3.0 (2); 3.0 or greater (3) (new character) [**ordered**].

27. Skull length: orbit length, ratio: less than 3.0 (0); 3.0 to less than 4.0 (1) 4.0 to less than 5.0 (2); 5.0 or greater (3) (new character) [**ordered**].

28. Skull width: orbit width, ratio: less than 2.5 (0); 2.5 to less than 3.5 (1); 3.5 or greater (2) (new character) [**ordered**].

29. Skull length: supratemporal fenestra length, ratio: less than 6.0 (0); 6.0 to less than 7.0 (1); 7.0 to less than 8.0 (2) 8.0 or greater (3) (new character) [**ordered**].

30. Skull width: supratemporal fenestra width, ratio: less than 3.0 (0); 3.0 to less than 5.0 (1); 5.0 to less than 6.0 (2); 6.0 or greater (3) (new character) [**ordered**].

31. Premaxilla, maximum mediolateral width of paired premaxillae relative to that of the rostrum at the level of alveoli 4 or 5: premaxillae equal or narrower (0); rostrum narrower (1) (Jouve, 2009).

32. Premaxilla, anterior to nares: narrower than, or equal to, twice the anterior nasal mediolateral width (0); broader than twice the anterior nasal width (1) (Clark *et al.*, 1994) (quantified).

33. Premaxilla-maxilla, distance between the anterior tip of the snout and the anteriormost position of the premaxilla-maxilla suture in dorsal view, relative to the distance between the anteriormost position of the premaxilla-maxilla suture and the posterodorsal extremity of the premaxilla in dorsal view: distance between the tip of the snout and the anteriormost position of the premaxilla-maxilla suture larger (0); distances approximately equal (1); distance between the anteriormost position of the premaxilla-maxilla suture and the posterodorsal extremity of the premaxilla larger (2) (Jouve, 2004) [**ordered**].

34. Premaxilla-maxilla suture, small foramen in lateral surface (not for large mandibular teeth): absent (0); present (1) (Pol, 1999).

35. Premaxilla, projection of the internarial bar relative to the main body of premaxilla and narial opening: does not project anterior to the main body of the premaxilla (0); strongly projected anteriorly from narial opening, extending anterior to main body of maxilla (1) (de Andrade *et al.*, 2011b).

36. Premaxilla, participation in internarial bar: forming at least the anterior half (0); with little participation (1) (Clark *et al.*, 1994) (replaced 'ventral' with 'anterior' in character state 0).

37. Premaxilla, ventral edge relative to maxilla: lower than ventral edge of maxilla, with dorsal contour of anterior part of dentary strongly concave to accommodate (0); at same height as ventral edge of maxilla (1); premaxilla ventral edge dorsal to maxilla (2) (Ortega *et al.*, 2000) (character state 2 added here) [**ordered**].

38. Premaxilla, perinarial crests: absent (0); present as well-defined and distinct ridges, cornering the lateral to posterior borders of the naris (1) (de Andrade *et al.*, 2011b).

39. Premaxilla, notch on lateral edge of external nares: absent (0); present on the dorsal half of the lateral edge of the external nares (1) (Pol, 1999).

40. Premaxilla, perinarial fossa: absent (0); present (1) (Pol and Apesteguía, 2005)

41. Premaxilla, postnarial fossa: absent (0); present (1) (de Andrade *et al.*, 2011b).

42. Premaxilla-maxilla, suture: confluent ventrally (0); opened contact on ventral edge of rostrum (1) (Clark *et al.*, 1994).

43. Premaxilla-maxilla contact, orientation in dorsal view, whether or not posterodorsal process is present: anteromedially directed (0); posteromedially directed (1) (Schwarz and Salisbury, 2005) (added 'whether or not posterodorsal process is present').

44. Premaxilla, posterodorsal process: absent (0); present, extending posteriorly and wedging between maxillae and nasals (1) (Pol, 1999).

45. Premaxilla, orientation of anterior alveolar margin: vertical (0); out-turned (1) (Sereno *et al.*, 2001) (character state 1 modified from 'inturned').

46. Maxillae, posterior palatal branches anterior to palatines: do not meet (0); meet (1) (Clark *et al.*, 1994).

47. Maxilla-premaxilla, suture in palatal view medial to alveolar region: sinusoidal, posteromedially directed on lateral half and anteromedially directed along medial region (0);

posteromedially-directed (1) (Pol, 1999) (character states 'anteromedially directed' and 'premaxillae-maxillae suture U-shaped' removed.

48. Maxilla-premaxilla, lateral fossa excavating alveolus of last premaxillary tooth: absent (0); present (1) (Larsson and Sues, 2007).

49. Maxilla, depression on posterolateral surface, laterally positioned: absent (0); present (1) (Wu *et al.*, 1997) (added 'on posterolateral').

50. Maxilla, depression on anterolateral surface, medially positioned: absent (0); present (1) (new character).

51. Maxilla, lateral surface of jugal process (posterior portion): heavily striated (0); ornamented, like rest of rostrum (1); smooth (2) (new character).

52. Maxilla, ventral edge in lateral view: straight or convex (0); sinusoidal (1) (Ortega *et al.*, 2000).

53. Maxilla and premaxilla, general shape of external surface: single plane facing laterally (0); with ventral region facing laterally and dorsal region facing dorsolaterally (1) (Pol, 1999).

54. Maxilla, presence of occlusal pit for reception of enlarged dentary tooth anterior to dental arcade (or M2): present (0); absent (1) (new character) (Martin *et al.*, 2014c).

55. Maxilla, evaginated alveolar edges: absent (0); present (1) (Gasparini *et al.*, 2006).

56. Maxilla, lateral surface, unsculpted region along alveolar margin: absent (0); present (1) (Wu and Sues, 1996).

57. Maxilla, sculpturing of palatal surface: absent, palatal surface smooth (0); present anteriorly, absent posteriorly (1); present throughout, palatal surface ornamented with ridges (2) (Ortega *et al.*, 2000) [**ordered**].

58. Maxilla, foramen on palatal surface, dorso-medial to enlarged 5th tooth: absent (0); present (1); develops elongate groove (2) (new character) [**ordered**].

59. Maxillary teeth, dental implantation, middle teeth: confluent, located in dental groove (0); in isolated alveoli (1) (new character).

60. Maxillary teeth, dental implantation, posterior teeth: confluent, located in dental groove (0); in isolated alveoli (1) (new character).

61. Maxilla, palatine process: absent (0); present, next to the anterior border of suborbital fenestrae (1) (de Andrade and Bertini, 2008).

62. Maxilla-nasal, suture, orientation with respect to snout lateral margins: parallel (0); oblique (1) (new character).

63. Nasal, participation in dorsal margin of external nares: present (0); absent (1) (new character).

64. Nasal participation in margins of external nares: present posteriorly (0); present posteriorly and medially (1) (Clark *et al.*, 1994).

65. Nasals: paired and unfused (0); partially or completely fused (1) (Gasparini *et al.*, 2006) (added 'and unfused' to character state 0).

66. Nasal, lateral border posterior to external nares: concave (0); straight (1); convex (2); sinusoidal (3) (character states 2 and 3 added) (Pol, 1999).

67. Nasal, lateral edges: sub-parallel (0); oblique to one another, converging anteriorly (1) (Pol, 1999).

68. Nasal, participation in antorbital fenestra: present (0); absent (1) (Ortega *et al.*, 2000).

69. Nasal, posterior portion of the dorsal surface: anteroposteriorly crenulated (0); smooth or sculpted as rest of rostrum (1) (new character).

70. Nasals, posterior mediolateral widening adjacent to the maxilla (anterior to contact with peri-orbital elements): abrupt (0); gradual (constant) (1); (new character) (Lauprasert *et al.*, 2011).

71. Nasal-lacrimal contact: present (0); absent (1) (Clark *et al.*, 1994).

72. Nasal-lacrimal contact: along medial surface of lacrimal (0); lacrimal forms a point contact with nasal (1) (Clark *et al.*, 1994) (changed character state 1 from 'along medial and anterior surfaces of lacrimal' to 'forms a point contact with nasal').

73. Nasal, posterior tips of nasals: converge along the sagittal plane (0); separated by anterior projection of frontals (1) (Ortega *et al.*, 2000).

74. Nasal, posterior portion and anterior portion of frontal, midline anteroposterior depression: absent (0); present (1) (Montefeltro *et al.*, 2011).

75. Lacrimal, total anteroposterior length relative to anteroposterior length of prefrontal: longer (0); shorter or equal to (1) (Brochu, 1999) (combined states 1 and 2).

76. Lacrimal, shape: anteroposteriorly longer than mediolaterally broad (0); as anteroposteriorly long as mediolaterally broad (1) (Sereno and Larsson, 2009).

77. Lacrimal, posterior extent and relationship with jugal: extending posteroventrally, widely contacting jugal (0); tapering posteroventrally, does not contact jugal or only point contact with jugal (1) (Zaher *et al.*, 2006).

78. Lacrimal and jugal, anterior margins: confluent, with no notch at the anterior contact (0); jugal edge convex, producing an anterior notch at contact (filled with maxilla) (1) (Larsson and Sues, 2007).

79. Jugal, anterior extension below orbit, in dorsolateral view: does not extend beyond anterior margin of orbit (0); extends beyond anterior margin (1) (Pol, 1999).

80. Jugal, dorsoventral depth of orbital portion in relation to infratemporal portion: almost the same to less than twice the depth (0); orbital portion twice the depth of the infratemporal portion (1) (Clark *et al.*, 1994) (added 'to less than twice the depth' to character state 0).

81. Jugal, foramen on the lateral surface near the anterior margin: absent (0); present (1) (Zaher *et al.*, 2006).

82. Jugal, anterior process length relative to infratemporal fenestrae anteroposterior length: 1.0 or less times the length (0); longer than 1.0 times the length (1) (Larsson and Sues, 2007) (Changed character states 0 and 1 to define state boundary ratio).

83. Jugal, orientation of base of postorbital process: directed posterodorsally (0); directed dorsally (1) (Pol, 1999).

84. Jugal, location of postorbital process relative to main jugal body: anteriorly placed (0); in the middle (1); posteriorly positioned (2) (Pol, 1999) [**ordered**].

85. Jugal portion of postorbital bar, relative to lateral surface of jugal: flush with lateral surface of jugal (0); inset (1) (Ortega *et al.*, 2000).

86. Jugal, anterior fossa: bordered by ornamented ridge (0); continuous with lateral surface (1) (new character).

87. Jugal, anteroposterior ridge on lateral surface below infratemporal fenestrae: absent (0); present (1) (Pol and Norell, 2004b).

88. Jugal-ectopterygoid, suture ridge: absent (0); present (1) (Montefeltro *et al.*, 2011).

89. Preorbital elements, anterior palpebral bone: no notable depression or projection (0); marked depression, developing into an incipient lateral projection (1); marked depression forming a prominent lateral projection for the support of the anterior palpebral (2) (Sereno and Larsson, 2009) (character state 0 added here) [**ordered**].

90. Prefrontal, lateral development: reduced, no notable lateral projection (0); enlarged, extending laterally or posterolaterally over orbit (1) (Gasparini *et al.*, 2006) (changed to 'laterally or posterolaterally' in state 1).

91. Prefrontal, anterior morphology: tapers anteriorly to a point (0); anteriorly broad (1) (new character).

92. Prefrontal-frontal sutures, form paired dorsal crests: absent (0); present (1) (Pol and Powell, 2011).

93. Prefrontal-lacrimal suture, crest: absent (0); present, situated anterior to orbit (1) (de Andrade *et al.*, 2011b) (changed 'dorsal' to 'anterior' in character state 1).

94. Prefrontal and lacrimal around orbits: forming flat rims (0); evaginated, forming elevated rims from the dorsal surface of the skull (1) (Gasparini *et al.*, 2006).

95. Prefrontal pillars (ventral process): not contacting palate (0); contacting palate (1) (Clark *et al.*, 1994).

96. Frontals: unfused (0); fused (1) (Clark *et al.*, 1994) (changed to indicate degree of fusion).

97. Frontal, mediolateral width of paired frontals between orbits: broader than nasals (0) equal or narrower than nasals (1) (Clark *et al.*, 1994) (added 'equal or' to character state 1).

98. Frontals, mediolateral width between orbits: narrower than posterior end (posterior end flares laterally posterior to orbits) (0); equal width or broader than posterior end (1) (new character) (Sweetman *et al.*, 2015).

99. Frontal, morphology of anteriormost border of anterior process: truncated (0); wedge-like (1); bifurcated (2) (character state 2 added here) (de Andrade *et al.*, 2011b) [**ordered**].

100. Frontals, dorsal surface: flat (0); with anteroposterior ridge along midline suture (1) (Clark *et al.*, 1994) (added 'along midline suture' to character state 1) [**ordered**] (note that this character might change relating to ontogeny (Schwarz and Salisbury, 2005)).

101. Frontal, dorsal anteroposterior ridge(s): restricted to the posterior portion (0); restricted to median portion (1); restricted to anterior portion (2); occupy entire length of frontal (3) (Montefeltro *et al.*, 2011) (character state 3 added).

102. Frontal, anterior extension of anterior margin: level with, or anterior to, the orbits (0); does not reach the anterior margin of the orbits (1) (de Andrade *et al.*, 2011b).

103. Frontal, participation in orbit border: forming great part of posterior, medial and anterior (or anteromedial) regions (0); restricted to posterior and posteromedial region (1); restricted to medial margin (2) (Montefeltro *et al.*, 2013) (character state 'restricted to the posterior region' removed; character states 1 and 2 added here) [**ordered**].

104. Frontal, transverse ridge crossing anteromedial to the orbits: absent (0); present (1) (Pol *et al.*, 2009).

105. Frontal, participation in supratemporal fenestra: absent (0); present (1) (new character).

106. Frontal, participation in supratemporal fenestra: anteromedially (0), anteriorly only (1) (new character).

107. Frontal, anterior ramus with respect to the anterior tip of the prefrontal: does not extend past the anterior tip (0); extends beyond the anterior tip of the prefrontal (1) (Sereno *et al.*, 2001) (modified states from 'ending anteriorly' and 'ending posteriorly' to remove potential gap between states).

108. Frontal, lateral margin relative to the skull surface: flush (0); elevated, forming ridged orbital margins (1) (Brochu, 1999).

109. Frontal, anterior process constriction with respect to main body of frontal, excluding sagittal projection into nasals anterior to orbits: absent, lateral edges parallel to sub-parallel (0); present, anterior portion mediolaterally constricted, with convergent lateral margins (1) (Montefeltro *et al.*, 2013) (added 'with respect to main body of frontal, excluding sagittal projection into nasals anterior to orbits').

110. Postorbital, anterolateral process: absent or poorly-developed (0); well-developed, long and distally acute (1) (Clark *et al.*, 1994).

111. Postorbital-jugal contact, configuration: postorbital medial to jugal (0); postorbital dorsal to jugal (1) (Clark *et al.*, 1994).

112. Parietal-postorbital suture: absent from the dorsal surface of the skull roof (0); present on the dorsal surface of the skull roof (1) (character broken down into characters 107-109) (Clark *et al.*, 1994).

113. Parietal-postorbital suture: absent from the supratemporal fossa (0); present within the supratemporal fossa (1) (new character).

114. Parietal-postorbital suture within the supratemporal fossa: present within the ventral region (0); broadly present (1) (new character).

115. Parietal, dorsal surface: projects dorsally, relative to the skull roof (0); same level as squamosal (1); depressed relative to the squamosal (2) (de Andrade *et al.*, 2011b) (character state 2 added here) [**ordered**].

116. Parietal, posterior region dorsal surface: smooth (0); presenting a anteroposterior dorsal ridge (1); marked ventral deflection ('bevelled') in posterior portion (2); sculpted as with the rest of the skull table (3) (Montefeltro *et al.*, 2013) (added 'anteroposterior' to character state 1; added character states 2 and 3 here).

117. Parietal-squamosal emargination (anterior concavity at suture contact), posterior margin in dorsal view: absent (0); present (1) (Wilkinson *et al.*, 2008).

118. Supratemporal roof, dorsal surface: postorbital and squamosal with flat shelves extending laterally beyond quadrate contact (0); lateral edge terminating medial or immediately dorsal to medial-most point of contact with quadrate (1) (Clark *et al.*, 1994) (character state 'complex' removed; character state 1 added).

119. Supratemporal fenestra, medial border: flat, sculpted region (or unsculpted if rest of cranial table unsculpted) (0); forming a low sagittal crest (rims) posteriorly (1); forming a low sagittal crest (rims) along full length (2) (Clark *et al.*, 1994) (character state 1 added here) [**ordered**].

120. Supratemporal fenestra, dermal bone overhang: absent (0); present (1) (Norell, 1988).

121. Supratemporal fenestra, dermal bone overhang: present only medially and posteriorly (0); present about the entire edge (1) (Norell, 1988).

122. Supratemporal fenestra, shallow fossa at anteromedial corner: present (0); absent, corner smooth (1) (Brochu, 1999).

123. Supratemporal medial rims: continuous with orbital rims (0); separated from orbital rims by the postorbital bar (1) (new character).

124. Supratemporal medial rims, extend posteriorly to contact posterior skull margin: present (0); absent (1) (new character).

125. Supratemporal fenestra, relative contribution of frontal and parietal to medial margin: parietal with equal or greater contribution (0); frontal excluded from margin (1) (new character).

126. Supratemporal fenestrae, minimum width between fenestrae, with respect to maximum width of cranial table: one third or less of total width (0); more than one third of total width (1) (new character) (Schwarz and Salisbury, 2005).

127. Orbitotemporal channel, size of the dorsal aperture: area of foramen less than or equal to 30% of that of the internal supratemporal fenestra (0); larger than 30% of the internal supratemporal fenestrae area (1) (Montefeltro *et al.*, 2013).

128. Postorbital bar between orbit and supratemporal fossa, shape: broad and solid, as broad as dorsal surface of the cranial table lateral to the supratemporal fenestra (0); much narrower (1); much narrower and connected to orbit via a thin, superficial furrow in postorbital (2) (Clark *et al.*, 1994) (replaced 'with broadly sculpted dorsal surface if sculpture present' with size-related quantifier in character state 0; removed 'sculpting restricted to anterior surface' from character state 1; added character state 2) [**ordered**].

129. Postorbital bar between orbit and supratemporal fenestra, external texture: sculpted (0); unsculpted (1) (Clark *et al.*, 1994).

130. Postorbital bar, lateral surface formed by: postorbital and jugal (0); only by postorbital (1) (Gasparini *et al.*, 2006).

131. Postorbital bar, shape: transversely flattened (0); transversely broad, with elliptical cross-section (1); slender and cylindrical (2) (Clark *et al.*, 1994).

132. Postorbital bar, shape of dorsal end nearing skull table: continuous with dorsal part of postorbital (0); dorsal part of postorbital bar constricted, distinct from the dorsal part of the postorbital (1) (Clark *et al.*, 1994).

133. Cranial table (skull roof), width with respect to ventral portion of skull: as wide as ventral portion of skull (quadrates covered by squamosal) (0); narrower, but still covering more than half of the mediolateral region of quadrates (1); narrower, exposing more than half of mediolateral region of quadrate (2) (Wu *et al.*, 1997) (added 'more than half' to states 1 and 2) [**ordered**].

134. Squamosal and postorbital, lateral margins, dorsal view excluding posterolateral process: parallel (0); diverging posteriorly (1); medially concave (2); converging posteriorly (3) (Ortega *et al.*, 2000) (character state 2 added; added 'excluding the squamosal posterolateral process to character state 1).

135. Squamosal, lateral surface, longitudinal groove for attachment of the upper ear lid: absent (0); present (1) (Clark and Sues, 2002).

136. Squamosal groove for upper ear lid: ventral edge is laterally displaced relative to dorsal edge (0); ventral edge is directly beneath dorsal edge (1) (Clark and Sues, 2002).

137. Squamosal, dorsal edge of groove for dorsal ear lid: parallel to ventral edge (0); dorsal margin with a medial curvature (1) (Montefeltro *et al.*, 2013).

138. Squamosal, dorsolateral edge: straight and parallel to skull roof (0); bevelled ventrally, with anterolateral notch (1) (new character) (Schwarz and Salisbury, 2005).

139. Squamosal, posterolateral process: present (0); absent (1) (new character) (Buscalioni and Sanz, 1990b).

140. Squamosal, posterolateral process: level with skull table (0); depressed from skull table (1) (Sereno and Larsson, 2009).

141. Squamosal, posterolateral process projection: ventrally directed, confluent with ventral rim of groove for the earflap (0); posteriorly directed and parallel to skull roof (1) (Ortega *et al.*, 2000) (removed character state 2).

142. Squamosal, posterolateral process, ornamentation: absent (0); present (1) (Larsson and Sues, 2007).

143. Squamosal, posterolateral process, distal end: tapered and pointed (0); broad and rounded (1) (Larsson and Sues, 2007).

144. Squamosal, anterior process extending anteriorly to the orbital margin, overlapping the postorbital, in lateral view: absent (0); present (1) (Turner and Buckley, 2008).

145. Squamosal, obliquely-oriented ridge on dorsal surface: present (0); absent (1) (new character).

146. Squamosal, oblique ridge on dorsal surface, position with respect to the supratemporal fenestra: posterior to supratemporal fenestra (0); posterolateral or lateral to supratemporal fenestra (1) (new character).

147. Squamosal-parietal suture: flat, not elevated from the skull table (0); forms a well-developed anteroposterior groove (often bounded by elevated ridges) (1) (new character) (Buffetaut, 1983).

148. Squamosal, anterior portion nearing orbital edge: sculpted or unsculpted, consistent with the rest of the skull table (0); sculpting pattern changes (1) (new character).

149. Quadratojugal, ornamentation at base (dorsolateral surface): absent (0); present (1) (Pol, 1999).

150. Quadratojugal, length of anterior process relative to the lower temporal bar: absent or less than one third of lower temporal bar (0); one third to one half the length of the lower temporal bar (1); long, greater than half of the lower temporal bar (2) (Larsson and Sues, 2007) (changed character states to close gap between 'short' and 'half' of length of lower temporal bar) [**ordered**].

151. Quadratojugal, shape of posterolateral end and relationship with quadrate: acute or rounded, tightly overlapping quadrate (0); sinusoidal ventral edge, and wide and rounded posterior edge slightly overhanging lateral surface of quadrate (1) (Pol and Norell, 2004a).

152. Quadratojugal, contribution to the lateral temporal fenestra, in dorsal view: extensive contact with the ventral and posterior margins (0); contributes to the posterior and dorsal margin (1); only contributes to the posterior margin (2) (new character).

153. Quadratojugal-postorbital contact, in lateral view: not in contact (0); small, point contact (1); broad contact between the quadratojugal and the posterior portion of the postorbital descending flange (2) (Clark *et al.*, 1994) (added character state 0 here) [**ordered**].

154. Infratemporal fenestra, posterior margin, dorsal view: straight (0); with an anterior projection, forming an acute angle (1) (Ortega *et al.*, 2000) (added 'forming an acute angle' to character state 1).

155. Quadrate, posterior edge: broad medial to tympanum, gently concave (0); narrow dorsal to otoccipital contact, strongly concave (1) (Clark *et al.*, 1994).

156. Quadrate, dorsal surface fenestration: absent (0); present (1) (Clark *et al.*, 1994).

157. Otic aperture (not including additional quadrate fenestrae): open posteriorly (0); closed posteriorly by quadrate and otoccipital (1) (Clark *et al.*, 1994).

158. Quadrate, distal body: anterior margin oriented at a right angle in relation to quadratojugal (0); anterior margin gently slopes relative to quadratojugal (1) (Montefeltro *et al.*, 2011).

159. Quadrate, pterygoid ramus: with flat ventral edge (0); with deep groove on ventral surface (1); rod-like (2) (Clark *et al.*, 1994) (character state 2 added here).

160. Quadrate, anterodorsal ramus in ventral view: developed, forming more than or equal to 50% of the lateral edge of the internal supratemporal fenestra (0); restricted, forming less than 50% of the lateral edge of the supratemporal fenestra (1) (Montefeltro *et al.*, 2011).

161. Quadrate, ventral surface: smooth, with simple muscle scars (0); with multiple developed ridges (1) (Ősi *et al.*, 2007).

162. Quadrate, condyles: with poorly-developed intercondylar groove (0); medial condyle expands ventrally, being separated from the lateral condyle by a deep intercondylar groove (1) (Ortega *et al.*, 2000).

163. Quadrate, development of distal body ventral to otoccipital-quadrate contact: distinct, developing posteroventrally to contact (0); indistinct, not surpassing contact (1) (Wu *et al.*, 1997)

(added ‘developing posteroventrally to contact’ to character state 0, and ‘not surpassing contact’ to character state 1).

164. Quadrate, dorsoventral height of the proximal region: less than or equal to 50% of the skull roof total width (0); more than 50% of the skull roof total width (1) (Montefeltro *et al.*, 2013) (added ‘or equal to’ to character state 0).

165. Cranio-quadrate canal: opened laterally (0); closed laterally (1) (Clark *et al.*, 1994).

166. Ectopterygoid-maxilla, contact: present (0); absent (1) (new character).

167. Ectopterygoid, contribution to postorbital bar: absent (0); present (1) (Sereno and Larsson, 2009).

168. Ectopterygoid, main axis orientation: mediolaterally or slightly anterolaterally (0); anteroposteriorly, subparallel to anteroposterior axis of skull (1) (Pol *et al.*, 2004) (changed laterally to mediolaterally in character state 0, and anteriorly to ‘anteroposteriorly’ in character state 1).

169. Ectopterygoid, extent of medial projection on the ventral surface of pterygoid flanges: barely extended (0); widely extended, covering approximately the lateral half of the ventral surface of the pterygoid flanges (1) (Zaher *et al.*, 2006).

170. Ectopterygoid, anterior process: developed (0); reduced or absent (1) (Pol, 1999).

171. Ectopterygoid, posterior process: developed (0); reduced or absent (1) (Pol, 1999).

172. Palatines, palatal processes: do not meet on palate below narial passage (0); meet ventral to narial passage, forming part of secondary palate (1) (Clark *et al.*, 1994).

173. Palatine-maxilla, suture when fused at midline: palatine anteriorly rounded (0); palatine anteriorly pointed (1); suture transverse to midline axis (2) (Brochu, 1999) (character state ‘palatine invaginated’ removed).

174. Interfenestral bar, anterior half between suborbital fenestrae, lateral margins: parallel to subparallel (0); flared anteriorly (1) (Pol *et al.*, 2009) (added ‘lateral margins’).

175. Interfenestral bar, posterior half between suborbital fenestrae, lateral margins: flared posteriorly (0); parallel to subparallel (1); converge posteriorly (2) (Pol *et al.*, 2009) (added 'lateral margins'; character state 2 added here) [**ordered**].

176. Palatines, anteroposterior axis: run parasagittally (0); diverge laterally, becoming rod-like and forming palatine bars posteriorly (1) (Martinelli, 2003)

177. Palatine-pterygoid, contact on palate: run parasagittally (0); palatines firmly sutured to pterygoids (1) (Pol and Norell, 2004a).

178. Pterygoids, contact with one another on palate: not in contact anterior to basisphenoid on the palate (0); pterygoids in contact (1) (Wu *et al.*, 1997).

179. Pterygoid, role of primary palate in forming choanal opening: forms posterior half of choanal opening (0); forms posterior, lateral, and part of anterior margin of choana (1); completely encloses choana (2) (Clark *et al.*, 1994) [**ordered**].

180. Pterygoid, participation in the suborbital fenestra, ventral view: forms margin of suborbital fenestra (0); excluded from suborbital fenestra by ectopterygoid-palatine contact (1) (Turner and Sertich, 2010).

181. Choanae, anterior edge, location: situated between suborbital fenestrae (or anteriorly) (0); near posterior edge of suborbital fenestrae (1) (Clark *et al.*, 1994).

182. Choanal opening, conformation in palate: continuous with pterygoid ventral surface except for anterior and anterolateral borders (0); opens into palate through deep choanal groove (1) (Clark *et al.*, 1994).

183. Choanal groove: undivided (0); partially septated (1); completely septated (2) (Clark *et al.*, 1994) [**ordered**].

184. Pterygoid, quadrate process: well-developed, extending posterolaterally beyond anterior margin of basioccipital (0); poorly-developed, only present as an incipient projection (1) (Pol, 1999)

(added ‘extending posterolaterally beyond anterior margin of basioccipital’ to character state 0, and ‘only present as an incipient projection’ to character state 1).

185. Pterygoid, quadrate ramus, in ventral view: narrow and bar-like (0); broad and laminar (1) (Wu *et al*., 1997) (added ‘bar-like’ to character state 0, and ‘laminar’ to character state 1).

186. Pterygoid, palatal surface: smooth (0); sculpted (1) (Clark *et al.*, 1994).

187. Pterygoid flanges: mediolaterally expanded, laterally surpassing the quadrate medial condyle (0); relatively short, and do not reach laterally to the level of the quadrate medial condyle (1) (Ősi *et al.*, 2007).

188. Basisphenoid, ventral exposure on braincase: exposed on ventral surface of braincase (0); virtually excluded from ventral surface by pterygoid and basioccipital (1) (Clark *et al.*, 1994).

189. Basisphenoid, lateral exposure on braincase: absent (0); present (1) (Pol, 1999).

190. Basisphenoid: ventral surface continuous with surrounding bones (0); body ventrally developed and separated from the remaining elements by a posteroventral step formed by a sulcus separating it from the main occipital plane, forming a postchoanal pterygoid-basisphenoid tuberosity (1) (Montefeltro *et al.*, 2011).

191. Basisphenoid, ventral surface, mediolateral size relative to basioccipital: shorter than basioccipital (0); equal or longer than basioccipital (1) (Clark *et al.*, 1994) (added ‘mediolateral’).

192. Basioccipital: without well-developed bilateral tuberosities (0); with large, pendulous tubera (1) (Clark *et al.*, 1994).

193. Basioccipital, midline crest on basioccipital plate below occipital condyle: absent (0); present (1) (Turner and Sertich, 2010).

194. Basioccipital and ventral part of otoccipital, orientation (when skull held horizontally): posteriorly (0); posteroventrally (1) (Gomani, 1997).

195. Otoccipital, ventrolateral contact with quadrate: very narrow, otoccipital only abuts quadrate (0); broad, ventrolateral margin of otoccipital extensively contacts ventromedial portion of

quadrate (1) (Clark *et al.*, 1994) (added 'otoccipital only abuts quadrate' to character state 0, and 'ventrolateral margin of otoccipital extensively contacts ventromedial portion of quadrate' to character state 1).

196. Supraoccipital, posterodorsal exposure in skull roof: absent (0); present (1) (Ortega *et al.*, 2000).

197. Supraoccipital, posterodorsal exposure: exposed in midline portion of posterior region of skull table (0); restricted to a thin surface attached to posteriormost portion of parietal and squamosal (1) (Montefeltro *et al.*, 2011).

198. Supraoccipital, relationship with foramen magnum: forms dorsal edge (0); otoccipitals meet dorsally, separating the foramen magnum from the supraoccipital (1) (Clark *et al.*, 1994).

199. Cranial nerves IX-XI, passage through braincase: all pass through common large foramen vagi in otoccipital (0); cranial nerve IX passes medial to nerves X and XI in separate passage (1) (Clark *et al.*, 1994).

200. Mastoid antrum, location: does not extend into supraoccipital (0); extends through transverse canal in supraoccipital to connect middle ear regions (1) (Clark *et al.*, 1994).

Mandibular Characters

201. Mandible, outer surface sculpture, lateral surface: absent (0); present (1) (Montefeltro *et al.*, 2011).

202. Mandible, outer surface sculpture, ventral surface: present on dentary (0); present on dentary and splenial (1) (Montefeltro *et al.*, 2011).

203. Mandibular symphysis, anteroposterior length relative to mediolateral width: short, length and width subequal or shorter than wide (0); proportionally long, longer than wide (1); extremely long, length at least five times its width (2) (de Andrade *et al.*, 2011b) [**ordered**].

204. Mandibular symphysis, posterior extension, terminating medial to the dentary alveoli: short, up to the D5 (0); to the D5-D6 (1); to the D7 or greater in length (new character) [**ordered**].

205. Mandibular symphysis, lateral view: shallow and tapering dorsoventrally anteriorly (0); deep and tapering dorsoventrally anteriorly (1); shallow and anterior margin convex (2) (Wu and Sues, 1996) (character state 'deep and anteriorly convex' removed).

206. Mandibular symphysis, shape, in ventral view: tapering mediolaterally anteriorly, forming an angle (0); U-shaped, smoothly curving anteriorly (1); lateral edges anteroposteriorly oriented with convex anterolateral cornier and extensive, transversely oriented anterior edge (2) (Pol, 1999).

207. External mandibular fenestra: absent (0); present (1) (Clark *et al.*, 1994).

208. External mandibular fenestra, size: present as a diminutive passage, less than 50% of the total size of the lateral temporal fenestra (0); present as an evident fenestra, 50% or greater than the total size of the lateral temporal fenestra (1) (Clark *et al.*, 1994) (quantified both character states).

209. External mandibular fenestra, orientation of main axis: horizontal to sub-horizontal (0); inclined, directed anteroventrally-posterodorsally (de Andrade *et al.*, 2011b) (added 'to sub-horizontal to character state 0).

210. External mandibular fenestra, shape: subcircular to elliptical (0); triangular (1) (de Andrade *et al.*, 2011b) (character states 'highly elliptic, anteroposterior axis much longer than dorso-ventral axis, three time or more, but both ends rounded', 'slit-like, proportionally very long and both ends acute' and 'teardrop-like' removed.)

211. Jaw joint, location of dorsal edge: level with or dorsolateral to occipital condyle (0); ventrolateral occipital condyle (1) (Wu and Sues, 1996).

212. Dentary, lateral surface adjacent to seventh alveolus: smooth (0); with lateral concavity for reception of enlarged maxillary tooth (1) (Buckley and Brochu, 1999).

213. Dentary, lateral surface below alveolar margin, at middle to posterior region of tooth row: vertically oriented, continuous with rest of lateral surface of the dentaries (0); flat surface exposed

dorsolaterally, divided by ridge from the rest of the lateral surface of the dentary (1); flat, unsculpted surface confluent with rest of the lateral surface (2) (Pol and Apesteguía, 2005) (character state 2 added here).

214. Dentary, relative to external mandibular fenestra: extends posteriorly beneath mandibular fenestra, posteriorly exceeding anterior margin (0); does not extend beneath fenestra, either terminating anteriorly to fenestra or only forming a point contact (1) (Clark *et al.*, 1994).

215. Dentary, mediolateral compression and ventrolateral surface anterior to mandibular fenestra (or of anterior portion posterior to symphysis if fenestra is absent): compressed and flat (0); uncompressed and convex (1) (Ortega *et al.*, 1996a) (added 'mediolateral').

216. Dentary, sculpted below the tooth row: lacking sculpting (0); present (1) (Pol, 1999).

217. Dentary alveoli: all independent of one another (0); some confluent (1); all confluent, within continuous alveolar groove (2) (new character) [**ordered**].

218. Dental alveoli, transitional shape morphology from circular to sub-circular or oval: absent (0); present (1) (new character).

219. Dentary alveoli, transitional shape morphology: posteriorly from D4 (0); posteriorly from D5 (1) (new character).

220. Dentary, distinct foramina on occlusal surface, lingual to dental arcade: absent (0); present (1) (new character).

221. Dentary, distinct foramina on occlusal surface, lingual to dental arcade: at D2-D3 (0); at D4 or positioned more posteriorly (1) (new character).

222. Dentary, external alveolar margins, dorsal edge: vertically festooned, forming raised rims about each alveolus (0); flat (1) (new character).

223. Dentary, internal alveolar margins: forming raised rims (0); flat and confluent with dentary occlusal surface (1) (new character).

224. Dentary, anterior portion, lateral margin shape in dorsoventral view: straight (0); distinctly spatulate, with abrupt lateral expansion (1); laterally convex (2) (new character).

225. Dentary, diastema (gap) between D7 and D8: present (0); absent (1) (new character).

226. Dentary, pitted ornamentation of external surface: absent (0); present (1) (new character).

227. Dentary, grooved ornamentation of external surface: absent (0); present (1) (new character).

228. Dentary, inter-alveolar septae within anterior dental arcade (D4-D8): present (0); absent (1) (new character).

229. Dentary, symphysis and dentary arcade lateral to symphysis, in dorsoventral view: parallel (0); oblique (1) (new character).

230. Dentary, occlusal surface: smooth (0); anteroposteriorly crenulated (1) (new character).

231. Dentary, obliquely inclined crenulations posterodorsal to D8-D9: present (0); absent (1) (new character).

232. Dentary, dorsolateral edge: slightly concave or straight and subparallel to anteroposterior axis of skull (0); sinusoidal, with two concave waves (1) (Ortega *et al.*, 1996a) (character state 'with single dorsal expansion and concave posteriorly' removed).

233. Splenial, involvement in symphysis, in ventral view: not involved (0); involved (1) (Clark *et al.*, 1994)

234. Splenial, contact with dentary, in ventral view: confluent (0); dorsally inset (1) (new character).

235. Splenial, posterior to symphysis: approximately constant mediolateral thickness throughout element (0); more robust posterodorsally (1) (Ortega *et al.*, 1996a) (changed character state 'thin' to 'approximately constant thickness throughout element'; changed character state 1 to 'posterodorsally').

236. Angular and posterior surangular, strong pitted pattern: absent (0); present (1); lateral surface with rugose pattern instead of pits (2) (de Andrade *et al.*, 2011b) (character state 2 added here).

237. Surangular, dorsal edge in lateral view: mostly straight (0); arched dorsally, excluding articular projection (1) (Clark *et al.*, 1994).

238. Surangular, anteroposterior ridge along the dorsolateral surface: absent (0); present (1) (Pol and Norell, 2004a).

239. Surangular, extension toward posterior end of retroarticular process: along entire length (0); pinched off anterior to posterior tip (Norell, 1988).

240. Articular, posterior ridge on glenoid fossa: posterior margin well-developed, evidently high (0); posterior margin poorly delimited, crest absent (1) (Pol and Apesteguía, 2005).

241. Articular, medial process articulating with otoccipital and basisphenoid: absent (0); present (1) (Clark *et al.*, 1994).

242. Retroarticular process: absent or extremely reduced (0); posteroventrally projecting and paddle-shaped (1); pointed, projects posteriorly and ventrally recurved (2); projects posteriorly and dorsally recurved (3) (Clark *et al.*, 1994) (character states 'with an extensive rounded, wide, and flat (or slightly concave) surface projected posteroventrally and facing dorsomedially' and 'posteriorly elongated, triangular, and facing dorsally' removed; character states 2 and 3 added).

Dental Characters

243. Premaxillary teeth, number: five or more (0); four or fewer (1) (Wu and Sues, 1996) (character states 'six', 'three', and 'two' removed, and replaced with 'or more' and 'or fewer in remaining character states).

244. Posterior premaxillary teeth, apicobasal length: less than 1.5 times the size of the anterior teeth (0); 1.5 times or greater than anterior teeth (1) (Clark *et al.*, 1994) (quantified and set character state boundary).

245. Maxillary teeth, mesiodistal margin carinae: absent or with smooth and crenulated carinae (0); with denticulate carinae (ziphodont condition) (1) (Ortega *et al.*, 1996a) (character state 'with tubercular heterogenic denticles' removed).

246. Maxillary tooth rows, middle to posterior elements: crowns not mesiodistally compressed, subcircular in cross-section (0); crowns slightly compressed mesiodistally (mesiodistal to labiolingual diameter ratio more than 0.5 at mid-height) (1); crowns highly compressed mesiodistally (mesiodistal to labiolingual diameter ratio less than or equal to 0.5 at mid-height) (2) (Pol, 1999) [**ordered**].

247. Maxillary tooth rows, mesiodistal compression of middle to posterior elements: absent, or symmetrical compression (0); asymmetrical compression, occurring only along the distal margin giving teeth a teardrop shape (1) (de Andrade and Bertini, 2008) (added 'or symmetrical compression' to character state 0).

248. Maxillary teeth, middle to posterior elements, ridged ornamentation on enamel surface: absent (0); present (1) (de Andrade *et al.*, 2011b).

249. Maxillary teeth, enamel surface: smooth or slightly crenulated (0); with ridges at base of crown (often extending apically) (1) (Turner and Sertich, 2010).

250. Maxillary teeth, striations on labial and lingual faces: present (0); absent (1) (new character) (Martin *et al.*, 2014c).

251. Cheek teeth, base (i.e., immediately apical to root), with respect to remainder of tooth crown: not constricted (0); constricted (1) (new character) (Martin *et al.*, 2014c).

252. Maxillary teeth, width of root with respect to crown: narrower (0); wider in anterior teeth and equal in posterior teeth (1) (Ortega *et al.*, 2000) (changed character state 1 to 'wider in anterior teeth, equal in posterior teeth'; removed 'or equal' from character state 0).

253. Maxillary teeth, posterior teeth, mediolaterally compressed lanceolate-shaped morphotype (sometimes called 'leaf-shaped'), visible in labial or lingual view, with wide crown tapering apically

to a sharp point (note that the point can often be abraded): present (0); absent (1) (new character) (Schwarz and Salisbury, 2005).

254. Maxillary teeth, low-crowned and strongly labiolingually compressed morphotypes, forming a crown that is mesiodistally broader than it is apicobasally tall: present, apical margins oriented at less than 45° from horizontal (0); absent (1) (new character) (Schwarz and Salisbury, 2005).

255. Tooth, present at premaxilla-maxilla contact with transitional size-based morphology: absent (0); present (1) (Turner and Sertich, 2010) (added 'size-based').

256. Maxillary teeth, size variation waves: absent, no tooth size variation (0); one wave of enlarged teeth (1); enlarged maxillary teeth occur in two waves (festooned) (2) (Clark *et al.*, 1994).

257. Enlarged maxillary teeth (at least 1.5 times the apicobasal size of remaining teeth): present at M2 and/or M3 (0); present at M4 and/or M5 (1) (Martin *et al.*, 2010).

258. Maxillary tooth 5, apicobasal size relative to adjacent maxillary teeth: subequal, or less than 4.0 times the size of adjacent teeth (0); hypertrophied, at least 4.0 times the size of adjacent teeth (1) (new character).

259. Maxillary tooth 5, hypertrophied: directed posteroventrally (0); directed ventrally (1) (new character).

260. Maxillary teeth 6 and 7: continuous with tooth row (0); dorsally inset (1) (new character).

261. Maxillary teeth, bulbous tooth morphotype (tribodont): present (0); absent (1) (Sweetman *et al.*, 2015).

262. Dentary teeth, anterior teeth (opposite premaxilla-maxilla contact) apicobasal length, relative to rest of dentary teeth: no more than twice the length (0); more than twice the length (1) (Clark *et al.*, 1994).

263. Dentary teeth, posterior teeth: occlude medial to opposing maxillary teeth (0); occlude lateral to, or interlock with, opposing maxillary teeth (1) (new character) (Sweetman *et al.*, 2015).

Axial Characters

264. Vertebrae, centra shape along axial column: cylindrical throughout (0); grade continuously from cylindrical to elongated spool-shaped (1); spool-shaped throughout (2) (Buscalioni and Sanz, 1988) (character state 1 added) [**ordered**].

265. Cervical vertebrae: amphicoelous or amphiplatyan (0); procoelous, and posterior centrum face (condyle) with a central depression ('semi-procoely') (1); fully procoelous (2) (Clark *et al.*, 1994) (character state 1 added) [**ordered**].

266. Cervical vertebrae, number: 6 or fewer (0); 7 (1); 8 or more (2) (new character) [**ordered**].

267. Atlas, intercentrum size: mediolaterally wider than anteroposteriorly long (0); subequal diameters or anteroposteriorly longer (Clark *et al.*, 1994).

268. Cervical vertebrae, neural spine: absent, or extremely reduced (0); present, distinct from centrum body (1) (new character).

269. Cervical vertebrae, neural spines: rod-like and elongate (0); short and transversely flattened (1) (new character).

270. Cervical and dorsal vertebrae, hypapophyses or anterior keels: absent (0); present (1) (Buscalioni and Sanz, 1988) (character states modified to present or absent).

271. Dorsal vertebrae: amphicoelous or amphiplatyan (0); procoelous (1) (Clark *et al.*, 1994) (replaced 'trunk' with 'dorsal').

272. Dorsal vertebrae, number: 14 or fewer (0); 15-16 (1); 17 or more (2) (new character) [**ordered**].

273. Posterior dorsal vertebrae, transverse process shape: dorsoventrally low and laminar (0); dorsoventrally high (1) (Buscalioni and Sanz, 1988).

274. Sacral vertebrae, number: two (0); three or more (1) (Buscalioni and Sanz, 1988).

275. Sacral vertebrae, orientation of transverse processes: project laterally (horizontally) (0); deflected markedly ventrally (1) (Gasparini *et al.*, 2006).

276. Caudal vertebrae, number: less than 50 (0); 50 or more (1) (new character).

277. Caudal vertebrae: amphicoelous or amphiplatyan (0); procoelous (1) (new character) (Salisbury and Frey, 2001).

278. Caudal vertebrae, first: same morphology as rest of caudal series (0); biconvex (1) (new character) (Salisbury and Frey, 2001).

279. Caudal vertebrae, anteroposterior ridge/lamina separating centrum and neural arch: present (0); absent (1) (new character; note that this could be an ontogenetic feature).

Appendicular Characters

280. Scapula, proximodorsal edge in lateral view: flat and confluent with scapular shaft (0); forms a distinct crest (1) (new character).

281. Coracoid, medial process: elongate posteromedial process (0); distally expanded ventromedial process (1) (Wu and Sues, 1996).

282. Coracoid, distal expansion: equal to or larger than the proximal expansion (0); less expanded than the proximal region (1) (Pol *et al.*, 2012).

283. Humerus, circular depression on the posterior surface of the proximal end, for the insertion of the *M. scapulohumeralis caudalis*: absent (0); present (1) (Pol *et al.*, 2012).

284. Humerus, lateral and medial surfaces of distal end: flat and anteroposteriorly broad, similar in anteroposterior length to the transverse width of the distal end of the humerus (0); convex and reduced in comparison with the transverse width of the distal humerus (1) (Pol *et al.*, 2012).

285. Forelimb:hindlimb length, ratio: less than 0.7 (0); 0.7 to less than 0.8 (1); 0.8 or greater (2) (new character) [**ordered**].

286. Humerus:femur length, ratio: less than 0.75 (0); 0.75 to less than 1.0 (1); 1.0 or greater (2) (new character) [**ordered**].

287. Ulna, morphology of olecranon process: narrow and subangular (0); wide and rounded (1) (Brochu, 1999).

288. Radius:humerus length, ratio: less than 0.6 (0); 0.6 to less than 0.75 (1); 0.75 or greater (2) (new character) [**ordered**].

289. Radius:tibia length, ratio: less than 0.6 (0); 0.6 to less than 0.7 (1); 0.7 or greater (2) (new character) [**ordered**].

290. Radiale, proximal end, shape: expanded symmetrically, similar to distal end (0); more expanded laterally than medially ("hatchet shaped") (1) (Buscalioni and Sanz, 1988).

291. Ilium, anterior (preacetabular) process, length relative to posterior (postacetabular) process: greater than 75% the length of the posterior process (0); 75% or less the length of the posterior process (1); completely absent (2) (Clark *et al.*, 1994) (changed 'similar in length' to 'greater than 75% of the length of the posterior process' in character state 0; changed 'one-quarter to 75% in character state 1) [**ordered**].

292. Ilium, development of the posterior (postacetabular) process: well-developed as a distinct process that extends anteroposteriorly for 60% or more of the acetabular length (0); extremely reduced or absent, extending anteroposteriorly less than 60% of the acetabular length (1) (Pol *et al.*, 2012) (character state 1 changed to 'less than 60%' to remove gap between 50-60%).

293. Ilium, posterior end of the postacetabular process: tapering posteriorly to an acute tip (0); subrectangular with a vertically oriented posterior margin (1) (Pol *et al.*, 2012) (removed 'with its dorsoventral height being at least 60% of the height at the origin of the postacetabular process' from character state 1).

294. Pubis, shape: rod-like without expanded distal end (0); with anterodorsally-posteroventrally expanded distal end (1) (Clark *et al.*, 1994) (added 'anterodorsally-posteroventrally' to character state 1).

295. Pubis, anterior process: absent (0); present (1) (Clark *et al.*, 1994).

296. Femur, proximal development of greater trochanter: prominent, ridge-like lateral border that separates the lateral surface of the proximal femur from a flat posterior surface reaching down to the level of the fourth trochanter (0); proximodistally short trochanteric surface lacking a distinct ridge, terminating well above the fourth trochanter (1) (Pol *et al.*, 2012).

297. Femur, femoral head: mediolaterally flattened (0); hemispherical (1) (new character).

298. Tibia, distal projection of articular surfaces: medial region of distal articular surface extends further distally than the lateral region, forming a strongly oblique distal margin of the tibia (0); medial and lateral regions sub-equally extended, with distal margin sub-horizontally oriented (1) (Pol *et al.*, 2012).

299. Tibia, posterior surface of shaft: flattened and confluent with fibula (0); twists posteriorly, leaving a void between the tibia and fibula (1) (new character).

300. Tibia:femur length, ratio: less than 0.9 (0); 0.9 to less than 1.0 (1); 1.0 or greater (2) (new character) [**ordered**].

301. Astragalus, anterior margin of the tibial facet: forming a well-defined ridge that reaches medially the ball-shaped region for the articulation of metatarsal I-II and closes the proximomedial corner of the anterior hollow of the astragalus (0); forming a low ridge that is medially separated by a notch from the ball-shaped region for the articulation of the metatarsals I-II, failing to close the proximomedial corner of the anterior hollow (1) (Pol *et al.*, 2012).

302. Distal tarsals, digits 2-4, dorsal surface: longitudinally grooved (0); smooth and flat (1) (new character).

303. Metatarsals I-IV: equidimensional (0); metatarsal I shorter than metatarsals II-IV (1) (new character).

Osteoderm Characters

304. Osteoderms, dorsal surface: entirely sculpted (0); partially or completely unsculpted (1) (new character).

305. Presacral armour: cervical and dorsal trunk shields undifferentiated, morphology grading continuously (0); cervical shields clearly differentiated from dorsa trunk shields by size and general morphology (regardless of contact between nuchal and trunk series) (1); anteriormost cervical osteoderms developed into distinct shield (2) (de Andrade *et al.*, 2011b) (character state 2 added) [**ordered**].

306. Nuchal osteoderms: consistent morphology along series (0); vary substantially in size in a random fashion (1); systematically increase in size posteriorly (2) (new character).

307. Nuchal osteoderms, with size variation: nuchals no less than 50% the size of dorsal osteoderms (0); some smaller than one half of the size of the dorsal osteoderms (1) (new character).

308. Dorsal osteoderms, shape: rounded or ovate (0); subrectangular (mediolaterally wider than anteroposteriorly long) (1); subtriangular (2); square (3) (Clark *et al.*, 1994) (character state 2 added).

309. Dorsal osteoderms, articular anterior process: absent (0); present (1) (Clark *et al.*, 1994).

310. Dorsal osteoderms, articular anterior process: as discrete convexity on anterior margin (0); well-developed process located anterolaterally ('peg and socket' articulation) (1) (Clark *et al.*, 1994).

311. Dorsal osteoderms, anteroposterior keel on anterior part of dorsal surface: absent (0); present (1) (new character).

312. Dorsal osteoderms, anteroposterior keel on posterior part of dorsal surface: absent (0); present (1) (new character).

313. Dorsal and cervical osteoderms: some or all imbricated (0); not in contact (1) (new character).

314. Dorsal osteoderms, sutured anterior and posterior contacts: present (0); absent (1) (new character).

315. Dorsal primary osteoderms , rows: two parallel rows (0); four rows or more (1) (Clark *et al.*, 1994) (character state 'more than four rows' removed).

316. Dorsal osteoderms, accessory osteoderms (i.e., osteoderms not forming part of the dorsal shield): absent (0); present (1) (Turner and Sertich, 2010).

317. Dorsal osteoderms, dorsal keel: same morphology in anteriormost dorsal osteoderms as remainder of dorsal series (0); keel shifts laterally in more posterior dorsal osteoderms (1) (new character).

318. Dorsal osteoderms, anterior edge of dorsal surface (i.e., articular surface, if present): sculpted, undifferentiated from main osteoderm body (0); unsculpted (1) (new character).

319. Dorsal osteoderms, outline in dorsal aspect (excluding peg articulation): symmetrical about anteroposterior axis (0); asymmetrical (1) (new character).

320. Dorsal osteoderms, mediolateral contacts: contact but not sutured (0); sutured (1) (new character).

321. Dorsal osteoderms, ventral to dorsal vertebrae beneath trunk: absent (0); present (1) (Clark *et al.*, 1994).

322. Caudal osteoderms: absent (0) present on dorsal surface only (1); completely surrounding tail (2) (Clark *et al.*, 1994) [**ordered**].

323. Caudal osteoderms: ovate (0); subcircular (1); subrectangular (2) (new character).

324. Caudal osteoderms, bearing anteroposterior ridge: present (0); absent (1) (new character).

325. Caudal osteoderms, anteroposterior ridge: present medially (0); forms a distinct lateral step in posterior-most elements (1) (new character)

326. Caudal osteoderms, geometry: continuous from short to elongate oval (0); continuous from subrectangular (rounded corners) to suboval (1); isometric (equal geometry along series) (2) (new character).

327. Caudal osteoderms, medial and lateral edges: serrated (0); smooth (1) (new character).

328. Caudal osteoderms, secondary osteoderms: present (0); absent (1) (new character).

329. Caudal osteoderms, anteroposterior ridges: same morphology along series (0); becoming more pronounced posteriorly, coincident with a decrease in osteoderm size (1) (new character).

Appendix 7 – Character codings for taxa used in phylogenetic analysis (see Chapter 4)

Protosuchus_richardsoni

1120100000102?00001101?2022213112100100001000??000000?011?11?001?111?11?001110000
?10000?100000?00100?1200?0000010?100000?1??1010000?111000????001?0000120000111?0?
0??0?????????01000????1?00?100?00??01??1?001001101001O????1???10????00?0?10101011?0
001001100?0??11100200?101100000?0100000021000000011000100121311100010000112221??11
0

Hoplosuchus_kayi

0?0010001210101????101010311??0???0?1000?0?????000200????????1?????11????0????100?12
000?????0???0??0???0???0?01???100???????????02?010??01100?01?0???1?1?00?02??011???0?
????10011?000?101??????????????0?0?0?0???10???10??????0?00?1??0???0??????????????11?
?????1??1?2?????0?000???0???0?1?22??????????01?1?110?10?00000001110120121111

Amphicotylus_lucasii

1121112011002?00111211200032331110000110111111011011101120111000001?1100111000?00
?121?00210110011010?0110?00100111130000?0??1010011?20??100011101?001212200?010??10
0?11??001011?10001020000011??1110????????1?????0?????????????????????????????????010001
010?111210?11?????????????????????10???

Eutretauranosuchus_delfsi

1121012112002?00111210200032231000?0001011111?110010?00000111??011?1100101011100
1??1000111101?10020?011101000001013100110??000000202211100011111?0012022111?10?11
0010001010201011001O2?000100001010?1??111?2111000?01?10??????1?10?1??01011100?0101
0001010?1112?0?1101???????0??????????????0??????????????0?????1100?????1??????????

Pholidosaurus_purbeckensis

10201012??002?00011?00?020?2?01??0??1????0??1???0001??0??????0??0???11??100??01?0???
110?11?000????10?0??1010?10???13000100???000101?12111000001?1?00?20??1110????1?11?0
????1???0111?1??000?1??0??010??10??2?1??????0???????????1????????1?0????0010?00010?00
11?0???01?????????0?????????????????????????1?????????????11????0?????????????

Pachycheilosuchus_trinquei

111??0????00100???0?????????????????????????????????000101010011?0?????1?????0?????0??1?1
0?0???0???1?110??100??00?????13??0??1????????2?????????????????????????1?????????????
??????????????????????11???????10100?0????01?0100?0?1101010101000?001?1????000??0?0110
??0?0???011?11111000?11?00101?2101?1011011101???02??31100001?00110111?001?

Theriosuchus_pusillus

1120012210011000101111110111110120011000001111?0001101000?0101011011100010101110100111?011000011102100001001000001?10020?100010100201010010010101?100100210???1?1?
??0?1100110101111011101010111011?101??1112110????12?10111100021110101111020??010002100001100011?0100101?1010?0000011?101??10100?1?111011211000030?000000?101022001111

Theriosuchus_ibericus

1120002???0???0010????????????0??0?1??000?01???01101100022000?????????????????1?11?011110???????1??113?0?10?10?????210?2???010???????10111001001000010??0????1??1?10100????12?102100?00211111011100 2???10?1011111010100111011???0???10?00?????101??2??????

Theriosuchus_sympiestodon

11???0????0???00101?????????????????????????????110110000??0?1?????????????????????????????????1?0111?0010?10??0??11?020?10101?0????2?11?001001?00?00?????01????1?000?????

??????1?201100100???????1???????11???????10???110110120100000?110?????????1111111010
?1111010??

Theriosuchus_guimarotae

1120012210001000001211110121110120011010001111000011010?001010112111111?0?101?000
?101110110?0011102100001001100000?110020?1?10001002010?0010010101?100102?101111100
000011111111110111110201010100011110 1??1111111101012010111100021110101010020 00?010
0021000110101101010010??1010?00?0001?1010?10???111??1?0021?00???11111?????10?0?2???
11?

Theriosuchus_grandinaris

???0??22110?2??????????????????0120011000001 0?0?0001?01?0??1??101111?11000?1?1???????
?????00????1??0??0????0?0??
??????????????????????????????1112?1???????????0?????0111?0???100???????000??0001?010??
0???0??

Theriosuchus_sp.

??
??
??????????????????????????1?121??????02?1?0101100011110 1000????????????????????????
??

Alligatorellus_sp.

??
??
??
??
????????????00??????????1???????101??00???0101101??0000??1??????

Alligatorellus_bavaricus

12100022100111012010101112102100?011100000?????000200??1?????00101100100001001001?

01110?000000?11010?10010000000??121000?1??01?210212011001????11?110?0001??01???0?0

????????????????????????????????0????0?????0????00?1??????????????????????00????2?0000001

0?1100?0?01?1201???0?1??00???1????1101111??11100011110121l0?1101000?1001200111?

Alligatorellus_beaumonti

1210002210012?012001101112101100201l100000?????000200??1?????001011?1100011001001?

01110?000000?11010200010000000?130010?11001?210212011000????11?11010001??01???0?0

????????????????????????????????0????0????00????00?1????????0?00?????100000??0200000001

0?0100?0?01?1201?0?0?20100??1010?021?221101??1?00110101101O?1101001?10012001101

Atoposaurus_jourdani

0?00002?10002?00200010?30100??00?0???0?000?????000200??1?????0???11?1????0???1?0???1

110?0???00?11?00???010?0?00???000000?1???1?2102100???0??????1?0?0?0?????????????????

????????????????????????0????0??????????????????????????00?????????????????????????11??

???????2?0?0?0?20111??1?????000210???1110101001?????????????????0?????1?

Atoposaurus_oberndorferi

0?0??02?????????????????1?0?00??0?????1???????????00?????1?????????????????????10????????

??2??0??

??????????????????????????0?1??0?????00??????????0?00?1???1100????????0????????10??0???

??2?1???001???1??1????011022?101111010101?????????????????????0?????1?

Alligatorium_meyeri

1110012210012?00101010111210110O?01?100000?????0??110??1?????001110?1100000000000??

01110?000000?11011010011001000O?130?20?11000?10020201?100000001?10010011?101???0?0

??????????????????????????????0????1?????1111?00111?????0???00????0???000?1?0?000000?

0?1100?0?01?1?0110???2????????0???0??0?20???????10?1?1100130?00000???010121???1?

Alligatorium_franconicum

1120012211002?00100010?020311200??1?10?00??????????110????????000?21?110000000??????

???0?000000?11010?00011011000??1300?0????00?20??020???00000001????1???????????0?????

??????????????????????????????1?????0??

??????????1?????1????????????1101202?????0?00???100?10?1100001011?1?1???1?

Montsecosuchus_depereti

11100022??002?00100011130221320 0?0?????00???????0001?????????0??010?1101000111?0??1

11?1?000000?11010?10011000000??020100?1??01?00011100?000000001?00020111?1?1?0?000?

??????????????????????????????100??101???0???00??1????????0?00?1???0?1??????3?????????

??????0?????1?1?0???10100???001?0000110201????010001002100?1111010?0101000001?

Wannchampsus_kirpachi

1120002???012?00101211110211220??0???????????0??0001??0???11?1??11??11010010011?100

111001100010110113000100100001001102 0?10000?0100020101000001?0110020121011110100 0

0?110011?100111011000000111011111 10?1012110???002?1?10???00211001 0?11??2000??0??11

011011110100111?1?1??1111?????10????10??0??1???????????00???210????????1??????????

Shamosuchus_djadochtaensis

1120002???002?00101110110132120 1?00?2????01????000011?11???1?1??011?111?100011100?0

1?101?10001?11011300010010000101100 00?0?00000201100001110010002012101110010000

0?110011??00112011000000111001 10?10?111???0???002?11?????0?2?10????01000010100??010

0001??10100101?1?2?11111?????0????010??022????????????100???1100100????0111?????1?

Koumpiodontosuchus_aprosdokii

1120012222002?00101111101032320010001000011 1?1?1001100?0000?011??01?1000000001001
?01100??11000?11000?000110100000?131000?1??0000011023100000100 01?001201210?110??0?
01100101101101120100110110100011 0?1??1012200???002?10????????2?10?1??10002000?0010?
?0101100101?0?0000??

Brillanceausuchus_babouriensis

1120002?11012?00111111111013103010000200110 11??1100011011011 1?11??30?1001101001???
?11??0?010001111010?000100000011113101 0?1010100100022101101001001110201 2??111??10
000?110011?120112011000010110100111 1?01010010???012?0100???002?11?10?010?20?0??310
01100?11010110101?0021111?12???0?0?1?????2?220?????????1??0000?00?0000000?010?????0
1?

Appendix 8 – Full European and North American stage-level subsampling results for different tetrapod groups

Non-marine, Europe

Bin name	Midpoint	Aves			
		Raw genera	Collections	Subsampled richness	Good's u
K12	68.3	1	1	NA	NA
K11	77.05	NA	NA	NA	NA
K10	84.65	2	2	1.66	1
K9	87.55	1	1	NA	NA
K8	91.4	NA	NA	NA	NA
K7	96.55	NA	NA	NA	NA
K6	105.8	1	1	NA	NA
K5	118.5	NA	NA	NA	NA
K4	127.5	5	5	3.33	0.571
K3	133.2	NA	NA	NA	NA
K2	138.3	NA	NA	NA	NA
K1	142.85	NA	NA	NA	NA
J11	148.15	1	7	1	1
J10	153.25	NA	NA	NA	NA
J9	158.45	NA	NA	NA	NA
J8	162.95	NA	NA	NA	NA
J7	166.2	NA	NA	NA	NA
J6	169.65	NA	NA	NA	NA
J5	173.6	NA	NA	NA	NA
J4	179.3	NA	NA	NA	NA
J3	186.3	NA	NA	NA	NA
J2	193.05	NA	NA	NA	NA
J1	199.05	NA	NA	NA	NA

Table 79. Stage level subsampled (SQS) diversity results for European Aves.

Bin name	Midpoint	Choristoderes			
		Raw genera	Collections	Subsampled richness	Good's u
K12	68.3	NA	NA	NA	NA
K11	77.05	NA	NA	NA	NA
K10	84.65	NA	NA	NA	NA
K9	87.55	NA	NA	NA	NA
K8	91.4	NA	NA	NA	NA
K7	96.55	NA	NA	NA	NA
K6	105.8	NA	NA	NA	NA
K5	118.5	NA	NA	NA	NA
K4	127.5	NA	NA	NA	NA
K3	133.2	NA	NA	NA	NA
K2	138.3	NA	NA	NA	NA
K1	142.85	NA	NA	NA	NA
J11	148.15	1	1	NA	NA
J10	153.25	1	1	NA	NA
J9	158.45	NA	NA	NA	NA
J8	162.95	NA	NA	NA	NA
J7	166.2	1	4	1	1
J6	169.65	NA	NA	NA	NA
J5	173.6	NA	NA	NA	NA
J4	179.3	NA	NA	NA	NA
J3	186.3	NA	NA	NA	NA
J2	193.05	NA	NA	NA	NA
J1	199.05	NA	NA	NA	NA

Table 80. Stage level subsampled (SQS) diversity results for European Choristoderes.

Bin name	Midpoint	Crocodyliformes			
		Raw genera	Collections	Subsampled richness	Good's u
K12	68.3	8	35	3.14	0.944
K11	77.05	NA	NA	NA	NA
K10	84.65	2	1	NA	NA
K9	87.55	NA	NA	NA	NA
K8	91.4	NA	NA	NA	NA
K7	96.55	NA	NA	NA	NA
K6	105.8	NA	NA	NA	NA
K5	118.5	NA	NA	NA	NA
K4	127.5	10	23	4.42	0.783
K3	133.2	3	6	2.3	0.833
K2	138.3	5	7	3.82	0.429
K1	142.85	6	27	2.32	0.969
J11	148.15	6	11	3.67	0.727
J10	153.25	6	10	2.54	0.867
J9	158.45	1	1	NA	NA
J8	162.95	NA	NA	NA	NA
J7	166.2	1	1	NA	NA
J6	169.65	NA	NA	NA	NA
J5	173.6	NA	NA	NA	NA
J4	179.3	NA	NA	NA	NA
J3	186.3	NA	NA	NA	NA
J2	193.05	NA	NA	NA	NA
J1	199.05	1	1	NA	NA

Table 81. Stage level subsampled (SQS) diversity results for European non-marine Crocodyliformes.

Bin name	Midpoint	Lepidosauria			
		Raw genera	Collections	Subsampled richness	Good's u
K12	68.3	3	3	2.17	0.5
K11	77.05	NA	NA	NA	NA
K10	84.65	NA	NA	NA	NA
K9	87.55	NA	NA	NA	NA
K8	91.4	NA	NA	NA	NA
K7	96.55	NA	NA	NA	NA
K6	105.8	NA	NA	NA	NA
K5	118.5	NA	NA	NA	NA
K4	127.5	8	12	3.07	0.533
K3	133.2	1	1	NA	NA
K2	138.3	NA	NA	NA	NA
K1	142.85	10	28	6.56	0.933
J11	148.15	4	5	2.58	0.714
J10	153.25	9	9	5.48	0.417
J9	158.45	1	1	NA	NA
J8	162.95	NA	NA	NA	NA
J7	166.2	4	7	2.52	0.714
J6	169.65	NA	NA	NA	NA
J5	173.6	NA	NA	NA	NA
J4	179.3	1	3	1	1
J3	186.3	NA	NA	NA	NA
J2	193.05	NA	NA	NA	NA
J1	199.05	NA	NA	NA	NA

Table 82. Stage level subsampled (SQS) diversity results for European non-marine Lepidosauria.

Bin name	Midpoint	Lissamphibia			
		Raw genera	Collections	Subsampled richness	Good's u
K12	68.3	5	12	2.11	0.949
K11	77.05	NA	NA	NA	NA
K10	84.65	2	1	NA	NA
K9	87.55	NA	NA	NA	NA
K8	91.4	NA	NA	NA	NA
K7	96.55	NA	NA	NA	NA
K6	105.8	NA	NA	NA	NA
K5	118.5	NA	NA	NA	NA
K4	127.5	11	12	6.22	0.533
K3	133.2	NA	NA	NA	NA
K2	138.3	NA	NA	NA	NA
K1	142.85	3	9	3	1
J11	148.15	NA	NA	NA	NA
J10	153.25	1	1	NA	NA
J9	158.45	NA	NA	NA	NA
J8	162.95	NA	NA	NA	NA
J7	166.2	4	9	1.54	0.727
J6	169.65	NA	NA	NA	NA
J5	173.6	NA	NA	NA	NA
J4	179.3	NA	NA	NA	NA
J3	186.3	NA	NA	NA	NA
J2	193.05	NA	NA	NA	NA
J1	199.05	NA	NA	NA	NA

Table 83. Stage level subsampled (SQS) diversity results for European Lissamphibia.

Bin name	Midpoint	Mammaliaformes			
		Raw genera	Collections	Subsampled richness	Good's u
K12	68.3	10	13	4.71	0.562
K11	77.05	NA	NA	NA	NA
K10	84.65	NA	NA	NA	NA
K9	87.55	NA	NA	NA	NA
K8	91.4	NA	NA	NA	NA
K7	96.55	NA	NA	NA	NA
K6	105.8	NA	NA	NA	NA
K5	118.5	NA	NA	NA	NA
K4	127.5	10	10	3.67	0.749
K3	133.2	1	1	NA	NA
K2	138.3	4	4	3.28	1
K1	142.85	23	29	8.73	0.828
J11	148.15	NA	NA	NA	NA
J10	153.25	21	1	NA	NA
J9	158.45	NA	NA	NA	NA
J8	162.95	NA	NA	NA	NA
J7	166.2	23	16	13.27	0.707
J6	169.65	NA	NA	NA	NA
J5	173.6	NA	NA	NA	NA
J4	179.3	NA	NA	NA	NA
J3	186.3	NA	NA	NA	NA
J2	193.05	NA	NA	NA	NA
J1	199.05	NA	NA	NA	NA

Table 84. Stage level subsampled (SQS) diversity results for European Mammaliaformes.

Bin name	Midpoint	Ornithischia			
		Raw genera	Collections	Subsampled richness	Good's u
K12	68.3	16	67	3.81	0.868
K11	77.05	NA	NA	NA	NA
K10	84.65	3	3	2.36	0.5
K9	87.55	NA	NA	NA	NA
K8	91.4	NA	NA	NA	NA
K7	96.55	NA	NA	NA	NA
K6	105.8	2	2	NA	NA
K5	118.5	2	2	NA	NA
K4	127.5	7	27	2.35	0.897
K3	133.2	2	5	1.26	1
K2	138.3	5	21	2.28	1
K1	142.85	9	30	2.54	0.848
J11	148.15	5	8	2.12	0.75
J10	153.25	5	11	2.02	0.636
J9	158.45	3	3	NA	NA
J8	162.95	3	5	2.23	0.8
J7	166.2	1	1	NA	NA
J6	169.65	NA	NA	NA	NA
J5	173.6	NA	NA	NA	NA
J4	179.3	1	1	NA	NA
J3	186.3	1	1	NA	NA
J2	193.05	1	4	1	1
J1	199.05	NA	NA	NA	NA

Table 85. Stage level subsampled (SQS) diversity results for European Ornithischia.

Bin name	Midpoint	Pterosauria			
		Raw genera	Collections	Subsampled richness	Good's u
K12	68.3	2	3	1.67	0.667
K11	77.05	NA	NA	NA	NA
K10	84.65	1	1	NA	NA
K9	87.55	NA	NA	NA	NA
K8	91.4	NA	NA	NA	NA
K7	96.55	NA	NA	NA	NA
K6	105.8	7	11	3.2	0.909
K5	118.5	NA	NA	NA	NA
K4	127.5	4	7	2.64	0.681
K3	133.2	1	2	1	1
K2	138.3	2	2	NA	NA
K1	142.85	5	6	NA	NA
J11	148.15	11	18	3.01	0.774
J10	153.25	8	15	3.85	0.778
J9	158.45	2	2	NA	NA
J8	162.95	NA	NA	NA	NA
J7	166.2	2	7	1.08	0.909
J6	169.65	NA	NA	NA	NA
J5	173.6	NA	NA	NA	NA
J4	179.3	3	51	1.46	1
J3	186.3	NA	NA	NA	NA
J2	193.05	NA	NA	NA	NA
J1	199.05	2	2	NA	NA

Table 86. Stage level subsampled (SQS) diversity results for European Pterosauria.

Bin name	Midpoint	Sauropodomorpha			
		Raw genera	Collections	Subsampled richness	Good's u
K12	68.3	4	28	1.71	0.969
K11	77.05	NA	NA	NA	NA
K10	84.65	NA	NA	NA	NA
K9	87.55	NA	NA	NA	NA
K8	91.4	NA	NA	NA	NA
K7	96.55	NA	NA	NA	NA
K6	105.8	1	1	NA	NA
K5	118.5	1	1	NA	NA
K4	127.5	1	1	NA	NA
K3	133.2	NA	NA	NA	NA
K2	138.3	2	2	1.52	0.667
K1	142.85	1	1	NA	NA
J11	148.15	4	5	2.45	0.4
J10	153.25	7	14	3.87	0.643
J9	158.45	NA	NA	NA	NA
J8	162.95	3	3	NA	NA
J7	166.2	2	15	1.12	0.937
J6	169.65	1	1	NA	NA
J5	173.6	NA	NA	NA	NA
J4	179.3	1	1	NA	NA
J3	186.3	NA	NA	NA	NA
J2	193.05	NA	NA	NA	NA
J1	199.05	NA	NA	NA	NA

Table 87. Stage level subsampled (SQS) diversity results for European Sauropodomorpha.

Bin name	Midpoint	Testudines			
		Raw genera	Collections	Subsampled richness	Good's u
K12	68.3	5	10	2.77	0.6
K11	77.05	NA	NA	NA	NA
K10	84.65	1	1	NA	NA
K9	87.55	NA	NA	NA	NA
K8	91.4	NA	NA	NA	NA
K7	96.55	NA	NA	NA	NA
K6	105.8	NA	NA	NA	NA
K5	118.5	NA	NA	NA	NA
K4	127.5	4	4	NA	NA
K3	133.2	2	2	1.74	0.667
K2	138.3	8	8	5.58	0.455
K1	142.85	8	16	2.51	0.923
J11	148.15	11	23	4.04	0.943
J10	153.25	12	27	3.98	0.904
J9	158.45	NA	NA	NA	NA
J8	162.95	NA	NA	NA	NA
J7	166.2	1	1	NA	NA
J6	169.65	NA	NA	NA	NA
J5	173.6	NA	NA	NA	NA
J4	179.3	NA	NA	NA	NA
J3	186.3	NA	NA	NA	NA
J2	193.05	NA	NA	NA	NA
J1	199.05	NA	NA	NA	NA

Table 88. Stage level subsampled (SQS) diversity results for European Testudines.

Bin name	Midpoint	Theropoda			
		Raw genera	Collections	Subsampled richness	Good's u
K12	68.3	15	26	5.85	0.724
K11	77.05	NA	NA	NA	NA
K10	84.65	1	1	NA	NA
K9	87.55	NA	NA	NA	NA
K8	91.4	NA	NA	NA	NA
K7	96.55	NA	NA	NA	NA
K6	105.8	2	2	NA	NA
K5	118.5	NA	NA	NA	NA
K4	127.5	9	9	NA	NA
K3	133.2	NA	NA	NA	NA
K2	138.3	4	5	3.01	0.4
K1	142.85	4	13	1.41	0.923
J11	148.15	5	7	3.84	0.571
J10	153.25	10	14	5.89	0.687
J9	158.45	2	4	1.5	0.75
J8	162.95	3	7	1.8	0.875
J7	166.2	7	19	2.06	0.7
J6	169.65	3	6	2.02	0.667
J5	173.6	NA	NA	NA	NA
J4	179.3	NA	NA	NA	NA
J3	186.3	NA	NA	NA	NA
J2	193.05	1	2	1	1
J1	199.05	1	1	NA	NA

Table 89. Stage level subsampled (SQS) diversity results for European Theropoda.

Marine, Europe

Bin name	Midpoint	Chelonioides			
		Raw genera	Collections	Subsampled richness	Good's u
J1	199.05	NA	NA	NA	NA
J2	193.05	NA	NA	NA	NA
J3	186.3	NA	NA	NA	NA
J4	179.3	NA	NA	NA	NA
J5	173.6	NA	NA	NA	NA
J6	169.65	NA	NA	NA	NA
J7	166.2	NA	NA	NA	NA
J8	162.95	NA	NA	NA	NA
J9	158.45	NA	NA	NA	NA
J10	153.25	NA	NA	NA	NA
J11	148.15	NA	NA	NA	NA
K1	142.85	NA	NA	NA	NA
K2	138.3	NA	NA	NA	NA
K3	133.2	NA	NA	NA	NA
K4	127.5	NA	NA	NA	NA
K5	118.5	NA	NA	NA	NA
K6	105.8	1	1	NA	NA
K7	96.55	NA	NA	NA	NA
K8	91.4	NA	NA	NA	NA
K9	87.55	NA	NA	NA	NA
K10	84.65	NA	NA	NA	NA
K11	77.05	NA	NA	NA	NA
K12	68.3	NA	NA	NA	NA

Figure 64. Stage level subsampled (SQS) diversity results for European Chelonioidea.

Bin name	Midpoint	Crocodyliformes			
		Raw	Collections	Subsampled	Good's u
J1	199.05	NA	NA	NA	NA
J2	193.05	NA	NA	NA	NA
J3	186.3	NA	NA	NA	NA
J4	179.3	4	29	1.55	0.955
J5	173.6	NA	NA	NA	NA
J6	169.65	NA	NA	NA	NA
J7	166.2	3	18	1.5	0.966
J8	162.95	7	23	2.08	0.955
J9	158.45	6	13	2.56	0.812
J10	153.25	12	43	2.77	0.941
J11	148.15	8	17	3.82	0.913
K1	142.85	NA	NA	NA	NA
K2	138.3	2	4	1.85	1
K3	133.2	1	1	NA	NA
K4	127.5	NA	NA	NA	NA
K5	118.5	1	1	NA	NA
K6	105.8	NA	NA	NA	NA
K7	96.55	NA	NA	NA	NA
K8	91.4	NA	NA	NA	NA
K9	87.55	NA	NA	NA	NA
K10	84.65	NA	NA	NA	NA
K11	77.05	NA	NA	NA	NA
K12	68.3	1	3	1	1

Table 90. Stage level subsampled (SQS) diversity results for European marine Crocodyliformes.

Bin name	Midpoint	Ichthyopterygia			
		Raw genera	Collections	Subsampled richness	Good's u
J1	199.05	3	12	1.7	1
J2	193.05	4	11	1.73	0.923
J3	186.3	2	5	1.59	1
J4	179.3	7	31	1.91	0.947
J5	173.6	1	2	1	1
J6	169.65	NA	NA	NA	NA
J7	166.2	NA	NA	NA	NA
J8	162.95	3	10	1.54	0.9
J9	158.45	1	1	NA	NA
J10	153.25	4	10	2.6	1
J11	148.15	10	16	3.78	0.722
K1	142.85	1	1	NA	NA
K2	138.3	1	1	NA	NA
K3	133.2	2	4	1.5	0.75
K4	127.5	2	2	NA	NA
K5	118.5	1	1	NA	NA
K6	105.8	3	8	1.83	0.875
K7	96.55	NA	NA	NA	NA
K8	91.4	NA	NA	NA	NA
K9	87.55	NA	NA	NA	NA
K10	84.65	NA	NA	NA	NA
K11	77.05	NA	NA	NA	NA
K12	68.3	NA	NA	NA	NA

Table 91. Stage level subsampled (SQS) diversity results for European Ichthyopterygia.

Bin name	Midpoint	Sauropterygia			
		Raw genera	Collections	Subsampled richness	Good's u
J1	199.05	8	12	4.22	0.643
J2	193.05	5	8	2.78	0.667
J3	186.3	3	3	NA	NA
J4	179.3	9	28	3.14	0.85
J5	173.6	NA	NA	NA	NA
J6	169.65	1	1	NA	NA
J7	166.2	1	2	1	1
J8	162.95	11	45	3.7	0.92
J9	158.45	3	7	1.61	0.714
J10	153.25	6	26	2.29	0.929
J11	148.15	7	22	1.91	0.826
K1	142.85	3	3	NA	NA
K2	138.3	1	5	1	1
K3	133.2	1	1	NA	NA
K4	127.5	2	2	NA	NA
K5	118.5	2	2	NA	NA
K6	105.8	2	3	1.64	0.667
K7	96.55	NA	NA	NA	NA
K8	91.4	NA	NA	NA	NA
K9	87.55	NA	NA	NA	NA
K10	84.65	1	1	NA	NA
K11	77.05	NA	NA	NA	NA
K12	68.3	NA	NA	NA	NA

Table 92. Stage level subsampled (SQS) diversity results for European Sauropterygia.

Bin name	Midpoint	Aves			
		Raw genera	Collections	Subsampled richness	Good's u
K12	68.3	16	24	6.05	0.656
K11	77.05	2	5	1.5	0.8
K10	84.65	2	2	NA	NA
K9	87.55	2	2	NA	NA
K8	91.4	NA	NA	NA	NA
K7	96.55	NA	NA	NA	NA
K6	105.8	NA	NA	NA	NA
K5	118.5	NA	NA	NA	NA
K4	127.5	NA	NA	NA	NA
K3	133.2	NA	NA	NA	NA
K2	138.3	NA	NA	NA	NA
K1	142.85	NA	NA	NA	NA
J11	148.15	NA	NA	NA	NA
J10	153.25	NA	NA	NA	NA
J9	158.45	NA	NA	NA	NA
J8	162.95	NA	NA	NA	NA
J7	166.2	NA	NA	NA	NA
J6	169.65	NA	NA	NA	NA
J5	173.6	NA	NA	NA	NA
J4	179.3	NA	NA	NA	NA
J3	186.3	NA	NA	NA	NA
J2	193.05	NA	NA	NA	NA
J1	199.05	NA	NA	NA	NA

Table 93. Stage level subsampled (SQS) diversity results for North American Aves.

Bin name	Midpoint	Choristoderes			
		Raw genera	Collections	Subsampled richness	Good's u
K12	68.3	1	43	1	1
K11	77.05	2	21	1.14	0.982
K10	84.65	NA	NA	NA	NA
K9	87.55	NA	NA	NA	NA
K8	91.4	NA	NA	NA	NA
K7	96.55	NA	NA	NA	NA
K6	105.8	NA	NA	NA	NA
K5	118.5	NA	NA	NA	NA
K4	127.5	NA	NA	NA	NA
K3	133.2	NA	NA	NA	NA
K2	138.3	NA	NA	NA	NA
K1	142.85	NA	NA	NA	NA
J11	148.15	1	2	1	1
J10	153.25	NA	NA	NA	NA
J9	158.45	NA	NA	NA	NA
J8	162.95	NA	NA	NA	NA
J7	166.2	1	NA	NA	NA
J6	169.65	NA	NA	NA	NA
J5	173.6	NA	NA	NA	NA
J4	179.3	NA	NA	NA	NA
J3	186.3	NA	NA	NA	NA
J2	193.05	NA	NA	NA	NA
J1	199.05	NA	NA	NA	NA

Table 94. Stage level subsampled (SQS) diversity results for North American Choristodera.

Bin name	Midpoint	Crocodyliformes			
		Raw genera	Collections	Subsampled richness	Good's u
K12	68.3	10	181	2.18	0.964
K11	77.05	4	45	1.55	0.969
K10	84.65	1	1	NA	NA
K9	87.55	NA	NA	NA	NA
K8	91.4	NA	NA	NA	NA
K7	96.55	1	2	1	1
K6	105.8	NA	NA	NA	NA
K5	118.5	1	1	NA	NA
K4	127.5	NA	NA	NA	NA
K3	133.2	NA	NA	NA	NA
K2	138.3	NA	NA	NA	NA
K1	142.85	NA	NA	NA	NA
J11	148.15	4	6	2.52	0.5
J10	153.25	3	7	2.15	0.857
J9	158.45	NA	NA	NA	NA
J8	162.95	1	1	NA	NA
J7	166.2	NA	NA	NA	NA
J6	169.65	NA	NA	NA	NA
J5	173.6	NA	NA	NA	NA
J4	179.3	NA	NA	NA	NA
J3	186.3	NA	NA	NA	NA
J2	193.05	NA	NA	NA	NA
J1	199.05	1	10	1	1

Table 95. Stage level subsampled (SQS) diversity results for North American non-marine Crocodyliformes.

Bin name	Midpoint	Lepidosauria			
		Raw genera	Collections	Subsampled richness	Good's u
K12	68.3	23	137	7.92	0.953
K11	77.05	21	83	6.21	0.863
K10	84.65	5	6	NA	NA
K9	87.55	NA	NA	NA	NA
K8	91.4	1	1	NA	NA
K7	96.55	5	14	3.87	0.894
K6	105.8	NA	NA	NA	NA
K5	118.5	NA	NA	NA	NA
K4	127.5	NA	NA	NA	NA
K3	133.2	NA	NA	NA	NA
K2	138.3	NA	NA	NA	NA
K1	142.85	NA	NA	NA	NA
J11	148.15	5	6	NA	NA
J10	153.25	4	6	2.53	0.5
J9	158.45	NA	NA	NA	NA
J8	162.95	NA	NA	NA	NA
J7	166.2	NA	NA	NA	NA
J6	169.65	NA	NA	NA	NA
J5	173.6	NA	NA	NA	NA
J4	179.3	NA	NA	NA	NA
J3	186.3	NA	NA	NA	NA
J2	193.05	NA	NA	NA	NA
J1	199.05	1	6	1	1

Table 96. Stage level subsampled (SQS) diversity results for North American non-marine Lepidosauria.

Bin name	Midpoint	Lissamphibia			
		Raw genera	Collections	Subsampled richness	Good's u
K12	68.3	15	195	3.84	0.988
K11	77.05	7	146	2.62	0.987
K10	84.65	1	2	1	1
K9	87.55	NA	NA	NA	NA
K8	91.4	1	1	NA	NA
K7	96.55	1	2	1	1
K6	105.8	NA	NA	NA	NA
K5	118.5	NA	NA	NA	NA
K4	127.5	NA	NA	NA	NA
K3	133.2	NA	NA	NA	NA
K2	138.3	NA	NA	NA	NA
K1	142.85	NA	NA	NA	NA
J11	148.15	NA	NA	NA	NA
J10	153.25	3	2	NA	NA
J9	158.45	NA	NA	NA	NA
J8	162.95	NA	NA	NA	NA
J7	166.2	NA	NA	NA	NA
J6	169.65	NA	NA	NA	NA
J5	173.6	NA	NA	NA	NA
J4	179.3	NA	NA	NA	NA
J3	186.3	NA	NA	NA	NA
J2	193.05	NA	NA	NA	NA
J1	199.05	NA	NA	NA	NA

Table 97. Stage level subsampled (SQS) diversity results for North American Lissamphibia.

Bin name	Midpoint	Mammaliaformes			
		Raw genera	Collections	Subsampled richness	Good's u
K12	68.3	45	510	7.32	0.986
K11	77.05	27	126	6.23	0.976
K10	84.65	15	14	11.85	0.421
K9	87.55	2	2	NA	NA
K8	91.4	5	8	2.83	0.867
K7	96.55	15	82	7.82	0.963
K6	105.8	1	1	NA	NA
K5	118.5	1	1	NA	NA
K4	127.5	NA	NA	NA	NA
K3	133.2	NA	NA	NA	NA
K2	138.3	NA	NA	NA	NA
K1	142.85	NA	NA	NA	NA
J11	148.15	9	4	NA	NA
J10	153.25	5	2	NA	NA
J9	158.45	NA	NA	NA	NA
J8	162.95	NA	NA	NA	NA
J7	166.2	NA	NA	NA	NA
J6	169.65	NA	NA	NA	NA
J5	173.6	NA	NA	NA	NA
J4	179.3	NA	NA	NA	NA
J3	186.3	NA	NA	NA	NA
J2	193.05	NA	NA	NA	NA
J1	199.05	1	1	NA	NA

Table 98. Stage level subsampled (SQS) diversity results for North American Mammaliaformes.

Bin name	Midpoint	Ornithischia			
		Raw genera	Collections	Subsampled richness	Good's u
K12	68.3	35	215	3.61	0.966
K11	77.05	23	50	4.73	0.902
K10	84.65	9	11	5.19	0.429
K9	87.55	2	NA	NA	NA
K8	91.4	NA	NA	NA	NA
K7	96.55	1	5	1	1
K6	105.8	7	14	3.08	0.942
K5	118.5	2	2	1.75	0.667
K4	127.5	6	9	4.01	0.7
K3	133.2	NA	NA	NA	NA
K2	138.3	1	NA	NA	NA
K1	142.85	NA	NA	NA	NA
J11	148.15	7	10	3.64	0.882
J10	153.25	7	20	2.6	0.909
J9	158.45	NA	NA	NA	NA
J8	162.95	NA	NA	NA	NA
J7	166.2	NA	NA	NA	NA
J6	169.65	NA	NA	NA	NA
J5	173.6	NA	NA	NA	NA
J4	179.3	NA	NA	NA	NA
J3	186.3	NA	NA	NA	NA
J2	193.05	NA	NA	NA	NA
J1	199.05	NA	NA	NA	NA

Table 99. Stage level subsampled (SQS) diversity results for North American Ornithischia.

Bin name	Midpoint	Pterosauria			
		Raw genera	Collections	Subsampled richness	Good's u
K12	68.3	1	6	1	1
K11	77.05	1	2	1	1
K10	84.65	1	2	1	1
K9	87.55	1	1	NA	NA
K8	91.4	NA	NA	NA	NA
K7	96.55	NA	NA	NA	NA
K6	105.8	1	1	NA	NA
K5	118.5	NA	NA	NA	NA
K4	127.5	NA	NA	NA	NA
K3	133.2	NA	NA	NA	NA
K2	138.3	NA	NA	NA	NA
K1	142.85	NA	NA	NA	NA
J11	148.15	1	1	NA	NA
J10	153.25	1	1	NA	NA
J9	158.45	NA	NA	NA	NA
J8	162.95	NA	NA	NA	NA
J7	166.2	NA	NA	NA	NA
J6	169.65	NA	NA	NA	NA
J5	173.6	NA	NA	NA	NA
J4	179.3	NA	NA	NA	NA
J3	186.3	NA	NA	NA	NA
J2	193.05	NA	NA	NA	NA
J1	199.05	NA	NA	NA	NA

Table 100. Stage level subsampled (SQS) diversity results for North American Pterosauria.

Bin name	Midpoint	Sauropodomorpha			
		Raw genera	Collections	Subsampled richness	Good's u
K12	68.3	1	21	1	1
K11	77.05	NA	NA	NA	NA
K10	84.65	NA	NA	NA	NA
K9	87.55	NA	NA	NA	NA
K8	91.4	NA	NA	NA	NA
K7	96.55	NA	NA	NA	NA
K6	105.8	1	2	1	1
K5	118.5	1	1	NA	NA
K4	127.5	2	4	1.84	1
K3	133.2	NA	NA	NA	NA
K2	138.3	NA	NA	NA	NA
K1	142.85	NA	NA	NA	NA
J11	148.15	7	22	2.74	0.935
J10	153.25	8	46	3.16	0.939
J9	158.45	1	1	NA	NA
J8	162.95	NA	NA	NA	NA
J7	166.2	NA	NA	NA	NA
J6	169.65	NA	NA	NA	NA
J5	173.6	NA	NA	NA	NA
J4	179.3	NA	NA	NA	NA
J3	186.3	NA	NA	NA	NA
J2	193.05	NA	NA	NA	NA
J1	199.05	1	3	1	1

Table 101. Stage level subsampled (SQS) diversity results for North American Sauropodomorpha.

Bin name	Midpoint	Testudines			
		Raw genera	Collections	Subsampled richness	Good's u
K12	68.3	36	166	5.08	0.981
K11	77.05	11	35	3.17	0.969
K10	84.65	4	5	3.01	0.4
K9	87.55	NA	NA	NA	NA
K8	91.4	NA	NA	NA	NA
K7	96.55	NA	NA	NA	NA
K6	105.8	2	4	1.5	0.807
K5	118.5	1	1	NA	NA
K4	127.5	NA	NA	NA	NA
K3	133.2	NA	NA	NA	NA
K2	138.3	NA	NA	NA	NA
K1	142.85	NA	NA	NA	NA
J11	148.15	3	5	2.17	0.9
J10	153.25	1	4	1	1
J9	158.45	NA	NA	NA	NA
J8	162.95	NA	NA	NA	NA
J7	166.2	NA	NA	NA	NA
J6	169.65	NA	NA	NA	NA
J5	173.6	NA	NA	NA	NA
J4	179.3	NA	NA	NA	NA
J3	186.3	NA	NA	NA	NA
J2	193.05	NA	NA	NA	NA
J1	199.05	NA	NA	NA	NA

Table 102. Stage level subsampled (SQS) diversity results for North American Testudines.

Bin name	Midpoint	Theropoda			
		Raw genera	Collections	Subsampled richness	Good's u
K12	68.3	27	333	4.5	0.974
K11	77.05	18	212	3.57	0.97
K10	84.65	5	7	3.25	0.429
K9	87.55	NA	NA	NA	NA
K8	91.4	NA	NA	NA	NA
K7	96.55	2	2	NA	NA
K6	105.8	3	23	1.43	0.957
K5	118.5	3	4	2.5	0.5
K4	127.5	5	8	3.63	0.75
K3	133.2	NA	NA	NA	NA
K2	138.3	NA	NA	NA	NA
K1	142.85	NA	NA	NA	NA
J11	148.15	7	14	3.69	0.714
J10	153.25	8	30	1.94	0.871
J9	158.45	NA	NA	NA	NA
J8	162.95	NA	NA	NA	NA
J7	166.2	NA	NA	NA	NA
J6	169.65	NA	NA	NA	NA
J5	173.6	NA	NA	NA	NA
J4	179.3	NA	NA	NA	NA
J3	186.3	NA	NA	NA	NA
J2	193.05	NA	NA	NA	NA
J1	199.05	1	1	NA	NA

Table 103. Stage level subsampled (SQS) diversity results for North American Theropoda.

Bin name	Midpoint	Chelonioides			
		Raw genera	Collections	Subsampled richness	Good's u
K12	68.3	6	17	2.5	0.842
K11	77.05	1	8	1	1
K10	84.65	5	3	3.58	0.571
K9	87.55	NA	NA	NA	NA
K8	91.4	NA	NA	NA	NA
K7	96.55	NA	NA	NA	NA
K6	105.8	NA	NA	NA	NA
K5	118.5	NA	NA	NA	NA
K4	127.5	NA	NA	NA	NA
K3	133.2	NA	NA	NA	NA
K2	138.3	NA	NA	NA	NA
K1	142.85	NA	NA	NA	NA
J11	148.15	NA	NA	NA	NA
J10	153.25	NA	NA	NA	NA
J9	158.45	NA	NA	NA	NA
J8	162.95	NA	NA	NA	NA
J7	166.2	NA	NA	NA	NA
J6	169.65	NA	NA	NA	NA
J5	173.6	NA	NA	NA	NA
J4	179.3	NA	NA	NA	NA
J3	186.3	NA	NA	NA	NA
J2	193.05	NA	NA	NA	NA
J1	199.05	NA	NA	NA	NA

Table 104. Stage level subsampled (SQS) diversity results for North American Chelonioidea.

Bin name	Midpoint	Crocodyliformes			
		Raw genera	Collections	Subsampled richness	Good's u
K12	68.3	3	26	1.59	0.967
K11	77.05	NA	NA	NA	NA
K10	84.65	NA	NA	NA	NA
K9	87.55	NA	NA	NA	NA
K8	91.4	NA	NA	NA	NA
K7	96.55	NA	NA	NA	NA
K6	105.8	NA	NA	NA	NA
K5	118.5	NA	NA	NA	NA
K4	127.5	NA	NA	NA	NA
K3	133.2	NA	NA	NA	NA
K2	138.3	NA	NA	NA	NA
K1	142.85	NA	NA	NA	NA
J11	148.15	NA	NA	NA	NA
J10	153.25	NA	NA	NA	NA
J9	158.45	NA	NA	NA	NA
J8	162.95	NA	NA	NA	NA
J7	166.2	NA	NA	NA	NA
J6	169.65	NA	NA	NA	NA
J5	173.6	NA	NA	NA	NA
J4	179.3	NA	NA	NA	NA
J3	186.3	NA	NA	NA	NA
J2	193.05	NA	NA	NA	NA
J1	199.05	NA	NA	NA	NA

Table 105. Stage level subsampled (SQS) diversity results for North American marine Crocodyliformes.

Bin name	Midpoint	Ichthyopterygia			
		Raw genera	Collections	Subsampled richness	Good's u
K12	68.3	NA	NA	NA	NA
K11	77.05	NA	NA	NA	NA
K10	84.65	NA	NA	NA	NA
K9	87.55	NA	NA	NA	NA
K8	91.4	NA	NA	NA	NA
K7	96.55	NA	NA	NA	NA
K6	105.8	1	2	1	1
K5	118.5	NA	NA	NA	NA
K4	127.5	NA	NA	NA	NA
K3	133.2	NA	NA	NA	NA
K2	138.3	NA	NA	NA	NA
K1	142.85	NA	NA	NA	NA
J11	148.15	1	1	NA	NA
J10	153.25	NA	NA	NA	NA
J9	158.45	3	3	NA	NA
J8	162.95	NA	NA	NA	NA
J7	166.2	NA	NA	NA	NA
J6	169.65	NA	NA	NA	NA
J5	173.6	NA	NA	NA	NA
J4	179.3	NA	NA	NA	NA
J3	186.3	NA	NA	NA	NA
J2	193.05	1	1	NA	NA
J1	199.05	NA	NA	NA	NA

Table 106. Stage level subsampled (SQS) diversity results for North American Ichthyopterygia.

Bin name	Midpoint	Sauropterygia			
		Raw genera	Collections	Subsampled richness	Good's u
K12	68.3	5	9	2.86	0.667
K11	77.05	NA	NA	NA	NA
K10	84.65	NA	NA	NA	NA
K9	87.55	NA	NA	NA	NA
K8	91.4	NA	NA	NA	NA
K7	96.55	1	1	NA	NA
K6	105.8	1	1	NA	NA
K5	118.5	NA	NA	NA	NA
K4	127.5	NA	NA	NA	NA
K3	133.2	NA	NA	NA	NA
K2	138.3	NA	NA	NA	NA
K1	142.85	NA	NA	NA	NA
J11	148.15	NA	NA	NA	NA
J10	153.25	NA	NA	NA	NA
J9	158.45	3	9	2.03	0.9
J8	162.95	1	1	NA	NA
J7	166.2	NA	NA	NA	NA
J6	169.65	NA	NA	NA	NA
J5	173.6	NA	NA	NA	NA
J4	179.3	NA	NA	NA	NA
J3	186.3	NA	NA	NA	NA
J2	193.05	NA	NA	NA	NA
J1	199.05	NA	NA	NA	NA

Table 107. Stage level subsampled (SQS) diversity results for North American Sauropterygia.

Appendix 9 – Full results of the SQS results for tetrapod groups when varying the quorum level.

10 myr Quorum level	0.1	0.2	0.3	0.4	0.5	0.6	0.7	0.8	0.9
K8	1.72	1.69	1.71	1.75	1.88	2.06	2.57	3.13	NA
K7	2.37	2.38	2.34	2.33	2.3	NA	NA	NA	NA
K6	NA	NA	NA	NA	NA	NA	NA	NA	NA
K5	NA	NA	NA	NA	NA	NA	NA	NA	NA
K4	NA	NA	NA	NA	NA	NA	NA	NA	NA
K3	1.33	1.33	1.34	1.34	1.34	1.35	2	2	2
K2	NA	NA	NA	NA	NA	NA	NA	NA	NA
K1	2.22	2.25	2.24	2.22	2.25	2.56	2.7	2.68	2.9
J6	2.82	2.74	2.91	3.16	3.61	4.18	5	6.06	8.13
J5	2.16	2.17	2.16	2.28	2.5	2.91	3.54	4.19	6.42
J4	1.88	1.84	1.93	1.84	1.96	2.13	2.49	2.78	4.03
J3	1.43	1.41	1.39	1.41	1.42	1.5	1.68	1.68	2.24
J2	NA	NA	NA	NA	NA	NA	NA	NA	NA
J1	NA	NA	NA	NA	NA	NA	NA	NA	NA

Stage Quorum level	0.1	0.2	0.3	0.4	0.5	0.6	0.7	0.8	0.9
K12	1.73	1.72	1.73	1.75	1.89	2.07	2.55	3.06	NA
K11	NA	NA	NA	NA	NA	NA	NA	NA	NA
K10	NA	NA	NA	NA	NA	NA	NA	NA	NA
K9	NA	NA	NA	NA	NA	NA	NA	NA	NA
K8	NA	NA	NA	NA	NA	NA	NA	NA	NA
K7	NA	NA	NA	NA	NA	NA	NA	NA	NA
K6	NA	NA	NA	NA	NA	NA	NA	NA	NA
K5	NA	NA	NA	NA	NA	NA	NA	NA	NA
K4	NA	NA	NA	NA	NA	NA	NA	NA	NA
K3	NA	NA	NA	NA	NA	NA	NA	NA	NA
K2	1.83	1.84	1.85	1.81	1.83	1.85	2	2	2
K1	1.73	1.74	1.74	1.74	1.74	1.73	NA	NA	NA
J11	2.9	2.85	3.08	3.21	3.55	4.04	4.78	5.4	6.54
J10	2.49	2.49	2.58	2.82	3.16	3.8	4.78	6.07	8.46
J9	2.23	2.24	2.24	2.5	2.8	3.38	3.99	4.76	NA
J8	1.94	1.92	1.99	2.04	2.2	2.45	2.89	3.31	4.41
J7	1.58	1.62	1.63	1.62	1.63	1.66	1.96	2.06	2.38
J6	NA	NA	NA	NA	NA	NA	NA	NA	NA
J5	NA	NA	NA	NA	NA	NA	NA	NA	NA
J4	1.43	1.42	1.4	1.41	1.43	1.53	1.69	1.73	2.21
J3	NA	NA	NA	NA	NA	NA	NA	NA	NA
J2	NA	NA	NA	NA	NA	NA	NA	NA	NA
J1	NA	NA	NA	NA	NA	NA	NA	NA	NA

Table 108. SQS results when the quorum is varied at increments of 0.1 for marine Crocodyliformes at 10 million year (top) and Stage (bottom) time bin intervals.

10 myr Quorum level	0.1	0.2	0.3	0.4	0.5	0.6	0.7	0.8	0.9
K8	3.8	4.05	4.37	5.02	6.07	7.8	10.59	15.64	24.45
K7	3.57	3.67	4.22	4.63	5.54	6.95	9.24	12.06	NA
K6	8.36	12.53	19.93	NA	NA	NA	NA	NA	NA
K5	3.74	4.04	5.19	6.58	8.61	11.69	NA	NA	NA
K4	5.08	5.68	7.31	NA	NA	NA	NA	NA	NA
K3	2.8	2.7	2.92	3.36	3.63	4.72	5.79	7.12	NA
K2	3.56	3.63	3.8	4.32	4.84	5.67	7.16	9.12	NA
K1	2.61	2.54	2.61	2.81	3.21	3.69	4.28	5.09	NA
J6	2.56	2.72	2.98	3.27	3.81	5	6.77	9.48	NA
J5	2.19	2.2	2.27	2.36	2.67	NA	NA	NA	NA
J4	NA	NA	NA	NA	NA	NA	NA	NA	NA
J3	NA	NA	NA	NA	NA	NA	NA	NA	NA
J2	NA	NA	NA	NA	NA	NA	NA	NA	NA
J1	2.06	2.05	2.07	2.12	2.28	2.83	3.61	NA	NA

Stage Quorum level	0.1	0.2	0.3	0.4	0.5	0.6	0.7	0.8	0.9
K12	3.76	4.04	4.44	5.1	5.87	7.69	10.49	15.16	24.95
K11	1.62	1.58	1.51	1.52	1.6	1.71	2.1	2.26	NA
K10	4.17	4.55	5.42	6.83	NA	NA	NA	NA	NA
K9	NA	NA	NA	NA	NA	NA	NA	NA	NA
K8	NA	NA	NA	NA	NA	NA	NA	NA	NA
K7	1	1	1	1	1	1	1	1	1
K6	1	1	1	1	1	1	1	1	1
K5	NA	NA	NA	NA	NA	NA	NA	NA	NA
K4	3.49	3.67	3.93	4.26	4.89	5.89	7.15	NA	NA
K3	2.3	2.35	2.29	2.31	2.24	2.6	2.7	2.71	NA
K2	3.37	3.32	3.38	3.82	NA	NA	NA	NA	NA
K1	2.26	2.3	2.26	2.32	2.54	2.99	3.34	3.83	4.3
J11	3.52	3.56	4.17	5.08	6.36	NA	NA	NA	NA
J10	2.98	2.92	3.24	3.34	3.64	4.33	5.4	6.36	NA
J9	2.67	2.59	2.57	2.74	3.32	NA	NA	NA	NA
J8	1.51	1.5	1.51	1.49	1.51	1.51	1.77	NA	NA
J7	NA	NA	NA	NA	NA	NA	NA	NA	NA
J6	NA	NA	NA	NA	NA	NA	NA	NA	NA
J5	NA	NA	NA	NA	NA	NA	NA	NA	NA
J4	NA	NA	NA	NA	NA	NA	NA	NA	NA
J3	NA	NA	NA	NA	NA	NA	NA	NA	NA
J2	3.07	3.11	3.12	3.09	NA	NA	NA	NA	NA
J1	1	1	1	1	1	1	1	1	1

Table 109. SQS results when the quorum is varied at increments of 0.1 for non-marine Crocodyliformes at 10 million year (top) and Stage (bottom) time bin intervals.

10 myr									
Quorum level	**0.1**	**0.2**	**0.3**	**0.4**	**0.5**	**0.6**	**0.7**	**0.8**	**0.9**
K8	NA	NA	NA	NA	NA	NA	NA	NA	NA
K7	NA	NA	NA	NA	NA	NA	NA	NA	NA
K6	NA	NA	NA	NA	NA	NA	NA	NA	NA
K5	1.51	1.47	1.48	1.47	1.5	1.59	1.84	NA	NA
K4	1.43	1.42	1.45	1.5	1.46	1.53	1.82	2.13	3.14
K3	1.65	1.7	1.67	1.64	1.67	1.84	2.16	NA	NA
K2	2.83	2.77	2.76	3.07	3.44	3.79	NA	NA	NA
K1	NA	NA	NA	NA	NA	NA	NA	NA	NA
J6	2.65	2.73	2.9	3.06	3.45	4.18	5.06	6.37	NA
J5	2	2.07	2.1	2.18	2.24	2.78	3.45	4.14	NA
J4	1.76	1.77	1.75	1.75	1.73	1.73	NA	NA	NA
J3	1.77	1.78	1.84	1.86	1.95	2.24	2.59	2.91	4.18
J2	1.58	1.61	1.59	1.6	1.6	1.59	1.89	1.91	1.88
J1	1.74	1.74	1.71	1.71	1.7	1.98	2.15	2.31	2.68

Stage									
Quorum level	**0.1**	**0.2**	**0.3**	**0.4**	**0.5**	**0.6**	**0.7**	**0.8**	**0.9**
K12	NA	NA	NA	NA	NA	NA	NA	NA	NA
K11	NA	NA	NA	NA	NA	NA	NA	NA	NA
K10	NA	NA	NA	NA	NA	NA	NA	NA	NA
K9	NA	NA	NA	NA	NA	NA	NA	NA	NA
K8	NA	NA	NA	NA	NA	NA	NA	NA	NA
K7	NA	NA	NA	NA	NA	NA	NA	NA	NA
K6	1.28	1.31	1.32	1.29	1.29	1.32	1.51	1.64	1.98
K5	NA	NA	NA	NA	NA	NA	NA	NA	NA
K4	NA	NA	NA	NA	NA	NA	NA	NA	NA
K3	1.49	1.46	1.51	1.5	1.48	1.5	1.66	NA	NA
K2	NA	NA	NA	NA	NA	NA	NA	NA	NA
K1	NA	NA	NA	NA	NA	NA	NA	NA	NA
J11	2.53	2.59	2.75	3.1	3.54	4.58	5.73	7.81	NA
J10	2.61	2.6	2.64	2.59	2.93	3.09	3.45	3.55	3.81
J9	NA	NA	NA	NA	NA	NA	NA	NA	NA
J8	1.56	1.53	1.52	1.56	1.56	1.71	2	2.12	2.47
J7	NA	NA	NA	NA	NA	NA	NA	NA	NA
J6	1.76	1.76	1.73	1.76	1.76	1.77	NA	NA	NA
J5	1	1	1	1	1	1	1	1	1
J4	1.88	1.88	1.94	1.89	2.1	2.41	2.8	3.21	4.53
J3	1.6	1.58	1.58	1.61	1.61	1.57	1.89	1.9	1.89
J2	1.74	1.75	1.71	1.73	1.81	1.98	2.32	2.46	2.96
J1	1.59	1.65	1.64	1.62	1.63	1.73	1.95	2.01	2.4

Table 110. SQS results when the quorum is varied at increments of 0.1 for Ichthyosauria at 10 million year (top) and Stage (bottom) time bin intervals.

10 myr									
Quorum level	**0.1**	**0.2**	**0.3**	**0.4**	**0.5**	**0.6**	**0.7**	**0.8**	**0.9**
K8	5.32	6.22	7.29	8.23	9.17	10.89	13.03	15.89	NA
K7	6.67	8.89	10.71	13.18	17.35	25.33	37.54	NA	NA
K6	7.14	NA	NA	NA	NA	NA	NA	NA	NA
K5	5.75	5.93	6.25	6.26	NA	NA	NA	NA	NA
K4	5.87	8.21	NA	NA	NA	NA	NA	NA	NA
K3	2.61	2.7	2.7	2.82	3.09	3.36	3.96	NA	NA
K2	4.74	5.43	8.34	NA	NA	NA	NA	NA	NA
K1	5.58	5.92	6.49	7.68	8.43	9.01	10.48	12.07	NA
J6	3.13	3.16	3.46	4.02	4.77	5.75	6.87	8.65	12.04
J5	NA	NA	NA	NA	NA	NA	NA	NA	NA
J4	3.04	3.08	3.04	3.28	3.78	4.07	NA	NA	NA
J3	3.06	3.03	2.96	3.22	NA	NA	NA	NA	NA
J2	NA	NA	NA	NA	NA	NA	NA	NA	NA
J1	1.4	1.41	1.39	1.37	1.39	1.43	1.44	1.46	1.6

Stage									
Quorum level	**0.1**	**0.2**	**0.3**	**0.4**	**0.5**	**0.6**	**0.7**	**0.8**	**0.9**
K12	5.38	6.19	7.3	8.24	9.16	11.23	13.08	16.1	NA
K11	4.38	4.82	5.56	6.22	7.4	9.73	13.07	NA	NA
K10	3.92	4.02	4.09	NA	NA	NA	NA	NA	NA
K9	NA	NA	NA	NA	NA	NA	NA	NA	NA
K8	NA	NA	NA	NA	NA	NA	NA	NA	NA
K7	3.92	3.75	3.81	3.89	4.06	4.24	NA	NA	NA
K6	NA	NA	NA	NA	NA	NA	NA	NA	NA
K5	NA	NA	NA	NA	NA	NA	NA	NA	NA
K4	3.52	3.7	4.3	5.87	6.94	NA	NA	NA	NA
K3	NA	NA	NA	NA	NA	NA	NA	NA	NA
K2	3	3	3	3	3	NA	NA	NA	NA
K1	6.15	6.33	7.18	7.54	8.15	8.74	9.44	10.44	NA
J11	4.36	4.63	5.08	5.35	6.25	NA	NA	NA	NA
J10	3.66	4.26	5.16	7.15	NA	NA	NA	NA	NA
J9	NA	NA	NA	NA	NA	NA	NA	NA	NA
J8	NA	NA	NA	NA	NA	NA	NA	NA	NA
J7	2.94	2.97	3.02	3.29	3.74	4.07	NA	NA	NA
J6	NA	NA	NA	NA	NA	NA	NA	NA	NA
J5	NA	NA	NA	NA	NA	NA	NA	NA	NA
J4	1	1	1	1	1	1	1	1	1
J3	NA	NA	NA	NA	NA	NA	NA	NA	NA
J2	NA	NA	NA	NA	NA	NA	NA	NA	NA
J1	1	1	1	1	1	1	1	1	1

Table 111. SQS results when the quorum is varied at increments of 0.1 for non-marine Lepidosauromorpha at 10 million year (top) and Stage (bottom) time bin intervals.

10 myr Quorum level	0.1	0.2	0.3	0.4	0.5	0.6	0.7	0.8	0.9
K8	3.53	3.64	4	4.48	4.71	5.61	6.89	8.26	11.41
K7	2.13	2.14	2.26	2.32	2.58	2.99	3.64	4.21	5.78
K6	4.58	4.6	5.25	5.89	6.6	8.13	9.72	10.93	NA
K5	2.39	2.41	2.42	2.59	2.91	3.48	4.31	NA	NA
K4	2.34	2.4	2.41	2.41	2.64	3.03	3.4	NA	NA
K3	3.86	3.96	3.96	4.31	NA	NA	NA	NA	NA
K2	3.97	5.01	5.84	6.75	8.18	NA	NA	NA	NA
K1	5.59	5.52	5.54	5.47	5.47	5.85	NA	NA	NA
J6	5.13	5.17	NA	NA	NA	NA	NA	NA	NA
J5	3.94	3.96	3.9	NA	NA	NA	NA	NA	NA
J4	2.08	2.06	2.05	2.19	2.41	3.13	4.22	NA	NA
J3	NA	NA	NA	NA	NA	NA	NA	NA	NA
J2	NA	NA	NA	NA	NA	NA	NA	NA	NA
J1	NA	NA	NA	NA	NA	NA	NA	NA	NA

Stage Quorum level	0.1	0.2	0.3	0.4	0.5	0.6	0.7	0.8	0.9
K12	3.44	3.77	4.06	4.52	4.85	5.68	6.83	8.27	11.23
K11	2.53	2.58	2.68	2.72	2.81	3.02	3.47	3.92	4.77
K10	1.98	2.08	1.99	2.8	2.98	NA	NA	NA	NA
K9	3.15	3.18	3.36	3.8	4.33	5.26	6.21	7.29	8.04
K8	NA	NA	NA	NA	NA	NA	NA	NA	NA
K7	1	1	1	1	1	1	1	1	1
K6	NA	NA	NA	NA	NA	NA	NA	NA	NA
K5	NA	NA	NA	NA	NA	NA	NA	NA	NA
K4	3.16	3.44	4.06	5.21	6.38	7.81	NA	NA	NA
K3	NA	NA	NA	NA	NA	NA	NA	NA	NA
K2	NA	NA	NA	NA	NA	NA	NA	NA	NA
K1	5.5	5.6	5.43	5.55	5.49	5.81	NA	NA	NA
J11	NA	NA	NA	NA	NA	NA	NA	NA	NA
J10	NA	NA	NA	NA	NA	NA	NA	NA	NA
J9	NA	NA	NA	NA	NA	NA	NA	NA	NA
J8	NA	NA	NA	NA	NA	NA	NA	NA	NA
J7	2.09	2.04	2.09	2.18	2.42	3.22	4.13	NA	NA
J6	NA	NA	NA	NA	NA	NA	NA	NA	NA
J5	NA	NA	NA	NA	NA	NA	NA	NA	NA
J4	NA	NA	NA	NA	NA	NA	NA	NA	NA
J3	NA	NA	NA	NA	NA	NA	NA	NA	NA
J2	NA	NA	NA	NA	NA	NA	NA	NA	NA
J1	NA	NA	NA	NA	NA	NA	NA	NA	NA

Table 112. SQS results when the quorum is varied at increments of 0.1 for Lissamphibia at 10 million year (top) and Stage (bottom) time bin intervals.

10 myr Quorum level	0.1	0.2	0.3	0.4	0.5	0.6	0.7	0.8	0.9
K8	4.65	5.26	6.47	7.37	8.89	10.87	13.86	17.53	27.3
K7	4.39	5.28	6.33	7.58	9.51	12.6	17.14	24.49	43.04
K6	5.08	5.27	5.85	6.54	7.46	9.24	12.16	14.62	NA
K5	4.89	5.69	6.77	7.82	9.47	11.49	14.29	17.72	NA
K4	4.06	4.43	4.88	5.53	6.3	8.33	10.81	NA	NA
K3	6.54	7.85	9.67	NA	NA	NA	NA	NA	NA
K2	4.24	4.71	5.53	6.71	8.39	11.2	NA	NA	NA
K1	6.25	8.01	11.16	15.38	19.09	23.95	31.03	NA	NA
J6	5	5.53	6.71	8.18	10.77	15.78	23.01	NA	NA
J5	6.05	9.2	12.48	NA	NA	NA	NA	NA	NA
J4	7.52	9.92	12.31	13.75	16.32	18.99	NA	NA	NA
J3	NA	NA	NA	NA	NA	NA	NA	NA	NA
J2	NA	NA	NA	NA	NA	NA	NA	NA	NA
J1	3.45	3.48	3.59	3.87	4.29	4.84	5.82	6.99	NA

Stage Quorum level	0.1	0.2	0.3	0.4	0.5	0.6	0.7	0.8	0.9
K12	4.8	5.26	6.37	7.63	8.88	10.96	13.81	17.36	27.69
K11	4.52	4.88	5.74	6.64	7.34	8.68	10.19	12.2	16.3
K10	7.78	9.44	11.01	12.75	NA	NA	NA	NA	NA
K9	4.48	4.83	5.28	5.93	7.36	8.86	10.13	12.23	NA
K8	2.8	2.8	2.92	2.84	3.18	3.6	3.82	4.05	NA
K7	5.34	5.96	7.01	7.8	8.6	9.95	11.22	12.04	NA
K6	NA	NA	NA	NA	NA	NA	NA	NA	NA
K5	NA	NA	NA	NA	NA	NA	NA	NA	NA
K4	4.62	5.3	6.45	7.6	10.07	NA	NA	NA	NA
K3	NA	NA	NA	NA	NA	NA	NA	NA	NA
K2	4.78	4.64	5.22	5.29	5.61	5.73	5.97	NA	NA
K1	5	6.39	8.99	11.71	14.81	18.13	22.45	NA	NA
J11	NA	NA	NA	NA	NA	NA	NA	NA	NA
J10	9.42	11.76	13.93	16.75	NA	NA	NA	NA	NA
J9	4.36	5.26	6.17	NA	NA	NA	NA	NA	NA
J8	5.94	6.73	7	NA	NA	NA	NA	NA	NA
J7	7.36	9.99	12.15	13.87	16.21	18.71	NA	NA	NA
J6	NA	NA	NA	NA	NA	NA	NA	NA	NA
J5	NA	NA	NA	NA	NA	NA	NA	NA	NA
J4	NA	NA	NA	NA	NA	NA	NA	NA	NA
J3	NA	NA	NA	NA	NA	NA	NA	NA	NA
J2	1.97	1.97	1.99	2.03	2.02	2.16	2.53	2.53	NA
J1	NA	NA	NA	NA	NA	NA	NA	NA	NA

Table 113. SQS results when the quorum is varied at increments of 0.1 for Mammaliaformes at 10 million year (top) and Stage (bottom) time bin intervals.

10 myr Quorum level	0.1	0.2	0.3	0.4	0.5	0.6	0.7	0.8	0.9
K8	3.52	3.72	4.5	5.27	6.33	9.32	13.13	20.11	40.88
K7	4.7	5.77	7.41	11	15.16	23.43	36.67	57.96	NA
K6	4.02	4.86	6.68	9.71	NA	NA	NA	NA	NA
K5	3.73	4.11	4.69	5.66	7.29	NA	NA	NA	NA
K4	5.26	6.01	7.73	11.08	16.35	NA	NA	NA	NA
K3	2.9	2.87	3.14	3.51	3.99	5.04	7.01	11.02	NA
K2	3.27	3.29	3.76	4.23	5.19	7.02	9.35	13.24	NA
K1	2.6	2.67	3	3.46	4.09	5.16	7.14	10.16	NA
J6	2.76	2.89	3.11	3.38	3.78	4.63	5.67	7.83	14.26
J5	5.09	5.6	7.12	9.05	10.88	NA	NA	NA	NA
J4	NA	NA	NA	NA	NA	NA	NA	NA	NA
J3	NA	NA	NA	NA	NA	NA	NA	NA	NA
J2	NA	NA	NA	NA	NA	NA	NA	NA	NA
J1	3.28	3.25	3.69	4.13	4.56	5.48	6.3	7.66	NA

Stage Quorum level	0.1	0.2	0.3	0.4	0.5	0.6	0.7	0.8	0.9
K12	3.44	3.86	4.25	5.2	6.57	8.92	13.2	20.17	41.51
K11	3.38	3.51	3.96	4.67	5.91	7.76	10.51	14.16	NA
K10	3.87	4.57	5.97	NA	NA	NA	NA	NA	NA
K9	2.49	2.48	2.54	2.5	2.73	NA	NA	NA	NA
K8	NA	NA	NA	NA	NA	NA	NA	NA	NA
K7	1	1	1	1	1	1	1	1	1
K6	3.89	4.03	4.85	5.74	7.26	NA	NA	NA	NA
K5	3.73	3.75	3.83	NA	NA	NA	NA	NA	NA
K4	3.48	3.52	4.07	4.56	5.66	7.49	10.13	NA	NA
K3	1.25	1.26	1.23	1.27	1.24	1.25	1.74	1.73	1.74
K2	2.74	2.65	2.89	2.98	3.38	4.22	4.8	5.61	NA
K1	2.13	2.28	2.32	2.48	2.91	3.5	4.27	5.68	NA
J11	2.94	2.93	3.36	3.78	4.41	5.54	7.36	9.02	NA
J10	3.18	3.16	3.4	3.82	4.11	4.93	6.06	8.19	NA
J9	NA	NA	NA	NA	NA	NA	NA	NA	NA
J8	2.35	2.29	2.24	2.25	2.62	2.91	3.27	3.52	NA
J7	NA	NA	NA	NA	NA	NA	NA	NA	NA
J6	NA	NA	NA	NA	NA	NA	NA	NA	NA
J5	NA	NA	NA	NA	NA	NA	NA	NA	NA
J4	NA	NA	NA	NA	NA	NA	NA	NA	NA
J3	NA	NA	NA	NA	NA	NA	NA	NA	NA
J2	2.31	2.25	2.24	2.23	2.51	2.9	3.2	NA	NA
J1	NA	NA	NA	NA	NA	NA	NA	NA	NA

Table 114. SQS results when the quorum is varied at increments of 0.1 for Ornithischia at 10 million year (top) and Stage (bottom) time bin intervals.

10 myr Quorum level	0.1	0.2	0.3	0.4	0.5	0.6	0.7	0.8	0.9
K8	2.12	2.15	2.12	2.32	2.68	3.2	4.11	NA	NA
K7	2.96	3.03	3.55	4.27	5.23	6.95	NA	NA	NA
K6	2.04	2.02	2.01	2.2	2.41	2.88	3.56	4.28	NA
K5	3.12	3.12	3.39	3.63	3.9	4.49	4.89	NA	NA
K4	3.28	3.48	4.03	4.29	5.29	7.16	10.6	NA	NA
K3	8.21	11.81	17.01	NA	NA	NA	NA	NA	NA
K2	2.08	2.09	2.13	2.09	2.32	2.69	3.11	NA	NA
K1	5.46	5.94	6.77	NA	NA	NA	NA	NA	NA
J6	3.26	3.3	3.64	4.59	5.42	7.68	10.82	NA	NA
J5	NA	NA	NA	NA	NA	NA	NA	NA	NA
J4	1.08	1.09	1.1	1.07	1.09	1.1	1.16	1.17	1.58
J3	1.48	1.46	1.47	1.45	1.47	1.55	1.82	1.87	2.29
J2	NA	NA	NA	NA	NA	NA	NA	NA	NA
J1	2.37	2.36	2.34	2.32	2.35	NA	NA	NA	NA

Stage Quorum level	0.1	0.2	0.3	0.4	0.5	0.6	0.7	0.8	0.9
K12	2.12	2.18	2.13	2.3	2.64	3.2	4.01	NA	NA
K11	1	1	1	1	1	1	1	1	1
K10	2.35	2.33	2.33	2.29	2.29	NA	NA	NA	NA
K9	NA	NA	NA	NA	NA	NA	NA	NA	NA
K8	NA	NA	NA	NA	NA	NA	NA	NA	NA
K7	NA	NA	NA	NA	NA	NA	NA	NA	NA
K6	3.04	3.07	3.75	4.07	4.86	5.7	6.5	7.13	NA
K5	2.99	2.91	2.98	3.69	NA	NA	NA	NA	NA
K4	3.2	3.1	3.1	3.36	NA	NA	NA	NA	NA
K3	1	1	1	1	1	1	1	1	1
K2	NA	NA	NA	NA	NA	NA	NA	NA	NA
K1	3.66	3.66	3.73	NA	NA	NA	NA	NA	NA
J11	2.84	2.74	3.05	3.43	3.81	4.96	7.55	NA	NA
J10	3.59	3.72	4.1	5	5.74	6.81	7.96	NA	NA
J9	NA	NA	NA	NA	NA	NA	NA	NA	NA
J8	NA	NA	NA	NA	NA	NA	NA	NA	NA
J7	1.1	1.1	1.1	1.09	1.09	1.09	1.17	1.19	1.58
J6	NA	NA	NA	NA	NA	NA	NA	NA	NA
J5	NA	NA	NA	NA	NA	NA	NA	NA	NA
J4	1.46	1.46	1.47	1.48	1.46	1.55	1.82	1.9	2.27
J3	NA	NA	NA	NA	NA	NA	NA	NA	NA
J2	NA	NA	NA	NA	NA	NA	NA	NA	NA
J1	NA	NA	NA	NA	NA	NA	NA	NA	NA

Table 115. SQS results when the quorum is varied at increments of 0.1 for Pterosauria at 10 million year (top) and Stage (bottom) time bin intervals.

10 myr Quorum level	0.1	0.2	0.3	0.4	0.5	0.6	0.7	0.8	0.9
K8	2.79	2.76	2.97	3.26	3.87	4.95	6.96	10.54	NA
K7	5.28	5.89	7.07	8.75	10.18	NA	NA	NA	NA
K6	7.58	11.03	NA	NA	NA	NA	NA	NA	NA
K5	3.24	3.26	3.74	4.57	5.45	NA	NA	NA	NA
K4	4.3	4.86	5.87	NA	NA	NA	NA	NA	NA
K3	3.44	3.45	3.76	4.22	5.03	6.08	NA	NA	NA
K2	5.31	5.26	6.03	6.11	NA	NA	NA	NA	NA
K1	3.54	3.56	NA	NA	NA	NA	NA	NA	NA
J6	3.14	3.19	3.51	3.79	4.34	5.33	6.74	8.94	14.24
J5	4.62	5.01	6.13	7.77	10.27	NA	NA	NA	NA
J4	1.53	1.59	1.53	1.57	1.56	1.73	2.18	3.4	NA
J3	NA	NA	NA	NA	NA	NA	NA	NA	NA
J2	NA	NA	NA	NA	NA	NA	NA	NA	NA
J1	2.51	2.52	2.74	3.09	3.47	4.5	6.98	12.89	NA

Stage Quorum level	0.1	0.2	0.3	0.4	0.5	0.6	0.7	0.8	0.9
K12	2.75	2.81	2.91	3.38	3.92	5.09	6.94	10.42	NA
K11	NA	NA	NA	NA	NA	NA	NA	NA	NA
K10	NA	NA	NA	NA	NA	NA	NA	NA	NA
K9	NA	NA	NA	NA	NA	NA	NA	NA	NA
K8	NA	NA	NA	NA	NA	NA	NA	NA	NA
K7	NA	NA	NA	NA	NA	NA	NA	NA	NA
K6	1.97	1.99	2.02	2.01	2.04	NA	NA	NA	NA
K5	NA	NA	NA	NA	NA	NA	NA	NA	NA
K4	3.55	3.57	3.58	3.88	3.97	NA	NA	NA	NA
K3	NA	NA	NA	NA	NA	NA	NA	NA	NA
K2	1.47	1.5	1.48	1.51	1.54	1.46	NA	NA	NA
K1	NA	NA	NA	NA	NA	NA	NA	NA	NA
J11	2.96	3.03	3.34	4.05	4.87	6.08	7.89	10.04	14.95
J10	4.22	4.46	4.67	5.41	5.83	7.06	8.61	11.76	NA
J9	3.11	3	3.12	3.6	4.12	5.14	NA	NA	NA
J8	3.57	3.55	4.01	4.74	NA	NA	NA	NA	NA
J7	1.45	1.48	1.46	1.44	1.43	1.54	1.82	2.51	NA
J6	NA	NA	NA	NA	NA	NA	NA	NA	NA
J5	NA	NA	NA	NA	NA	NA	NA	NA	NA
J4	NA	NA	NA	NA	NA	NA	NA	NA	NA
J3	NA	NA	NA	NA	NA	NA	NA	NA	NA
J2	1.82	1.82	1.85	1.85	1.97	2.19	2.59	3.07	4.78
J1	3.02	3.12	3.2	3.8	4.1	4.65	NA	NA	NA

Table 116. SQS results when the quorum is varied at increments of 0.1 for Sauropodomorpha at 10 million year (top) and Stage (bottom) time bin intervals.

10 myr Quorum level	0.1	0.2	0.3	0.4	0.5	0.6	0.7	0.8	0.9
K8	3.62	3.53	3.96	4.44	5.11	6.25	7.86	8.73	NA
K7	3.17	3.29	3.57	4.07	4.68	5.92	7.32	NA	NA
K6	3.05	3.32	4.02	5.03	6.34	8.88	NA	NA	NA
K5	2.76	2.77	3.01	3.22	3.58	4.34	5.2	NA	NA
K4	3.35	3.36	4.22	4.66	5.29	NA	NA	NA	NA
K3	2.15	2.17	2.12	2.62	2.87	3.61	3.85	NA	NA
K2	2.48	2.47	2.49	2.49	2.74	NA	NA	NA	NA
K1	2.2	2.12	2.19	2.24	2.49	3.12	3.69	4.41	NA
J6	2.01	1.93	2.11	2.07	2.26	2.76	3.4	9.28	7.03
J5	3.48	3.5	3.93	4.45	4.99	6.18	7.37	NA	NA
J4	2.36	2.37	2.3	2.32	2.37	NA	NA	7.11	NA
J3	2.93	2.93	3.04	3.39	4.02	4.74	5.68	NA	NA
J2	NA	NA	NA	NA	NA	NA	NA	NA	NA
J1	3.27	3.33	3.81	4.42	5.08	6.49	8.31	NA	NA

Stage Quorum level	0.1	0.2	0.3	0.4	0.5	0.6	0.7	0.8	0.9
K12	3.6	3.56	4.08	4.45	5.17	6.22	7.94	NA	NA
K11	NA	NA	NA	NA	NA	NA	NA	NA	NA
K10	3.05	2.91	3	3.21	NA	NA	NA	NA	NA
K9	NA	NA	NA	NA	NA	NA	NA	NA	NA
K8	NA	NA	NA	NA	NA	NA	NA	NA	NA
K7	NA	NA	NA	NA	NA	NA	NA	NA	NA
K6	2.66	2.68	2.67	2.68	NA	NA	NA	NA	NA
K5	NA	NA	NA	NA	NA	NA	NA	NA	NA
K4	NA	NA	NA	NA	NA	NA	NA	NA	NA
K3	NA	NA	NA	NA	NA	NA	NA	NA	NA
K2	1.31	1.3	1.31	1.33	1.33	1.32	1.48	1.51	NA
K1	NA	NA	NA	NA	NA	NA	NA	NA	NA
J11	2.27	2.22	2.25	2.34	2.67	3.11	4.05	5.75	NA
J10	2.13	2.1	2.04	2.18	2.32	2.61	3.18	3.6	4.58
J9	3.22	3.24	3.37	3.73	4	4.68	5.61	6.58	NA
J8	3.32	3.3	3.53	3.81	4.3	5.03	5.84	7.08	9.91
J7	1	1	1	1	1	1	1	1	1
J6	NA	NA	NA	NA	NA	NA	NA	NA	NA
J5	NA	NA	NA	NA	NA	NA	NA	NA	NA
J4	2.89	2.87	3.01	3.36	3.73	4.55	5.89	NA	NA
J3	NA	NA	NA	NA	NA	NA	NA	NA	NA
J2	2.52	2.65	2.55	2.8	2.99	3.47	NA	NA	NA
J1	3.03	3.03	3.64	4.29	4.81	5.92	NA	NA	NA

Table 117. SQS results when the quorum is varied at increments of 0.1 for Sauropterygia at 10 million year (top) and Stage (bottom) time bin intervals.

10 myr Quorum level	0.1	0.2	0.3	0.4	0.5	0.6	0.7	0.8	0.9
K8	4.29	4.77	5.88	7.18	8.65	12.83	18.79	29.47	NA
K7	3.72	3.91	4.32	5.03	5.76	7.39	9.38	13.09	21.35
K6	5.93	6.48	8.29	9.93	11.79	15.64	NA	NA	NA
K5	3.59	3.59	4.37	4.83	5.68	NA	NA	NA	NA
K4	4.73	5.33	6.64	8.22	10.05	13.08	NA	NA	NA
K3	8.66	NA	NA	NA	NA	NA	NA	NA	NA
K2	5.83	6.67	7.93	8.96	10.38	NA	NA	NA	NA
K1	3.6	3.75	4.22	4.55	5.41	6.39	8.29	11.48	NA
J6	3.06	3.12	3.38	3.83	4.35	5.64	7.17	8.96	13.89
J5	1.88	1.86	1.86	1.87	2.04	2.48	3.36	4.29	NA
J4	NA	NA	NA	NA	NA	NA	NA	NA	NA
J3	NA	NA	NA	NA	NA	NA	NA	NA	NA
J2	NA	NA	NA	NA	NA	NA	NA	NA	NA
J1	NA	NA	NA	NA	NA	NA	NA	NA	NA

Stage Quorum level	0.1	0.2	0.3	0.4	0.5	0.6	0.7	0.8	0.9
K12	4.26	5	5.67	6.86	8.54	12.49	18.59	29.67	NA
K11	3.02	3.02	3.03	3.3	3.45	3.95	4.53	5.11	6.82
K10	6.38	7.43	8.44	9.63	NA	NA	NA	NA	NA
K9	NA	NA	NA	NA	NA	NA	NA	NA	NA
K8	NA	NA	NA	NA	NA	NA	NA	NA	NA
K7	NA	NA	NA	NA	NA	NA	NA	NA	NA
K6	3.51	3.5	4.39	5.28	6.24	NA	NA	NA	NA
K5	NA	NA	NA	NA	NA	NA	NA	NA	NA
K4	5.06	5.06	NA	NA	NA	NA	NA	NA	NA
K3	2.39	2.42	2.42	2.42	2.43	NA	NA	NA	NA
K2	4.58	4.79	5.86	6.49	NA	NA	NA	NA	NA
K1	2.73	2.75	2.94	3.06	3.61	4.33	5.2	6.69	NA
J11	3.62	3.68	4.18	4.52	5.3	6.2	7.87	9.76	13.21
J10	3.41	3.45	3.71	4.39	4.91	5.86	7.1	8.15	10.75
J9	1.87	1.85	1.91	1.88	1.96	2.22	2.56	NA	NA
J8	1.87	1.85	1.84	1.84	1.78	2.08	2.53	2.59	NA
J7	NA	NA	NA	NA	NA	NA	NA	NA	NA
J6	NA	NA	NA	NA	NA	NA	NA	NA	NA
J5	NA	NA	NA	NA	NA	NA	NA	NA	NA
J4	NA	NA	NA	NA	NA	NA	NA	NA	NA
J3	NA	NA	NA	NA	NA	NA	NA	NA	NA
J2	NA	NA	NA	NA	NA	NA	NA	NA	NA
J1	NA	NA	NA	NA	NA	NA	NA	NA	NA

Table 118. SQS results when the quorum is varied at increments of 0.1 for Testudines at 10 million year (top) and Stage (bottom) time bin intervals.

10 myr Quorum level	0.1	0.2	0.3	0.4	0.5	0.6	0.7	0.8	0.9
K8	4.76	5.38	6.51	8	10.29	13.89	19.21	32.72	NA
K7	4.7	5.54	6.57	7.69	9.5	12.25	18.26	29.49	NA
K6	6.63	7.74	10.76	15.23	NA	NA	NA	NA	NA
K5	4.56	5.19	6.22	7.24	8.84	11.89	NA	NA	NA
K4	3.37	3.62	4.08	4.81	6.33	8.61	12.07	NA	NA
K3	4.97	6.34	7.7	10.32	14.3	18.51	NA	NA	NA
K2	8.18	10.45	12.78	15.41	17.96	NA	NA	NA	NA
K1	2.77	2.72	2.85	3.24	3.59	4.52	5.71	6.87	NA
J6	2.35	2.33	2.58	2.67	3.16	4.1	5.62	8.27	15.79
J5	4.49	5.18	6.27	8.27	11.9	NA	NA	NA	NA
J4	2.18	2.14	2.17	2.3	2.57	3.17	5.27	NA	NA
J3	NA	NA	NA	NA	NA	NA	NA	NA	NA
J2	NA	NA	NA	NA	NA	NA	NA	NA	NA
J1	2.43	2.46	2.63	2.7	3.03	3.52	4.26	5.02	6.38

Stage Quorum level	0.1	0.2	0.3	0.4	0.5	0.6	0.7	0.8	0.9
K12	4.79	5.31	6.65	7.89	10.08	13.54	19.9	32.41	NA
K11	3.19	3.2	3.36	3.59	3.92	4.57	5.32	6.26	9.14
K10	7.22	NA	NA	NA	NA	NA	NA	NA	NA
K9	2.02	2.01	1.98	2.02	1.97	2.44	NA	NA	NA
K8	NA	NA	NA	NA	NA	NA	NA	NA	NA
K7	NA	NA	NA	NA	NA	NA	NA	NA	NA
K6	2.57	2.64	2.7	2.9	3.46	NA	NA	NA	NA
K5	3.18	3.2	3.09	3.18	NA	NA	NA	NA	NA
K4	11.81	15.01	NA	NA	NA	NA	NA	NA	NA
K3	NA	NA	NA	NA	NA	NA	NA	NA	NA
K2	3	2.97	3.03	3.01	NA	NA	NA	NA	NA
K1	1.4	1.38	1.41	1.44	1.45	1.59	1.96	2.2	2.74
J11	4.75	5.11	5.64	6.76	8.11	10.58	13.27	NA	NA
J10	2.78	2.63	3.04	3.42	3.99	4.9	6.63	8.98	NA
J9	4	4.26	5.2	5.91	6.89	NA	NA	NA	NA
J8	4.2	4.09	4.86	6.11	NA	NA	NA	NA	NA
J7	2.02	2.04	1.99	2.03	2.32	2.83	4.43	NA	NA
J6	2.03	1.96	1.98	2.02	2.01	2.03	NA	NA	NA
J5	NA	NA	NA	NA	NA	NA	NA	NA	NA
J4	NA	NA	NA	NA	NA	NA	NA	NA	NA
J3	NA	NA	NA	NA	NA	NA	NA	NA	NA
J2	1.79	1.83	1.8	1.8	1.78	2.1	2.5	2.88	NA
J1	2.5	2.53	2.5	2.48	NA	NA	NA	NA	NA

Table 119. SQS results when the quorum is varied at increments of 0.1 for Theropoda at 10 million year (top) and Stage (bottom) time bin intervals.

Appendix 10 – Full model-fitting results for all tetrapod groups and extrinsic parameters including sampling proxies and environmental factors.

Genus diversity	AICc		Spearman's rank			Pearson's PMCC		
	Likelihood	Weight	rho	p-value	adjusted p-value	r	p-value	adjusted p-value
Non-marine area	67.763	0.166	0.393	0.396	0.56025	**0.655**	0.110	0.330
Sea-level (Miller)	70.450	0.043	-0.357	0.444	0.56025	-0.403	0.370	0.550
Oxygen	67.453	0.193	**0.679**	0.110	0.495	**0.674**	0.097	0.330
Carbon	**66.341**	**0.337**	0.071	0.906	0.906	**0.731**	0.062	0.330
Strontium	71.600	0.024	0.321	0.498	0.560	0.113	0.809	0.942
Sulphur	68.968	0.091	-0.393	0.396	0.560	**-0.568**	0.184	0.331
Sea-surface temp.	68.796	0.099	**-0.739**	0.058	0.495	**-0.582**	0.171	0.331
TBF	71.682	0.023	0.393	0.396	0.560	0.034	0.942	0.942
TBC	71.635	0.024	**0.571**	0.200	0.560	0.088	0.850	0.942

SQS diversity	AICc		Spearman's rank			Pearson's PMCC		
	Likelihood	Weight	rho	p-value	adjusted p-value	r	p-value	adjusted p-value
Non-marine area	62.550	0.224	0.393	0.396	0.554	**0.705**	0.077	0.254
Sea-level (Miller)	66.630	0.029	-0.393	0.396	0.554	-0.316	0.491	0.573
Oxygen	64.086	0.104	**0.857**	**0.024**	0.168	**0.612**	0.145	0.254
Carbon	**61.135**	**0.455**	-0.107	0.840	0.840	**0.768**	**0.044**	0.254
Strontium	67.127	0.023	0.143	0.783	0.840	-0.183	0.695	0.695
Sulphur	63.655	0.129	**-0.571**	0.200	0.467	**-0.641**	0.121	0.254
Sea-surface temp.	66.256	0.035	**-0.739**	0.058	0.203	-0.383	0.397	0.556

Table 120. Model fitting results for raw taxonomic diversity and subsampled diversity for Aves at the genus level.

Genus diversity	AICc		Spearman's rank			Pearson's PMCC		
	Likelihood	Weight	rho	p-value	adjusted p-value	r	p-value	adjusted p-value
Non-marine area	-3.643	0.000	NA	NA	NA	**0.933**	0.235	0.470
Sea-level (Miller)	-7.717	0.000	NA	NA	NA	**-0.983**	0.117	0.470
Oxygen	-4.012	0.000	NA	NA	NA	**0.941**	0.220	0.470
Carbon	1.707	0.000	NA	NA	NA	-0.477	0.684	0.684
Strontium	0.169	0.000	NA	NA	NA	**0.733**	0.476	0.595
Sulphur	-0.996	0.000	NA	NA	NA	**-0.828**	0.379	0.577
SQS diversity	-4.504	0.000	NA	NA	NA	**0.950**	0.202	0.470
Sea-surface temp.	0.963	0.000	NA	NA	NA	**-0.630**	0.566	0.629
MBF	**-26.260**	**1.000**	NA	NA	NA	**1.000**	**0.005**	**0.050**
MBC	-0.660	0.000	NA	NA	NA	**0.806**	0.404	0.577

SQS diversity	AICc		Spearman's rank			Pearson's PMCC		
	Likelihood	Weight	rho	p-value	adjusted p-value	r	p-value	adjusted p-value
Non-marine area	-12.265	0.037	NA	NA	NA	-0.165	0.895	0.895
Sea-level (Miller)	-12.283	0.037	NA	NA	NA	-0.182	0.883	0.895
Oxygen	**-17.425**	**0.483**	NA	NA	NA	**-0.909**	0.274	0.895
Carbon	-12.494	0.041	NA	NA	NA	-0.314	0.797	0.895
Strontium	-13.149	0.057	NA	NA	NA	**-0.525**	0.648	0.895
Sulphur	-15.044	0.147	NA	NA	NA	**-0.784**	0.426	0.895
SQS diversity	-15.123	0.153	NA	NA	NA	**-0.790**	0.420	0.895
Sea-surface temp.	-12.670	0.045	NA	NA	NA	0.388	0.747	0.895

Table 121. Model fitting results for raw taxonomic diversity and subsampled diversity for Chelonioidea at the genus level.

Genus diversity	AICc		Spearman's rank			Pearson's PMCC		
	Likelihood	Weight	rho	p-value	adjusted p-value	r	p-value	adjusted p-value
Non-marine area	-8.356	0.145	NA	NA	NA	**0.904**	0.281	0.930
Sea-level (Miller)	-3.248	0.011	NA	NA	NA	0.004	0.998	0.930
Oxygen	-4.007	0.016	NA	NA	NA	0.473	0.686	0.930
Carbon	-6.192	0.049	NA	NA	NA	**0.791**	0.419	0.930
Strontium	-6.106	0.047	NA	NA	NA	**-0.784**	0.427	0.930
Sulphur	**-11.476**	**0.689**	NA	NA	NA	**-0.967**	0.163	0.930
Sea-surface temp.	-4.111	0.017	NA	NA	NA	**0.500**	0.667	0.930
TBF	-3.511	0.013	NA	NA	NA	-0.290	0.813	0.930
TBC	-3.472	0.013	NA	NA	NA	-0.268	0.827	0.930

SQS diversity	AICc		Spearman's rank			Pearson's PMCC		
	Likelihood	Weight	rho	p-value	adjusted p-value	r	p-value	adjusted p-value
Non-marine area	-17.538	0.000	NA	NA	NA	**0.984**	0.114	0.399
Sea-level (Miller)	-7.391	0.000	NA	NA	NA	-0.255	0.836	0.836
Oxygen	-9.088	0.000	NA	NA	NA	**0.685**	0.520	0.684
Carbon	-8.558	0.000	NA	NA	NA	**0.605**	0.586	0.684
Strontium	-12.732	0.000	NA	NA	NA	**-0.918**	0.260	0.607
Sulphur	**-38.622**	**1.000**	NA	NA	NA	**-1.000**	**0.003**	**0.021**
Sea-surface temp.	-9.269	0.000	NA	NA	NA	**0.707**	0.500	0.684

Table 122. Model fitting results for raw taxonomic diversity and subsampled diversity for Choristodera at the genus level.

Genus diversity	AICc		Spearman's rank			Pearson's PMCC		
	Likelihood	Weight	rho	p-value	adjusted p-value	r	p-value	adjusted p-value
Non-marine area	56.179	0.005	0.024	0.977	0.977	-0.076	0.859	0.947
Sea-level (Miller)	52.968	0.027	0.179	0.713	0.977	0.231	0.619	0.884
Oxygen	53.931	0.016	-0.429	0.299	0.748	-0.499	0.208	0.520
Carbon	56.216	0.005	-0.071	0.882	0.977	0.032	0.939	0.947
Strontium	53.360	0.022	**-0.595**	0.132	0.440	**-0.549**	0.159	0.520
Sulphur	55.172	0.009	-0.119	0.793	0.977	-0.351	0.394	0.788
SQS diversity	55.615	0.007	-0.048	0.935	0.977	-0.271	0.516	0.860
Sea-surface temp.	56.218	0.005	0.347	0.399	0.798	-0.028	0.947	0.947
MBF	**47.221**	**0.472**	**0.905**	**0.005**	**0.050**	**0.822**	**0.012**	0.065
MBC	47.406	0.431	**0.762**	**0.037**	0.185	**0.817**	**0.013**	0.065

SQS diversity	AICc		Spearman's rank			Pearson's PMCC		
	Likelihood	Weight	rho	p-value	adjusted p-value	r	p-value	adjusted p-value
Non-marine area	24.390	0.104	-0.452	0.268	0.634	-0.326	0.430	0.678
Sea-level (Miller)	24.208	0.114	0.393	0.396	0.634	0.380	0.400	0.678
Oxygen	**22.741**	**0.237**	**-0.524**	0.197	0.634	**-0.522**	0.184	0.678
Carbon	24.674	0.090	-0.405	0.327	0.634	-0.272	0.514	0.678
Strontium	24.876	0.081	-0.238	0.582	0.776	-0.225	0.593	0.678
Sulphur	25.068	0.074	0.000	1.000	1.000	-0.166	0.695	0.695
SQS diversity	24.362	0.105	-0.071	0.882	1.000	-0.331	0.423	0.678
Sea-surface temp.	23.118	0.196	-0.491	0.217	0.634	-0.488	0.220	0.678

Table 123. Model fitting results for raw taxonomic diversity and subsampled diversity for marine Crocodyliformes at the genus level.

Genus diversity	AICc		Spearman's rank			Pearson's PMCC		
	Likelihood	Weight	rho	p-value	adjusted p-value	r	p-value	adjusted p-value
Non-marine area	95.712	0.016	0.105	0.750	0.750	0.012	0.970	0.970
Sea-level (Miller)	**88.697**	**0.529**	0.345	0.299	0.610	0.156	0.647	0.830
Oxygen	95.228	0.020	-0.175	0.588	0.714	-0.199	0.535	0.830
Carbon	93.662	0.044	**0.552**	0.067	0.603	0.396	0.202	0.830
Strontium	94.686	0.026	-0.252	0.430	0.645	-0.287	0.367	0.830
Sulphur	94.853	0.024	0.343	0.276	0.610	0.263	0.409	0.830
Sea-surface temp.	89.906	0.289	0.303	0.339	0.610	**0.619**	**0.032**	0.288
TBF	95.490	0.018	0.154	0.635	0.714	0.136	0.674	0.830
TBC	95.573	0.017	0.427	0.169	0.610	0.108	0.738	0.830

SQS diversity	AICc		Spearman's rank			Pearson's PMCC		
	Likelihood	Weight	rho	p-value	adjusted p-value	r	p-value	adjusted p-value
Non-marine area	35.785	0.008	-0.358	0.313	0.677	**-0.589**	0.073	0.152
Sea-level (Miller)	**26.285**	**0.969**	**0.750**	**0.025**	0.175	**0.846**	**0.004**	**0.028**
Oxygen	39.235	0.001	-0.030	0.946	0.946	-0.278	0.437	0.612
Carbon	39.565	0.001	0.309	0.387	0.677	0.215	0.551	0.643
Strontium	40.035	0.001	-0.055	0.892	0.946	-0.016	0.965	0.965
Sulphur	35.294	0.011	0.467	0.178	0.623	**0.615**	0.059	0.152
Sea-surface temp.	36.141	0.007	0.043	0.906	0.946	**0.568**	0.087	0.152

Table 124. Model fitting results for raw taxonomic diversity and subsampled diversity for non-marine Crocodyliformes at the genus level.

Genus diversity	AICc		Spearman's rank			Pearson's PMCC		
	Likelihood	Weight	rho	p-value	adjusted p-value	r	p-value	adjusted p-value
Non-marine area	62.204	0.000	0.219	0.517	0.989	0.141	0.679	0.860
Sea-level (Miller)	51.632	0.065	0.349	0.396	0.989	0.122	0.774	0.860
Oxygen	61.974	0.000	0.027	0.936	0.989	-0.200	0.555	0.860
Carbon	62.397	0.000	0.205	0.544	0.989	0.050	0.883	0.883
Strontium	62.120	0.000	0.005	0.989	0.989	-0.166	0.627	0.860
Sulphur	61.761	0.000	-0.105	0.759	0.989	-0.242	0.473	0.860
SQS diversity	61.909	0.000	0.005	0.989	0.989	-0.214	0.527	0.860
Sea-surface temp.	62.241	0.000	-0.060	0.861	0.989	-0.129	0.706	0.860
MBF	54.881	0.013	**0.534**	0.090	0.450	**0.705**	**0.015**	0.075
MBC	**46.330**	**0.920**	**0.676**	**0.022**	0.220	**0.877**	**0.000**	0.040

SQS diversity	AICc		Spearman's rank			Pearson's PMCC		
	Likelihood	Weight	rho	p-value	adjusted p-value	r	p-value	adjusted p-value
Non-marine area	24.673	0.082	-0.091	0.811	0.906	-0.184	0.610	0.962
Sea-level (Miller)	26.646	0.031	0.071	0.906	0.906	0.054	0.909	0.962
Oxygen	25.016	0.069	0.139	0.707	0.906	-0.017	0.962	0.962
Carbon	23.354	0.158	-0.127	0.733	0.906	-0.392	0.263	0.962
Strontium	24.686	0.081	-0.236	0.514	0.906	-0.181	0.617	0.962
Sulphur	25.002	0.069	0.224	0.537	0.906	0.041	0.910	0.962
SQS diversity	**21.403**	**0.420**	-0.370	0.296	0.906	**-0.551**	0.099	0.792
Sea-surface temp.	24.479	0.090	-0.317	0.372	0.906	-0.229	0.524	0.962

Table 125. Model fitting results for raw taxonomic diversity and subsampled diversity for Ichthyosauria at the genus level.

Genus diversity	AICc		Spearman's rank			Pearson's PMCC		
	Likelihood	Weight	rho	p-value	adjusted p-value	r	p-value	adjusted p-value
Non-marine area	122.161	0.000	-0.020	0.952	0.952	-0.406	0.150	0.270
Sea-level (Miller)	**101.473**	**0.915**	0.400	0.225	0.405	0.244	0.471	0.672
Oxygen	124.654	0.000	-0.095	0.750	0.844	-0.041	0.891	0.891
Carbon	124.413	0.000	0.130	0.660	0.844	0.137	0.641	0.721
Strontium	120.722	0.000	0.398	0.160	0.405	0.496	0.071	0.213
Sulphur	124.182	0.000	0.178	0.542	0.813	0.186	0.523	0.672
Sea-surface temp.	121.820	0.000	**-0.601**	**0.023**	**0.207**	-0.430	0.125	0.270
TBF	114.558	0.001	0.380	0.181	0.405	**0.717**	**0.004**	**0.017**
TBC	106.252	0.084	0.442	0.116	0.405	**0.855**	**0.000**	**0.001**

SQS diversity	AICc		Spearman's rank			Pearson's PMCC		
	Likelihood	Weight	rho	p-value	adjusted p-value	r	p-value	adjusted p-value
Non-marine area	48.369	0.114	**-0.650**	0.067	0.469	**-0.530**	0.142	0.850
Sea-level (Miller)	44.663	**0.727**	0.214	0.662	0.912	0.089	0.850	0.850
Oxygen	50.885	0.032	0.117	0.776	0.912	0.222	0.565	0.850
Carbon	51.291	0.026	0.117	0.776	0.912	-0.075	0.848	0.850
Strontium	50.990	0.031	0.067	0.880	0.912	0.196	0.614	0.850
Sulphur	51.158	0.028	-0.050	0.912	0.912	0.142	0.716	0.850
Sea-surface temp.	50.396	0.041	-0.477	0.194	0.679	-0.316	0.408	0.850

Table 126. Model fitting results for raw taxonomic diversity and subsampled diversity for non-marine Lepidosauria at the genus level.

Genus diversity	AICc		Spearman's rank			Pearson's PMCC		
	Likelihood	Weight	rho	p-value	adjusted p-value	r	p-value	adjusted p-value
Non-marine area	1.851	0.096	-0.112	0.733	1.000	-0.223	0.485	0.847
Sea-level (Miller)	0.988	0.148	-0.182	0.595	1.000	-0.162	0.634	0.847
Oxygen	2.434	0.072	0.000	1.000	1.000	-0.050	0.877	0.877
Carbon	2.400	0.073	0.084	0.800	1.000	0.074	0.820	0.877
Strontium	2.144	0.083	-0.147	0.651	1.000	-0.162	0.614	0.847
Sulphur	**0.331**	**0.206**	0.483	0.115	1.000	0.404	0.193	0.847
Sea-surface temp.	1.366	0.123	-0.028	0.931	1.000	0.296	0.351	0.847
TBF	1.426	0.119	0.322	0.308	1.000	0.288	0.364	0.847
TBC	2.218	0.080	0.301	0.343	1.000	0.143	0.659	0.847

SQS diversity	AICc		Spearman's rank			Pearson's PMCC		
	Likelihood	Weight	rho	p-value	adjusted p-value	r	p-value	adjusted p-value
Non-marine area	43.344	0.063	0.317	0.410	0.810	0.457	0.216	0.756
Sea-level (Miller)	44.298	0.039	-0.150	0.708	0.810	-0.347	0.360	0.788
Oxygen	**38.260**	**0.796**	**0.700**	**0.043**	0.301	**0.742**	**0.022**	0.154
Carbon	44.994	0.027	-0.100	0.810	0.810	-0.224	0.563	0.788
Strontium	44.811	0.030	-0.100	0.810	0.810	-0.263	0.495	0.788
Sulphur	45.447	0.022	0.133	0.744	0.810	-0.029	0.940	0.940
Sea-surface temp.	45.332	0.023	0.102	0.795	0.810	0.116	0.766	0.894

Table 127. Model fitting results for raw taxonomic diversity and subsampled diversity for Lissamphibia at the genus level.

Genus diversity	AICc		Spearman's rank			Pearson's PMCC		
	Likelihood	Weight	rho	p-value	adjusted p-value	r	p-value	adjusted p-value
Non-marine area	10.913	0.005	-0.341	0.233	0.374	-0.298	0.301	0.677
Sea-level (Miller)	6.766	0.038	0.327	0.327	0.374	0.121	0.722	0.812
Oxygen	7.959	0.021	**-0.587**	**0.030**	**0.135**	**-0.512**	0.061	0.183
Carbon	11.609	0.003	0.327	0.253	0.374	0.205	0.481	0.722
Strontium	11.542	0.004	0.257	0.374	0.374	0.216	0.458	0.722
Sulphur	11.938	0.003	0.257	0.374	0.374	0.139	0.635	0.812
Sea-surface temp.	11.914	0.003	-0.325	0.257	0.374	0.036	0.902	0.902
TBF	**0.597**	**0.836**	**0.596**	**0.028**	0.135	**0.751**	**0.002**	**0.018**
TBC	5.114	0.087	0.451	0.108	0.324	**0.631**	**0.016**	0.072

SQS diversity	AICc		Spearman's rank			Pearson's PMCC		
	Likelihood	Weight	rho	p-value	adjusted p-value	r	p-value	adjusted p-value
Non-marine area	61.508	0.006	**-0.527**	0.123	0.431	-0.187	0.605	0.671
Sea-level (Miller)	**51.394**	**0.931**	-0.450	0.230	0.537	**-0.666**	**0.050**	0.301
Oxygen	61.416	0.006	0.261	0.470	0.658	0.209	0.562	0.671
Carbon	57.946	0.035	-0.358	0.313	0.548	**-0.569**	0.086	0.301
Strontium	61.533	0.006	-0.091	0.811	0.811	-0.180	0.618	0.671
Sulphur	61.623	0.006	-0.152	0.682	0.796	-0.154	0.671	0.671
Sea-surface temp.	60.478	0.010	**-0.675**	**0.032**	0.224	-0.360	0.307	0.671

Table 128. Model fitting results for raw taxonomic diversity and subsampled diversity for Mammaliaformes at the genus level.

Genus diversity	AICc		Spearman's rank			Pearson's PMCC		
	Likelihood	Weight	rho	p-value	adjusted p-value	r	p-value	adjusted p-value
Non-marine area	17.268	0.000	0.077	0.817	0.834	-0.107	0.741	0.953
Sea-level (Miller)	10.340	0.001	0.176	0.632	0.834	-0.003	0.992	0.992
Oxygen	16.798	0.000	-0.371	0.237	0.711	-0.222	0.487	0.851
Carbon	16.503	0.000	0.224	0.485	0.834	0.269	0.397	0.851
Strontium	16.448	0.000	0.070	0.834	0.834	0.277	0.383	0.851
Sulphur	17.361	0.000	-0.077	0.817	0.834	-0.061	0.850	0.957
Sea-surface temp.	16.993	0.000	-0.215	0.502	0.834	-0.184	0.567	0.851
TBF	**-4.803**	**0.987**	**0.811**	**0.002**	**0.021**	**0.918**	**0.000**	0.002
TBC	3.982	0.012	**0.720**	**0.011**	**0.050**	**0.821**	**0.001**	0.005

SQS diversity	AICc		Spearman's rank			Pearson's PMCC		
	Likelihood	Weight	rho	p-value	adjusted p-value	r	p-value	adjusted p-value
Non-marine area	62.274	0.132	-0.327	0.327	0.681	-0.401	0.221	0.751
Sea-level (Miller)	**60.106**	**0.391**	0.200	0.584	0.681	0.047	0.898	0.898
Oxygen	61.272	0.218	**-0.509**	0.114	0.613	-0.484	0.132	0.751
Carbon	63.912	0.058	0.191	0.576	0.681	0.163	0.633	0.898
Strontium	64.075	0.054	0.082	0.818	0.818	-0.109	0.749	0.898
Sulphur	64.179	0.051	0.255	0.451	0.681	-0.050	0.884	0.898
Sea-surface temp.	62.942	0.095	0.440	0.175	0.613	0.330	0.322	0.751

Table 129. Model fitting results for raw taxonomic diversity and subsampled diversity for Ornithischia at the genus level.

Genus diversity	AICc		Spearman's rank			Pearson's PMCC		
	Likelihood	Weight	rho	p-value	adjusted p-value	r	p-value	adjusted p-value
Non-marine area	15.578	0.040	0.137	0.656	0.738	0.180	0.556	0.757
Sea-level (Miller)	14.918	0.055	0.200	0.558	0.717	0.115	0.736	0.828
Oxygen	16.004	0.032	-0.011	0.978	0.978	-0.014	0.963	0.963
Carbon	12.841	0.155	0.335	0.263	0.592	0.465	0.109	0.491
Strontium	15.646	0.038	0.181	0.554	0.717	-0.165	0.589	0.757
Sulphur	**10.504**	**0.500**	**-0.500**	0.085	0.455	**-0.587**	**0.035**	0.315
Sea-surface temp.	14.591	0.065	-0.365	0.221	0.592	-0.321	0.285	0.641
TBF	15.315	0.045	0.187	0.541	0.717	0.228	0.455	0.757
TBC	14.418	0.071	0.478	0.101	0.455	0.339	0.257	0.641

SQS diversity	AICc		Spearman's rank			Pearson's PMCC		
	Likelihood	Weight	rho	p-value	adjusted p-value	r	p-value	adjusted p-value
Non-marine area	40.617	0.022	0.188	0.608	0.796	-0.309	0.385	0.594
Sea-level (Miller)	**33.261**	**0.872**	**0.714**	0.058	0.406	**0.647**	0.083	0.581
Oxygen	39.834	0.033	-0.297	0.407	0.796	-0.405	0.246	0.594
Carbon	41.043	0.018	0.152	0.682	0.796	0.237	0.509	0.594
Strontium	40.923	0.019	0.261	0.470	0.796	0.260	0.469	0.594
Sulphur	41.520	0.014	-0.091	0.811	0.811	-0.101	0.782	0.782
Sea-surface temp.	40.515	0.023	-0.285	0.427	0.796	-0.324	0.362	0.594

Table 130. Model fitting results for raw taxonomic diversity and subsampled diversity for Pterosauria at the genus level.

Genus diversity	AICc		Spearman's rank			Pearson's PMCC		
	Likelihood	Weight	rho	p-value	adjusted p-value	r	p-value	adjusted p-value
Non-marine area	11.286	0.047	0.390	0.189	0.819	0.212	0.486	0.875
Sea-level (Miller)	**6.250**	**0.587**	0.364	0.273	0.819	0.248	0.463	0.875
Oxygen	11.770	0.037	-0.093	0.765	0.906	-0.094	0.760	0.977
Carbon	11.641	0.040	0.247	0.415	0.826	0.136	0.657	0.977
Strontium	11.885	0.035	-0.038	0.906	0.906	-0.008	0.979	0.979
Sulphur	11.864	0.035	0.170	0.579	0.869	-0.041	0.894	0.979
Sea-surface temp.	11.277	0.048	-0.061	0.844	0.906	-0.214	0.483	0.875
TBF	11.107	0.052	0.225	0.459	0.826	0.241	0.428	0.875
TBC	9.440	0.119	0.549	0.055	0.495	0.414	0.160	0.875

SQS diversity	AICc		Spearman's rank			Pearson's PMCC		
	Likelihood	Weight	rho	p-value	adjusted p-value	r	p-value	adjusted p-value
Non-marine area	44.139	0.115	-0.283	0.463	0.810	-0.415	0.267	0.564
Sea-level (Miller)	**41.191**	**0.501**	0.310	0.462	0.810	0.457	0.255	0.564
Oxygen	44.841	0.081	0.350	0.359	0.810	0.324	0.395	0.564
Carbon	45.159	0.069	0.050	0.912	0.912	0.270	0.483	0.564
Strontium	44.998	0.075	0.183	0.644	0.902	0.299	0.435	0.564
Sulphur	45.710	0.052	0.050	0.912	0.912	0.119	0.761	0.761
Sea-surface temp.	44.264	0.108	**-0.586**	0.097	0.679	-0.400	0.285	0.564

Table 131. Model fitting results for raw taxonomic diversity and subsampled diversity for Sauropodomorpha at the genus level.

Genus diversity	AICc		Spearman's rank			Pearson's PMCC		
	Likelihood	Weight	rho	p-value	adjusted p-value	r	p-value	adjusted p-value
Non-marine area	8.389	0.0094	0.182	0.532	0.756	0.005	0.986	0.986
Sea-level (Miller)	8.799	0.0077	0.191	0.576	0.756	0.216	0.524	0.986
Oxygen	8.100	0.0109	-0.156	0.594	0.756	-0.143	0.626	0.986
Carbon	7.828	0.0125	0.319	0.267	0.756	0.198	0.497	0.986
Strontium	8.380	0.0095	-0.073	0.808	0.898	0.026	0.930	0.986
Sulphur	8.312	0.0098	0.152	0.605	0.756	0.074	0.802	0.986
SQS diversity	8.386	0.0094	0.011	0.976	0.976	-0.015	0.959	0.986
Sea-surface temp.	7.410	0.0154	0.181	0.535	0.756	0.260	0.370	0.986
MBF	3.624	0.1020	0.464	0.097	0.485	**0.537**	**0.048**	0.240
MBC	**-0.529**	**0.8135**	**0.767**	**0.002**	**0.020**	**0.686**	**0.007**	0.070

SQS diversity	AICc		Spearman's rank			Pearson's PMCC		
	Likelihood	Weight	rho	p-value	adjusted p-value	r	p-value	adjusted p-value
Non-marine area	45.749	0.057	0.159	0.604	0.906	0.004	0.990	0.990
Sea-level (Miller)	**41.820**	**0.409**	0.055	0.882	0.906	0.065	0.850	0.985
Oxygen	45.604	0.062	-0.192	0.529	0.906	-0.105	0.732	0.985
Carbon	45.609	0.061	0.264	0.384	0.906	0.104	0.736	0.985
Strontium	45.711	0.058	0.038	0.906	0.906	0.054	0.862	0.985
Sulphur	45.678	0.059	0.165	0.591	0.906	0.074	0.810	0.985
SQS diversity	45.350	0.070	0.088	0.779	0.906	0.174	0.570	0.985
Sea-surface temp.	43.034	0.223	**0.624**	**0.023**	0.184	0.434	0.138	0.985

Table 132. Model fitting results for raw taxonomic diversity and subsampled diversity for Sauropterygia at the genus level.

Genus diversity	AICc		Spearman's rank			Pearson's PMCC		
	Likelihood	Weight	rho	p-value	adjusted p-value	r	p-value	adjusted p-value
Non-marine area	9.157	0.076	**0.527**	0.123	0.410	0.287	0.421	0.621
Sea-level (Miller)	10.007	0.049	0.067	0.865	0.865	-0.033	0.928	0.928
Oxygen	9.207	0.074	-0.309	0.387	0.639	-0.279	0.435	0.621
Carbon	9.173	0.075	0.224	0.537	0.639	0.285	0.425	0.621
Strontium	9.004	0.082	0.285	0.427	0.639	0.310	0.383	0.621
Sulphur	9.904	0.052	0.224	0.537	0.639	0.106	0.770	0.928
SQS diversity	7.836	0.146	0.467	0.178	0.445	0.443	0.200	0.621
Sea-surface temp.	9.985	0.050	-0.202	0.575	0.639	-0.058	0.874	0.928
TBF	7.301	0.191	**0.600**	0.073	0.410	0.488	0.153	0.621
TBC	**7.167**	**0.205**	**0.564**	0.096	0.410	0.498	0.143	0.621

SQS diversity	AICc		Spearman's rank			Pearson's PMCC		
	Likelihood	Weight	rho	p-value	adjusted p-value	r	p-value	adjusted p-value
Non-marine area	51.961	0.134	0.433	0.250	0.880	0.300	0.432	0.891
Sea-level (Miller)	52.796	0.088	-0.083	0.843	0.880	-0.042	0.915	0.915
Oxygen	52.742	0.091	-0.067	0.880	0.880	-0.088	0.821	0.915
Carbon	52.378	0.109	0.150	0.708	0.880	0.217	0.575	0.891
Strontium	52.558	0.099	0.200	0.613	0.880	0.167	0.668	0.891
Sulphur	52.257	0.115	0.350	0.359	0.880	0.244	0.526	0.891
SQS diversity	52.442	0.105	0.083	0.843	0.880	0.201	0.605	0.891
Sea-surface temp.	**50.648**	**0.258**	0.343	0.366	0.880	0.462	0.210	0.891

Table 133. Model fitting results for raw taxonomic diversity and subsampled diversity for Testudines at the genus level.

Genus diversity	AICc		Spearman's rank			Pearson's PMCC		
	Likelihood	Weight	rho	p-value	adjusted p-value	r	p-value	adjusted p-value
Non-marine area	7.321	0.013	-0.315	0.320	0.497	-0.393	0.206	0.371
Sea-level (Miller)	6.072	0.025	0.418	0.203	0.457	0.450	0.165	0.371
Oxygen	9.335	0.005	0.418	0.203	0.457	0.009	0.978	0.978
Carbon	4.032	0.069	0.385	0.750	0.844	**0.598**	0.040	0.120
Strontium	9.307	0.005	-0.042	0.904	0.904	-0.049	0.880	0.978
Sulphur	9.186	0.005	0.308	0.331	0.497	0.112	0.730	0.978
Sea-surface temp.	9.255	0.005	-0.225	0.481	0.618	-0.082	0.799	0.978
TBF	1.493	0.246	**0.531**	0.079	0.356	**0.693**	**0.013**	0.059
TBC	**-0.372**	**0.626**	**0.790**	**0.004**	**0.036**	**0.745**	**0.005**	**0.045**

SQS diversity	AICc		Spearman's rank			Pearson's PMCC		
	Likelihood	Weight	rho	p-value	adjusted p-value	r	p-value	adjusted p-value
Non-marine area	78.525	0.033	0.021	0.956	0.968	0.019	0.954	0.954
Sea-level (Miller)	**72.931**	**0.534**	-0.018	0.968	0.968	0.037	0.915	0.954
Oxygen	76.875	0.074	0.462	0.134	0.620	0.359	0.252	0.637
Carbon	75.665	0.136	0.420	0.177	0.620	0.461	0.132	0.637
Strontium	77.866	0.045	-0.126	0.700	0.968	-0.232	0.469	0.821
Sulphur	78.408	0.035	0.133	0.683	0.968	0.100	0.757	0.954
Sea-surface temp.	77.011	0.069	0.127	0.695	0.968	0.345	0.273	0.637

Table 134. Model fitting results for raw taxonomic diversity and subsampled diversity for Theropoda at the genus level.

Appendix 11 – Appendix 11 – Spatial diversity (SQSPt, SQSPs, SQSRc, SQSRu) results for subsampled non-marine crocodyliforms (Chapter 4).

Bin	Collections	Raw Genera	Subsampled diversity	Good's u
Maastrichtian	32	6	1.83	0.937
Campanian	NA	NA	NA	NA
Santonian	NA	NA	NA	NA
Coniacian	NA	NA	NA	NA
Turonian	NA	NA	NA	NA
Cenomanian	NA	NA	NA	NA
Albian	2	1	1	1
Aptian	1	1	NA	NA
Barremian	NA	NA	NA	NA
Hauterivian	NA	NA	NA	NA
Valanginian	NA	NA	NA	NA
Berriasian	NA	NA	NA	NA
Tithonian	2	1	1	1
Kimmeridgian	1	1	NA	NA
Oxfordian	NA	NA	NA	NA
Callovian	NA	NA	NA	NA
Bathonian	NA	NA	NA	NA
Bajocian	NA	NA	NA	NA
Aalenian	NA	NA	NA	NA
Toarcian	NA	NA	NA	NA
Pliensbachian	NA	NA	NA	NA
Sinemurian	NA	NA	NA	NA
Hettangian	NA	NA	NA	NA

Table 135. Regional subsampled non-marine crocodyliform diversity (SQSPs) in Africa.

	Asia			
Bin	**Collections**	**Raw genera**	**Subsampled diversity**	**Good's u**
Maastrichtian	14	8	NA	NA
Campanian	NA	NA	4.42	0.733
Santonian	1	2	NA	NA
Coniacian	NA	NA	NA	NA
Turonian	NA	NA	NA	NA
Cenomanian	NA	NA	NA	NA
Albian	NA	NA	NA	NA
Aptian	1	1	NA	NA
Barremian	NA	NA	NA	NA
Hauterivian	NA	NA	NA	NA
Valanginian	NA	NA	NA	NA
Berriasian	NA	NA	NA	NA
Tithonian	3	3	NA	NA
Kimmeridgian	NA	NA	NA	NA
Oxfordian	6	4	NA	NA
Callovian	3	1	2.15	0.571
Bathonian	NA	NA	1	1
Bajocian	NA	NA	NA	NA
Aalenian	NA	NA	NA	NA
Toarcian	NA	NA	NA	NA
Pliensbachian	NA	NA	NA	NA
Sinemurian	5	4	NA	NA
Hettangian	NA	NA	3.07	0.4

Table 136. Regional subsampled non-marine crocodyliform diversity (SQSPs) in Asia.

	Europe			
Bin	**Collections**	**Raw genera**	**Subsampled diversity**	**Good's u**
Maastrichtian	35	8	3.09	NA
Campanian	NA	NA	NA	0.944
Santonian	1	2	NA	NA
Coniacian	NA	NA	NA	NA
Turonian	NA	NA	NA	NA
Cenomanian	NA	NA	NA	NA
Albian	NA	NA	NA	NA
Aptian	NA	NA	NA	NA
Barremian	23	10	4.32	NA
Hauterivian	6	3	2.31	0.783
Valanginian	7	5	3.8	0.833
Berriasian	27	6	2.32	0.429
Tithonian	11	6	3.77	0.969
Kimmeridgian	10	6	2.57	0.727
Oxfordian	1	1	NA	0.867
Callovian	NA	NA	NA	NA
Bathonian	1	1	NA	NA
Bajocian	NA	NA	NA	NA
Aalenian	NA	NA	NA	NA
Toarcian	NA	NA	NA	NA
Pliensbachian	NA	NA	NA	NA
Sinemurian	NA	NA	NA	NA
Hettangian	1	1	NA	NA

Table 137. Regional subsampled non-marine crocodyliform diversity (SQSPs) in Europe.

	North America			
Bin	**Collections**	**Raw genera**	**Subsampled diversity**	**Good's u**
Maastrichtian	181	10	2.23	0.964
Campanian	45	4	1.59	0.969
Santonian	1	1	NA	NA
Coniacian	NA	NA	NA	NA
Turonian	NA	NA	NA	NA
Cenomanian	2	1	1	1
Albian	NA	NA	NA	NA
Aptian	1	1	NA	NA
Barremian	NA	NA	NA	NA
Hauterivian	NA	NA	NA	NA
Valanginian	NA	NA	NA	NA
Berriasian	NA	NA	NA	NA
Tithonian	6	4	2.5	0.5
Kimmeridgian	7	3	2.15	0.857
Oxfordian	NA	NA	NA	NA
Callovian	1	1	NA	NA
Bathonian	NA	NA	NA	NA
Bajocian	NA	NA	NA	NA
Aalenian	NA	NA	NA	NA
Toarcian	NA	NA	NA	NA
Pliensbachian	NA	NA	NA	NA
Sinemurian	NA	NA	NA	NA
Hettangian	10	1	1	1

Table 138. Regional subsampled non-marine crocodyliform diversity (SQSPs) in North America.

	South America			
Bin	**Collections**	**Raw genera**	**Subsampled diversity**	**Good's u**
Maastrichtian	6	4	2.61	0.714
Campanian	NA	NA	NA	NA
Santonian	10	6	3.03	0.636
Coniacian	NA	NA	NA	NA
Turonian	NA	NA	NA	NA
Cenomanian	NA	NA	NA	NA
Albian	NA	NA	NA	NA
Aptian	1	NA	NA	NA
Barremian	NA	NA	NA	NA
Hauterivian	NA	NA	NA	NA
Valanginian	NA	NA	NA	NA
Berriasian	NA	NA	NA	NA
Tithonian	NA	NA	NA	NA
Kimmeridgian	NA	NA	NA	NA
Oxfordian	NA	NA	NA	NA
Callovian	NA	NA	NA	NA
Bathonian	NA	NA	NA	NA
Bajocian	NA	NA	NA	NA
Aalenian	NA	NA	NA	NA
Toarcian	NA	NA	NA	NA
Pliensbachian	NA	NA	NA	NA
Sinemurian	NA	NA	NA	NA
Hettangian	NA	NA	NA	NA

Table 139. Regional subsampled non-marine crocodyliform diversity (SQSPs) in South America.

Africa				
Bin	**Collections**	**Raw Genera**	**Subsampled diversity**	**Good's u**
K8	32	6	1.78	0.937
K7	1	1	NA	NA
K6	1	2	NA	NA
K5	15	12	NA	NA
K4	4	3	2.15	0.5
K3	7	2	1.6	0.94
K2	NA	NA	NA	NA
K1	NA	NA	NA	NA
J6	3	2	1.53	0.667
J5	NA	NA	NA	NA
J4	2	1	1	1
J3	NA	NA	NA	NA
J2	NA	NA	NA	NA
J1	4	2	1.48	0.75

Table 140. SQSPt results on a regional level for Africa.

Asia				
Bin	**Collections**	**Raw genera**	**Subsampled diversity**	**Good's u**
K8	14	8	4.33	0.733
K7	8	6	4.03	0.556
K6	5	7	4.96	0.444
K5	1	1	NA	NA
K4	NA	NA	NA	NA
K3	1	1	NA	NA
K2	1	2	NA	NA
K1	NA	NA	NA	NA
J6	2	3	NA	NA
J5	9	4	1.66	0.7
J4	NA	NA	NA	NA
J3	NA	NA	NA	NA
J2	NA	NA	NA	NA
J1	4	4	3.11	0.4

Table 141. SQSPt results on a regional level for Asia.

Europe				
Bin	**Collections**	**Raw genera**	**Subsampled diversity**	**Good's u**
K8	35	8	3.12	0.944
K7	16	6	3.63	0.889
K6	1	2	NA	NA
K5	NA	NA	NA	NA
K4	4	3	2.4	0.5
K3	10	3	1.58	1
K2	33	10	3.95	0.879
K1	33	9	2.88	0.9
J6	17	8	3.11	0.923
J5	1	1	NA	NA
J4	1	1	NA	NA
J3	NA	NA	NA	NA
J2	NA	NA	NA	NA
J1	1	1	NA	NA

Table 142. SQSPt results on a regional level for Europe.

North America				
Bin	**Collections**	**Raw genera**	**Subsampled diversity**	**Good's u**
K8	181	10	2.15	0.964
K7	75	9	2.21	0.947
K6	4	2	1.46	0.75
K5	9	5	1.91	0.8
K4	3	3	NA	NA
K3	4	4	NA	NA
K2	NA	NA	NA	NA
K1	NA	NA	NA	NA
J6	36	7	1.91	0.919
J5	1	1	NA	NA
J4	NA	NA	NA	NA
J3	NA	NA	NA	NA
J2	NA	NA	NA	NA
J1	10	1	1	1

Table 143. SQSPt results on a regional level for North America.

South America				
Bin	**Collections**	**Raw genera**	**Subsampled diversity**	**Good's u**
K8	5	4	2.95	0.4
K7	4	3	2.32	0.5
K6	43	24	9.08	0.605
K5	3	1	1	1
K4	5	4	3.3	0.4
K3	5	3	1.63	0.8
K2	NA	NA	NA	NA
K1	NA	NA	NA	NA
J6	1	1	NA	NA
J5	1	1	NA	NA
J4	NA	NA	NA	NA
J3	NA	NA	NA	NA
J2	NA	NA	NA	NA
J1	NA	NA	NA	NA

Table 144. SQSPt results on a regional level for South America.

Europe

Bin	Collections	Raw genera	Subsampled diversity (SQSRc)	Standard deviation (SQSRc)	Good's u	Subsampled diversity (SQSRu)	Standard deviation (SQSRu)	Good's u
K8	26	8	1.611	0.025	0.944	1.712	0.027	0.978
K7	10	6	1.583	0.023	0.889	1.919	0.03	0.933
K6	1	2	NA	NA	NA	NA	NA	NA
K5	NA	NA	NA	NA	NA	NA	NA	NA
K4	3	3	NA	NA	0.5	NA	NA	0.5
K3	6	3	0.982	0.021	1	1.377	0.016	0.92
K2	22	10	2.05	0.028	0.879	1.86	0.032	0.878
K1	22	9	1.252	0.034	0.9	1.193	0.03	0.92
J6	15	8	2.276	0.027	0.923	2.087	0.023	0.97
J5	1	1	NA	NA	NA	NA	NA	NA
J4	1	1	NA	NA	NA	NA	NA	NA
J3	NA	NA	NA	NA	NA	NA	NA	NA
J2	NA	NA	NA	NA	NA	NA	NA	NA
J1	1	1	NA	NA	NA	NA	NA	NA

Table 145. SQSRc and SQSRu results on a regional level for Europe.

Asia

Bin	Collections	Raw genera	Subsampled diversity (SQSRc)	Standard deviation (SQSRc)	Good's u	Subsampled diversity (SQSRu)	Standard deviation (SQSRu)	Good's u
K8	12	8	3.014	0.026	0.733	2.565	0.036	0.75
K7	7	6	2.85	0.025	0.556	2.495	0.041	0.583
K6	5	7	NA	NA	0.444	2.878	0.043	0.643
K5	1	1	NA	NA	NA	0.9	0.02	1
K4	NA	NA	NA	NA	NA	0.895	0.022	0.6
K3	1	1	NA	NA	NA	5.347	0.04	0.6875
K2	1	2	NA	NA	NA	3.267	0.032	0.75
K1	NA	NA	NA	NA	NA	0.898	0.021	1
J6	2	3	NA	NA	NA	1.038	0.027	0.75
J5	9	5	0.967	0.024	0.636	0.993	0.025	0.769
J4	NA	NA	NA	NA	NA	NA	NA	NA
J3	NA	NA	NA	NA	NA	NA	NA	NA
J2	NA	NA	NA	NA	NA	NA	NA	NA
J1	4	4	NA	NA	0.4	NA	NA	0.4

Table 146. SQSRc and SQSRu results on a regional level for Asia.

Africa

Bin	Collections	Raw genera	Subsampled diversity (SQSRc)	Standard deviation (SQSRc)	Good's u	Subsampled diversity (SQSRu)	Standard deviation (SQSRu)	Good's u
K8	29	6	1.022	0.026	0.938	1.022	0.026	0.938
K7	1	1	NA	NA	NA	NA	NA	NA
K6	1	2	NA	NA	NA	NA	NA	NA
K5	13	12	8.295	0.022	0.47	6.371	0.049	0.619
K4	4	3	NA	NA	0.5	1.848	0.031	0.824
K3	6	2	0.918	0.019	1	1.939	0.028	0.733
K2	NA	NA	NA	NA	NA	NA	NA	NA
K1	NA	NA	NA	NA	NA	NA	NA	NA
J6	3	2	0.719	0.018	0.667	0.719	0.018	0.667
J5	NA	NA	NA	NA	NA	NA	NA	NA
J4	NA	NA	NA	NA	NA	NA	NA	NA
J3	NA	NA	NA	NA	NA	NA	NA	NA
J2	NA	NA	NA	NA	NA	NA	NA	NA
J1	4	2	0.836	0.018	0.75	0.836	0.018	0.75

Table 147. SQSRc and SQSRu results on a regional level for Africa.

North America

Bin	Collections	Raw genera	Subsampled diversity (SQSRc)	Standard deviation (SQSRc)	Good's u	Subsampled diversity (SQSRu)	Standard deviation (SQSRu)	Good's u
K8	122	10	0.986	0.022	0.967	0.986	0.022	0.967
K7	68	9	1.085	0.025	0.947	1.085	0.025	0.947
K6	4	2	0.836	0.019	0.75	0.884	0.014	0.833
K5	8	5	1.734	0.031	0.8	1.468	0.02	0.857
K4	3	3	NA	NA	NA	0.899	0.02	0.75
K3	4	4	NA	NA	NA	0.966	0.028	0.571
K2	NA	NA	NA	NA	NA	NA	NA	NA
K1	NA	NA	NA	NA	NA	NA	NA	NA
J6	31	7	0.997	0.02	0.919	0.997	0.02	0.919
J5	1	1	NA	NA	NA	NA	NA	NA
J4	NA	NA	NA	NA	NA	NA	NA	NA
J3	NA	NA	NA	NA	NA	NA	NA	NA
J2	NA	NA	NA	NA	NA	0.835	0.018	0.75
J1	10	1	1	0	1	0.947	0.021	0.929

Table 148. SQSRc and SQSRu results on a regional level for North America.

South America

Bin	Collections	Raw genera	Subsampled diversity (SQSRc)	Standard deviation (SQSRc)	Good's u	Subsampled diversity (SQSRu)	Standard deviation (SQSRu)	Good's u
K8	6	4	1.79	0.021	0.714	4.484	0.043	0.647
K7	3	2	0.717	0.021	0.667	2.887	0.049	0.643
K6	30	25	NA	NA	0.333	NA	NA	0.371
K5	2	1	NA	NA	1	0.836	0.017	0.75
K4	4	4	NA	NA	0.4	NA	NA	0.286
K3	4	3	1.603	0.021	0.8	3.404	0.017	0.571
K2	NA	NA	NA	NA	NA	NA	NA	NA
K1	NA	NA	NA	NA	NA	NA	NA	NA
J6	1	1	NA	NA	NA	NA	NA	NA
J5	NA	NA	NA	NA	NA	NA	NA	NA
J4	NA	NA	NA	NA	NA	NA	NA	NA
J3	NA	NA	NA	NA	NA	NA	NA	NA
J2	NA	NA	NA	NA	NA	NA	NA	NA
J1	NA	NA	NA	NA	NA	NA	NA	NA

Table 149. SQSRc and SQSRu results on a regional level for South America.

Appendix 12 - Complete results of phylogenetic diversity analyses for Crocodyliformes (Chapter 4).

Species				
Time bin	Equal	First-app	Random	Mean
Hettangian	29	13	19	20.33
Sinemurian	26	10	16	17.33
Pliensbachian	56	23	40	39.67
Toarcian	48	14	29	30.33
Aalenian	60	27	42	43.00
Bajocian	63	39	53	51.67
Bathonian	72	47	60	59.67
Callovian	67	45	55	55.67
Oxfordian	85	73	81	79.67
Kimmeridgian	75	66	75	72.00
Tithonian	54	47	54	51.67
Berriasian	46	39	46	43.67
Valanginian	44	37	44	41.67
Hauterivian	52	45	50	49.00
Barremian	118	111	122	117.00
Aptian	71	60	6	45.67
Albian	71	62	67	66.67
Cenomanian	67	58	63	62.67
Turonian	63	55	59	59.00
Coniacian	64	57	60	60.33
Santonian	51	50	50	50.33
Campanian	37	37	37	37.00

Table 150. Phylogenetic diversity (species) for all Crocodyliformes at the stage level (PDEs).

Genera				
Time bin	Equal	First-app	Random	Mean
Hettangian	20	12	16	16.00
Sinemurian	19	11	15	15.00
Pliensbachian	26	16	22	21.33
Toarcian	24	14	20	19.33
Aalenian	33	24	30	29.00
Bajocian	33	25	31	29.67
Bathonian	39	31	35	35.00
Callovian	44	38	42	41.33
Oxfordian	58	49	54	53.67
Kimmeridgian	52	45	48	48.33
Tithonian	40	34	36	36.67
Berriasian	39	33	35	35.67
Valanginian	38	32	34	34.67
Hauterivian	43	38	41	40.67
Barremian	95	92	97	94.67
Aptian	66	60	64	63.33
Albian	64	59	62	61.67
Cenomanian	67	62	67	65.33
Turonian	65	61	65	63.67
Coniacian	64	63	64	63.67
Santonian	44	44	44	44.00
Campanian	34	34	34	34.00

Table 151. Phylogenetic diversity (genera) for all Crocodyliformes at the stage level (PDEs).

10 million year time bin (PDEt)

	Equal	First-app	Random	Mean
J1	29	13	19	20.33
J2	66	36	60	54.00
J3	75	44	59	59.33
J4	96	85	96	92.33
J5	138	143	146	142.33
J6	127	121	137	128.33
K1	46	39	46	43.67
K2	128	124	132	128.00
K3	86	76	82	81.33
K4	96	92	95	94.33
K5	98	92	95	95.00
K6	90	97	93	93.33
K7	55	56	56	55.67
K8	NA	NA	NA	NA

Table 152. Phylogenetic diversity (species) for all Crocodyliformes at the 10 million year time bin level (PDEt).

	Equal	First-app	Random	Mean
J1	20	12	16	16.00
J2	32	23	31	28.67
J3	42	34	40	38.67
J4	46	42	44	44.00
J5	84	79	85	82.67
J6	68	65	64	65.67
K1	39	33	35	35.67
K2	102	100	106	102.67
K3	79	74	78	77.00
K4	85	83	85	84.33
K5	93	91	96	93.33
K6	67	71	67	68.33
K7	44	44	44	44.00
K8	NA	NA	NA	NA

Table 153. Phylogenetic diversity (genera) for all Crocodyliformes at the 10 million year time bin level (PDEt).

Appendix 13 – Full results from model fitting procedure between crocodyliform diversity estimates and extrinsic sampling and environmental parameters (Chapter 4).

Marine Variable	AICc	Akaike weights	Spearman's rho	p-value	Pearson's PMCC	p-value
NMA	71.956	0.051	-0.081	0.804	-0.018	0.955
Sea level (Haq)	71.960	0.051	0.027	0.936	0.008	0.981
Sea level (Miller)	**68.048**	**0.361**	0.193	0.549	0.042	0.903
FMF	71.907	0.052	-0.182	0.571	0.067	0.837
$\delta^{18}O$	71.406	0.067	0.228	0.477	-0.212	0.507
$\delta^{13}C$	70.510	0.105	-0.382	0.221	0.337	0.284
$^{87}Sr/^{86}Sr$	70.734	0.094	-0.165	0.609	-0.312	0.324
$\delta^{34}S$	70.735	0.094	0.172	0.594	-0.312	0.324
SQS diversity	71.777	0.056	-0.127	0.694	0.123	0.703
SST	71.407	0.067	-0.127	0.694	-0.212	0.508

Non-marine Variable	AICc	Akaike weights	Spearman's rho	p-value	Pearson's PMCC	p-value
NMA	95.712	0.016	0.105	0.750	0.012	0.970
Sea level (Haq)	95.179	0.020	0.357	0.256	0.209	0.515
Sea level (Miller)	**88.697**	**0.522**	0.345	0.299	0.156	0.647
FMF	94.649	0.027	-0.210	0.514	-0.291	0.358
$\delta^{18}O$	95.228	0.020	-0.175	0.588	-0.199	0.535
$\delta^{13}C$	93.662	0.044	**0.552**	0.067	0.396	0.202
$^{87}Sr/^{86}Sr$	94.686	0.026	-0.252	0.430	-0.287	0.367
$\delta^{34}S$	94.853	0.024	0.343	0.276	0.263	0.409
SQS diversity	95.699	0.016	0.203	0.528	0.035	0.913
SST	89.906	0.285	0.303	0.339	0.619	0.032

Table 154. Model fitting results for marine (top) and non-marine (bottom) crocodyliform raw taxonomic diversity and extrinsic environmental and sampling variables.

Marine

Variable	AICc	Akaike weights	Spearman's rho	p-value	Pearson's PMCC	p-value
NMA	24.498	0.017	0.321	0.498	0.214	0.645
Sea level (Haq)	22.571	0.045	0.357	0.444	0.525	0.227
Sea level (Miller)	**18.053**	**0.433**	**0.929**	**0.007**	**0.787**	**0.036**
FMF	23.502	0.028	0.321	0.498	0.415	0.354
$\delta^{18}O$	23.151	0.034	-0.429	0.354	-0.461	0.298
$\delta^{13}C$	**19.082**	**0.259**	**0.786**	**0.048**	**0.748**	0.053
$^{87}Sr/^{86}Sr$	24.711	0.016	-0.143	0.783	-0.127	0.786
$\delta^{34}S$	20.913	0.104	**-0.643**	0.139	**-0.654**	0.111
SQS diversity	22.595	0.045	0.286	0.556	**0.522**	0.229
SST	24.352	0.019	-0.143	0.783	-0.256	0.580

Non-marine

Variable	AICc	Akaike weights	Spearman's rho	p-value	Pearson's PMCC	p-value
NMA	40.078	0.033	0.000	1.000	0.046	0.906
Sea level (Haq)	40.097	0.032	-0.100	0.810	-0.010	0.980
Sea level (Miller)	40.096	0.032	0.117	0.776	0.013	0.974
FMF	38.726	0.064	-0.267	0.493	-0.376	0.319
$\delta^{18}O$	39.731	0.039	0.267	0.493	0.200	0.606
$\delta^{13}C$	40.080	0.033	-0.117	0.776	-0.045	0.909
$^{87}Sr/^{86}Sr$	39.073	0.054	0.150	0.708	0.328	0.389
$\delta^{34}S$	37.051	0.149	**0.650**	0.067	**0.536**	0.137
SQS diversity	39.940	0.035	-0.100	0.810	-0.132	0.735
SST	**34.513**	**0.529**	**-0.567**	0.121	**-0.680**	**0.044**

Marine (excluding Metriorhynchoidea)

Variable	AICc	Akaike weights	Spearman's rho	p-value	Pearson's PMCC	p-value
NMA	17.809	0.007	0.300	0.683	0.467	0.428
Sea level (Haq)	**10.424**	**0.278**	**0.900**	0.083	**0.906**	**0.034**
Sea level (Miller)	16.810	0.011	**0.600**	0.350	**0.600**	0.285
FMF	18.760	0.004	0.300	0.683	0.232	0.707
$\delta^{18}O$	18.417	0.005	-0.100	0.950	-0.342	0.574
$\delta^{13}C$	**8.722**	**0.650**	**0.900**	0.083	**0.934**	**0.020**
$^{87}Sr/^{86}Sr$	16.641	0.012	0.300	0.683	0.617	0.267
$\delta^{34}S$	18.224	0.006	**-0.700**	0.233	-0.388	0.519
SQS diversity	17.522	0.008	0.100	0.950	**0.511**	0.379
SST	15.805	0.019	**-0.700**	0.233	-0.690	0.197

Table 155. Model fitting results for marine (top) and non-marine (middle) and marine excluding Metriorhynchoidea (bottom) subsampled crocodyliform diversity (SQSPs) and extrinsic environmental and sampling variables.

Marine Variable	AICc	Akaike weights	Spearman's rho	p-value	Pearson's PMCC	p-value
NMA	24.390	0.081	-0.452	0.268	-0.326	0.430
Sea level (Haq)	22.961	0.166	0.071	0.882	**0.503**	0.204
Sea level (Miller)	24.208	0.089	0.393	0.396	0.380	0.400
FMF	25.288	0.052	0.048	0.935	0.018	0.966
$\delta^{18}O$	22.741	0.185	**-0.524**	0.197	**-0.522**	0.184
$\delta^{13}C$	24.674	0.070	-0.405	0.327	-0.272	0.514
$^{87}Sr/^{86}Sr$	24.876	0.064	-0.238	0.582	-0.225	0.593
$\delta^{34}S$	25.068	0.058	0.000	1.000	-0.166	0.695
SQS diversity	24.362	0.082	-0.071	0.882	-0.331	0.423
SST	23.118	0.153	-0.491	0.217	-0.488	0.220

Non-marine Variable	AICc	Akaike weights	Spearman's rho	p-value	Pearson's PMCC	p-value
NMA	35.785	0.008	-0.358	0.313	**-0.589**	0.073
Sea level (Haq)	34.907	0.013	**0.564**	0.096	**0.634**	**0.049**
Sea level (Miller)	**26.285**	**0.949**	**0.750**	**0.025**	**0.846**	**0.004**
FMF	39.596	0.001	-0.224	0.537	-0.208	0.565
$\delta^{18}O$	39.235	0.001	-0.030	0.946	-0.278	0.437
$\delta^{13}C$	39.565	0.001	0.309	0.387	0.215	0.551
$^{87}Sr/^{86}Sr$	40.035	0.001	-0.055	0.892	-0.016	0.965
$\delta^{34}S$	35.294	0.010	0.467	0.178	**0.615**	0.059
SQS diversity	35.785	0.008	0.055	0.892	-0.301	0.398
SST	36.141	0.007	0.043	0.906	**0.568**	0.087

Table 156. Model fitting results for marine (top) and non-marine (bottom) subsampled crocodyliform diversity (SQSPt) and extrinsic environmental and sampling variables.

Marine Variable	AICc	Akaike weights	Spearman's rho	p-value	Pearson's PMCC	p-value
NMA	22.843	0.044	0.071	0.906	0.074	0.875
Sea level (Haq)	20.009	0.183	0.214	0.662	**0.580**	0.172
Sea level (Miller)	22.611	0.050	0.371	0.497	**0.643**	0.169
FMF	22.861	0.044	0.286	0.556	0.054	0.908
$\delta^{18}O$	22.358	0.056	0.143	0.783	-0.268	0.561
$\delta^{13}C$	22.801	0.045	-0.143	0.783	0.107	0.819
$^{87}Sr/^{86}Sr$	19.725	0.210	**-0.714**	0.088	**-0.602**	0.152
$\delta^{34}S$	**19.458**	**0.240**	**-0.786**	**0.048**	**-0.622**	0.136
SQS diversity	22.664	0.048	0.464	0.302	-0.175	0.708
SST	21.696	0.079	**-0.631**	0.129	-0.395	0.381

Non-marine Variable	AICc	Akaike weights	Spearman's rho	p-value	Pearson's PMCC	p-value
NMA	45.663	0.009	-0.067	0.880	-0.380	0.314
Sea level (Haq)	42.896	0.037	**0.583**	0.108	**0.567**	0.111
Sea level (Miller)	38.558	0.328	0.310	0.462	**0.704**	0.051
FMF	45.663	0.009	-0.233	0.552	-0.278	0.468
$\delta^{18}O$	44.810	0.014	0.017	0.982	-0.401	0.285
$\delta^{13}C$	45.619	0.010	0.450	0.230	0.286	0.455
$^{87}Sr/^{86}Sr$	46.292	0.007	-0.333	0.385	-0.103	0.791
$\delta^{34}S$	42.653	0.042	0.217	0.581	0.583	0.100
SQS diversity	45.467	0.010	0.000	1.000	-0.312	0.414
SST	**37.585**	**0.533**	0.271	0.480	**0.790**	**0.011**

Table 157. Model fitting results for marine (top) and non-marine (bottom) subsampled crocodyliform diversity (SQSRc) and extrinsic environmental and sampling variables.

Non-marine Variable	AICc	Akaike weights	Spearman's rho	p-value	Pearson's PMCC	p-value
NMA	75.796	0.001	0.049	0.886	-0.021	0.948
Sea level (Haq)	75.003	0.002	0.280	0.379	0.254	0.426
Sea level (Miller)	**62.944**	**0.735**	0.430	0.218	0.436	0.208
FMF	73.975	0.003	0.231	0.471	0.376	0.229
$\delta^{18}O$	75.799	0.001	-0.112	0.733	-0.013	0.967
$\delta^{13}C$	**65.284**	**0.228**	**0.762**	**0.006**	**0.764**	**0.004**
$^{87}Sr/^{86}Sr$	73.825	0.003	0.343	0.276	0.390	0.211
$\delta^{34}S$	75.002	0.002	0.357	0.256	0.254	0.426
SQS diversity	69.884	0.023	0.406	0.193	**0.624**	**0.030**
SST	75.554	0.001	-0.286	0.368	-0.143	0.658

Table 158. Model fitting results for non-marine subsampled crocodyliform diversity (SQSRu) and extrinsic environmental and sampling variables.

Genera (all)

Variable	AICc	Akaike weights	Spearman's rho	p-value	Pearson's PMCC	p-value
NMA	101.332	0.013	-0.182	0.595	-0.291	0.385
Sea level (Haq)	97.331	0.093	**0.682**	**0.025**	**0.603**	**0.049**
Sea level (Miller)	**92.938**	**0.836**	**0.745**	**0.012**	**0.757**	**0.007**
FMF	102.155	0.008	0.391	0.237	0.117	0.731
$\delta^{18}O$	101.881	0.010	0.091	0.797	0.195	0.565
$\delta^{13}C$	102.257	0.008	0.218	0.521	0.068	0.843
$^{87}Sr/^{86}Sr$	102.197	0.008	-0.100	0.776	0.100	0.770
$\delta^{34}S$	102.261	0.008	-0.409	0.214	0.065	0.849
SQS diversity	102.208	0.008	0.373	0.261	0.095	0.781
SST	102.041	0.009	0.382	0.248	0.155	0.650

Species (all)

Variable	AICc	Akaike weights	Spearman's rho	p-value	Pearson's PMCC	p-value
NMA	107.113	0.011	0.264	0.435	0.020	0.954
Sea level (Haq)	102.817	0.097	**0.600**	0.056	**0.569**	0.068
Sea level (Miller)	**98.587**	**0.805**	**0.645**	**0.037**	**0.735**	**0.010**
FMF	107.098	0.011	0.018	0.968	-0.042	0.903
$\delta^{18}O$	107.055	0.012	-0.355	0.286	-0.075	0.825
$\delta^{13}C$	106.681	0.014	0.373	0.261	0.197	0.561
$^{87}Sr/^{86}Sr$	107.051	0.012	-0.291	0.386	-0.077	0.821
$\delta^{34}S$	107.117	0.011	-0.155	0.654	0.006	0.987
SQS diversity	107.098	0.011	-0.036	0.924	-0.042	0.903
SST	106.527	0.015	0.609	0.052	0.229	0.499

Table 159. Model fitting results for total crocodyliform phylogenetic diversity (PDEs) at the genus (top) and species (bottom) levels and extrinsic environmental and sampling variables.

Genera Variable	AICc	Akaike weights	Spearman's rho	p-value	Pearson's PMCC	p-value
NMA	61.986	0.175	0.345	0.299	0.423	0.194
Sea level (Haq)	64.141	0.060	-0.027	0.946	-0.041	0.906
Sea level (Miller)	64.144	0.060	-0.100	0.776	-0.037	0.914
FMF	64.144	0.059	0.209	0.539	0.024	0.945
$\delta^{18}O$	64.073	0.062	0.009	0.989	0.088	0.796
$\delta^{13}C$	63.199	0.096	0.109	0.755	0.289	0.389
$^{87}Sr/^{86}Sr$	**61.392**	**0.236**	**-0.500**	0.121	-0.472	0.143
$\delta^{34}S$	64.127	0.060	0.000	1.000	-0.055	0.873
SQS diversity	63.954	0.066	0.064	0.860	0.136	0.690
SST	62.622	0.128	0.491	0.129	0.361	0.275

Species Variable	AICc	Akaike weights	Spearman's rho	p-value	Pearson's PMCC	p-value
NMA	81.603	0.107	0.255	0.451	0.220	0.515
Sea level (Haq)	82.151	0.081	0.173	0.614	0.004	0.992
Sea level (Miller)	82.143	0.081	-0.018	0.968	0.029	0.934
FMF	81.771	0.098	0.082	0.818	-0.184	0.588
$\delta^{18}O$	82.151	0.081	-0.073	0.839	0.006	0.986
$\delta^{13}C$	82.144	0.081	-0.073	0.839	-0.027	0.938
$^{87}Sr/^{86}Sr$	81.861	0.094	-0.073	0.839	-0.162	0.635
$\delta^{34}S$	81.210	0.130	0.282	0.402	0.286	0.393
SQS diversity	81.880	0.093	0.045	0.903	-0.156	0.647
SST	**80.875**	**0.154**	0.318	0.341	0.331	0.320

Table 160. Model fitting results for marine crocodyliform phylogenetic diversity (PDEs) at the genus (top) and species (bottom) levels and extrinsic environmental and sampling variables.

Genera Variable	AICc	Akaike weights	Spearman's rho	p-value	Pearson's PMCC	p-value
NMA	96.047	0.035	-0.565	0.070	-0.522	0.100
Sea level (Haq)	94.191	0.088	**0.770**	**0.006**	**0.620**	**0.042**
Sea level (Miller)	**89.704**	**0.827**	**0.642**	**0.033**	**0.769**	**0.006**
FMF	99.517	0.006	0.077	0.821	0.045	0.896
$\delta^{18}O$	98.677	0.009	0.155	0.649	0.274	0.414
$\delta^{13}C$	99.380	0.007	-0.159	0.640	-0.120	0.726
$^{87}Sr/^{86}Sr$	98.649	0.009	0.205	0.545	0.279	0.406
$\delta^{34}S$	99.118	0.007	-0.036	0.915	0.194	0.568
SQS diversity	99.536	0.006	0.141	0.679	-0.016	0.962
SST	99.517	0.006	0.241	0.474	0.044	0.897

Species Variable	AICc	Akaike weights	Spearman's rho	p-value	Pearson's PMCC	p-value
NMA	103.322	0.008	-0.236	0.486	-0.406	0.215
Sea level (Haq)	98.038	0.114	**0.855**	**0.002**	**0.695**	**0.018**
Sea level (Miller)	**94.021**	**0.852**	**0.873**	**0.001**	**0.801**	**0.003**
FMF	105.229	0.003	0.300	0.371	0.082	0.810
$\delta^{18}O$	104.825	0.004	0.009	0.989	0.206	0.543
$\delta^{13}C$	105.297	0.003	0.245	0.468	-0.024	0.944
$^{87}Sr/^{86}Sr$	104.147	0.005	0.309	0.356	0.316	0.344
$\delta^{34}S$	105.057	0.003	-0.164	0.634	0.149	0.662
SQS diversity	105.280	0.003	0.491	0.129	0.046	0.893
SST	105.266	0.003	-0.055	0.882	-0.059	0.864

Table 161. Model fitting results for mpm=marine crocodyliform phylogenetic diversity (PDEs) at the genus (top) and species (bottom) levels and extrinsic environmental and sampling variables.

Genera (all)

Variable	AICc	Akaike weights	Spearman's rho	p-value	Pearson's PMCC	p-value
NMA	117.613	0.000	-0.224	0.485	-0.263	0.409
Sea level (Haq)	114.237	0.000	**0.608**	**0.040**	**0.545**	0.067
Sea level (Miller)	**97.926**	**0.999**	0.382	0.279	0.444	0.199
FMF	118.295	0.000	0.203	0.528	0.122	0.707
$\delta^{18}O$	118.446	0.000	-0.063	0.852	-0.048	0.882
$\delta^{13}C$	117.639	0.000	0.315	0.320	0.259	0.416
$^{87}Sr/^{86}Sr$	118.430	0.000	0.063	0.852	-0.060	0.853
$\delta^{34}S$	118.413	0.000	-0.196	0.543	-0.071	0.826
SQS diversity	118.435	0.000	-0.070	0.834	-0.056	0.862
SST	118.378	0.000	0.225	0.481	0.089	0.783

Species (all)

Variable	AICc	Akaike weights	Spearman's rho	p-value	Pearson's PMCC	p-value
NMA	125.122	0.000	-0.119	0.716	-0.077	0.813
Sea level (Haq)	122.206	0.000	**0.545**	**0.071**	0.469	0.124
Sea level (Miller)	**105.651**	**0.999**	0.188	0.608	0.140	0.700
FMF	125.177	0.000	0.000	1.000	-0.037	0.910
$\delta^{18}O$	124.799	0.000	-0.224	0.485	-0.180	0.576
$\delta^{13}C$	124.721	0.000	0.203	0.528	0.196	0.541
$^{87}Sr/^{86}Sr$	120.917	0.000	-0.364	0.246	-0.548	0.065
$\delta^{34}S$	123.540	0.000	-0.238	0.457	-0.359	0.252
SQS diversity	124.660	0.000	-0.147	0.651	-0.208	0.516
SST	125.139	0.000	0.148	0.647	-0.067	0.835

Table 162. Model fitting results for total crocodyliform phylogenetic diversity (PDEt) at the genus (top) and species (bottom) levels and extrinsic environmental and sampling variables.

Genera

Variable	AICc	Akaike weights	Spearman's rho	p-value	Pearson's PMCC	p-value
NMA	81.707	0.006	-0.035	0.921	0.149	0.644
Sea level (Haq)	81.962	0.005	-0.133	0.683	-0.034	0.916
Sea level (Miller)	**71.474**	**0.942**	-0.224	0.537	-0.186	0.608
FMF	81.829	0.005	-0.168	0.604	-0.110	0.733
$\delta^{18}O$	81.962	0.005	0.154	0.635	-0.035	0.915
$\delta^{13}C$	80.426	0.011	0.042	0.904	0.348	0.268
$^{87}Sr/^{86}Sr$	80.753	0.009	-0.385	0.218	-0.311	0.325
$\delta^{34}S$	81.133	0.008	-0.154	0.635	-0.261	0.413
SQS diversity	81.972	0.005	-0.280	0.379	-0.020	0.952
SST	81.976	0.005	0.169	0.600	0.004	0.990

Species

Variable	AICc	Akaike weights	Spearman's rho	p-value	Pearson's PMCC	p-value
NMA	125.122	0.000	-0.119	0.716	0.469	0.124
Sea level (Haq)	122.206	0.000	**0.545**	0.071	0.140	0.700
Sea level (Miller)	**105.651**	**0.999**	0.188	0.608	-0.037	0.910
FMF	125.177	0.000	0.000	1.000	-0.180	0.576
$\delta^{18}O$	124.799	0.000	-0.224	0.485	0.196	0.541
$\delta^{13}C$	124.721	0.000	0.203	0.528	**-0.548**	0.065
$^{87}Sr/^{86}Sr$	120.917	0.000	-0.364	0.246	-0.359	0.252
$\delta^{34}S$	123.540	0.000	-0.238	0.457	-0.208	0.516
SQS diversity	124.660	0.000	-0.147	0.651	-0.208	0.516
SST	125.139	0.000	0.148	0.647	-0.067	0.835

Genera

Variable	AICc	Akaike weights	Spearman's rho	p-value	Pearson's PMCC	p-value
NMA	65.473	0.017	0.413	0.185	0.455	0.137
Sea level (Haq)	68.256	0.004	0.119	0.716	0.011	0.973
Sea level (Miller)	**57.590**	**0.873**	0.394	0.263	0.272	0.446
FMF	67.018	0.008	0.301	0.343	0.313	0.322
$\delta^{18}O$	68.197	0.004	0.112	0.733	0.071	0.827
$\delta^{13}C$	64.758	0.024	0.231	0.471	0.503	0.096
$^{87}Sr/^{86}Sr$	67.987	0.005	-0.098	0.766	-0.149	0.643
$\delta^{34}S$	65.863	0.014	-0.427	0.169	-0.425	0.168
SQS diversity	63.487	0.046	**0.531**	0.079	**0.573**	0.052
SST	67.835	0.005	0.035	0.914	-0.186	0.563

Species

Variable	AICc	Akaike weights	Spearman's rho	p-value	Pearson's PMCC	p-value
NMA	95.574	0.000	0.021	0.956	0.290	0.360
Sea level (Haq)	95.821	0.000	-0.224	0.485	-0.256	0.423
Sea level (Miller)	**79.244**	**0.998**	-0.164	0.657	-0.278	0.436
FMF	96.425	0.000	0.056	0.869	-0.131	0.686
$\delta^{18}O$	96.594	0.000	0.112	0.733	-0.056	0.863
$\delta^{13}C$	96.531	0.000	-0.175	0.588	-0.091	0.777
$^{87}Sr/^{86}Sr$	96.516	0.000	-0.098	0.766	-0.098	0.762
$\delta^{34}S$	96.631	0.000	0.007	0.991	-0.009	0.979
SQS diversity	96.624	0.000	0.252	0.430	0.025	0.939
SST	96.021	0.000	-0.190	0.554	-0.223	0.486

Table 163. Model fitting results for marine crocodyliform phylogenetic diversity (PDEt) including (top two) and excluding (bottom two) Metriorhynchoidea at the genus and species levels and extrinsic environmental and sampling variables.

Genera Variable	AICc	Akaike weights	Spearman's rho	p-value	Pearson's PMCC	p-value
NMA	114.977	0.000	-0.189	0.558	-0.337	0.284
Sea level (Haq)	112.070	0.000	**0.713**	**0.012**	**0.552**	0.063
Sea level (Miller)	**96.101**	**0.999**	0.479	0.166	0.479	0.161
FMF	116.335	0.000	0.112	0.733	0.087	0.788
$\delta^{18}O$	116.395	0.000	-0.175	0.588	-0.051	0.875
$\delta^{13}C$	116.264	0.000	0.280	0.379	0.116	0.720
$^{87}Sr/^{86}Sr$	116.422	0.000	0.091	0.783	0.019	0.952
$\delta^{34}S$	116.423	0.000	-0.119	0.716	0.016	0.961
SQS diversity	116.178	0.000	-0.119	0.716	-0.143	0.657
SST	116.337	0.000	0.239	0.454	0.086	0.791

Species Variable	AICc	Akaike weights	Spearman's rho	p-value	Pearson's PMCC	p-value
NMA	123.325	0.000	-0.224	0.485	-0.219	0.495
Sea level (Haq)	119.797	0.000	**0.552**	0.067	**0.539**	0.071
Sea level (Miller)	**102.374**	**1.000**	0.442	0.204	0.402	0.250
FMF	123.851	0.000	0.252	0.430	0.072	0.825
$\delta^{18}O$	123.880	0.000	-0.028	0.939	-0.052	0.872
$\delta^{13}C$	123.295	0.000	0.217	0.499	0.224	0.484
$^{87}Sr/^{86}Sr$	123.461	0.000	0.091	0.783	-0.192	0.550
$\delta^{34}S$	123.761	0.000	-0.196	0.543	-0.112	0.729
SQS diversity	123.795	0.000	0.056	0.869	-0.099	0.760
SST	123.725	0.000	0.092	0.777	0.125	0.700

Table 164. Model fitting results for non-marine crocodyliform diversity at the genus (top) and species (bottom) levels and extrinsic environmental and sampling parameters.